

<b>REPORT DOCUMENTATION PAGE</b>	1. REPORT NO. NSF/RA 780619	2.	3. Recipient's Accession No. <b>PH300508</b>
4. Title and Subtitle Microzonation for Safer Construction, Research and Application, Proceedings of the Second International Conference, Vol. 3, (San Francisco, 11/26/78 - 12/1/78)		5. Report Date 1978	
7. Author(s)		6.	
9. Performing Organization Name and Address University of Washington at Seattle Seattle, Washington 98105		8. Performing Organization Rept. No.	
12. Sponsoring Organization Name and Address Engineering and Applied Science (EAS) National Science Foundation 1800 G Street, N.W. Washington, D.C. 20550		10. Project/Task/Work Unit No.	
15. Supplementary Notes		11. Contract(C) or Grant(G) No. (C) (G) PFR7723228	
16. Abstract (Limit: 200 words) Proceedings of three conference sessions are presented. The first dealt with engineering mechanics and structural design. General topics include the need for a comprehensive approach in establishing design earthquakes, building on isolators, and selecting buildings for strong-motion instrumentation. Specialized subjects encompass spectra response studies, effective peak acceleration, and influence of soil structure interaction effects on large panel prefabrication buildings. Offshore microzonation constituted the theme of the second session. An overview of microzonation of offshore areas was followed by presentation of factors influencing seismic exposure evaluation for offshore areas and various considerations in offshore platform design. Reports were presented on the Baltimore Canyon and Southern California coastal region. Various technical aspects of offshore structures were described, and guidelines given for designing offshore structures for an earthquake environment. The final session dealt with urban planning, socio-economics, and government responsibility. Issues discussed include policy and administrative implications of microzonation, earthquake and insurance, and the role of the U.S. Geological Survey in geologic hazards warning.		13. Type of Report & Period Covered	
17. Document Analysis a. Descriptors Urban planning Hazards Earthquakes  b. Identifiers/Open-Ended Terms Baltimore Canyon Southern California coastal region Microzonation  c. COSATI Field/Group		14.	
18. Availability Statement NTIS		19. Security Class (This Report)	21. No. of Pages 399
		20. Security Class (This Page)	22. Price A17-A01



**PROCEEDINGS OF  
THE SECOND INTERNATIONAL CONFERENCE ON  
MICROZONATION  
FOR SAFER CONSTRUCTION—RESEARCH AND APPLICATION**



**VOLUME**

**III**

*Any opinions, findings, conclusions  
or recommendations expressed in this  
publication are those of the author(s)  
and do not necessarily reflect the views  
of the National Science Foundation.*

**Sponsored by:  
National Science Foundation  
UNESCO  
American Society of Civil Engineers  
Earthquake Engineering Research Institute  
Seismological Society of America  
Universities Council for Earthquake Engineering Research**

**SAN FRANCISCO, CALIFORNIA, U.S.A.**

**ii**

**NOVEMBER 26-DECEMBER 1, 1978**





# TABLE OF CONTENTS

## VOLUME I

STATE-OF-THE-ART SESSION		Page
C. Kisslinger	Seismicity and Global Tectonics as a Framework for Microzonation . . . . .	3
P. C. Jennings D. V. Helmberger	Strong-Motion Seismology . . . . .	27
N. C. Donovan	Soil & Geologic Effects on Site Response . . . . .	55
M. A. Sherif I. Ishibashi	Soil Dynamics Considerations for Microzonation . . . . .	81
A. S. Veletsos	Soil-Structure Interaction for Buildings during Earthquakes . . . . .	111
L. S. Cluff	Geologic Considerations for Seismic Microzonation . . . . .	135
V. J. Murphy	Geophysical Engineering Investigative Techniques for Site Characterization . . . . .	153
J. R. Hutton D. S. Mileti	Social Aspects of Earthquakes . . . . .	179
H. J. Lagorio E. E. Botsai	Urban Design and Earthquakes . . . . .	193
K. V. Steinbrugge	Earthquake Insurance and Microzonation . . . . .	203
N. S. Remmer	Government Responsibility in Microzonation . . . . .	215

## MICROZONATION SESSION

### Progress on Seismic Zonation in the San Francisco Bay Region

E. E. Brabb R. D. Borchardt	1. Introduction and Summary . . . . .	229
D. G. Herd	2. Neotectonic Framework of Central Coastal California and Its Implications to Microzonation of the San Francisco Bay Region . . . . .	231
R. D. Borchardt J. F. Gibbs T. E. Fumal	3. Progress on Ground Motion Predictions for the San Francisco Bay Region, California . . . . .	241
R. J. Archuleta W. B. Joyner D. M. Boore	4. A Methodology for Predicting Ground Motion at Specific Sites . . . . .	255

T. L. Youd J. C. Tinsley D. M. Perkins E. J. King R. F. Preston	5. Liquefaction Potential Map of San Fernando Valley, California . . . . .	267
D. K. Keefer G. F. Wieczorek E. L. Harp D. H. Tuel	6. Preliminary Assessment of Seismically Induced Landslide Susceptibility . . . . .	279
S. T. Algermissen K. V. Steinbrugge	7. Earthquake Losses to Buildings in the San Francisco Bay Area . . . . .	291
W. J. Kockelman E. E. Brabb	8. Examples of Seismic Zonation in the San Francisco Bay Region . . . . .	303
J. B. Perkins	9. The Use of Earthquake and Related Information in Regional Planning--What We've Done and Where We're Going . . . . .	315
W. G. Milne D. H. Weichert	The Sensitivity of Seismic Risk Maps to the Choice of Earthquake Parameters in the Georgia Strait Region of British Columbia . . . . .	323
J. A. Fischer J. G. McWhorter	The Microzonation of New York State: Progress Report No. 2 . . . . .	329
J. Kuroiwa E. Deza H. Jaén J. Kogan	Microzonation Methods and Techniques Used in Peru	341
E. L. Harp R. C. Wilson G. F. Wieczorek D. K. Keefer	Landslides from the February 4, 1976 Guatemala Earthquake: Implications for Seismic Hazard Reduction in the Guatemala City Area . . . . .	353
S. T. Mau C. S. Kao	A Risk Model for Seismic Zoning of Taiwan . . . . .	367
H. K. Acharya	Ground Motion Attenuation in the Philippines . . . . .	379
K. Moazami-Goudarzi H. Parhikhteh	A Quantitative Seismotectonic Study of the Iranian Plateau . . . . .	391
N. Mândrescu	The Vrancea Earthquake of March 4, 1977 and the Seismic Microzonation of Bucharest . . . . .	399
J. Petrovski	Need for Experimental Evidence in Development of Seismic Microzoning Methods . . . . .	413
S. Hattori	A New Proposal of the Seismic Risk Map Based on the Maximum Earthquake Motions, the Ground Characteristics and the Temporal Variations of the Seismicity	421
E. Shima	Seismic Microzoning Map of Tokyo . . . . .	433

S. Yoshikawa Y. T. Iwasaki M. Tai	Microzoning of Osaka Region . . . . .	445
D. R. Packer L. S. Cluff D. P. Schwartz F. H. Swan, III I. M. Idriss	Auburn Dam - A Case History of Earthquake Evaluation for a Critical Facility . . . . .	457
E. J. Bell D. T. Trexler J. W. Bell	Computer-Simulated Composite Earthquake Hazard Model for Reno, Nevada . . . . .	471
A. S. Patwardhan D. D. Tillson R. L. Nowack	Zonation for Critical Facilities Based on Two-Level Earthquakes . . . . .	485
W. W. Hays S. T. Algermissen R. D. Miller K. W. King	Preliminary Ground Response Maps for the Salt Lake City, Utah, Area . . . . .	497
C. E. Glass	Application of Regionalized Variables to Micro- zonation . . . . .	509
J. L. Alonso L. Urbina	A New Microzonation Technique for Design Purposes	523
A. S. Patwardhan L. S. Cluff	The Concept of Residual Risk in Earthquake Risk Assessments . . . . .	535
S. Murakami K. Midorikawa	Land Use Technique for Microzonation . . . . .	547
J. G. Anderson M. D. Trifunac	Application of Seismic Risk Procedures to Problems in Microzonation . . . . .	559
B. A. Schell	Seismotectonic Microzoning for Earthquake Risk Reduction . . . . .	571
A Report on the Miyagiken-oki, Japan, Earthquake of June 12, 1978		
	Abstract . . . . .	587
H. Kobayashi K. Seo S. Midorikawa	I. Strong Ground Motions and Seismic Microzoning	588
Y. Yoshimi I. Tohno K. Tokimatsu	II. Geotechnical Aspects of Damage . . . . .	600
T. Katayama	III. Damage to Lifeline Utility Systems (A) . . .	606
H. Shibata	IV. Damage to Lifeline Utility Systems (B) . . .	612

Index of Authors

VOLUME II

GEOLOGY, SEISMOLOGY, GEOPHYSICS AND SITE EFFECTS SESSION

B. A. Bolt	Fallacies in Current Ground Motion Prediction . . .	617
E. W. Hart	Zoning for the Hazard of Surface Fault Rupture in California . . . . .	635
M. R. Ploessel	High-Resolution Geophysical Surveys, A Technique for Microzonation of the Continental Shelf . . . .	647
L. Esteva E. Bazán	Seismicity and Seismic Risk Related to Subduction Zones . . . . .	657
W. D. Page W. U. Savage J. N. Alt L. S. Cluff D. Tocher	Seismic Hazards along the Makran Coast of Iran and Pakistan: The Importance of Regional Tectonics and Geologic Assessment . . . . .	669
S. Kh. Negmatullaev G. S. Seleznyov D. W. Simpson C. Rojahn	Engineering and Seismological Observations at Dams	681
R. A. Wiggins G. A. Frazier J. Sweet R. Apsel	Modeling Strong Motions from Major Earthquakes . .	693
F. T. Wu	Prediction of Strong Ground Motion Using Small Earthquakes . . . . .	701
T. Iwasaki T. Katayama K. Kawashima M. Saeki	Statistical Analysis of Strong-Motion Acceleration Records Obtained in Japan . . . . .	705
A. F. Shakal M. N. Toksöz	Analysis of Source and Medium Effects on Strong Motion Observations . . . . .	717
F. J. Sánchez-Sesma	Ground Motion Amplification due to Canyons of Arbitrary Shape . . . . .	729
E. Mardiross	A Method for Assessment of Seismic Design Motions	739
A. M. Rogers W. W. Hays	Preliminary Evaluation of Site Transfer Functions Developed from Earthquakes and Nuclear Explosions	753
K. Kudo	The Contribution of Love Waves to Strong Ground Motions . . . . .	765
I. S. Oweis	The Relevancy of One Dimensional Shear Models in Predicting Surface Acceleration . . . . .	777

N. Goto Y. Ohta H. Kagami	Deep Shear Wave Velocity Measurement for Evaluation of 1-10 Sec Seismic Input Motions . . . . .	793
K. Sadigh M. S. Power R. R. Youngs	Peak Horizontal and Vertical Accelerations, Velocities, and Displacements on Deep Soil Sites during Moderately Strong Earthquakes . . . . .	801
F. J. Sabina I. Herrera R. England	Theory of Connectivity: Applications to Scattering of Seismic Waves. I. SH Wave Motion . . . . .	813
S. Midorikawa H. Kobayashi	On Estimation of Strong Earthquake Motions with Regard to Fault Rupture . . . . .	825

SOIL DYNAMICS, SOIL-STRUCTURE INTERACTION AND GROUND EFFECTS SESSION

W. D. L. Finn Y. P. Vaid S. K. Bhatia	Constant Volume Cyclic Simple Shear Testing . . . . .	839
Y. Yoshimi K. Tokimatsu	Two-Dimensional Pore Pressure Changes in Sand Deposits during Earthquakes . . . . .	853
A. S. Arya P. Nandakumaran V. K. Puri S. Mukerjee	Verification of Liquefaction Potential by Field Blast Tests . . . . .	865
H. Dezfulian S. R. Prager	Use of Penetration Data for Evaluation of Liquefaction Potential . . . . .	873
T. Iwasaki F. Tatsuoka K. Tokida S. Yasuda	A Practical Method for Assessing Soil Liquefaction Potential Based on Case Studies at Various Sites in Japan . . . . .	885
K. Ishihara K. Ogawa	Liquefaction Susceptibility Map of Downtown Tokyo	897
J. Isenberg D. K. Vaughan	Three-Dimensional Nonlinear Analysis of Soil-Structure Interaction in a Nuclear Power Plant Containment Structure . . . . .	911
E. Alarcón J. Domínguez A. Martín F. Paris	Boundary Methods in Soil-Structure Interaction . . . . .	921
Y. Sugimura	Seismic Shear Strain Induced in Soil Deposits . . . . .	933
R. D. Singh W. S. Gardner R. Dobry	Post Cyclic Loading Behavior of Soft Clays . . . . .	945

S. Nemat-Nasser A. Shokooch	A New Approach for the Analysis of Liquefaction of Sand in Cyclic Shearing . . . . .	957
K. Tanimoto M. Nishi T. Noda	A Study of Shear Deformation Process of Sandy Soils by the Observation of Acoustic Emission Response . . . . .	971
W. P. Grant I. Arango D. N. Clayton	Geotechnical Data at Selected Strong Motion Accelerograph Sites . . . . .	983
Y. Shioi T. Furuya M. Okahara	Recent Earthquake Resistant Design Methods for Different Types of Foundations in Japan . . . . .	1001
W. F. Marcuson, III R. F. Ballard, Jr. S. S. Cooper	Comparison of Penetration Resistance Values to In Situ Shear Wave Velocities . . . . .	1013
C. M. Duke G. C. Liang	Site Effects from Fourier Transforms . . . . .	1025
A. M. Abdel-Ghaffar R. F. Scott	Dynamic Characteristics of an Earth Dam from Two Recorded Earthquake Motions . . . . .	1037
B. Tucker J. King K. Aki J. Brune I. Nersesov W. Prothero G. Shpilker G. Self	A Preliminary Report on a Study of the Seismic Response of Three Sediment-Filled Valleys in the Garm Region of the USSR . . . . .	1051
K. W. Campbell	Empirical Synthesis of Seismic Velocity Profiles from Geotechnical Data . . . . .	1063
S. D. Werner H. S. Ts'ao	Effect of Local Site Conditions on Spectral Amplification Factors . . . . .	1077
I. Lam C. F. Tsai G. R. Martin	Determination of Site Dependent Spectra Using Non-linear Analysis . . . . .	1089
M. L. Traubenik J. E. Valera W. H. Roth	Effects of Soil Inertia Forces on Design of Buried Pipelines Crossing Faults . . . . .	1105
C. B. Crouse B. E. Turner	Analysis of Ground Motion Spectra . . . . .	1117

Index of Authors

VOLUME III

ENGINEERING MECHANICS AND STRUCTURAL DESIGN SESSION

G. C. Hart C. Rojahn	Selection of Buildings for Strong-Motion Instrumentation Using Zonation Information and Decision Theory . . . . .	1135
V. V. Bertero S. A. Mahin	Need for a Comprehensive Approach in Establishing Design Earthquakes . . . . .	1145
A. R. Chandrasekaran D. K. Paul	Velocity Response Spectra for Sites on Rock or Soil	1157
P. C. Chen J. H. Chen	Generation of Floor Response Spectra Directly from Free-Field Design Spectra . . . . .	1169
T. Hisada Y. Ohsaki M. Watabe T. Ohta	Design Spectra for Stiff Structures on Rock . . . .	1187
A. H. Hadjian	On the Correlation of the Components of Strong Ground Motion . . . . .	1199
T. Iwasaki K. Kawashima	Seismic Analysis of a Highway Bridge Utilizing Strong-Motion Acceleration Records . . . . .	1211
G. C. Delfosse J. C. Miranda	Buildings on Isolators for Earthquake Protection	1223
W. J. Hall J. R. Morgan N. M. Newmark	Traveling Seismic Waves and Structural Response . .	1235
R. V. Whitman	Effective Peak Acceleration . . . . .	1247
B. Mohraz M. L. Eskijian	A Study of Earthquake Response Spectra for Offshore Platforms . . . . .	1257
J. Petrovski	Influence of Soil-Structure Interaction Effects on Dynamic Response of Large Panel Prefabricated Buildings . . . . .	1269

OFFSHORE MICROZONATION SESSION

I. M. Idriss L. S. Cluff A. S. Patwardhan	Microzonation of Offshore Areas - An Overview . . .	1281
A. S. Patwardhan	Factors Influencing Seismic Exposure Evaluation for Offshore Areas . . . . .	1291
R. G. Bea M. R. Akky	Seismic Exposure and Reliability Considerations in Offshore Platform Design . . . . .	1307

J. A. Fischer C. T. Spiker	Preliminary Microzonation of the Baltimore Canyon Lease Area . . . . .	1329
L. A. Selzer R. T. Eguchi T. K. Hasselman	Seismic Risk Evaluation of Southern California Coastal Region . . . . .	1341
J. R. Benjamin F. A. Webster C. Kircher	The Uncertainty in Seismic Loading and Response Criteria . . . . .	1369
D. Nair J. B. Weidler R. A. Hayes	Inelastic Seismic Design Considerations for Offshore Platforms . . . . .	1383
H. Kappler G. I. Schuëller	The Influence of Microzonation on the Reliability- Based Design of Offshore Structures . . . . .	1399
B. J. Watt R. C. Byrd	Aseismic Design Considerations for Concrete Gravity Platforms . . . . .	1409
Y. Moriwaki E. H. Doyle	Site Effects on Microzonation in Offshore Areas . .	1433
H. J. Swanger D. M. Boore	Importance of Surface Waves in Strong Ground Motion in the Period Range of 1 to 10 Seconds . . . . .	1447
J. Kallaby W. W. Mitchell	Guidelines for Design of Offshore Structures for Earthquake Environment . . . . .	1459

URBAN PLANNING, SOCIO-ECONOMICS AND GOVERNMENT RESPONSIBILITY SESSION

R. A. Olson	The Policy and Administrative Implications of Seismic Microzonation: Toward Logic or Confusion	1475
M. Abolafia A. L. Kafka	Toward a Measure of Socio-Seismicity . . . . .	1489
E. Kuribayashi T. Tazaki	An Evaluation Study on the Distribution of Property Losses Caused by Earthquakes . . . . .	1499
H. C. Cochrane	Potential for Inflated Building Costs after Disaster . . . . .	1511
R. Themptander	Earthquake and Insurance . . . . .	1525
D. R. Nichols R. A. Matthews	The U.S. Geological Survey's Role in Geologic- Related Hazards Warning . . . . .	1531

Index of Authors



***ENGINEERING MECHANICS AND  
STRUCTURAL DESIGN SESSION***



SELECTION OF BUILDINGS FOR STRONG-MOTION INSTRUMENTATION  
USING ZONATION INFORMATION AND DECISION THEORY

by

G. C. HART<sup>I</sup> and C. Rojahn<sup>II</sup>

ABSTRACT

Decision theory is used to determine which buildings should be given first priority for instrumentation in the various seismically active areas of California. The expected severity of ground shaking at each location and its probability of occurrence can be defined in terms of peak acceleration, Modified Mercalli Intensity, earthquake magnitude and epicentral distance, or some other measure of strong ground shaking. Building classes must be identified, and the value of obtaining a building response record for each building type can be quantified according to professional engineering judgment. Using this information, decision theory can be used to calculate the expected value of instrumenting buildings of a particular class at various locations. The locations are then ranked in order of preference for each building class. This procedure can be extended to instrumentation programs in other regions.

INTRODUCTION

In 1971 the State of California enacted a law (4) establishing a state-wide Strong-Motion Instrumentation Program to assure the development of a scientifically sound distribution of strong-motion instruments throughout the State. The law stipulates that the instruments are to be located in representative geologic environments and representative structures throughout the State, and that the California Division of Mines and Geology (CDMG), with the advice of an ad-hoc advisory board, should organize and monitor the program. Funding is provided by a 0.007 percent (7¢ per \$1000) assessment of estimated construction costs collected statewide from building permits.

The basic objectives for the building instrumentation phase of the program, originally set forth in an unpublished paper by R.B. Matthiesen and C. Rojahn, were adopted by the advisory board in mid-1973 as follows: to place a high priority on instrumenting buildings in Zone III of the Preliminary Map of the Maximum Expectable Earthquake Intensity in California (1) and a lower priority on instrumenting buildings in Zone II; to place the highest priority on instrumenting buildings within 5 miles of the major faults along which there is significant activity; to seek the assistance of the Structural Engineers Association of California in selecting buildings to be instrumented under the program; to select representative types and heights of buildings; and to instrument many buildings moderately rather than a few buildings highly using remote-recording accelerograph systems with accelerometers located so as best to record both translational and torsional response of each building. With these objectives and at the request of the advisory board, a specially appointed ad-hoc committee (the Subcommittee on Instrumentation for Buildings) developed a series of guidelines defining where, which types of, and how buildings should be instrumented under the State program.

---

<sup>I</sup> Associate Professor, Mechanics and Structures Department, University of California, Los Angeles.

<sup>II</sup> Research Civil Engineer, U.S. Geological Survey, Menlo Park, California.

Those guidelines are discussed in detail in reference (3) and are now being implemented by CDMG.

The original guidelines were not based on formal decision theory, but rather on knowledge developed from experience in earthquake engineering. More specifically, they were based on a knowledge of strong-motion seismicity, structural dynamics, and strong-motion instrumentation. The guidelines have proven to be valuable and have provided the basis for selecting more than 35 buildings instrumented so far statewide under the program. At this time, however, since current projections indicate that approximately six buildings per year will continue to be instrumented under the program, we believe it is prudent to select future buildings using a more systematic procedure that incorporates the fundamental elements of decision theory (2).

The procedure presented in this paper suggests the types of information needed to select buildings for instrumentation and indicates where this information fits into the decision process. The procedure is flexible enough to enable the decisionmaker to incorporate new developments in various technical fields over the years and to utilize knowledge gained from future earthquakes.

#### GENERAL DISCUSSION OF DECISION THEORY

As an introduction to the basic parts of a decision problem, consider the following discussion regarding the decision to instrument a specified building at a specified site in order to measure strong-motion earthquake response. The person making the decision has two courses of action available--to instrument the building or not to. Whatever action is taken, nature will also provide two alternatives--a strongly felt earthquake will occur (i.e., one which will be strong enough to provide measurable building response), or it will not. In decision theory terminology, one says that, in this example, there are two possible states of nature. One of the tasks facing decisionmakers is assessing the likelihood or probability of each possible state of nature. Each conjunction of a state of nature and an action chosen by the decisionmaker results in what is called a consequence. In this example, each of the two possible actions may occur in conjunction with either of the possible states of nature. Therefore, there are four possible consequences: 1) the building is instrumented and an earthquake occurs; 2) the building is instrumented and no earthquake occurs; 3) the building is not instrumented and an earthquake occurs; and 4) the building is not instrumented and no earthquake occurs.

One of the most important aspects in decision theory is that different decisionmakers, whether they be persons, committees, or organizations, will react to the four consequences in different ways. In a decision problem, it is necessary to quantify the degree of preference associated with the occurrence of each consequence. This degree of preference is quantified using a measure known as "utility." The process of quantifying the relative utilities for the consequences is begun by assigning arbitrary values to the best and worst consequences. Utilities to the intermediate consequences are then assigned by weighting preferences and will vary between decisionmakers. One of the explanations for why different decisionmakers make different decisions is that they assign different utilities.

The decisionmaker must next assign probabilities to the occurrence of the possible states of nature. In this example, probabilities associated with site seismicity must be determined.

Having identified the possible courses of action and states of nature, having assigned probabilities to the occurrence of the possible states of nature, and having assigned different utilities for each possible consequence, the decisionmaker can then calculate the relative expected degree of preference, i.e., the expected utility associated with each possible course of action. The expected utility associated with a decision to instrument the building is:

$$U_I = U_{I,E}p(E) + U_{I,NE}p(NE)$$

where  $U_I$  = expected utility of instrumenting the building

$U_{I,E}$  = utility of instrumenting the building and an earthquake occurs (i.e., consequence 1 occurs)

$U_{I,NE}$  = utility of instrumenting the building and no earthquake occurs (i.e., consequence 2 occurs)

$p(E)$  = probability of an earthquake occurring in an established time span

$p(NE)$  = probability of no earthquake occurring in an established time span

Similarly, the expected utility associated with a decision not to instrument the building is:

$$U_{NI} = U_{NI,E}p(E) + U_{NI,NE}p(NE)$$

where  $U_{NI}$  = expected utility of not instrumenting the building

$U_{NI,E}$  = utility of not instrumenting the building and an earthquake occurs (i.e., consequence 3 occurs)

$U_{NI,NE}$  = utility of not instrumenting the building and no earthquake occurs (i.e., consequence 4 occurs)

The decisionmaker would choose the course of action that produced the largest expected utility.

In summary, three basic components of the decision problem include: 1) identification of the possible courses of action; 2) description of the possible states of nature and the assignment of the associated probabilities of occurrence; and 3) quantification of the relative utility associated with the consequence of each action and each state of nature.

#### IDENTIFICATION OF POSSIBLE COURSES OF ACTION

The decisionmaker must clearly identify the possible courses of action. In selecting buildings for strong-motion instrumentation, the types of buildings that are to be instrumented must be defined. In the California program, for example, desired building types have been defined in terms of structural framing system (open frame, continuous frame, box, shear-wall, precast element, or combination), construction material (reinforced concrete, steel, wood, or masonry), and number of stories (3). The owner or function of the building could also be potentially important (e.g., hospital, government building, or private building), and the decisionmaker may wish to expand the definition of desired building types to reflect this factor. The selection of the detail that is used in describing the types of buildings

is at least partly influenced by two factors: 1) the decisionmaker's ability to describe the states of nature and their different effects on the building types, and 2) the ability of the decisionmaker to define the utility associated with the occurrence of each state of nature on each building type.

#### STATES OF NATURE AND THEIR PROBABILITY OF OCCURRENCE

The state of nature must be described in terms that address problems inherent in building response. The state of nature--an earthquake occurs or no earthquake occurs--used in the general discussion on decision theory does not reflect the severity of ground shaking, which is the most important parameter affecting building response. In general, the severity of ground shaking is dependent on earthquake magnitude, distance from the building site to the source of energy release, depth and type of faulting, regional and local geology, and other site conditions. The two most common measures used to describe the severity of ground shaking are peak ground acceleration at the site and Modified Mercalli Intensity (MMI) at the site. With regard to the first measure, three possible states of nature might be:

1. No earthquake occurs in 10 years with a peak ground acceleration at the building site greater than 10 percent of gravity.
2. One earthquake occurs in 10 years with a peak ground acceleration at the building site between 10 and 30 percent of gravity.
3. One earthquake occurs in 10 years with a peak ground acceleration at the building site between 30 and 50 percent of gravity.

As an alternative, the severity of strong ground shaking may be described in terms of MMI (e.g., the number of events in which MMI at the site was equal to or greater than VI in a specified time period), magnitude (e.g., the number of times a magnitude 5 or greater earthquake occurred within 100 km of the site in a specified time period), or some other measure such as one based on strong-motion response spectra data (e.g., site motion described in terms of the number of cycles of building motion above a specified threshold level of response). In all cases, the states of nature must incorporate the time variable because the probability of the existence of the state of nature is a function of the time span over which the occurrence is viewed.

In general, the description of the state of nature must incorporate all items which the decisionmaker feels are necessary to define the motion of the building site or, alternatively, the building response. This description can assume a multitude of variations because individual decisionmakers will usually differ on what is necessary at any given time (present or future). The description can include the occurrence of more than one earthquake in more than one order. For example, a state of nature could be defined as: one earthquake occurs in the years 1980 through 1984 with a peak site ground acceleration between 10 and 30 percent of gravity, and one earthquake occurs in the years 1985 through 1989 with a peak site ground acceleration between 30 and 50 percent of gravity.

For each state of nature, it is necessary to define a probability of occurrence. Because the probability of occurrence must be numerically evaluated, it influences the description of a state of nature. If historical data or professional insight is not adequate to obtain a reliable probability estimate, then the description of the state of nature must be modified.

## QUANTIFICATION OF RELATIVE UTILITY

The relative utility or value associated with each consequence may be a function of time. At any one time, one type or level of building response may be important to fill a gap in our knowledge, but at some later date, this gap may be closed and, therefore, the utility will have decreased. The assignment of utilities can be very difficult. It requires in many respects a quantification of ignorance and a projection of future value. The value of human life can enter here, as can personal or national priorities. A building official, for example, might place a higher priority on measurements of earthquake response of unreinforced masonry buildings than would a university professor or design engineer, who might be interested in only the response of buildings designed in accordance with current standards and codes.

## ILLUSTRATION OF THE USE OF THE PROCEDURE

The following example is intended to facilitate understanding of the development of the component parts of the decision problem. Although the example utilizes our experience, it is intended only to demonstrate the procedure and is not to be used in planning.

This example concerns the selection of buildings to be instrumented in eight cities in southern California (table 1). The cities are all located within Zone III (zone of maximum expected intensity) of the Preliminary Map of Maximum Expectable Earthquake Intensity in California (1). Four of the cities--Los Angeles, Long Beach, Anaheim, and Santa Ana--are among the ten most populated cities in the state of California; the others were selected on the basis of size and estimated level of local earthquake activity.

There are three possible actions (table 2) for each city: 1) instrumentation of a one- or two-story building; 2) instrumentation of a three- to six-story building; and 3) instrumentation of a seven- to fifteen-story building. This example, then, is concerned with the evaluation of the expected utility associated with each of 24 possible actions.

The states of nature are based on the rates of occurrence of magnitude 5 and greater earthquakes occurring within specific distance ranges of the selected cities. State of nature 1 is the occurrence within the next 5 years of at least one magnitude 5 or greater earthquake with an epicentral distance to the city hall of 0 to 10 km. State of nature 2 is the occurrence within the next 5 years of at least one magnitude 5 or greater earthquake with an epicentral distance to the city hall of 10 to 25 km. State of nature 3 is the occurrence within the next 5 years of at least one magnitude 5 or greater earthquake with an epicentral distance to the city hall of 25 to 50 km.

The historical earthquake activity (1932 to 1975) for each city in table 2 were determined from the California Institute of Technology earthquake data tape (table 3). These data are for magnitude 5 or greater earthquakes and are listed in terms of the number of earthquakes per year occurring in various distance ranges from the city halls of the eight selected cities. For example, for El Centro, there are 0.1136 earthquakes per year in the distance range 0 to 10 km. The corresponding return period, on the average, is one earthquake every 8.8 years. For a particular city hall site, the number of earthquakes per year is highly dependent on the epicentral distance range. Table 4 indicates this in another form by showing the percent of earthquakes within a 100-km radius of the city hall associated with each epicentral distance range. For example, 43.48% of all Long Beach

earthquakes (with an epicentral distance less than 100 km) are within the distance range 10 to 25 km, whereas only 4.44% of all earthquakes for El Centro are within this same distance range.

The probability of occurrence of each state of nature for each city is calculated using the equation:

$$p = 1 - e^{-(L/T)}$$

where  $p$  = probability of occurrence of at least one earthquake of magnitude 5 or greater in the next  $L$  years.

$L$  = number of years under future consideration (5 in this example)

$T$  = return period of state of nature (1 divided by the number of events per year)

For example, considering El Centro and the 0- to 10-km epicentral distance range, it follows that:

$$p = 1.0 - e^{-(5/8.80)} = 0.433$$

The utility associated with each consequence must now be assigned. The utility matrix (table 5) relating each epicentral distance range and each of the three building heights is based on the preference ratings assigned for the state of California program (3). The number in each row and column of the matrix corresponds to the utility associated with the consequence defined by that row and column. The utilities are assumed to be the same for each city.

The components of the decision problem have now been defined, and expected utilities can be calculated. The expected utility of action number 7 (table 2), for example, on the basis of the states of nature defined above, probabilities computed from table 3, and utilities from table 5, is:

$U_7$  = expected utility for action 7, which is to instrument a one- or two-story building in El Centro.

$$\begin{aligned} &= (\text{probability of occurrence of state of nature 1}) \times (\text{utility of state of nature 1 and action 7}) \\ &+ (\text{probability of occurrence of state of nature 2}) \times (\text{utility of state of nature 2 and action 7}) \\ &+ (\text{probability of occurrence of state of nature 3}) \times (\text{utility of state of nature 3 and action 7}) \end{aligned}$$

$$= (0.433)(16) + (0.203)(12) + (0.796)(0)$$

$$= 9.375$$

The expected utility associated with each of the other 23 possible actions have been calculated similarly (tables 6 and 7). The ranking of the possible actions shown in these tables is dependent on building site and the number of stories. Because the parameters used in the procedure need further study, this ranking is considered to be only preliminary.

## CONCLUSIONS

This procedure for the rational selection of buildings for strong-



motion instrumentation uses decision theory and zonation information. One of the primary advantages of the procedure is that it incorporates professional experience in all of its phases. On the basis of past experience, the earthquake engineer must work with the structural engineer to define states of nature that are meaningful to both parties and calculate probabilities of occurrence for each state of nature. These probabilities should be based on available historical earthquake data and/or analytical modeling techniques. The professional structural engineer must then define what utility is to be assigned to each consequence relating an action and a state of nature. The final ranking of actions is highly dependent on these utilities, and, therefore, the role of the engineer is critical.

The procedure presented is general in nature. The definition of components will vary with each problem and will be influenced by the goals of the nation, state, or organization making the decision.

#### ACKNOWLEDGMENTS

The authors gratefully acknowledge the assistance of Sampson Huang and the financial support provided by the National Science Foundation.

#### REFERENCES

- (1) Alfors, J. T., Burnett, J. L., and Gay, T. E., Jr., 1973, Urban geology master plan for California: California Division of Mines and Geology Bulletin 198, p. 20.
- (2) Benjamin, J. R., and Cornell, C. A., 1970, Probability, statistics, and decision for civil engineers: New York, McGraw Hill, 684 p.
- (3) Rojahn, C., 1976, California building strong-motion earthquake instrumentation program: Proceedings, ASCE-EMD Special Conference on the Dynamic Response of Structures, University of California at Los Angeles, p. 40-60.
- (4) SB 1374, Chapter 8 of Division 2 of the Public Resources Code, State of California.

Table 1.- Southern California cities selected for example problem

	<u>Population</u>	<u>Latitude</u>	<u>Longitude</u>
Anaheim	200,100	33°50.1'N	117°54.8'W
China Lake	21,000	35°43.5'N	117°37.0'W
El Centro	22,650	32°47.5'N	115°33.6'W
Long Beach	343,000	33°46.5'N	118°11.1'W
Los Angeles	2,754,500	34°03.5'N	118°15.0'W
Oxnard	92,100	34°12.3'N	119°10.5'W
Santa Ana	180,000	33°45.8'N	117°51.9'W
San Bernardino	103,600	34°06.5'N	117°18.6'W

Table 2.- Possible actions for example problem

<u>Action number</u>	<u>Action to instrument</u>
	Anaheim
1	One- or two-story building
2	Three- to six-story building
3	Seven- to fifteen-story building
	China Lake
4	One- or two-story building
5	Three- to six-story building
6	Seven- to fifteen-story building
	El Centro
7	One- or two-story building
8	Three- to six-story building
9	Seven- to fifteen-story building
	Long Beach
10	One- or two-story building
11	Three- to six-story building
12	Seven- to fifteen-story building
	Los Angeles
13	One- or two-story building
14	Three- to six-story building
15	Seven- to fifteen-story building
	Oxnard
16	One- or two-story building
17	Three- to six-story building
18	Seven- to fifteen-story building
	Santa Ana
19	One- or two-story building
20	Three- to six-story building
21	Seven- to fifteen-story building
	San Bernardino
22	One- or two-story building
23	Three- to six-story building
24	Seven- to fifteen-story building

Table 3.- Number of earthquakes of magnitude 5 or greater per year

Location	Number of earthquakes per year in range (kilometers)				
	0-10	10-25	25-50	50-75	75-100
Anaheim	0.0	0.2045	0.1364	0.0455	0.1818
China Lake	.0	.0455	.1818	.0	.1591
El Centro	.1136	.0455	.3182	.3409	.2045
Long Beach	.0455	.2273	.0455	.1364	.0682
Los Angeles	.0	.0227	.3636	.1136	.0455
Oxnard	.0	.0227	.0682	.0227	.5000
Santa Ana	.0	.2727	.1136	.0455	.2273
San Bernardino	.0	.0	.1136	.0682	.5456
San Diego	.0	.0	.0	.0227	.1364

Table 4.- Percent of observed earthquakes at different distances from city hall site (magnitude 5 or greater)

Location	Percent of earthquakes in range (kilometers)				
	0-10	10-25	25-50	50-75	75-100
Anaheim	0.0	36.0	24.0	8.0	32.0
China Lake	.0	11.76	47.06	.0	41.18
El Centro	11.11	4.44	31.11	33.33	20.0
Long Beach	8.70	43.48	8.70	26.09	13.04
Los Angeles	.0	4.17	66.67	20.83	8.33
Oxnard	.0	3.70	11.11	3.70	81.48
Santa Ana	.0	41.38	17.24	6.90	34.48
San Bernardino	.0	.0	15.63	9.38	75.0
San Diego	.0	.0	.0	14.29	85.71

Table 5.- Utility matrix for example problem

Distance from city hall site to epicenter	Number of building stories		
	1-2	3-6	7-15
0-10 km	16	16	4
10-25 km	12	16	12
25-50 km	0	0	10

Table 6.- Expected utility and ranking of possible actions

Rank	Location	Building height (stories)	Utility	Action number
1	Long Beach	3-6	14.1216	11
2	Santa Ana	7-15	13.2634	21
3	Anaheim	7-15	12.6276	3
4	El Centro	7-15	12.1382	9
5	Santa Ana	3-6	11.9072	20
6	Long Beach	1-2	11.4052	10
7	Long Beach	7-15	10.9982	12
8	Anaheim	3-6	10.2448	2
9	El Centro	3-6	10.1888	8
10	Los Angeles	7-15	9.6636	15
11	El Centro	1-2	9.3748	7
12	Santa Ana	1-2	8.9304	19
13	China Lake	7-15	8.4130	6
14	Anaheim	1-2	7.6836	1
15	Oxnard	7-15	4.4084	18
16	San Bernadino	7-15	4.3330	24
17	China Lake	3-6	3.2560	5
18	China Lake	1-2	2.4420	4
19 Tied	Los Angeles	3-6	1.7168	14
19 Tied	Oxnard	3-6	1.7168	17
21 Tied	Los Angeles	1-2	1.2876	13
21 Tied	Oxnard	1-2	1.2876	16
23 Tied	San Bernardino	3-6	0.0	23
23 Tied	San Bernardino	1-2	0.0	22

Table 7.- Ranking of sites by building height

Rank	Building Height		
	7-15 story	3-6 story	1-2 story
1	Santa Ana (13.2634)	Long Beach (14.1216)	Long Beach (11.4052)
2	Anaheim (13.2634)	Santa Ana (11.9072)	El Centro (9.3748)
3	El Centro (12.1382)	Anaheim (10.2448)	Santa Ana (8.9304)
4	Long Beach (10.9982)	El Centro (10.2448)	Anaheim (7.6836)
5	Los Angeles (9.6636)	China Lake (3.2560)	China Lake (2.4420)
6	China Lake (8.4130)	Los Angeles (1.7168)	Los Angeles (1.2876)
7	Oxnard (4.4084)	Oxnard (1.7168)	Oxnard (1.2876)
8	San Bernardino (4.3330)	San Bernardino (0.0)	San Bernardino (0.0)

## NEED FOR A COMPREHENSIVE APPROACH IN ESTABLISHING DESIGN EARTHQUAKES

by

V. V. Bertero<sup>I</sup> and S. A. Mahin<sup>II</sup>

## ABSTRACT

A logical approach to the seismic-resistant design of structures is comprehensive design. Difficulties encountered in applying this approach arise from uncertainties regarding details of the critical ground motion, and the inherent sensitivity of the response of structural systems to variations of these details. Design earthquakes for serviceability, damageability, and collapse limit states are discussed. When serviceability controls, the most facilitative and reliable approach of specifying design earthquakes is based on smoothed response spectra. The use and reliability of standard linear-elastic design response spectra (LEDRS) are reviewed. When damageability or collapse controls design, design earthquakes are often specified using inelastic design response spectra (IDRS) derived directly by modifying LEDRS. The use of these IDRS are shown to be unreliable for certain cases and another approach is suggested. The need for a comprehensive approach is stressed and research needs are discussed.

## INTRODUCTION

Establishment of design earthquakes is one of the most important steps in designing building structures to resist the effects of earthquake ground shaking. During the past three decades, there has been considerable advancement in various specialized fields related to earthquake ground motions and structural response. Despite these advances, there has been no corresponding improvement in the reliability with which structures can be designed to resist the effects of seismic ground shaking. One of the reasons for this is that most attempts at specifying design earthquakes have been based on the concerns of only a single specialized discipline, rather than integrating the knowledge and requirements of the various disciplines involved in seismic-resistant design.

The need for a more comprehensive approach for establishing design earthquakes has recently been pointed out (1-3). Biggs, Hansen, and Holley (1) indicate that in addition to problems related to uncertainties regarding details of potential ground motions and the sensitivity of structural response to variations of these details, inadequate consideration has been given to earthquake risk and associated costs. Bertero and Bresler (2) have also suggested that an efficient design must reconcile the total cost of a structure (including initial, maintenance, and damage repair costs) against the probability of events that can lead to undesirable modes of behavior (inadmissible limit states). Such limit states may range in practice from superficial damage to collapse, and have generally been grouped into two categories: 1) serviceability, where damage should be limited to prevent functional failure under normal service loads and frequent ground shaking; and 2) collapse, where life safety should be protected under maximum credible overloads and ground shaking. A third category, damageability, was suggested (2) in which structural and nonstructural damage should be limited to economically

---

I Professor of Civil Engineering, University of California, Berkeley.

II Assistant Professor of Civil Engineering, University of California, Berkeley.

acceptable levels. The comprehensive design philosophy provides a logical basis for considering these factors in design and construction (2).

Practical problems also arise in defining design earthquakes. For example, the design earthquake is intended to be a set of design forces or a ground motion that induces a "critical" response in the structure. However, even for a given site and specific structural system, that seismic excitation will depend not only on the characteristics and likelihood of the various types of ground motions that might be experienced at the site, but also, on the dynamic and mechanical characteristics of the building-foundation-soil system, and on the severity of structural response that can be tolerated. Thus, even for a given site and known structure there is no unique design earthquake, and different considerations may be needed to develop design earthquakes for serviceability, damageability, and collapse limit states. The interrelationships between the design earthquake and the requirements of different limit states and other aspects of seismic-resistant design are illustrated in the flow chart of Fig. 1.

This paper focuses on the overall problems of establishing design earthquakes for structures and the need for a comprehensive approach to resolve these problems. Present methods of prescribing design earthquakes and factors that should be considered in defining them for the three categories of limit states are discussed. The reliability of procedures suggested for establishing damageability and collapse limit state design earthquakes is evaluated. Recommendations for additional research are presented.

#### PRESENT METHODS OF PRESCRIBING DESIGN EARTHQUAKES

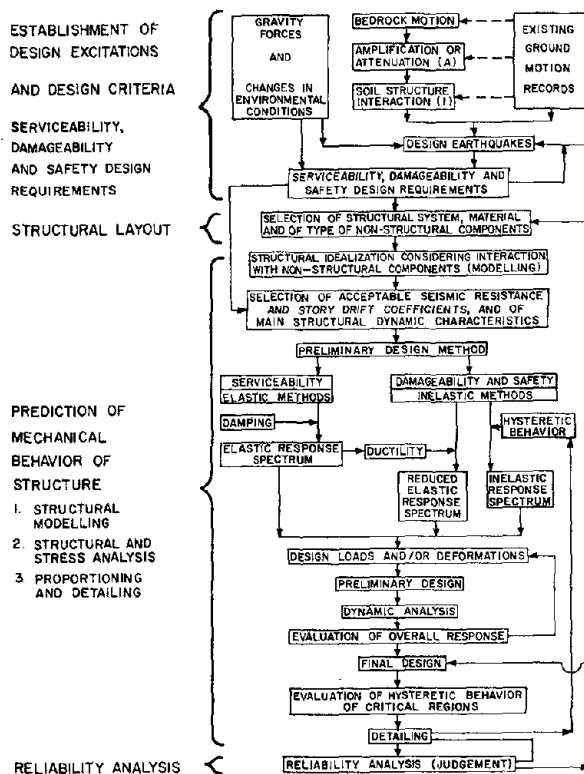


FIG. 1 FLOW DIAGRAM OF GENERAL ASPECTS AND STEPS INVOLVED IN SEISMIC-RESISTANT DESIGN

The ground motion experienced at a site is a complex function of the type and characteristics of the source mechanism, the nature of the intervening geological structure, and the topographical and soil conditions near the site. A common design simplification is to consider only nonconcurrent action of horizontal, translational ground motion components. For sites near an earthquake source, it may be necessary to base structural response evaluations on the simultaneous action of all six components (4) and to consider realistically nonlinear soil-structure interaction rather than to use predicted free-field ground motions. Instrumentation should be installed to obtain records of all components of ground motion and building response in future earthquakes.

Design earthquakes are specified in a number of ways. For example, in preliminary design smoothed response spectra are often used. On the other hand, it may be

necessary to specify an ensemble of ground motion time histories in order to proportion and detail critical regions during final design or to study the reliability of a given design or structure. An evaluation of current methods for prescribing design earthquakes has been reported in (5), and is summarized below.

Serviceability Limit States. -- Seismic codes have specified design earthquakes in terms of a building code zone, a site intensity factor, or, as a peak or effective site acceleration. Reliance on such indices alone, however, is generally inadequate and methods using response spectrum, accelerograms or random vibration theory have recently been suggested. Advantages and disadvantages of these methods are discussed in (1), (3), and (5).

In cases where serviceability limit states control design, structures should remain essentially in their elastic range. For these cases and for structures located at moderate distances from earthquake sources, it is generally agreed that the most reliable and convenient way to specify design earthquakes is by smoothed, linear-elastic design response spectrum (LEDRS). Design based on random vibrational analysis is of interest because of its rationality, but requires further development before implementing it in practice. LEDRS can be constructed from statistical analysis of elastic spectra derived for appropriate accelerograms (real or simulated), or, by scaling the peak ground acceleration, velocity, and displacement using spectral amplification factors statistically derived for various amounts of damping (6). When only estimates of peak ground acceleration are available, it has been suggested that reasonable values for the peak ground velocity and displacement may be obtained by multiplying the ground acceleration (expressed as a fraction of gravity) by 1.22 m/sec (48 in./sec) and 0.91 m (36.0 in.), respectively (7).

Simple methods for constructing LEDRS have been based on so-called standard severe earthquake motions obtained at moderate distances from the causative fault. For building sites located near such faults, however, LEDRS should be based on realistic maximum values of effective ground acceleration, velocity, and displacement. These values should be determined from analysis of available records and/or from theoretical predictions based on the appropriate faulting process (8). If realistic estimates of these values cannot be made, the critical earthquake ground motion should be determined from techniques suggested in (9) and (10). Further studies on the subject of spectral amplification factors for different amounts of damping are also needed. Significant differences have been found between the values of the ratio of maximum elastic responses for different amounts of damping and those for presently suggested amplification factors (8).

In conclusion, LEDRS are the best way of specifying design earthquakes for serviceability limit states. However, establishment of the proper LEDRS for a specific building is a problem that requires considerable engineering knowledge and judgment. A detailed discussion of these problems is presented in (3), which indicates that LEDRS cannot be defined without considering the amount of viscous damping, the allowable stresses and strains, and the method of evaluating the dynamic characteristics of the structure. Even for the case of linear-elastic structural behavior, a comprehensive approach to design earthquakes is required.

Ultimate Limit States. -- In most cases it is economically unfeasible to design buildings located near faults for the forces indicated by LEDRS based on the largest expected ground spectrum. Lower design forces may be used

if it is possible to utilize a building's ability to absorb and dissipate energy by inelastic deformations. However, to ensure safety against collapse or to avoid extensive damage, inelastic deformations must be limited. Current code procedures, based on equivalent static forces and elastic analysis, anticipate some inelastic behavior under severe ground shaking, but do not always result in satisfactory designs (1).

One improvement over simple code procedures is to specify the design earthquakes for ultimate limit states using simplified inelastic design response spectra (IDRS). Derivation of such IDRS using nonlinear dynamic analyses of realistic structural models subjected to appropriate accelerograms is generally unfeasible in most preliminary designs due to modeling problems and excessive computational effort (11). Simple methods which directly modify LEDRS to obtain IDRS using factors based on the elasto-perfectly plastic (EPP) response of single-degree-of-freedom (SDOF) systems (7,12) are more often used (13). Use of these types of IDRS permits design for specified ductility and drift ratios. However, these methods are based on limited numbers of ground motion records, and as their proposers have pointed out, they should be used with caution when applying them to sites that can be subjected to different kinds of ground motions. Furthermore, they may not be suitable for multidegree-of-freedom (MDOF) systems, or in cases where actual hysteretic behavior is likely to differ from the assumed elasto-plastic idealization (7,8).

The Applied Technology Council has studied a procedure utilizing IDRS derived directly from LEDRS (13). This method is based on elastic modal analysis, where ductility ratios are computed on the basis of peak elastic distortion and yield limit distortion. This procedure is questionable since actual, local, inelastic distortions may differ significantly (1). Studies carried out at Berkeley (8,14) have also shown that the types of excitations that induce the maximum response in elastic and inelastic systems are fundamentally different. The information used for computing IDRS from LEDRS, although necessary, is insufficient for predicting maximum inelastic dynamic response. Information should be complemented with data on the duration of strong ground shaking and the number, sequence, and characteristics of intense, relatively long-duration acceleration pulses that can be expected.

1. Duration of strong ground shaking. -- The degree of damage to be expected in any structure that is strained beyond its elastic limit depends on the duration of strong shaking. Smoothed LEDRS on which IDRS are based usually depend on estimates of the peak ground response and viscous damping, and not on the duration of ground motion. Although results obtained (11) using artificial accelerograms with different durations show that the influence of duration was not large, quantitative results obtained in other recent studies (8,14) clearly show the opposite. A review (5) of the principles governing hysteretic behavior and failures of actual structures under generalized dynamic excitations confirms the importance of earthquake duration.

2. Number, sequence, and characteristics of intense, long-duration acceleration pulses. -- The need for this information is evident in the results obtained by applying vibration theory to SDOF systems (8). In the linear-elastic case, the critical dynamic excitation is periodic, having a frequency equal to that of the system, which induces an engineering resonance phenomenon. For this type of excitation, the dynamic magnification operator,  $D$ , can reach a maximum value approximately equal to  $1/(2\xi)$ , where  $\xi$  is the damping ratio. Thus, for values of  $\xi$  ranging from 2% to 10%,  $D$  can attain



values ranging from 25 to 5. For elasto-plastic systems, short periodic acceleration pulses are not generally critical since the large amount of energy dissipated by even small inelastic deformations is equivalent to very large values of  $\xi$ .

Severe long-duration acceleration pulses are not usually crucial for linear-elastic system because the largest value of  $D$  for an impulsive excitation is only 2. In an inelastic system, however, such long pulses can become critical. This is particularly true for a structure having a yielding resistance,  $R_y$ , equal to or less than the inertial force corresponding to the effective ground acceleration of the pulse,  $\ddot{X}_e$ , i.e.  $R_y \leq M\ddot{X}_e$ , where  $M$  is the mass of the structure. The larger the  $\ddot{X}_e$  of a pulse with respect to  $R_y$  or the shorter the rise time to the peak acceleration or the longer the pulse duration relative to the fundamental period of the structure, the larger the amount of inelastic deformations. Furthermore, repeated applications of such pulses can lead to failure due to low-cycle fatigue, incremental (crawling) collapse, or a combination of the two (5). Thus, quantitative specification of the inelastic design earthquake requires determining 1) the severity of the long acceleration pulses that can be developed; and 2) the manner in which these pulses can be defined.

Severe, long-duration (about 0.66 sec) acceleration pulses were recorded near the fault of the 1971 San Fernando earthquake (14). These pulses resulted in very large incremental ground velocities [1.4 m/sec (55 in./sec) for the derived Pacoima Dam (DPD) record and 1.7 m/sec (67.6 in./sec) for the Van Norman record], which were close to the theoretical limits of the peak near-fault particle velocity that has been placed in the range of 1-1.5 m/sec (40-59 in./sec) (7,15,16). The record obtained in Bucharest during the 1977 Romanian earthquake also contains a large sine wave-like pulse with a peak acceleration of 0.20g and a duration of about 1.7 sec. (17). This resulted in an incremental velocity of the order of 1.2 m/sec (47 in./sec), which is very high for a site located at a distance of about 200 km (125 mi) from the focus. Thus, LEDRS and IDRS based on ground spectra derived from standard earthquake records may be questionable for structures irrespective of their location to the earthquake source.

#### RELIABILITY OF IDRS DERIVED DIRECTLY FROM PROPOSED LEDRS

Several nonlinear dynamic analyses of SDOF and MDOF systems have been performed to assess the reliability of two representative methods [Newmark and Hall (7) and ATC (18)] of constructing IDRS directly from LEDRS for structures located where seismic ground motions containing severe, long-duration acceleration pulses are possible. Analysis of some of the results obtained for the first approach are summarized below. Reference 19 gives a more detailed discussion of these results.

Application of IDRS to SDOF Systems. -- The displacement ductility demands for ideal EPP-SDOF systems were computed for a variety of ground motion records and compared with the ductility values used in deriving the IDRS.

1. Comparison of ductility demands for different ground motions with specified ductility values. -- A series of ten accelerograms was used to compute required ductilities of EPP-SDOF systems designed using the basic Newmark-Hall IDRS with a specified ductility of 4, 5% damping, and a ratio of peak ground velocity to acceleration of 1.22 m/sec/g (48 in./sec/g). The accelerograms selected were representative of strong earthquake ground motions recorded on firm ground at moderate epicentral distances. The

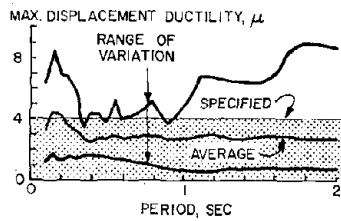


FIG. 2 DUCTILITY VARIATION FOR EPP-SDOF SYSTEMS DESIGNED ACCORDING TO NEWMARK-HALL IDRS FOR  $\mu = 4$  AND  $\xi = 0.05$  -- TEN NORMALIZED RECORDS

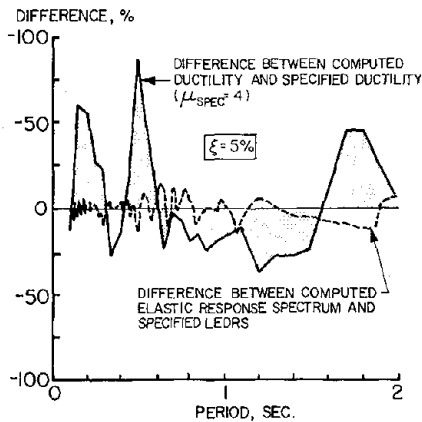


FIG. 3 DIFFERENCE BETWEEN COMPUTED AND SPECIFIED DUCTILITIES AND RESPONSE SPECTRA -- SIMULATED GROUND MOTION

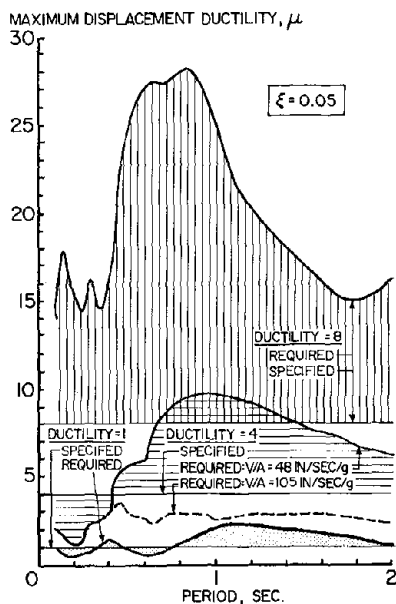


FIG. 4 REQUIRED AND SPECIFIED DUCTILITIES -- DPD RECORD (S-16°-E)

average displacement ductility demand computed from these records is plotted in Fig. 2. Maximum ductility is on the average nearly 25% lower than the specified value of 4, except in the short period range. However, the computed ductilities were very sensitive to the ground motion record; ductility demands in excess of 8 were computed for some records and the systems did not yield at all for other records.

It is possible that the discrepancies between computed and specified ductilities were due to variations between the LEDRS used to derive the IDRS and the elastic spectra of the actual ground motions used in the analyses. To investigate this possibility, a spectrum compatible ground motion record was generated (20). The difference between the controlling LEDRS and the elastic spectrum of the simulated record, Fig. 3, was small and never exceeded 13%. However, the difference between the computed displacement ductility demand for this record and the value of 4 specified in the IDRS was much larger; the maximum difference being more than 80%.

Results from near-fault, pulse-like ground motion records are presented in Fig. 4, which shows the values obtained using the DPD record. The required displacement ductilities tend to be substantially larger than the values specified. This discrepancy increases with increasing ductility demands so that for a specified ductility of 8, ductility demands of nearly 30 were required in some period ranges. Since the ground spectrum used to derive the LEDRS was based on a ratio of peak ground velocity to acceleration considerably smaller than that observed for this record, one might expect the computed ductilities to be much larger than the specified values outside of the short period range. Results for systems designed with the Newmark-Hall IDRS modified to reflect the actual ratio of peak ground velocity to acceleration of 2.67 m/sec/g (105 in./sec/g) are also shown in Fig. 4. In this case, the required ductilities were smaller than the specified values for all periods. Thus, it could be concluded that such IDRS lead to conservative design values if the governing ground spectrum is based on actual maximum values of acceleration, velocity, and displacement, rather than on standard values.

2. Comparison of ductility demands for different values of viscous damping ratio with specified ductility value. -- The direct derivation of Newmark-Hall IDRS from LEDRS implies that viscous damping affects inelastic response to exactly the same extent as elastic response. To investigate this, IDRS constructed using a specified ductility of 4, and LEDRS derived for the basic ground spectrum shape and 2%, 5%, and 10% damping were used to derive strengths of ideal EPP-SDOF systems. The required ductilities computed for these EPP systems subjected to the El Centro and DPD records are shown in Fig. 5. Since the same specified ductility was used in constructing each IDRS, the design forces became increasingly unconservative as the viscous damping ratio increased. This was particularly true for the DPD record, where inelastic response was dominated by a large inelastic excursion due to the severe, long-duration acceleration pulse. Newmark and his associates have recommended that this technique not be used for damping ratios in excess of 5%.

Application of IDRS to MDOF Systems. -- Because it is difficult to idealize conventional multistory buildings as EPP-SDOF systems, IDRS based on the inelastic response of simple SDOF systems are not directly applicable to MDOF systems (7). A number of investigations have attempted to estimate preliminary design forces for MDOF systems using elastic root-mean-square modal superposition techniques based on initial elastic dynamic characteristics of a structure and an IDRS (8,13,21,22). In general, such methods have been found to have serious defects. For example, a ten-story, three-bay frame was designed (21) using a Newmark-Hall type IDRS with a specified ductility of 4 and a ground velocity 31% higher than the basic Newmark-Hall recommendation. A series of inelastic analyses of this frame has been performed considering different accelerograms and amounts of viscous damping (8). The roof and first floor displacement time histories of this frame subjected to the El Centro and DPD records (normalized to 0.5g) are shown in Fig. 6 along with the accelerograms. While inelastic response was satisfactory for the El Centro record, it was not for the DPD record. Damping had a far more significant effect on elastic response than on inelastic

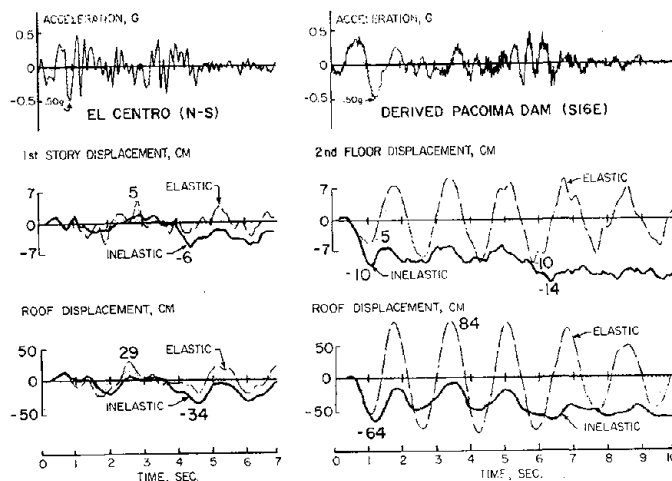
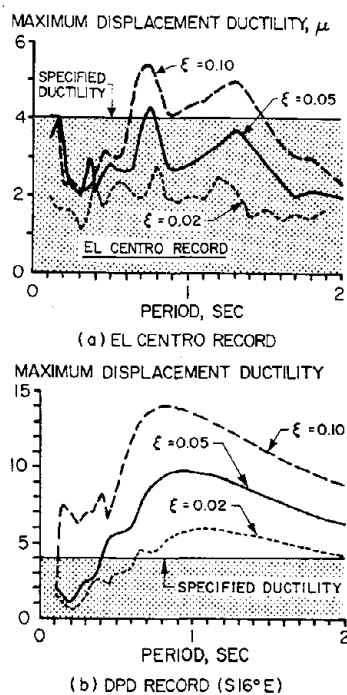


FIG. 6 DISPLACEMENT TIME HISTORIES OF 10-STORY FRAME FOR 5% DAMPING

FIG. 5 EFFECT OF DAMPING ON DUCTILITY DEMANDS

response (8). Use of modal superposition to determine design forces also failed to achieve desirable distributions of local member inelastic deformations and to limit these to acceptable values at certain critical locations. Similar conclusions were reported in other studies (22).

#### CONCLUSIONS AND RECOMMENDATIONS

The need for a comprehensive approach to the problem of establishing design earthquakes has been shown. In addition to essential information regarding detailed characteristics of the various types of ground motions that may be expected at a site, specification of design earthquakes must account for uncertainties regarding these excitations, the mechanical and dynamic characteristics of the whole building-foundation-soil system, earthquake-related costs, and the extent of damage that can be tolerated.

Comprehensive Approach for Serviceability Limit States. -- For elastic design, a design earthquake based on smoothed elastic design response spectrum is the most reliable and convenient approach for preliminary design. However, the ground spectrum must be appropriate to the site, not based just on standard values. Values selected for the damping ratio, determination of allowable stresses, and computation of natural periods and internal forces must be consistent with the expected behavior. Additional research is needed to refine spectral amplification factors and determine ground spectrum values, especially for near-fault sites.

Comprehensive Approach for Ultimate Limit States. -- Derivation of rational and reliable IDRS requires full characterization of expected severe ground motions at the site, and expected and/or acceptable responses of the structure. The former requires estimation of not only the intensity, frequency content, and probability of seismic excitations, but also the duration of strong shaking and the number, sequence, and characteristics of intense, relatively long-duration acceleration pulses. Current IDRS do not account for the duration of strong shaking. Information on this topic is needed to ascertain the maximum inelastic deformation excursion, as well as the maximum number of reversals of inelastic deformations, so that the structure's critical regions may be adequately proportioned and detailed. Data for most seismic regions of the U.S. remain scarce.

Research is needed to establish bounds on the number and dynamic characteristics of possible severe, long-duration acceleration pulses, e.g. the largest incremental velocity and the associated effective acceleration that can be developed according to the dynamic mechanical characteristics of the soil. While there is considerable analytical work to predict dynamic response of soils, experimental corroboration of the analytical models and results is urgently needed. Better estimates of the characteristics of these pulses will enable the design engineer to determine an upper bound on the energy that can be transmitted to the foundation of the structure. Methods for constructing IDRS, as well as LEDRS, should reflect the larger ground spectrum values recorded at near-fault sites.

Ultimate limit state design criteria are not only controlled by the energy dissipation capacity of the structural system, but also by damageability. Thus, selection of a design ductility factor without considering structural flexibility (period), type of structural and nonstructural systems, or earthquake type (magnitude, source distance, duration, etc.) is generally unacceptable. Even for a specific structural system, the acceptable ductility will vary depending on whether nonstructural or structural damage

controls. If nonstructural damage controls, the allowable ductility will decrease with increasing structural flexibility (period). Comprehensive studies to determine more reliable methods for establishing values of acceptable ductility are needed, particularly for flexible structures (5,19).

The economic impact of designing structures for either seismic resistance coefficients or design ductility ratios higher than those presently assumed should be assessed. Such studies will require examining the uncertainties involved in selecting values of all parameters pertinent to the design process. To do this, the interrelationship of these parameters must be considered. For example, in designing for strength, the computed internal forces determined from critical design excitations should be reconciled with the actual strength of structural elements. Present methods of designing sections, regions, and whole structures include several factors that usually lead to significant overstrength (3,23). Thus, by taking a conservative approach, looking at each side of the design strength equation independently, one may arrive at an unreasonable, uneconomical design.

Extensive studies will be required to obtain all the information necessary to establish reliable design earthquakes under ultimate limit states. Until this is done, the following procedure may be implemented. For the case of SDOF systems, charts similar to those derived and presented in (8) and (14) and illustrated in Fig. 7 should be prepared. These charts should consider different hysteretic models (at least bounds on possible stiffness degradation and strain-hardening) and all seismic ground motions previously recorded at similar sites, as well as those that can be obtained from theoretical faulting mechanisms. Statistical analysis of the results, along with values of acceptable ductility, could be used to formulate inelastic design earthquakes in the form of IDRS ( $C_y$  vs.  $T$ , as illustrated in Fig. 8); see also (11).

IDRS derived for SDOF systems may be used only as design guidelines for MDOF systems. The response of different MDOF systems to severe ground

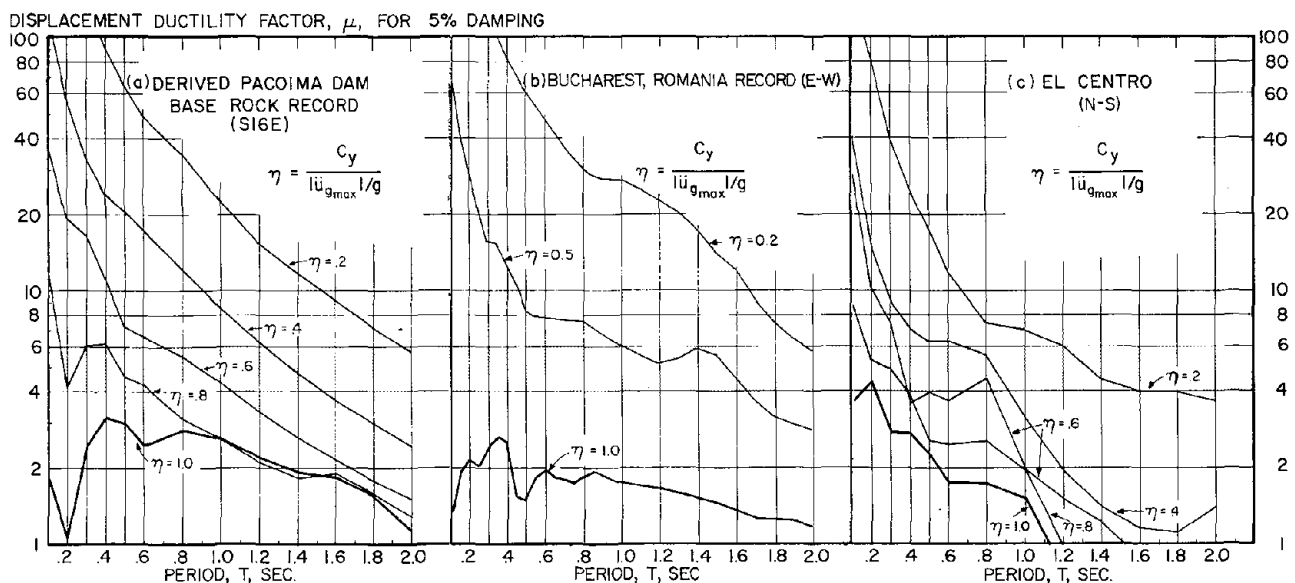


FIG. 7 DISPLACEMENT DUCTILITY REQUIREMENTS FOR SDOF SYSTEMS WITH 5% DAMPING

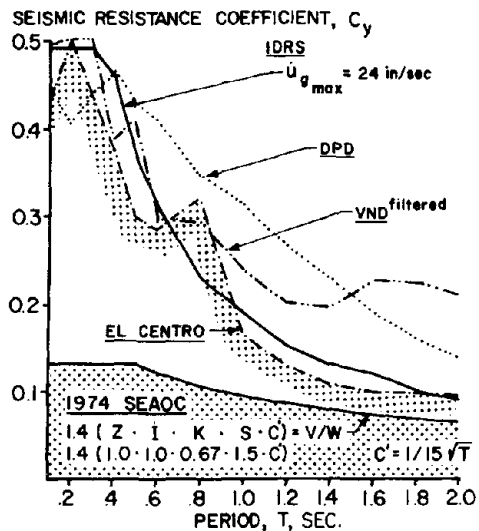


FIG. 8  $C_y$  VS.  $T$  FOR  $\ddot{X}_e = 0.5g$ ,  
 $\xi = 5\%$ , AND  $\mu = 4$

motions should be investigated to determine ways in which IDRS for SDOF systems can be modified for MDOF systems, or to formulate inelastic design procedures for these systems. Only comprehensive analyses and studies of all the factors that are involved in the design process can lead to more reliable and practical IDRS.

#### ACKNOWLEDGMENT

The sponsorship of the National Science Foundation under Grant No. ENV76-01419, subproject S-22066 is gratefully acknowledged. The assistance of L. Tsai and L. Hashizume in preparing the manuscript is appreciated.

#### REFERENCES

1. Biggs, J. M., R. J. Hansen, and M. J. Holley, Jr., "On Methods of Structural Analysis and Design for Earthquakes," Structural and Geotechnical Mechanics, ed. W. J. Hall, Prentice-Hall, Englewood Cliffs, New Jersey, 1971.
2. Bertero, V. V. and B. Bresler, "Failure Criteria (Limit States)," panel discussion paper, Sixth World Conference on Earthquake Engineering, New Delhi, January 1977; also, Report No. UCB/EERC-77/06, Earthquake Engineering Research Center, University of California, Berkeley, February 1977.
3. Housner, G. W. and P. C. Jennings, "Earthquake Design Criteria for Structures," Report No. EERL 77-06, Earthquake Engineering Research Laboratory, California Institute of Technology, Pasadena, November 1977.
4. Rosenblueth, E., "The Six Components of Earthquakes," Journal of the Structural Division, ASCE, vol. 102, no. ST2, 1976.
5. Bertero, V. V. "State-of-the-Art in Establishing Design Earthquakes," Proceedings, Workshop on Earthquake-Resistant R/C Building Construction, University of California, Berkeley, July 1977.
6. Newmark, N., J. Blume, and K. Kapur, "Seismic Design Spectra for Nuclear Power Plants," Journal of the Power Division, ASCE, vol. 99, no. P02, November 1973.
7. Newmark, N. M. and W. J. Hall, "Procedures and Criteria for Earthquake Resistant Design," Building Practices for Disaster Mitigation, Building Science Series 46, U.S. Dept. of Commerce, National Bureau of Standards, Washington, D. C., February 1973.

8. Bertero, V. V., R. A. Herrera, and S. A. Mahin, "Establishment of Design Earthquakes--Evaluation of Present Methods," Proceedings, International Symposium on Earthquake Structural Engineering, St. Louis, August 1976.
9. Drenik, R. F., P. C. Wang, and W. Wang, "Case Study of Critical Excitations and Response Structures," Report No. POLY EE/EP-73-DID, Polytechnic Institute of New York, November 1975.
10. Hoshiya, M., S. Shibata, and T. Nishiwaka, "Upper Bound of Response Spectrum," Proceedings, Fifth European Conference on Earthquake Engineering, Istanbul, vol. 1, September 1975.
11. Murakami, M. and J. Penzien, "Nonlinear Response Spectra for Probabilistic Seismic Design of Reinforced Concrete Structures," Proceedings, U.S. - Japan Cooperative Research Program in Earthquake Engineering, Assn. for Science Documents Information, Tokyo, 1976.
12. Veletsos, A. S. and N. M. Newmark, "Effect of Inelastic Behavior on the Response of Simple Systems to Earthquake Motions," Proceedings, Second World Conference on Earthquake Engineering, Tokyo, vol. 2, 1960.
13. "An Evaluation of Response Spectrum Approach to Seismic Design of Buildings," Applied Technology Council, San Francisco, September 1974.
14. Bertero, V. V., S. A. Mahin, and R. A. Herrera, "Aseismic Design Implications of Near-Fault San Fernando Earthquake Records," International Journal of Earthquake Engineering and Structural Dynamics, vol. 6, 1978.
15. Ambraseys, N. M., "Maximum Intensity of Ground Movements Caused by Faulting," Proceedings, Fourth World Conference on Earthquake Engineering, Santiago, Chile, vol. 1, 1969.
16. Brune, J. N., "Tectonic Stress and the Spectra of Seismic Shear Waves from Earthquakes," Journal of Geophysical Research, vol. 75, 1970.
17. "Earthquake in Romania, March 4, 1971," Newsletter, Earthquake Engineering Research Institute, vol. 11, no. 3B, May 1977.
18. Final Review Draft of Recommended Comprehensive Seismic Design Provisions for Buildings, Applied Technology Council, ATC-3-05, Palo Alto, California, January 1977.
19. Mahin, S. A. and V. V. Bertero, "An Evaluation of Inelastic Seismic Design Spectra," preprint from ASCE Spring Convention and Exhibit, Pittsburgh, April 1978.
20. Gasparini, D. A. and E. H. Vanmarke, "Simulated Earthquake Motions Compatible with Prescribed Response Spectra," Publication R76-4, Dept. of Civil Engineering, Massachusetts Institute of Technology, Cambridge, January 1976.
21. Bertero, V. V. and H. Kamil, "Nonlinear Seismic Design of Multistory Frames," Canadian Journal of Civil Engineering, vol. 2, Ottawa, December 1975.

22. Anagnostopoulos, S. A., R. W. Haviland, and J. M. Biggs, "Use of Inelastic Spectra in Aseismic Design," Journal of the Structural Division, ASCE, vol. 104, no. ST1, January 1978.
23. Bertero, V. V., "Strength and Deformation Capacities of Buildings," Proceedings, Symposium on Structural Engineering and Structural Mechanics, University of California, Berkeley, August 1977.



## VELOCITY RESPONSE SPECTRA FOR SITES ON ROCK OR SOIL

A.R. Chandrasekaran<sup>I</sup> and D.K. Paul<sup>II</sup>

## ABSTRACT

For aseismic design of structures, information of ground motion in the form of response spectra is used almost invariably since it conveniently represents the combined influence of amplitude of ground acceleration, frequency content, and to some extent the duration of ground shaking on different structures. Several investigators have studied the shape of response spectra for different site conditions and different confidence levels using different methods of normalisation. A new criteria for selecting normalising parameter has been suggested in this study for velocity response spectra based on least standard deviation. Based on the study, spectrum shapes corresponding to various confidence levels have been proposed for rock and alluvial sites.

## INTRODUCTION

Several investigators have proposed shape of average response spectra using different methods of normalisation. Housner (9) was the first to propose such an average response spectra using spectral intensity as normalising factor. Subsequently several other investigators (2,3,6,7,8,10,11,12,13,14,15,18 and 19) used peak ground acceleration to normalise the response spectra. Later other parameters like peak ground velocity,  $ad/v^2$  (where  $a$ ,  $v$  and  $d$  are the peak ground acceleration, velocity and displacement respectively), and spectral intensity were used to normalise the response spectra. A comparison of such different types of normalisation have been made by some authors (3,5,10). Out of these, peak ground acceleration was used widely to normalise response spectra since this parameter is readily available from the accelerogram and used as a measure of intensity. Further, there also exists several statistical relationships for determining the expected peak ground acceleration at a site. The peak velocity representing the integrated effect of a accelerogram is not much influenced by a few stray high peaks of acceleration of the record. It has been shown that the same spectra can be achieved by accelerograms having different peak accelerations (4). Therefore peak ground acceleration alone should not always be considered for normalisation.

A new criteria for selecting normalising parameter has been suggested in this study for velocity response spectra based on least standard deviation. The standard deviations

---

I	Professor	)	School of Research and Training
		)	in Earthquake Engineering
II	Reader	)	University of Roorkee
		)	Roorkee, U.P.,
		)	INDIA

corresponding to various normalisations have been compared by equating the area under the velocity spectra. The normalising parameter showing least standard deviation over the major portion of the period range was considered as the best. Separate studies were made for alluvial and rock site. Using this normalisation, spectrum shapes corresponding to various confidence levels have been proposed for rock and alluvial sites.

#### DATA ANALYSED

It is considered that the ground motion is greatly influenced by the type of soil condition where it is recorded. Therefore, the available strong motion earthquake data (1,16, 17) have been broadly classified into two groups, one recorded on rock sites and other on alluvial sites. In this classification, where the depth of bed rock is very shallow, it was considered as a rock site.

Thirty one strong motion earthquake records classified under rock site obtained from four earthquake events were considered in spectra analysis for rock site. Since large number of records are from only San Fernando earthquake, the sample is somewhat influenced by this earthquake. The magnitude of records considered ranged from 5.25 to 6.6, epicentral distance ranged from 7 to 62 km. Selection of accelerogram records were limited to those in which the peak ground acceleration is greater than 0.05g.

Fifty earthquake records that were reported to be recorded on alluvial site, taken from thirteen earthquake events were considered for spectra analysis. This sample of records is also influenced by San Fernando earthquake. The magnitude of records considered ranged from 5.3 to 7.7 and epicentral distances ranges from 18 to 124 km. The selection of accelerogram records were limited to those in which the peak ground acceleration is greater than 0.04g.

#### NORMALISATION OF SPECTRA

It was seen that normalisation with reference to non-dimensional factor  $ad/v^2$  (where  $a$  = peak ground acceleration,  $v$  = peak ground velocity and  $d$  = peak ground displacement) gives very large standard deviation (3) throughout the period range and therefore this parameter has not been considered for normalising in this study. Since the peak ground displacement is very sensitive to the method of base line correction applied for an accelerogram, it has also not been considered as a parameter for normalisation. The other parameters like peak ground acceleration, peak ground velocity, spectral intensity corresponding to zero percent,  $SI_0$ , and spectral intensity corresponding to five percent,  $SI_5$ , have been considered for normalizing the velocity spectra. Standard deviation at each time period for all the dampings and different normalisation have been calculated by the following expression,

$$\sigma_j = \sqrt{\frac{(x_{ij} - \bar{x}_j)^2}{n - 1}} \quad \dots (1)$$

where  $x_{ij}$  is the  $i$ th sample value at  $j$ th time period,  $\bar{x}_j$  is the corresponding mean value at  $j$ th time period and  $n$  is the number of samples. Different confidence response spectrum were obtained by the expression

$$y_j = \bar{x}_j + c\sigma_j \quad \dots (2)$$

where  $c$  is a constant (13) for a confidence level.

The comparison of different normalisations have been made by equating the area under the average spectra equal to each other. In this study, the normalising parameter showing least standard deviation over the major portion of the period range is considered as the best.

### Alluvial Site

Figure 1 shows the standard deviation curves of spectral values for different dampings corresponding to different normalisation for alluvial site. It is seen that the standard deviation curves corresponding to peak ground velocity and peak ground acceleration is close to each other. The curves corresponding to both peak ground velocity and peak ground acceleration show minimum deviation from mean. The curves corresponding to peak ground acceleration show minimum deviation in shorter period range and that for peak ground velocity in the longer period range for all the dampings. The curves corresponding to spectral intensity show large deviation. On this basis, the best normalisation could be achieved by using peak ground velocity or peak ground acceleration for obtaining average velocity response spectra (AVRS) for alluvial site.

The AVRS have been obtained using different normalisation. To make a comparison between the AVRS, the area under the curves corresponding to different normalisation were matched to obtain the multiplying factors. The AVRS curves corresponding to different normalisation are shown in Fig. 2. The AVRS curves corresponding to normalisation with respect to peak ground velocity and peak ground acceleration have almost the same shape. Similarly, the AVRS curves corresponding to normalisation  $SI_0$  and  $SI_5$  have almost the same shape. The shape corresponding to  $SI_{15}$  is, however, very much different from 'a' and 'v'. Similar behaviour is also seen for standard deviation curves. The shape of AVRS curves depend upon the normalisation. Therefore, selection of proper normalising factor should be considered while arriving at AVRS curves. In the present study, peak ground velocity is taken as the normalising factor since it gives nondimensional velocity spectra. Based on above, different confidence level velocity response spectra curves normalised to 1 cm/s peak ground velocity have

been obtained and shown in figure 3. 1.0 cm/s peak ground velocity correspond to average value of  $7.0 \text{ cm/s}^2$  peak ground acceleration, 10.0 cm spectral intensity,  $SI_0$  and 6.4 cm spectral intensity,  $SI_5$  respectively. This would mean that 1.0g peak ground acceleration will correspond to 145 cm/s peak ground velocity, 1400 cm spectral intensity,  $SI_0$  and 900 cm spectral intensity,  $SI_5$ .

### Rock Site

Fig. 4 shows the standard deviation curves of spectral values for different damping corresponding to different normalisation for rock site. It is seen that the standard deviation curve corresponding to normalisation with  $SI_0$  and  $SI_5$  are close to each other and show minimum deviation whereas the curves corresponding to normalisation with respect to 'a' and 'v' show large deviations for rock site. The curves corresponding to  $SI_0$  show least deviation almost throughout the period range for zero percent and 2 percent damping whereas  $SI_5$  show least deviation almost throughout the period range for higher dampings.

The AVRS curves corresponding to different normalisation are shown in Fig. 5. The average curves corresponding to peak ground acceleration and peak ground velocity as normalising factors have almost the same shape. Similarly, the AVRS curves corresponding to normalisation  $SI_0$  and  $SI_5$  have almost the same shape. The shape corresponding to spectral intensity is, however, very much different from 'a' and 'v'. The same fact is evident from the standard deviation curves also. On the basis of least standard deviation, the best normalisation could be achieved by using  $SI_0$  or  $SI_5$  for obtaining the AVRS for rock site. Since standard deviation curve for both the spectral intensity are close, the spectral intensity corresponding to zero percent damping has been considered as normalising factor in this study for rock site. Using the  $SI_0$  normalising factor, the shape of velocity response has been obtained for different confidence levels and is shown in Fig. 6. These are expressed with respect to a peak ground velocity of 1 cm/s by using a relation that 1 cm/s velocity corresponds to 4.35 cm  $SI_0$  for rock sites. It has been found that for rock site 1.0 cm/s peak ground velocity correspond to  $11.65 \text{ cm/s}^2$  peak ground acceleration, 4.35 cm  $SI_0$  and 2.62 cm  $SI_5$ . This would mean that 1.0g peak ground acceleration will correspond to 84.0 cm/s peak ground velocity, 366 cm  $SI_0$  and 190 cm  $SI_5$ .

### CONCLUSIONS

The shape of average velocity response spectra (AVRS) very much depends upon the method of normalisation and therefore proper normalisation should be adopted. A new criteria based on least standard deviation has been suggested for selecting the proper method of normalisation of response spectra. On this basis, spectra for rock sites corresponding to

normalisation  $SI_0$  and  $SI_5$  give least deviation and either of them may be adopted for normalisation whereas for alluvial sites peak ground acceleration (a) and velocity (v) give least deviation and either of them may be adopted for normalisation of response spectra for alluvial site. In this study, velocity response spectra for various confidence level, normalised to peak ground velocity of 1 cm/s have been recommended for rock and alluvial site for aseismic design of structures. Depending upon the risk and importance of structures, different confidence level velocity response spectra may be selected.

It was observed that for rock site 1.0 g peak ground velocity corresponds to 84 cm/s peak ground velocity, 366 cm spectral intensity ( $SI_0$ ) and 190 cm spectral intensity ( $SI_5$ ). In case of alluvium 1.0 g peak ground velocity corresponds to 145 cm/s peak ground velocity, 1400 cm spectral intensity corresponding to zero percent damping, and 900 cm spectral intensity corresponding to 5 percent damping.

The mean response velocity is almost flat beyond 1.0 second time period and has a approximate amplification of 1.75, 1.25, 1.0, 0.85 and 0.7 corresponding to 0, 2, 5, 10, 20 percent damping for rock site. The corresponding amplification for alluvial soil are 3.0, 2.1, 1.75, 1.5 and 1.15 respectively for the same dampings. It may therefore be concluded that site characteristics influence the shape of response spectra to a great extent. The amplification is more in alluvial soil than on rock site.

It is interesting to note for any type of site condition, for the normalisation corresponding to 'a' and 'v', the shape of spectra almost coincide with each other.

#### ACKNOWLEDGEMENT

Authors are thankful to Mr. Nem Kumar, Research Assistant for his assistance in preparation of this paper.

#### REFERENCES

1. Analysis of Strong Motion Earthquake Accelerograms, (1972-73), Vol. III, Earthquake Engineering Research Laboratory, California, Institute of Technology, Pasadena, California.
2. Blume, J.A., R.L. Sharpe and J.S. Dalal, (1972), Recommendations for Shape of Earthquake Response Spectra, Wash-1254, USAEC Contract no. At-(49-5)-3011, John A. Blume and Associates, San Francisco, California.
3. Chandrasekaran, A.R. and D.K. Paul, (1973), Response for Alluvial Soils, Symposium on Nuclear Science and Engineering, Bhabha Atomic Research Centre, Bombay.

4. Chandrasekaran, A.R., (1977), Response Spectra, Panel Paper, Sixth World Conference on Earthquake Engineering, New Delhi, Jan.
5. Dalal, J.S. and P.R. Perumalswami, (1977), Significance of Seismic Response Spectrum Normalisation in Nuclear Power Plant Design, Fourth International Conference on Structural Mechanics in Reactor Technology, Paper No. K1/5, San Francisco, Aug.
6. Design Response Spectra for Seismic Design of Nuclear Power Plant, (1973), US Atomic Energy Commission Regulatory Guide, 1.60, Directorate of Regulation Standards, October.
7. Hall, W.J., B. Mohraz and N.M. Newmark, (1975), Statistical Analysis of Earthquake Response Spectra, Third International Conference on Structural Mechanics and Reactor Technology, London.
8. Hayashi, S., H. Tsuchida and E. Kurata, (1971), Average Response Spectra for Various Subsoil Conditions, Third Joint Meeting, U.S. - Japan Panel on Wind and Seismic Effects, UJNF Tokyo, May 10-12.
9. Housner, G.W. (1959), Behaviour of Structures During Earthquakes, Proceedings American Society of Civil Engineers, Journal of Engineering Mechanics Division, Vol. 85, pp. 109-129.
10. Khanna, R., D.K. Paul, Brijesh Chandra (1977), Site Dependent Spectra for Aseismic Design, Bulletin, Indian Society of Earthquake Technology, Vol. 14, No. 3, Sept.
11. Kuribayashi, E., I. Toshio, I. Yitaka and T. Katurari (1970), Effects of Seismic and Subsoil Conditions on Earthquake Response Spectra, Microzonation Conference, Vol. II.
12. Mohraz, B., W.J. Hall and N.M. Newmark (1972), A study of Vertical and Horizontal Earthquake Spectra, Wash-1255, USAEC Contract No. AT-(49-5)-2667, Nathan M. Newmark Consulting Engineering Services, Urbana, Illinois.
13. Newmark, N.M. (1973), Consulting Engg. Service, A Study of Vertical and Horizontal Earthquake Spectra, USAEC Contract No. AT-(49-5)-2667, Wash 1255, April.
14. Newmark, N.M., J.A. Blume and Kanwar, Kapur (1973), Design Response Spectra for Nuclear Power Plants, Structural Engineers ASCE Conference, San Francisco, California, April.

15. Seed, H.B., C. Ugas and J. Lysmer (1974), Site Dependent Spectra for Earthquake Resistant Design, Earthquake Engg. Research Centre, Report No. EERC 74-12, University of California, Berkeley.
16. Strong Motion Earthquake Accelerograms Digitised and Plotted Data (1972-73), Vol. II, Earthquake Engineering Research Laboratory, California Institute of Technology, Pasadena, California.
17. Strong Motion Instrumental Data on the San Fernando Earthquake of Feb. 9, 1971 (1971), Edited Hudson, D.E., Earthquake Engineering Research Laboratory, California Institute of Technology, Pasadena, California.
18. Trifunac, M.D. (1973), Analysis of Strong Earthquake Ground Motion for Prediction of Response Spectra, International J. of Earthquake Engg. and Structural Dynamics, Vol. 2, No. 1, p. 59-69.
19. Trifunac, M.D. and J.G. Anderson (1977), Preliminary Empirical Models for Scaling Absolute Acceleration Spectra, Report No. CE 77-03, University of Southern California, Department of Civil Engineering, Los Angeles, California.

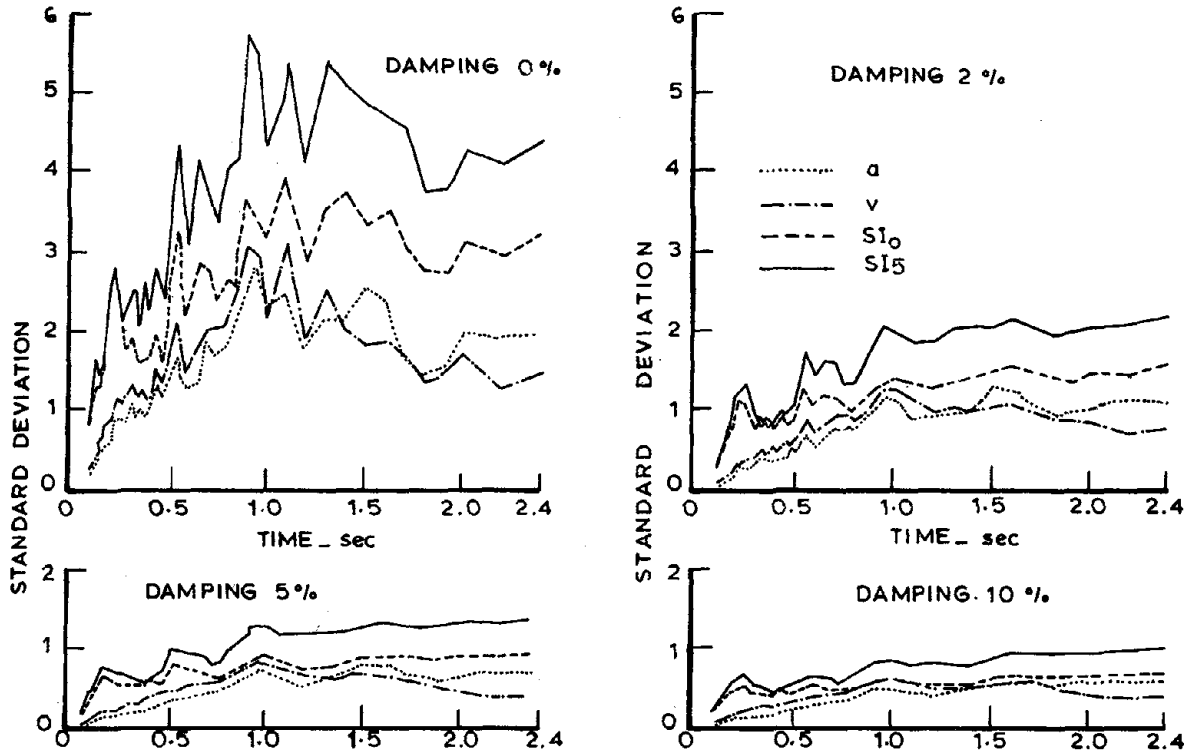


FIG.1-STANDARD DEVIATION CURVES FOR DIFFERENT NORMALISATION AND DAMPING (ALLUVIAL SITE)

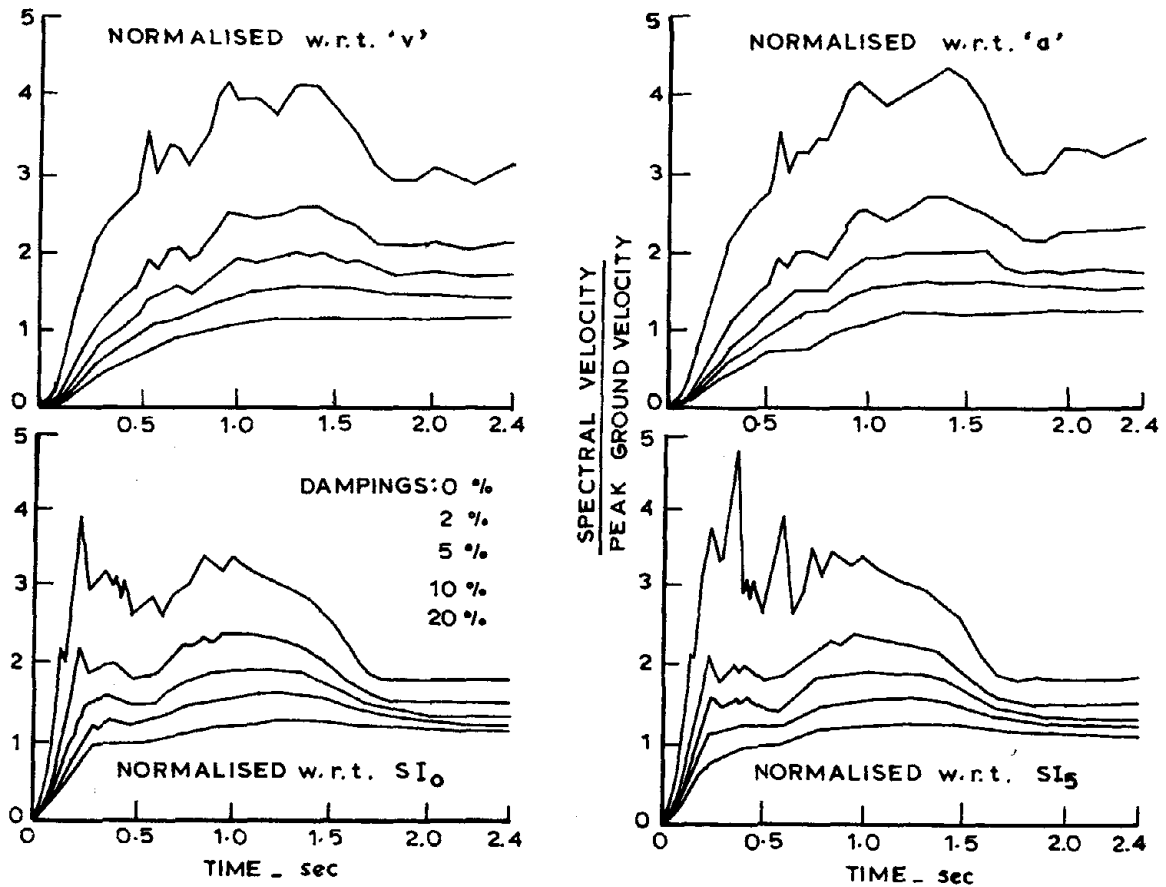


FIG. 2 - AVERAGE VELOCITY RESPONSE SPECTRA FOR DIFFERENT NORMALISATION (ALLUVIAL SITE)



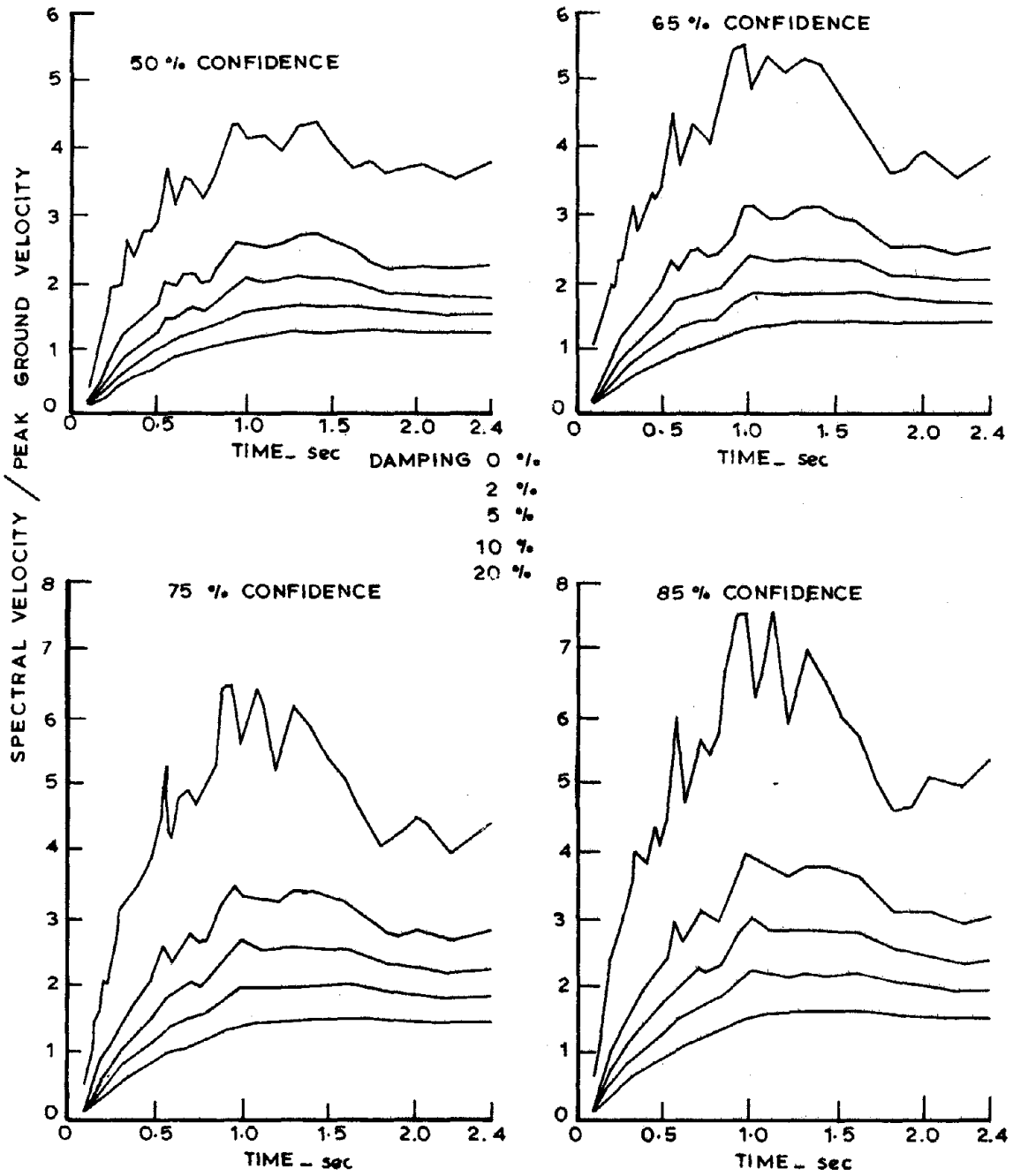


FIG.3- VELOCITY RESPONSE SPECTRA FOR VARIOUS CONFIDENCE LEVEL (ALLUVIAL SITE)

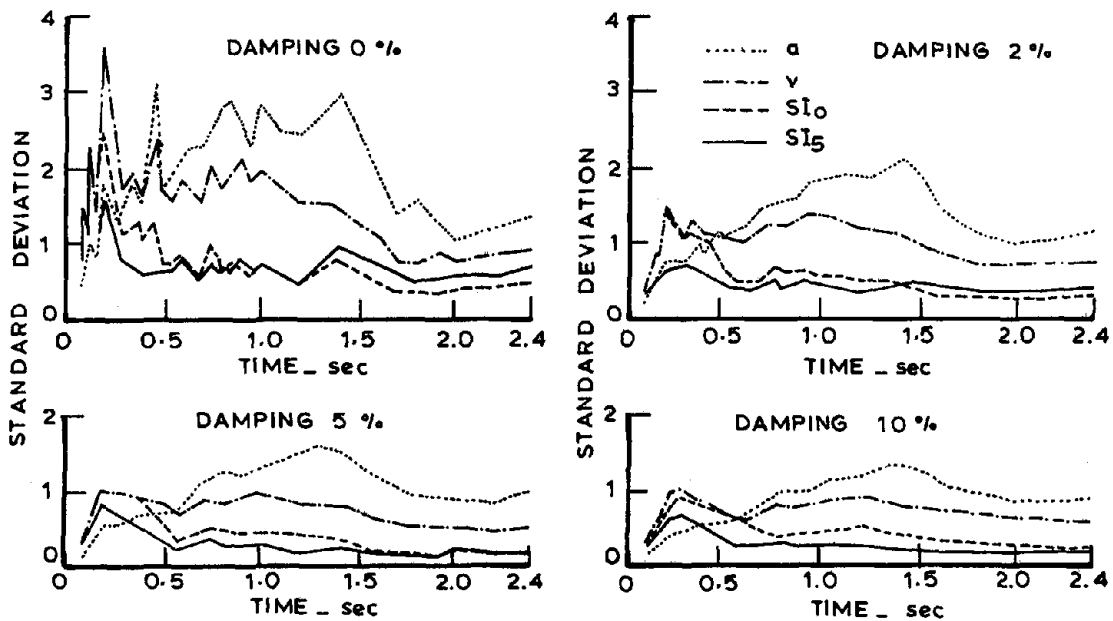


FIG.4 \_ STANDARD DEVIATION CURVES FOR DIFFERENT NORMALISATION AND DAMPING (ROCK SITE)

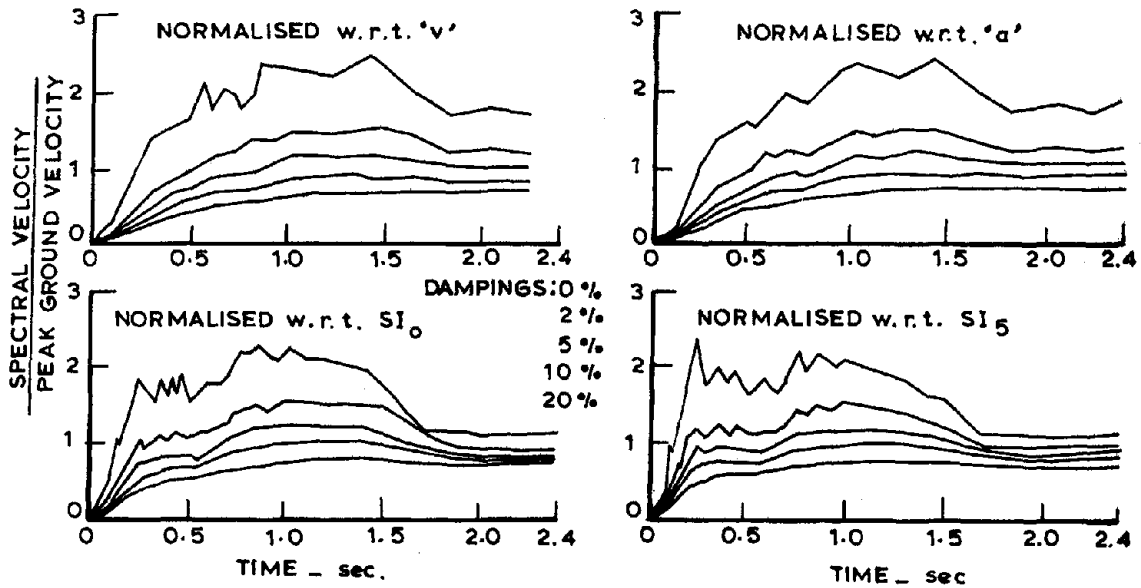
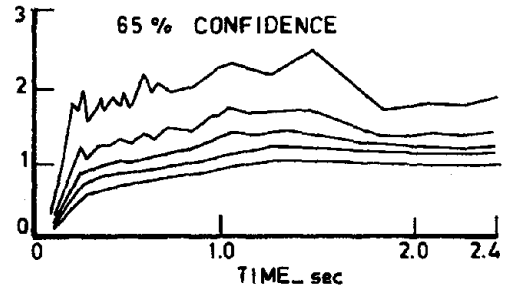
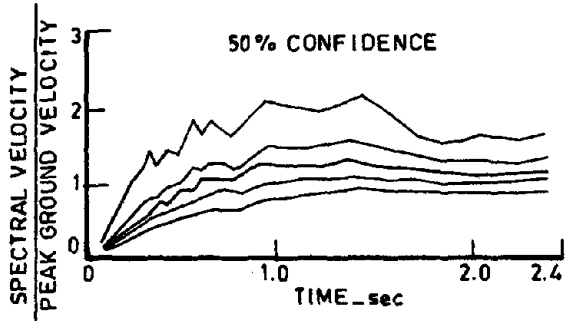


FIG. 5 \_ AVERAGE VELOCITY RESPONSE SPECTRA FOR VARIOUS NORMALISATION (ALLUVIAL SITE)



DAMPINGS  
 0 %  
 2 %  
 5 %  
 10 %  
 20 %

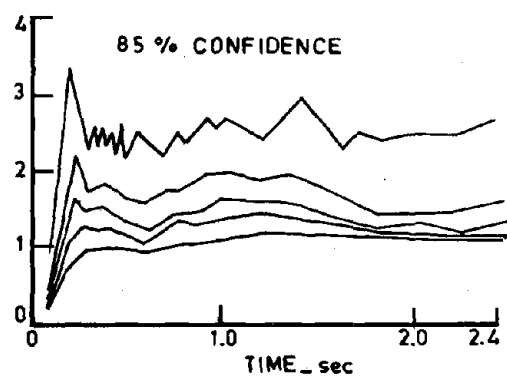
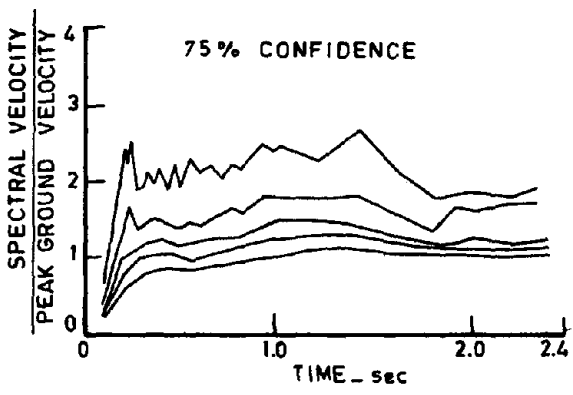


FIG.6\_VELOCITY RESPONSE SPECTRA FOR VARIOUS CONFIDENCE LEVEL (ROCK SITE)

1169

**INTENTIONALLY BLANK**

GENERATION OF FLOOR RESPONSE SPECTRA DIRECTLY FROM  
FREE-FIELD DESIGN SPECTRA

P. C. Chen\*

J. H. Chen\*\*

ABSTRACT

An approach which utilizes recent developments in the theories of probabilistic structural dynamics and random processes was studied for generating floor response spectra directly from free-field design spectra. The approach considers earthquakes as stochastic processes and computes free-field power spectra from free-field design spectra using the extreme value theorem of stochastic processes. The power spectra of the response of linear systems are then determined using random vibration theory and the method of complex response. The floor response spectra of the structures are obtained by using response power spectra of a linear system through relations between power and response spectra.

Numerical examples are provided to illustrate the application of the direct method for generating floor response spectra of a nuclear facility. The NRC free-field design spectra are used as input excitations. The generated floor response spectra are compared with spectra obtained by the time-history method using six distinct NRC spectrum-compatible synthetic earthquakes, and are shown to provide a reliable method for determining seismic forces for equipment design.

\*Engineering Specialist, Research and Engineering,  
Bechtel National, Inc., San Francisco, California

\*\*Graduate Student of Civil Engineering, University  
of California, Berkeley, California

## INTRODUCTION

In recent years there has been considerable interest in developing methodologies which compute floor response spectra directly from free-field design spectra for seismic design of equipment. This spur of interest was due to 1) uncertainties associated with the use of spectrum-compatible time-histories and 2) high cost incurred when the time-history method is used for computing floor response spectra. Many researchers have investigated the direct approach for generating floor response spectra without using the time-history approach either by the amplification functions of a two-mass dynamic system (1, 2, 3, 4, 5, 6, 7), the Fourier Transform technique (8, 9, 10) or the random vibration theory of linear systems (11, 12, 13). All of these methods for directly generating floor response spectra have major shortcomings. An approach developed by Romo-Organista, et al (14, 15) for analyzing soil-structure interaction in a random seismic environment does not have the shortcomings of other methods and was used in this investigation to investigate its capability for directly generating floor response spectra for equipment design.

## APPROACH

The approach taken in this investigation for generating floor response spectra directly from free-field design spectra is termed the direct method and is shown in Figure 1. The direct method has the following features:

- o Earthquakes are considered as random processes
- o The extreme value theorem of stochastic processes is used to develop the relations between free-field response and power spectra.
- o Power spectra of the response of a linear system to stochastic processes are determined by random vibration theory.
- o Floor response spectra are obtained using the response power spectra of the response of a linear system through relations between response and power spectra.

The consideration of earthquakes as random processes is well recognized, as is the application of random vibration theory for

determining power spectra of the response of linear systems when the power spectra of excitations are known. The new and key feature of the approach discussed in this paper for computing floor response spectra directly from free-field design spectra is the use of extreme value theorem for establishing relations between response and power spectra. The justifications for using the extreme value theorem to establish the above relations are: 1) the structural responses are random processes and, 2) any response spectral value which is the maximum response of a linear oscillator can be interpreted as the extreme value of the response.

Mathematical details of the extreme value theorem of random processes and its use for establishing relations between response and power spectra are given in References 14, 16, and 17.

## NUMERICAL RESULTS

A mathematical model (Figure 2) was used to establish the applicability of the approach taken for generating floor response spectra directly from free-field design spectra. The same model was also used for computing floor response spectra using the time-history approach. Floor response spectra with damping ratios of 0.02 and 0.05 were computed at nodal points 4, 7 and 9. The natural frequencies and modal participation factors of this model are given in Table 1.

The NRC horizontal free-field design spectra (Figure 3) (18) with a maximum acceleration of 0.25g were used in both the direct and time-history approaches for determining the floor response spectra. In the direct approach, the NRC design spectra were considered as the average response spectra of a random process which is an ensemble of all possible motions that might occur at the site. In the time-history method, six distinct spectrum-compatible synthetic earthquakes were used. This is because earthquakes are considered as random processes and more than one synthetic time-history should be used in order to make a meaningful comparisons of floor response spectra obtained by the direct and time-history methods. The response spectrum of each of these six synthetic earthquakes envelops the NRC free-field design spectrum for a 0.02 damping ratio (Figure 4).

In order to assess the accuracy of the direct method, floor response spectra with damping ratios of 0.02 and 0.05 were generated and compared using both the direct and time-history methods. Because the floor response spectral values determined by six spectrum-compatible synthetic time-histories differ by more than 30% (Table 2)

and earthquakes are considered as random processes, the mean value of the response spectral values obtained from the time-history approach were compared with those obtained by the direct method.

The floor acceleration response spectra obtained by both the time-history and direct methods are compared in Figure 5. In each of these figures, the dotted line is the mean spectral values from the six synthetic earthquakes, the solid line is the mean value from the direct method, and the dot-dashed and dashed lines are the upper and lower 90% confidence levels, respectively. The confidence levels are provided to estimate the statistical dispersion of response spectral values obtained by the direct method.

A comparison of these response spectra illustrates that the direct method accurately predicts the frequency values at which peak and lowest (valley) responses occur. For a damping ratio of 0.02, the magnitudes of the spectra predicted by both approaches are in good agreement. For damping ratio of 0.05, the direct method gives higher peak responses and lower responses at valleys than the time-history method. The difference in peak spectral values at higher resonant frequencies is progressively less. In frequency ranges where no peaks and valleys occur, the agreement is excellent.

Comparisons of the predicted response spectra for the cases studied indicate that the seismic analysis results obtained by the direct method generally agree well with the mean of those obtained using six synthetic earthquakes. In some cases, higher peak acceleration responses are predicted using the direct method than using the time-history method. If the peak accelerations are used directly as equivalent static forces for equipment design, higher costs will be incurred. However, these higher costs can usually be avoided by using a lower design acceleration. This is achieved when equipment is designed to avoid resonance with structural frequencies.

It should also be noted that the lower responses at valleys in the response spectra predicted by the direct method will not result in an unconservative equipment design. The common practice of smoothing and widening predicted response spectra when defining equipment design spectra such as shown in Figure 6 will account for these differences. Therefore, the response spectra obtained by the direct method can be used for practical design purposes.

From the point of view of computational cost, it is more expensive to compute floor response spectra by the time-history approach than the direct method presented herein. The cost of computing floor response spectra with damping ratios of 0.02, 0.05, and 0.07 at three mass points of the mathematical model in this study was \$64



by the time-history approach using one synthetic earthquake. The corresponding cost incurred by the direct method was only \$7. It is therefore apparent that the direct method is quite cost-effective compared to the time-history approach.

## CONCLUSIONS

The accuracy and cost-effectiveness of the direct method presented in this study establish its capability of generating the floor response spectra for equipment design. Furthermore, the low cost of the direct method makes it suitable for parametric seismic studies to determine the effects on structural response of variations in plan layout and material properties such as damping and stiffness.

The advantages of the direct method are:

- o It computes floor response spectra directly from free-field design spectra, thereby eliminating the need for generating spectrum-compatible synthetic earthquakes and for performing time-history analyses.
- o By considering the free-field design spectra as the average response spectra of a random process, all possible motions whose response spectra are compatible with the free-field design spectra are implicitly considered. This is important because the time-history approach, which considered only one earthquake, may lead to non-conservative designs. Therefore, the direct method provides more reliable equipment design requirements.
- o It is cost-effective compared to the time-history approach.

## REFERENCES

1. Biggs, J. M., and Roesset, J. M., "Seismic Analysis of Equipment Mounted on a Massive Structure, "Seismic Design for Nuclear Power Plants, edited by R. J. Hansen, MIT Press, Cambridge, Mass. 1970.
2. Biggs, J. M., "Seismic Response Spectra for Equipment Design in Nuclear Power Plants", presented at the First International Conference on Structural Mechanics in Reactor Technology, Berlin, September, 1971.
3. Thomas, C. S., "Comparison of Methods for Generating Seismic Floor Response Spectra", MIT, Department of Civil Engineering, June, 1972.
4. Kapur, K. K., and Shao, L. C., "Generation of Seismic Floor Response Spectra for Equipment Design", Proceedings of Speciality Conference on Structural Design of Nuclear Plant Facilities, Chicago, Ill., December, 1973.
5. Sato, H., Komazaki, M., and Ohri, M., "An Extensive Study on A Single Method for Estimating Response Spectrum Based on A Simulated Spectrum", Transactions of the 4th International Conference on Structural Mechanics in Reactor Technology, San Francisco, August, 1977.
6. Schmitz, D. and Peters, K., "Direct Evaluation of Floor Response Spectra from a Given Ground Response Spectrum", Transactions of the 4th International Conference on Structural Mechanics in Reactor Technology, San Francisco, August, 1977.
7. Peters, K., and Schmitz, D., "The Problem of Resonance in the Evaluation of Floor Response Spectra", Transactions of the 4th International Conference on Structural Mechanics in Reactor Technology, San Francisco, August, 1977.
8. Scanlan, R. H., and Sachs, K., "Earthquake Time Histories and Response Spectra", Journal of The Engineering Mechanics Division, Vol. 100, No. EM4, August, 1974.
9. Scanlan, R. H., and Sachs, K., "Floor Response Spectra for Multi-Degree-of Freedom Systems by Fourier Transform", Proceedings of 3rd International Conference on Structural Mechanics in Reactor Technology, London, September, 1975.

## REFERENCES

10. Scanlan, R. H., and Sachs, K., "Development of Compatible Secondary Spectra Without Time History", Transactions of the 4th International Conference on Structural Mechanics in Reactor Technology, San Francisco, August, 1977.
11. Singh, M. P., Singh, S., and Chu, S. L., "Stochastic Concepts in Seismic Design of Nuclear Power Plant", Proceedings of the 2nd International Conference on Structural Mechanics in Reactor Technology, Berlin, September, 1973.
12. Singh, M. P., "Generation of Seismic Floor Spectra", Journal of the Engineering Mechanics Division, Vol. 101, No. EM5, October, 1975.
13. Singh, M. P., and Chu, S. L., "Stochastic Consideration in Seismic Analysis of Structures", Earthquakes Engineering and Structural Dynamics, Vol. 4, 1975.
14. Romo-Organista, M. P., "Soil-Structure Interaction in a Random Seismic Environment", Ph.D Thesis, University of California, Berkeley, California, 1977.
15. Romo-Organista, M. P., Lysmer, J. and Seed, H. B., "Finite Element Random Vibration Method for Soil-Structure Interaction Analysis", Transactions of the 4th International Conference on Structural Mechanics in Reactor Technology, San Francisco, August, 1977.
16. Clough, R. W. and Penzien, J., Dynamic of Structures, McGraw-Hill Book Company, 1975.
17. Gasparini, D. and Vanmarcke, E. H., "Simulated Earthquake Motions Compatible with Prescribed Response Spectra", M.I.T., Department of Civil Engineering Research Report No. R76-4, January, 1976.
18. "Design Response Spectra for Seismic Design of Nuclear Power Plants", Regulatory Guide 1.60, Revision 1, U.S. Nuclear Regulatory Commission, December, 1973.

TABLE 1  
DYNAMIC CHARACTERISTICS OF MATHEMATICAL MODEL

	NATURAL FREQUENCY (CPS)	MODAL PARTICIPATION FACTOR
MODE		
1	4.81	80.90
2	9.11	88.26
3	16.07	24.70
4	22.31	17.50
5	25.54	32.11
6	38.30	16.86
7	46.53	8.36
8	58.18	5.49

N	FREQ	SIMQKE 1	SIMQKE 2	SIMQKE 3	SIMQKE 4	SIMQKE 5	SIMQKE 6
1	.200	.809E-01	.961E-01	.715E-01	.775E-01	.900E-01	.937E-01
2	.300	.164E+00	.205E+00	.204E+00	.145E+00	.210E+00	.172E+00
3	.400	.202E+00	.158E+00	.278E+00	.213E+00	.231E+00	.234E+00
4	.500	.267E+00	.200E+00	.297E+00	.268E+00	.279E+00	.248E+00
5	.600	.300E+00	.310E+00	.295E+00	.313E+00	.355E+00	.343E+00
6	.700	.380E+00	.368E+00	.325E+00	.335E+00	.332E+00	.374E+00
7	.800	.463E+00	.391E+00	.426E+00	.462E+00	.463E+00	.429E+00
8	.900	.506E+00	.445E+00	.358E+00	.540E+00	.406E+00	.426E+00
9	1.000	.538E+00	.547E+00	.518E+00	.558E+00	.595E+00	.524E+00
10	1.100	.586E+00	.595E+00	.596E+00	.599E+00	.621E+00	.641E+00
11	1.200	.714E+00	.646E+00	.599E+00	.703E+00	.527E+00	.648E+00
12	1.300	.839E+00	.787E+00	.762E+00	.730E+00	.790E+00	.708E+00
13	1.400	.878E+00	.759E+00	.811E+00	.755E+00	.696E+00	.757E+00
14	1.500	.951E+00	.872E+00	.812E+00	.910E+00	.853E+00	.822E+00
15	1.600	.100E+01	.937E+00	.825E+00	.854E+00	.920E+00	.908E+00
16	1.800	.130E+01	.108E+01	.116E+01	.117E+01	.103E+01	.109E+01
17	2.000	.124E+01	.122E+01	.115E+01	.128E+01	.102E+01	.137E+01
18	2.200	.152E+01	.137E+01	.149E+01	.152E+01	.145E+01	.147E+01
19	2.400	.152E+01	.174E+01	.177E+01	.154E+01	.167E+01	.190E+01
20	2.420	.155E+01	.178E+01	.168E+01	.153E+01	.175E+01	.200E+01
21	2.600	.188E+01	.200E+01	.178E+01	.175E+01	.203E+01	.190E+01
22	2.800	.204E+01	.195E+01	.213E+01	.200E+01	.165E+01	.194E+01
23	3.000	.219E+01	.207E+01	.213E+01	.242E+01	.229E+01	.244E+01
24	3.300	.240E+01	.279E+01	.289E+01	.257E+01	.243E+01	.292E+01
25	3.600	.323E+01	.306E+01	.305E+01	.297E+01	.314E+01	.332E+01
26	4.000	.506E+01	.470E+01	.440E+01	.393E+01	.411E+01	.533E+01
27	4.400	.687E+01	.696E+01	.750E+01	.748E+01	.821E+01	.784E+01
28	4.470	.648E+01	.804E+01	.813E+01	.846E+01	.839E+01	.795E+01
29	4.700	.992E+01	.100E+02	.912E+01	.940E+01	.979E+01	.109E+02
30	4.810	.103E+02	.104E+02	.836E+01	.901E+01	.922E+01	.104E+02
31	5.000	.104E+02	.109E+02	.977E+01	.101E+02	.697E+01	.959E+01
32	5.500	.548E+01	.619E+01	.630E+01	.617E+01	.743E+01	.576E+01
33	6.000	.584E+01	.529E+01	.561E+01	.536E+01	.488E+01	.569E+01
34	6.500	.499E+01	.422E+01	.409E+01	.417E+01	.429E+01	.471E+01
35	7.000	.441E+01	.395E+01	.421E+01	.360E+01	.362E+01	.409E+01
36	7.500	.492E+01	.539E+01	.493E+01	.419E+01	.423E+01	.409E+01
37	8.000	.504E+01	.517E+01	.527E+01	.435E+01	.460E+01	.445E+01
38	8.500	.462E+01	.558E+01	.569E+01	.492E+01	.490E+01	.548E+01
39	9.000	.670E+01	.672E+01	.543E+01	.622E+01	.577E+01	.610E+01
40	10.000	.450E+01	.393E+01	.312E+01	.379E+01	.422E+01	.366E+01
41	11.000	.248E+01	.255E+01	.247E+01	.260E+01	.233E+01	.251E+01
42	12.000	.266E+01	.215E+01	.191E+01	.205E+01	.200E+01	.207E+01
43	13.000	.198E+01	.176E+01	.183E+01	.204E+01	.161E+01	.178E+01
44	14.000	.181E+01	.185E+01	.146E+01	.169E+01	.136E+01	.171E+01
45	15.000	.191E+01	.168E+01	.142E+01	.174E+01	.151E+01	.155E+01
46	16.500	.167E+01	.157E+01	.125E+01	.154E+01	.170E+01	.157E+01
47	18.000	.162E+01	.144E+01	.131E+01	.140E+01	.142E+01	.142E+01
48	20.000	.158E+01	.137E+01	.121E+01	.132E+01	.120E+01	.128E+01
49	22.000	.151E+01	.128E+01	.119E+01	.129E+01	.117E+01	.124E+01
50	25.000	.142E+01	.130E+01	.119E+01	.126E+01	.112E+01	.119E+01
51	28.000	.139E+01	.128E+01	.118E+01	.125E+01	.111E+01	.117E+01
52	33.000	.134E+01	.126E+01	.116E+01	.123E+01	.110E+01	.116E+01

Reproduced from  
best available copy.



TABLE 2 RESPONSE ACCELERATIONS BY SYNTHETIC EARTHQUAKES  
AT NODE 9, DAMPING RATIO=0.02

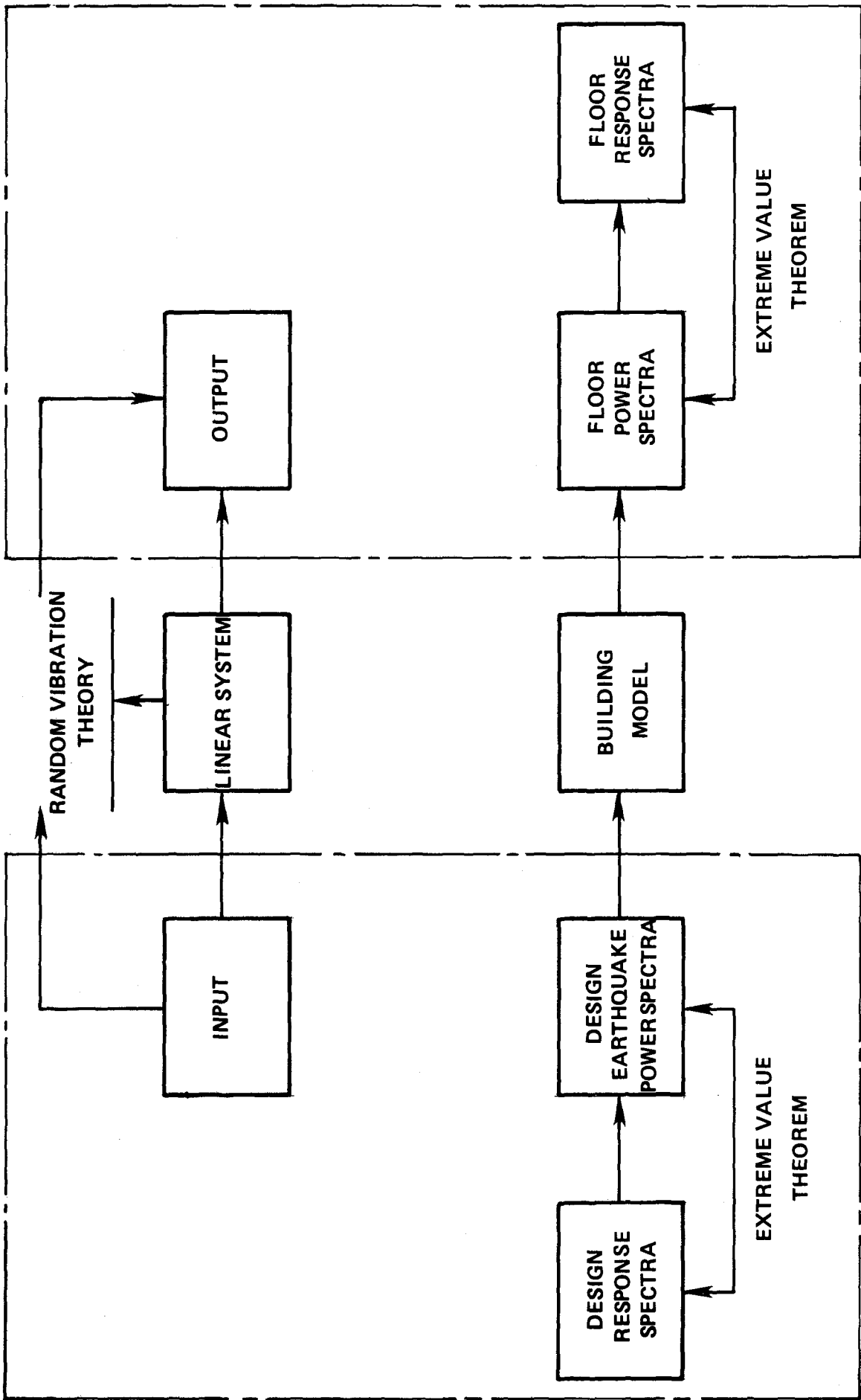
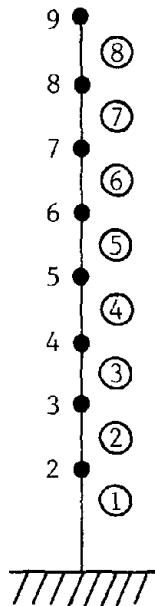


FIGURE 1 SCHEMATIC REPRESENTATION OF DIRECT METHOD FOR GENERATING FLOOR RESPONSE SPECTRA



The diagram shows a vertical structural member fixed at the base (node 1, elevation -26'-0"). Nodes 2 through 9 are spaced vertically. Node 2 is at 0'-0", node 3 at 18'-0", node 4 at 36'-0", node 5 at 60'-0", node 6 at 80'-0", node 7 at 110'-0", node 8 at 153'-0", and node 9 at 195'-0". Each node is marked with a circled number. The member is supported by a fixed base indicated by hatching.

Elev.	WEIGHT (kips)	AREA (ft <sup>2</sup> )	SHEAR AREA (ft <sup>2</sup> )	I (ft <sup>4</sup> )
195'-0"	31,700	3,180	1,100	13,140,530
153'-0"	23,740	3,180	1,100	13,140,530
110'-0"	35,500	3,700	1,475	13,488,265
80'-0"	56,730	14,300	7,033	62,907,890
60'-0"	108,300	18,926	10,055	63,058,160
36'-0"	94,120	16,900	9,520	72,437,030
18'-0"	81,710	15,950	10,200	73,262,500
0'-0"	104,839	19,790	12,718	91,209,000
-26'-0"				

**FIGURE 2 MATHEMATICAL MODEL STUDIED**

$$E = 519,840 \text{ k/ft}^2, \nu = 0.3$$

\* 7% MATERIAL DAMPING RATIO FOR STRUCTURAL ELEMENTS

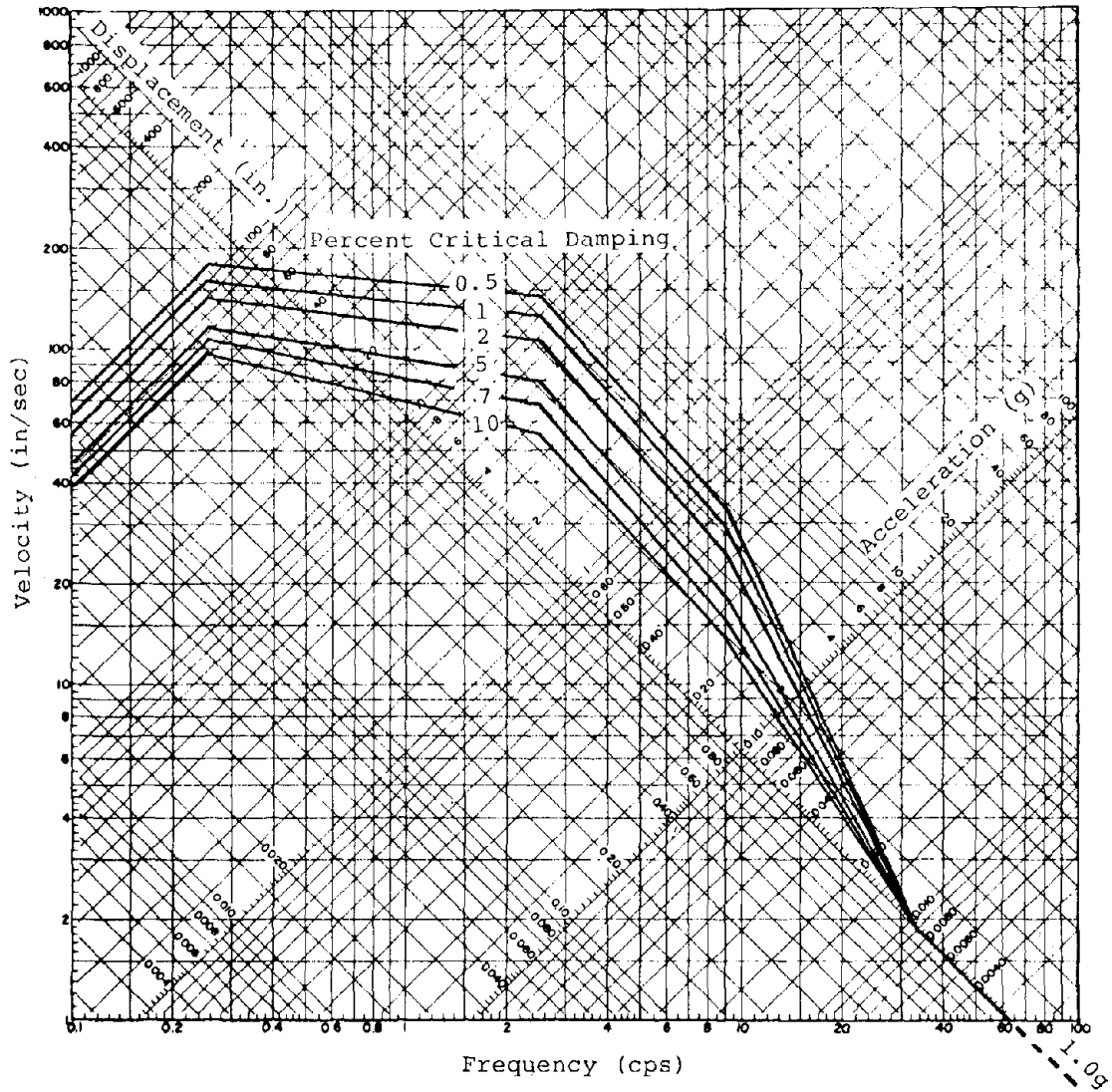


**FIGURE 3 HORIZONTAL DESIGN SPECTRA FOR PEAK HORIZONTAL  
GROUND ACCELERATION OF 1.0g**



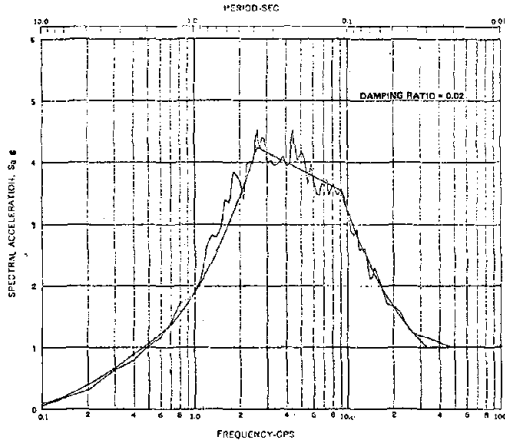


**FIGURE 4.a ACCELERATION RESPONSE SPECTRUM OF SYNTHETIC TIME HISTORY - SIMOKE 1**

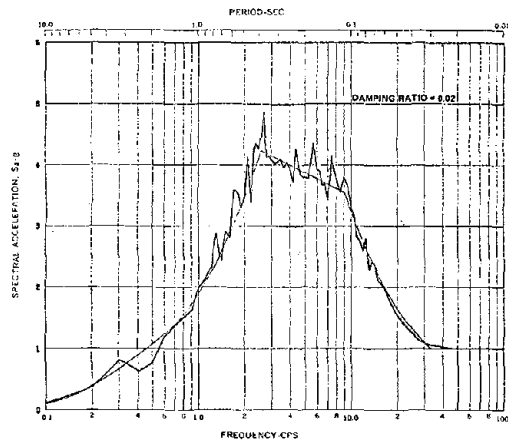


**FIGURE 4.b ACCELERATION RESPONSE SPECTRUM OF SYNTHETIC TIME HISTORY - SIMOKE 2**

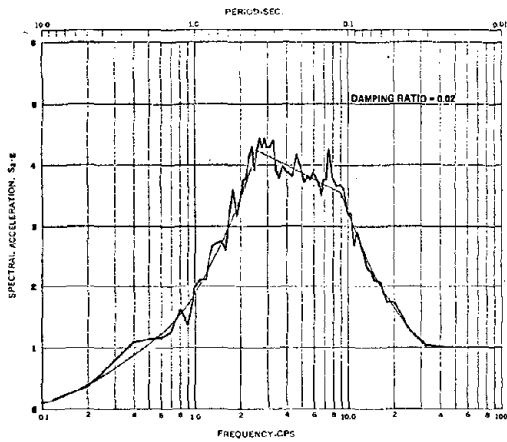


**FIGURE 4.c ACCELERATION RESPONSE SPECTRUM OF SYNTHETIC TIME HISTORY - SIMOKE 3**

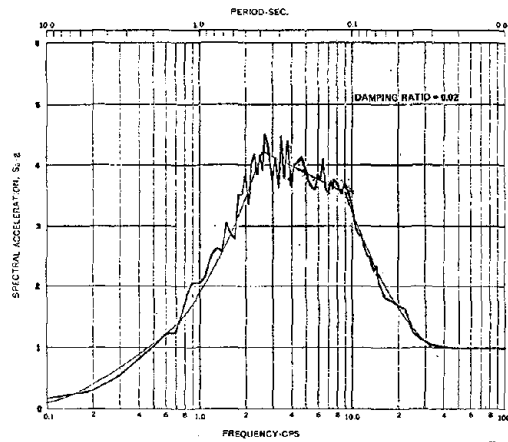


**FIGURE 4.d ACCELERATION RESPONSE SPECTRUM OF SYNTHETIC TIME HISTORY - SIMOKE 4**

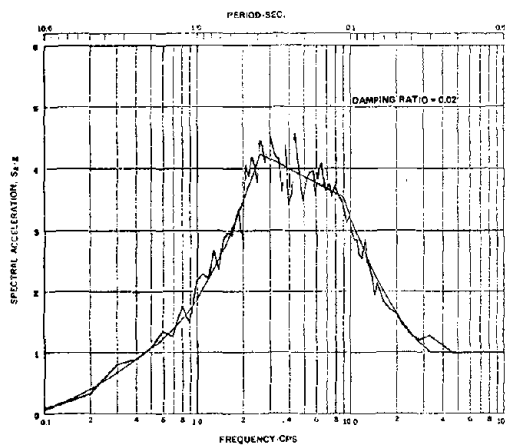


**FIGURE 4.e ACCELERATION RESPONSE SPECTRUM OF SYNTHETIC TIME HISTORY - SIMOKE 5**

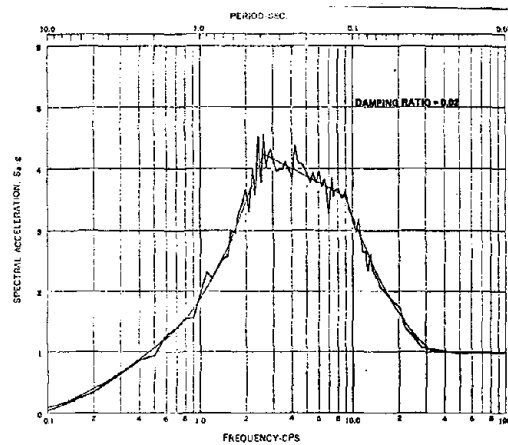


**FIGURE 4.f ACCELERATION RESPONSE SPECTRUM OF SYNTHETIC TIME HISTORY - SIMOKE 6**

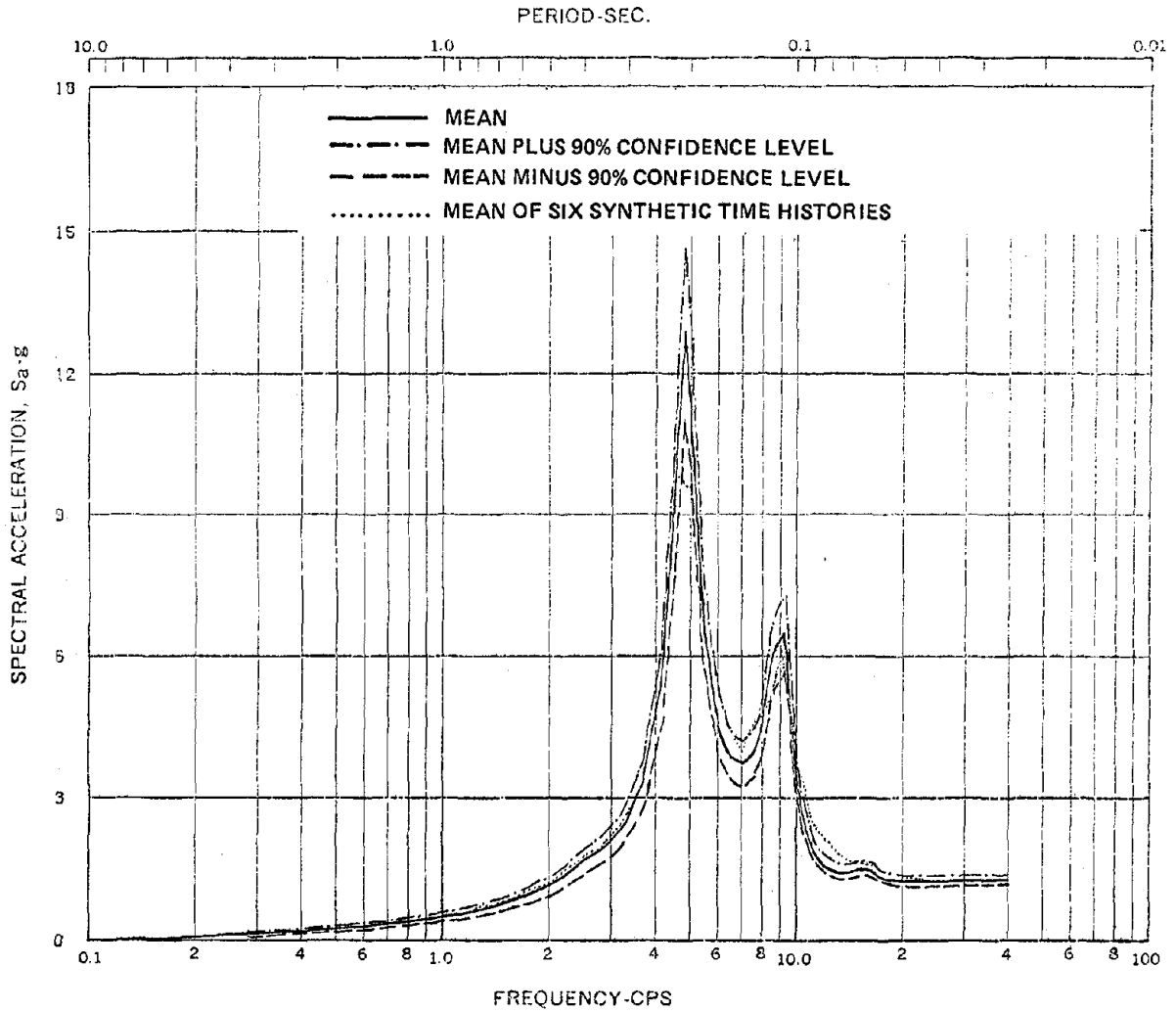


**FIGURE 5.a ACCELERATION RESPONSE SPECTRA AT NODE NO. 9,  
DAMPING RATIO=0.02**

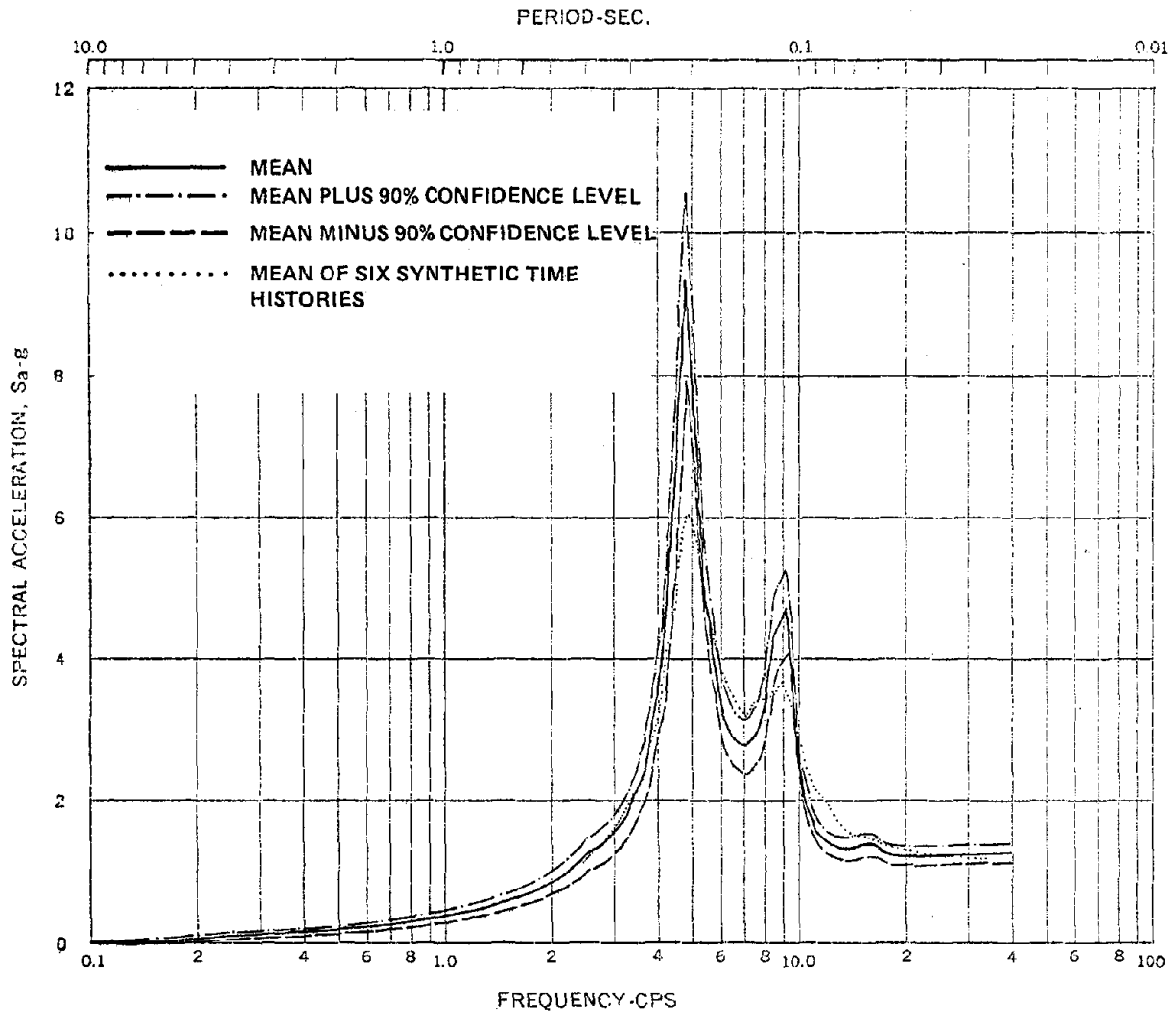


**FIGURE 5.b ACCELERATION RESPONSE SPECTRA AT NODE NO. 9,  
DAMPING RATIO=0.05**

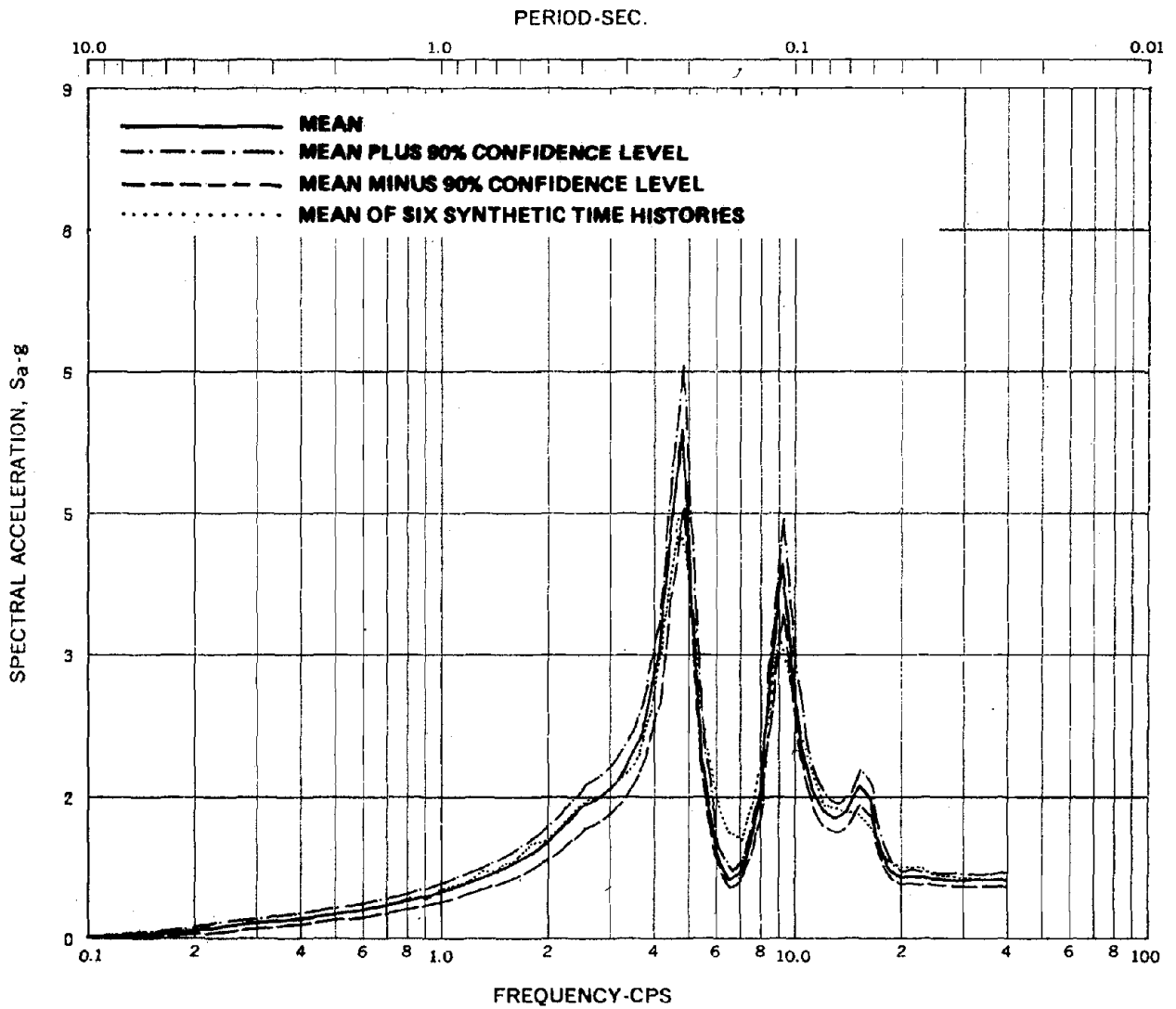


**FIGURE 5.c ACCELERATION RESPONSE SPECTRA AT NODE NO. 7,  
DAMPING RATIO=0.02**

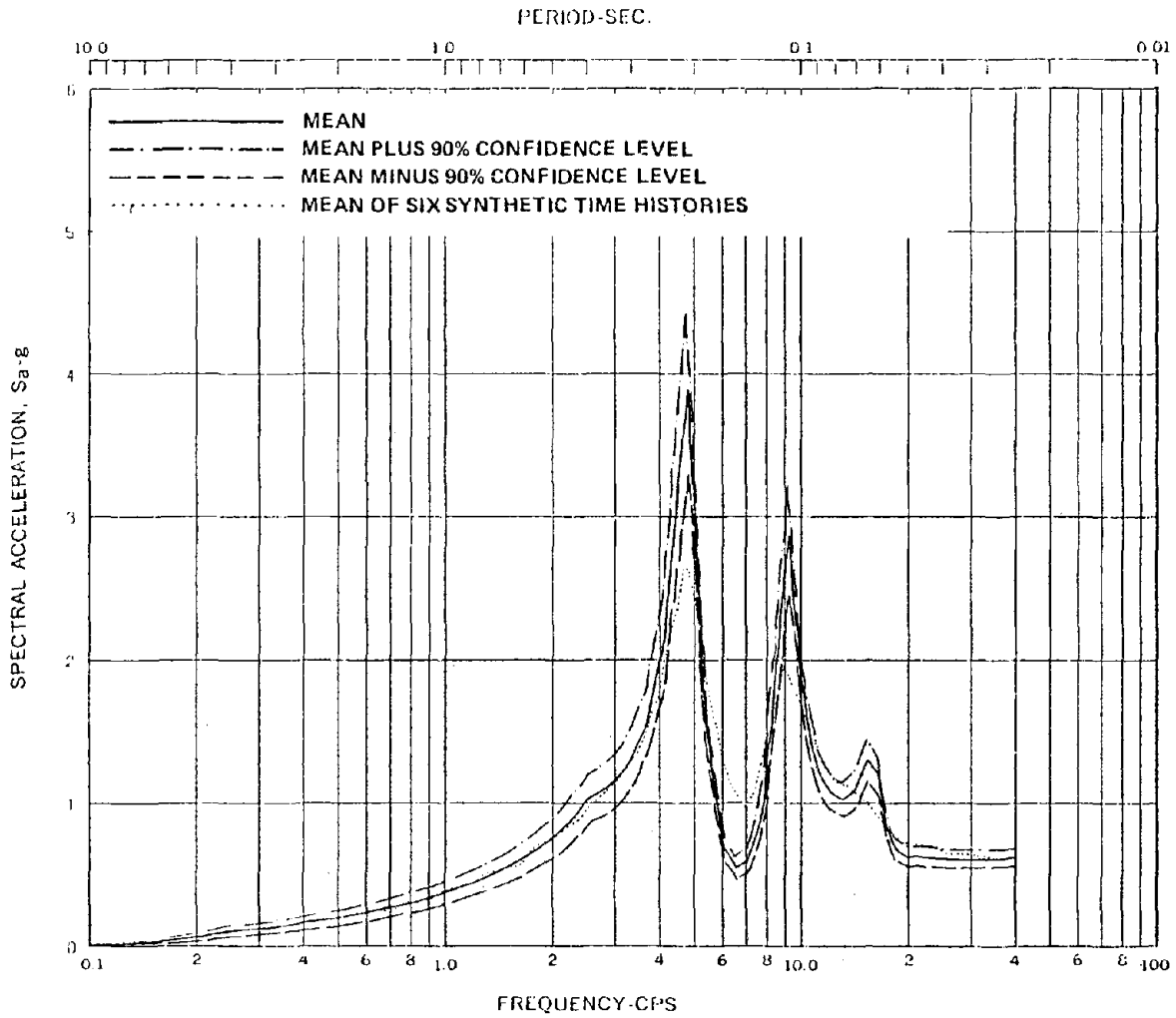
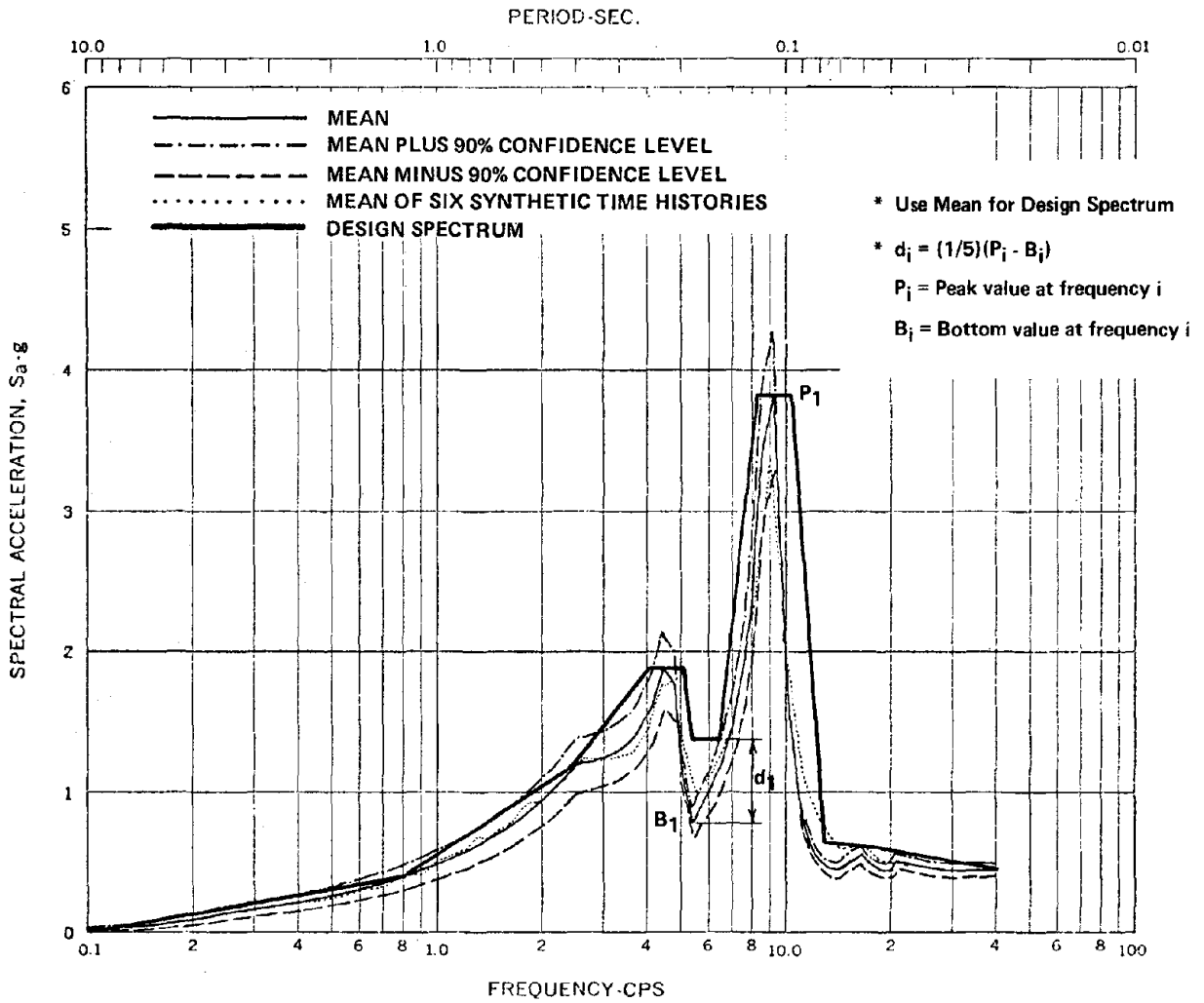


FIGURE 5d ACCELERATION RESPONSE SPECTRA NODE NO. 7,

DAMPING RATIO=0.05



**FIGURE 6 ACCELERATION RESPONSE SPECTRA AT NODE NO. 4,  
DAMPING RATIO=0.02**

## DESIGN SPECTRA FOR STIFF STRUCTURES ON ROCK

by

T. Hisada<sup>I</sup>, Y. Ohsaki<sup>II</sup>, M. Watabe<sup>III</sup> and T. Ohta<sup>IV</sup>

## ABSTRACT

Standard response spectra are proposed for stiff structures such as nuclear power facilities to be constructed on rock sites. The proposal is principally based on accumulated informations on peak accelerations of ground motions in near-fields, as well as on analyses of approximately 50 accelerograms obtained on rock outcroppings and actuated by considerable strong earthquakes with intermediate or far epicentral distances. The dependences of significant parameters in response spectra on magnitudes and epicentral distances are closely examined on the basis of those informations to obtain essential values required to construct standard response spectra. A considerable extent of engineering judgement is also exercised for the refinement of final shapes of the response spectra. The proposed response spectrum is defined for each of 3x3 matrix in terms of magnitude 6,7,8 and near, intermediate, and far epicentral distance, whereas the definitions of near, intermediate, and far earthquakes are, in turn, dependent on the magnitude of each earthquake.

## FREE ROCK SURFACE

The proposed standard response spectra are defined for ground motions at a free rock surface as is illustrated in Fig.1. This free rock surface is defined followingly; (i) surface should be horizontal and flat exposed surface of rock, extending over a reasonably wide area, above which neither surface layer nor structure is present,

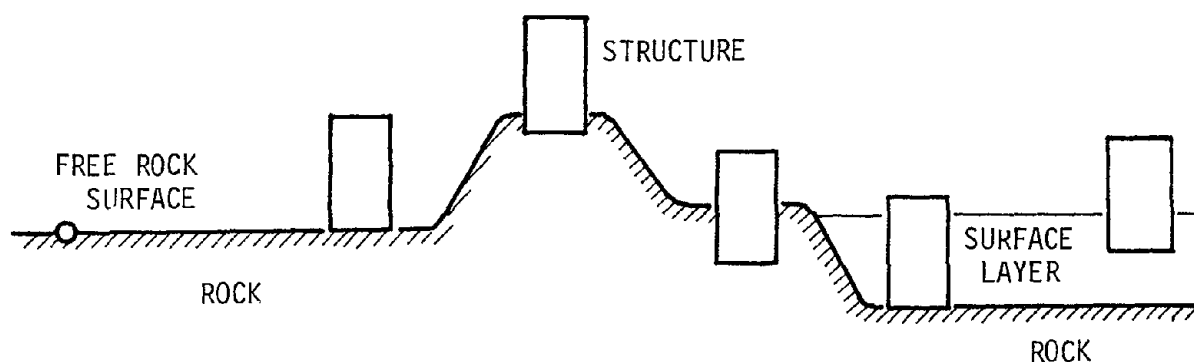


Fig.1 Definition of Free Rock Surface

(ii) the rock should be firm, intact (not significantly weathered nor fissured) and what has been formed in principle in the Tertiary or earlier

I Director, Kajima Institute of Construction Technology, Tokyo, Japan

II Professor, Faculty of Engineering, University of Tokyo, Tokyo, Japan

III Director, Structural Engineering Department, Building Research Institute, Tokyo, Japan

IV Senior Research Engineer, Kajima Institute of Construction Technology, Tokyo, Japan

geological era, having shear wave velocity larger than approximately 700 m/sec, (iii) where such surface can not be identified within or around the proposed site, it should reasonably be assumed.

If, as shown in Fig.1, (i) the rock surface undulates, (ii) it is weathered or overlain by soil layers, (iii) a structure is to be constructed on the rock surface, or (iv) furthermore, the structure is to be embedded into the rock these effects should be taken into consideration separately, by applying adequate modification to the proposed, original response spectra.

#### STANDARD RESPONSE SPECTRA

The proposed standard response spectra consist of a curve, AB, and three straight-line segments BC, CD, and DE in tripartite representation as shown in Fig.2. The first one, AB, is such a curve that will develop a straight line between points A and B, when a pseudo-acceleration response spectrum is drawn with arithmetic axes.

The periods  $T$  in sec and velocity responses  $S_v$  in cm/sec at control points A, B, C, D, and E are as given in Table 1, with the following conditions:

- i) for horizontal ground motions at the free rock surface,
- ii) scaled to 10 cm/sec ground velocity, and
- iii) represented for 5 percent of critical damping.

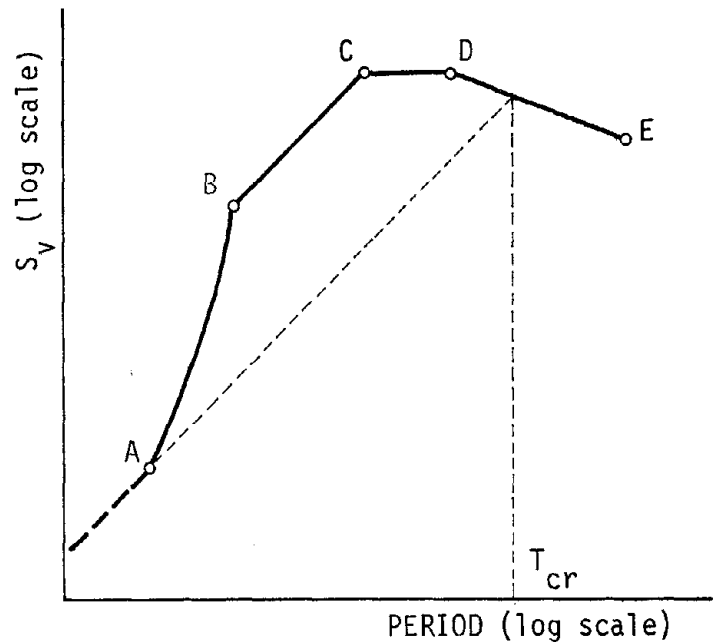


Fig.2 Control Points in Response Spectra

#### VARIATIONS TO STANDARD RESPONSE SPECTRA

Design earthquakes for a specific structure should be deliberately selected by scientists and engineers concerned. As far as nuclear power facilities are concerned, the regulatory guide for selection of design earthquakes is provided elsewhere (1). If design earthquakes thus selected are of magnitudes and epicentral distances different from those specified in Table 1, the logarithmic response spectra should be determined by linear interpolation in terms of magnitudes and by logarithmic interpolation in terms of distances, respectively. However for near-field earthquake ground motions with shorter epicentral distances than defined in Table 1, the response spectra remain the same as the indicated NEAR in Table 1.

For damping factors other than 5%, it is recommendable to multiply the specified, spectral values by the factor(2)

$$\eta = \frac{1}{\sqrt{1 + 17(h-0.05)\exp(-2.5T/T_0)}} \quad \text{for } T \geq 0.07 \text{ sec.} \quad [1]$$

$$\eta = 1.0 \quad \text{for } T = 0.02 \text{ sec.}$$

where  $h$  : damping factor in decimal fraction



Table 1 : Horizontal Standard Response Spectra (Damping Factor 5%)

Field	Magni- tude, M	Epicentral Distance $\Delta$ (km)	Control Points									
			A		B		C		D		E	
			$T_A$	$S_V$	$T_B$	$S_V$	$T_C$	$S_V$	$T_D$	$S_V$	$T_E$	$S_V$
Near	8	25	0.02	0.6	0.10	10	0.30	30	0.50	30	2.0	12
	7	10		0.7	0.09	10	0.22	24	0.45	24		7
	6	5		1.2	0.07	12	0.13	21	0.35	21		3
Inter- mediate	8	120		0.5	0.20	18	0.35	32	1.00	32		26
	7	45		0.5	0.13	11	0.33	28	0.80	28		19
	6	15		0.6	0.08	8	0.25	24	0.60	24		12
Far	8	350		0.5	0.22	26	0.37	44	1.20	44		42
	7	150		0.5	0.14	15	0.35	38	0.90	38		32
	6	60		0.5	0.10	10	0.33	33	0.70	33		20

$T$  : period at control point in Table 1 in sec.

$T_0$  : duration of ground motion

$$= 10^{0.31 \cdot M - 1.2} \text{ in sec. (3)}$$

$M$  : magnitude

For evaluating peak velocities of rock motions due to design earthquakes, it is recommended at the present state to use Kanai's empirical formula(4)

$$v_{\text{peak}} = 10^{0.61M - P \log_{10} X - Q} \quad [2]$$

where

$v_{\text{peak}}$  : peak velocity amplitude in cm/sec at free rock surface

$M$  : magnitude

$P = 1.66 + 3.60/X$ ,  $Q = 0.631 + 1.83/X$

$X$  : focal distance in kilometers

Eq.[2] is well known as an expression for evaluating intensities of earthquake ground motions, indicating smaller scatter between computed and observed values than any other similar expressions in terms of peak velocity or acceleration. In addition, it has long been pointed out that velocity characteristics of earthquake motions are more closely correlated with damage potential than peak accelerations(5). Under such considerations, the priority is given to velocity over acceleration in the representation of standard response spectra in Table 1.

To employ eq.[2], it is required to have information on the focal depth  $D$  for computing the focal distance  $X$ . If such seismotectonic information is unfortunately not available, alternatively the following equation is recommended to obtain the focal depth  $D$  in terms of magnitude.

$$D = 10^{0.353M - 1.435} \text{ in Kilometers} \quad [3]$$

Fig.3 is a diagrammatic representation of design response spectra defined in Table 1 on the basis of eq.[2] and eq.[3]. In Fig.4, furthermore, the same response spectra are shown in the form of normalized acceleration response spectra,  $\bar{q}_a(T)$ .

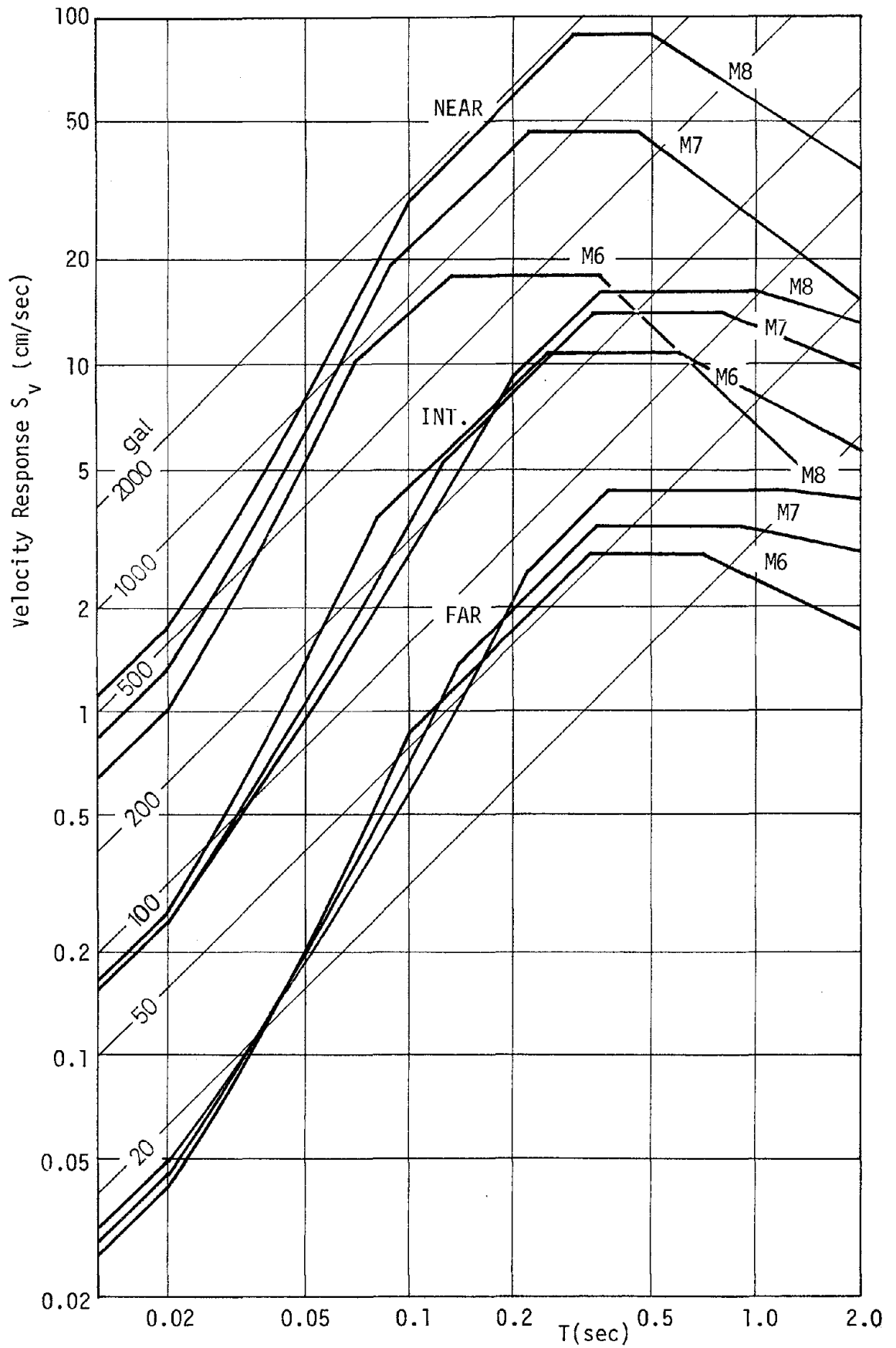
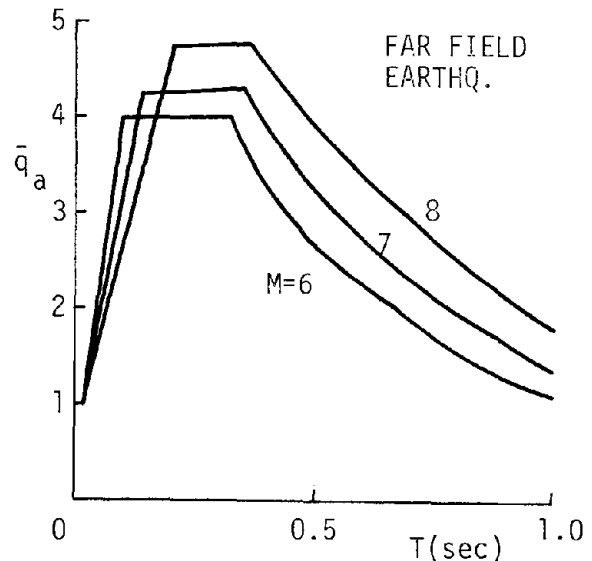
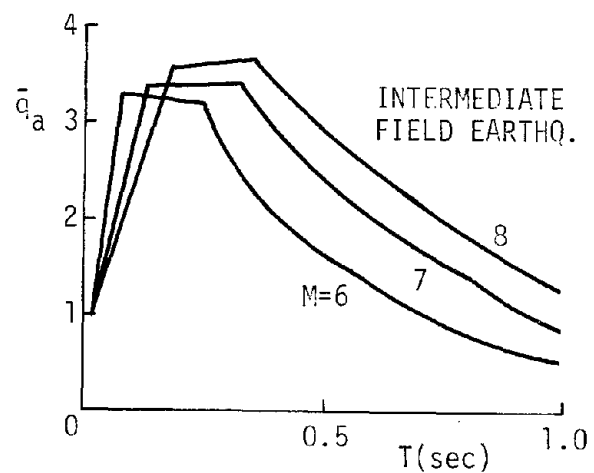
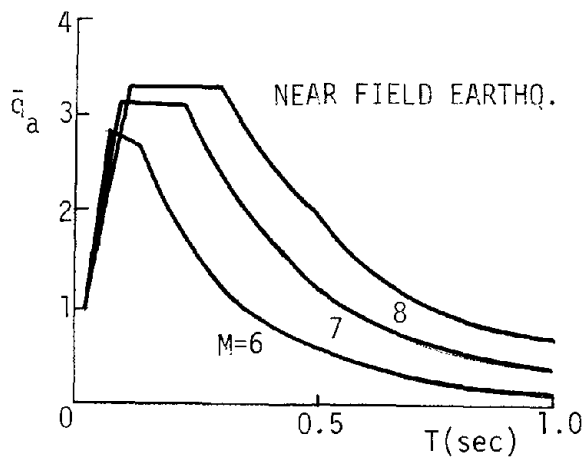


Fig.3 Design Response Spectra as Defined in Table 1.



#### FIT TO OBSERVED, CHARACTERISTIC VALUES

1) *Field Classification* : Traditionally, peak accelerations during earthquakes have been estimated in Japan by observing the overturning of tombstones, simply assuming that the ratio of peak acceleration,  $\alpha$ , to acceleration of gravity,  $g$ , may approximately be represented by  $\alpha/g > B/H$ , where  $B$  and  $H$  are the width and the height of an overturned tombstone.

In the events of recent earthquakes, the same observations were also made in a large number of cemeteries which are close to each causative fault and where rock can be encountered at shallow depths. The estimated peak accelerations are plotted in Fig.5 (6) in terms of distances from the faults. Some fact may be found from Fig.5 that peak accelerations remain constant in epicentral areas within certain boundaries, beyond which peak accelerations tend to attenuate gradually.

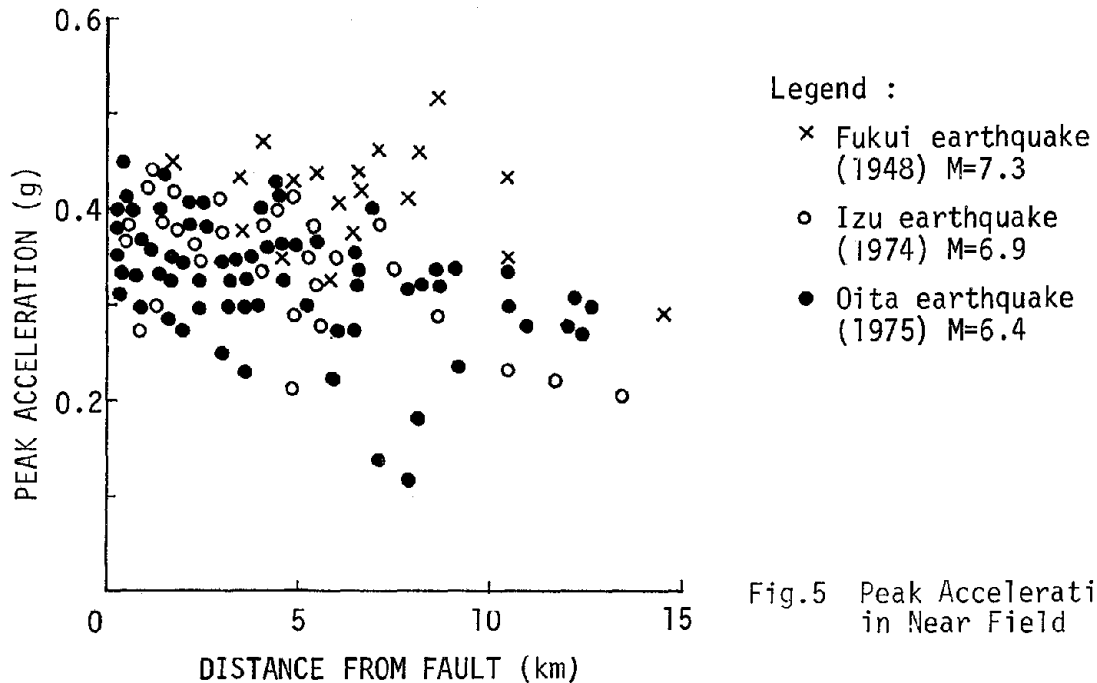
In view of the results shown in Fig.5, the range with truncated peak accelerations is referred to as near-field in this paper, and in the third column of Table 1, the boundary distance is defined for each magnitude of near-field earthquake with due conservatism.

The epicentral distances, which yield peak velocities of approximately 5 and 1 cm/sec by eq. [2], are simply assumed to represent intermediate and far fields, respectively. One of empirical formulae which represent the radius of sphere,  $r$ , enveloping the foci of after-shocks as a function of the magnitude of main shock,  $M$ , is (7)

$$r = 10^{0.353M - 1.134} \quad \text{in kilometers.} \quad [4]$$

Fig.4 Normalized Absolute Acceleration Response Spectra

The epicentral distances representing intermediate and far fields in Table 1 are approximately equal to 2 times and 8 times the radius in eq. [4], respectively.



2) *Accelerations in Near-Field* : Peak accelerations of rock motions in the near-field are estimated as shown in Fig.6 (7,8) based on the observations of tombstone behaviors as described above and of damage to buildings. Pseudo-accelerations at control point A for the near field are as shown by solid line in Fig.6. It is considered here that, whereas the solid line is somewhat lower than the upper bound of plotted 'peak' accelerations, the former might be reasonably sufficient for representing 'effective' peak accelerations for the purposes of structural design.

3) *Amplification* : As a basis of judgement in constructing standard spectra, characteristics of acceleration and velocity response spectra of ground motions listed in Table 2 have been closely examined. Except five records from foreign countries, all were obtained recently in Japan on the free rock surfaces with shear wave velocity larger than approximately 1,000 m/sec.

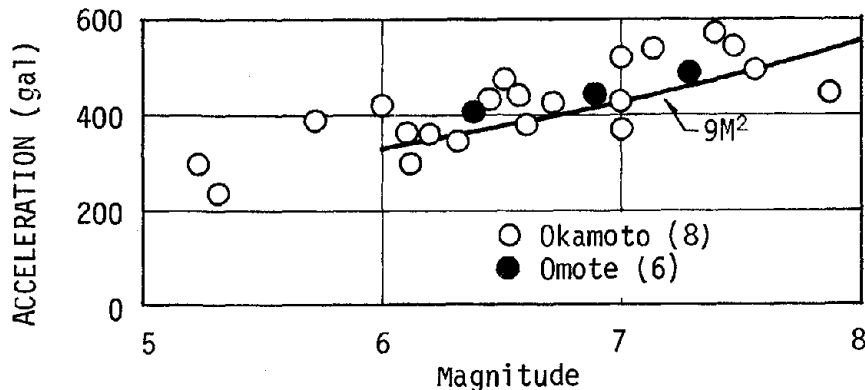


Table 2 : List of Observed Earthquake Motions

Earthquake No.	M	$\Delta$ (km)	Max. Acceleration(gal)		Category
			NS	EW	
L3 - 1	5.3	15	64.4	68.0	5 - I
L3 - 2	4.9	15	145.4	285.7	
P1 - 1	5.3	12	81.8	102.8	
P4 - 1	5.4	13	139.0	194.4	
Q10- 1	5.4	4.3	204.0	403.0	
Q10- 2	4.7	6.4	221.0	88.0	
Q10- 3	4.5	5.7	287.0	90.0	
Q10- 4	4.9	5.0	158.0	218.0	
P5 - 1	6.3	13	630.0	490.0	6 - I
Q1 - 8	6.4	39	36.0	62.0	
Q4 - 2	5.8	14	117.0	86.0	
D1 - 3	6.9	60	35.0	33.0	7 - I
J2 - 1	6.6	40	8.5	12.7	
P3 - 1	6.6	9	1148.1	1054.9	
P6 - 1	7.7	43	152.0	175.0	8 - I
B1 - 2	4.8	30	25.2	27.0	5 - F
B1 -12	5.2	40	79.8	36.8	
J1 - 1	5.1	30	10.9	-	
L2 - 1	4.8	30	77.4	-	
Q6 - 1	4.8	53	-	27.0	
Q7 - 1	5.0	66	53.0	-	
B1 - 6	6.2	80	60.0	54.0	6 - F
B1 - 7	6.2	110	8.0	12.1	
B1 - 8	5.5	60	56.3	46.6	
B1 - 9	6.0	60	18.4	29.1	
B1 -10	5.7	60	34.2	33.5	
B1 -11	5.5	50	82.1	42.1	
D1 - 2	5.5	40	60.0	35.0	
M1 - 1	6.2	65	50.9	130.6	
P2 - 1	5.6	31	264.3	340.8	
Q1 - 3	5.9	127	33.0	44.0	
Q1 - 4	6.3	84	50.0	47.0	
Q1 - 6	5.7	122	44.0	33.0	
Q1 - 7	6.0	89	52.1	31.0	
Q1 - 9	6.2	111	39.0	30.0	
Q6 - 2	6.2	90	152.0	78.0	
C4 - 1	7.2	245	11.3	14.4	7 - F
C4 - 2	6.9	110	14.1	11.6	
F1 - 1	6.6	145	11.6	-	
K1 - 1	6.6	95	-	26.1	
L4 - 1	6.9	140	33.8	30.4	
L5 - 1	6.9	140	25.8	-	
Q1 - 5	7.2	103	113.0	93.0	
Q1 - 1	7.9	183	116.0	95.0	8 - F
Q1 - 2	7.5	211	91.0	77.0	
Q5 - 1	7.9	234	-	4.5	

Column line for category in Table 2 indicates the magnitude of earthquake and epicentral distance of observation station, i.e., for instance, Category 7-I implies that the magnitude is within the range of  $M=6.5$  to  $7.4$ , and the station is located at the epicentral distance belonging to the intermediate field as represented in Table 1. Observed records in far field are placed under the category with symbol F.

To illustrate the fit to observed, characteristic values, Fig.7,8, and 9 are shown in the followings. In Fig.7, max. velocity response amplifications,  $\bar{q}_v$ , due to observed rock motions are compared with corresponding values defined in Table 1, i.e.,  $S_v$ 's at control point C or D divided

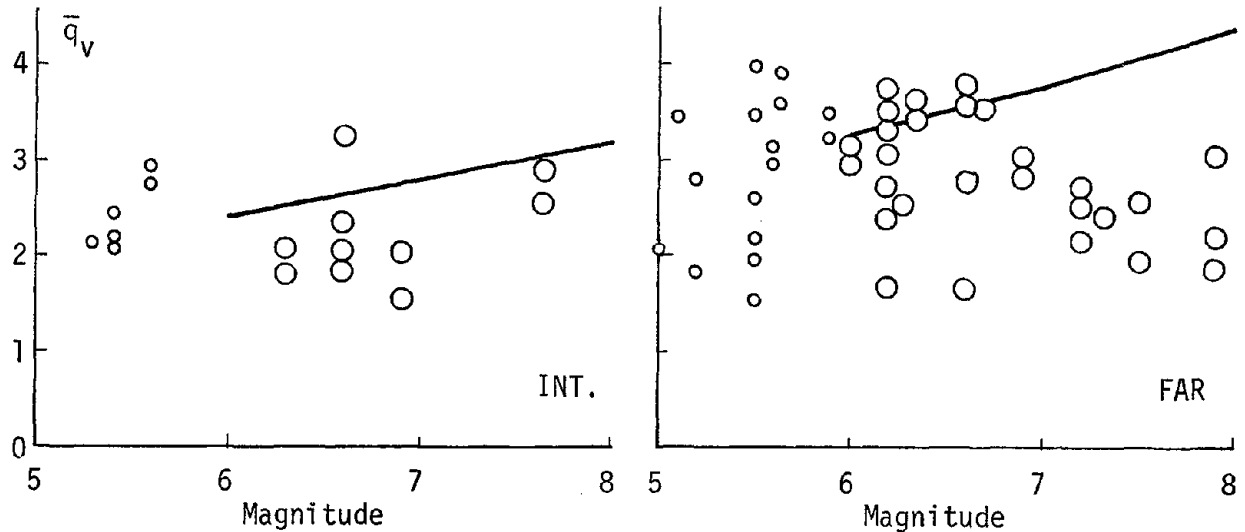


Fig.7 Response Amplification Factor  $\bar{q}_v$  in velocity

by 10 cm/sec, for intermediate and far fields. In Fig.8 relation between magnitudes of earthquakes observed and predominant periods for maximum response accelerations are shown, together with the periods indicated in Table 1, as the control points B and C where the maximum response accelerations are expected in the proposed standard response spectra.

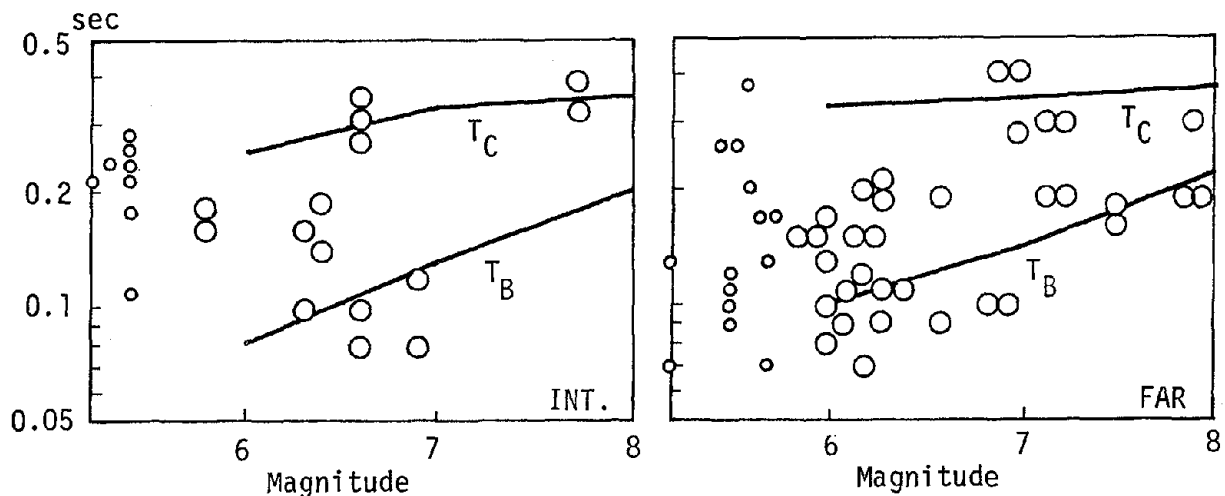


Fig.8 Periods for Max. Response Acceleration and Magnitudes

The period at which normalized acceleration response curve becomes equal to unity in its decreasing portion, i.e.,  $T_{CR}$  in Fig.2, is frequently referred to as critical period. Fig.9 compares critical periods in actual response spectra and the same periods implicitly represented in the proposed standard response spectra. Incidentally, the straight line DE in the proposed standard response spectra has been determined in consideration of Fig.9,

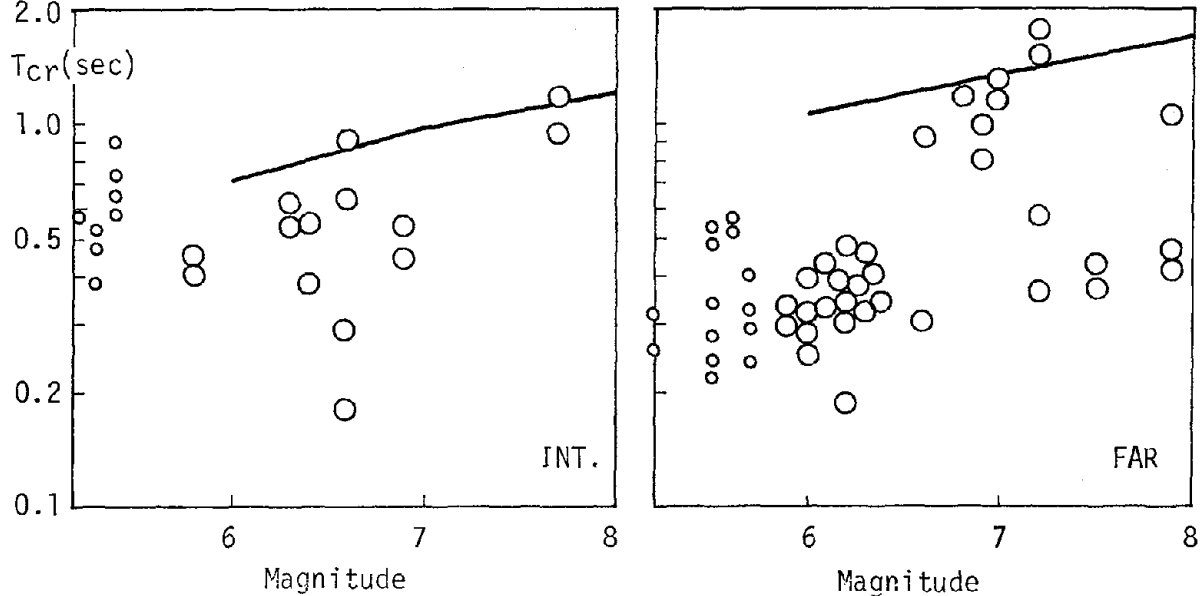


Fig.9 Critical Periods and Magnitudes

whereas characteristics of displacement response spectra are not taken into account in this proposal.

In these figures, plotted points are not completely enveloped by proposed parameters; however, the extent of envelopment seems to be reasonable.

4) *Extrapolation to Near-Field Parameters* : Actually, no information is available on spectral characteristics of rock motions in the near field such as defined in this proposal. The lack of these materials has required inevitably the most intuitive judgement.

In completing the proposed system of standard spectra, it has been intended primarily to determine near-field parameters by as reasonable and smooth extrapolation as possible of intermediate and far field parameters on logarithmically scaled diagrams. In Fig.10 is shown an example of such extrapolation with respect to the periods of control point C.

5) *Relation Between Response Amplification and Damping Factor* : As the background for the proposed eq.[1], the effect of damping factor to response spectral values has been analyzed, utilizing 135 horizontal components of accelerograms. Ratios of pseudo-velocity response values with specific damping factor to those of 5% have been obtained for each accelerogram and in each period. These values have been averaged in each

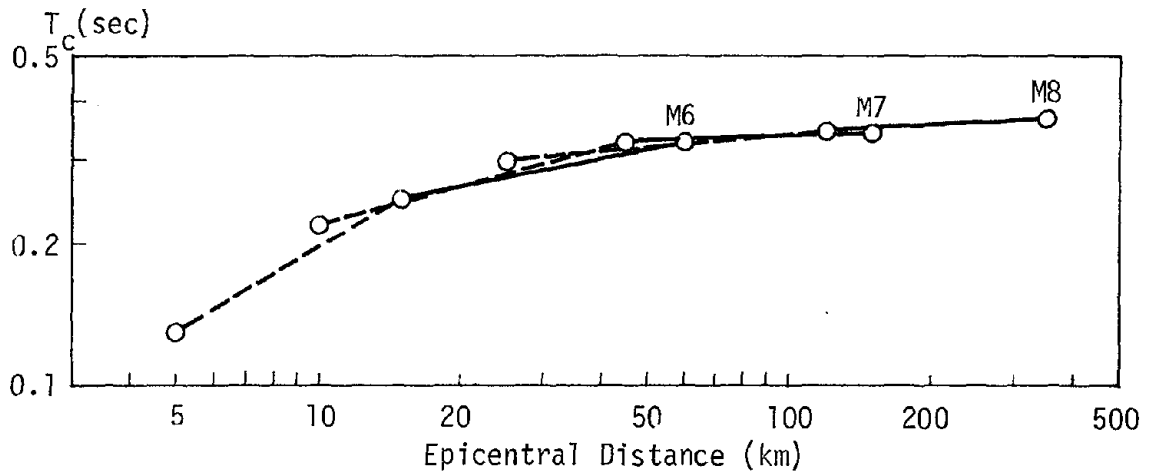


Fig.10 Relation Between Control Point C and Epicentral Distance

period the result of which have been shown in Fig.11. Solid lines in Fig.11 indicate the values of the proposed modification factor in eq.[1] as parameters of magnitudes.

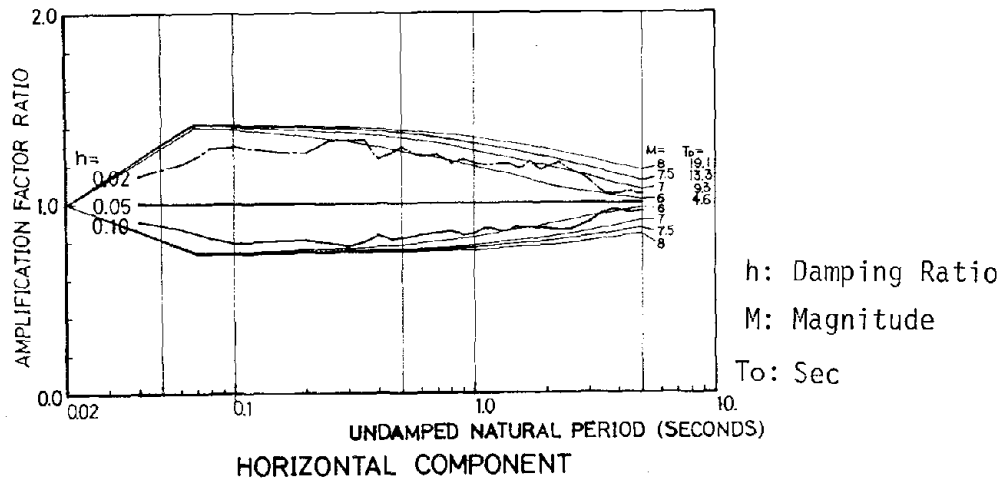


Fig.11 Effect of Damping, Normalized by Responses with 5% Damping Ratio

#### COMPARISON OF PROPOSED AND OBSERVED RESPONSE SPECTRA

According to the instructions suggested in VARIATIONS TO STANDARD RESPONSE SPECTRA, are shown in Fig.12 some standard response spectra due to some earthquakes with epicentral distances and magnitudes identical with those of real strong motion earthquakes, the response spectra of which have also been shown in the same figure for comparison.

#### CONCLUDING REMARKS

Standard response spectra of earthquake motions on the free rock surface are proposed for design purpose of stiff structures (with fundamental period less than 2.0 sec).



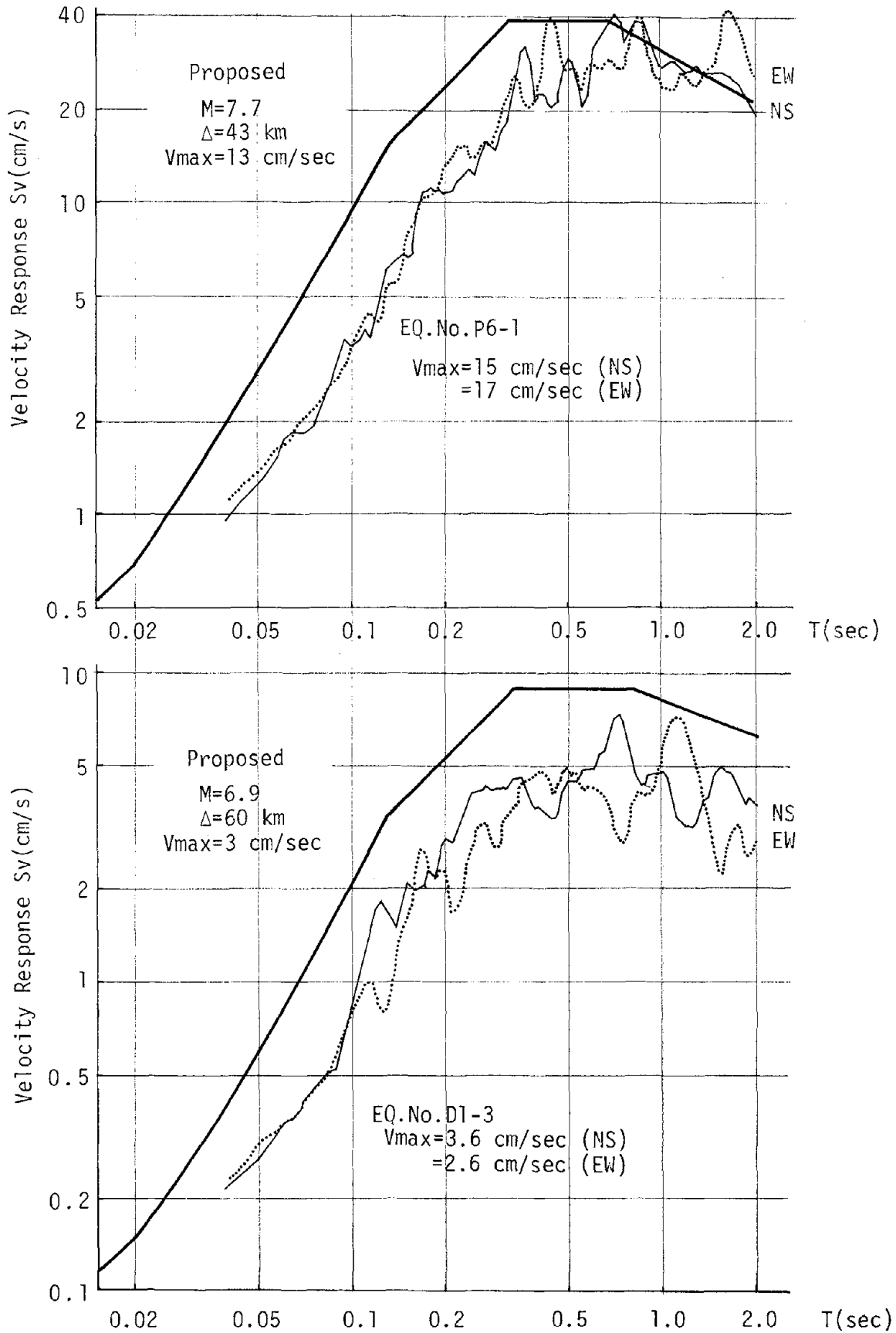


Fig.12 Comparison Between Standard Response Spectrum and Real Earthquake Response Spectra

The proposed system of response spectra will never be complete one from rigorous scientific viewpoint until sufficient instrumental records of strong ground motions, in particular due to real near-field-earthquakes, are available, however for practical design purpose, a number of concepts presented in this proposal may be regarded as new and instructive.

This year of 1978, a few intense earthquakes have occurred successively near Tokyo and north-east part of Japan. It is hoped that the proposal will be revised and up-to-dated based on the most recent records of rock motions due to these earthquakes.

#### ACKNOWLEDGEMENTS

The authors wish to thank Mr. R. Iwasaki, University of Tokyo, Mr. H. Ando, Kajima Institute of Construction Technology, and Mr. M. Todo, Toda Construction Co. Ltd. for their helpful contribution during the progress of this study.

#### BIBLIOGRAPHY

- (1) Regulatory Guide of Design Earthquake Ground Motions for Nuclear Power Facilities, Interim Report of the Aseismic Design Committee, Science and Technology Agency, Japanese Government, March 1975
- (2) Ohsaki, Y., Watabe, M. and Uchiki, T. : Relationship between Damping Factor and Shape of Response Spectrum, Reports of the Annual Meeting of Architectural Institute of Japan, September 1978
- (3) Hisada, T. and Ando, H. : On Relationship between Duration and Magnitude of Earthquake Motions, Kajima Institute of Construction Technology, June 1973
- (4) Kanai, K. and Suzuki, T. : Expectancy of the Maximum Velocity Amplitude of Earthquake Motions at Bedrock, Bull. Earthquake Research Institute, University of Tokyo, XLVI, 1968
- (5) Tanabashi, R. : Hypothesis on Damage Potential of Earthquake and Resistant Capacity of Building, Bull. Architectural Institute of Japan, No.599, May 1935
- (6) Omote, S. and Muto, A. : On Maximum Accelerations in Near-Field, Part 2, Reports of the Annual Meeting of Architectural Institute of Japan, October 1976
- (7) Iida, K. : Earthquake Magnitude, Earthquake Fault, and Source Dimensions, Journal of Earth Science, Nagoya University, Vo.13, October 1965
- (8) Okamoto, S. : Aseismic Engineering, Ohm-sha Co., Inc., September 1971

ON THE CORRELATION OF THE  
COMPONENTS OF STRONG GROUND MOTION

by

A. H. Hadjian<sup>I</sup>

## ABSTRACT

Nine earthquakes have been studied in an attempt to identify the correlation between any two components of ground motion. Since in general accelerographs are oriented arbitrarily (in a seismological sense), the recorded motions are only a set out of a multitude of other possibilities. Thus, any statistical study of ground motion should also consider these other possibilities. This approach, as used herein, shows that the three components of ground motion are correlated in a special way, rather than being "statistically independent." The correlation of the two horizontal components can be made either zero or a maximum for some orientations of the accelerograph. In fact, these orientations are separated by  $45^\circ$ . For some orientation of the accelerograph, the vertical component of motion is usually maximally correlated with one horizontal component and zero correlated with the other component. Under these circumstances, it seems that it would be contradicting nature to insist that the three components of ground motion are "statistically independent."

## INTRODUCTION

In the seismic analysis of important structures, such as nuclear power plant facilities, the simultaneous input of the three translational components of ground motion is being used more frequently. It is also common practice to generate artificial time-histories that are either "compatible" with some design (smooth) spectra or satisfy certain constraints required by regulatory bodies. Newmark et al (1), introduced the notion of "statistically independent" components of ground motion but did not provide either a definition of the term or the basis for the requirement. The intent of the requirement (private discussions with Newmark) was to assure that different time histories with characteristics similar to observed motions would be used in the different directions for structural calculations. Nonetheless, attempts have been made by others to mathematically define statistical independence (2). It seems that the presently accepted definition as proposed by Chen (2) is that the correlation coefficient of any two components of ground motion be equal to or less than 0.16 (3). Refer to Appendix A for details of this calculation. The fact that the three components of ground motion are generated at the same source, travel through the same geologic formations and are recorded at the same point on the ground surface all at the same time suggests that the three components of ground motion must have a special dependence rather than be "statistically independent." Another study (4) similar to the present one explored other characteristics of ground motion components.

## ACCELEROGRAPH ORIENTATION

Except for experimental purposes, accelerographs are usually oriented along principal axes of structures or parallel to some convenient reference

---

I Principal Engineer, Bechtel Power Corp., Los Angeles Power Division,  
Norwalk, California 90650

line. This being the case, it is very likely that any statistical study of recorded ground motions could miss some inherent characteristic of the motions, simply because most all accelerographs located in buildings in a given locality would tend to be parallel to the orientation of the streets. Recent research on strong ground motion recordings has taken special steps to ensure, for example, that the orientation of instruments is parallel to adjacent fault traces. This is not really necessary if one is willing to accept errors due to the digitization process. Given the three components of ground motion, the time history space vector can be generated and then decomposed into any desired orientation without losing the basic information recorded during the earthquake. Fig. 1a shows an example of the trace of the horizontal vector of a recorded motion. The figure is based on assuming a straight line motion during the digitization time interval (0.02 sec. in this example). The similarity to a seismoscope record is obvious. The same motion was rotated through two different angles (Figures 1b and 1c) by first calculating the horizontal vector and then decomposing it to two orthogonal components. Taking into account the change in the orientation angle, the three "seismoscopic" records are otherwise the same, as would be expected. Thus, three accelerographs located at the same point and oriented as shown in Fig. 1 would have provided the same information despite the fact that the "recorded" ground motion components would have been somewhat different as shown in Fig. 2. Even though the motions are different in detail, overall characteristics are similar and any one set would have been used as acceptable component motions recorded at Golden Gate Park in 1957. Thus, a given recording at a site is only one of a multitude of motions that would have been recorded if some other instrument orientation had been chosen.

#### CORRELATION COEFFICIENTS OF GROUND MOTIONS

Records of nine earthquakes, as digitized and processed by the Earthquake Engineering Research Laboratory, California Institute of Technology, have been used to explore the correlation characteristics of ground motion components. Since all of these records could have been recorded at any other orientation, the two horizontal components of each earthquake has been vectorially combined and then decomposed into  $10^{\circ}$  incremental orientations starting with the as recorded orientation at  $0^{\circ}$ . Obviously at  $90^{\circ}$  rotation, the correlation is the same as for the original records (except for a sign change) since the N-S motion becomes the new E-W motion and the E-W motion becomes the new N-S motion. The correlation coefficient at each instrument orientation is calculated and plotted as shown in Fig. 3a. For each orientation, the two horizontal "components" are compared to the vertical motion resulting in correlation coefficients that vary also with the angle of orientation as shown in Figs. 3b and 3c. The other eight earthquakes show very similar characteristics and thus curves similar to Fig. 3 will not be presented for the other events. However, summary tables will be provided. Parenthetically, it must be observed that the "new" time-history components that have been generated for selected orientations of the accelerograph do not have any attributes that one could have detected to make them any dissimilar from the as recorded components. The comment made regarding Fig. 2 is applicable also to all nine events studied: even though the motions are different in detail, overall characteristics are similar and any one set would have been used, without any questioning, as the appropriate motion at the recorded site. Returning to Fig. 3, the following is to be noted:

(a) Depending on the orientation of the instrument, the correlation coefficient can be made either zero or some maximum value for any two of

the three components. For the Golden Gate horizontal motion, this occurs at  $11.5^\circ$  and  $56.5^\circ$  from the as recorded orientation. The corresponding time-history records appear in Fig. 2.

(b) The maximum correlation and the zero correlation of the horizontal components are separated by  $45^\circ$ .

(c) The maximum and the zero correlations of each of the horizontal components with the vertical does not show a similar definite property. However, the separation for the records studied is given roughly by  $90^\circ \pm 15^\circ$ .

(d) The zero and maximum correlations of each of the two horizontal components with the vertical are separated by  $90^\circ$ . In fact, these two curves are mirror images separated by  $90^\circ$ .

(e) The as recorded correlation coefficients for the Golden Gate records are  $-0.124$ ,  $-0.249$  and  $0.10$  and thus do not satisfy the  $0.16$  criteria (2,3). More importantly, there is no other orientation that would satisfy this criteria. The "best" orientation occurs at  $77^\circ$  with the following correlation coefficients:  $0.233$ ,  $0.163$ , and  $0.233$ . In other words, it is an impossible task to meet the adopted criteria for a real record in any orientation of the accelerograph! In fact, this criteria will not be satisfied for any of the records studied unless, for the  $0^\circ$  to  $90^\circ$  orientation range, two of the three curves are always below  $0.16$ . The conclusion is obvious: although any two components can be maximally or zero correlated, for all three correlation coefficients to be less than  $0.16$  is an impossibility for those records that cross this "barrier" at some orientation of the accelerograph.

Table 1 is a summary of the earthquakes studied. Reading across this table one can see immediately the as recorded correlation of the two horizontal components, the maximum possible correlation and, of course, the zero correlation. Table 2 lists the "best" correlation coefficients for all three possible correlations with the associated rotation angles.

#### PEAK ACCELERATIONS AND RESPONSE SPECTRA

Peak acceleration and response spectra are two often used attributes of strong ground motion. The as recorded accelerations are often used to conduct statistical analysis. Based on the findings of the previous section, it would be useful to investigate the peak accelerations of the horizontal components at maximum and zero correlations. Table 3 lists these values and their times of occurrence. Also shown are the ratios of the peak accelerations of the two horizontal components. As has been known all along, the peak accelerations usually occur at different times. It is to be noted that the re-oriented components of motion do peak at about the same time frame as the recorded components with a few exceptions. This is not an unexpected result following the discussion of Fig. 2: the general character of the motion does not change. However, two changes deserve mention:

(a) Except for the 1940 El Centro record (A001), the peak horizontal acceleration of the re-oriented motions are larger than the as recorded peaks (these are designated with an asterisk in the table) with the zero correlated motion dominating this increase. The changes themselves are small (last column). The small sample used in this study does not justify further discussion of this observation.

(b) Except for the Kern County earthquake of 1952 recorded at the Hollywood Storage P.E. lot, the ratio of the peak accelerations of the two horizontal components are invariably larger for the case of zero correlation than for maximum correlation. The trend is definite even for this small sample. More on this later.

Fig. 4 shows a comparison of response spectra of the two horizontal components of the as recorded, maximum and zero correlations. As with the time-history records, these response spectra are very much similar in overall characteristics. (The response spectra of all nine events studied are very much similar to the one shown in Fig. 4). However, an important difference is noticeable between the spectra of the maximum correlated motions and zero correlated motions. Whereas in the former, the significant peaks and valleys between 2 and 10 Hz. almost always fall under each other, in the latter case there is a definite relative shift of the peaks. This is as it should be as a direct result of the correlations. The movement of the peaks for the zero correlation case are to the left and to the right of their positions held when the motions were maximally correlated. It should be noted that the differences between the spectra of the zero correlation and the as recorded are small since the re-orientation of the accelerograph is only for a small angle of  $11.5^\circ$ .

#### DISCUSSION

Although not part of this study, it is tempting to suggest one explanation for the observations made by a rather simplistic model. Referring to Fig. 5 and assuming horizontally propagating waves, the orientation of the accelerograph would either selectively record one or the other type of waves shown on each axis (Fig. 5a) or mix these waves such that each axis would contain some part of all the types of waves shown (Fig. 5b). Thus, maximum correlation would be expected from Fig. 5b orientation of the accelerograph and zero correlation from Fig. 5a orientation. This type of reasoning could also explain the peak acceleration ratio of the horizontal components. As shown in Table 3, this ratio is larger when the components are zero correlated than when they are maximally correlated. The distinct amplitudes of each type of wave could well be the cause of this trend. Similar arguments can also be advanced for any other non-horizontally propagating wave trains. In fact, these types of studies may help determine, from experimental evidence, the "mix" of strong ground motion. This type of endeavor, although lies in the domain of seismology, would benefit structural engineering. The interest of the latter in these potential findings lies in the need to correctly use ground motion data for the calculation of the response of embedded and underground structures and structures with large foundation plan dimensions.

Returning to the basic concern of the structural engineer in the statistical correlation of ground motion components, the important question should not be whether the input motions used are correlated or not, but rather if this correlation has any bearing on the response of structures. Referring to Fig. 4, one can argue that, given the response spectra of Figs. 4b and 4c, a symmetrical structure of fundamental frequency at about 4.5 cps would respond more strongly if the input motions were not "statistically independent" (Fig. 4b). This type of evaluation is beyond the scope of the present paper.

#### CONCLUSIONS

Although the number of earthquakes studied does not lend itself to a detailed evaluation of the problem, the results presented can be used to make several conclusions and recommendations:

(a) The definition of "statistical independence" of the components of ground motion as being equivalent to a correlation coefficient of 0.16 or less is, in general, an unrealizable attribute of recorded ground motions.

(b) If anything, the three components of ground motion are statistically dependent, in a special way. Based on the orientation of the accelerometer, the two horizontal motions, for example, can be made to be zero correlated or maximally correlated.

(c) Any statistical study should be done in the framework of the physics of the problem. In this particular context, the as recorded data used by Chen (2) was one of many other possible orientations and therefore did not reflect the true character of the problem. In fact, the reported statistical manipulations have created a contradiction in nature by neglecting the spectrum of all other equally likely correlations.

(d) For the structural engineer, the more important question is whether the correlation of ground motion components has any bearing on the response of the structure. "Statistical independence" could well result in less severe response.

(e) The potential of the approach used herein to study the "mix" of waves making up strong ground motion should be explored. The need to know this "mix" is becoming more urgent.

(f) This study needs to be expanded to a larger sample to generate more definite answers, provided, of course, that the concept of the correlation coefficient as used is appropriate to the study of the dependence or independence of the components of ground motion (See Appendix A).

#### ACKNOWLEDGEMENTS

The author would like to thank S. T. Lin for the generation of all data used in this paper.

#### APPENDIX A - CORRELATION COEFFICIENT

Chen (2) judges the statistical independence of any two of the components of ground motion  $x_1(t)$  and  $x_2(t)$  by the correlation coefficient given by

$$\rho_{12} = \frac{E [(x_1 - m_1)(x_2 - m_2)]}{\sigma_1 \sigma_2} \quad (1)$$

where  $E$  = the mathematical expectation;  $m_1$ ,  $m_2$ ,  $\sigma_1$ , and  $\sigma_2$  equal the mean values and standard deviations of  $x_1(t)$  and  $x_2(t)$  respectively, and the numerator of Eq. 1 is known as the covariance. The correlation coefficient is also referred to as the normalized covariance since it is obtained by dividing the covariance with the product of the standard deviations. The normalization produces correlation coefficients that lie between +1 and -1. There are two ways that one can interpret Eq. 1. Since we are dealing with earthquake motions, we will start with the discussion of a time dependent stochastic process.

Assume that  $N$ -S components of all recorded ground motions are sample functions of the ensemble of a particular stochastic process. Within the present context, similar ensembles exist for the E-W and vertical components as well. Considering only one of these three ensembles, the amplitudes of acceleration, at a given time  $t=t_1$  can then be treated as a random variable, and statistical estimates of the mean and ensemble moments can then be made. Similar estimates can also be made for any other time  $t=t_2$ . Given these two random variables  $x_1(t_1)$  and  $x_1(t_2)$  the ensemble covariance can be estimated by

$$\text{Cov}(x_1(t_1), x_1(t_2)) = \sigma^2(t_1, t_2) = \frac{1}{N} \sum_{j=1}^N (x_1^j(t_1) - m_1(t_1)) (x_1^j(t_2) - m_1(t_2)) \quad (2)$$

The correlation coefficient between the two random variables at times  $t_1$  and  $t_2$  is then given by

$$\rho_{11} = \frac{\text{Cov}(x_1(t_1), x_1(t_2))}{\sigma_1(t_1) \sigma_1(t_2)} \quad (3)$$

The above concept can be extended for use in cross correlation studies between two stochastic processes and, as mentioned above, the E-W or the vertical components of all recorded motions can be considered the second stochastic process. Equations similar to Eqs. 2 and 3 are defined by simply substituting  $x_2$  for  $x_1$ . The correlation coefficient then between one random variable at  $t=t_1$ , (of the first stochastic process) and a second random variable at  $t=t_2$  (of the second stochastic process) can be estimated by

$$\rho_{12} = \frac{\text{Cov}(x_1(t_1), x_2(t_2))}{\sigma_1(t_1) \sigma_2(t_2)} \quad (4)$$

Instead of using two time variables  $t=t_1$  and  $t=t_2$ , it is common practice to introduce a time variable  $\tau=t_2 - t_1$  and the above correlations defined in terms of  $t_1$  and  $\tau$ . If it can then be assumed that these correlations are functions of  $\tau$  only (i.e., they are independent of the reference time  $t=t_1$ ), then the stochastic processes  $x_1(t)$  and  $x_2(t)$  are said to be stationary. In other words, the properties are invariant under a shift of the time scale.

To evaluate any of the above equations requires a large number of sample functions. Given only one sample function in each ensemble, it is still possible to obtain averages with respect to time along the one available sample, thus substituting the ensemble averages by temporal averages. There is a subclass of stationary stochastic processes where the ensemble averages are equal to the corresponding temporal averages of a single sample function. These processes are known as ergodic processes and Eq. 1 can only be valid under this assumption, since  $x_1(t)$  and  $x_2(t)$  are any two of the components of motion of a given earthquake.

The second way of interpreting Eq. 1 has nothing to do with time dependency. It is very much like observing simultaneously two outcomes of an experiment. A commonly used example is the compressive strength of concrete (denoted by  $x_1$ ) and modulus of elasticity (denoted by  $x_2$ ) of many concrete test cylinders presumably prepared under similar conditions. Within our context,  $x_1$  and  $x_2$  are the simultaneous amplitudes of accelerations at any time of the two components of motion. The ordering of these paired amplitudes is, of course, immaterial as long as the two quantities are measured simultaneously and used as a pair. However, since the components of ground motion data are usually digitized at equal time intervals, the pair,  $x_1$  and  $x_2$ , are the simultaneously occurring amplitudes of acceleration at each time step, irrespective of how the pairs are ordered. Thus, with this interpretation, Eq. 1 gives the appropriate correlation coefficient except that  $x_1$  and  $x_2$  should not be shown as functions of time, otherwise the first interpretation must be adopted.



## REFERENCES

1. Newmark, N. M., Blume, J. A., and Kapur, K. K., "Seismic Design Spectra for Nuclear Power Plants," J. of the Power Division, ASCE, Vol. 99:P02, Nov. 1973, pp. 287-303.
2. Chen, G., "Definition of Statistically Independent Time Histories," J. of the Structural Div., ASCE, Vol. 101:ST2, Feb. 1975, pp. 449-451.
3. ASME Section 3, Rules for Construction of Nuclear Power Plant Components, Division 1 - Appendices, Appendix X.
4. Penzien, J. and Watabe, M., "Characteristics of 3-Dimensional Earthquake Ground Motions," Earthquake Engineering and Structural Dynamics, Vol. 3, pp. 365-373 (1975).

Table 1. Correlation coefficients of nine recorded earthquakes

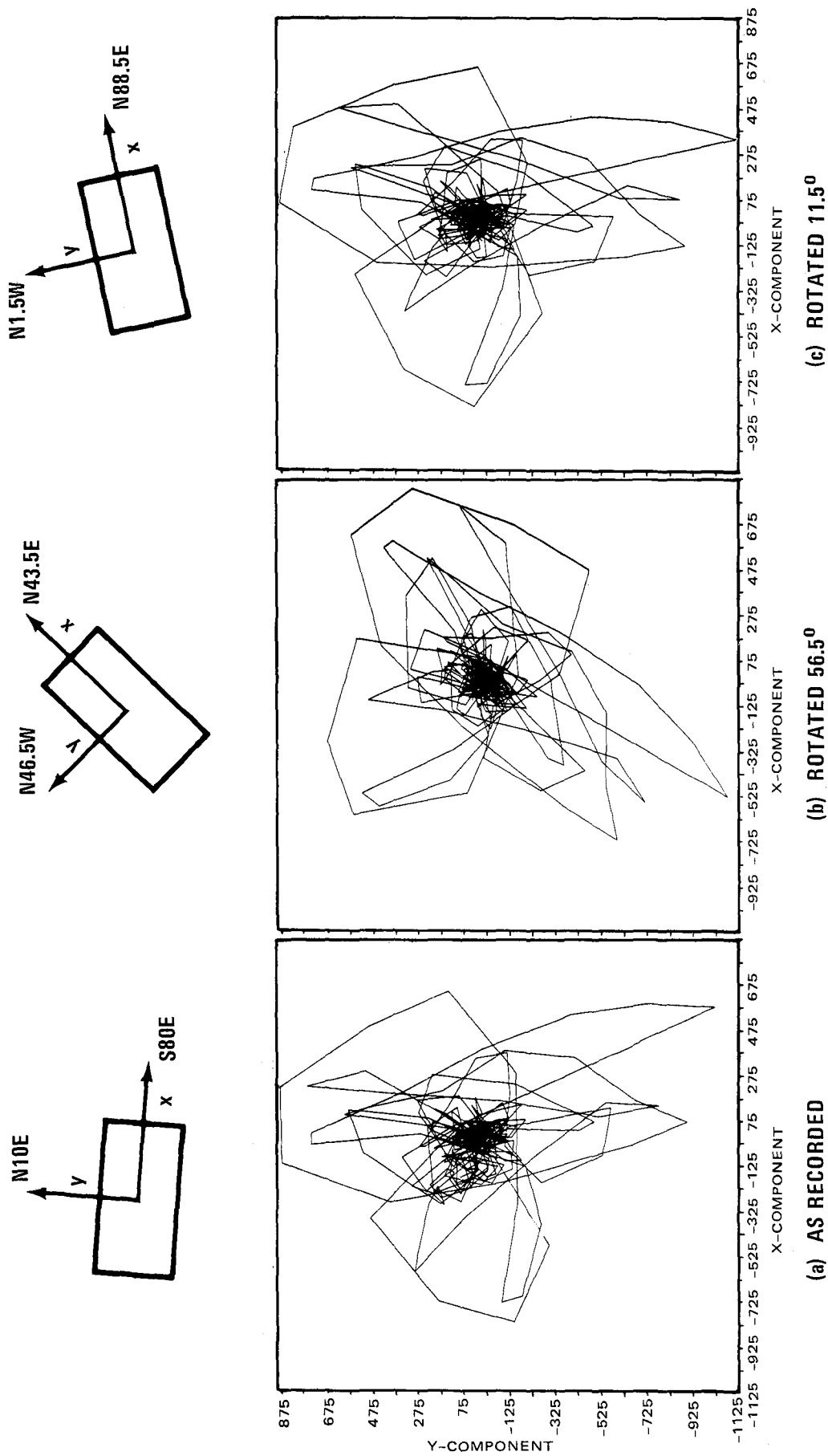
CIT DESIGNATION	EARTHQUAKE NAME & DATE	AS RECORDED CORRELATIONS			MAX. CORRELATION HORIZ. COMPONENTS		ZERO CORRELATION HORIZ. COMPONENTS		
		x	y	z	xy	yz	zx	$\alpha$	$\beta$
A001	El Centro 1940	S00E	S90W	Vert.	-.178	.059	-.066	22.1	67.1
								-.244	0.0
								.077	-.077
								-.046	.026
A004	Taft 1952	N21E	S69E	Vert.	.124	.293	.138	9.0	54.0
								.130	0.0
								.274	0.071
								.180	0.302
A007	Kern County 1952 Hollywood Storage P. E. Lot	N90E	S00W	Vert.	.087	.254	.005	89.3	44.3
								-.087	0.0
								-.002	0.186
								.254	0.174
A009	Ferndale-Eureka 1954	N44E	N46W	Vert.	.370	.254	.265	76.6	31.6
								-.407	0.0
								-.227	0.058
								.290	0.308
A014	S.F. 1957 Alexander Bldg.	N09W	N81E	Vert.	-.171	-.237	0.194	11.4	56.4
								-0.185	0.0
								-0.264	-0.27
								0.152	-0.088
A015	S.F. 1957 Golden Gate	N10E	S80E	Vert.	-.124	-.249	0.100	56.5	11.5
								0.305	0.0
								-0.227	-.257
								-0.188	.033
A019	Borrego 1968	S00W	S90W	Vert.	.063	-.120	-.065	52.7	7.7
								-.231	0.0
								-.007	-0.108
								-.127	-0.077
D057	San Fernando Hollywood Storage Basement	N90E	S90W	Vert.	-.105	-.232	-.019	56.1	11.1
								-.267	0.0
								-.094	-0.226
								-.179	-0.053
D058	San Fernando Hollywood Storage P.E. Lot	N90E	S00W	Vert.	-.191	-.106	-.155	65.0	20.0
								-.289	0.0
								-.195	-0.174
								-.013	0.114

Table 2. "Best" overall correlations

CIT DESIGNATION	CORRELATION	AS RECORDED °° ORIENTATION	"BEST" ORIENTATION	
			COEFFICIENT	ANGLE
A001	xy	-.178	-.08	58°
	yz	-.059	-.08	
	zx	-.066	.01	
A004	xy	.124	.118	22°
	yz	.293	.233	
	zx	.138	.233	
A007	xy	.087	-.01	46°
	yz	.254	.18	
	zx	.005	.18	
A009	xy	.370	.282	11°
	yz	.254	.200	
	zx	.265	.282	
A014	xy	-.171	.150	83°
	yz	-.237	-.215	
	zx	.194	-.215	
A015	xy	-.124	.233	17°
	yz	-.249	-.163	
	zx	.100	-.233	
A019	xy	.063	-.075	17°
	yz	-.120	-.090	
	zx	-.065	-.090	
D057	xy	.105	-.178	32°
	yz	-.232	-.178	
	zx	-.019	-.110	
D058	xy	.191	.115	9°
	yz	-.106	-.138	
	zx	.155	.138	

Table 3. Peak accelerations (cm/sec<sup>2</sup>) and time of occurrence (sec)

CIT DESIGNATION	COMPONENT	TIME	AS RECORDED		MAXIMUM CORRELATION				ZERO CORRELATION				PEAK HORIZ. AS RECORDED PEAK
			ACC.	RATIO	TIME	ACC.	RATIO	ANGLE	TIME	ACC.	RATIO	ANGLE	
A001	x	2.14	341.7*	1.63	2.14	294.2	1.25	22.1°	1.92	-181.2	1.86	67.1°	1.00
	y	11.46	210.1		11.46	236.3		2.14	-337.9				
	z	1.0	-206.3		-	-		-	-				
A004	x	9.12	152.7	1.15	9.10	159.2	1.03	9.0°	3.72	215.1*	1.52	54.0°	1.22
	y	3.72	175.9		3.72	154.4		4.22	141.8				
	z	9.78	102.9		-	-		-	-				
A007	x	13.00	41.2	1.41	13.32	-58.2*	1.42	89.3°	12.94	54.9	1.11	44.3°	1.00
	y	13.32	-58.1		13.00	-41.0		12.68	-49.3				
	z	18.08	-20.3		-	-		-	-				
A009	x	6.90	155.7	1.27	7.14	198.9	1.19	76.6°	7.18	199.4*	1.23	31.6°	1.01
	y	7.12	197.3		6.88	-167.4		7.10	162.7				
	z	8.02	-41.9		-	-		-	-				
A014	x	2.70	41.8	1.09	2.70	41.6	1.19	11.4°	2.20	35.4	1.32	56.4°	1.09
	y	2.06	-45.4		2.06	-49.6*		2.06	-46.6				
	z	0.16	-30.0		-	-		-	-				
A015	x	1.36	-81.8	1.26	1.78	84.5	1.23	56.5°	1.36	-83.3	1.34	11.5°	1.09
	y	1.46	-102.8		1.46	-104.3		1.46	-112.0*				
	z	1.20	37.2		-	-		-	-				
A019	x	8.56	-127.8	2.27	8.56	84.2	1.15	52.7°	8.56	-127.8*	2.19	7.7°	1.00
	y	15.02	-56.3		8.56	96.5		15.02	-58.3				
	z	7.42	-29.7		-	-		-	-				
D057	x	3.52	148.2	1.43	7.10	-118.4	1.33	56.1°	7.08	-146.4	1.50	11.1°	1.06
	y	4.70	103.8		3.54	-157.8*		4.70	97.7				
	z	5.28	-49.8		-	-		-	-				
D058	x	3.38	-207.0	1.24	2.76	191.0	1.10	65.0°	3.38	-208.6*	1.53	20.0°	1.01
	y	2.78	167.3		3.52	-173.9		2.84	-136.3				
	z	3.54	87.0		-	-		-	-				



(a) AS RECORDED

(b) ROTATED 56.5°

(c) ROTATED 11.5°

FIGURE 1. THREE ORIENTATIONS OF ACCELEROGRAPHS - SAN FRANCISCO EARTHQUAKE OF 1957, GOLDEN GATE PARK, HORIZONTAL VECTOR.

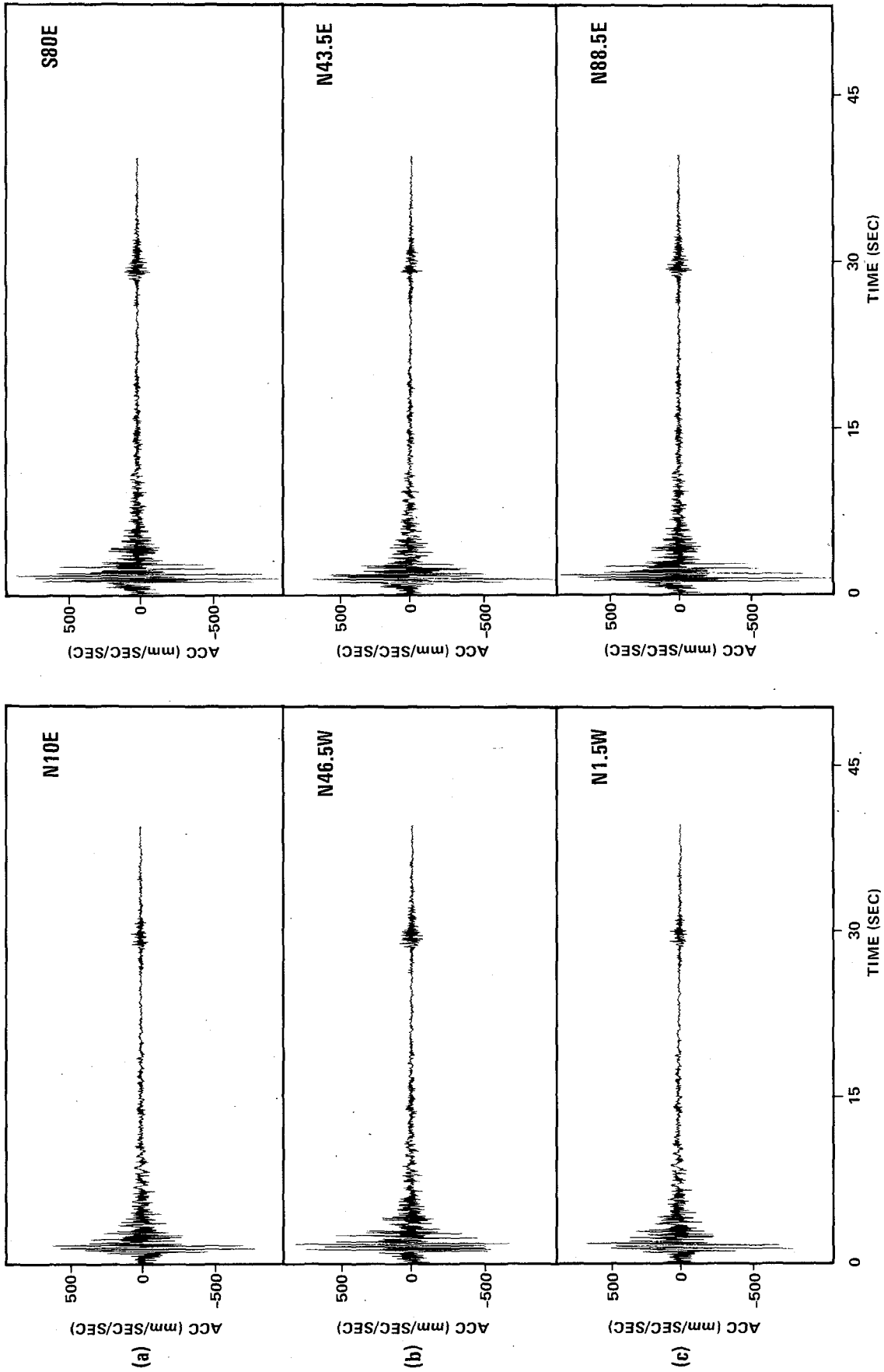


FIGURE 2. TWO HORIZONTAL COMPONENTS OF GROUND MOTION RECORDED AT GOLDEN GATE, SAN FRANCISCO EARTHQUAKE, 1957. ACCELEROGRAPH ORIENTATIONS CORRESPOND TO FIGURE 1

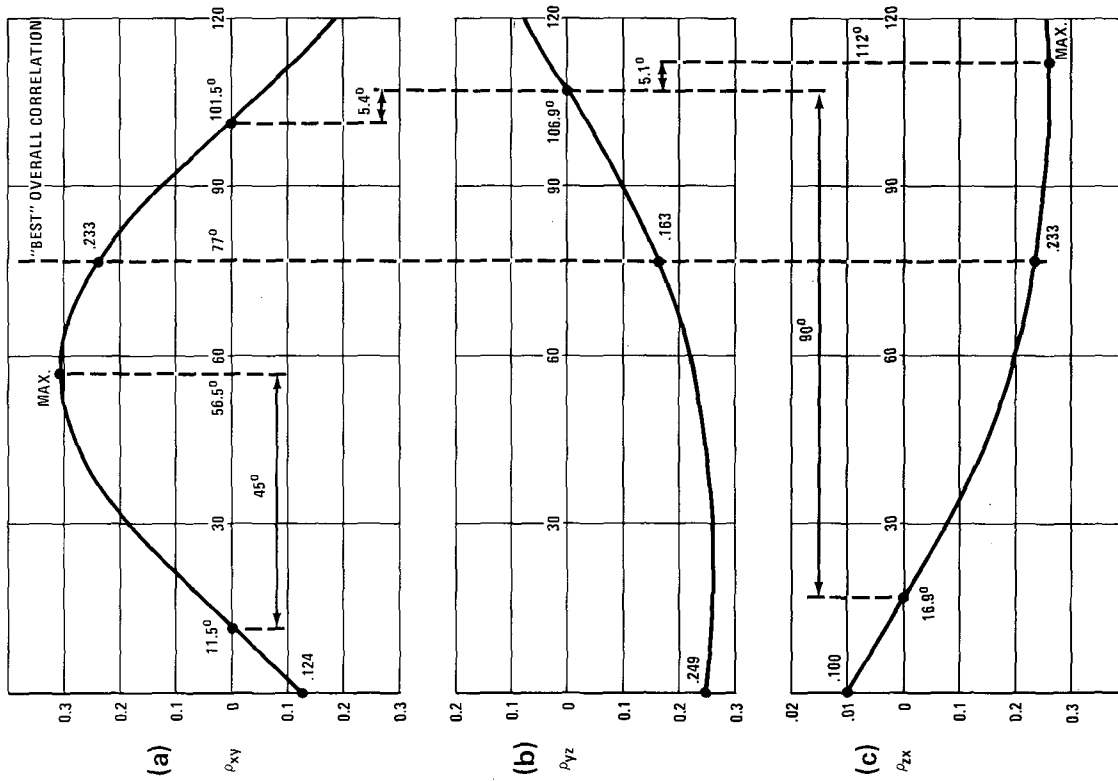


FIGURE 3. CORRELATION COEFFICIENTS FOR A RANGE OF ACCELEROGRAPH ORIENTATIONS - SAN FRANCISCO EARTHQUAKE OF 1957, GOLDEN GATE PARK

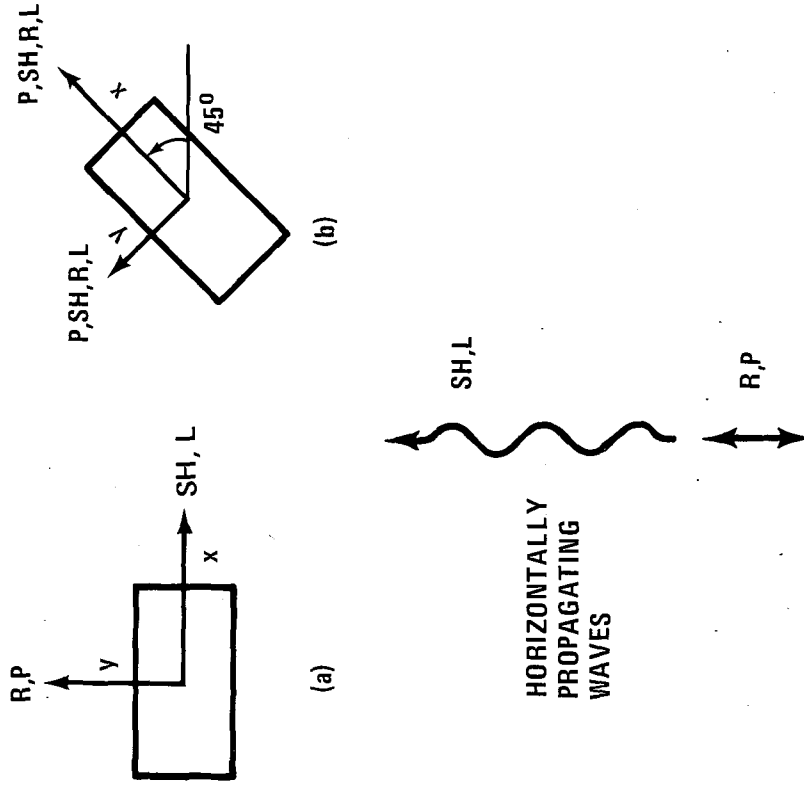


FIGURE 5. SIMPLIFIED MODEL TO EXPLAIN POSSIBLE CORRELATIONS

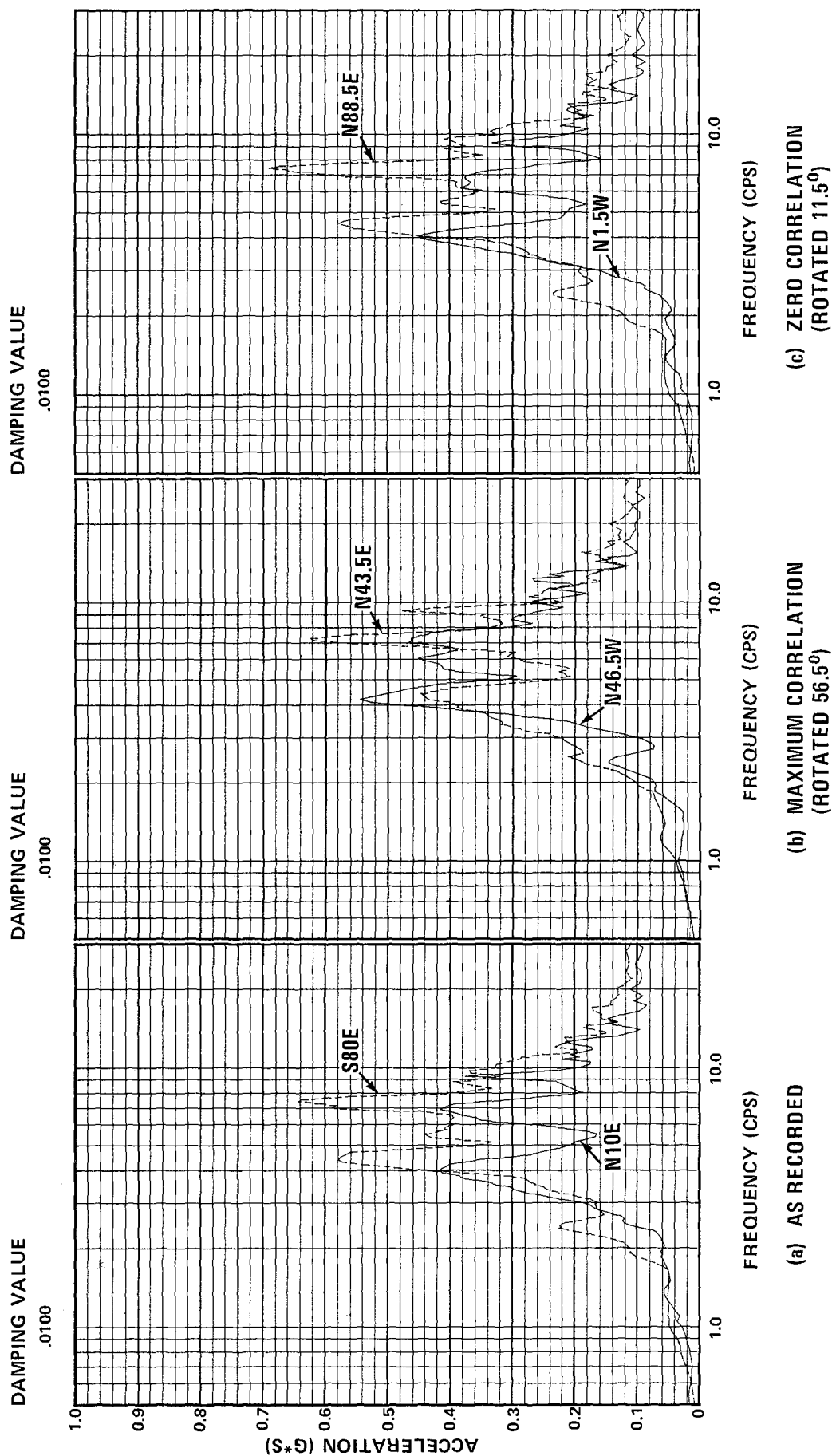


FIGURE 4. COMPARISON OF RESPONSE SPECTRA OF THE TWO HORIZONTAL COMPONENTS – SAN FRANCISCO EARTHQUAKE OF 1957, GOLDEN GATE PARK

SEISMIC ANALYSIS OF A HIGHWAY BRIDGE UTILIZING STRONG-MOTION  
ACCELERATION RECORDS

by

Toshio IWASAKI<sup>I</sup> and Kazuhiko KAWASHIMA<sup>II</sup>

## ABSTRACT

In analyzing seismic behavior of highway bridges constructed on soft soil deposits, it is important to take account of soil-structure interaction effects. In this paper, seismic response of a bridge pier-foundation is investigated based on earthquake acceleration records measured simultaneously on the pier crest and on the ground surface near that bridge. Four motions were used in the analysis, i.e., two were induced by two earthquakes with magnitudes of 7.5 and 6.6, respectively; and two by their aftershocks. In the former two earthquakes, the maximum accelerations were 186 and 438 gals on the ground surface, and 310 and 230 gals on the pier top, respectively. Analyses of frequency characteristics of the motions showed that the predominant frequencies of pier-foundation were always approximately identical with the fundamental natural frequency of the subsoil. Analyses of micro-tremors measured at the sites revealed that the natural frequency of the pier-foundation system is higher than the fundamental natural frequency of the subsoil. Analytical models were formulated to calculate the seismic response of the pier-foundation assuming the subsoil and pier-foundation to be a shear column model with an equivalent linear shear modulus and an elastically supported beam on the subsoil, respectively. Bedrock motions were computed from the measured ground surface motions and then applied to the bedrock of the analytical model. The seismic responses of pier-foundation were thus calculated and compared with the measured records giving a good agreement.

## INTRODUCTION

In the past, numerous highway bridges have suffered extensive damages due to strong motion earthquakes. Seismic damages to bridges consisting of simply supported girders or trusses rested on massive piers and abutments were commonly caused by foundation failures resulting from excessive ground deformations and/or loss of stability and bearing capacity of the foundation soils. As a direct result, the substructures often tilted, settled, or sometimes overturned, and these large displacements of the supports caused relative shifting of the superstructures, induced failures of the bearing supports, and even caused dislodging of the spans from their supports.

It has been well recognized from these evidences that the influences of surrounding subsurface ground are very important for the seismic responses of foundations deeply embedded in the ground, and considerable interests were concentrated on the soil-structure interaction effects of such structures through model experiments and theoretical analyses. However very limited researches have been undertaken in studying seismic responses of actual foundations during high intensity seismic excitations since only few data

---

I Chief, Ground Vibration Section, Earthquake Disaster Prevention Division, Public Works Research Institute, Ministry of Construction, Chiba, Japan  
II Research Engineer, Ground Vibration Section, Earthquake Disaster Prevention Division, Public Works Research Institute, Ministry of Construction, Chiba, Japan

have been available for such purposes. This investigation presents the results of observation of seismic motions on a bridge pier and on the ground surface nearby with high accelerations which were measured during four earthquakes, and also correlates the pier motions measured with the pier motions analyzed using the ground surface acceleration records.

#### STRUCTURAL AND SITE CONDITIONS OF THE BRIDGE

The Itajima Bridge studied is a five-spanned simply-supported plate girder bridge as shown in Fig. 1. The strong-motion-acceleration observations have been conducted since 1966 at a crest of one of the piers and on the free-field ground surface located about 200m apart from the pier. Two SMAC-B2 type accelerographs are set at the both sites to measure accelerations in the longitudinal, transverse and vertical directions of the bridge axis.

Ground surveys were performed at the both sites and informations on soil profile, N-value of standard penetration test, and shear wave velocities were obtained. Figure 2 shows the soil profiles and N-values at the sites. It is recognized from the results that the ground conditions are essentially the same between the two sites, i.e., the soil profiles consist of upper soft loam to fine sand formations with the averaged N-value of approximately 7 and lower stiff gravel formations with the averaged N-values of 30 or more. It is also recognized that the ground condition seems to be continuous between the two sites. The shear wave velocities of the upper and lower formations were estimated to be approximately 130 and 480 m/sec., respectively. The gravel formations were assumed to be the base-rock at the sites in calculating seismic responses of the ground and foundation in the following paragraph.

#### STRONG-MOTION-ACCELERATION RECORDS

Four simultaneous strong-motion-acceleration records have been obtained at the Itajima Bridge as summarized in Table 1 which were induced by four earthquakes, i.e., main and after shocks of both the Hyuganada Earthquake of April 1, 1968 and the Bungosuido Earthquake of August 6, 1968, which are designated herein as A, B, C and D Earthquakes, respectively. Figures 3, 4 and 5 show the acceleration records thus obtained in the longitudinal and transverse directions of the bridge axis. In the D-Earthquake, accelerations on the pier could not be unfortunately recorded and only the maximum value of acceleration was obtained. It should be noted here that although the seismic response accelerations achieved at the pier crest were very high, superstructures and foundations of the Itajima Bridge suffered no structural damages through any of these four earthquakes.

Figure 6 represents amplifications of maximum accelerations between the ground surface and the crest of pier. It can be recognized from this result that the amplifications of maximum accelerations are very much different between the Hyuganada Earthquake (A and B -Earthquakes) and the Bungosuido Earthquake (C and D -Earthquakes), i.e., the amplification factors are in the range of 1.1 - 1.7 in the case of A and B -Earthquakes, whereas they are in the range of 0.4 - 0.6 in the C and D -Earthquakes. The frequency characteristics of the motions were then investigated. Predominant frequencies of the records are summarized in Table 2, based on the power spectra presented in Fig. 7. It is understood from the result that in the A-Earthquake the predominant frequencies of the ground is approximately equal to that of the pier motion, namely, approximately 1.5 Hz in the longitudinal motion and 1.3 Hz in the transverse motion. Also the wave forms of all the four acceleration records during the A-Earthquake are very simple with one predominant



frequency. It is also understood from the Table 2 that in the B-Earthquake the predominant frequencies of both the ground and pier motions are approximately 1.6 Hz in the transverse direction. In the longitudinal direction, however, the pier motion has several predominant frequencies. The most predominant one is approximately 1.8 Hz which is again very close to the predominant frequency of the ground motion of 1.9 Hz. As is the case of A-Earthquake, the acceleration records on the ground in the both directions and the acceleration record on the pier top in the transverse direction are very simple with a single predominant frequency. On the other hand, the records during the C-Earthquake are somewhat different from those for the A and B-Earthquakes described as above. The most predominant frequencies of the ground motions are approximately 3.7 Hz in both the longitudinal and transverse directions which are different from those of pier motions, i.e., approximately 1.4 Hz in both directions. It should be noted here, however, that the ground motions have a predominant frequency close to the 1.4 Hz although they are not the most predominant.

It can be recognized from these results that the acceleration records of pier always contain the motions in the range of 1.3 - 1.7 Hz as the most predominant ones in both the longitudinal and transverse directions. The frequencies in the range of 1.3 - 1.7 Hz, however, can not be considered to be the natural frequency of the substructure, since microtremor analyses conducted during both daytime and midnight revealed that the natural frequencies of the foundation are approximately 3.8 Hz and 3.2 Hz in the longitudinal and transverse directions, respectively (refer to Table 3). On the other hand, the fundamental natural frequency of the subsurface ground on the gravel formation would be estimated approximately as

$$f_{s1} = \frac{V_S}{4H} \approx \frac{130}{4 \times 18} = 1.8 \text{ (Hz)} \quad (1)$$

where

$f_{s1}$  : fundamental natural frequency of the subsoil during shear vibration (Hz)

$V_S$  : average shear wave velocity of the subsoil (m/sec.)

$H$  : thickness of the subsurface ground (m)

which is considered to correspond to the lowest frequency of the subsurface ground during low-amplitude vibrations. Assuming that the shear wave velocity decreases to 70 percent of original during the high amplitude vibrations, the lowest frequency of the subsurface ground would be estimated by Eq. (1) as approximately 1.3 Hz. It would be deduced from these considerations that the most predominant frequency that is always contained in the motions of the pier is significantly influenced by the lowest natural frequency of the subsurface ground so that the pier vibrates almost in accordance with the motion of the subsurface ground nearby.

#### ANALYTICAL PROCEDURE OF THE FOUNDATION

An discrete analytical model as shown in Fig. 8 was formulated to calculate earthquake responses of the embedded foundation. The equation of motions of the system can be written as

$$\begin{aligned} & (\underline{M}_p + \underline{M}_e) \ddot{\underline{u}}_p + \underline{C}_p \dot{\underline{u}}_p + \underline{K}_p \underline{u}_p \\ & + \underline{C}_e (\dot{\underline{u}}_p - \dot{\underline{u}}_g) + \underline{K}_e (\underline{u}_p - \underline{u}_g) = \underline{0} \end{aligned} \quad (2)$$

where,

- $\underline{M}_p$  : mass matrix of the foundation  
 $\underline{M}_e$  : mass matrix of surrounding soils  
 $\underline{C}_p$  : damping matrix of the foundation  
 $\underline{K}_p$  : stiffness matrix of the foundation  
 $\underline{C}_e$  : damping matrix expressing radiational dampings  
 $\underline{K}_e$  : stiffness matrix expressing springs between foundation and surrounding soils  
 $\underline{u}_p, \dot{\underline{u}}_p, \ddot{\underline{u}}_p$  : absolute displacement, velocity and acceleration vectors of foundation  
 $\underline{u}_g, \dot{\underline{u}}_g$  : absolute displacement and velocity vectors of subsurface ground

in which the subsurface ground motions of  $\underline{u}_g$  and  $\dot{\underline{u}}_g$  are assumed to be specified. Denoting as

$$\begin{aligned}
 \underline{M} &= \underline{M}_p + \underline{M}_e \\
 \underline{C} &= \underline{C}_p + \underline{C}_e \\
 \underline{K} &= \underline{K}_p + \underline{K}_e
 \end{aligned} \tag{3}$$

Eq. (2) can be written as

$$\underline{M} \ddot{\underline{u}}_p + \underline{C} \dot{\underline{u}}_p + \underline{K} \underline{u}_p = \underline{C}_e \dot{\underline{u}}_g + \underline{K}_e \underline{u}_g \tag{4}$$

The vector  $\underline{u}_p$  can be conveniently decomposed into a quasi-static displacement vector  $\underline{u}_{ps}$  and a dynamic displacement vector  $\underline{u}_{pd}$ , i.e.,

$$\underline{u}_p = \underline{u}_{pd} + \underline{u}_{ps} \tag{5}$$

By definition of quasi-static displacement in the form as

$$\underline{K} \underline{u}_{ps} + \underline{K}_e \underline{u}_g = \underline{0} \tag{6}$$

$\underline{u}_{ps}$  can be written as

$$\underline{u}_{ps} = -\underline{K}^{-1} \underline{K}_e \underline{u}_g \equiv -\underline{K}_s \underline{u}_g \tag{7}$$

Substitutions of Eqs. (5) and (6) into Eq. (4) gives

$$\underline{M} \ddot{\underline{u}}_{pd} + \underline{C} \dot{\underline{u}}_{pd} + \underline{K} \underline{u}_{pd} = \underline{M} \underline{K}_s \ddot{\underline{u}}_g + (\underline{C}_e + \underline{C} \underline{K}_s) \dot{\underline{u}}_g \tag{8}$$

Usually the damping term on the right hand side of Eq. (8) is less significant comparing with the inertia terms so that it can be dropped from the equation without introducing significant errors. Then Eq. (8) can be written as

$$\underline{M} \ddot{\underline{u}}_{pd} + \underline{C} \dot{\underline{u}}_{pd} + \underline{K} \underline{u}_{pd} = \underline{M} \underline{K}_s \ddot{\underline{u}}_g \tag{9}$$

Eq. (9) can be solved by mode-superposition procedures provided that the damping matrix on the left hand side of the equation is assumed to be triangularized in the same manner as the mass and stiffness matrixes in the form of damping ratio of critical, i.e.,

$$\begin{aligned}
 \underline{\Phi}^T \underline{M} \underline{\Phi} &= \underline{I} \\
 \underline{\Phi}^T \underline{K} \underline{\Phi} &= \underline{\Omega}^2 \\
 \underline{\Phi}^T \underline{C} \underline{\Phi} &= \underline{A}^2
 \end{aligned} \tag{10}$$

where

$$\begin{aligned}
 \underline{\Phi} &: \text{modal matrix} \\
 \underline{I} &: \text{identity matrix} \\
 \underline{\Omega}^2 &= \text{diag } (\omega_i^2) \\
 \underline{A}^2 &= \text{diag } (2 h_i \omega_i) \\
 \omega_i &: \text{i-th undamped natural frequency} \\
 h_i &: \text{i-th damping ratio of critical}
 \end{aligned}$$

Then denoting  $\underline{u}_{pd}$ ,  $\dot{\underline{u}}_{pd}$  and  $\ddot{\underline{u}}_{pd}$  by the normal coordinates as

$$\underline{u}_{pd} = \underline{\Phi} \underline{x}, \quad \dot{\underline{u}}_{pd} = \underline{\Phi} \dot{\underline{x}}, \quad \ddot{\underline{u}}_{pd} = \underline{\Phi} \ddot{\underline{x}} \tag{11}$$

Eq. (9) can be written in the following form.

$$\ddot{\underline{x}} + \underline{A} \dot{\underline{x}} + \underline{\Omega}^2 \underline{x} = \underline{R} \tag{12}$$

where

$$\underline{R} = -\underline{\Phi}^T \underline{M} \ddot{\underline{u}}_{pd} \tag{13}$$

Equation (12) is a uncoupled equation of motion and the i-th normal coordinate can be solved by the Duhamel Integration as

$$x_i = \frac{1}{\omega_i \sqrt{1-h_i^2}} \int_0^t R_i(\tau) e^{-h_i \omega_i (t-\tau)} \sin(\sqrt{1-h_i^2} \omega_i (t-\tau)) d\tau \tag{14}$$

#### CALCULATION OF PIER MOTIONS

The pier motions were computed by using the analytical procedure described in the preceeding paragraph based on the measured ground motions for the A, B and C-Earthquakes and they were compared with the measured motions. The correlations were conducted only for the motions in the longitudinal direction since conditions of the shoes in this direction was considered to be well defined as compared with the complex conditions in the transverse direction, i.e., in the longitudinal direction one of the two girders supported on the pier was rigidly connected to the pier and another girder was supported by the movable shoe.

The base-rock motions was computed from the measured ground surface motions by the deconvolution procedure taking account of the strain dependence of the shear moduli and hysteretic damping ratios of the subsoils. The subsoils and foundation were idealized by an one-dimensional shear column model with equivalent linear soil properties and one-dimensional elastic beam supported elastically by the surrounding subsoils, respectively. The weight of a girder rigidly supported by the pier was idealized as an additional mass lumped at the crest of pier. In the analyses the effects of another girder which is supported by movable shoe were disregarded since it was considered general that the frictional forces acting at the movable shoe being rela-

tively less significant. The lowest natural frequencies of the pier and surrounding subsoils thus estimated are shown in Table 4.

The response accelerations of pier were then calculated based on Eq. (2) by applying the base-rock motions at the bottom of the shear column model of subsoils. The comparative plots of both the theoretical and measured accelerations at the crest of pier are shown in Fig. 9 for the A, B and C-Earthquakes. The damping ratios assumed in the analyses are shown in Table 4. It is recognized from the results that fairly good agreements are obtained for the motions in the A and B-Earthquakes. On the other hand, a poor correlation was achieved for the motion in the C-Earthquake and further precise investigations are needed to clarify the frequency characteristics of the foundation.

#### CONCLUSIONS

Based on the results presented, the following conclusions may be deduced:

- (1) Seismic responses of the deeply embedded foundation are significantly influenced by the effects of surrounding subsurface soils. Provided that the lowest natural frequency of foundation be smaller than the lowest natural frequency of the surrounding subsoils, the motions of foundation are significantly prescribed by the motions of the surrounding subsoils.
- (2) Seismic response accelerations of the foundation can be calculated with fairly good accuracy by the analytical procedure presented herein from the free-field ground accelerations measured near the foundation for earthquakes which induce ground accelerations at the bridge site with the most predominant frequencies lower than the fundamental natural frequency of the foundation.

#### REFERENCES:

- 1) Iwasaki, T.: Earthquake-Resistant Design of Bridges in Japan, Bulletin of Public Works Research Institute, Volume 29, Public Works Research Institute, Ministry of Construction, May 1973.
- 2) Kuribayashi, E. and Iwasaki, T.: Dynamic Properties of Highway Bridges, 5th World Conference on Earthquake Engineering, Roma, December 1972.
- 3) Iwasaki, T., Kawashima, K. and Takagi, Y.: Influences of The Surrounding Subsoils on Seismic Responses of Highway Bridge Foundation, Technical Memorandum No. 1372, Public Works Research Institute, Ministry of Construction, May 1978 (in Japanese).

Table 1 STRONG MOTION ACCELERATION RECORDS AT ITAJIMA BRIDGE

Earthquake No.	Earthquake	Date	Richter Magnitude	Epicentral Distance (km)	Maximum Accelerations (Gal)			
					Pier Motion		Ground Surface Motion	
					Longitudinal*	Transverse*	Longitudinal*	Transverse*
A	The Hyuganada Earthquake	April 1, 1978	7.5	100	219	310	170	186
B	The Hyuganada Earthquake (Aftershock)	April 1, 1978	6.3	100	39	66	35	42
C	The Bungosuido Earthquake	August 6, 1978	6.6	11	230	198	438	365
D	The Bungosuido Earthquake (Aftershock)	August 6, 1978	5.3	11	100	63	220	165

(Note) Longitudinal and transverse directions to the bridge axis.

Table 2 PREDOMINANT FREQUENCIES OF STRONG MOTION ACCELERATION RECORDS MEASURED ON PIER CREST AND GROUND NEARBY AT THE ITAJIMA BRIDGE (HZ)

Earthquake No.	Longitudinal Direction		Transverse Direction	
	On Ground	On Pier Crest	On Ground	On Pier Crest
A	1.5	1.5	1.3	1.3
B	1.9	1.8, 2.0, 2.3, 3.7	1.6	1.6
C	3.7	1.4	3.7, 4.4	1.4
D	4.2	-	4.4	-

Table 3 PREDOMINANT FREQUENCIES ON THE PIER CREST AND GROUND SURFACE NEARBY ESTIMATED FROM MICROTREMOR ANALYSES

Location Direction	Ground Surface where Ground Motions were Measured	Ground Surface around the Pier	Top of Pier
Longitudinal	2.3	-	3.8
Transverse	3.0	2.0	3.2
Vertical	4.5	4.0	6.0

Table 4 LOWEST NATURAL FREQUENCIES AND DAMPING RATIOS ASSUMED

Earthquake No.	Lowest Natural Frequency (Hz)		Hysteretic Damping Ratio of Subsoils (%)	Radiation Damping Ratio (%)
	Ground	Pier		
A	1.6	2.75	10	20
B	1.90	3.06	5	20
C	1.59	2.66	8 - 12	20

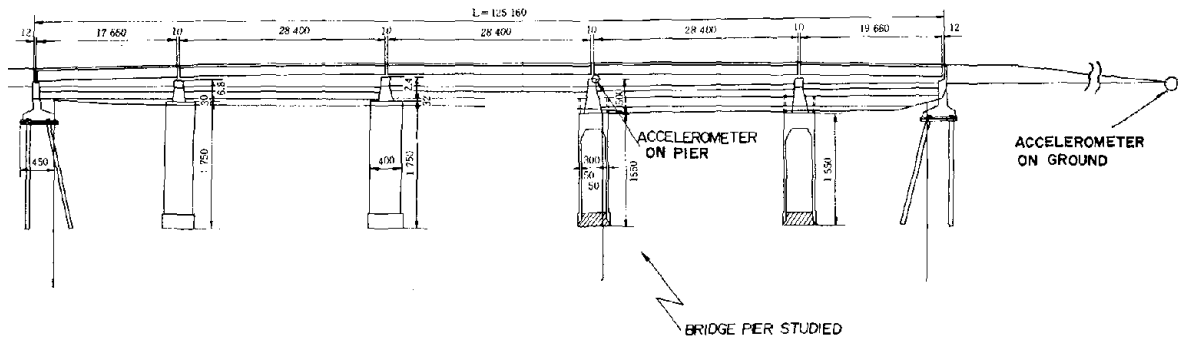


Fig. 1 GENERAL VIEW OF THE ITAJIMA BRIDGE

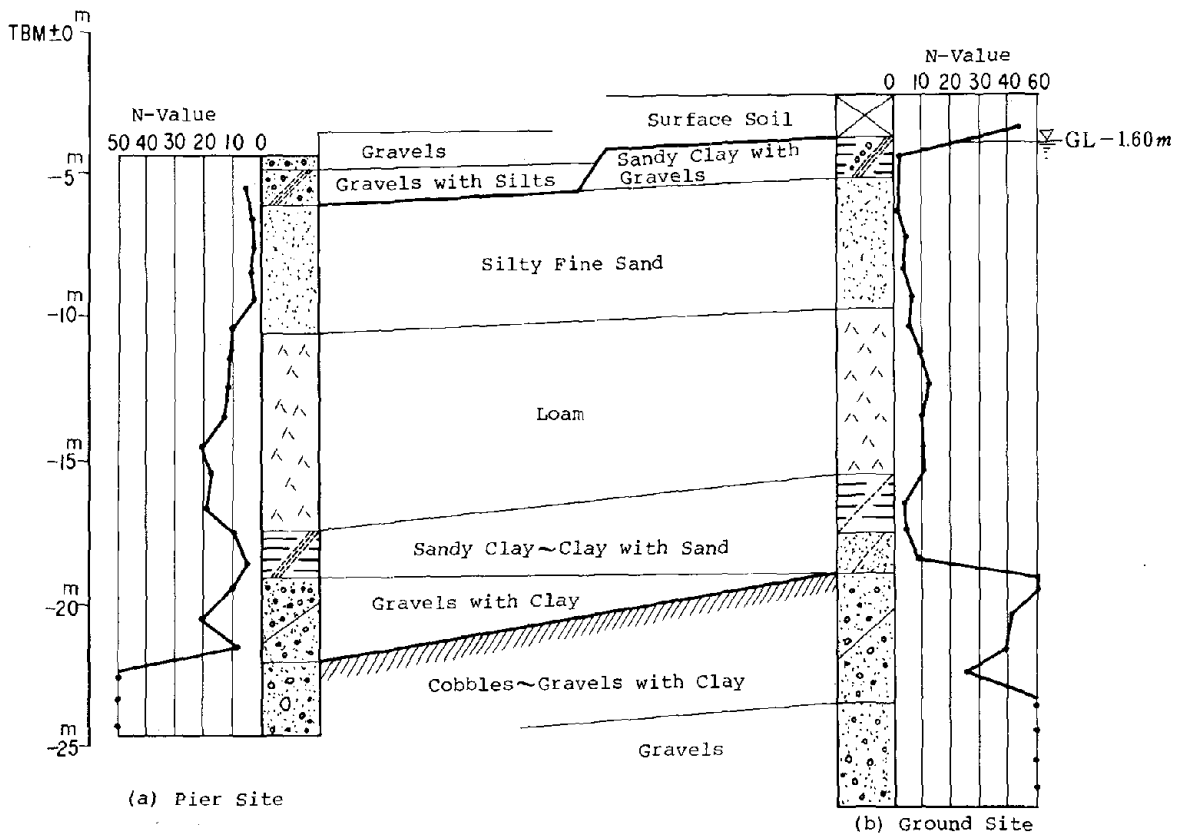


Fig. 2 SOIL PROFILE AT THE PIER SITE AND THE GROUND SITE

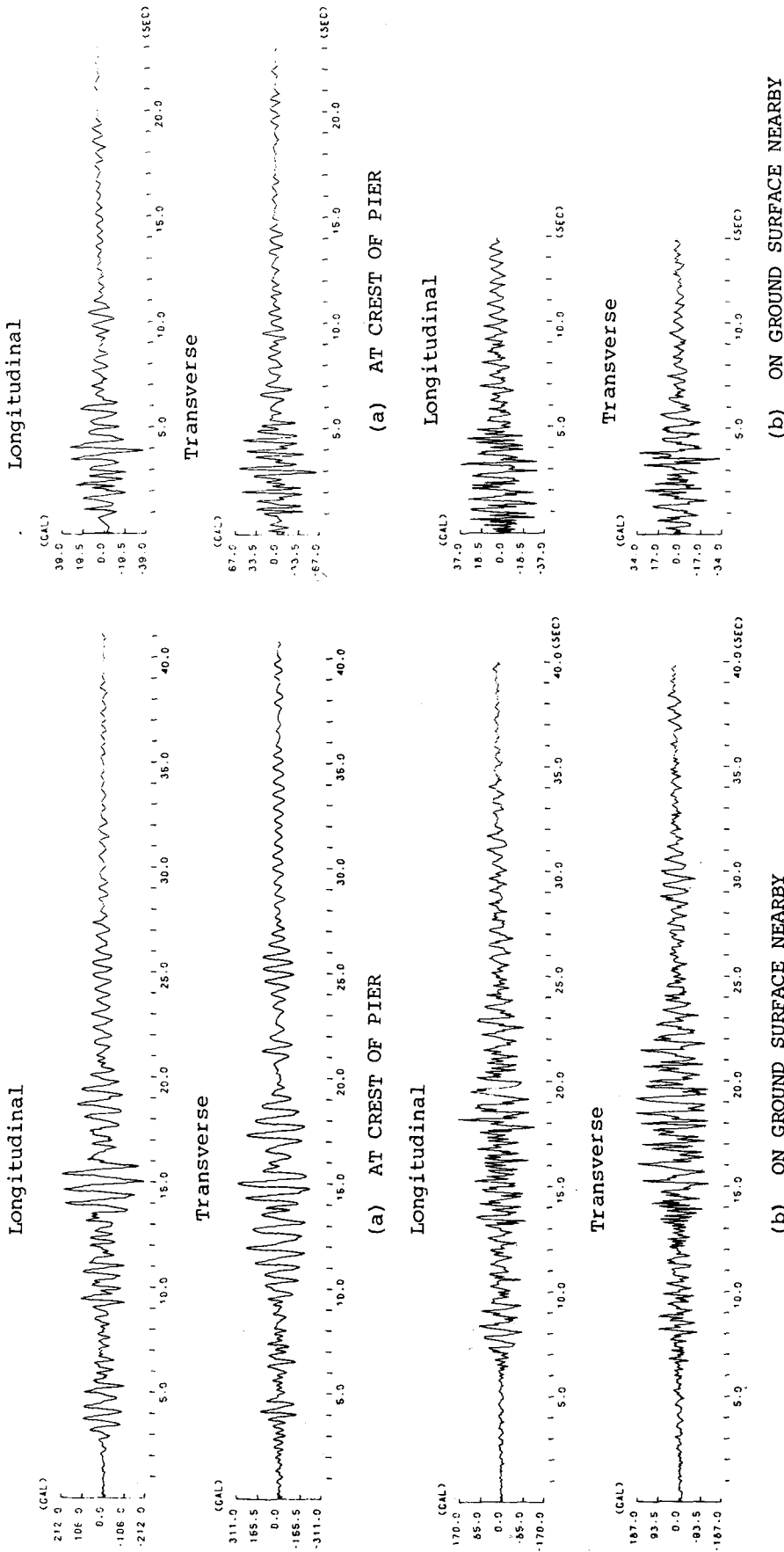


Fig. 3 ACCELERATION RECORDS AT THE ITAJIMA BRIDGE DURING THE HYUGANADA EARTHQUAKE OF APRIL 1, 1968 (A-EARTHQUAKE)

Fig. 4 ACCELERATION RECORDS AT THE ITAJIMA BRIDGE DURING AN AFTERSHOCK OF THE HYUGANADA EARTHQUAKE OF APRIL 1, 1968 (B-EARTHQUAKE)

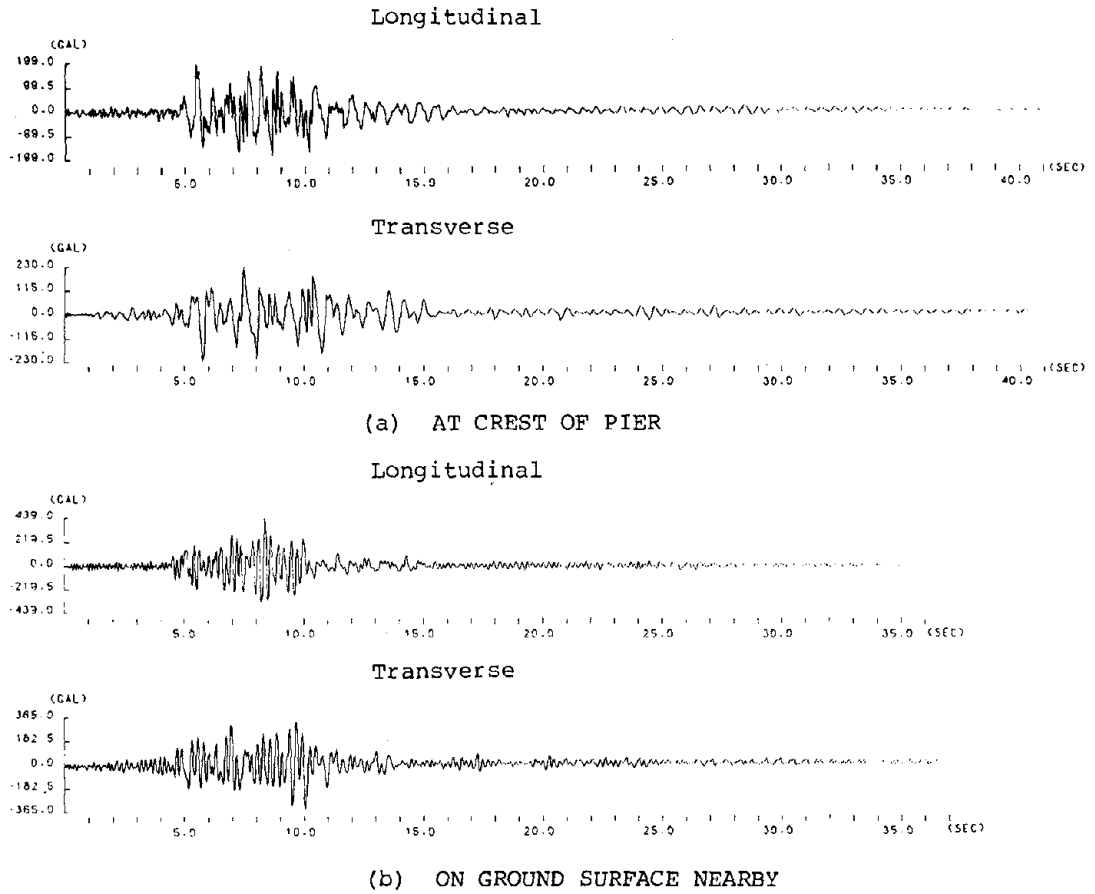


Fig. 5 ACCELERATION RECORDS AT THE ITAJIMA BRIDGE DURING THE BUNGOSUIDO EARTHQUAKE OF AUGUST 6, 1968 (C-EARTHQUAKE)

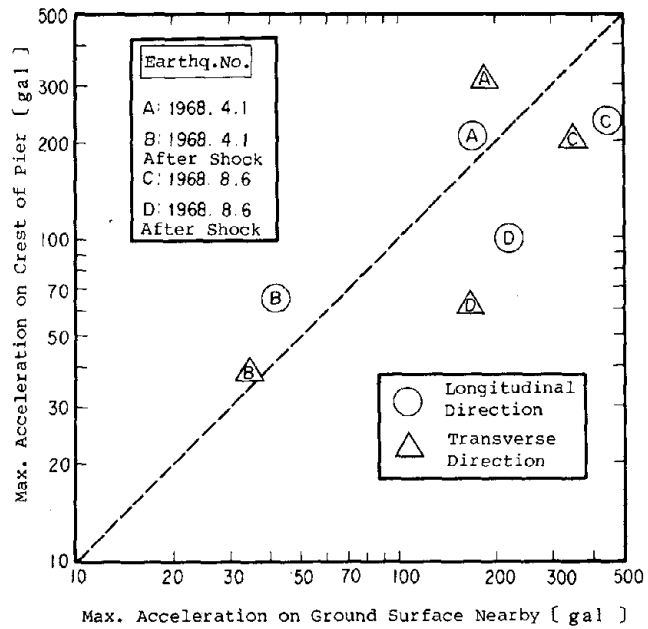


Fig. 6 AMPLIFICATIONS OF MAXIMUM ACCELERATION BETWEEN THE CREST OF PIER AND GROUND SURFACE NEARBY



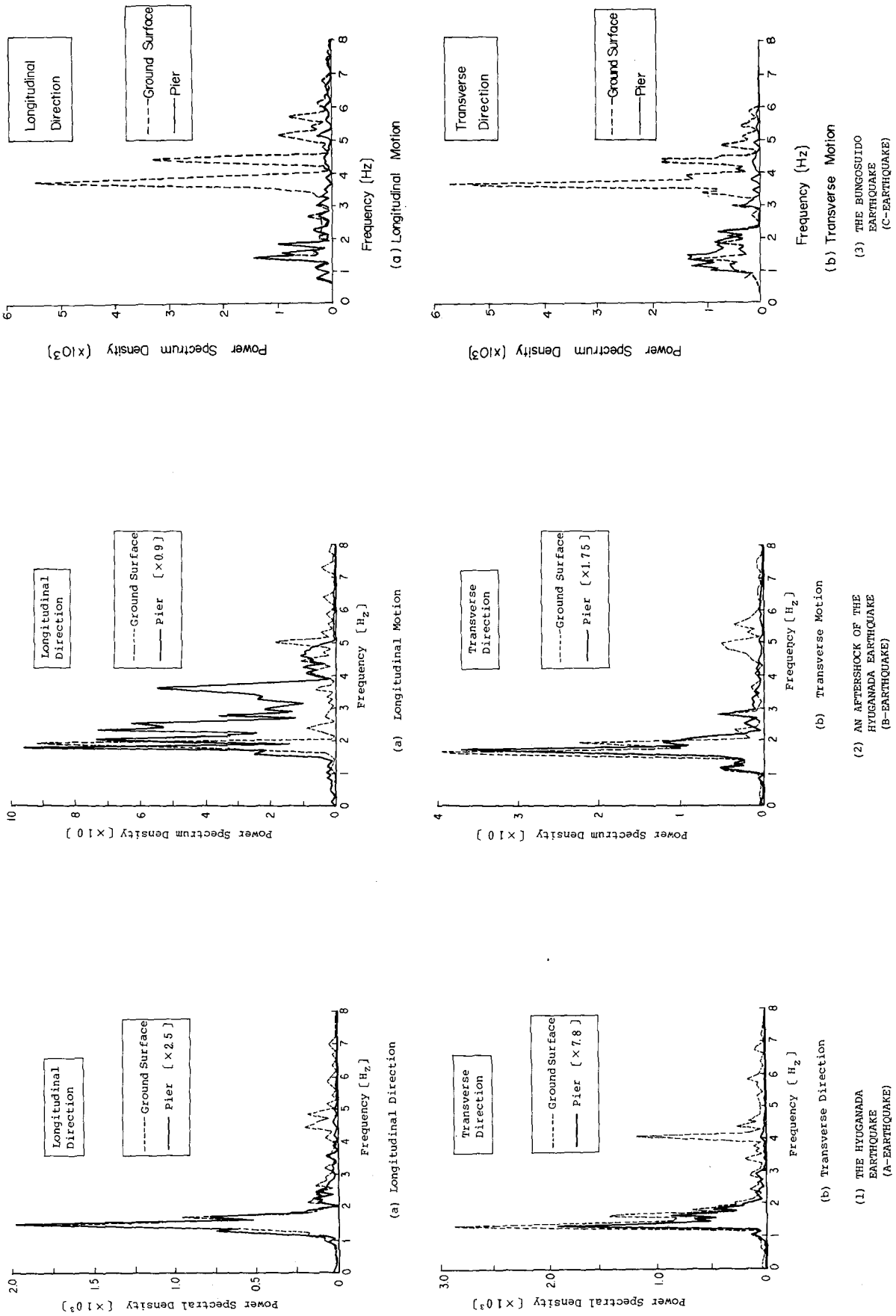


Fig. 7 POWER SPECTRA OF ACCELERATION RECORDS AT THE ITAJIMA BRIDGE

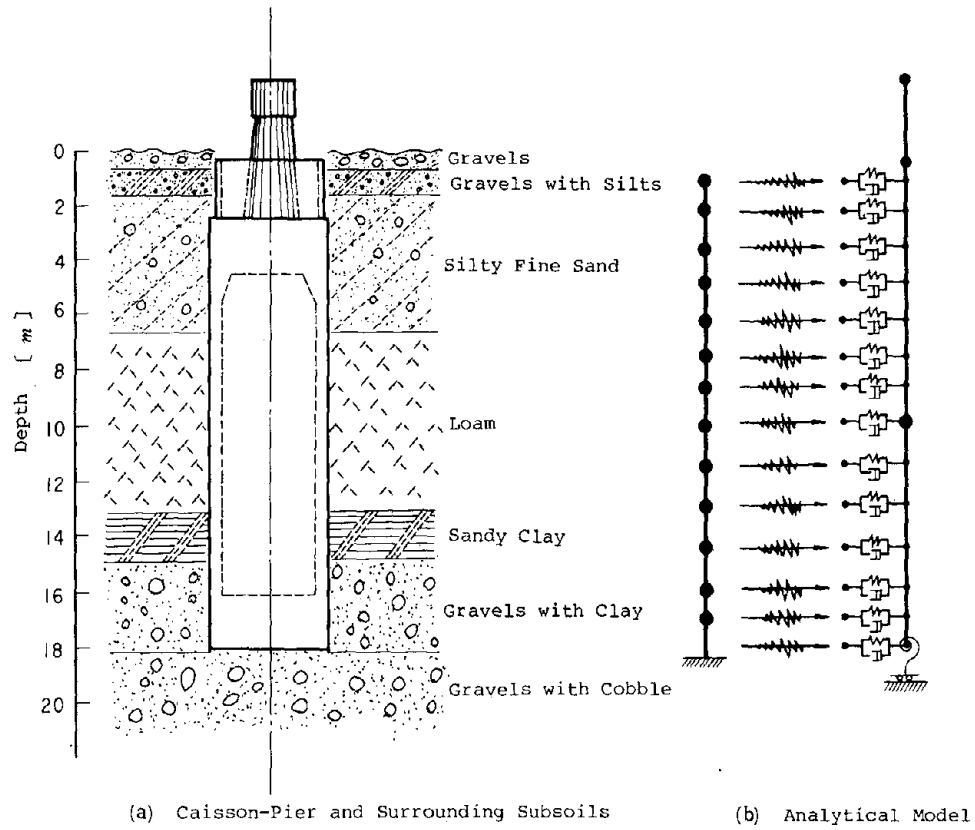


Fig. 8 ANALYTICAL MODEL OF FOUNDATION OF THE ITAJIMA BRIDGE

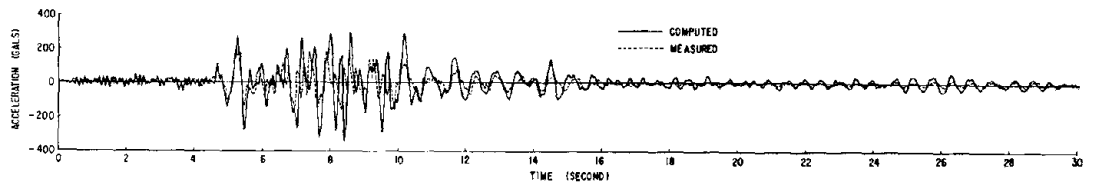
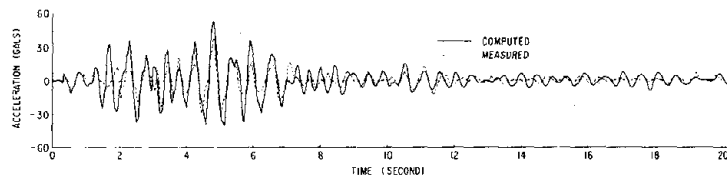
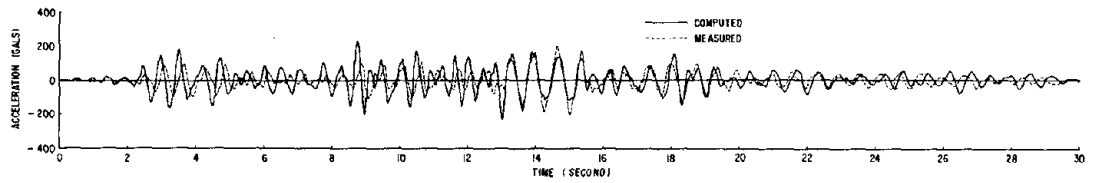


Fig. 9 CORRELATIONS OF SEISMIC RESPONSE ACCELERATION AT THE CREST OF ITAJIMA BRIDGE (LONGITUDINAL ACCELERATIONS)

## BUILDINGS ON ISOLATORS FOR EARTHQUAKE PROTECTION

by

G.C.DELFOSSE<sup>I</sup> and J.C.MIRANDA<sup>II</sup>

## ABSTRACT

A strong revival of interest is presently observed in earthquake isolation technology. An Aseismic Building Isolation System (A.B.I.S.) must satisfy four basic criteria of effectiveness. A particular type of A.B.I.S., called GAPEC SYSTEM, was extensively tested at the Centre National de la Recherche Scientifique in Marseille, France and at the John A. Blume Earthquake Engineering Center at Stanford University, California. Tests have shown that the GAPEC SYSTEM satisfies the four basic criteria of effectiveness; in particular, acceleration response, shears and overturning moments are reduced by a factor of four to eight for buildings mounted on isolators. Isolation techniques are not more expensive than classical reinforcing systems and different applications of A.B.I.S. have been put in practice.

## INTRODUCTION

A new trend for earthquake-resistant structures has developed in the last few decades, which intends to confine the seismic energy to a limited area of the structure which acts as a shock absorber. In the 1930's, Martel, Green and Jacobsen presented some aspects of a flexible story and Fintel and Khan (1968) described a shock-absorbing soft story concept (1). These authors observed that the upper stories of many buildings, when subjected to strong earthquakes, had suffered only minimum damage when the first story was flexible enough to accommodate large distortions.

In Fintel and Khan's method, the entire building should remain within the elastic range, except the columns of the soft story which undergo elastoplastic behaviour. As a consequence, the building would stay in a displaced position after the quake.

A further step is to install a perfectly soft elastic story so that the building is restored to its original position after the seismic event. According to the laws of structural dynamics, such a story would increase the natural periods of the buildings and decrease the acceleration response correspondingly. Thanks to the latest progress in rubber technology, such a soft story can now be constructed.

## FUNDAMENTALS OF ASEISMIC BUILDING ISOLATION SYSTEMS.

An Aseismic Building Isolation System (A.B.I.S.) must satisfy four basic criteria of effectiveness :

- 1.- A low horizontal acceleration response of the building under a given seismic load.
- 2.- A predominantly translational behaviour of the building.

---

I Head, Structural Dynamics Department, Centre National de la Recherche Scientifique (C.N.R.S.) Marseille, France.

II Docteur-Ingénieur, Ministerio de Planificación Urbana, Managua, Nicaragua.

3.- No amplification of the vertical motion with respect to the ground motion.

4.- A satisfactory accommodation to the large displacements which can take place.

The first criterion is obvious. Low acceleration responses lead to reduced shears and overturning moments and consequently to minimum damage. The structural materials work essentially in the elastic range and always remain capable of withstanding successive shocks.

The second criterion excludes rotational motions about the principal horizontal axes of the building. The whole building then moves like a quasi-rigid body with three main consequences : a) drift between stories is reduced, resulting in little or no non-structural damage, b) the base rocking is strongly decreased which entails a lesser risk of large irregular settling in the foundation soil and c) no significant coupling exists between the vertical and horizontal motions which enables a substantial simplification of the design.

The third criterion aims to prevent the vertical amplification which can result from the practical dispositions employed to satisfy the criteria 1 and 2. Considering that buildings are constructed to withstand high vertical forces, the third criterion is a minimum isolation requirement permitting vertical seismic forces to be transmitted through the structure without attenuation nor amplification.

The fourth criterion concerns the building stability under large displacements which can occur during strong earthquakes. Stability is obviously a basic parameter when designing any earthquake resistant system.

#### PRACTICAL IMPLEMENTATION OF AN EFFECTIVE A.B.I.S.

The most practical method of implementing a really effective A.B.I.S. is to mount the buildings on energy absorption devices called isolators which are located between the first floor and the basement or between the first floor and the ground level, if no basement exists (fig. 1).

Isolators consist of laminated layers of rubber and steel plates strongly bonded together during the rubber vulcanizing process. Their main feature is a relatively high stiffness in the vertical direction and around the two principal horizontal axes and a low stiffness in the horizontal plane and around the vertical axis. Lateral stiffness of isolators is currently five hundred times less than the vertical one and one hundred times less than the horizontal stiffness of the first story concrete columns ; the structure of the isolators permits the separate control of horizontal and vertical stiffness. Isolators have a quasi-linear behaviour up to 10% compressive strain ratio and up to 100% shear strain ratio. Thanks to a special chemical composition, the rubber employed is efficiently protected against air oxygen and the steel plates are covered with highly resistant paints. Thus the isolators have a life expectancy at least as long as that of the building which they protect. Finally, in spite of the fact that isolators are strongly attached to the structure, provisions are made to change them if necessary, without excessive work.

Let us see now how a building mounted on isolators meets the four basic criteria mentioned above.

## DYNAMIC CHARACTERISTICS OF A BUILDING ON ISOLATORS.

1.- It is well known that the natural periods increase if the stiffness of the connection between the structure and the ground is decreased. This characteristic is a direct consequence of the dynamic equilibrium equations and has been utilized for some time in the field of machinery isolations. The absolute maximum acceleration response of a multiple-degree of freedom system submitted to a ground acceleration  $a(t)$  is expressed by the formula :

$$(1) \quad |\ddot{u}(t)|_{\max} = \sum_j \phi_j^2 X_j S_{a_j}$$

where

$$(2) \quad S_{a_j} = \omega_j \left| \int_0^t a(\tau) \exp[-\xi_j \omega_j (t-\tau)] \sin \omega_j (t-\tau) d\tau \right|_{\max}.$$

represents the spectral acceleration in the  $j^{\text{th}}$  mode  $X_j$  and  $\phi_j$ ,  $\omega_j$  and  $\xi_j$  are respectively the modal participation factor, the natural circular frequency and the equivalent viscous damping ratio of the  $j^{\text{th}}$  mode. As far as an isolation system is concerned, we have to consider two distinct types of acceleration response spectra in view of the range of the predominant natural periods (fig.2). Type I is illustrated by the El Centro 1940 California Earthquake SOOE component with predominant periods in the range 0.25 - 0.6 seconds ; it corresponds to a "classical" strong earthquake recorded on firm soil at a relatively short distance from the epicenter. The type II refers to the long period earthquakes like, for instance, the 1977 Romania earthquake N-S component with a predominant period of 1 second or more ; the magnitude was 7.2, similar to the El Centro magnitude, but the corresponding accelerogram was recorded in Bucarest at 80 miles from the epicenter and on soft soil. These two earthquake types radically differ by their period content, but have a common characteristic : the absolute maximum acceleration response always decreases when the natural period increases above the predominant periods and they correspond to similar spectral acceleration, when the natural period is high enough.

Since we have observed that by decreasing the stiffness of the supporting elements we increase the natural periods, we have to design the isolators accordingly. The lateral stiffness of the isolators may be expressed as :

$$(3) \quad K_x = \sum_N GA/L_c$$

where  $G$  is the shear modulus of rubber,  $A$  the cross-sectional area of rubber,  $L_c$  the total thickness of rubber. The summation is extended to the number  $N$  of isolators.  $A$  is determined by the maximum permissible compression stress  $\bar{\sigma}$  under static load and  $G$  depends on the quality of the rubber ; the usual values are  $\bar{\sigma} = 1200$  psi and  $G = 85$  psi. We see that  $L_c$  is the parameter which determines  $K_x$  and thus the natural periods of the building.  $L_c$  is roughly proportional to the square of the first natural period and would be, for example, 4 times greater for a period of 2s. than for a period of 1s.

2.- The low lateral stiffness of isolators brings about rigid body modes of vibration. Indeed let us bear in mind that the first two natural frequencies of a free-free structure (a simple beam for instance) are zero, the first mode corresponding to a rigid body translational motion and the second

mode to a rigid body rotational motion (2). A structure with low-stiffness supporting elements tends to behave like a free-free structure and consequently, we have to wait for a first mode with predominant rigid translation and a second one with a predominant rigid rocking motion. In connection with this, Miranda (3) investigated a typical building of 46' x 46' in plan with 5, 10, 15 and 20 stories and two kinds of structural system : frames only and shear walls only. He found that three basic parameters control the behaviour of a building mounted on isolators :

a) The slenderness ratio  $e$  which is the ratio between the height of the building and the dimension in plan parallel to the displacement.

b) The mean horizontal stiffness  $K_M$  which is the arithmetic mean of the story stiffnesses and,

c) The horizontal stiffness  $K_{IX}$  of the isolators.

From Miranda's work it appears clearly that a building mounted on isolators exhibits two rigid modes : the first is translational and the second - which he designates as 1bis - is rotational ; the higher modes have a shape similar to that of the rigidly fixed buildings with nevertheless a non-zero displacement at the base. Miranda showed that when  $e$  or  $K_M$  decreases or  $K_{IX}$  increases, the participation factors  $\phi_i$  of the formula (1) decrease and the higher modes have a decreasing part in the whole response. At the same time, the first mode shape was found to be a straight line whose base value increases and top value decreases, when the basic parameter  $e$ ,  $K_M$  and  $K_{IX}$  vary as indicated above. From this situation, we can envisage two cases of buildings on isolators :

Case A. Low or stiff buildings ; for instance, low buildings up to 10 stories or shear-wall buildings up to  $e$  value of 2. These buildings show a predominant translational rigid body motion with an exclusive participation of the first mode ; they benefit fully from the decrease of acceleration response resulting from the increase of natural periods.

Case B. High or flexible buildings ; for instance, buildings above 10 stories or framed buildings with  $e$  value above 2. For these buildings, the participation of the higher modes has a double effect :

a) it increases the first natural period and consequently diminishes the acceleration response,

b) due to the fact that modes number 1bis and 2 are rotational and flexural their participation increases the acceleration response. In case of particularly flexible or slender structures, this effect may overcome the effect (a) above and the net difference between these effects has to be cancelled by lower lateral stiffness of the isolators.

A parallel has often been made between isolators and soft soil. Indeed both of them increase the natural periods and lower the acceleration response if the slenderness or flexibility effects mentioned above do not overcome this latter effect. But the analogy stops there, since the vertical, horizontal and rotational stiffness properties of a soil vary in the same direction. It means that if a soil is soft in the horizontal direction, it is also soft in the vertical and rotational directions, resulting in a strong coupling between the vertical and horizontal responses and large flexural displacements.

3.- The ability to independently control the lateral stiffness of isolators without affecting the vertical stiffness finds another application which is

related to the vertical response. It is generally possible to design the vertical stiffness  $K_{zz}$  of the isolators so that the fundamental period in the vertical direction is low enough to prevent amplification ; this dynamic aspect of the design meets the requirement we mentioned in the description of isolators, which necessitates high vertical stiffness to limit the vertical static deflection. In addition, damping introduced by isolators, nearly 5% of critical, largely contributes, in any situation, to reduce the vertical response.

4.- Displacements at the base of the building are roughly proportional to the square of the first natural period. Consequently, large displacements may be associated with low accelerations that result from high natural periods. Now we can better understand the behaviour of a building mounted on isolators through the energy dissipation concept. In a rigidly fixed building, the seismic energy input resulting from the ground motion is mainly dissipated by a general elasto-plastic distortion of the structure ; on the contrary, if the building is mounted on isolators, the seismic energy is dissipated essentially through the lateral displacement of the structure; the higher the first natural period, the slower is the displacement.

We can obtain an approximate measure of stability under large displacements by the following considerations. Let  $W$  and  $H$  represent the weight and height of the building,  $S_0$  the base shear and  $u_x$  the first floor lateral  $XX$  displacement. If the building moves like a rigid body, the base moment around the horizontal axis  $YY$  may be written as :

$$(4) \quad M_y = S_0 H/2 + W u_x$$

or, observing that, with an effective isolation system,  $S_0$  is a fraction  $\beta$  of  $W$ , for instance  $\beta < 0,5$  :

$$(5) \quad M_y = W (\beta H/2 + u_x)$$

It is easy to verify that in all practical applications,  $u_x$  is negligible compared with  $\beta H/2$ . Consequently, the load eccentricity resulting from large displacement has no influence on the building stability.

If the first floor is stiff enough, the isolators are rigidly connected together and work as a single unit to resist the moment of formula (5). The additional compressive stress in isolator (i) may be expressed as :

$$(6) \quad (\sigma_z)_i = M_y a_{xi} / I_y$$

in which  $a_{xi}$  is the distance of the isolator (i) from the vertical plane as defined by the  $YY$  axis and the center of mass,  $I_y$  is the quadratic moment of inertia of the isolators with respect to the  $YY$  axis of the building. The total compressive stress in the isolator (i) may be written as :

$$(7) \quad (\sigma)_i = Q_i / A_i + (\sigma_z)_i$$

Where  $Q_i$  is the vertical load on the isolator (i) and  $A_i$  the rubber cross-sectional area.

If  $(\sigma_a)_i$  is the buckling stress of the isolator (i), the ratio  $(\sigma_a)_i / \sigma_c$  represents a measure of the local stability at point i.

If the calculations are made for each isolator, a measure of the general stability of the structure may thus be obtained.

The moment in the isolators appears as a destabilizing factor and an experimental approach can eliminate its effects. The relative lateral displacement  $u_x$  of one isolator end may be expressed as the following sum of two functions :

$$(8) \quad u_x = \theta/k_x + F(m)$$

where  $k_x$  is the lateral stiffness of the isolator,  $\theta$  and  $m$  respectively the shear and bending moment in the isolator, bearing in mind that the latter depends both of  $\theta$  and  $u_x$ . The figure (3) shows typical shear curves obtained for an 8 inch diameter isolator submitted to a variable vertical load  $Q$ . Each curve has three branches: a branch O A limited by  $(u_{x0})$  and corresponding to the sole action of the shear  $\theta$  ; when  $\theta$  and  $u_x$  increase, the moment increases and  $u_x$  increases faster : it is the branch AB of the curve ; the branch BC, where  $u_x$  tends to infinity with no appreciable increase of shear, corresponds to buckling of the isolator ; the value  $(u_x)_{cr}$  is the critical lateral displacement corresponding to the vertical load  $Q$ . We see on figure 3 that when  $Q$  increases the limiting values  $(u_{x0})$  and  $(u_x)_{cr}$  decrease. In order to avoid the risk of buckling, it is advisable to limit the lateral displacement to the value  $(u_{x0})$  and to limit the vertical load to a reasonable value, for instance, one third of the buckling load  $(\varphi)_{cr} = A \sigma_{cr}$  without shear.

#### LARGE SCALE COMPARATIVE TESTS AND THEORETICAL INVESTIGATIONS.

Numerous tests were performed since 1973 on the shaking-table of the Laboratory of Mechanics and Acoustics at the Centre National de la Recherche Scientifique in Marseille, France, on a particular type of A.B.I.S. called the GAPEC SYSTEM (4) (5). Sizes of the 20 story scale-model are 4' x 2'3" in plan and 10'4" in height ; weight is 2068 Lbs. Tests were carried out with and without isolators ; figure 4 shows the response accelerations, shears and overturning moments when the model is excited by the 1952 Taft California Earthquake, N21E component orthogonally to the longer side, with a maximum ground acceleration of 0.1g. We see that when the structure is mounted on isolators, the acceleration at the top and the shear and overturning moment at the base are all decreased by a factor of about 8 ; at the same time, the first natural period has increased from 0.10s without isolators to 0.18s with isolators. Similar tests were performed on the shaking-table of the John A. Blume Earthquake Engineering Center at Stanford University (6) with a scale-model made of four 1-1/4" thick steel floors connected by four 1.5" x 0.75" steel columns at each story ; sizes of the model are 3' x 3' in plan and 6'-5" in height. The weight of each floor is 460 Lbs and the total weight is 1900 Lbs. Tests were carried out with and without isolators ; the figure 5 shows the first three mode shapes and we find again a straight line almost parallel to the vertical axis for the first mode with isolators, and a straight inclined line for the mode 1bis which does not exist without isolators. Damping was measured to be 0.6% of critical without isolators and 6% of critical with isolators for the first mode ; similar values were found for the mode nb. 1bis. The first natural period increased from 0.23s without isolators to 0.47s with isolators. The scale-model was excited by two types of earthquakes : San-Francisco (1957), S80E component and El-Centro (1940), S00E component. The best results were obtained with the latter, i.e. with the highest magnitude. The figure 6



shows the response-accelerations, shears and overturning moments ; we see, that top accelerations, base shears and overturning moments are reduced by a factor of about five when the structure is mounted on isolators with a predominant translational behaviour.

Moreover, dynamic responses were computed for a great variety of buildings with and without isolators, using the normal mode method (3) (4) (5). The results confirm the experimental work described above.

#### SPECIAL PROBLEMS ARISING FROM AN A.B.I.S.

The first problem arising from an A.B.I.S. is the wind sensitivity. For tall buildings, the low lateral stiffness of isolators can introduce some discomfort to the occupants during wind action. In this case, some isolators can be fitted with wind-stabilizers which are simple rods or bolts designed to break when the base shear reaches a minimum value corresponding to the elastic resistance capacity of the structure without isolators. After the earthquake, the wind-stabilizers can be easily changed.

Another problem is the necessary clearance for the pipes crossing the interface which is the space where the isolators are located. Elevator shaft crossing the interface would be suspended from the top of the building or near the center of mass. This condition would have to be fulfilled, even when the building is rigidly fixed to the ground.

#### COST OF AN A.B.I.S.

The general decrease of shears and overturning moments in a building fitted with an A.B.I.S. results in large savings in the design of structural elements and specially in foundation. These savings more than compensate the cost of isolators when severe earthquake requirements are obligatory. However, in view of the fact that after an earthquake shock, the building will remain in use without important repair, an effective A.B.I.S. is undoubtedly much cheaper than any classical strengthening system.

#### PRACTICAL USE AND FIELD APPLICATION OF A.B.I.S.

The H.Pestalozzi school, built in Skopje, Yougoslavia, in 1969, was mounted on 54 isolators of dimensions 2'-4" x 2'-4" x 1'-2" (7). In view of the engineering lessons acquired from recent earthquakes and the tremendous progress in rubber technology in the last ten years, a large revival of interest has been recently observed for aseismic building isolation systems. For instance, french nuclear plants are mounted on isolators in seismic zones and several buildings including dwelling houses and a recording studio have been recently built on isolators for a designed VIII M.M. earthquake.

In fact three distinct types of problems may be solved by an A.B.I.S. Problems of the type I are the most common ; they concern buildings with ordinary requirements of security against earthquakes (coefficient I = 1.0 of U.B.C. 1976 earthquake regulations) ; these buildings are usually protected by strengthening the resisting elements and applying the ductility requirements. It is well known that the philosophy of such a type of protection is no collapse should take place, but permissible major structural and non-structural damage may occur when the building is submitted to a major earthquake (8). In this case, an A.B.I.S. can undoubtedly solve the problem with higher security and cheaper costs.

Problems of type II concern the buildings in which high security is involved (coefficient I = 1.25 or 1.50 of U.B.C. 1976 earthquake regulations). These are buildings whose continued operation or security after an earthquake is essential to the community such as hospitals, administrative buildings, nuclear power plants, electric generating stations, water tanks and so on or those buildings that contain high human concentration such as schools, hotels, auditorium and so on. The high security involved in this type of buildings cannot be achieved at reasonable costs by strengthening techniques and an A.B.I.S. is the ideal solution.

Finally, problems of type III concern special structures which cannot be protected at the required level by usual strengthening techniques. These are, for instance, electrical facilities such as high voltage circuit breakers, pipes, airport control towers and so on. These structures are light, slender, top heavy and must resist very strong earthquakes with no interruption in service. This type of problem can presently be solved only by an isolation technology using specifically designed isolators.

#### CONCLUSION.

If an Aseismic Building Isolation System satisfies the four basic requirements, it can solve a great variety of earthquake protection problems with greatly increased security and at generally cheaper costs than classical strengthening techniques. A full protection may be obtained when it is required, due to the fact that the isolators and the structural materials of an elastically suspended building work in the elastic range only. Finally, the isolation technology may solve special dynamic problems related to light slender structures with high earthquake protection requirements.

#### BIBLIOGRAPHY.

- 1 FINTEL Mark, KHAN Fazlur R. "Shock-absorbing soft story concept for multistory earthquake structures". 64th Annual ACI Convention, Los Angeles, March 7, 1968.
- 2 MEIROVITCH Leonard. "Analytical Methods in Vibrations". The Macmillan Company, 1967.
- 3 MIRANDA Julio. "Comportement dynamique des bâtiments montés sur une suspension élastique. Cas de l'excitation sismique". Thèse de Docteur-Ingénieur. Faculté des Sciences de l'Université d'Aix-Marseille, 1978.
- 4 DELFOSSE G.C. "The GAPEC SYSTEM : a new highly effective aseismic system". Proceedings of the VI World Conference on Earthquake Engineering, New-Dehli, 1977.
- 5 DELFOSSE G.C. "The GAPEC SYSTEM : a new aseismic building method founded on old principles". Seminar on Constructions in seismic zones, Bergamo-Udine, 10-13 May, 1978.
- 6 SHAH Haresh C. "Measurements of dynamic characteristics of a scale-model structure with and without GAPEC isolators Summary". The John A. Blume E.E.C., Stanford University, March 1978.

- 7 PETROWSKI J., JURUKOVSKI D., SIMOVSKI V. "Dynamic Response of Building with isolation on rubber cushions". Seminar on Constructions in seismic zones, Bergamo-Udine, 10-13 May, 1978.
- 8 FINTEL Mark. "Resistance to earthquake. Philosophy, ductility and details". Publication A.C.I.S.P.-36. Response of Multistory Concrete Structures to lateral Forces. Paper SP36-5 A.C.I. Detroit, 1973.

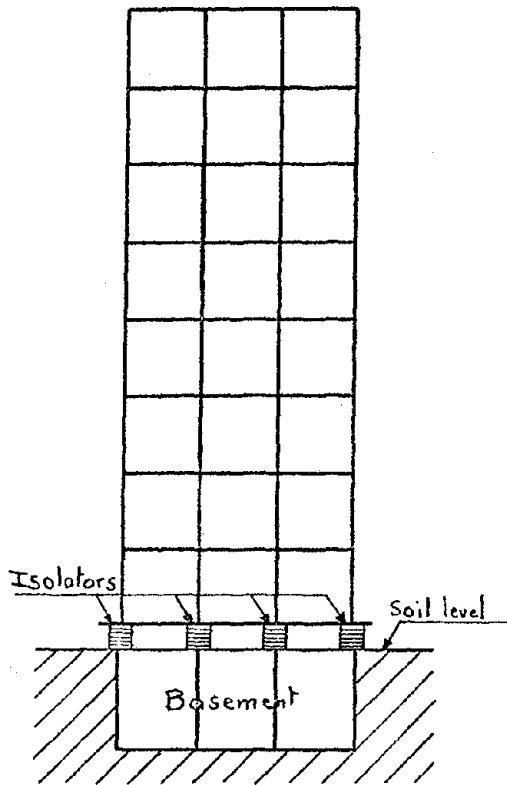


Fig.1- Schematic view of a building on isolators

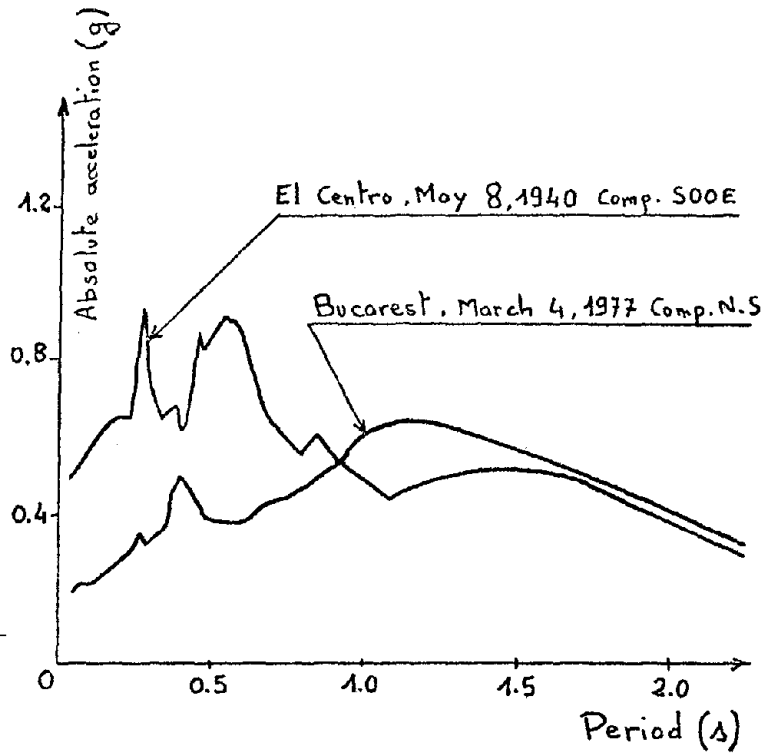


Fig.2- Short and long period absolute acceleration response spectra ; damping 5% of critical

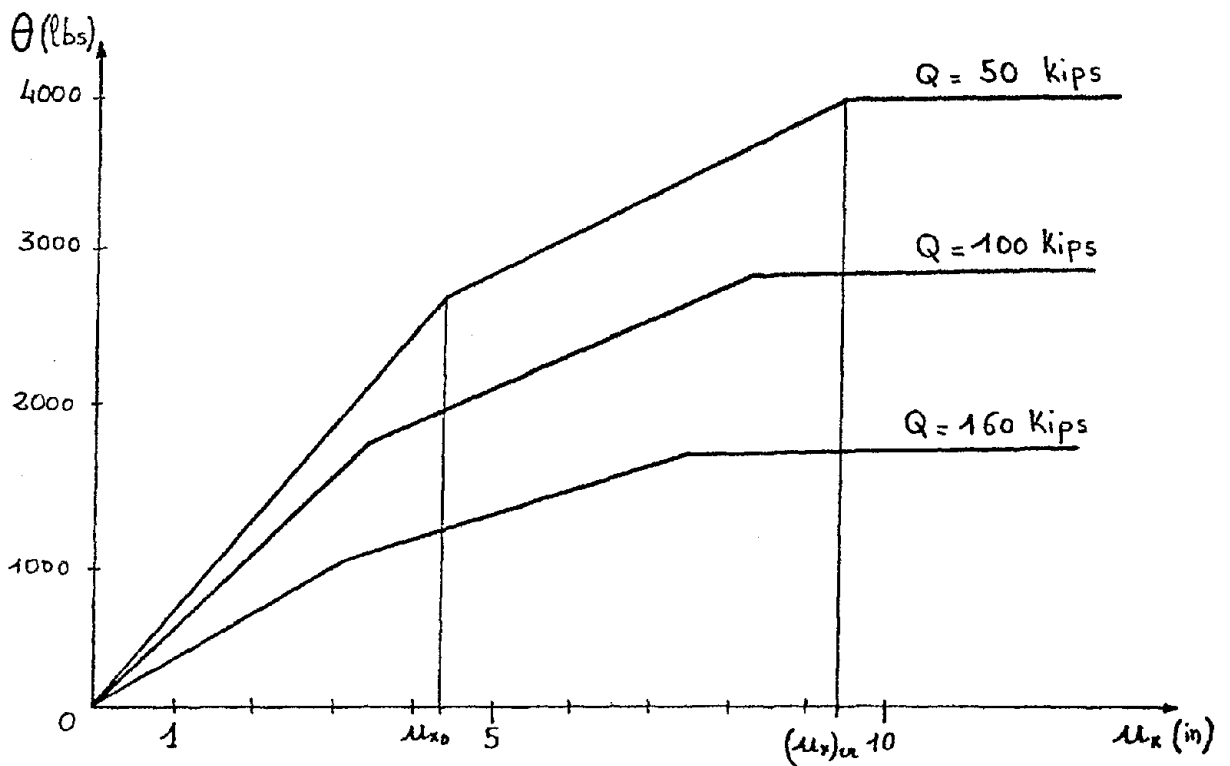


Fig.3.- Typical shear curves for a 8 inch diameter isolator with vertical load Q.

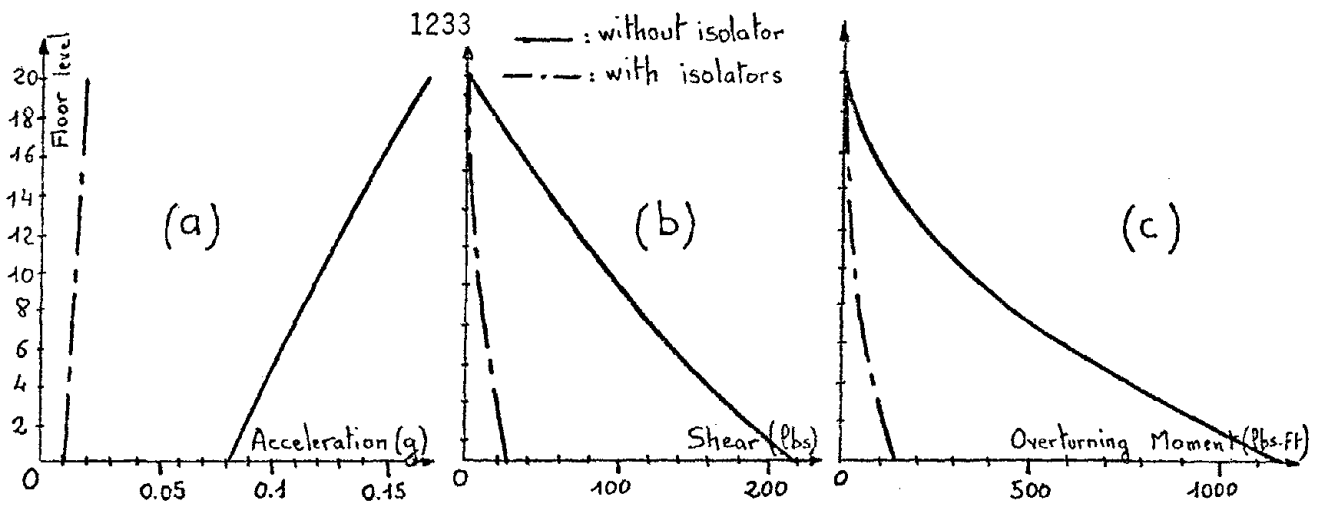


Fig.4.- French C.N.R.S. scale model with and without isolators (a) Réponse accelerations, (b) shears, (c) overturning moments.

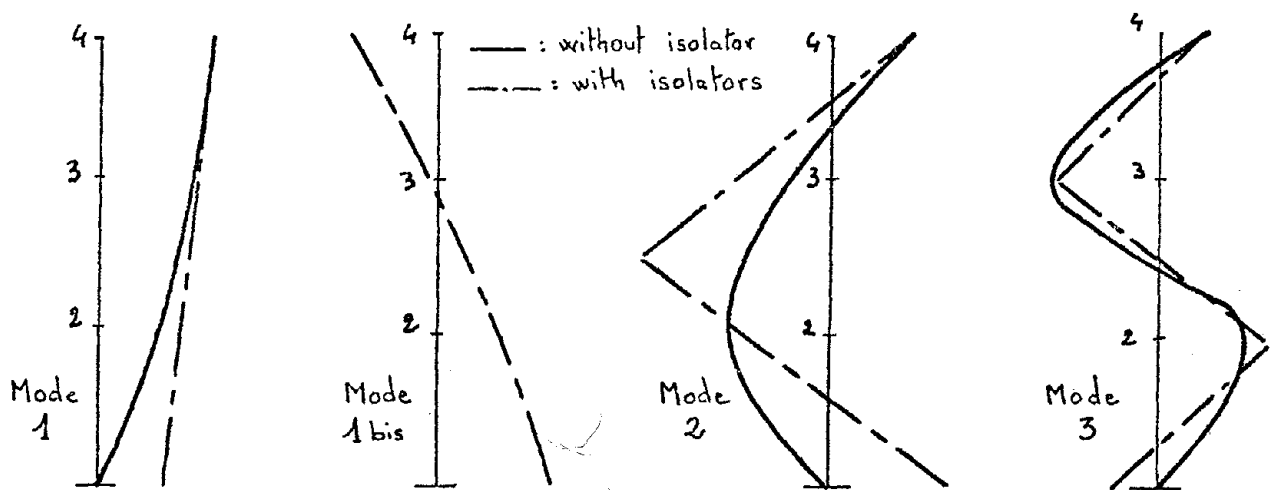


Fig.5.- Stanford University scale-model. Mode shapes with and without isolators.

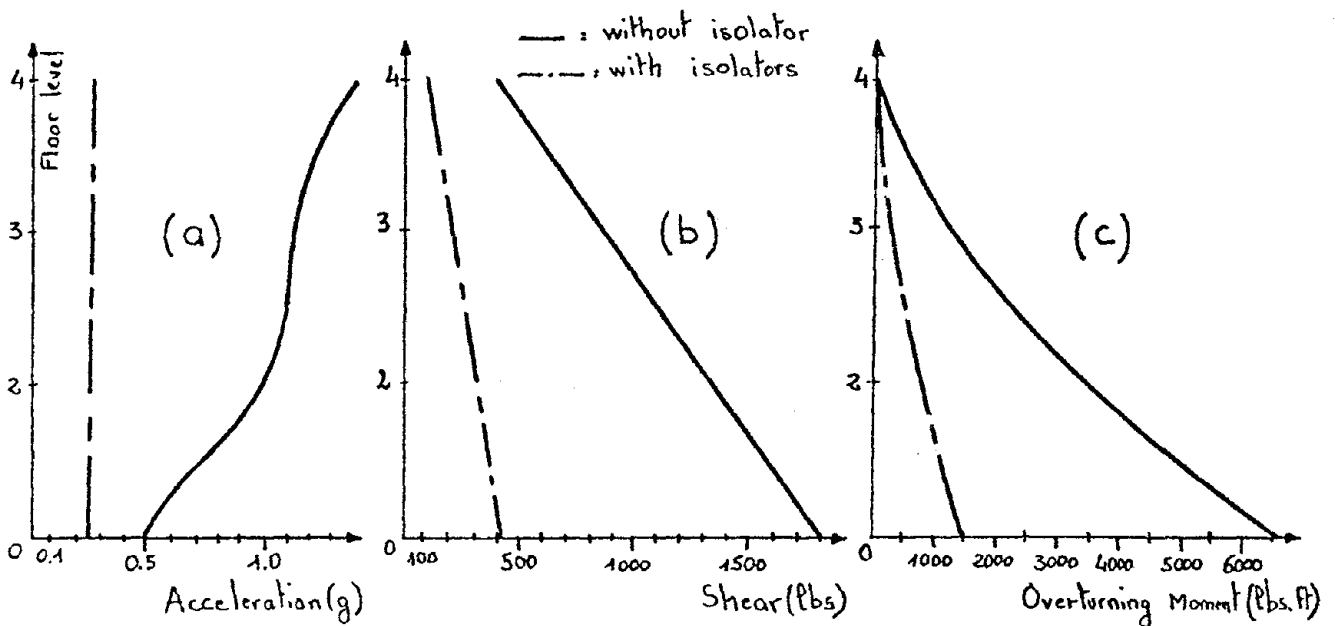


Fig.6.- Stanford University scale-model with and without isolators, (a) réponse accelerations, (b) shears, (c) overturning moments.

1234

**INTENTIONALLY BLANK**

## TRAVELING SEISMIC WAVES AND STRUCTURAL RESPONSE

by

W. J. Hall<sup>I</sup>, J. R. Morgan<sup>II</sup> and N. M. Newmark<sup>III</sup>

## ABSTRACT

Observations of earthquake damage indicate that buildings undergo rotational as well as translational motion, and that structures on large foundations respond with less intensity to ground shaking than do smaller structures. In 1969 Newmark (Ref. 1) developed a basis for determining torsional earthquake effects in symmetrical buildings, and in 1970 Yamahara (Ref. 2) offered an explanation of observed reductions in translational response of buildings as compared with free-field behavior. More recently the authors (Ref. 3) presented a numerical technique for computing reduced building response by averaging an acceleration record successively over a transit time.

The acceleration time-history is treated as a traveling seismic (shear) wave, and resulting translational and rotational motions of the base are obtained by using an averaging procedure. In this paper various combined responses are computed and compared, and the practical implications of the results obtained are discussed.

## INTRODUCTION

Studies of acceleration time-histories and corresponding computed responses for buildings suggest that the accelerations imparted to large structures approach an average of the free-field motion during some transit time related to building size. The so-called  $\tau$ -effect (Ref. 3) is a systematic attempt to reasonably account for the soil-structure interaction observed for large buildings.

The first paper that attempted to offer a rational explanation for observed reduction in response behavior apparently was that by Yamahara in 1970 (Ref. 2). An example of this reduced response can be seen in Fig. 1 which shows the response spectra of the Hollywood Storage Building and adjacent P.E. Lot for the 1971 San Fernando earthquake. This reduction is not as apparent for the distant 1952 Kern County earthquake for measurements made at the same site.

A measure of the effect of an earthquake on a large building can be obtained through calculation of a time-averaged acceleration over a transit

- 
- I Professor of Civil Engineering, University of Illinois, Urbana, Illinois 61801.
  - II Research Assistant in Civil Engineering, University of Illinois, Urbana, Illinois 61801.
  - III Professor of Civil Engineering and in the Center for Advanced Study, Emeritus, University of Illinois, Urbana, Illinois 61801.

time (Ref. 3). As used here the transit time,  $\tau$ , is the time required for a point on a wave to travel the length of the base of the structure (i.e.,  $\tau =$  the length of the base divided by the wave velocity). The concepts of the transit time ( $\tau$ ), the average translational acceleration ( $\ddot{\phi}$ ), and the average rotational acceleration ( $\ddot{\alpha}$ ) as a wave propagates over the base of a building are shown in Fig. 2. The torsional component of ground motion can be important in determining the base input for design; for this reason the rotation of the foundation, characterized by  $\arctan \dot{\alpha}$  ( $= \dot{\alpha}$ ), should not be ignored. The use of the least square fitting (Fig. 2) is not restricted to a straight line (i.e., the assumption of a rigid foundation) and indeed the averaging procedure presented applies whether or not the foundation is assumed rigid. In the case of a more realistic foundation (i.e., one having some degree of flexibility) one would expect less reduction than for a rigid foundation; nevertheless, reduction would still be expected to occur. Response curves for a real building would fall somewhere between those for a rigid foundation of the same size and those for a point. For a massive foundation the response curve would be much closer to that of a rigid foundation than to that of a point.

The acceleration at the edge of the building foundation due only to the rotation of the base is  $\ddot{\alpha}\tau/2$ . This torsional acceleration must be added to the average translational acceleration to obtain the total acceleration at the edge of the base ( $\ddot{\phi} + \ddot{\alpha}\tau/2$ ). Thus in the  $\tau$ -averaging procedure, discussed in detail in the next section, three time-histories are obtained for each acceleration time-history: (1) average translation acceleration ( $\ddot{\phi}$ ), (2) average rotational acceleration ( $\ddot{\alpha}\tau/2$ ), and (3) average total acceleration ( $\ddot{\phi} + \ddot{\alpha}\tau/2$ ). The third time-history is the algebraic sum in time (i.e., signs are observed) of the first two time-histories and therefore represents the total acceleration at the edge of the base. The other two time-histories represent the individual contributions of translational and torsional motions.

With these generated time-histories of averaged translational, rotational, and total accelerations the response of a single-degree-of-freedom system may be computed and presented in the form of response spectra.

#### THEORY AND PROCEDURE

The technique employed in the calculations is essentially a time-averaging of an acceleration time-history over a transit time,  $\tau$ . It should be noted that this procedure assumes that the ground motion propagates as a plane wave.

At a given point in time some portion of the acceleration time-history is positioned along the side of the foundation as shown in Fig. 2. As time progresses the acceleration time-history simply slides along the foundation such that at any time the accelerations imparted to the foundation are changed only slightly from those imparted at a time  $\Delta t$  earlier. The following theoretical derivation for computing translation and rotation by Newmark is an outgrowth of earlier studies on torsion in symmetrical buildings (Ref. 1).

Given an acceleration time-history,  $\ddot{\rho}$ , and applying the principle of least squares to obtain the average translational acceleration,  $\ddot{\phi}$ , and



the average slope of the fitted line,  $\ddot{\alpha}$  (which is related to the average rotational acceleration), one can obtain the following:

$$\int_A^B (\ddot{\phi} + \ddot{\alpha}t - \ddot{\rho})^2 dt = \text{minimum}$$

Setting  $\partial/\partial\ddot{\phi} = 0$  for the integral

$$2[\int \ddot{\phi} dt + \int \ddot{\alpha}t dt - \int \ddot{\rho} dt] = 0$$

and setting  $\partial/\partial\ddot{\alpha} = 0$  for the integral

$$2[\int \ddot{\phi}t dt + \int \ddot{\alpha}t^2 dt - \int \ddot{\rho}t dt] = 0$$

Noting that:  $\int \ddot{\alpha}t dt = \int \ddot{\phi}t dt = 0$  since  $A = -\tau/2$ ,  $B = \tau/2$

$$\int \ddot{\phi} dt = \dot{\phi}\{t(B) - t(A)\} = \dot{\phi}\tau$$

$$\int \ddot{\alpha}t^2 dt = \ddot{\alpha}\{1/3[t(B)^3 - t(A)^3]\} = \ddot{\alpha}\tau^3/12$$

$$\int \ddot{\rho} dt = \dot{\rho}(B) - \dot{\rho}(A)$$

$$\int \ddot{\rho}t dt \text{ integrating by parts}$$

$$= \tau/2[\dot{\rho}(B) + \dot{\rho}(A)] - [\rho(B) - \rho(A)]$$

Substituting into the above, one obtains:

$$\ddot{\phi} = 1/\tau\{\dot{\rho}(B) - \dot{\rho}(A)\} \quad \text{Eq. (1)}$$

$$\ddot{\alpha} 6/\tau^2\{\dot{\rho}(B) + \dot{\rho}(A)\} - 12/\tau^3\{\rho(B) - \rho(A)\} \quad \text{Eq. (2)}$$

Note that as  $\tau \rightarrow 0$ , using Taylor Series expansions for  $\dot{\rho}$  and  $\rho$ ,  $\ddot{\alpha} \rightarrow \ddot{\rho}(0)$  as would be expected. It should be noted that  $\ddot{\alpha}$ , the slope of the fitted acceleration curve, is the derivative of acceleration with respect to time and therefore has units of length/time<sup>3</sup>.

There are two time-histories resulting from the  $\tau$ -averaging procedure derived above; one of averaged translational acceleration,  $\dot{\phi}$ , and one of averaged rotational acceleration,  $\ddot{\alpha}$ . Elastic response spectra are computed from these two averaged time-histories using the Z-transform method as presented by Stagner and Hart in 1970 (Ref. 4). This procedure is a recursive relationship in the time domain for the elastic response of a single-degree-of-freedom oscillator to an arbitrary base motion.

In the aforementioned combinational technique it has been assumed that a simple superposition of the effects of translation and rotation can be used (i.e., that translational ground motion causes only translational response and rotational motion causes only rotational response). Furthermore,

it has been assumed that the ratio of torsional to translational frequencies is unity. It can be shown (Ref. 1) that the theoretical ratio is unity for a rectangular floor plan with equal uniformly distributed resistance in the two principal directions. If a more realistic resistance distribution pattern (e.g., corner columns or end walls and columns) is assumed the theoretical ratio of torsional to translational frequencies is greater than unity. The influence of torsion would be reduced, from that seen using  $\omega_{\text{torsion}}/\omega_{\text{translation}} = 1.0$ , if  $\omega_{\text{torsion}} > \omega_{\text{translation}}$  and therefore the assumption of  $\omega_{\text{torsion}}/\omega_{\text{translation}} = 1.0$  is conservative.

When considering translation alone, response in the high-frequency range is substantially lower if the  $\tau$  procedure is used. This reduction occurs at frequencies above 1 Hz and is shown in Fig. 3 for the Hollywood Storage P.E. Lot San Fernando record. This compares favorably with the computed responses for the Hollywood Storage Building Basement as compared to the adjacent P.E. Lot (Ref. 3). The averaging that occurs considering translation only is directly proportional to the building size (i.e., as the building gets larger the magnitude of the response reduction also increases). A more complete analysis includes the effects of both translational and rotational averaging. The rotational response is of greatest importance in the high-frequency range (Figs. 3 through 6), and therefore offsets somewhat the reduction computed from translation. The importance of rotational response increases with the size of the building and is as great or greater than the normal translational response in some regions (5-9 Hz for  $\tau = 0.08$ , 2.5-6 Hz for  $\tau = 0.16$ ).

Of special importance in making design recommendations is the effect of combined motion. It has been shown that, in the high-frequency region, consideration of translation alone would lead to response reduction and consideration of rotation alone would lead to response amplification. When considering combined motion one would expect the effects of translational averaging and rotation partially to offset each other, as indeed they do at high frequencies. However, it has been found that in the mid-frequency (2-8 Hz) range the combined response is somewhat greater than the normal computed response (Figs. 3 through 6).

#### SUMMARY

In this study the influence of building size on effective base motion during an earthquake was studied. Based on plane wave assumptions the effects of averaged translation and rotation on the overall combined response were computed. While the  $\tau$ -averaging method is not exact it constitutes one systematic and reasonable way to account for observed behavior. Comparison of the combined response curves (Figs. 3 through 6) to the standard response spectra reveals two trends. First, the averaging effects due to translation alone (i.e., response reduction at higher frequencies as reported in previous work) are offset somewhat by the added effects of torsion; however, significant reduction still can occur. Secondly and more important from a design point of view the torsional contribution to combined response in the mid-frequency range can be quite significant and result in substantial amplification. The magnitude of the amplification reported herein is an upper bound, as it assumes all of the motion corresponds to a vertical wave front propagating horizontally, whereas the real situation may be much less stringent.

In computing the combined response three different combinational methods have been considered. An algebraic summation of time-histories with the response computed from this combined time-history is the most rigorous and makes the best physical sense. On the other hand the traditional square root of the sum of squares of the responses (from spectra) yields essentially the same results and is easier to obtain. The absolute sum of responses is an overestimate of expected combined response and is the greatest of the computed responses.

An attempt was made to formulate a general procedure for constructing a design spectrum (including both translational averaging and torsion). As a result it is considered that a modification of a normal design spectra in the acceleration region will be sufficient to include the combined effects. In a first attempt to indicate the notion of the amplification arising from combined translational and torsional averaging, the regions and amounts of amplifications found as a part of this study are shown in Figs. 7 and 8. Transition zones are not shown since they cannot be accurately defined at this moment. The amplification values employed for the response spectra used for comparison purposes in Figs. 7 and 8 are taken from Ref. 5.

Certain trends were observed during this study which hold for records from different earthquakes and for sites on soil and rock. However, these trends can only be considered as qualitative at this time.

A more exhaustive study will be needed to establish firm recommendations about transition zones and high-frequency effects.

#### ACKNOWLEDGMENT

The work reported herein was accomplished in part under National Science Foundation (RANN and ASFA) Grants No. ENV 75-08456 and ENV 77-07190 and in part under Nuclear Regulatory Commission, Directorate of Research, sponsorship. Any opinions, findings, and conclusions or recommendations expressed in this publication are those of the authors and do not necessarily reflect the views of the National Science Foundation or the Nuclear Regulatory Commission.

#### REFERENCES

1. Newmark, N. M., "Torsion in Symmetrical Buildings", Proceedings of 4th World Conference on Earthquake Engineering, Santiago, Chile, 1969.
2. Yamahara, H., "Ground Motions during Earthquakes and Input Loss of Earthquake Power to an Excitation of Buildings", Soils and Foundations V. 10, No. 12, pp. 145-161, Tokyo, 1970.
3. Newmark, N. M., Hall, W. J. and J. R. Morgan, "Comparison of Building Response and Free-Field Motion in Earthquakes", Proceedings of 6th World Conference on Earthquake Engineering, New Delhi, India, 1977.

4. Stagner, J. R., and G. C. Hart, "Application of the Bilinear Z-Transform Method to Ground Motion Studies", Bulletin of the Seismological Society of America, V. 60, No. 3, pp. 809-817, June 1970.
5. Hall, W. J., Mohraz B., and N. M. Newmark, "Statistical Analyses of Earthquake Response Spectra", Transactions 3rd International Conference on Structural Mechanics in Reactor Technology, London, England, V. 4, Paper K 1/6, 11 pp., September 1975.

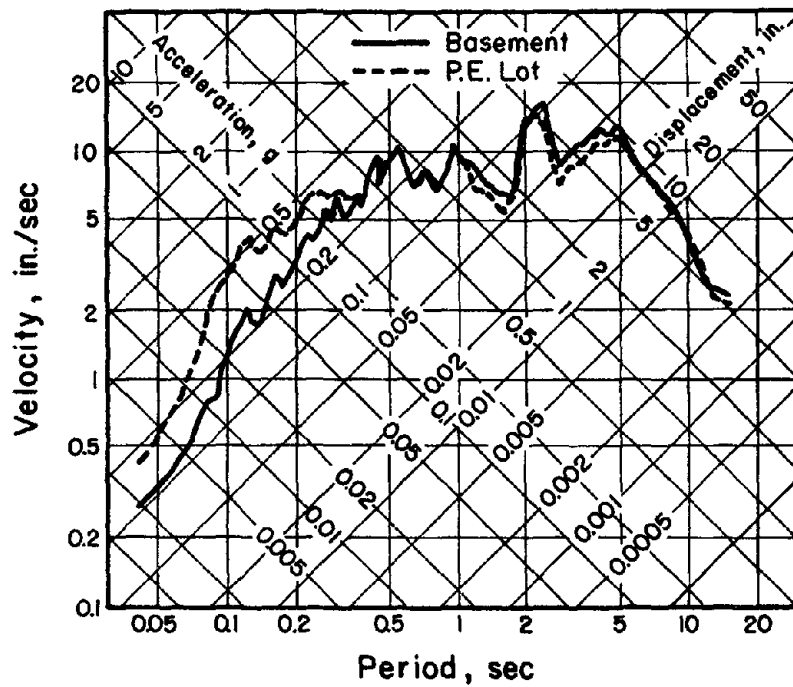


FIG. 1 HOLLYWOOD STORAGE BUILDING BASEMENT AND P.E. LOT, SAN FERNANDO EARTHQUAKE, 9 FEB, 1971-0600 PST, COMPONENT SOUTH, DAMPING 5% OF CRITICAL

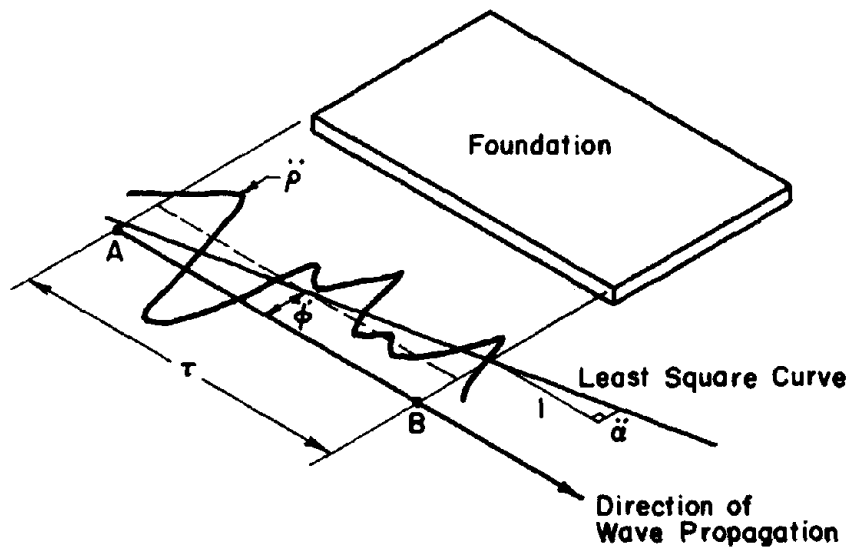


FIG. 2 BASE TRANSLATION AND ROTATION ARISING FROM TRAVELING SEISMIC WAVES

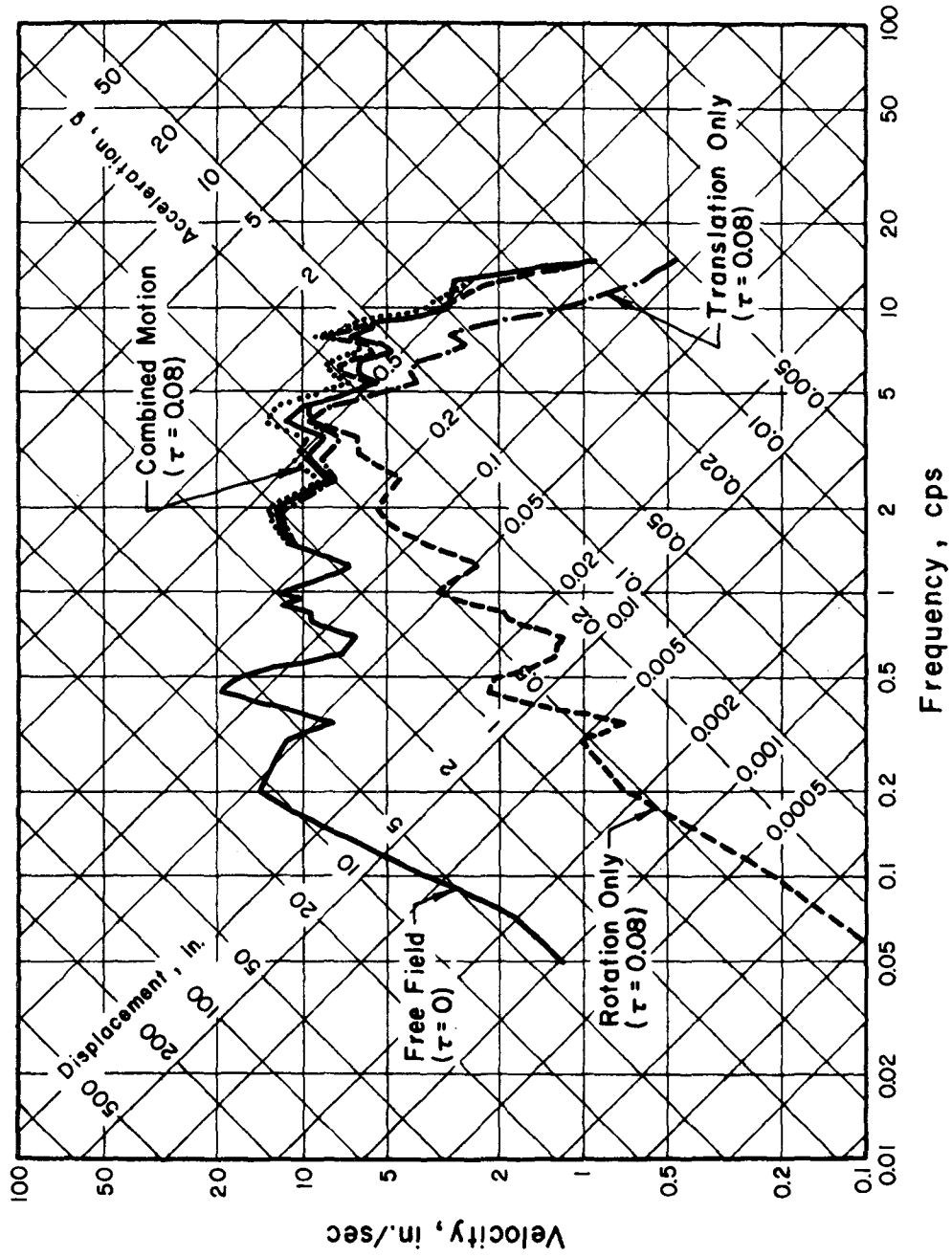


FIG. 3 HOLLYWOOD STORAGE P.E. LOT, SOOW, SAN FERNANDO EARTHQUAKE, 9 FEBRUARY 1971, SPECTRUM COMPUTED USING 2.0 PERCENT CRITICAL DAMPING

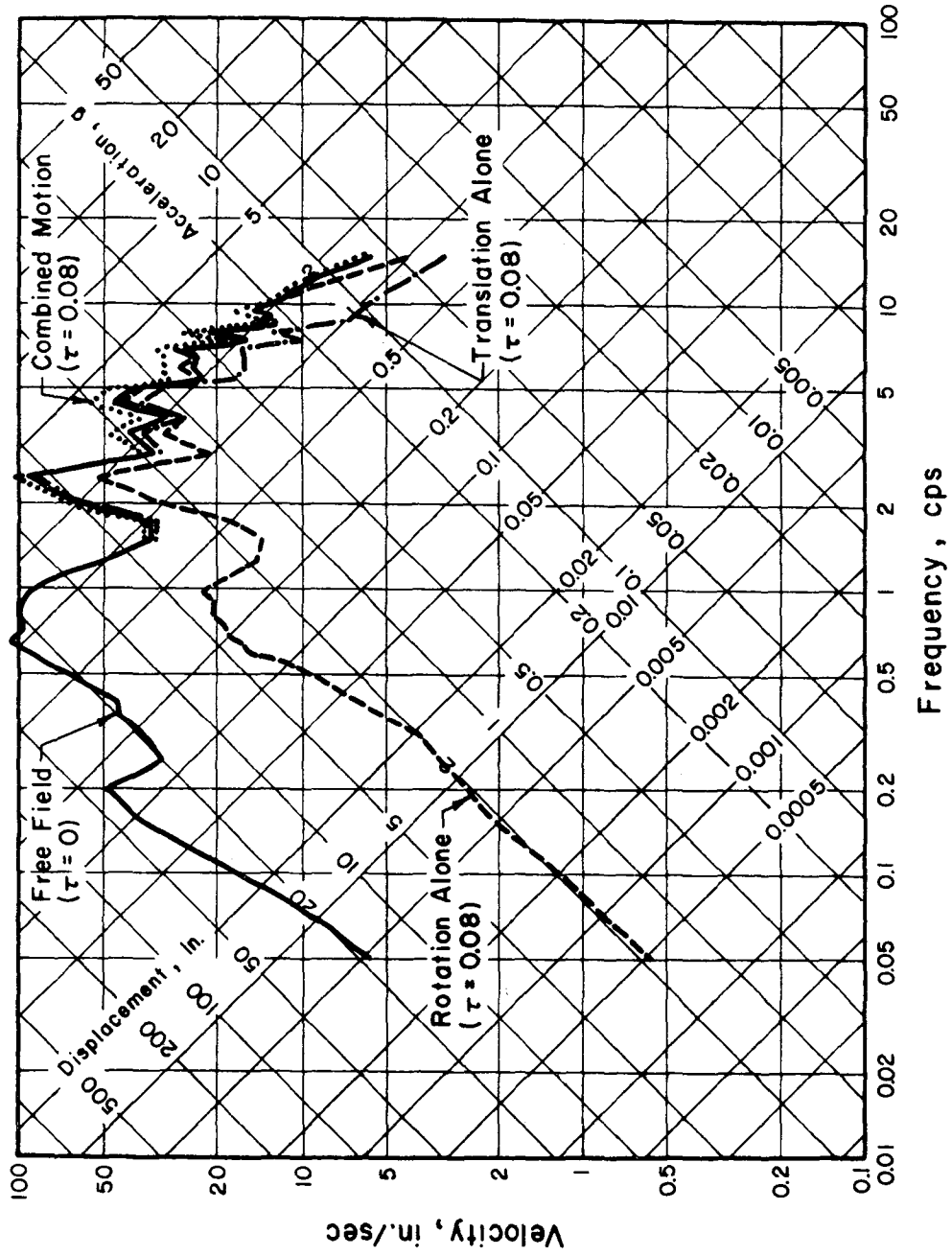


FIG. 4 PACOIMA DAM, S16E, SAN FERNANDO EARTHQUAKE, 9 FEBRUARY 1971, SPECTRUM COMPUTED USING 2% CRITICAL DAMPING

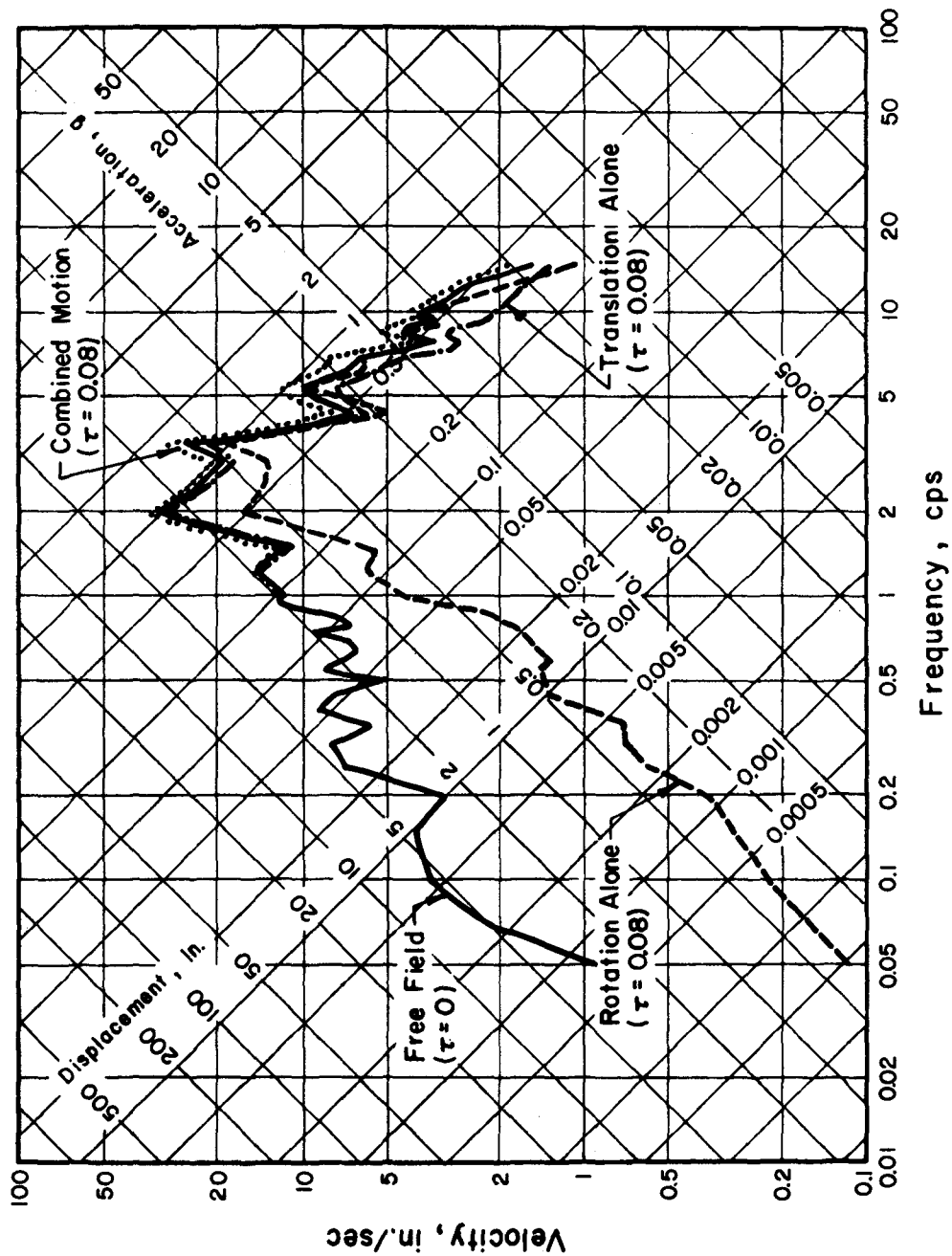


FIG. 5 CHOLAME, SHANDON, ARRAY NO. 5, N05W, PARKFIELD EARTHQUAKE, 27 JUNE 1966, SPECTRUM COMPUTED USING 2% CRITICAL DAMPING



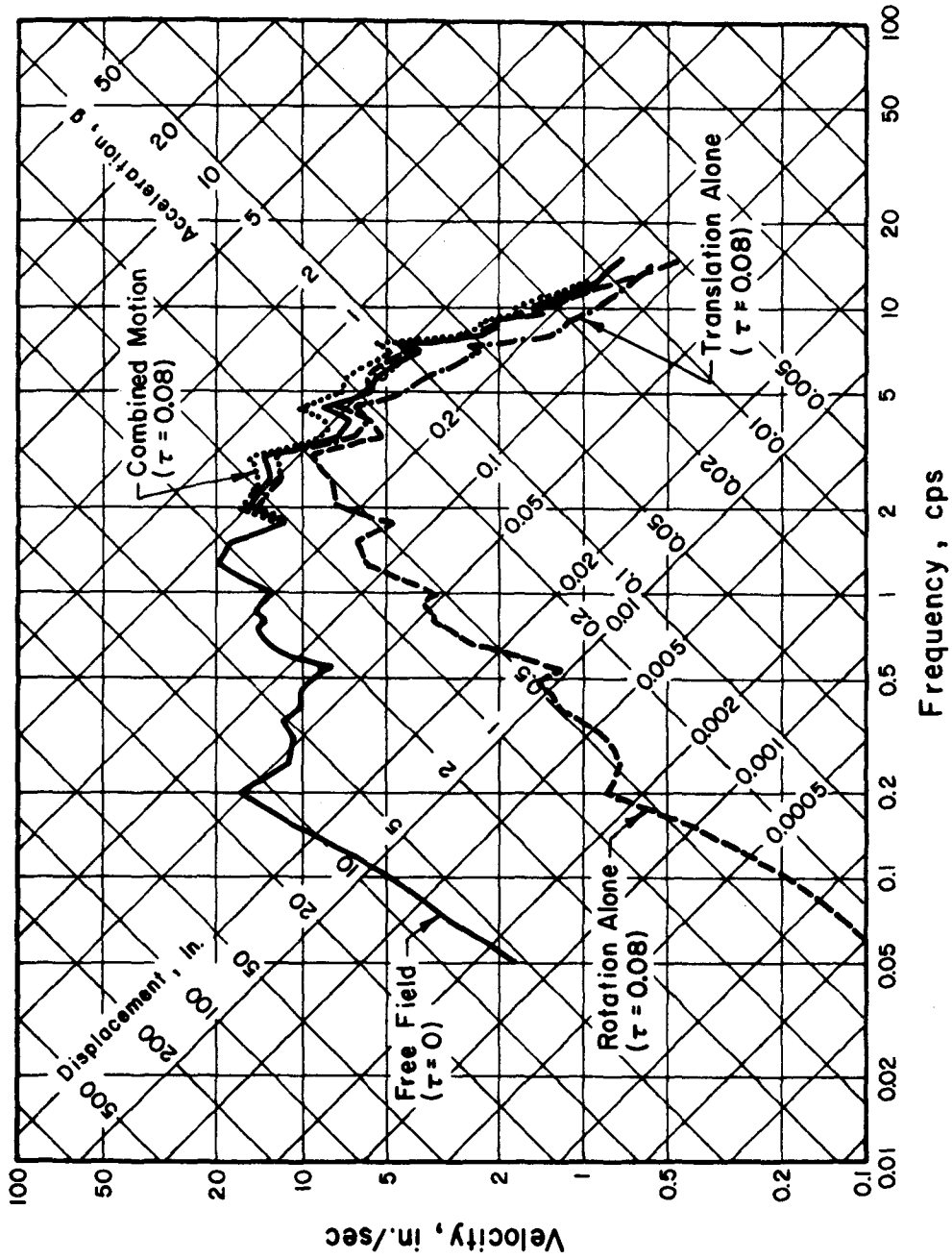


FIG. 6 TAFT LINCOLN SCHOOL, N21E, KERN COUNTY EARTHQUAKE, 21 JULY 1952, SPECTRUM COMPUTED USING 2.0 PERCENT CRITICAL DAMPING

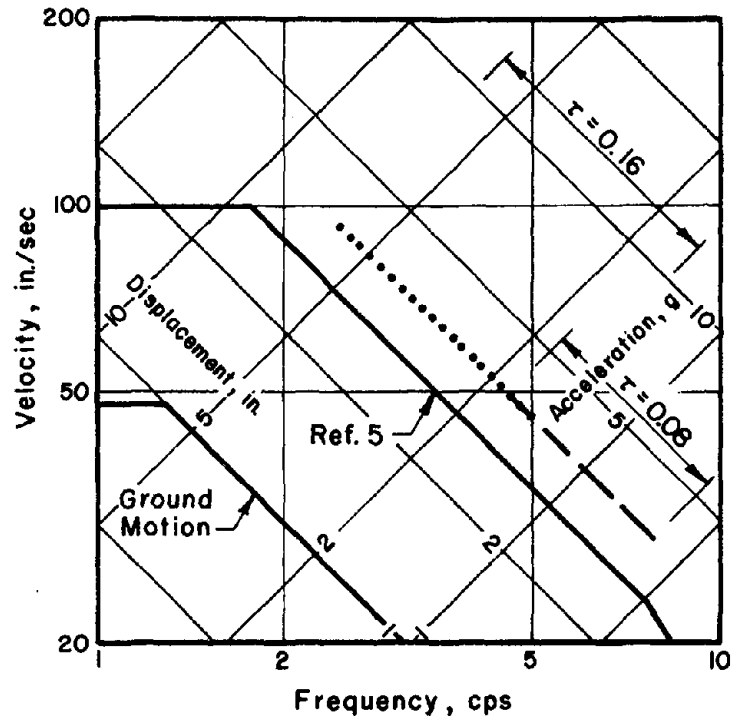


FIG. 7 ILLUSTRATION OF RESPONSE AMPLIFICATION ARISING FROM COMBINED TRANSLATION AND TORSION (50 PERCENTILE)

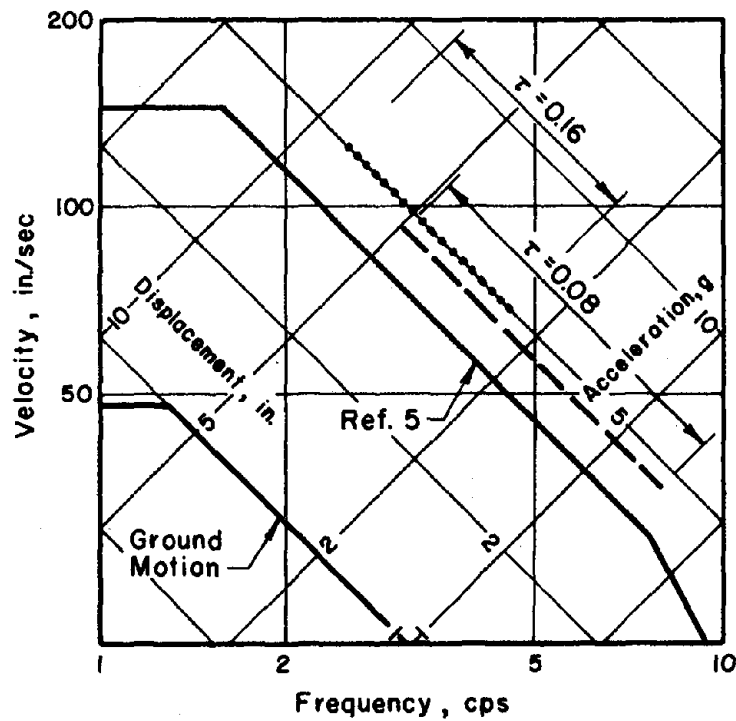


FIG. 8 ILLUSTRATION OF RESPONSE AMPLIFICATION ARISING FROM COMBINED TRANSLATION AND TORSION (84.1 PERCENTILE)

## EFFECTIVE PEAK ACCELERATION

by

Robert V. Whitman<sup>I</sup>

## ABSTRACT

A definition of effective peak acceleration (EPA) is developed in connection with cyclic mobility (liquefaction) of sands. Available data are used to relate EPA to the magnitude of an earthquake, and hence to develop an attenuation equation for EPA as a function of magnitude and epicentral distance. An example is given illustrating the use of this new attenuation equation in risk analysis, and the extension of this approach to structures is discussed.

## INTRODUCTION

In the development of zoning maps for ATC-3, the concept of effective peak acceleration (EPA) was introduced (4). Like other parameters such as "sustained peak acceleration", EPA is related to the damaging potential of a ground motion. EPA is less than peak acceleration (A) for two reasons: (a) very high frequencies, typified by spikes of high acceleration but very short duration, have little effect upon the response of most structures, and (b) for structures being strained into the inelastic range, duration of motion or number of cycles of straining has a great influence on the damage.

The concept of an EPA certainly is sound. However, thus far there is lack of systematic, quantitative definition of the parameter. Any specific definition for EPA ultimately must come from the study of the behavior of structures whose resistance deteriorates with successive cycles of loading. As a first step in this direction, the analogous problem of liquefaction of sands is considered.

## EPA FOR CYCLIC MOBILITY

The literature of geotechnical engineering contains much information relating duration of ground shaking to the likelihood of failure by cyclic mobility (liquefaction). Methods have been developed to account quantitatively for the difference between motions having the same peak acceleration but different durations. These results will be used to illustrate how EPA may be defined, how the ratio EPA/A may be evaluated, and how this result may be used in risk analysis.

## A DEFINITION FOR EPA

A key step in the analysis of cyclic mobility is to convert a chaotic-

---

<sup>I</sup>Professor of Civil Engineering, Massachusetts Institute of Technology, Cambridge, MA 02139

appearing time history of shear stress into an equivalent, periodic shear stress with a limited number of cycles. The procedures used for this purpose are based upon principles from fatigue analysis (1,5) and experimental studies have demonstrated the approximate validity of these procedures. As indicated in Fig. 1, there are a number of different equivalent combinations of peak uniform shear stress,  $\tau_{eq}$ , and number of cycles,  $N_{eq}$ , each of which is also equivalent to the original time history. The equivalent peak uniform shear stress may be either greater or less than the peak shear stress,  $\tau_{pk}$ , in the original time history, depending upon the corresponding number of cycles.

Close to ground surface where cyclic mobility is usually of greatest concern, the essential features in a time history of shear stress are proportional to the corresponding features in the time history of acceleration at the surface of the ground. Thus, the notions embodied in Fig. 1 may also be applied to determine equivalent combinations of uniform peak acceleration and number of cycles. That is:  $EPA/A \approx \tau_{eq}/\tau_{pk}$ . This leads to a definition for EPA as it applies to cyclic mobility:

EPA  $\equiv$  the peak acceleration in a series of uniform cycles which produce failure by cyclic mobility in some standard number of cycles -- say 10 cycles.

#### EPA/A AS A FUNCTION OF MAGNITUDE

Generalized data available in the literature may be used to develop an approximate relationship for this ratio. Fig. 2 reproduces data for the equivalent number of cycles in ground motion as a function of magnitude. These data were originally obtained by applying the previously-mentioned method for determining equivalent number of cycles to a set of recorded and artificially-generated time histories, assuming  $\tau_{eq}/\tau_{pk} \approx EPA/A = 0.65$ . While considerable scatter is apparent in Fig. 2, an average curve is drawn.

By repeating the analysis which led to the data in Fig. 2, curves for other values of EPA/A may be constructed. However, this may be accomplished approximately and much more simply by making use of the curves in Fig. 3. Just such curves, which give typical combinations of  $\tau_{eq}$  and  $N_{eq}$ , were used in the processing of time histories to obtain Fig. 2. The procedure used here may be explained with the help of Fig. 4.

1. Assume some M, and read  $N_{eq}$  from part (a).
2. Enter part (b) and find  $\tau_{eq}/\bar{\sigma}_{vo}$ , which is also  $0.65 \tau_{pk}/\bar{\sigma}_{vo}$ .
3. Assume some other  $\tau_{eq}/\tau_{pk}$ . For example,  $\tau_{eq}/\tau_{pk} = 0.80$  must correspond to  $\tau_{eq}/\bar{\sigma}_{vo}$  equal to  $0.80/0.65 = 1.23$  times the value in step 2. Read the new  $N_{eq}$ .
4. Plot these new values of  $\tau_{eq}/\tau_{pk}$  and  $N_{eq}$  in part (a).

Fig. 5 shows the resulting relations, using the curves in Fig. 3 for a relative density of 68%. Similar curves are obtained for other relative densities.

Finally, the relations plotted in Fig. 5 may be inverted so as to plot EPA/A vs. magnitude for various values of  $N_{eq}$ . These new relations are shown in Fig. 6, again for a relative density of 68%. Curves for  $N_{eq} = 10$  are also given for other relative densities, and the relation is seen to be quite similar in all cases, especially for  $M > 6$ . Several relations might be matched to these results; a convenient one is:

$$\frac{EPA}{A} [N_{eq} = 10] = 0.17e^{0.19M} \quad (1)$$

This curve is also shown on Fig. 6 for comparison. Note that the ratio of EPA to A increases with increasing magnitude, reflecting the increase in duration of ground shaking as magnitude increases. For this particular definition of EPA used here,  $EPA < A$  for  $M < 9.32$ . That is, EPA will almost always be less than A. It is also of interest that  $EPA < 0.65A$  for  $M < 7.05$ . The coefficient 0.65 was selected because so often the equivalent uniform shear stress is taken as 0.65 times the peak shear stress.

#### RISK ANALYSIS IN TERMS OF EPA

By combining Eq. (1) with an attenuation equation relating peak acceleration to magnitude and epicentral (or hypocentral) distance, it is possible to derive an attenuation equation for EPA. This new equation may then be used, in connection with standard techniques (2,3), to produce risk curves and risk maps for EPA.

To illustrate the nature of the results, a particular equation for peak acceleration will be used:

$$A = 18.4e^{0.69M_{\Delta}-0.8} \quad (2)$$

where A is in cm/sec<sup>2</sup> and  $\Delta$  is the epicentral distance in km. This equation is based upon Japanese experience and gives peak acceleration at the surface of "soft" soils (7). Combining Eqs. (1) and (2) gives:

$$EPA = 3.13e^{0.88M_{\Delta}-0.8} \quad (3)$$

Because of this particular form chosen for Eq. (1), the new attenuation equation for EPA contains just the same terms as the original attenuation equation but with different coefficients. This simplification permits use of existing computer programs for carrying out risk analysis, but is not essential to the basic method for analysing and mapping the risk of exceeding various levels of EPA.

Fig. 7 depicts a fault system assumed for an illustrative example, and gives the source parameters used for each of the two faults. Values of EPA, A and 0.65, corresponding to a mean recurrence interval of 500 years, were computed at various grid points in the vicinity of the assumed faults. At all points, EPA was, of course, less than A; this result simply reflects the definition of EPA used here. Of more interest is the comparison between EPA and 0.65A. Fig. 8 shows the variation of these quantities along two lines drawn perpendicular to the faults. Very close to the faults, where earthquakes of small magnitude can cause significant accelerations, EPA is less than 0.65A. On the other hand, well away from the faults EPA exceeds 0.65A, since only earthquakes of large magnitude cause significant motions at these distances. Greater differences may be expected in other situations.

#### SOME EXTENSIONS

Further study will lead to an improved attenuation equation for EPA as it relates to cyclic mobility in saturated sandy soils. An obvious step is to compute EPA directly for a large number of ground motions recorded at different distances from earthquakes of different magnitude, and then to relate EPA to magnitude and distance by regression analysis. Study must also be made of the sensitivity of the resulting attenuation equation to the form of the relation between EPA and  $N_{eq}$  (as in Fig. 3). This research is underway.

It would seem that the approach developed in connection with cyclic mobility might also be utilized for structures. For this purpose it is neces-

sary to develop relations equivalent to those in Fig. 3. There has, of course, already been much study of the effect of duration of ground motion upon the dynamic response of simple structures. [See Reference (8) for a summary of this work]. For an elastic structure subjected to random base motion, the peak response increases slowly. The function expressing this increase may be used to determine combinations of the intensity and duration of motion, all of which are expected to cause some selected level of response to be reached in a given type of structure. A curve drawn through these combinations is the required relation. Similar relations have also been determined for simple gravity-affected hysteretic structures.

If some particular duration is selected as a standard, a structurally-oriented definition of EPA may then be developed. For any ground motion, the EPA would be that intensity of shaking which, when applied over the standard duration, produces the same response as the actual motion. "Response" might mean some prescribed level of elastic distortion, reaching the collapse threshold in a non-linear structure, etc. Once the EPA is related to duration, then expressions connecting duration to magnitude may be used to determine the functional relation between EPA and magnitude.

Actually, research has shown that it is not duration itself which is important, but rather the ratio of duration to the natural period of the structure. This ratio is, in effect, the number of cycles in the response of the structure. This, the definition of EPA as applied to a structure becomes very similar to that developed here in connection with cyclic mobility.

The ultimate aim is to develop risk maps for use in connection with building codes. Thus one wants to map a very small number of parameters which, if used to determine lateral forces and minimum design requirements, lead to roughly equal risks for all buildings in all locations. The foregoing discussion suggests that potentially there is a different relation between EPA, magnitude and distance for each different type of structure, depending upon the period and inelastic characteristics of the structure. The aim of research must be to identify a few such relationships that can account satisfactorily for a wide range of conditions.

#### ACKNOWLEDGEMENTS

This study has been supported in part by Grant ENV73-03345 A-03 from the Division of Advanced Environmental Research and Technology of the National Science Foundation. Professor C.A. Cornell is principal investigator for the work under this grant. Betsy Schumacker, Lecturer in Civil Engineering, developed the computer program for risk analysis. Stephen A. Clifford and Alfredo Urzua-Moll, both graduate students, carried out the computations.

#### REFERENCES

1. Annaki, M. and Lee, K.L., 1976: "Equivalent Uniform Cycle Concept for Soil Dynamics", Liquefaction Problems in Geotechnical Engineering, ASCE Preprint 2752, pp. 227-254.
2. Algermissen, S.T., and Perkins, D.M., 1976: A Probabilistic Estimate of Maximum Acceleration in Rock in the Contiguous United States, U.S. Geological Survey Open File Report 76-416.
3. Cornell, C.A., 1968: "Engineering Seismic Risk Analysis", Bulletin, Seismological Society of America, Vol. 58, pp. 1583-1606.

4. Donovan, N.C., Bolt, B.A. and Whitman, R.V., 1978: "Development of Expectancy Maps and Risk Analysis", Journal, Structural Division, Proceedings, ASCE (in publication).
5. Lee, K.L., and Chan C.K., 1972: "Number of Equivalent Significant Cycles in Strong-Motion Earthquakes", Proceedings, International Conference on Microzonation, University of Washington, Seattle, WA, Vol. II, pp. 609-627.
6. Seed, H.B., 1976: "Evaluation of Soil Liquefaction Effects on Level Ground During Earthquakes", Liquefaction Problems in Geotechnical Engineering, ASCE, preprint 2752, pp. 1-104.
7. Ohashi, M., Iwasaki, T., Wakabayashi, S., and Tokida, K., 1977: "Statistical Analysis of Strong-Motion Acceleration Records", Proceedings, 9th Joint Meeting, U.S. - Japan Panel on Wind and Seismic Effects, U.S. Department of Commerce.
8. Vanmarcke, E.H., 1976: "Structural Response to Earthquakes", Chapter 8 in Seismic Risk and Engineering Decisions, C. Lumnitz and E. Rosenblueth, eds., Elsevier Scientific Publishing Company.

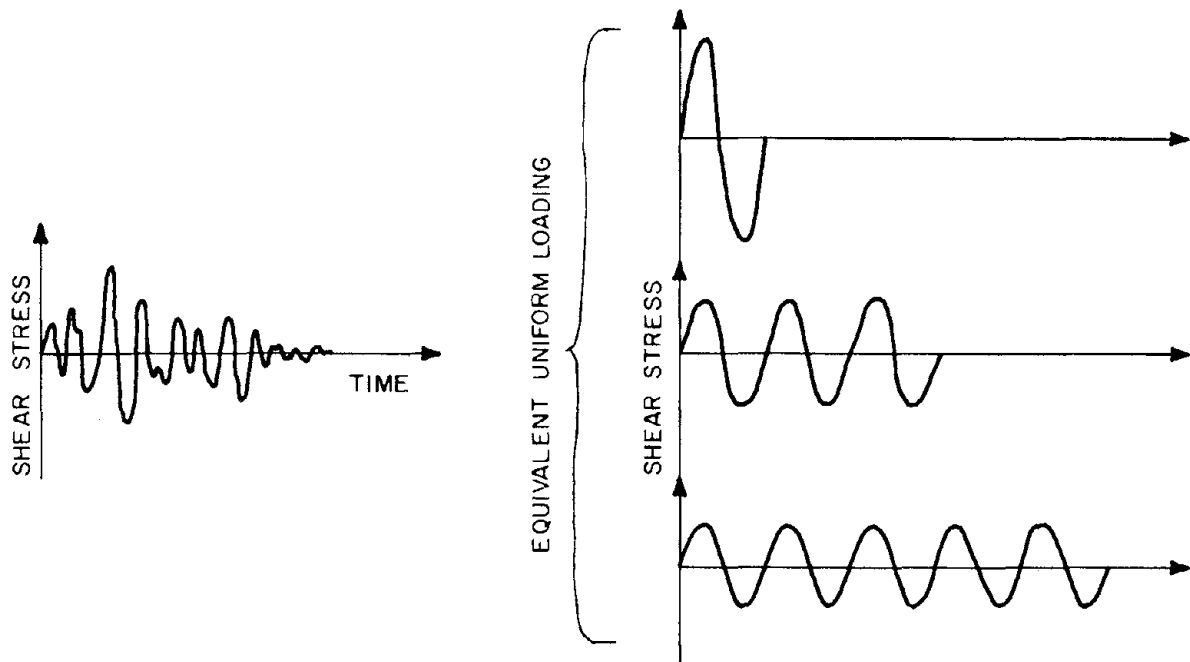


FIGURE 1 EQUIVALENT UNIFORM LOADINGS

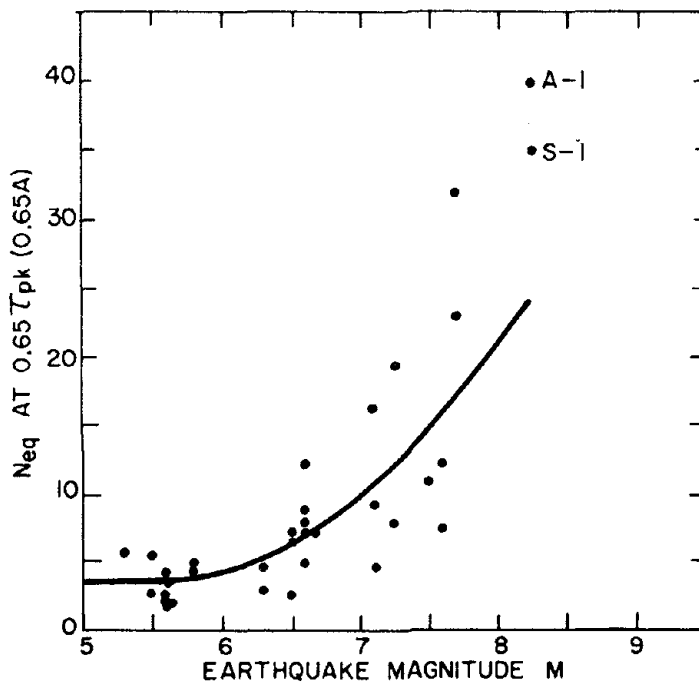


FIGURE 2 EQUIVALENT NUMBERS OF UNIFORM STRESS CYCLES (FROM SEED, 1976)



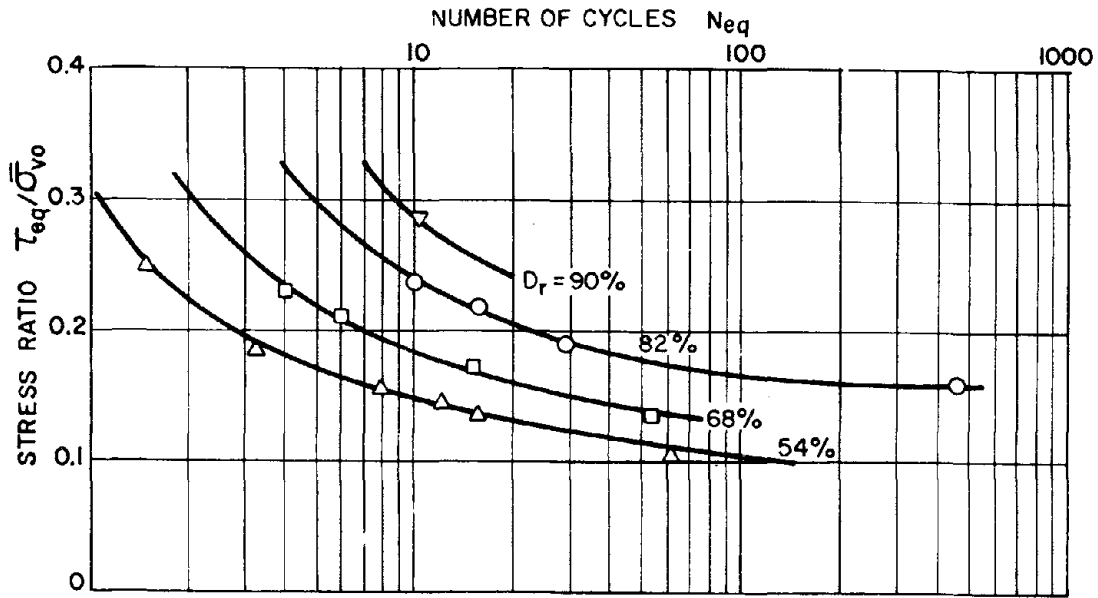


FIGURE 3 COMBINATIONS OF SHEAR STRESS AND NUMBER OF UNIFORM CYCLES CAUSING  $\bar{\sigma} = 0$ . TYPICAL RESULTS FROM SEED (1976)

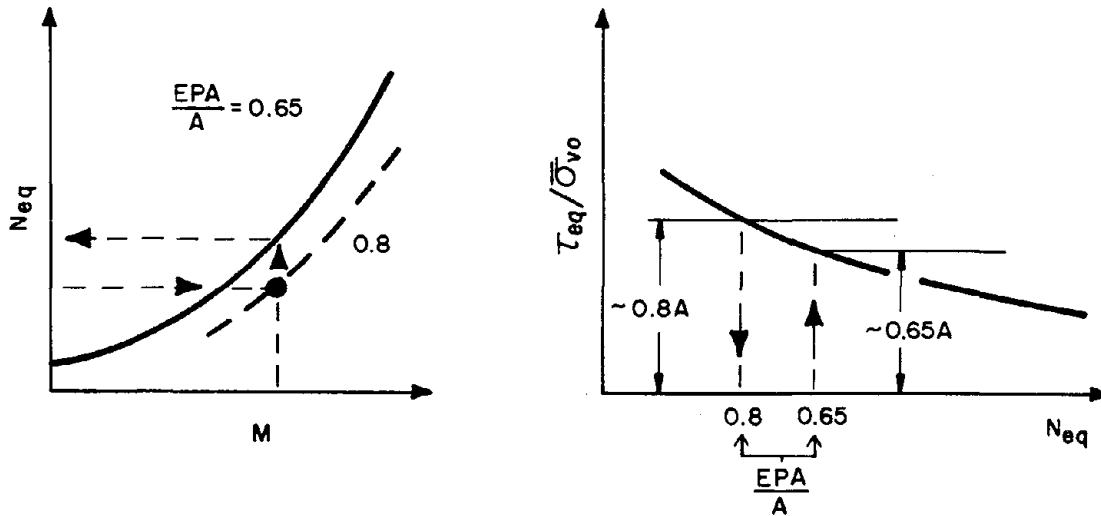


FIGURE 4 PROCEDURE FOR CONSTRUCTING  $N_{eq}$  vs  $M$  CURVES FOR OTHER  $\tau_{eq}/\tau_{pk}$

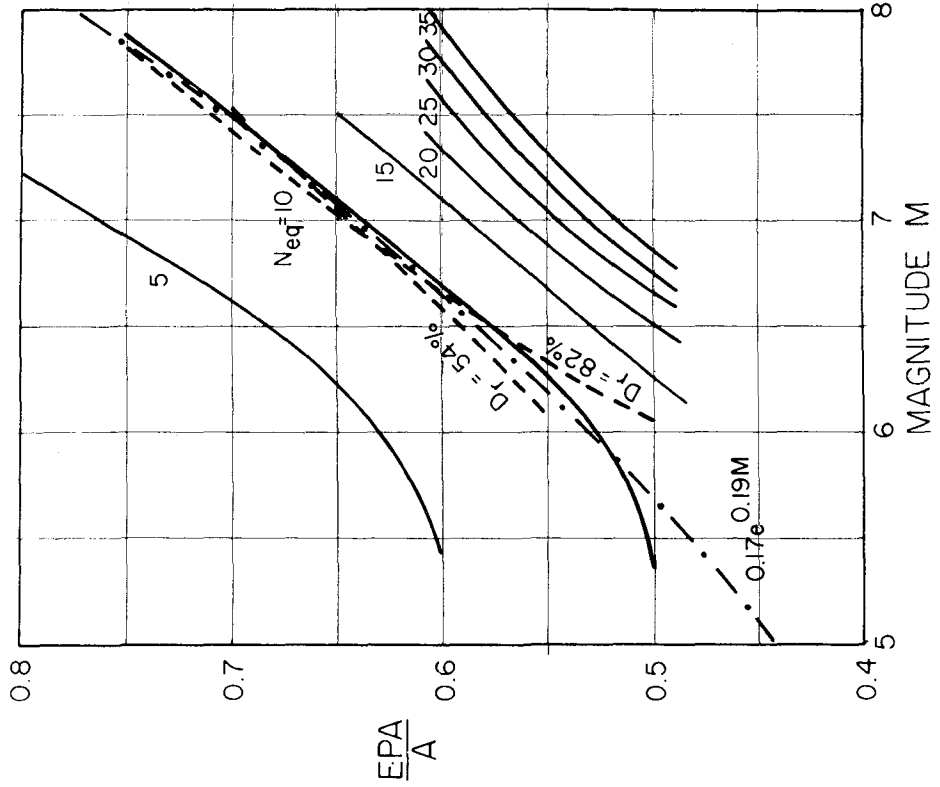


FIGURE 6 EPA/A vs. M FOR VARIOUS  $N_{eq}$  ( $D_r = 68\%$ )

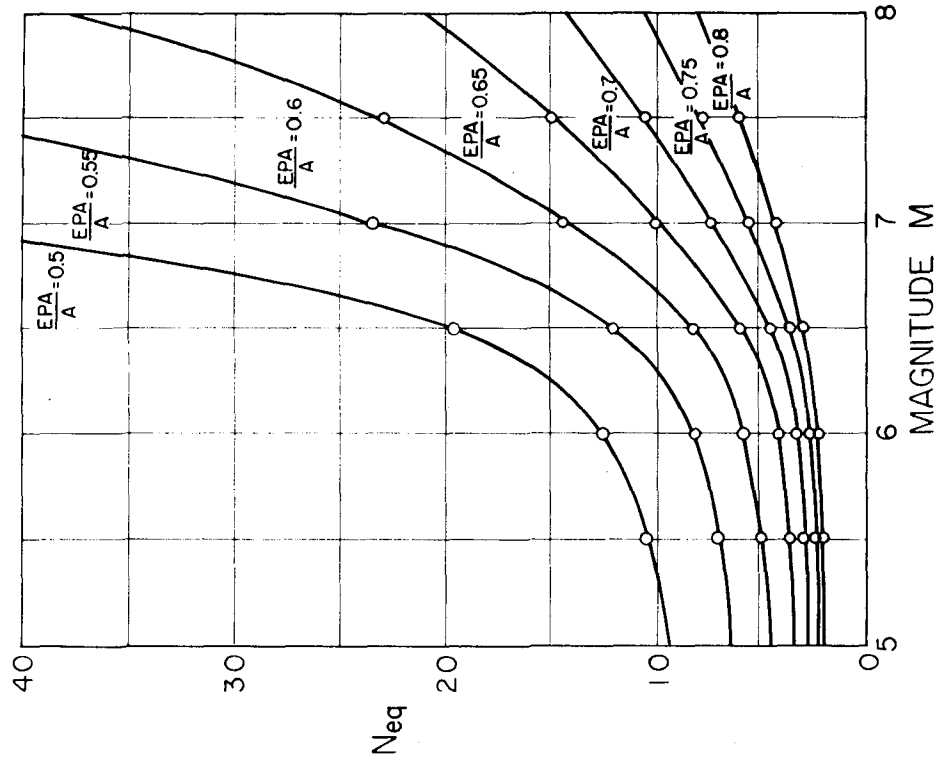


FIGURE 5  $N_{eq}$  vs. M FOR VARIOUS EPA/A ( $D_r = 68\%$ )

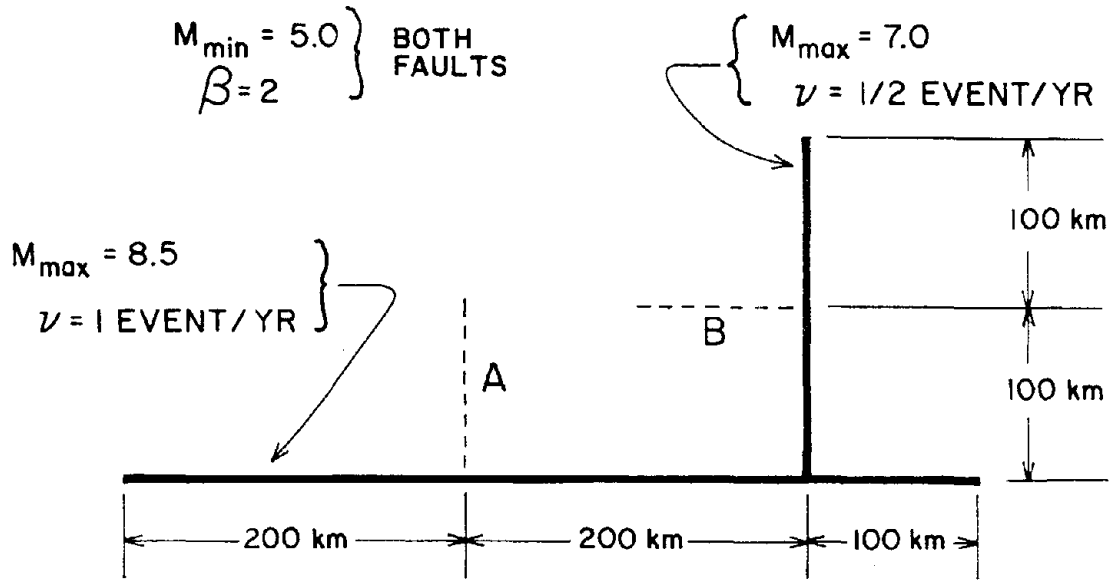


FIGURE 7 FAULT SYSTEM ASSUMED FOR EXAMPLE

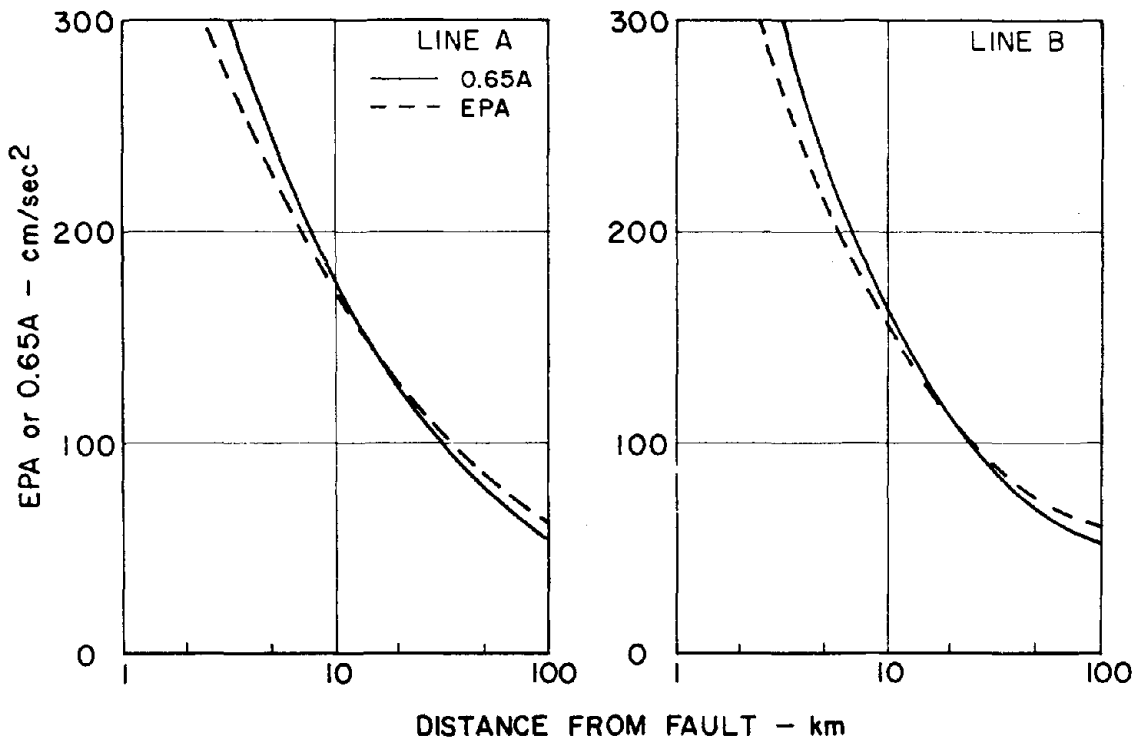


FIGURE 8 EPA AND 0.65A FOR MEAN RECURRENCE INTERVAL OF 500 YEARS

1256

**INTENTIONALLY BLANK**

# A STUDY OF EARTHQUAKE RESPONSE SPECTRA FOR OFFSHORE PLATFORMS

by

B. Mohraz<sup>I</sup> and M. L. Eskijian<sup>II</sup>

## ABSTRACT

This paper examines the earthquake ground motion and spectral amplification for the design of offshore platforms. Since offshore platforms are typically considered flexible structures and thus are sensitive to long periods of vibration, only records with long period oscillation characteristics were included in this statistical study. The long period oscillations of each record were examined by normalizing the Fourier amplitude spectral ordinates of the record, squaring the normalized ordinates, and then computing the area under the curve in the frequency range of interest. The areas provide a pseudo-measure of the power spectral density of the record in the specified frequency range.

The influences of site geology and duration of strong motion on spectral amplification are also investigated and compared with previous studies. The study indicates that substantial differences, particularly in the low frequency range of spectra, exist between the results of this and of previous studies.

## INTRODUCTION

The importance of the response spectrum technique in the aseismic design of structures and equipment is well-known to earthquake design engineers. Since its introduction in 1941 by Biot and Housner (1-3), a number of studies have been carried out to determine the shape and magnitude of earthquake design spectra (4-16). The majority of these studies were based on a statistical analysis of a number of actual earthquake ground motion records and their computed response spectra, and were carried out with the objective of developing recommendations for the earthquake design spectra for nuclear power plants. Most of these studies have used records selected on the basis that the horizontal peak ground acceleration is greater than or equal to 0.05 g's as a criterion for strong motion. While the use of such a limit is justified, there is a general belief that peak ground acceleration is primarily related to high frequency components of the motion (17); therefore, statistical summaries based on such record filtering may not be reliable in the low and even intermediate frequency regions of the spectrum. Although a design spectrum based on such statistical summaries would be satisfactory for structures with short natural periods, such as nuclear power plants, it would not necessarily be appropriate for structures with long periods of oscillation, such as offshore platforms. This study was undertaken to

---

I Associate Professor of Civil Engineering, School of Engineering and Applied Science, Southern Methodist University, Dallas, Texas 75275; Consultant, The Aerospace Corporation

II Member of the Technical Staff, The Aerospace Corporation, El Segundo, California, 90009

provide spectral amplification ratios specifically for offshore oil platform design. The hypothesis being investigated is that long duration earthquakes with above average energy content will govern design spectra of long period platform structures. Previous studies that include records without regard to duration and energy content are believed to result in design spectra too low in the displacement and velocity regions. In this study, the development of spectra is accomplished by selecting from the strong motion data base those records with duration and energy characteristics that are particularly important to platform design.

Earlier studies did not include the influences of such parameters as site geology, epicentral distance, peak ground acceleration, magnitude, and duration on ground motion and response spectra statistical summaries. Later studies (10, 11, 13, 18-22) considered the influence of some of these parameters, and showed that site geology strongly influences both ground motion and spectral amplifications. This study also considers the effects of site geology on spectral amplification.

#### RECORD SELECTION

Ground motion and response spectra data used in this study were selected from the records processed by the Earthquake Engineering Research Laboratory of the California Institute of Technology (23-25). Only ground or basement level, horizontal records were considered in this study.

In order to filter the records for strong motion characteristics, only those records with a peak horizontal ground acceleration equal to or greater than 0.05 g's and a bracketed duration equal to or greater than 5 sec were selected for the study. The bracketed duration requirement is defined as the time interval between the first and last acceleration peaks greater than 0.05 g's. This definition has been used in a number of past studies (26-28). The horizontal records remaining were then subjected to a filtering process designed to preserve records with long period oscillation potential. Each record of Fourier amplitude spectra was normalized, squared and then integrated between the frequencies of 0.125 and 3.0 Hz. This frequency range included the low and intermediate range of the design spectrum (10, 13). The integrand provides a pseudo-measure of the power spectral density of the record in the frequency range of interest. The computed integrands were then averaged, and those greater than the average were selected for the final regression analysis.

As mentioned previously, many earlier studies indicate that site geology strongly influences the spectral amplifications. In this study, the selected records were divided into two categories: (1) "hard"--those on rock or less than 30 ft of alluvium underlain by rock and (2) "soft"--those located on alluvium deposits greater than 30 ft. This classification was selected in order to be utilized with the ground motion maxima obtained from a companion seismic risk study (29; see also Selzer, et al. in these proceedings).

## METHODOLOGY AND DISCUSSION OF RESULTS

The methodology used in this study is basically the same as in previous studies (6, 10, 13). The spectral ordinates are normalized using maximum record values, and then a regression analysis is performed at discrete frequencies. Displacement spectral ordinates are used in the frequency range of 0.10 to 0.30 Hz, velocity ordinates from 0.30 to 3.0 Hz, and acceleration ordinates from 3.0 to 8.0 Hz. Within these three frequency ranges, amplification ratios for the respective ground motion parameters are fairly constant and are averaged to obtain final spectral amplification ratios. Regression is performed twice--once on a normal distribution of the data, and once on a log-normal distribution. A test for correlation of amplification ratio data for the normal and log-normal frequency distributions was performed. Similar to a previous study (13), the log-normal distribution provides a better fit of the data. In addition to the spectral amplification ratios, statistical summaries of ground motion were computed and are included here for comparison with other investigations, e.g., ratios of  $d/a$ ,  $v/a$  and  $ad/v^2$  ( $d$ ,  $v$ , and  $a$  denote displacement, velocity and acceleration, respectively). Results are presented in terms of the median (50 percentile) and the median plus one standard deviation (84.1 percentile).

Ground motion ratios for the two categories are presented in Table 1. For comparison, the results for "rock" (stations on rock deposits) and "alluvium" (stations on an unspecified thickness of alluvium) of a previous study (13) are presented.

Although the differences between the results of the two studies shown in Table 1 are partially due to the manner in which the sites are classified, it is believed that they are primarily caused by the filtering for long period oscillation characteristics. As one might expect, by the selection of records with long period oscillation, the ground displacements are increased. The  $v/a$  ratios for the "hard" and "soft" sites are also greater than the ratios for "rock" and "alluvium", although the increase is not as significant as that for the displacement ratio,  $d/a$ . The  $ad/v^2$  ratios indicate no general trend for the records with long period oscillations. Since this ratio is proportional to displacement, inversely proportional to the velocity squared, increases in  $d$  and  $v$  tend to offset each other. The depth of soil overburden is a significant factor in amplification, and also the duration of strong motion has a greater influence on the amplification for sites with shallow alluvium than for sites with deep alluvium.

Spectral amplifications for 2, 5 and 10 percent of critical damping are given in Table 2. The results of a previous study (13) are presented for comparison. The increase in the displacement amplification ratios is the result of selecting records with long period oscillation characteristics, whereas the increase in the acceleration amplification ratios is the result of selecting records with a duration of strong motion greater than 5 sec. This increase in the acceleration amplification ratios is consistent with the results from a previous study (22).

The spectral amplifications, particularly the 84.1 percentile, computed in this study are very similar for both site categories. In the

comparison study (13) there were appreciable differences in the amplification ratios for "rock" and "alluvium". In that study, the geological classification was more refined. With the introduction of the ground motion, the resulting spectra for the two categories of this study are substantially different.

Although the spectral amplification ratios presented herein are intended for use with the ground motion maxima from seismic risk studies (see ref. 29, for example), response spectra based on the log 50 percentile ground motion and 84.1 percentile amplification ratios are computed and presented for comparison to previous studies. To be consistent with other studies, ground motion is normalized to  $1.0 g^1_s$ , and velocity and displacement were computed from the  $v/a$  and  $ad/v^2$  ratios, respectively. The spectra for 2, 5 and 10 percent critical damping for "hard" and "soft" sites are given in Figures 1 and 2. A comparison of 5 percent critical damping spectra from this study and others is presented in Figure 3. This figure indicates that the spectra constructed from this study are generally higher in the velocity and displacement regions than spectra from other studies.

#### SUMMARY AND CONCLUSIONS

Regression analyses of ground motion and spectral amplifications for records with long period oscillation characteristics for two site categories are presented and compared to previous studies. The results indicate that displacement and velocity spectral bounds (based on the product of 50 percentile ground motion and 84.1 percentile amplification) are different from those of other investigations. The difference reflects mainly the influence of the long period oscillation characteristics of the record which is important in the design of flexible offshore platforms. The amplification ratios presented in this study are intended specifically for use with ground motion isoseismal maps (29) in preparing design response spectra for offshore platforms.

#### ACKNOWLEDGMENTS

The investigation reported herein is part of a study (29) performed by The Aerospace Corporation, for the U.S. Geological Survey, Department of the Interior.<sup>III</sup> The authors would like to express their appreciation to Mr. P. Stevens, principal investigator, and Mr. L. Selzer, Manager of the Design Evaluation Section, The Aerospace Corporation, for their suggestions during the course of this investigation.

---

III The views and conclusions contained in this document are those of the authors and should not be interpreted as necessarily representing the official policies, either expressed or implied, of the U.S. Government.



## REFERENCES

1. Biot, M. A., "A Mechanical Analyzer for the Prediction of Earthquake Stresses," Bull. Seism. Soc. Am., Vol. 31, No. 2 (1941).
2. Biot, M. A., "Analytical and Experimental Methods in Engineering Seismology," Proceedings of the American Society of Civil Engineers, Vol. 68 (1942).
3. Housner, G. W., "An Investigation of the Effects of Earthquakes on Buildings," Ph.D. Thesis, California Institute of Technology, Pasadena, California (1941).
4. Newmark, N.M. and W.J. Hall, "Seismic Design Criteria for Nuclear Reactor Facilities," Proceedings of the Fourth World Conference in Earthquake Engineering, Santiago, Chile (1969).
5. Blume, J.A., R.L. Sharpe, and J.S. Dalal, "Recommendations for Shape of Earthquake Response Spectra," John A. Blume & Associates, Engineers, San Francisco, California, USAEC Contract No. AT(49-5)-3011 (1972), (AEC Report WASH-1254, February 1973).
6. Mohraz, B., W.J. Hall, and N.M. Newmark, "A Study of Vertical and Horizontal Earthquake Spectra," Nathan M. Newmark Consulting Engineering Services, Urbana, Illinois (1972), (AEC Report WASH-1255, April 1973).
7. Newmark, N.M., J.A. Blume, and K.K. Kapur, "Seismic Design Spectra for Nuclear Power Plants," Journal of the Power Division, ASCE, Vol. 99, No. P02, Proc. Paper 10142 (1973).
8. Virdee, A.S. and R. L. Sharpe, "Present Seismic Code and Future Directions--SEAOC," Paper presented at the ASCE National Structural Engineering Meeting, April 22-26, Cincinnati, Ohio (1974).
9. Fallgren, R. B., P.C. Jennings, J. L. Smith and D.K. Ostrom, "Aseismic Design Criteria for Electrical Facilities," Journal of the Power Division, ASCE Vol. 100, No. P01 (1974).
10. Hall, W.J., B. Mohraz, and N.M. Newmark, "Statistical Studies of Vertical and Horizontal Earthquake Spectra," Nathan M. Newmark Consulting Engineering Services, Urbana, Illinois (1975), (NRC Report NUREG-0003, 1976).
11. Seed, H. B., C. Ugas, and J. Lysmer, "Site-Dependent Spectra for Earthquake-Resistance Design," Bull. Seism. Soc. Am., Vol. 66, No. 1 (1976).
12. Bolt, B. A., R.G. Johnston, J. Lefter, and M.A. Sozen, "The Study of Earthquake Questions Related to Veterans Administration Hospital Facilities," Bull. Seism. Soc. Am., Vol. 65, No. 4 (1975).

13. Mohraz, B., "A Study of Earthquake Response Spectra for Different Geological Conditions," Bull. Seism. Soc. Am., Vol. 66, No. 3 (1976).
14. Housner, G. W., "Design Spectrum," Chapter 5 in Earthquake Engineering, R. L. Weigel (ed.), Prentice-Hall, Inc., Englewood Cliffs, New Jersey (1970).
15. Housner, G. W., "Behavior of Structures During Earthquakes," Journal of the Engineering Mechanics Division, ASCE, Vol. 85, No. EM4 (1959).
16. "Design Response Spectra for Seismic Design of Nuclear Power Plants," Regulatory Guide 1.60, Directorate of Regulatory Standards, U.S. Atomic Energy Commission, Washington, D. C. (1973).
17. Dalal, J. S. and P. R. Perumalswami, "Significance of Seismic Response Spectrum Normalization in Nuclear Power Plant Design," Presented at the Fourth International Conference on Structural Mechanics in Reactor Technology, San Francisco, California, August 1977, and to be published in Nuclear Engineering and Design (1978).
18. McGuire, R. K., "Seismic Structural Response Risk Analysis, Incorporating Peak Response Regressions on Earthquake Magnitude and Distance," Structures Publication No. 399, Department of Civil Engineering, Massachusetts Institute of Technology, Cambridge, Massachusetts (1974).
19. Cherry, J. T., E. J. Halda, and K. G. Hamilton, "A Deterministic Approach to the Prediction of Free Field Ground Motion and Response Spectra from Stick-Slip Earthquakes," Systems Science and Software, La Jolla, California (1974).
20. Hall, W. J., B. Mohraz, and N. M. Newmark, "Statistical Analysis of Earthquake Response Spectra," Proceedings of the Third International Conference on Structure Mechanics in Reactor Technology, London, England (1975).
21. Mohraz, B., "Comments on Earthquake Response Spectra," Presented at the Fourth International Conference on Structural Mechanics in Reactor Technology, San Francisco, California, August 1977, and to be published in Nuclear Engineering and Design (1978).
22. Mohraz, B., "Influences of the Magnitude of the Earthquake and the Duration of Strong Motion on Earthquake Response Spectra," Proceedings of the Central American Conference on Earthquake Engineering, San Salvador (1978).
23. "Analysis of Strong Motion Earthquake Accelerograms--Digitized and Plotted Data, Vol. II: Corrected Accelerograms and Integrated Ground Velocity and Displacement Curves, Parts A through Y," Earthquake Engineering Research Laboratory, California Institute of Technology, Pasadena, California (1972-1974).

24. "Analysis of Strong Motion Earthquake Accelerograms, Vol. III-- Response Spectra, Parts A through Y, " Earthquake Engineering Research Laboratory, California Institute of Technology, Pasadena, California (1972-1974).
25. "Analysis of Strong Motion Earthquake Accelerograms, Vol. IV-- Fourier Amplitude Spectra, Parts A through Y, " Earthquake Engineering Research Laboratory, California Institute of Technology, Pasadena, California (1972-1974).
26. Page, R.A., D.M. Boore, W.B. Joyner, and H.M. Coulter, "Ground Motion Values for Use in the Seismic Design of the Trans-Alaska Pipeline System, " Geological Survey Circular 672, Washington, D.C. (1972).
27. Bolt, B.A., "Duration of Strong Ground Motion, " Proceedings, Fifth World Conference on Earthquake Engineering, Rome, Italy (1974).
28. Cloud, W.K., "Strong Motion During Earthquakes, " Proceedings, Fifth World Conference on Earthquake Engineering, Rome, Italy (1974).
29. "Environmental Design Data for Gulf of Alaska, Mid-Atlantic and Southern California Outer Continental Shelf Regions, " Summary Final Report prepared for the U.S.G.S. by The Aerospace Corporation (1977).
30. "API Recommended Practice for Planning, Designing, and Constructing Fixed Offshore Platforms, " API RP 2A, American Petroleum Institute, Eighth Edition (1977).

Table 1. Summary of Ground Motion Ratios (Log-Normal Distribution)

Classification	Number of Components	d/a (in/g)		v/a (in/sec)/g		ad/v <sup>2</sup>	
		Percentile					
		50%	84.1%	50%	84.1%	50%	84.1%
Hard	14	23	34	48	69	3.9	6.4
Soft	67	34	48	56	78	4.1	6.0
Rock* (Ref. 13)	13	8	15	24	38	5.3	11.0
Alluvium* (Ref. 13)	25	23	44	48	69	3.9	6.0

\* Based on the largest of the two horizontal components of peak ground acceleration.

Table 2. Summary of Spectral Amplifications (Log-Normal Distribution)

Classification	Damping (% of critical)	Displacement		Velocity		Acceleration	
		Percentile					
		50%	84.1%	50%	84.1%	50%	84.1%
Hard	2	2.73	3.52	1.67	2.34	2.78	4.03
	5	2.39	2.99	1.32	1.78	2.12	2.94
	10	2.00	2.41	1.04	1.34	1.70	2.27
Soft	2	2.67	3.52	1.60	2.22	3.04	4.08
	5	2.30	2.95	1.26	1.69	2.28	2.91
	10	1.92	2.39	0.99	1.29	1.80	2.20
Rock* (Ref. 13)	2	2.13	3.29	1.57	2.44	2.57	3.80
	5	1.83	2.71	1.28	1.90	1.98	2.82
	10	1.53	2.16	1.04	1.48	1.56	2.11
Alluvium* (Ref. 13)	2	2.51	3.43	1.84	2.77	2.60	3.55
	5	2.07	2.78	1.44	2.08	2.01	2.58
	10	1.68	2.19	1.13	1.58	1.62	1.99

\* Based on the largest of the two horizontal components of peak ground acceleration.

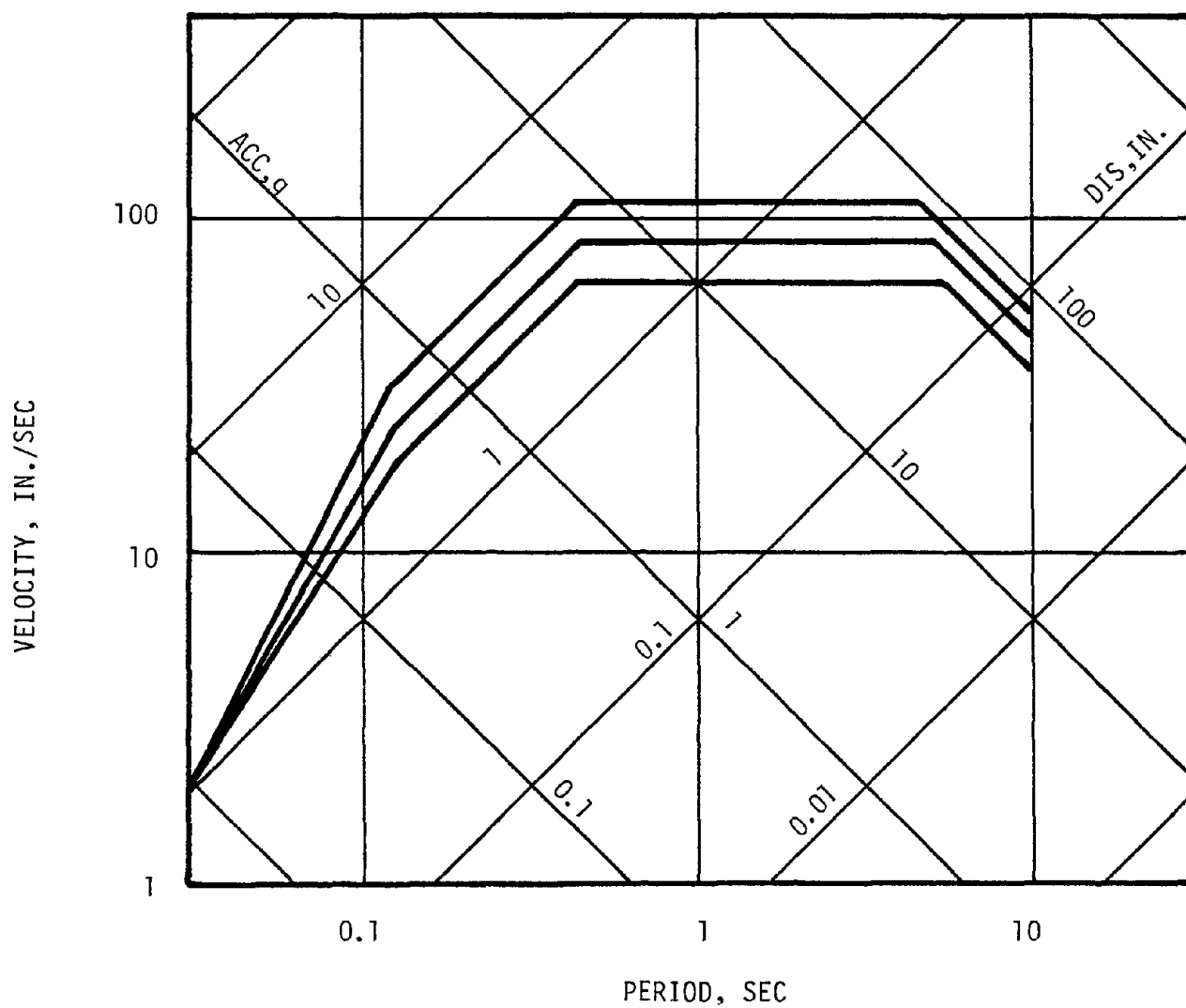


FIG. 1 - RESPONSE SPECTRA FOR 2, 5, AND 10 PERCENT OF CRITICAL DAMPING FOR "HARD" SITE. (Log-Normal 50 percentile ground motion and 84.1 percentile amplifications)

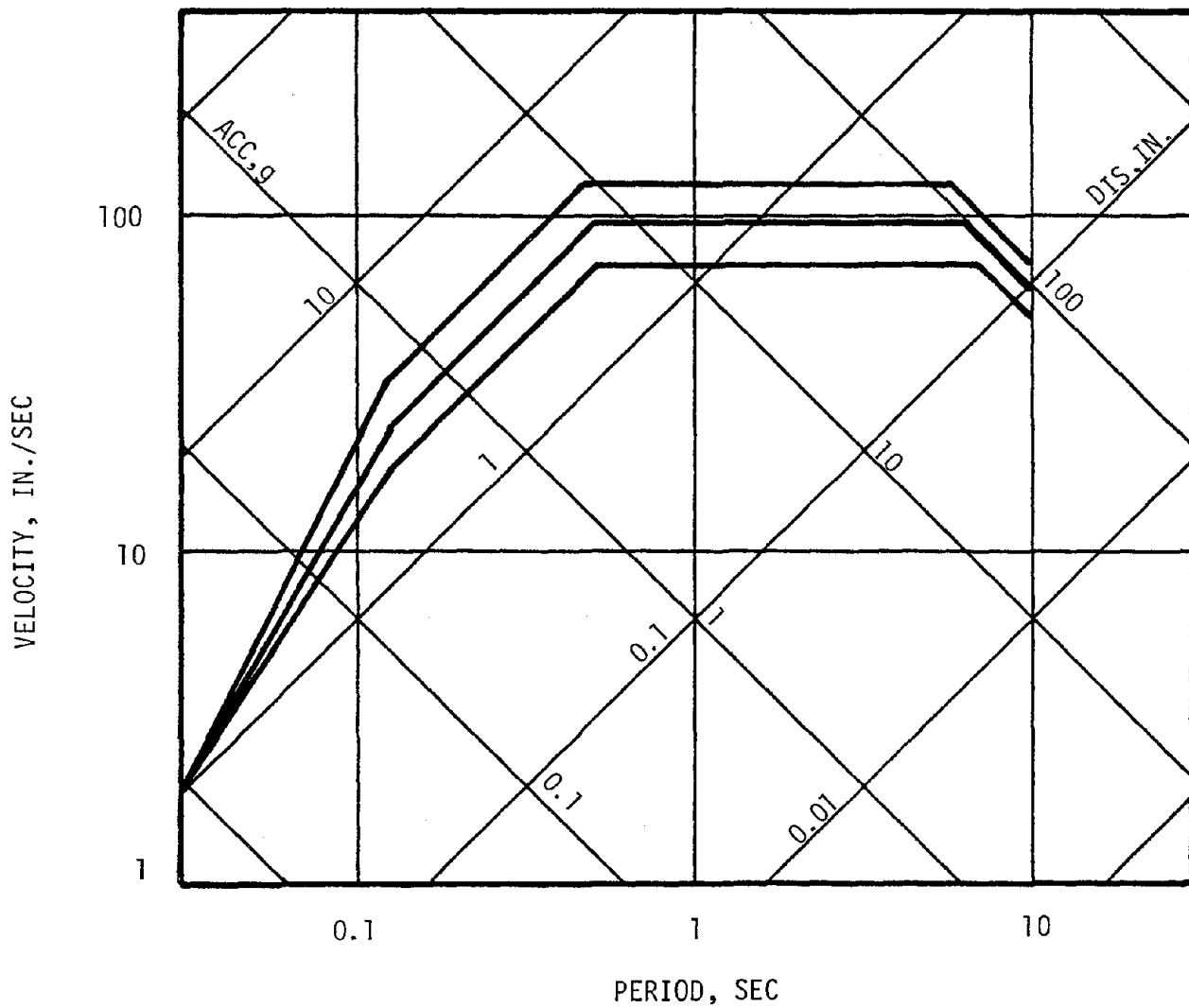
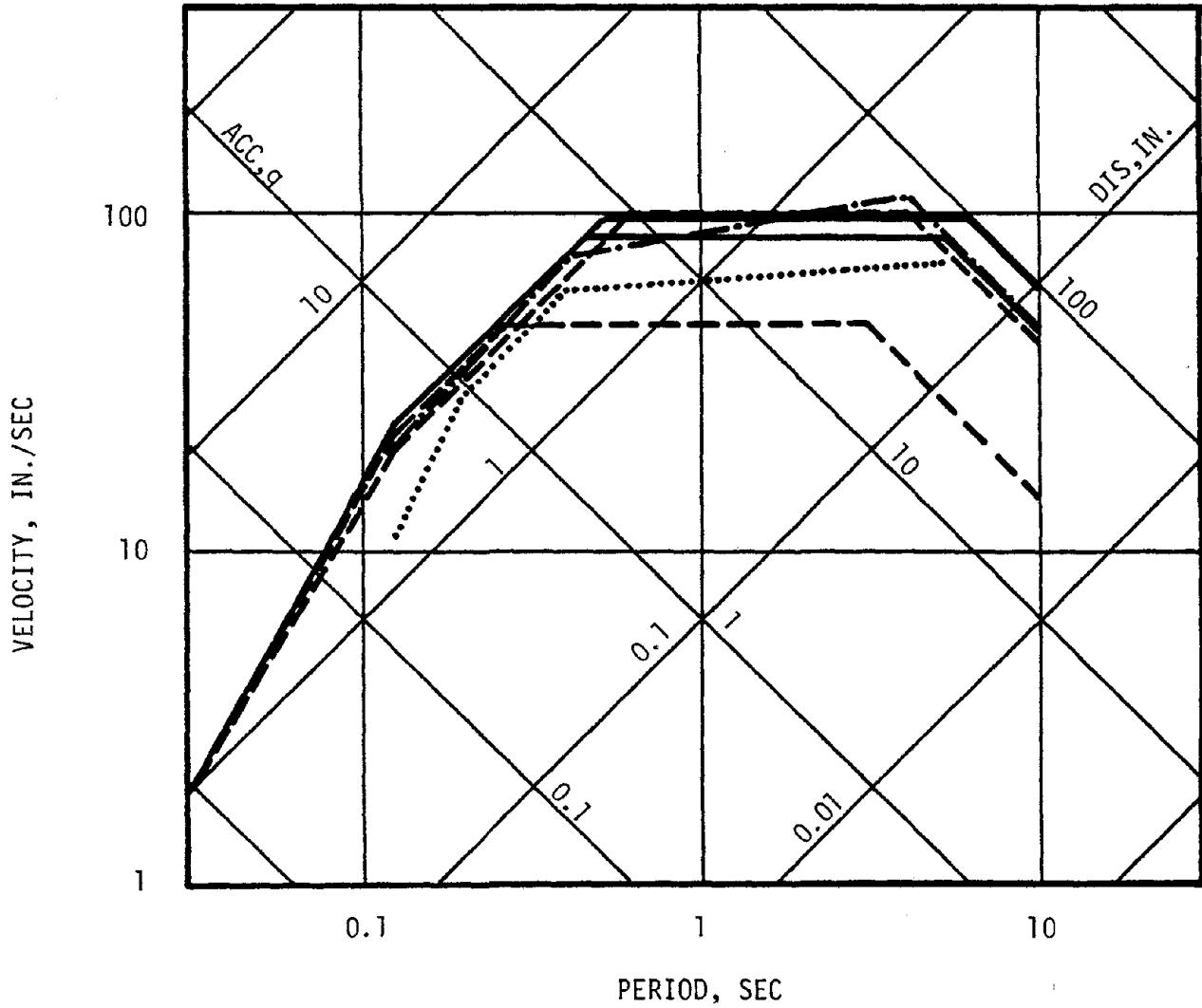


FIG. 2 - RESPONSE SPECTRA FOR 2, 5, AND 10 PERCENT OF CRITICAL DAMPING FOR "SOFT" SITE. (Log-Normal 50 percentile ground motion and 84.1 percentile amplifications)



- "HARD" AND "SOFT" THIS STUDY
- - - ROCK AND ALLUVIUM (REF. 13)
- · - · NRC REGULATORY GUIDE 1.60 (REF. 16)
- API RP 2A (REF. 30)

FIG. 3 - COMPARISON OF RESPONSE SPECTRA FOR 5 PERCENT OF CRITICAL DAMPING.

1268

**INTENTIONALLY BLANK**



INFLUENCE OF SOIL-STRUCTURE INTERACTION EFFECTS  
ON DYNAMIC RESPONSE OF LARGE PANNEL PREFABRICATED  
BUILDINGS

by  
Jakim Petrovski<sup>I</sup>

ABSTRACT

Assumption of fixed base of the structures into the soil media considering it as a rigid nondeformable media is widely used in the existing methods for structural dynamic response analysis. Presented experimental results from full-scale forced vibration studies of rigid structures are showing that this assumption has hardly an appropriate physical justification.

Using dynamic properties obtained from full-scale forced vibration study formulation of the mathematical model of five and twenty-two storey large pannel prefabricated buildings is performed.

Comparing the results from the respinse analysis of the fixed and flexible base model of the buildings, an increase of the base shear up to 50 percents is obtained. It is concluded that the influence of soil-structure interaction ought to be considered in the case of typified construction of large-pannel prefabricated buildings and similar rigid structures, in particular due to the effect of significant increase of lateral forces not considered in the existing seismic design codes.

INTRODUCTION

In order to find solution of the serious housing problems many European countries (USSR, France, Denmark, U.K., Germany, Romania, Yugoslavia and others) adopted large-pannel prefabricated structural system as favourable from both structural and constructional point of view (6). The system was developed initially for application in non-seismic zones and in most of the cases was automatically adopted for seismic zones with minor changes. Besides the structural problems connected with satisfactory determination of elastic and post-elastic structural behaviour, the influence of soil flexibility on the dynamic response of this type of rather stiff system is playing very important role. The system is usually used for mass construction and the design of different types of buildings is performed based on standard seismic code requirements in which the effect of soil flexibility influence on the structural response is not taken into account.

Studies on the influence of the soil media flexibility on the damage ratio of the large-pannel prefabricated structures in the past earthquakes (3,6) as well as recent forced vibration studies of the full-scale structures and strong motion records (4,5) had shown that the soil media flexibility has a significant influence on the dynamic response of this type of structures.

From the above evidence it appears that widely used assumption treating the structure fixed in the soil media hardly has any physical justification.

---

I Director and Professor, Institute of Earthquake Engineering and Engineering Seismology, University of Skopje, Yugoslavia.

In order to have more realistic prediction of the structural response, it will be desirable in the formulation of the mathematical models of the structural systems to include the soil media flexibility.

The soil media flexibility, or as it is commonly used soil-structure interaction, depends basically on the mechanism of energy transmission between the soil media and the structure itself. The primary effects of interaction phenomena consist in the resonant frequencies modification and the energy absorption increase.

#### SOIL-STRUCTURE INTERACTION PARAMETERS EVALUATION

An effort for evaluation of soil-structure interaction parameters from the dynamic response of embedded footings has been presented in (4) and (5). Basic assumptions in their evaluation is that the equivalent linear dynamic properties of the soil media are valid if they are obtained from the dynamic test simulating the embedment conditions and the excitation levels on the structural foundation model in the same soil conditions of the contact area as for the structural system considered.

Using approximate analytical solution for the coupled horizontal and rocking vibration of embedded footings (4) and field experimental results from the dynamic response of the foundation models, a reverse analytical procedure has been applied for evaluation of the equivalent linear dynamic properties of the soil media for different excitation levels. This procedure enables presentation of the nonlinear behaviour of the soil media with equivalent linear properties depending on the level of deformation involved in the system. In this manner the biggest insufficiency of the discrete model is exceeded. On Fig. 1 the diagrams of equivalent shear moduli of the subsoil and the side soil, dependent on the deformations in the soil-foundation system for rectangular footings, are given.

In order to check validity of the presented assumptions a full-scale forced vibration study of the five and twenty-two storey large panel prefabricated buildings founded in the same soil conditions was performed. For the magnitude of deformations on the foundation level and the diagrams on Fig. 1 the values for equivalent shear moduli were obtained. Values of the soil-structure interaction parameters could be now calculated for the particular case using corresponding equations to determine equivalent values of the shear moduli (4,5).

#### MATHEMATICAL MODEL FORMULATION

In order to determine the influence of the interaction phenomenon on the dynamic properties of the structure, an Euler beam model was developed. The differential equation for free vibration of a beam can be written in the following form:

$$EI \frac{\partial^4 U}{\partial x^4} + \bar{m} \frac{\partial^2 U}{\partial t^2} - \bar{m} r^2 \frac{\partial^2 U}{\partial t^2 \partial x^2} + \frac{\bar{m}}{K'A} (\bar{m} r^2 \frac{\partial^4 U}{\partial t^4} - EI \frac{\partial^4 U}{\partial x^2 \partial t^2}) \dots \dots \dots (1)$$

where:

- |  |                       |
|--|-----------------------|
| E = modulus of elasticity                    | K'A = effective shear |
| I = moment of inertia of the beam            | area of the section   |
| $\bar{m}$ = mass per unit length             |                       |
| r = radius of gyration of the cross section. |                       |

Using the Laplace transform, equation (1) can be transformed into the following form:

$$\phi''(x) + \left( a^4 r^2 + \frac{\bar{m} \omega^2}{K'AG} \right) \phi''(x) - a^4 \left( 1 - \frac{\bar{m} \omega^2 r^2}{K'AG} \right) \phi(x) = 0 \quad \dots\dots\dots(2)$$

where

$$a^4 = \frac{\bar{m} \omega^2}{EI}$$

and  $\omega$  is the characteristic frequency of vibration in radians per second. The solution of equation (2) can be obtained in a standard way by assuming a solution in a form

$$\phi(x) = C e^{sx} \quad \dots\dots\dots(3)$$

which leads to the final shape function expression

$$\phi(x) = D_1 \sin \delta x + D_2 \cos \delta x + D_3 \operatorname{sh} \epsilon x + D_4 \operatorname{ch} \epsilon x \quad \dots\dots\dots(4)$$

where  $\delta$  and  $\epsilon$  are functions of  $a$ .

From the boundary conditions of the beam for flexible base model, the following matrix equation can be written:

$$\begin{bmatrix} \frac{EI}{K_1} \delta^3 & -1 & -\frac{EI}{K_1} \epsilon^2 & -1 \\ \delta & -\frac{EI}{K_2} \delta^2 & +\epsilon & -\frac{EI}{K_2} \epsilon^2 \\ -\delta^2 \sin \delta_L & -\delta^2 \cos \delta_L & \epsilon^2 \operatorname{sh} \epsilon_L & \epsilon^2 \operatorname{ch} \epsilon_L \\ -\delta^3 \cos \delta_L & \delta^3 \sin \delta_L & \epsilon^3 \operatorname{ch} \epsilon_L & \epsilon^3 \operatorname{sh} \epsilon_L \end{bmatrix} \begin{Bmatrix} D_1 \\ D_2 \\ D_3 \\ D_4 \end{Bmatrix} = 0 \quad \dots\dots\dots(5)$$

For the coefficients to be nonzero, this equation requires that the determinant of the square matrix vanish; setting this determinant equal to zero provides the frequency equation from which the frequencies of vibration of the cantilever beam can be obtained. Expressing the coefficients  $D_2$ ,  $D_3$  and  $D_4$  from equation (5) in terms of only the first coefficient, the mode shape can be obtained from the equation (4).

#### DYNAMIC PROPERTIES OF THE BUILDINGS

In order to study the influence of the soil-structure interaction on the dynamic response of large-panel prefabricated buildings, forced-vibration full-scale study was performed on five and twenty-two storey buildings with typical floor plans and cross sections as shown in Figs. 2 and 3.

The resonant frequencies and damping coefficients for the first mode of vibration of the five and twenty-two storey buildings are given in Table 1. and experimental mode shapes are presented in the Figs. 3 and 4.

Direction	Five Storey Bldg.		Twenty-two Storey Bldg.	
	fr (c/s)	$\beta$ (%)	fr (c/s)	$\beta$ (%)
E - W	5.05	6.4-7.2	0.97	2.0
N - S	5.15	3.9-4.1	1.32	3.0

For checking of the validity of the evaluated soil-structure interaction parameters and formulation of the mathematical model using described procedure a fixed base and flexible base model of both buildings in transverse direction were analysed and the results are presented in the Figs. 4 and 5. It could be easily seen that for the fixed base model there is a significant difference in the mode shapes and the resonant frequencies differ for the five storey building for about 100% and for the twenty-two storey building for 12%. In the case of the flexible base model there is practically no difference in the mode shapes and the variation of the experimental and analytical resonant frequency is within 1 and 4.5% (Figs. 4 and 5).

#### DYNAMIC RESPONSE DIFFERENCE

For the five storey building the dynamic response for the fixed base and the flexible base model were analysed for the El Centro 1940 N-S component and Port Hueneme 1957 N-S component. Comparing the base shear for both models an increase of 49.4% for El Centro and 23% for Port Hueneme was obtained for the flexible base model in respect to the fixed base one.

#### CONCLUSIONS

The presented procedure for evaluation of the mathematical model of the structural system including soil-structure interaction effect is demonstrated comparing analytical and experimental dynamic properties of the studied large-panel buildings.

There is evidence of an increase of 20-50% of the base shear due to the interaction effect on the studied structural system. Significant increase of the inertia forces in the rigid structural systems could be obtained due to effect of soil media flexibility, producing large damage on the superstructure in the case of firm soil and large foundation differential settlements in the case of soft soil. For the last one this effect could be larger due to more intensive modification of the resonant frequencies and the smaller effect of the energy absorption.

The largest number of buildings in housing development in most of the countries are presenting low storey rigid structures, particularly those of large panel prefabricated buildings or similar. The existing design regulations and code of practice are neglecting the soil-structure interaction effect. Some of the intensive damage and collapse of the structural systems in the past earthquakes (Skopje, Anchorage, Niigata) could be better explained if the soil flexibility effect is considered. In order to minimize damage potential in the future construction it will be desirable to pay more attention studying the soil-structure interaction phenomenon and applying it in the codes for design and construction in the seismic areas.

## REFERENCES

1. Ambraseys, N.N. (1973), "Dynamics and Response of Foundation Materials in Epicentral Regions of Strong Earthquakes", Invited Paper, IWCEE, Rome, 1973.
2. Jurukovski, D., Petrovski, J. and Tashkov, Lj. (1978), "A Cantilever Beam Model of a Twenty-two Storey Building with Included Translation and Rotation of the Foundation", Preprints, VICEE, Dubrovnik, September, 1978.
3. Martemjanov, A.I. (1977), "Influence of the Foundation Design on Seismic Resistance of Large-Panel Prefabricated Buildings", (in Russian), Osnovaniya, Fundamenti i Mehanika Gruntov, No.6, Moscow, November, 1977.
4. Petrovski, J. (1977), "Prediction of Dynamic Response of Embedded Foundation", Preprints VIWCEE, New Delhi, January, 1977.
5. Petrovski, J. and Jurukovski, D. (1977), "Influence of Soil-Structure Interaction on Dynamic Response of Structures", Preprints VIWCEE, New Delhi, January, 1977.
6. Velkov, M. and Jurukovski, D. (1977), "Some Aspects of Application and Behaviour of Large-Panel Prefabricated Systems in Seismic Regions of Europe", Workshop on ERCBC, University of California, Berkeley, July 11-15, 1977.

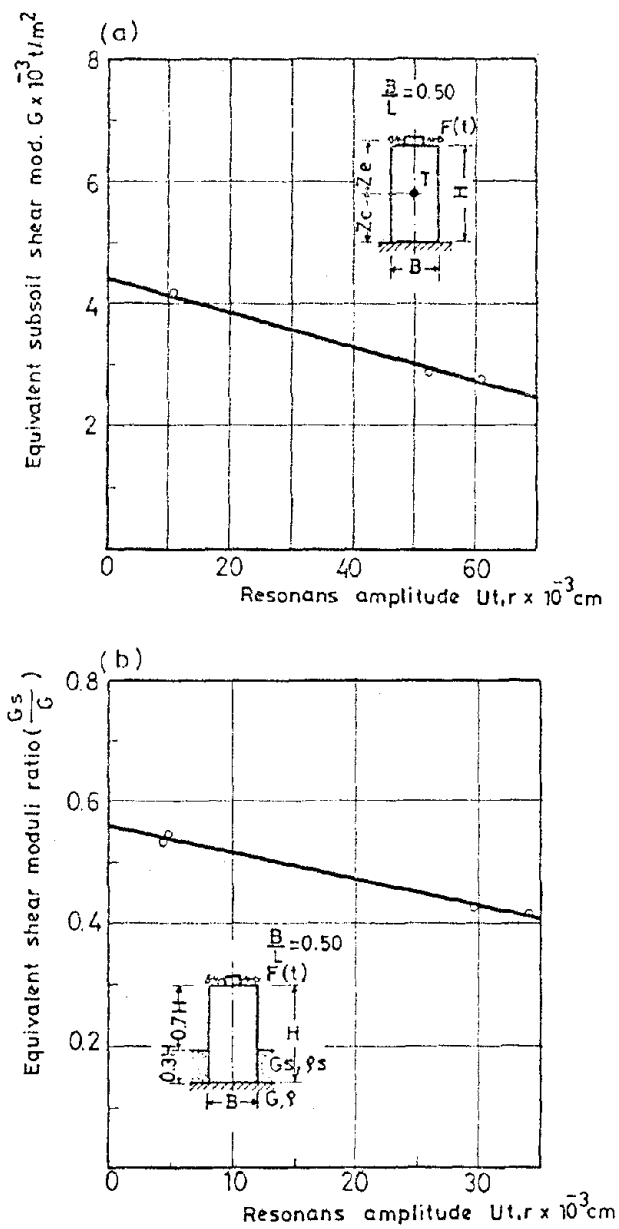


Figure 1. EQUIVALENT SHEAR MODULI FROM DYNAMIC RESPONSE OF FOOTINGS FOR SANDY GRAVEL

(a) Shear Moduli for Subsoil

(b) Shear Moduli Ratio for Sidesoil

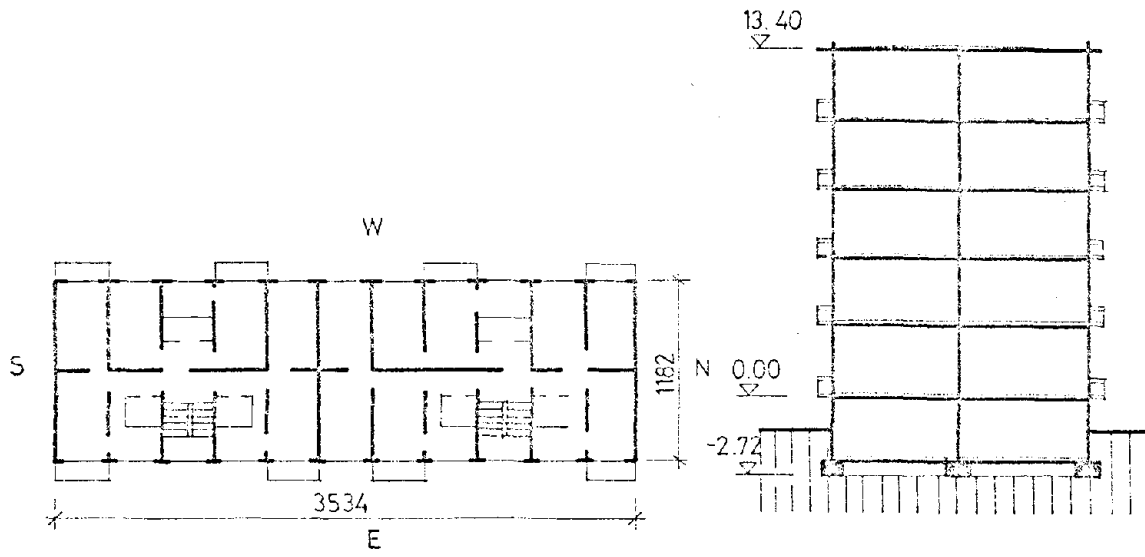


Figure 2. TYPICAL PLAN AND CROSS SECTION OF THE FIVE-STOREY BUILDING

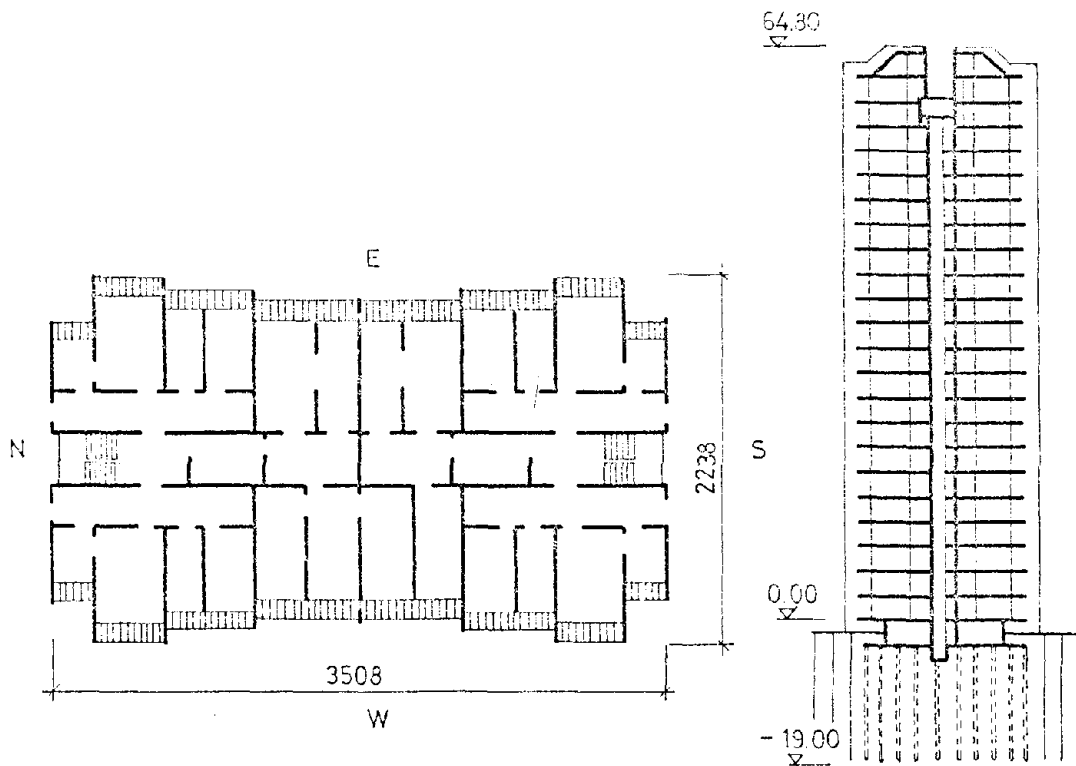


Figure 3. TYPICAL PLAN AND CROSS SECTION OF THE TWENTYTWO-STOREY BUILDING



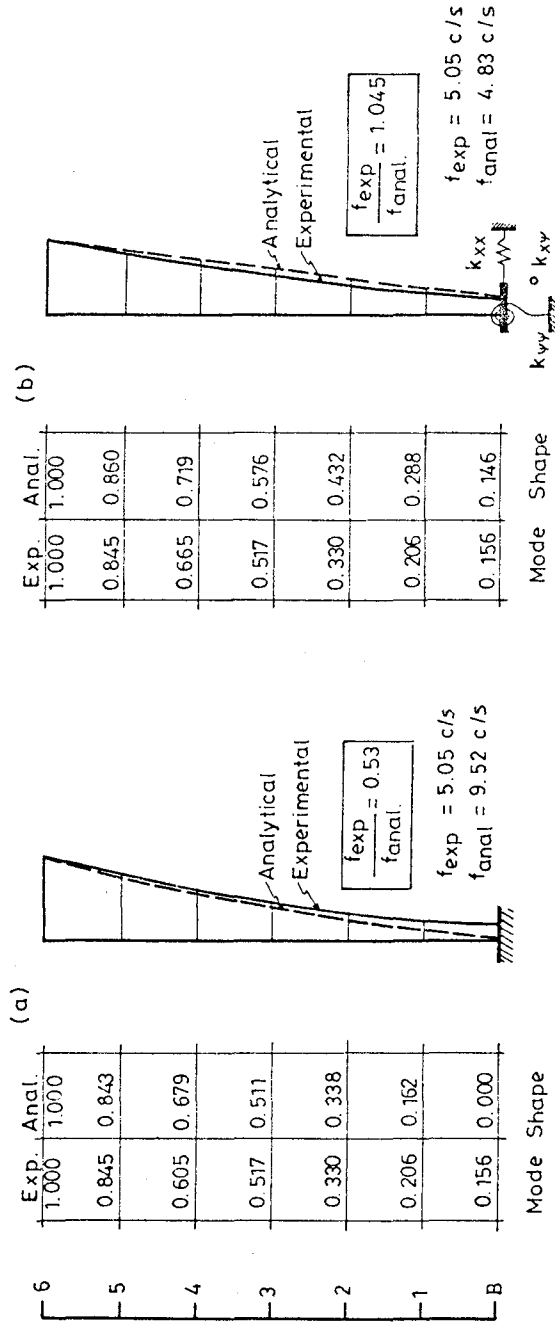


Figure 4. COMPARISON OF EXPERIMENTAL AND ANALYTICAL DYNAMIC PROPERTIES OF FIVE-STORY BUILDING

- (a) Fixed Base Model
- (b) Flexible Base Model



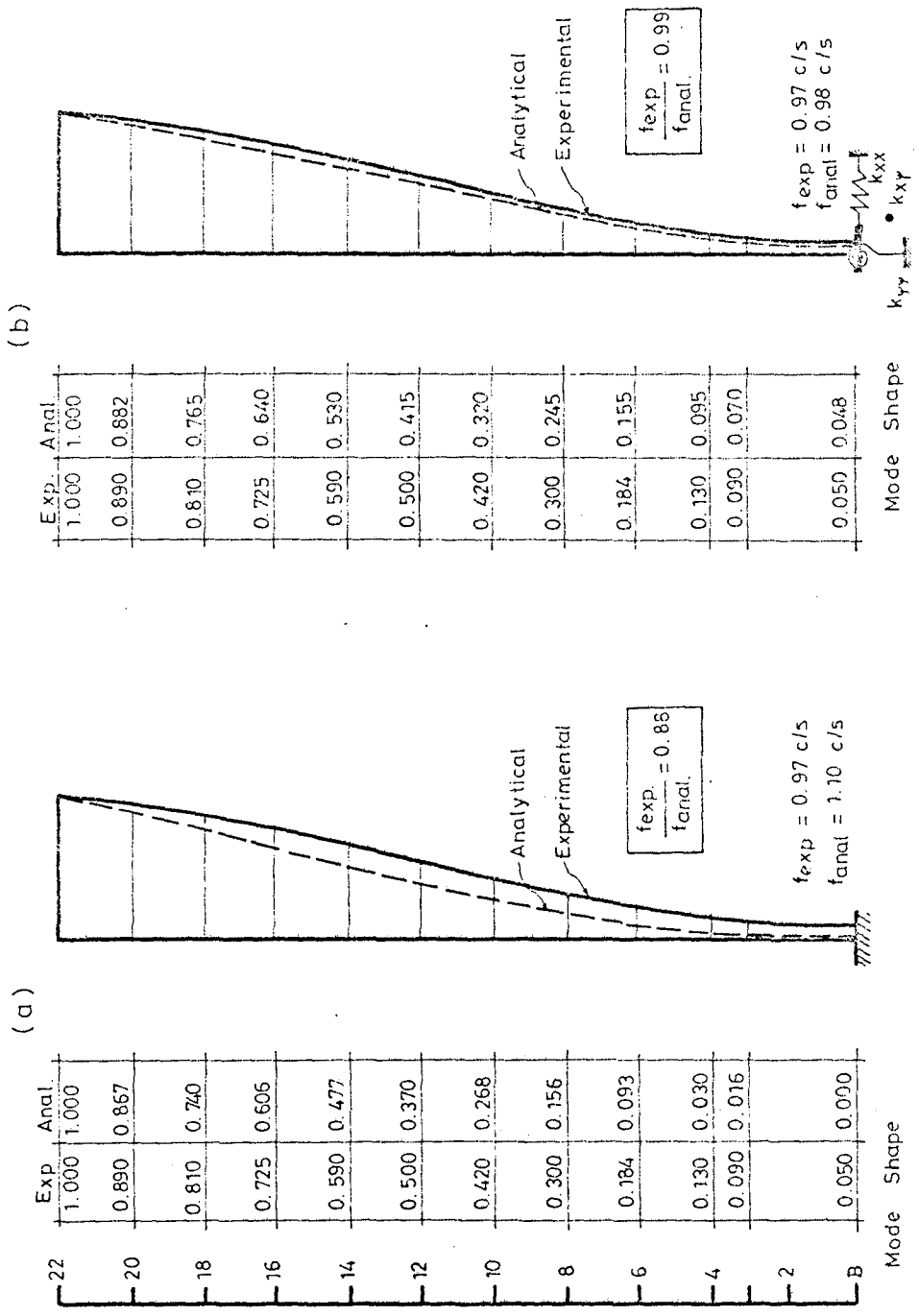
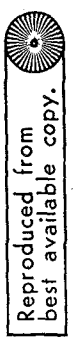


Figure 5. COMPARISON OF EXPERIMENTAL AND ANALYTICAL DYNAMIC PROPERTIES OF TWENTYTWO-STORY BUILDING

(a) Fixed Base Model  
 (b) Flexible Base Model



Reproduced from  
 best available copy.

1278

**INTENTIONALLY BLANK**

1279

# **OFFSHORE MICROZONATION SESSION**

**INTENTIONALLY BLANK**

1280

## MICROZONATION OF OFFSHORE AREAS - AN OVERVIEW

By

I. M. Idriss<sup>I</sup>, Lloyd S. Cluff<sup>II</sup>, and Ashok S. Patwardhan<sup>III</sup>

## ABSTRACT

In principle, the approach to and methods of microzonation of offshore areas are similar to those utilized for onshore areas. However, the differences in the range and characteristics of parameters used in defining the zonation criteria for comparable levels of safety or acceptable risk may yield zonation maps of a different character. These parameters include seismicity, earthquake recurrence intervals, subsurface conditions, and structural characteristics. Simplified subregional tectonic models may be used for seismic zonation, and the resulting zone may be somewhat larger in size than on land. To improve the accuracy of the results, it is necessary to pursue a program of investigation and collection of data in offshore environments.

Structural characteristics of major offshore structures (such as platforms) suggest that zonation be based on ground motion parameters such as peak velocity, spectral velocity, or spectral displacement rather than peak acceleration. It is advantageous to base the zonation on an evaluation of seismic exposure and to supplement the seismic exposure evaluations with representative subsurface data for microzonation.

## INTRODUCTION

During the past two decades, offshore areas have received increasing attention for development of petroleum resources, for construction of submarine pipelines, and for other purposes such as sea bed mining. Figure 1 shows some of the areas of major interest at present. Although these areas are in active seismicity regions, zonation and microzonation concepts have not been applied to them with the same degree of detail and geographic coverage as they have been on land. Primary reasons for this are:

(a) Offshore areas in zones of high seismic activity have not been subjected to sustained utilization until the past decade and there were too few locations to warrant zonation.

(b) Sufficient information regarding the different elements on which microzonation is commonly based (tectonic setting, earthquake recurrence intervals, subsurface conditions, and structural performance) have not been accumulated and analyzed on an areal basis.

---

I Principal, Woodward-Clyde Consultants, San Francisco, California

II Chief Engineering Geologist, Woodward-Clyde Consultants,  
San Francisco, California

III Associate, Woodward-Clyde Consultants, San Francisco, California

(c) Sufficient experience was not available on the performance of structural systems (such as platforms and pipelines) in an offshore seismic environment.

(d) Ideas on reliability of offshore structures and acceptable risk are still in a formative stage.

As a result of recent major design efforts and studies in some seismically active offshore regions, such as Southern California and Alaska, a clearer picture of the issues and methods for offshore microzonation have emerged that may be of value to owners, designers, and regulatory agencies. It is the objective of this paper to discuss these issues.

Figure 2 shows a schematic flow diagram of the different steps of a microzonation process. Current efforts at the microzonation of onshore areas have accomplished these steps to different degrees of completion. In principle, the steps followed in the microzonation of offshore areas are similar to those in the onshore areas. However, differences in the character of the elements noted in (b) above mandate differences in the microzonation patterns. A review of these differences is both instructive and of practical value.

#### PHYSICAL ENVIRONMENT

(a) Location - Offshore areas of current interest are shown in Fig. 1. The chief motivation for development of many of the areas is recovery of petroleum. Also shown in Fig. 1 are areas of major seismicity in the world. The coincidence of the two areas is remarkable and points to the need for a systematic study of the range and character of seismically induced forces on offshore structures. Most areas of interest extend from a few miles to approximately 200 miles from the shore, to which they are frequently connected by pipelines.

(b) Water - In the case of oil platforms, water depths have ranged from 50 ft to 800 ft, although in some cases platforms in water depths exceeding 1000 ft are being considered. Pipelines have been constructed or planned in water depths to 2000 ft. Sea bed mining has been studied for even greater depths.

The presence of water has a significant effect on the selection of type of structure, the selection of environmental loading--both static and transient--and on the response of the structure. In areas of low seismicity, the effects of waves and storms on structures and foundation soil stability (e.g., structural stresses, down slope movement, liquefaction) can be comparable to or exceed earthquake effects and make seismic microzonation relatively unimportant.

(c) Soil Characteristics - Available information on soil characteristics in offshore areas is limited to a few locations under active development (e.g., Gulf of Mexico, North Sea, Gulf of Alaska, Southern California). The range of material types and in situ index properties is similar to those on land, varying from rock and stiff soils to very soft deep alluvial materials. The deformational properties may show some

differences. Deeper sedimentary deposits and deposits normally consolidated to considerable depths are encountered more frequently than on land. Weak, near-surface materials with a potential for instability due to wave action are also encountered in several areas. Therefore, the seismic hazards that result from various soil properties may be different in an offshore environment and may influence the selection of microzonation criteria.

#### SEISMIC ENVIRONMENT

(a) Seismicity - The offshore areas experience varying levels of seismic activity ranging from low (e.g., Gulf of Mexico) to very high (e.g., the Aleutians). Many of the offshore areas of current interest (e.g., the entire circum-Pacific belt, Iran, Italy, Rumania, and Turkey) are located on or close to major plate boundaries and experience the effects of major tectonic activity. The average recurrence of large earthquakes ( $M_s > 7$ ) in these areas is high; the areas shown in Fig. 1 account for nearly 80 percent of the worldwide annual release of seismic energy (1).

Great earthquakes ( $M_s > 7.8$ ) tend to occur in a nonrandom pattern in space and time (2). This pattern results in "seismic gaps" during which no significant seismic activity is observed for a period of time (usually several tens of years). Although seismic gaps are recognized in onshore areas, they appear to be of greater significance in offshore areas, which incorporate more gap areas. Areas experiencing seismic gaps are believed to be areas of buildup of strain energy and have a higher likelihood of experiencing a great earthquake in the near future than the adjacent areas. The presence of gap areas and post-earthquake areas results in a seismic exposure function that is time dependent. Consequently, seismic zonation maps prepared on the basis of current levels of seismic exposure need to be prepared on a "real-time" basis and updated periodically.

There is a paucity of regional information on the location, geometry and rate of activity of earthquake sources such as the dipping sections of subducting plates (Benioff zones) or individual active faults in offshore areas. Therefore, offshore zonation has to be based on simpler, subregional tectonic models and may cover larger areas than on land.

(b) Ground Motions - A major difference between onshore and offshore areas is the lack of recorded ground motions in an offshore environment. A limited number of recordings of offshore earthquakes are available from onshore stations. An analysis of recordings from deep offshore earthquakes (focal depths greater than 20 km) show major differences in the source and attenuation characteristics of offshore ground motions vis-a-vis the motions from shallow, onshore earthquakes (3). It appears that for the deep, offshore sources, longer period motions ( $T > 1$  sec) are less dominant than for shallow, onshore sources. Also, motions generated by the deep earthquakes appear to attenuate at a slower rate than motions generated by shallow earthquakes (3) for all frequencies. The significant duration of these motions appears to be shorter than the duration of onshore earthquakes. The combined effect of these differences on seismic exposure and seismic zonation can be significant, as discussed below.

## SEISMIC EXPOSURE

The above-mentioned differences in earthquake source characteristics, recurrence, ground motions, and attenuation characteristics indicate seismic exposure patterns that differ from those obtained on land. Differences in the frequency contents of deep earthquake motions can lead to different spectral shapes for any given probability of exceedance. Based on available studies, it appears that in areas of high seismicity, such as near subduction zones where large, deeper earthquakes occur, the expected values of high frequency motions may be substantially higher in offshore areas within 200 km of the dominant sources, whereas values for longer period motions (e.g., spectral velocity at  $T = 5$  sec) may be substantially lower for all return periods.

## CONSIDERATIONS FOR ZONATION AND MICROZONATION

A zonation process is often undertaken with multiple objectives, such as:

(a) delineation of areas for which broad seismic exposure and seismic design inputs can be defined for both elastic and inelastic design.

(b) delineation of areas that have specific potentials for similar types of seismic hazards or have specific ranges of subsurface conditions.

(c) delineation of areas for which similar risk and performance criteria can be defined.

In the context of offshore development, objective (a) is of interest to owners for prebid analyses and comparative analyses of different areas. If approximate cost versus seismic design level relationships are available, the information is also of interest to a designer for comparing various platform types and design strategies. Objective (b) enables a refinement of the alternate designs and costs and, if other factors do not change, offers an opportunity for comparison between different locations. Objective (c) enables further refinement of the designs and an optimization of costs and expected performance. Each step offers progressively more detailed assessment of the safety and performance of the structure. None of the currently available zonation procedures, either on land or offshore, have accomplished all these objectives in an adequate manner.

At present, three studies are available on the seismic zonation of coastal waters in the United States (4, 5, 6). Two are based on a seismic exposure evaluation of an area (4, 5). The third study (6) provides a set of reference values of shaking and recommends design response spectra for three typical subsurface conditions.

More comprehensive studies have been conducted for specific areas. A recent example is the Offshore Alaska Seismic Exposure Study (OASES) (7), in which a comprehensive evaluation of seismic exposure was made for most offshore areas in Alaska in terms of a number of ground motion parameters including peak values (peak acceleration, peak velocity, and



displacement), RMS values, and spectral values (velocity and displacement). No other published studies on microzonation of offshore Alaska are available. The ASOC study provides a basis for such efforts. Site-specific studies have been made for offshore platform sites (in the North Sea, Southern California, and Gulf of Alaska), some of which are available in literature (8).

Zonation studies are helpful in providing an estimate of seismic exposure. This estimate may be utilized for overall strategies and for assessing, on a generic basis, the relative benefits of siting in one area versus another, and the relative costs of additional conservatism in design. A major consideration in seismic zonation for offshore areas is the choice of appropriate ground motion parameters. A majority of offshore structures have long natural periods ( $T = 2$  to 5 sec); structures with natural periods of 20 sec have been contemplated. Ground motion parameters that influence their behavior more significantly are peak velocity, peak displacement, and response spectral values. It is more appropriate, therefore, to formulate zonation and microzonation criteria and maps utilizing these parameters rather than peak acceleration, as is commonly done for onshore areas. If the dominant sources of seismic exposure are offshore and deeper ( $H > 20$  km), the longer period components of motion may show a different seismic exposure pattern. The API RP 2A earthquake provisions (6) utilize a parameter designated as "effective acceleration" for zonation. At present, the effective acceleration has not been related to seismic exposure. Additional work is needed in this area.

If the objective of zonation is to provide a basis for seismic design that will limit the probable damage to an acceptable value, the offshore areas have certain advantages in relation to onshore areas in that, in most cases, the types of structures are limited and the period of interest is relatively short (generally less than 40 years). The applicable design criteria can be defined on the basis of real-time expected seismicity levels to achieve desired levels of elastic strength and ductility. Limited available data indicate that in some areas the elastic design criteria can be based on an approximately 100-year return period ground motion for a 20- to 30-year useful life of the structure for a satisfactory design. The ductility criteria with respect to longer return period effects of earthquakes can be met by selecting an earthquake with a return period consistent with the acceptable risk in the area.

On the other hand, a handicap for a risk-based seismic zonation is the lack of a definitive relationship between the probabilities of damage and expected ground motions for offshore structures. This difficulty exists even for onshore structures, but to a considerably lesser extent because a large volume of observational data on damage versus ground motions is available from historical earthquakes.

Another ingredient of risk-based zonations is the definition of "acceptable risk". Different assessments of acceptable risk may be made by the regulators, owners, designers, and the public at large. Considerations governing acceptable risk in offshore areas are similar to those in other areas and include items such as the need to protect investment, the need to maximize public safety, and the need to minimize impact on the environment.

As shown in Fig. 3, additional information is required for microzonation. This information will consist of data on the type, extent and range of properties of subsurface materials, and presence of subregional or secondary earthquake sources. Generally, such information is acquired by drilling, in situ testing, and by geophysical techniques. In an offshore environment, acquisition of this information is very expensive, and the need for its acquisition over large areas is not likely to arise very often. Therefore, the prospect of complete microzonation of large offshore areas is rather remote at present. However, with a moderate outlay of resources, it may be possible to delineate specific microzones for the purpose of an assessment of potential for seismically induced hazards such as surface fault rupture, slope failure, or liquefaction. It may also be feasible to define ranges of soil response spectra applicable to a given microzone. Where possible, microzonation on the basis of subsurface data can be of help in the refinement of design strategies and risk assessments.

It has been suggested that, because the siting of major structures in the offshore environment is strongly influenced by factors such as location of oil reservoirs, and the structures may be few in number and located at considerable distances from one another, it may be advantageous to proceed directly to site-specific studies, once the broad seismic zones are established, and eliminate microzonation. Such may be the case if the structures are very few in number and do not require any auxiliary structures. Microzonation may be of benefit where a relative assessment of subregional seismic hazard is required and in cases where more than one site in the same zone needs to be evaluated.

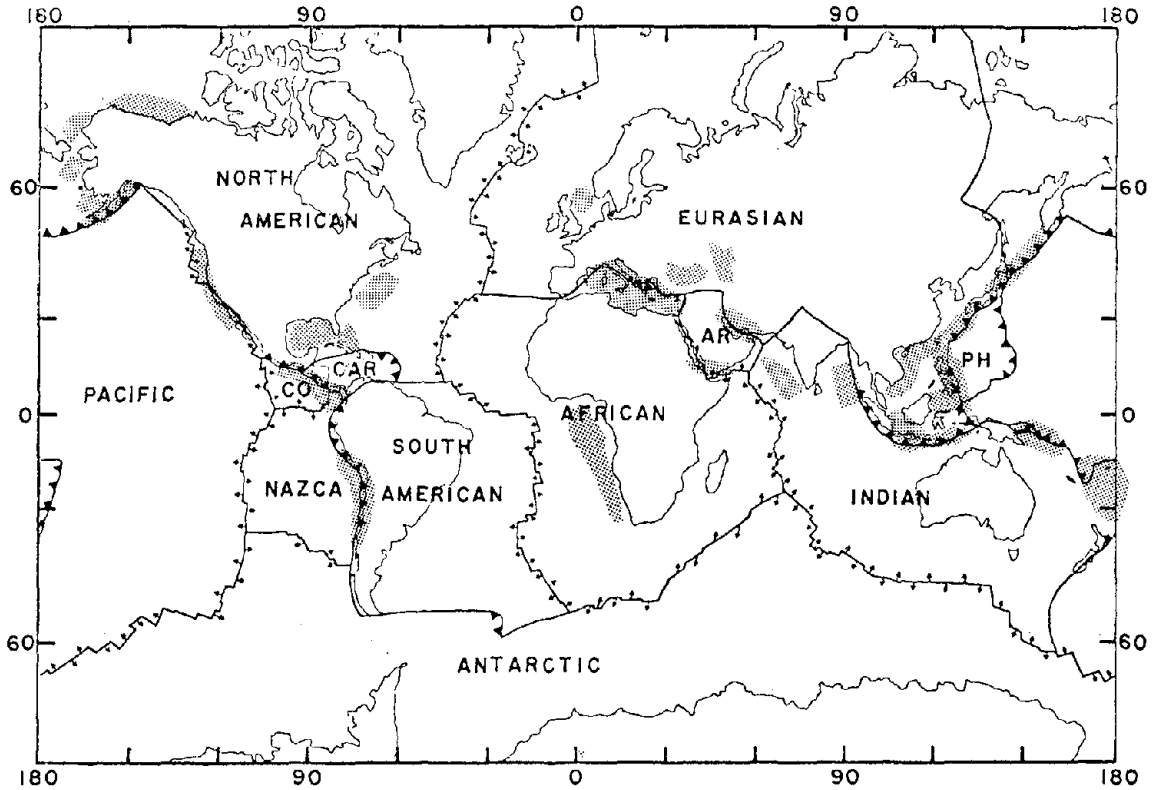
#### SUMMARY

In principle, the approach to and methods of microzonation of offshore areas are similar to those utilized for onshore areas. However, the differences in the range and characteristics of parameters used in defining the zonation criteria for comparable levels of safety or acceptable risk may yield zonation maps of a different character. These parameters include seismicity, earthquake recurrence intervals, subsurface conditions, and structural characteristics. Simplified subregional tectonic models may be used for seismic zonation, and the resulting zone may be somewhat larger in size than on land. To improve the accuracy of the results, it is necessary to pursue a program of investigation and collection of data in offshore environments.

Structural characteristics of major offshore structures (such as platforms) suggest that zonation be based on ground motion parameters such as peak velocity, spectral velocity or spectral displacement, rather than peak acceleration. It is advantageous to base the zonation on an evaluation of seismic exposure and to supplement the seismic exposure evaluations with representative subsurface data for microzonation. Ground motion relationships utilized in the evaluations should take note of significant differences that may exist between onshore and offshore areas.

## BIBLIOGRAPHY

1. Richter, C. F., 1958, Elementary seimology: W. H. Freeman & Company, San Francisco, California.
2. Kelleher, J. A., Sykes, L. R., and Oliver, J., 1973, Possible criteria for predicting earthquake locations and their application to major plate boundaries of the Pacific and the Caribbean: Journal of Geophysical Research, v. 78, no. 14, p. 2547-2585.
3. Patwardhan, A. S., Sadigh, K., Idriss, I. M., and Youngs, R., 1978, Attenuation of strong ground motion--effect of site conditions, transmission path characteristics, and focal depth: in press.
4. Algermissen, S. T., and Perkins, D. M., 1976, A probabilistic estimate of maximum acceleration in rock in the contiguous United States: U. S. Geological Survey Open-File Report 76-416, 45 p.
5. Applied Technology Council, 1977, Recommended comprehensive seismic design provisions for buildings: sponsored by National Science Foundation and National Bureau of Standards, 9th edition, November.
6. American Petroleum Institute, 1977, Recommended practice for planning, designing, and constructing fixed offshore platforms: API RP 2A, Section 2.10, 9th edition, November.
7. Alaska Subarctic Offshore Committee, 1978, Offshore Alaska Seismic Exposure Study, Vols. I through V: prepared by Woodward-Clyde Consultants, San Francisco, California.
8. Bea, R. G., 1976, Earthquake criteria for platforms in the Gulf of Alaska: Offshore Technology Conference Preprints, OTC 2675, Houston, Texas, May.



Source: Offshore areas Woodward-Clyde  
Consultants files (1978)



**EXPLANATION**  
 Major Offshore Areas of Current Interest  
 Major Plate Boundary  
 PACIFIC

Fig. 1. Major Offshore Areas of Current Interest and Areas of Major Tectonic Activity

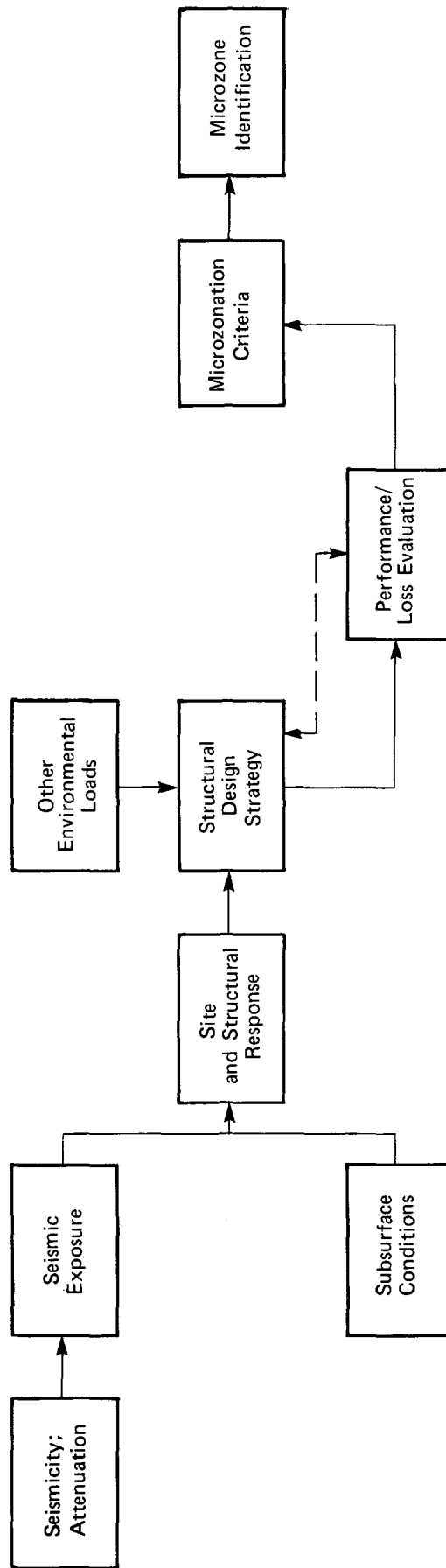


Fig. 2. Seismic Microzonation Procedure

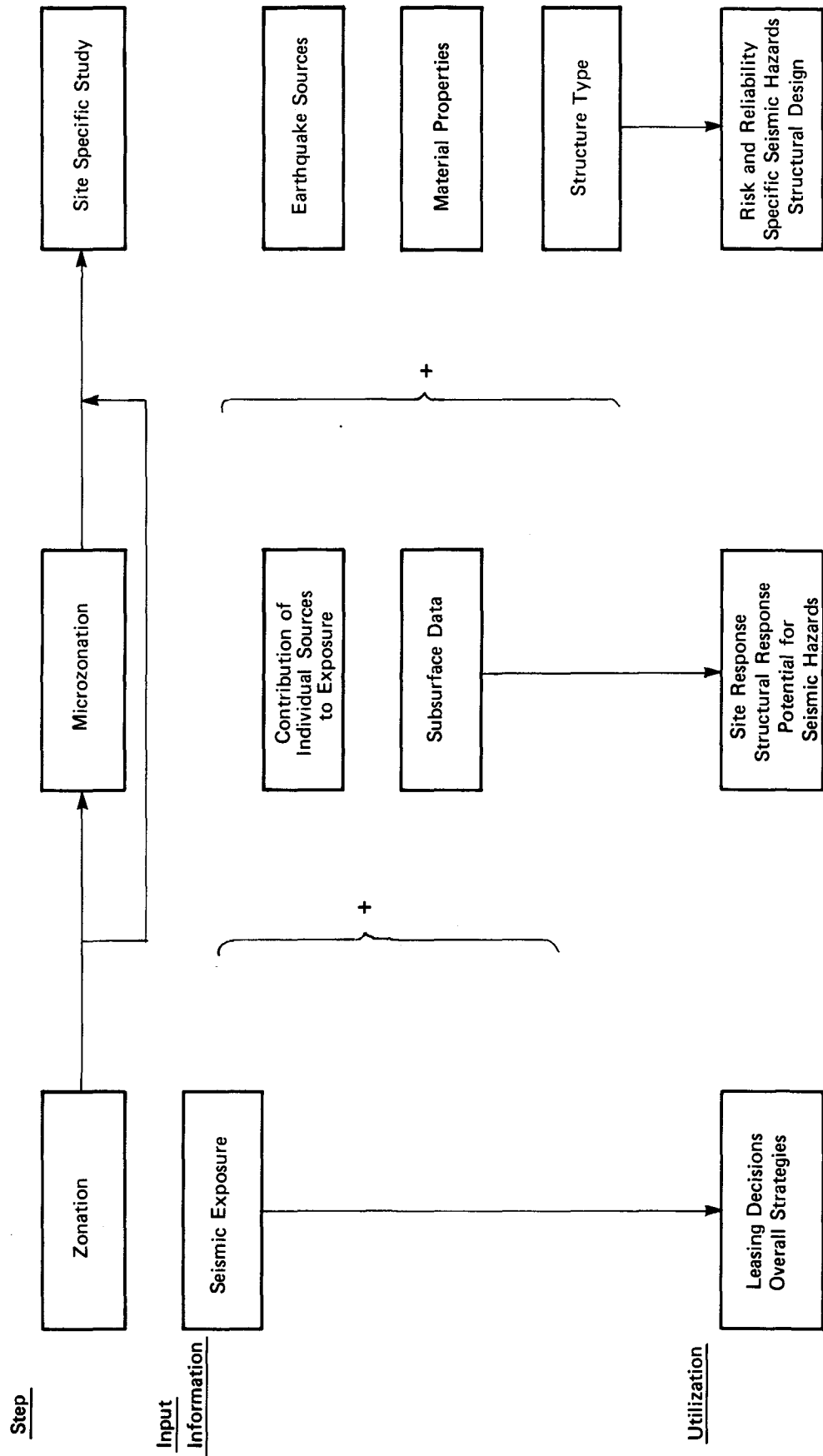


Fig. 3. Data and Utilization of Seismic Zonation and Microzonation in Offshore Areas

## FACTORS INFLUENCING SEISMIC EXPOSURE EVALUATION FOR OFFSHORE AREAS

By

Ashok S. Patwardhan<sup>I</sup>

## ABSTRACT

Seismic exposure evaluation is an essential step in seismic zonation, evaluation of seismically induced hazards, and risk-based design of offshore structures. The application of the results of a seismic exposure evaluation is based on calculated values of ground motion parameters which, in turn, are influenced by input parameters and the exposure evaluation model. The relative influence of various factors is discussed by examining seismic exposure in an example area (Gulf of Alaska). Major influencing factors include the source characterization, attenuation characteristics, and exposure evaluation procedure. A separation of the overall seismic exposure values into the contributions of different sources and factors enhances the value of a seismic exposure evaluation for a specific purpose.

## ROLE OF SEISMIC EXPOSURE EVALUATION IN OFFSHORE AREAS

Seismic exposure is defined as the exposure to earthquake effects at a given location expressed as the level of a ground motion parameter for a selected probability of exceedance. If planned with a sufficiently broad scope and in adequate depth, a seismic exposure evaluation can provide insights of value to offshore development. To name a few:

(a) Seismic exposure values can be useful for qualitative cost estimates and risk assessments necessary for pre-lease evaluations. They may serve to preclude certain structural configurations from consideration for certain lease areas. If a relationship between earthquake forces and platform costs were available, they could strongly impact bid strategy. If combined with an areal description of soil properties, the results can be used to identify tracts with potential foundation problems and to guide the selection of pipeline routes.

(b) Seismic exposure maps can provide a broad basis for seismic zonation and establish design guidelines for similar seismic risks in the various offshore areas. If seismic exposure values are calculated for various return periods (e.g., ranging from 50 to 1,000 years), they can provide the designer with an opportunity to assess the impact of added conservatism on facility cost.

(c) Identification of dominant factors can afford the research planner an opportunity to target research efforts where they will be most productive; e.g., earthquake sources, transmission paths, subsurface conditions, and exposure evaluation models.

---

<sup>I</sup> Associate, Woodward-Clyde Consultants, San Francisco, California

(d) A seismic exposure evaluation can provide one of the bases for a site-specific study. If a breakdown of the relative contributions to seismic exposure by different earthquake sources can be established, the bases for seismic design can be refined further.

(e) Finally, the first element of a reliability analysis is a probabilistic description of the environmental forces. A seismic exposure evaluation can provide this description for the earthquake loads.

Most applications of a seismic exposure evaluation are based on the calculated values of ground motion parameters which, in turn, are influenced by input parameters and the evaluation model. It is the objective of this paper to examine the relative significance of various input parameters. For illustration, examples are chosen from a recent comprehensive seismic exposure study, the Offshore Alaska Seismic Exposure Study (OASES), sponsored by ASOC (1).

#### SCOPE

The scope of a seismic exposure evaluation is governed by the proposed utilization with respect to structures, space, and time. Major offshore facilities include a wide range of structures varying from pipelines to platforms, which are flexible structures with long natural periods (typically 1 to 10 sec). The response of the facility and the stability of foundations is influenced by properties of subsurface materials. Published work (e.g., 2 and 3) indicates that significant differences exist in the characteristics of motions recorded on rock, stiff, and soft materials depending upon the magnitude, distances, material properties, and the motion itself. Different design strategies may require assessments for different probability levels. Thus, the desirable scope of an exposure evaluation should encompass:

(a) Calculation of seismic exposure values for ground motion parameters that have dominant influence on structural response in a given frequency range; e.g., peak values (peak acceleration and peak velocity), RMS values, and spectral values (velocity and displacement).

(b) Calculation of seismic exposure values for different site conditions.

(c) Calculation of seismic exposure values extending over a range of return periods.

#### EXPOSURE EVALUATION MODEL

The steps in a seismic exposure evaluation of offshore areas are shown in Fig. 1. They are: source seismicity, attenuation, and exposure evaluation. Figure 2 depicts a model in which the geometrical representations of the sources, earthquake events, and attenuation paths are consistent with the physical conditions in an offshore environment (1). All earthquake sources are represented by one or more dipping planes. For calculation purposes, both the earthquake source surface and the offshore area under investigation are discretized into grid cells. Each grid corner on the source is a potential earthquake hypocenter. Each



grid cell corner in the offshore area is a "site". An individual earthquake event is represented by a rectangular rupture surface whose size is a function of the size (surface wave magnitude,  $M_s$ ) of the earthquake. Vibratory ground motion is assumed to be generated along the rupture surface and propagated towards a site along the shortest path between the rupture surface and the site (designated as significant distance in Fig. 2).

The seismic exposure calculations begin by choosing and calculating a source for all the earthquake magnitudes and locations along the source by utilizing the recurrence relationship and attenuation relationships. The procedure is then repeated for the next source until all sources are exhausted. A relationship showing the combined probability of exceeding a given value of the ground motion parameter due to all sources is plotted as shown in Fig. 3(a). Similar relationships are established for other sites within the area. Selected values of ground motion parameters at each site corresponding to a given return period (probability of exceedance) can be utilized to construct a seismic exposure map. This geometrical scheme differs from most available models and may influence calculated ground motion values in high seismicity areas (4).

#### RELATIVE SIGNIFICANCE OF INFLUENCING FACTORS

Source-Related Parameters: The relative significance of the various parameters in Fig. 1 is discussed using the Gulf of Alaska area from OASES as an example area (1). Earthquake sources in the region are shown on Fig. 4. The dominant earthquake source is the Benioff zone, which underlies the area at a shallow depth (approximately 12 km). North of the lease area, the zone dips at approximately 30 degrees with depths varying between 13 and 62.5 km. Other earthquake sources include known individual faults. The geometrical scheme of Fig. 2 is a good representation of the sources in the area.

Similarly, a large number of offshore areas of current interest lie close to zones of major seismic activity, wherein the dominant cause of earthquakes is the relative movement between the plate boundaries which may be predominantly strike-slip (e.g., the San Andreas fault) or thrust motions (e.g., Benioff zone in southern Alaska). Other earthquake sources may include individual faults, fault zones, and volcanic areas. If the seismicity is associated with well-defined sources, the location and spacing between the sources produces an exposure pattern different from the case when the seismicity is uniformly distributed over a large area. In many offshore areas, it may be difficult to correlate all seismic activity with known sources. A combination of the two alternatives becomes appropriate wherein the tectonic model includes both known sources and "random" sources that represent sources of unknown location.

Similarly, characterization of an individual earthquake event as occurring at a point affects the seismic exposure significantly in comparison to the case when the same overall earthquake is modelled by a rupture surface over a finite area. In the model shown in Fig. 2, the size of the rupture area will be 12 x 6 km for  $M_s = 6$  and 400 x 200 km for  $M_s = 8$ , which indicates that the rupture surface may underlie practically an entire offshore area if earthquake magnitudes  $M_s \approx 7.8$ . Figure 5 shows

a comparison of the seismic exposure values for a site similar to a site in the example area obtained by using different seismic exposure models (4). Clearly, the association of a rupture surface with an earthquake event yields substantially higher values in high seismicity areas.

Recurrence of earthquakes can influence the seismic exposure at a site in a significant manner. In some major plate boundary areas, the occurrence of large earthquakes is highly non-random in location and time (5). This gives rise to "seismic gaps" in which no great earthquakes ( $M_s \approx 7.5$ ) have occurred for a period of time. It has been suggested (5) that the probability of occurrence of great earthquakes is higher in seismic gaps than in other areas which have experienced a great earthquake in the recent past. To evaluate the significance of seismic gaps to seismic exposure, calculations should be made to differentiate between the contributions of great, gap-filling earthquakes and of smaller, independent earthquakes.

Figures 3(a), (b), and (c) show the cumulative distribution functions for maximum acceleration ( $a_{max}$ ), maximum velocity ( $v_{max}$ ), and pseudorelative spectral velocity (PSV), respectively, for site A in Fig. 4. For each parameter, values are calculated for all sources (curve 1), for the dominant source (Benioff zone) (curve 2), and for the random source (curve 4). Also shown are the calculated exposure values due to the smaller earthquakes,  $M_s < 7.5$  (curve 5). A comparison between curves 2 and 5 is informative in that it provides a relative assessment of the contribution to seismic exposure by the "gap-filling" great earthquakes and the smaller magnitude earthquakes. The influence of change in the level of seismic activity on seismic exposure was evaluated by increasing the expected number of earthquakes of all magnitudes on the dominant source by a factor 2 (curve 3). A horizontal line is drawn (in Fig. 3) at a probability of exceedance of 0.33 (i.e., a 100-year return period for a 40-year period of interest), which gives the peak acceleration values of 193 cm/sec<sup>2</sup> for all sources, 175 cm/sec<sup>2</sup> for the Benioff zone, and 52 cm/sec<sup>2</sup> for the random source.

To ascertain the relative contribution of various sources, the probability of exceedance for a selected value of maximum acceleration can be examined. In Fig. 3(a) for a probability of exceedance  $p_a = 0.33$  for all sources, the maximum acceleration ( $a_{max}$ ) is 193 cm/sec<sup>2</sup>. For this value of  $a_{max}$ , the probability of exceedance on the Benioff zone,  $p_B$ , is 0.275. The probability of exceedance of the same  $a_{max}$  for sources other than the Benioff zone,  $p_r$ , can be obtained by assuming independence of events:

$$(1 - p_a) = (1 - p_B) (1 - p_r)$$

$$\text{or } p_r = 1 - \frac{(1 - 0.33)}{(1 - 0.275)} = 0.076 ; \text{ i.e., } 7.6\%$$

Similar calculations indicate that the Benioff zone contributes 83% of the expected peak acceleration and that approximately 38% of the seismic exposure due to the Benioff zone is contributed by earthquakes of magnitudes smaller than  $M_s = 7.5$ . An estimate of relative contributions

of different magnitude ranges and a knowledge of the appropriate distance to the Benioff zone at this site (approximately 12 km) provides useful information for inelastic design considerations or selection of input motions for analysis.

Relationships similar to those shown in Fig. 3 can also be used to estimate the variation in relative contributions of the various sources with return period. For example, the following table summarizes the relative contributions of various sources for return periods of 50, 100, and 500 years.

Return Period (Years)	500	100	50
Maximum Acceleration ( $a_{\max}$ ), cm/sec <sup>2</sup>	318	198	152
Probability of Exceedance of $a_{\max}$ due to:			
All sources ( $p_a$ )	0.08	0.33	0.55
Benioff zone ( $p_B$ )	0.06	0.275	0.45
Other sources ( $p_r$ )	0.02	0.08	0.182
Benioff zones, $M_s < 7.5$ ( $p_{Bs}$ )	0.019	0.08	0.19
Benioff zones, $M_s < 7.5$ (% of Benioff zone)	16.7	29.1	42

As can be seen from the table, as well as from Fig. 3, the contributions of smaller magnitude earthquakes to seismic exposure decrease with increasing return periods, a result that can be anticipated from the N-M relationship, the minimum distance of the Benioff zone from the site, and the attenuation relationship.

On the Benioff zone itself, an increase in the overall seismicity by a factor of 2 increases the 100-year return period value of maximum acceleration from 175 cm/sec<sup>2</sup> to 220 cm/sec<sup>2</sup>; i.e., by approximately 26%.

Similar assessments can be made for peak velocity,  $v_{\max}$  (see Fig. 3b) and pseudorelative spectral velocity, PSV ( $T = 1.5$  and 5 sec,  $\beta = 5\%$ ) (see Fig. 3c). The Benioff zone contributes nearly 82% of the exposure in case of maximum velocity and approximately 82 to 85% of the exposure in case of pseudorelative spectral velocity. The contributions of the random source appear to be somewhat higher for  $a_{\max}$  than for  $v_{\max}$  or PSV. Figure 4 shows a seismic exposure map for the example area for a 100-year return period. Figure 5 shows the range of calculated values of different parameters versus return period.

Attenuation Parameters: Physical conditions in the example areas suggest that two types of attenuation relationships should be utilized in the calculation of seismic exposure (1): transmission path A, applied to shallow earthquakes with focal depths less than 20 km; and transmission path B, applied to deeper earthquakes on the Benioff zone with focal depths greater than 20 km. A log normal distribution was used to account

for the uncertainty associated with the attenuation relationship. The relationships utilized for peak accelerations are shown in Fig. 6 (1).

Similar conditions appear to exist in other offshore areas close to the major plate boundary; e.g., the Aleutians (1). Analyses were made for one site in the Aleutians to evaluate the effect of variation in the type of relationship, depth of application, the width of distribution associated with the relationship, and site conditions.

Type and Depth of Application: The configuration of the dominant source for the investigated site, the Benioff zone, is similar to that shown in Fig. 2 with a shallow dipping portion at depths of approximately 20 km and a steeply dipping portion with depths varying between 20 km and 100 km (1). Correspondingly, three depths (0, 21, and 100 km) were utilized corresponding to cases (A), (B), and (C) in Figs. 7(a) and (b). Thus, case (A) represents the calculation of seismic exposure values using only transmission path B, case (C) represents calculations using only transmission path A, and case (B) represents the basic case consistent with the physical setting. Figures 7(a), (b), and (c) show that significant differences in the values of maximum acceleration, maximum velocity, and pseudorelative spectral velocity can be obtained depending upon the type of relationship used and the depth of application. The differences in calculated exposure values are larger in case of maximum acceleration and smaller in case of maximum velocity. A reversal in trends is observed in case of pseudorelative spectral velocities (Fig. 7c). The differences in exposure values are primarily attributable to the differences in the characteristics of motions associated with transmission paths A and B, in which long motions from deeper earthquakes (path B) appear to be less dominant than those from shallow earthquakes (path A) (1).

Site Conditions: Figures 8(a), (b), and (c) show the effect of using attenuation relationships for rock and stiff sites for calculating seismic exposure with respect to  $a_{max}$ ,  $v_{max}$ , and PSV ( $T = 1.5$  and 5 sec), respectively, for one site in the example area; i.e., the Gulf of Alaska area. For a 100-year return period, maximum accelerations for rock and stiff site conditions differ only slightly from each other than those for stiff sites, while maximum velocities are substantially higher for stiff site conditions. The spectral values are higher for rock site conditions. For a 100-year return period, the ratio of maximum accelerations for stiff to rock site conditions is approximately 1.0 and of maximum velocities is approximately 1.65. Spectral velocities for both periods ( $T = 1.5$  and 5 sec) are substantially higher for stiff sites than for rock sites for all return periods.

Dispersion: Seismic exposure calculations for a site in the Aleutians area using log normal distributions of widths equal to 0, 1, 2, 3, and 4 standard deviations with respect to the mean indicate that the values of peak acceleration, peak velocity, and pseudorelative spectral velocity for a selected probability of exceedance differ insignificantly (less than 5%) for distributions using widths three times the standard deviation or greater.

Exposure Evaluation Model: Figure 9 shows the influence of the exposure evaluation model on the calculated values. Three models by Der

Kiureghian, McGuire, and Stanford were evaluated (see 4 for details). As shown in the figure, significant differences can be obtained depending upon the source geometry and recurrence inputs.

#### SUMMARY

Seismic exposure evaluation is an essential step in seismic zonation, evaluation of seismically induced hazards, and risk-based design of offshore structures. The application of the results of a seismic exposure evaluation is based on calculated values of ground motion parameters which, in turn, are influenced by input parameters and the exposure evaluation model. The relative influence of various factors is discussed by examining seismic exposure in an example area (Gulf of Alaska). Major influencing factors include the source characterization, attenuation characteristics, and exposure evaluation procedure. A separation of the overall seismic exposure values into the contributions of different sources and factors enhances the value of a seismic exposure evaluation for a specific purpose.

#### ACKNOWLEDGEMENTS

The discussions presented in this paper are based on the Offshore Alaska Seismic Exposure Study conducted by Woodward-Clyde Consultants (WCC) for the Alaska Subarctic Offshore Committee (ASOC). Sincere thanks are due to ASOC for the support of the investigation and permission to publish the results. Sincere thanks are due to the Project Director, Dr. I. M. Idriss, and members of the project team, especially Dr. Khosrow Sadigh and Mr. John Hobgood of WCC and Dr. Christian P. Mortgat of Stanford University for substantial contributions to the work reported here. Sincere thanks are also due to Mr. Curtis E. Granberry of Exxon and Mr. Thomas P. Taylor of Mobil for useful discussions on the role and scope of seismic exposure evaluation for offshore areas.

#### BIBLIOGRAPHY

1. Alaska Subarctic Offshore Committee, 1978, Offshore Alaska Seismic Exposure Study, Vols. I through V: prepared by Woodward-Clyde Consultants, San Francisco, California.
2. Seed, H. B., Ugas, C., and Lysmer, J., 1974, Site-dependent spectra for earthquake-resistant design: EERC Report No. 74-12, November.
3. Idriss, I. M., and Power, M. S., 1977, Peak horizontal accelerations, velocities, and displacements on rock and stiff soil sites for moderately strong earthquakes: in press.
4. Mortgat, C. P., Patwardhan, A. S., and Idriss, I. M., 1978, Influence of seismicity modeling on seismic exposure evaluation: Seismological Society of America, Earthquake Notes, v. 49, no. 1, p. 51.
5. Kelleher, J. A., Sykes, L. R., and Oliver, J., 1973, Possible criteria for predicting earthquake locations and their application to major plate boundaries of the Pacific and the Caribbean: Journal of Geophysical Research, v. 78, no. 14, p. 2547-2585.

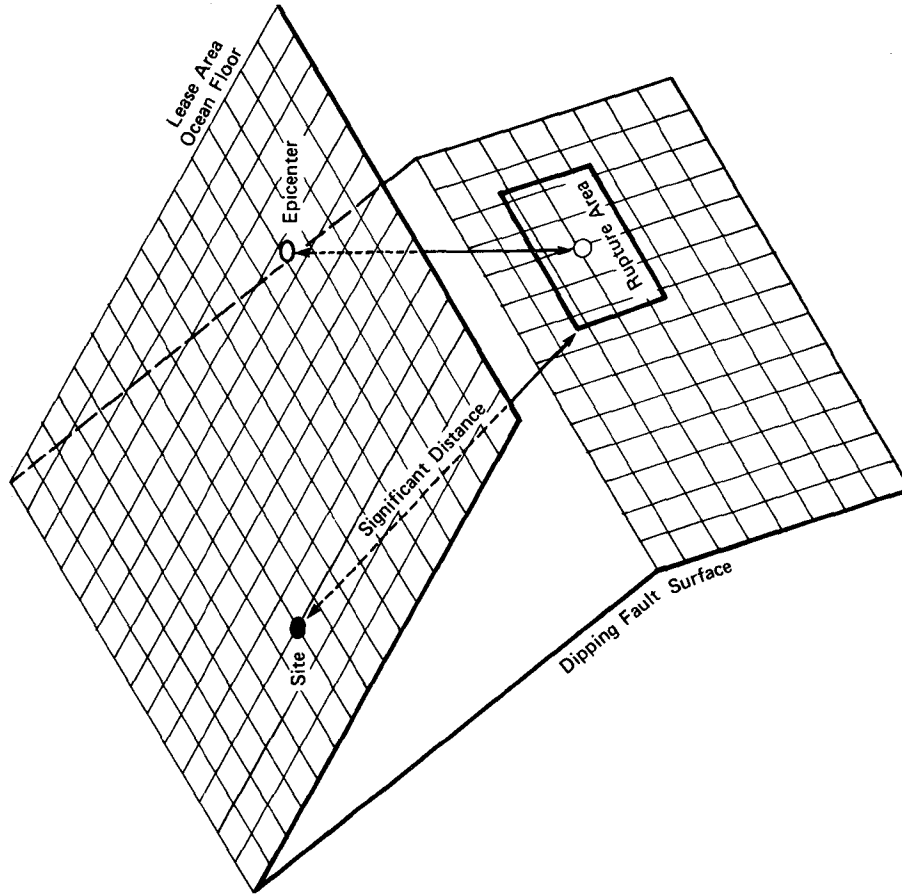


Fig. 2. Geometrical Representation of an Earthquake Source, Event and Transmission Path

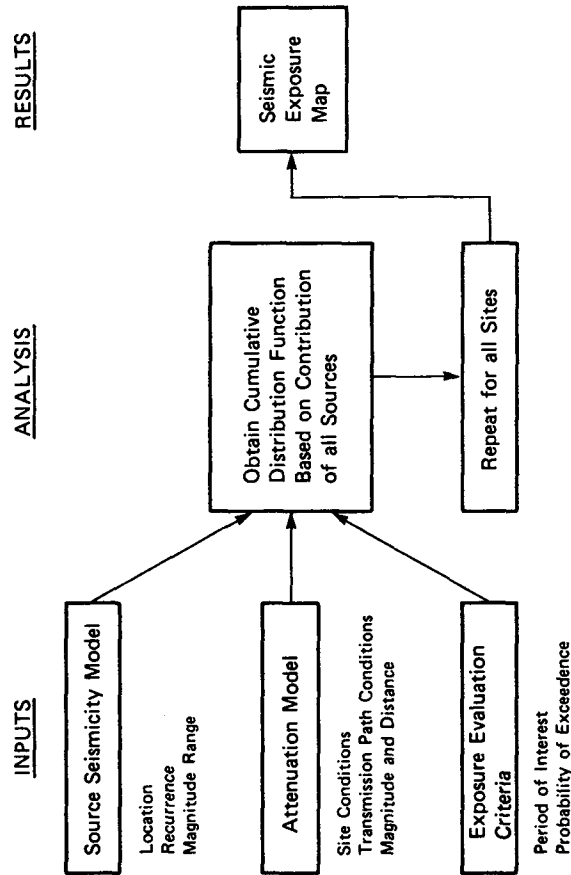
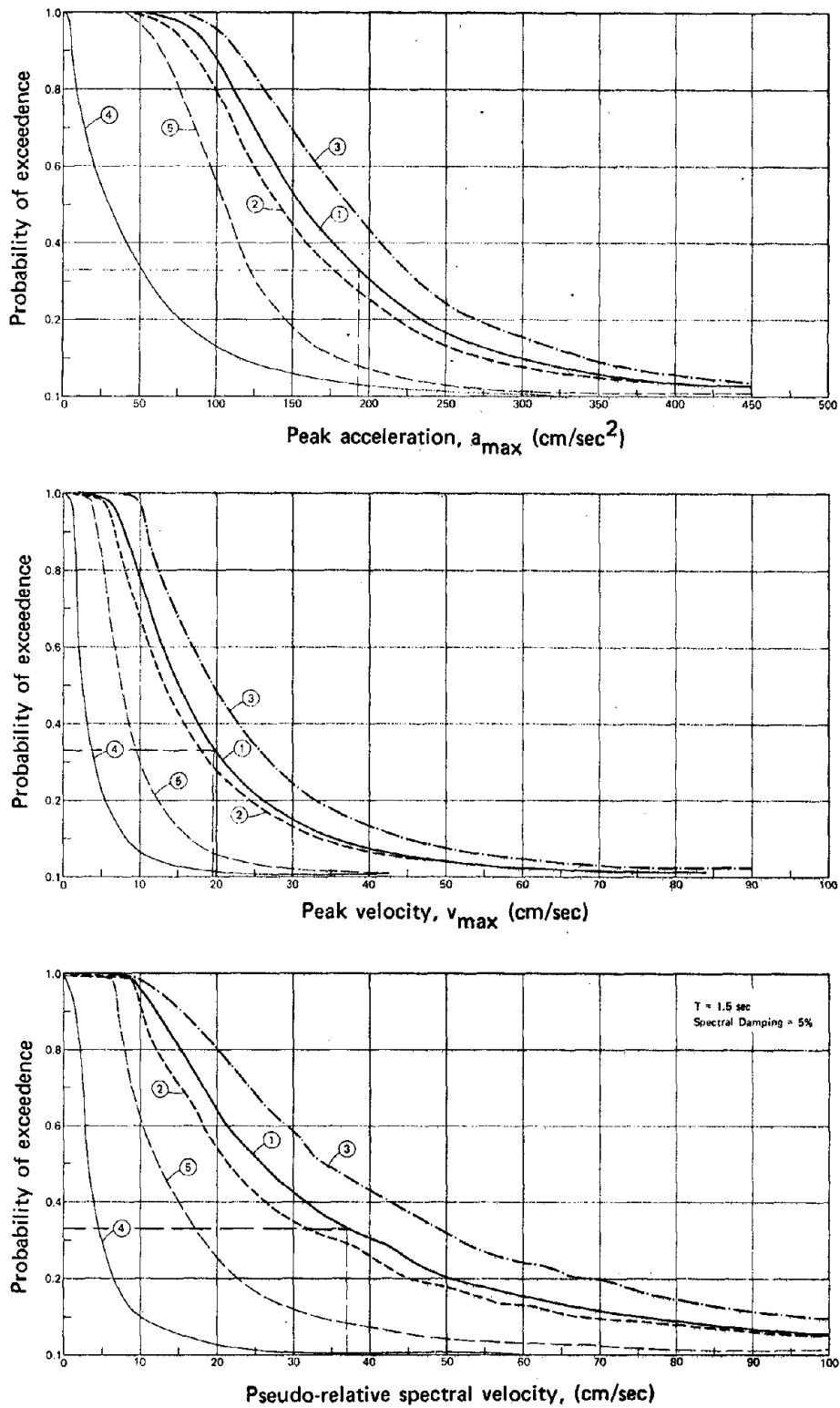


Fig. 1. Seismic Exposure Evaluation Model



**EXPLANATION**

Site A - Gulf of Alaska, See Fig. 4.

Based on ASOC (1)

- |                    |                           |
|--------------------|---------------------------|
| ① All sources      | ④ Random sources          |
| ② Benioff Zone     | ⑤ Benioff Zone, $M < 7.5$ |
| ③ Benioff Zone x 2 |                           |

**Fig. 3. Contributions of Different Sources and Influence of Seismicity on Seismic Exposure**

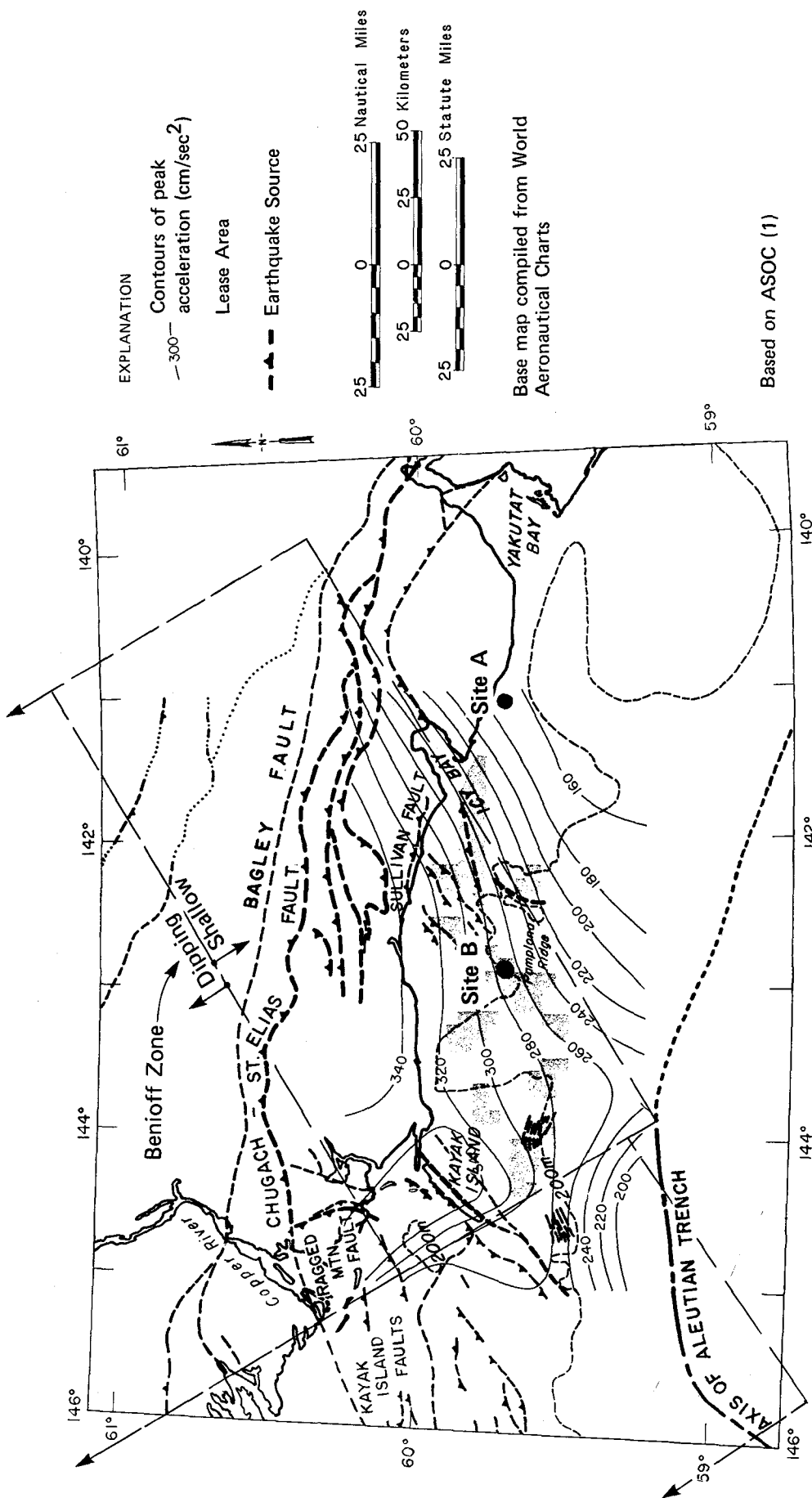


Fig. 4. Gulf of Alaska, Earthquake Sources and Seismic Exposure Map for Peak Acceleration (100 years return period, 40 years period of interest)



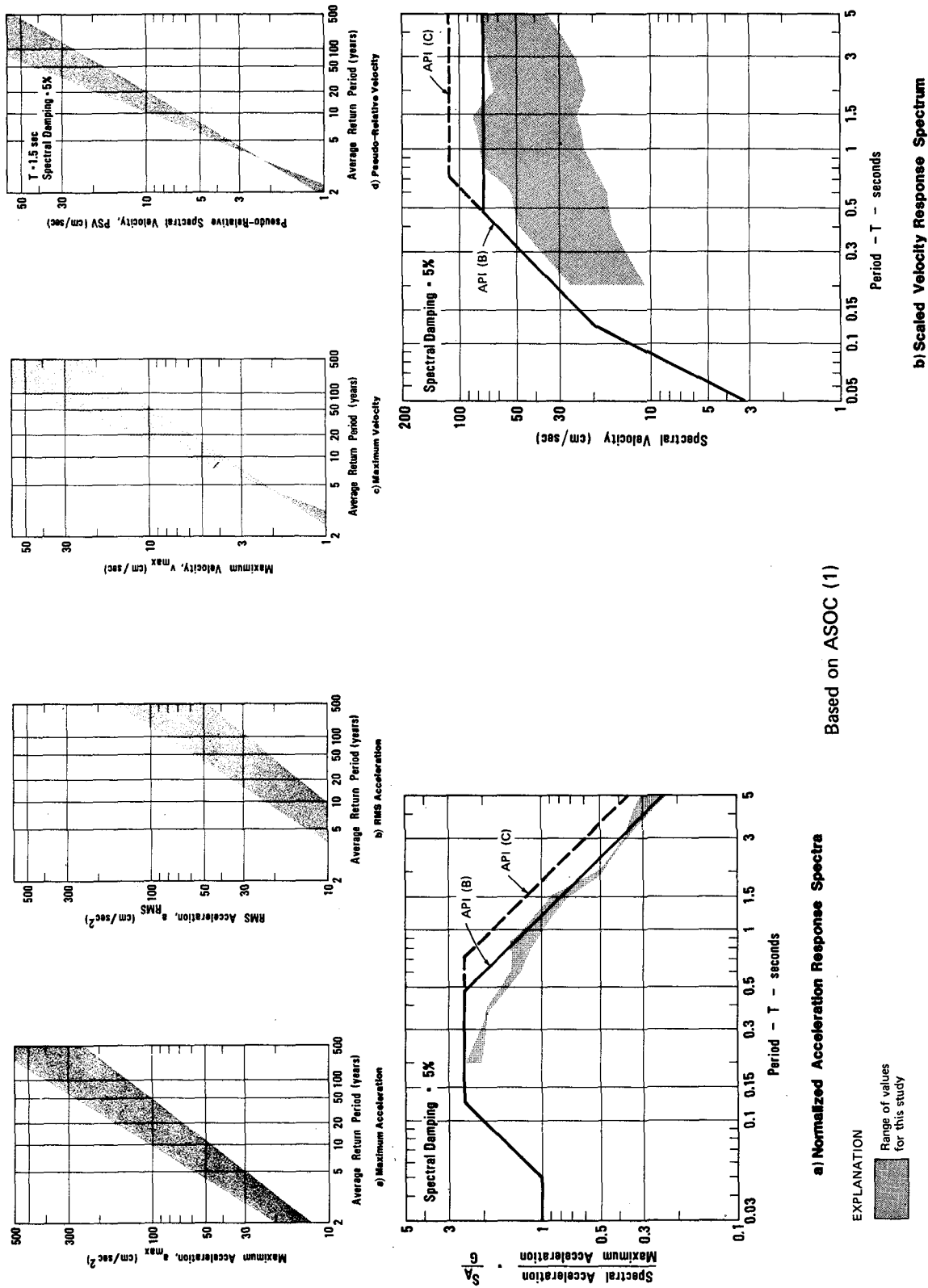
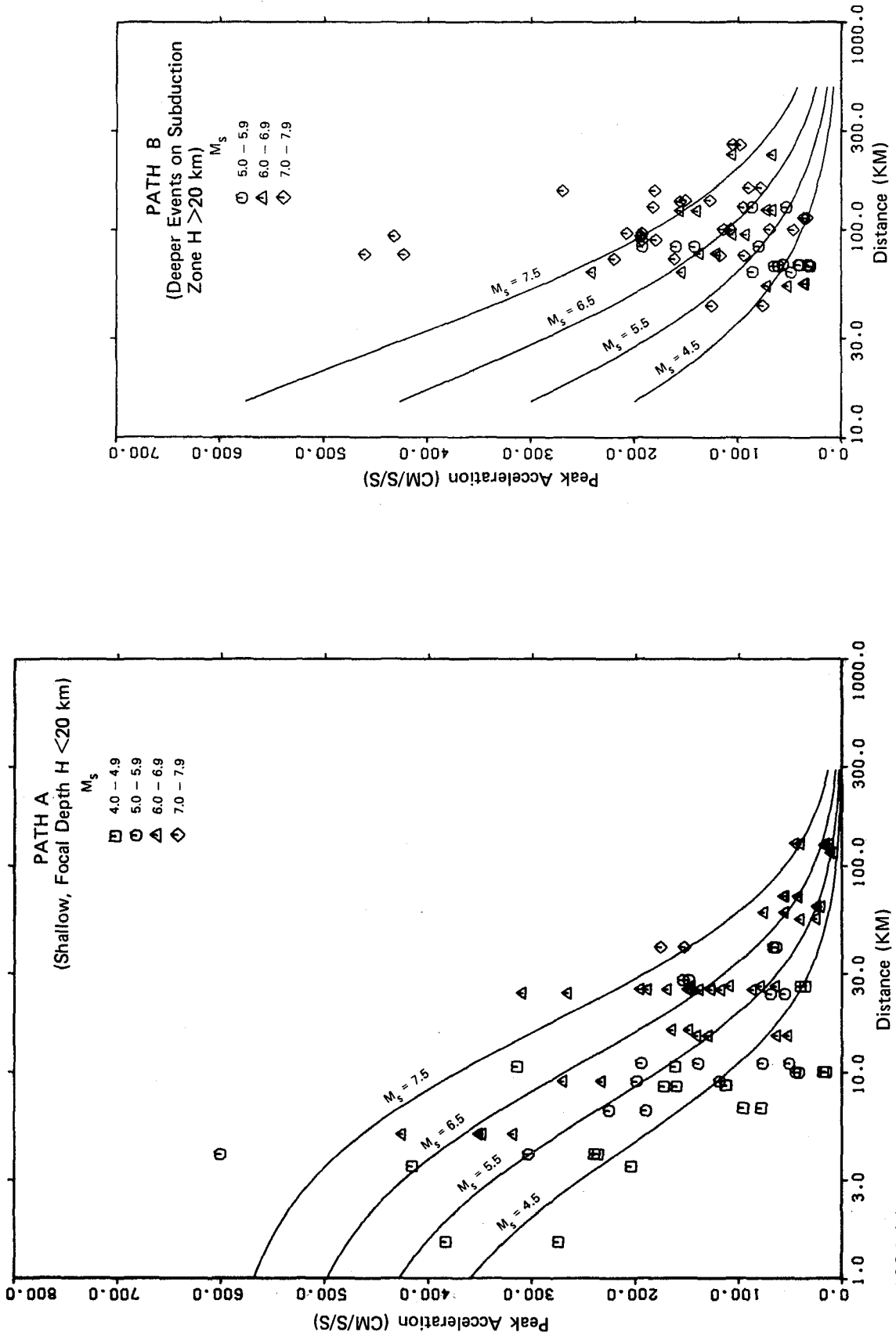
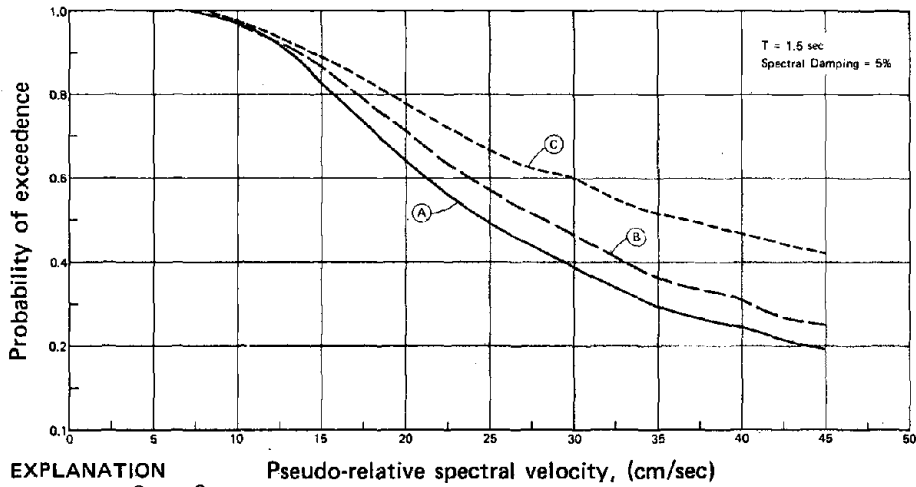
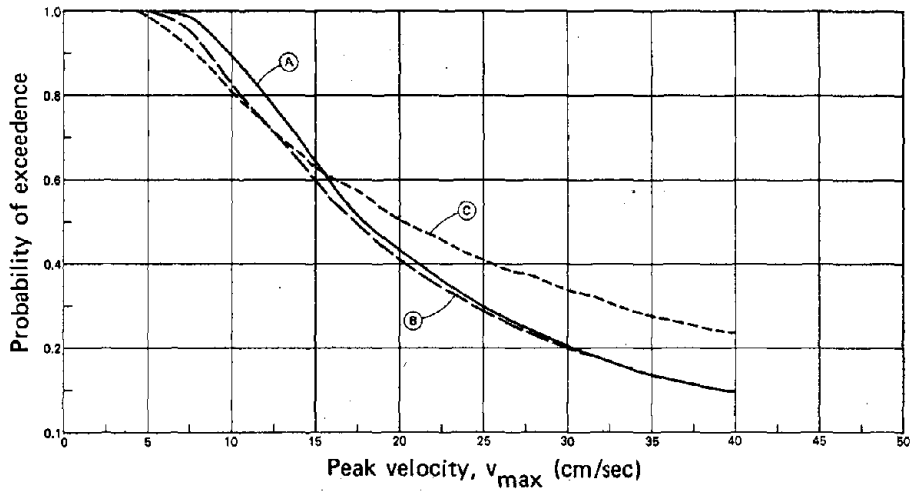
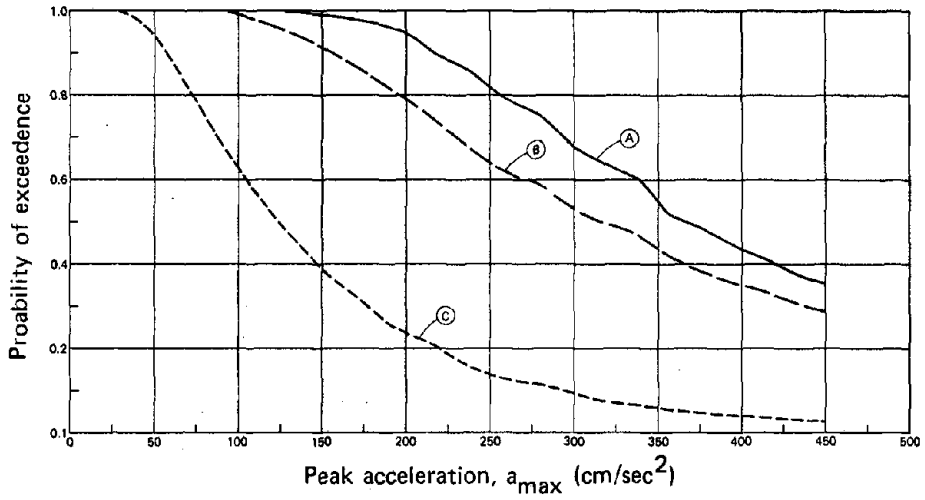


Fig. 5. Gulf of Alaska, Comparison of Seismic Exposure Values for Different Parameters



Based on ASOC (1)

Fig. 6. Attenuation Relationships for Shallow Earthquakes and Deeper Earthquakes on Subduction Zones in Offshore Alaska



**EXPLANATION**

Aleutians 158°W 56°N

Depth of application of attenuation

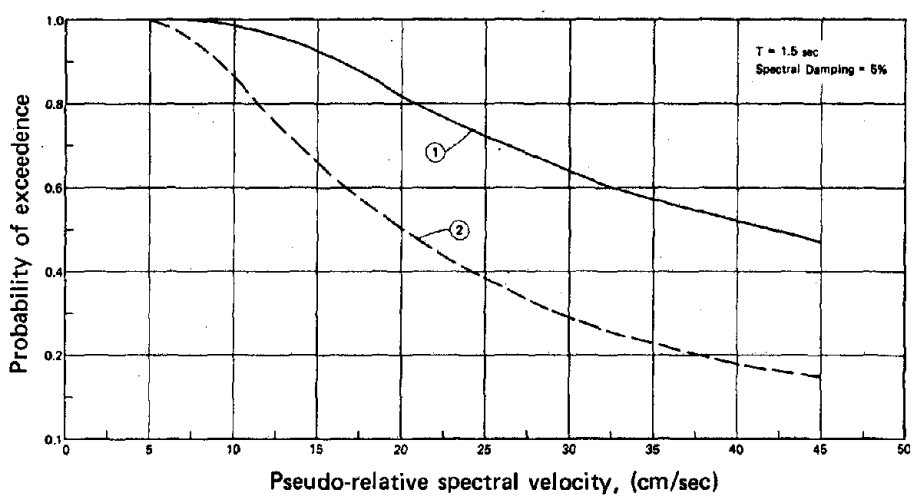
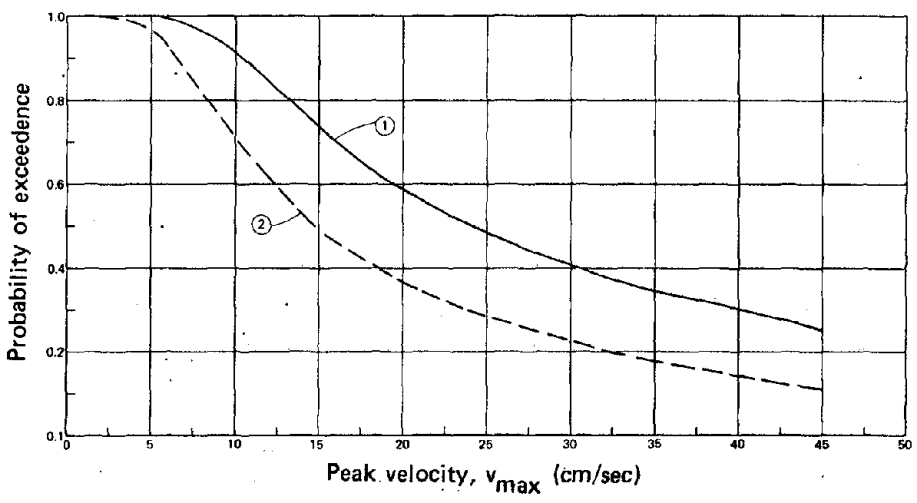
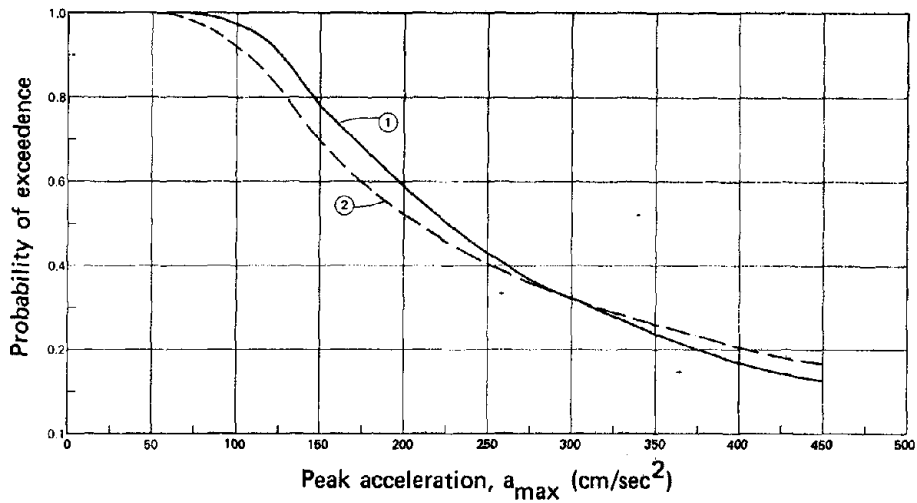
relationship transmission path B

(See Fig. 6)

Based on ASOC (1)

- (A) 0 km
- (B) 21 km
- (C) 100 km

Fig. 7. Influence of Type of Attenuation Relationship on Seismic Exposure



- EXPLANATION**  
 Site B — Gulf of Alaska, See Fig. 4.
- ① Stiff sites
  - ② Rock sites

Based on ASOC (1)

**Fig. 8. Influence of Site Conditions on Seismic Exposure**

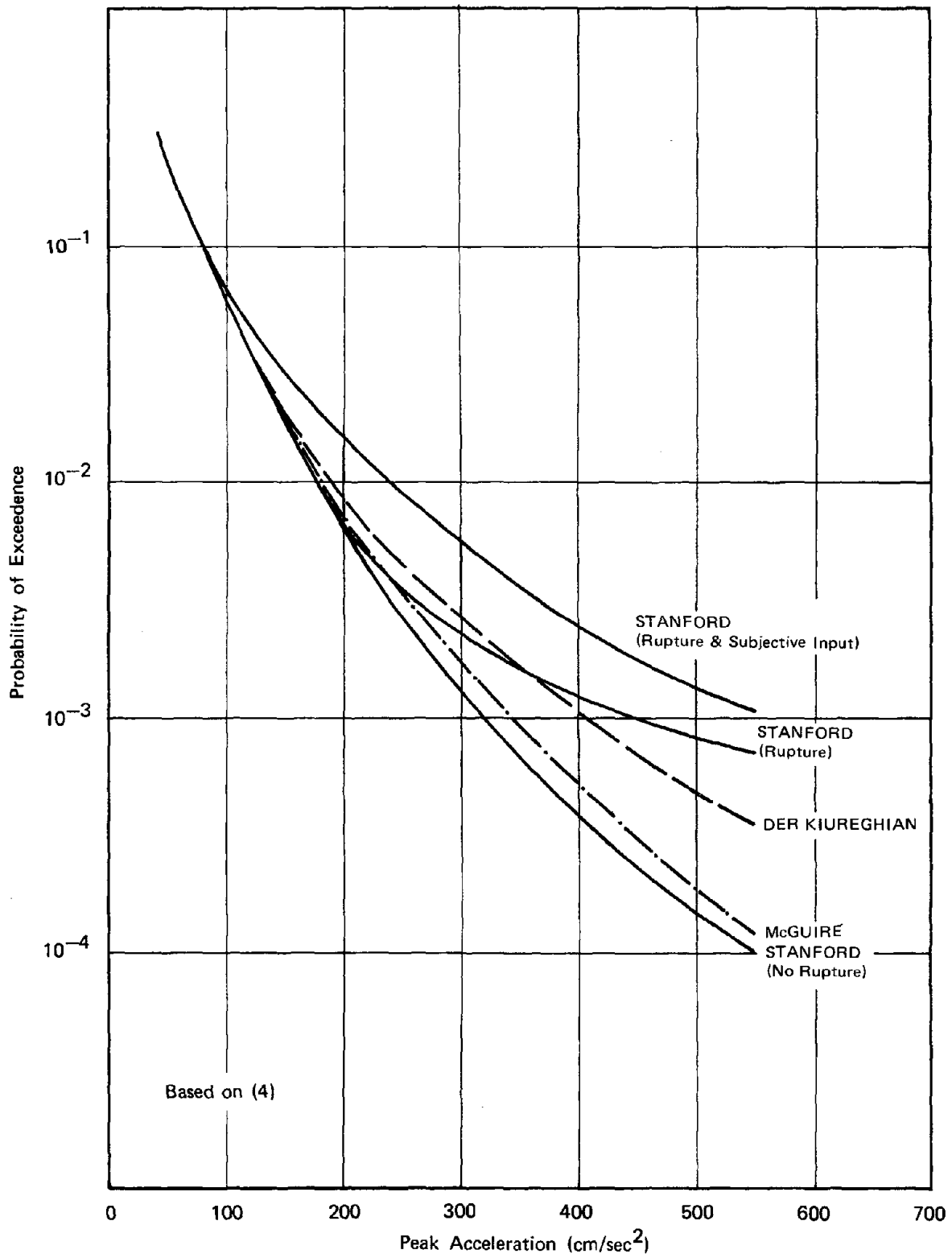


Fig. 9. Influence of Exposure Evaluation Model on Seismic Exposure Values

1306

**INTENTIONALLY BLANK**

SEISMIC EXPOSURE AND RELIABILITY CONSIDERATIONS  
IN OFFSHORE PLATFORM DESIGN

by  
R. G. Bea<sup>I</sup> and M. R. Akky<sup>II</sup>

ABSTRACT

Decisions on earthquake ground motions appropriate for design should include consideration of the structure design process and of the projected performance of structures designed by such a process. Seismic design conditions depend not only on geology and seismology, but as well on the characteristics of the structure which is to be designed and on the degree of reliability which is deemed desirable.

Seismic exposure results from a recently completed study of Alaskan Continental Shelf areas (1) are combined with results of a previous study of the performance and reliability characteristics of steel, tubular membered, template-type, pile-supported offshore platforms (2,3,4). Effective ground accelerations applicable to API's (5) normalized response spectra for design of offshore platforms are developed for two general locations - Eastern Gulf of Alaska and Lower Cook Inlet. These preliminary results indicate that substantial reductions in effective ground accelerations may be justified for Lower Cook Inlet. Current API values appear to be appropriate for the Eastern Gulf of Alaska area.

INTRODUCTION

In late 1976, the Alaska Subarctic Operators' Committee (composed of 21 oil companies) initiated the Offshore Alaska Seismic Exposure Study (OASES). The primary objective of this study was to characterize earthquake ground motions which might be experienced at offshore Alaskan sites. A variety of parameters were used to characterize the expected ground motions. Statistical and probabilistic methods were used to describe the variabilities and uncertainties associated with the ground motion parameters. The data, models, procedures, and judgement applied in development of these results are described in Reference (1).

The objective of this paper will be to take a portion of the results from OASES and translate them to design conditions for one class of offshore platform. A reliability and value assessment process will be used for this translation. The results will be expressed in the terms of the API's (5) effective ground accelerations and developed within the context of this particular design process.

API RP 2A

API RP 2A (5) utilizes the seismic zoning concept to describe the relative intensity of ground motions in a given geographical zone. Seismic zoning maps of the United States coastal areas developed by the U. S. Geological Survey (6) and the Applied Technology Council (7) were considered by API.

Figure 1 shows the Alaskan coastal waters divided into eight zones. Also shown are the regions included in OASES. The relative seismicity of each API zone is

- 
- I Chief Engineer, Ocean Engineering Group, Woodward-Clyde Consultants, Houston, Texas.
- II Sr. Project Engineer, Ocean Engineering Group, Woodward-Clyde Consultants, San Francisco, California.

characterized by using a factor of 1 through 5, the relative seismicity being higher factor numbers. The zone factors are linked to design coefficients called effective ground accelerations,  $G$  (see inset Figure 1). These accelerations are used to dimensionalize API's response spectra.

Figure 2 shows the normalized acceleration,  $S_a/G$ , response spectra used by API to characterize the distribution of energy with frequency. These spectra were based on studies primarily of Western U. S. records (8,9,10). The spectra are referenced to three types of local soil geological conditions: (A) Rock-like materials, (B) Shallow strong alluvium (less than 200 feet thick), and (C) Deep strong alluvium. Special studies are recommended for conditions which lie outside these general characterizations, particularly for deep soft soil conditions.

To determine the design forces appropriate for sizing the platform elements to meet strength requirements, the system is treated as a series of single-degree-of-freedom systems having the same natural frequencies as the platform system. The computed response is taken as the weighted linear superposition of the responses of these multiple single-degree-of-freedom systems. The weighting factors are composed of the ground motion participation factors and the natural mode shapes. Maximum response is calculated as the square root of the sum of the squares of the individual modal responses.

The API provides a description of three components of ground motion to be used. The major horizontal component (applied along a major axis of the platform) consists of the response spectrum shown in Figure 2 scaled by a design coefficient obtained from the seismic risk map shown in Figure 1. The minor horizontal component (acting in an orthogonal direction to the major axis of the structure) is taken as two-thirds of that assigned to the major horizontal component. A response spectrum of one-half the major horizontal component is assigned to the vertical component. These response spectra are intended to represent ground motions at elevations where pile and mat foundation elements receive the major effects of ground motion.

API structural design criteria are composed of two fundamental requirements: one for strength, and one for ductility. The strength requirement is based on the forces determined from the scaled response spectra and analysis procedure (environmental criteria). The members are designed so that the computed stresses do not exceed either buckling or minimum yield stresses. Special provisions are given for joints to insure that the strength of the joint exceeds that of the attached members. In addition, redundancy is provided so that alternate load redistribution paths may be developed in the event of primary member failures, loading reversals are considered, and details which incorporate abrupt changes in stiffness or strength are avoided.

The ductility requirement provides that the platform be stable under lateral deflections twice those calculated using the strength condition forces. Account is taken of the limited strength of framing that either buckles or yields, cyclic loadings, and the effects of vertical loadings acting through inelastic deformations.

## SEISMIC EXPOSURE

OASES results for two locations will be used to illustrate a translation of seismic exposure results to response spectra based environmental design criteria: the Eastern Gulf of Alaska (GOA) and Lower Cook Inlet (LCI). These locations are shown on Figure 1.



The GOA and LCI are bordered by the earth's most active seismic zone, the Circum-Pacific Belt. The primary cause of seismic activity is the relative motion between the Pacific and North American Plates. In this area, the boundary is characterized by two distinct styles of deformation. Along the eastern GOA to north of the Queen Charlotte Islands (API Zone 4, Figure 1), the two plates are sliding past each other along major right-lateral strike-slip fault systems.

Southwest of Prince William Sound and along the Aleutian Arc, the Pacific Plate is underthrusting the North American Plate. This develops the compressional forces that produce seismicity typical of Benioff Zones.

The transition zone between strike-slip and subduction motions is complex. The GOA study area is within this zone. The upper 7 to 12 kilometers of crust in this area is severely warped up and down and complexly faulted. Seismic data indicates that the Benioff Zone beneath this crust is nearly horizontal and generally underlies the entire area.

The LCI area lies within a large structurally dropped block, approximately 100 by 300 kilometers. The tectonics of this area are currently dominated by compression along the zone of underthrusting, with only minor deformation occurring within the LCI crust. Seismicity is dominated by the activity of the Benioff Zone which lies at a depth of approximately 50 to 100 kilometers beneath the study area.

The variation of four of the seismic exposure parameters mapped in OASES for the GOA with return period is shown in Figure 3. Those for LCI are shown in Figure 4. These values are for the offshore areas generally lying within 200 meter water depths and are applicable to firm alluvium soil conditions.

Figure 5 shows the comparison of OASES normalized acceleration response spectra and scaled velocity response spectra (for 100-year return interval) with those of API for the GOA. A similar comparison for LCI is given in Figure 6. Both of these areas fall within API relative seismicity zone 5. API response spectra for soils (B) and (C) are shown as they should bracket the soil conditions appropriate for comparisons with OASES results.

One of the major factors contributing to the GOA seismic exposure characterization is the expected level of seismicity on the dominant source, the shallow and dipping Benioff Zone. The GOA is considered to be a seismic gap (11,12), and the mean number of large earthquakes (surface wave magnitudes,  $M_s$ ,  $> 7.4$ ) utilized in the seismic exposure evaluation is 2.04. The upper range of maximum acceleration occurs in an area close to the junction between the shallow and deep Benioff Zone. This is an area influenced by attenuation relationships for shallow sources (similar to those derived from Western U. S. records) and for deep sources (derived from Japanese and South American records for similar tectonic conditions). Attenuation relationships associated with the deep Benioff sources give substantially higher values of maximum acceleration (1,13). The upper range of spectral velocity also occurs in the same area, which may be attributed to the influence of the shallow source attenuation relationship at relatively short distances. For a site with a maximum acceleration in the mid-range of that shown in Figure 3, the Benioff Zone contributes about 90 percent of the exposure, of which nearly 62 percent is contributed by earthquakes of magnitude greater than 7.5.

The LCI area is small in size which partially accounts for the narrow range of values shown. The probability of large earthquakes in LCI is estimated to be about 2.5 times lower than the GOA. The markedly lower spectral velocity values can be attributed to the dominant influence of the attenuation relationships for the deep

Benioff sources which control the seismic exposure of this area. As noted, these deeper sources (focal depths in excess of 20 km) develop recorded ground motions which have less amounts of energy in the longer period range (periods greater than about 1.5 sec). It has been postulated (13) that this observation is due to the existence of much less surface wave energy for deep sources as compared with that for shallow sources. The Benioff Zone contributes about 95 percent of the seismic exposure. Nearly all of this exposure is contributed by earthquakes of magnitudes less than 7.5. This is in significant contrast with the GOA.

## SEISMIC FORCES

The effects of earthquake ground motions on a structure are dependent upon the dynamic, strength, and deformation capacity of that structure. In this study, a conventional template-type, pile-supported drilling and production platform for 300 feet of water will be used to analyze the potential earthquake effects. The response characteristics of this platform have been extensively studied (3,4). The following paragraphs will summarize some of the important details of this particular structure.

The structure consists of two primary systems: a superstructure system, which is comprised of decks, supporting drilling and production equipment, and a template (or tower) which connects the decks with the seafloor; and a substructure system which is comprised of the soils and embedded foundation piles and well conductors (through which wells are drilled).

The template is composed of small diameter, steel, three-dimensionally trussed frame members. Leg diameters are 78 in. and brace diameters range from 24 in. to 48 in.

The substructure is taken to be comprised of firm, shallow alluvium type soils (API Soil Type B), 72-in., 2.5-in. wall thickness piles, and 24-in., 2-in. (equivalent) wall thickness conductors. The piles extend 250 feet into firm alluvium.

The platform system has a total dynamic weight,  $W$ , of 105,000 kips. Water contained in the legs and other elements accounts for 11,500 kips and participating in dynamic response (lateral, added mass) accounts for 28,000 kips.

The system has a fundamental period (broadside flexural) of 2.1 sec; a second mode (end-on flexural) period of 1.8 sec; and a first vertical mode period of 0.4 sec. Overall system damping (including foundation hysteretic and geometric contributions, hydrodynamic, and structural) was taken to be 5 percent of critical for low level excitations inducing forces less than elastic design load) and 10 percent of critical for high level excitations.

Elements of this platform were sized according to API guidelines (5). The dynamic response of the platform system was determined using a three-dimensional, elastic, time domain computer code, initially developed by Clough (14). The computer model lumps self-weight, imposed, and dynamic masses at the nodes, determines stiffness characteristics based on the elastic properties of the interconnected members, uses uniform modal damping to recognize the various forms of energy dissipation, and simulates support of the substructure by a series of linear-coupled elastic springs.

Earthquakes were input as three-dimensional acceleration time histories, applied uniformly across the base of the platform system. A wide variety of recorded and synthetic ground motions (firm alluvium), typical of Western U. S. records were used in the analyses. Analyses were performed for the first 40 seconds of input

ground motion time histories. Some 100 different analyses performed in the study lead to the following relationship between the maximum or peak value of resultant, horizontal base shear (BS max) and the peak ground velocity (V max) (referencing peak of one of horizontal input components):

$$\begin{array}{rcl} \text{BS max} & = & 430 \text{ (Vmax)} \\ \text{(kips)} & & \text{(cm/sec)} \end{array} \quad (1)$$

This is a mean correlation which has a coefficient of variation (COV) of about 20 percent (3).

In this study, the BS max will be used as the index of environmental effects on the platform system. As for most complex phenomena, a single index must fail to describe many of the details of the phenomena. In the case of the platform system studied, this index does appear to capture the majority of important gross strength and force effects.

As previously discussed, the OASES study indicates that LCI ground motions potentially have much lower amounts of energy in the long period range (due to contributions of seismic sources on deep Benioff), than either associated with Western U. S. recorded ground motions or appropriate for the GOA region. To approximate the potential effects of this factor on the forces induced in the study platform system, the following mean relationship has been used:

$$\begin{array}{rcl} \text{BS max} & = & 245 \text{ (Vmax)} \\ \text{(kips)} & & \text{(cm/sec)} \end{array} \quad (2)$$

This relationship has been derived from the response spectra developed for LCI (Figure 6) by ratioing the response spectra ordinates appropriate for shallow sources to those for LCI within the range of periods of primary interest to the dynamic response of the study platform. Future efforts could utilize the South American and Japanese recorded ground motions for deep source events as input to a study of platform response to more accurately determine this effect. Results for LCI will be developed for both of these relationships to determine the influence on design conditions.

Characterization of expected annual maximum resultant base shear forces developed on the study platform by the earthquake exposure projected for the range of GOA sites (Figure 3) is given in Figure 7 (based on equation 1). The 100-year BS max ranges from 23,200 kips to 5,800 kips. Similar results for LCI are shown in Figure 8 (based on equations 1 and 2).

At this point, it is important to recall that these forces have been derived from results of elastic analyses. For ground motions which develop forces in excess of the elastic (or pseudo-elastic) limit, inelastic action or ductility will act to limit or reduce the forces (15,16,17). This potential reduction in forces generated in the platform system during very intense ground motions will be introduced at a later stage in the analysis. Thus, the results shown in Figures 7 and 8 are appropriate for elastic structures or structures which have a ductility (ratio of maximum deformation to yield deformation of system) of one.

## STORM FORCES

Projected storm wave height conditions for the two study locations are quantified in Figure 9. The conditions are expressed as the probabilities of experiencing various values of expected maximum wave heights in any given year.

The 100-year expected maximum wave height for GOA is 110 feet and that of LCI is 30 feet. These results are based on information developed from oceanographic hindcasting models (18,19,20). These models utilize historical data on meteorology and wind fields of severe storms to make estimates of wind, wave, and current conditions which have been experienced in the past. Data measured in these two locations have provided a strong basis for calibrations of the hindcast models and quantifications of the reliability of the hindcast results.

Storm forces (wind, wave, current) developed on the study platform were computed in a manner similar to that previously described for earthquake induced forces. The storm waves were characterized as long-crested, two-dimensional, regular, wave forms described by heights and periods (periods based on height to length ratio of 1/10). Stokes' Fifth Order Theory was used to determine the time-space variation of wave particle velocities and accelerations. A storm and tide associated surface current of 4 feet per second decreasing linearly to zero at the mudline was assumed for both locations. The Morison force equation coupled with drag and inertia coefficients of 0.6 and 1.5, respectively, were used to compute the resultant hydrodynamic forces. A storm wind speed of 130 miles-per-hour was assumed. The mean relationships which were developed for peak horizontal resultant base shear (BS max) as a function of wave height (H) is:

$$\text{BS max} = 2.5 H^2 \quad (\text{for } H \geq 60 \text{ ft}) \quad (3)$$

(kips)      (ft)

and,

$$\text{BS max} = 30 H^{1.4} \quad (\text{for } H < 60 \text{ ft}) \quad (4)$$

The coefficient of variation associated with this relationship (based on plausible ranges in currents, wave periods, directionality, and projected area of the platform) is approximately 17 percent.

Characterization of projected expected annual BS max for GOA and LCI oceanographic conditions (Figure 9) are given in Figure 10 (based on equations 3 and 4).

## MODELING UNCERTAINTIES

In this study, two important sources of randomness are recognized: (1) natural or inherent variability; and (2) modeling deficiencies or uncertainties. Natural variabilities are due to fundamental variations in future storm tracks and conditions, or due to variations in future locations and intensities of earthquakes. The source of randomness has been expressed in development of the oceanographic and earthquake loading characterizations (Figures 7,8,10).

The second source of randomness, modeling uncertainties, is due fundamentally to the inability of our analytical models to accurately or precisely determine loadings and forces, given a description of the environmental conditions and the platform system characteristics. Analysis of this source of randomness has been developed previously (2,21). The analysis recognizes potential variabilities in wave form, currents, flow theory drag coefficients, and the effective projected area of the platform in computing hydrodynamic loadings. In addition, uncertainties in the characteristics of free-field ground motions, soil-water-structure interactions have been recognized in the analysis for earthquake induced forces.

The analysis indicates that unbiased estimators have been developed for both earthquake and oceanographic forces (ratio of actual to predicted force at 50th percentile is 1.0). The COV on the ratio of actual to predicted force is 66 and 82 percent for oceanographic and earthquake forces, respectively.

In subsequent parts of this study, these uncertainties will be combined with the natural or inherent variabilities. Results will be developed including and excluding modeling uncertainties to illustrate the importance of this factor.

## PLATFORM RESISTANCE

Results from a static, three-dimensional, inelastic analysis of the study platform system are summarized in Figure 11. To perform the analysis, a loading pattern was established for the platform system from results of the dynamic, elastic analyses of platform response to ground motions (22). Loadings were then sequentially increased, maintaining the established pattern of inertial loadings. Vertical loadings were included in the analysis.

A design level lateral loading ( $R_d$ ) of 25,000 kips is shown in reference to the succeeding damage states (DS) leading to collapse (inability to support vertical loads) of the system. Characteristics of the damage states are given on the figure. The characteristics utilized to describe the behavior of the tubular brace, joint, pile, and conductor elements have been given previously (2,3).

Overall system ductility, referenced to the deformation at the design load, is in the range of 2.5 to 3. The margin between the elastic design load and the inelastic collapse load is about 2.

Significant separation of yield and collapse level base shears and displacements from those of the design level are due to many factors including: system of framing, redundancy in the system, intentional factors-of-safety in the design process, extra strength added by other loading requirements or added at the prerogative of the designer, and the design-performance requirements for the tubular members and joints which comprise the majority of the elements of this platform system.

The earthquake induced force capacity characterization for the study platform system is summarized in Figure 12. Ultimate or collapse resistance ( $R_c$ ) (defined on a force, not deformation basis) is referenced to the elastic design load ( $R_d$ ) through the resistance ratio (RR). The variabilities in computed resistance were quantified using previously developed data and methods (2,23). The variabilities are due primarily to those of materials, fabrication, element strength, and performance of subsystems (composed of elements and joints). The median RR is 2.0 and the coefficient of variation about 28 percent.

Also shown on this figure is the description of RR for oceanographic loadings. Derivation of this description is detailed in reference (2). The median RR is 3.0 and the coefficient of variation is 53 percent. This difference in resistance characterization is due to the integration of actual experience with platforms in the field subjected to severe oceanographic loadings (approaching 3 times  $R_d$ ). Bayesian updating techniques have been used in this derivation (24). Such experience is indicating that either the platforms are stronger, the storm loadings are less, or some combination of the two.

Figure 11 indicates a possible alternative behavior for an offshore platform system. In this system there is a nominal separation between design and ultimate total lateral forces (22). However, the platform is designed to develop an overall system ductility of about 2. API guidelines (5) would allow such performance. The earlier yielding in this system compared with that of the study platform would have the effect of limiting the level of forces which could be induced in the system. For ground motions which would cause yielding of the alternative system, the induced forces would be approximately half of those of the non-yielding elastic (or pseudo-

elastic) system. Thus, even though the alternative system has only about half the capacity of the study platform (referring to ultimate lateral forces), its ductility would allow it to perform comparably in ground motions which would cause yielding of the alternative system when the yielding did not exceed the ductility limits and when the ground motions did not induce forces in the pseudo-elastic system which exceeded its capacity.

In an approximate way, the influence of system ductility can be entered into the analysis by generating inelastic response spectra in lieu of elastic response spectra such as are given in Figures 5 and 6 (15,17). For a given allowable ductility, such a spectra characterization would indicate the level of design lateral loading required for a given level of non-exceedance. In this study, this factor is introduced by reducing the earthquake induced forces above values in excess of the yield level lateral force by dividing by the system ductility. This factor, when coupled with the lower capacity ratio for the system (Figure 12, 50th percentile ratio close to unity) develops results which approximate those for the pseudo-elastic system. It is well to note that even in the case of the pseudo-elastic system, there is a limiting loading which can be developed in the system which is equal to the ultimate resistance of the system (4). This can be a very important factor in analysis of performance in very intense ground motions.

## RELIABILITY CHARACTERIZATIONS

Risks are an unavoidable fact of life for offshore structures. Projections of environmental conditions, loadings, and response of the platform system during its lifetime involves large uncertainties. Uncertainties lead to risk.

Reliability ( $P_s$ ) can be defined generally as the probability that the platform will perform adequately or acceptably during its lifetime. Risk ( $P_f$ ) is the compliment of reliability ( $P_f = 1 - P_s$ ). There can be many and multiple definitions of acceptable or unacceptable performance. The damage states expressed in Figure 11 are one such definition. In this analysis, consideration will be given to the damage state with the largest impacts - the ultimate or collapse damage state.

In a load ( $S$ ) and resistance ( $R$ ) format, reliability is defined as the probability that loading does not exceed resistance or strength. If the true future maximum loading condition could be determined precisely and the structure designed and constructed so that it had an assured or actual strength in excess of this maximum loading, then the structure would be absolutely reliable. However, the unknown future whims of Mother Nature and the uncertainties of the response and performance of man's structures combine to make absolute reliability a practical impossibility. Characterization of reliability provides a means through which uncertainties (which are recognized) can be examined and quantified, and rational decisions reached on design strategies which develop an acceptable level of reliability.

In this study, reliability has been computed as follows (25):

$$P_s = \phi \left[ \frac{\ln \left( \frac{\bar{R}}{\bar{S}} \sqrt{\frac{1 + V_S^2}{1 + V_R^2}} \right)}{\sqrt{\ln(1 + V_S^2)(1 + V_R^2)}} \right] \quad (5)$$

where:  $\phi [X]$  = tabulated normal cumulative probability of the standard variate,  $X$ , in the interval  $-\infty$  to  $x$ .

$\bar{R}$  = mean value of resistance (ultimate)

$\bar{S}$  = mean value of loading

$V_R = COV_R$  = coefficient of variation of the resistance (decimal)

$V_S = COV_S$  = coefficient of variation of the loading (decimal)

Figures 13 and 14 show platform reliability (as annual probability of failure,  $P_{fa}$ ), for various elastic design base shears ( $R_d$ ), for the two locations, and for earthquake induced forces. Figure 15 contains the same information for storm loadings. Figure 16 shows results for the combined environmental conditions (storms and earthquakes).

Results of the sensitivity studies are shown in Figures 17 and 18. Figure 17 illustrates the influences of not including modeling uncertainties. Figure 18 illustrates potential effects of the lower energy content in LCI long period ground motions.

It is to be noted that the reliability of the platform system in the combined environment (oceanographic and earthquake) has been computed assuming independence of the two loading environments, and simultaneous occurrence of significant oceanographic and earthquake loadings have been neglected.

## ASSESSMENT OF CHOICES

Before a design load can be selected, the level of desirable or acceptable reliability must be determined. This is an assessment of choices with the objective of making a decision on overall design strategy. Development of target reliabilities will not be dwelled upon here. Previous work (26,27,28) will be relied upon to supply this background.

In this study, two attacks at determining a target reliability will be used: (1) a cost optimization analysis, and (2) use of a computed historical reliability for a comparable type of operation (offshore oil drilling and production).

It has been shown (29) that the annual probability of failure that produces the lowest combination of initial cost and potential future losses resulting from platform loss of serviceability is:

$$P_{fao} = \frac{\Delta C_i}{E(PL) \times PVF \times 2.3} = \frac{1}{2.3 \times PVF \times \text{Cost Ratio}} \quad (6)$$

where:	$P_{fao}$	=	The annual probability of failure determined on the basis of minimizing the tangible costs associated with placement of the facility and those potential costs associated with a loss of serviceability (defined as failure here).
	Cost Ratio	=	The ratio of $E(PL)$ to $\Delta C_i$ , or $C_f$ to $\Delta C_i$
	$\Delta C_i$	=	The slope of the initial cost curve when plotted against the common log of the annual probability of failure
	$E(PL)=C_f$	=	The expected cost of facility loss of serviceability (cost of failure)
	PVF	=	The present value function intended to bring to present cost terms the costs of potential future losses.

Analyses (4,21,27) of the cost factors involved lead to a conclusion that the Cost Ratio for conventional operations based on structures of the type studied here lie in the range of 4 to 6. Consideration of operation lifetimes in the range of 20 to 50 years, and assuming reasonable present value functions and discount rates, the optimum computed annual probability of failure can be shown to fall in the range of 0.3 to 1.2 percent (26).

A reliability study of Gulf of Mexico platform hurricane loadings, platform resistance, and actual survival experience of platforms (2,21) indicates computed annual probabilities of failure for current design strategies (5) to lie in the range of one percent. Experience with operations in the Gulf of Mexico would indicate actual probabilities of failure almost an order of magnitude smaller than those computed (30). However, for the purposes of identifying an analytical target reliability, values in the range of 0.5 to 1 percent appear to be appropriate. Thus, the cost optimization analysis and computation of reliabilities for comparable operations give similar results.

## DESIGN CRITERIA

Design criteria consist of environmental criteria (load or force determining processes and parameters), and structural criteria (member sizing processes and parameters which determine strength and ductility). Design strategy is a particular combination of engineering practice and design criteria.

Design criteria are intended to result in desired strength and reliable performance of the structure. Strength or performance is comprised of two primary elements: ultimate capacity, and ductility. Ultimate capacity reflects the load carrying capabilities of the facility. Ductility reflects the deformation capacity of the facility.

Strength is determined by the design criteria, strategy, construction processes, and the verification-quality control processes. Designation of a desirable level of strength is determined as a result of a complex process of decisions which attempt to reach a balance between the costs of achieving a given level of strength and those costs which might be incurred if the strength (and ductility) are not great enough.

Design criteria must provide the designer with a simple, readily applied process and set of parameters which will guide him in engineering a structure to have



acceptable performance characteristics. The definition of earthquake design conditions (intense ground motion characterizations) is one part of an integrated process which has as its objective the attainment of a given level of strength and ductility in the facility. To be reasonable, the environmental criteria specification must be coupled to the remaining parts of the process.

For a given seismic exposure, earthquake criteria for offshore platforms should depend upon: (1) exposures due to other environmental hazards such as those due to storm winds, waves, and currents, (2) procedures used to configure and size the platform system elements, (3) projected response of the platform system when it is subjected to intense ground motions and other environmental loadings (primary concern is with extreme damage, hence the focus is on inelastic performance), (4) acceptability of the projected response for a given platform system and design strategy, and (5) assessment of the variabilities and uncertainties associated with projected environmental conditions and responses of the platform system to these conditions.

In this study, design strategy is embodied in API guidelines (5), and in the engineering practice used to develop the conventional, 300-ft water depth, template-type platform. Structural criteria is taken as that defined by API. Potential changes in environmental criteria are focused on the effective ground accelerations defined by API for GOA and LCI. Other parts of the response spectra force determining process are assumed unchanged. The desirable computed platform reliability (annual) is taken as 99.0 percent.

Table I summarizes the environmental criteria developed from these analyses. The parameters shown are for the analyses which include modeling uncertainties.

Wave heights and peak ground velocities to be used in three-dimensional, time-domain, elastic analyses (as described earlier for the example platform) are given in Table I. These quantities have been determined from elastic design resultant base shears tabulated for an annual reliability of 99.0 percent, and from the appropriate force equations (1-4). Return intervals for these design quantities are based on results given in Figures 3, 4, and 9. Peak ground accelerations are tabulated for the same return intervals as those determined for the peak ground velocities.

API response spectra based effective ground accelerations shown in the last column of Table I have been determined as follows. The elastic base shear,  $R_d$ , represents the resultant of two orthogonal base shear components,  $R_{dx}$  and  $R_{dy}$ , which are aligned with the two principal horizontal axes of the platform (broadside and endon). API provides that:

$$R_{dy} = \frac{2}{3} R_{dx} \quad (7)$$

(weaker component) (stronger component)

and,

$$R_d = \sqrt{R_{dx}^2 + R_{dy}^2} \quad (8)$$

Thus,

$$R_d = \sqrt{R_{dx}^2 + \left(\frac{2}{3} R_{dx}\right)^2} \quad (9)$$

and,

$$R_{dx} = 0.83 R_d \quad (10)$$

For the platform studied (x direction strong component coincident with broadside weaker axis of structure):

<u>Mode (x)</u>	<u>Period (sec)</u>	<u>Participation Factor</u>	<u>Sa/G</u>
1	2.0	0.622	0.59
2	0.7	0.333	1.40
3	0.5	0.34	1.85

The normalized spectral accelerations (Sa/G) were obtained from API guidelines for B-type soils. Thus,

$$Rdx = \frac{W G}{g} \sqrt{(0.622 \times 0.59)^2 + (0.333 \times 1.4)^2 + (0.034 \times 1.85)^2} \quad (11)$$

and,

$$G = 1.327 \times 10^{-5} (Rd) g \quad (12)$$

## SUMMARY

Table I indicates that API response spectra based effective ground accelerations for GOA fall in the range of 0.5 to 0.4 g, considering storm and earthquake effects. Those for LCI fall in the range of 0.07 to 0.08 g. These values compare with a current API G of 0.4 g for LCI and GOA. Thus, a substantial reduction may be appropriate for LCI. Note the comparisons of peak ground accelerations (at the return intervals for design peak velocities) with effective ground accelerations; in all cases the peak accelerations are substantially greater than the effective accelerations.

Figure 17 shows the very substantial influence of neglecting modeling uncertainties on the computed reliabilities. However, when one considers this same factor in deriving target reliabilities for design, values in the range of 99.5 (annually) result. Thus, the elastic design loads and the environmental criteria coupled to these loads remain about the same.

Figure 18 shows the potential effect of the lower energy content in LCI long period ground motions on computed reliabilities. For a computed target reliability of 99 percent, Rd would be reduced from 5,900 kips to 4,000 kips, and the API G from 0.08 g to 0.05 g. Such a reduction for LCI and other similar areas along the coasts of Alaska could be an important consideration for future efforts.

## REFERENCES

1. Woodward-Clyde Consultants, "Offshore Alaska Seismic Exposure Study," Prepared for Alaska Subarctic Operators' Committee (ASOC), Volumes I - V, March, 1978.
2. Marshall, P. W., and Bea, R. G., "Failure Modes of Offshore Platforms," Proceedings, BOSS '76, Vol. Two, Trondheim, August, 1976.
3. Bea, R. G., Audibert, J.M.E.A., and Akky, M. R., "Earthquake Response of Offshore Platforms," Presented at Session No. 12, Earthquake Response of Special Structures - State of the Art, ASCE Annual Convention, San Francisco, California, October, 1977.
4. Bea, R. G., "Earthquake Criteria for Platforms in the Gulf of Alaska," Journal of Petroleum Technology, March, 1978.

5. American Petroleum Institute, "API Recommended Practice for Planning, Designing, and Constructing Fixed Offshore Platforms," American Petroleum Institute, API RP 2A, Ninth Edition, Dallas, Texas, 1978.
6. Algermissen, S. T., and Perkins, D. M., "A Probabilistic Estimate of Maximum Acceleration in Rock of the Contiguous United States," U. S. Geological Survey, Open File Report 76-416, 1976.
7. ATC-3, Final Review Draft of Recommended Comprehensive Seismic Design Provisions for Buildings, Prepared by Applied Technology Council, Sponsored by the National Science Foundation and by the National Bureau of Standards, 1977.
8. Seed, H., Ugas, C., and Lysmer, J., "Site Dependent Spectra for Earthquake-Resistant Design," Bull. Seism. Soc. Amer., Vol. 66, No. 1, February, 1976.
9. Newmark, N. M., Blume, J. A., and Kapur, K. K., "Seismic Design Spectra for Nuclear Power Plants," Journal of the Power Division, ASCE, Vol. 99, No. PO2, November, 1973.
10. Mohraz, B., "A Study of Earthquake Response Spectra for Different Geological Conditions," Bull. of Seism. Soc. Amer., Vol. 66, No. 3, June, 1976.
11. Kelleher, J., Sykes, L., and Oliver, J., "Possible Criteria for Predicting Earthquake Locations and Their Application to Major Plate Boundaries of the Pacific and the Caribbean," J. Geo. Res., Vol. 78, No. 14, 1973.
12. Page, R. A., "Evaluation of Seismicity and Earthquake Shaking at Offshore Sites," Proceedings, Offshore Technology Conference, OTC 2354, 1975.
13. Idriss, I. M., "State-of-the-Art Report, Ground Motion Characterization," ASCE Geotechnical Engineering Division Specialty Conference, Earthquake Engineering and Soil Dynamics, Pasadena, California, June, 1978.
14. Clough, R. W., "Earthquake Effects on Offshore Platforms," Final Report on Investigation for Shell Oil Company, July, 1966.
15. Veletsos, A. S., Newmark, N. M., and Chelapati, C. V., "Deformation Spectra for Elastic and Elastoplastic Systems Subjected to Ground Shock and Earthquake Motions," Proceedings of the Third World Conference on Earthquake Engineering, New Zealand, 1965.
16. Veletsos, A. S., "Maximum Deformations of Certain Nonlinear Systems," Proceedings, Fourth World Conference on Earthquake Engineering, Santiago, 1969.
17. Whitman, R. V., and Protonotarios, J. N., "Inelastic Response to Site-Modified Ground Motions," Journal of the Geotechnical Engineering Division, Proceedings, ASCE, October, 1977.
18. Marine Advisers, Inc., "Group Oceanographic Survey, Gulf of Alaska, Phase I Area, Final Report, Vol. 4, Compensated Extreme Storms," A Report on Industry Cooperative Study to Standard Oil Co. of California, 1970.
19. Federal Power Commission, Bureau of Natural Gas, "Draft Environmental Impact Statement, Cook Inlet - California Project," Vol. 1, September, 1976.

20. Environmental Research Laboratories, "Environmental Assessment of the Alaskan Continental Shelf, Vol. II, Physical Oceanography and Meteorology," Boulder, Colorado, 1976.
21. Bea, R. G., "Earthquake Design Criteria for Offshore Platforms," Presented at Session No. 50, Probabilistic Methods in Earthquake Engineering, ASCE Annual Convention, San Francisco, California, October, 1977.
22. Kallaby, J., and Millman, D. N., "Inelastic Analysis of Fixed Offshore Platforms for Earthquake Loading," Offshore Technology Conference Preprints, OTC 2357, 1975.
23. Marshall, P. W., "Risk Factors for Offshore Structures," Journal of the Structural Division, ASCE, Vol. 95, No. ST12, 1969.
24. Tang, W. H., and Ang, A. H. S., "Modeling, Analysis and Updating of Uncertainties," ASCE National Structural Engineering Meeting, Preprint 2016, April 1973.
25. Ang, A. H. S., and Cornell, C. A., "Reliability Bases of Structural Safety and Design," Modern Concepts of Structural Safety and Design, ASCE National Structural Engineering Meeting, Preprint 2023, 1973.
26. Bea, R. G., "Development of Safe Environmental Criteria for Offshore Structures," Proceedings, Oceanology Int. Conf., Brighton, England, 1975.
27. Stahl, B., and Blenkarn, K. A., "Offshore Platform Reliability - A Parameter Study," Proceedings of the National Structural Engineering Conference, Methods of Structural Analysis, Madison, Wisconsin, August 1976.
28. Keeney, R. L., and Raiffa, H., Decisions With Multiple Objectives: Preferences and Value Tradeoffs, John Wiley and Sons, 1976.
29. Bea, R. G., and Dover, A. R., "Reliability Analyses for Offshore Platforms," Submitted for possible publication in Journal of the Waterways and Harbors Division, ASCE, July 1978.
30. Stahl, B., "Offshore Structure Reliability Engineering," Petroleum Engineer, October 1977.

TABLE 1: DESIGN ENVIRONMENTAL CONDITIONS  
Annual Probability of Failure, Pfa, 1%

Location	Type of Loading	Elastic Base Shear <sub>3</sub> (Rd) (10 <sup>3</sup> -kips)	Wave Height H (ft)	Wave Return Interval HRI (years)	Peak Ground Velocity Vmax (cm/sec)	Velocity Return Interval VRI (years)	Peak Ground Acc. at VRI Amax (g's)	API RP 2A Effective Ground Acc., G (g's)
Gulf of Alaska (Lower Bound)	Storms & Earthquakes	29.5	109	100	69	6666	0.54	0.39
	Storms	29.0	108	100	--	--	--	--
	Earthquakes	6.0	--	--	14	100	0.14	0.08
Gulf of Alaska (Upper Bound)	Storms & Earthquakes	38.0	123	350	88	200	0.51	0.50
	Storms	29.0	108	100	--	--	--	--
	Earthquakes	20.0	--	--	47	83	0.32	0.27
Lower Cook Inlet (Lower Bound)	Storms & Earthquakes	4.9	37	800	11	167	0.23	0.07
	Storms	3.5	29	80	--	--	--	--
	Earthquakes	4.0	--	--	9	100	0.20	0.05
Lower Cook Inlet (Upper Bound)	Storms & Earthquakes	5.9	43	6666	14	143	0.30	0.08
	Storms	3.5	29	80	--	--	--	--
	Earthquakes	5.0	--	--	12	100	0.25	0.07

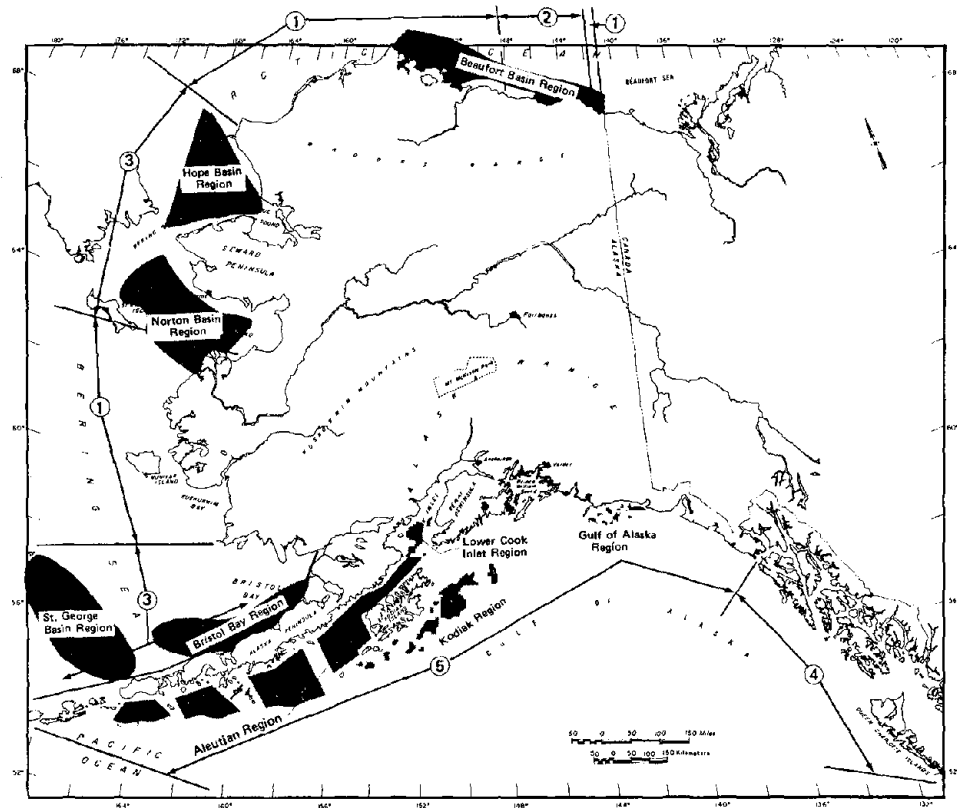


Fig. 1. Location of Seismic Exposure Study Area's Relative to API Seismic Zones

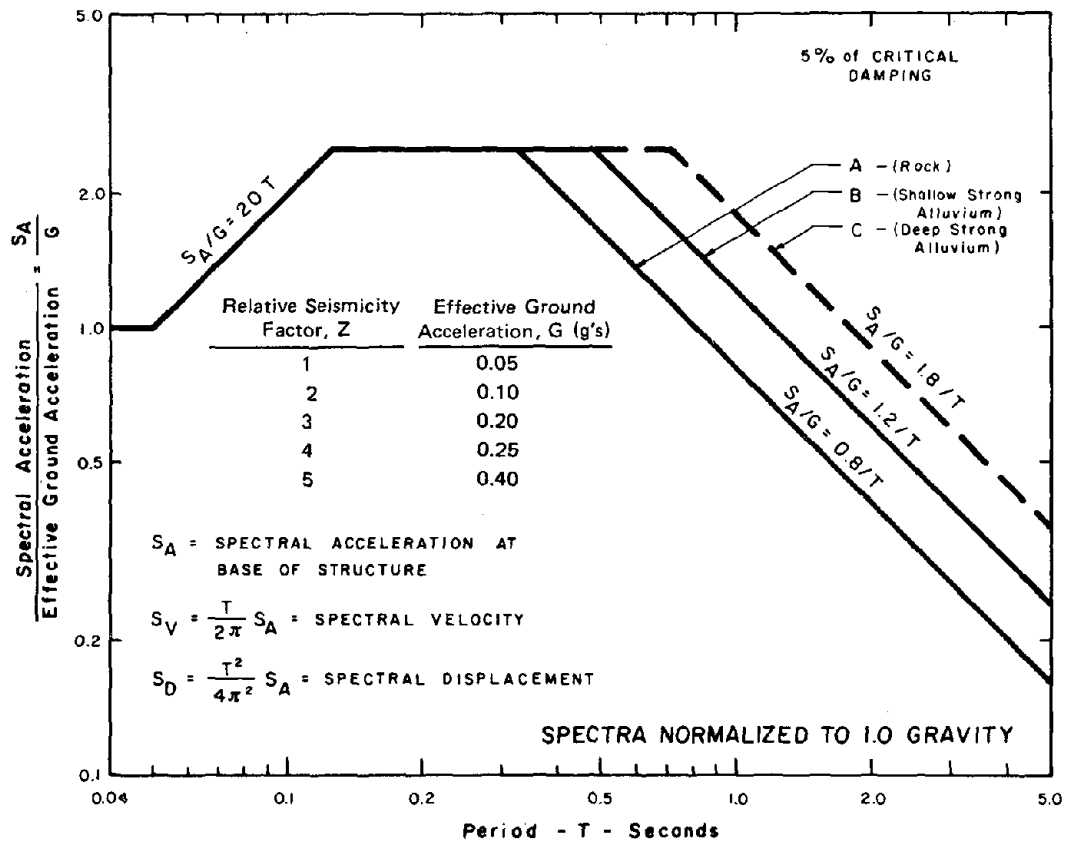


Fig. 2. API (1978) Design Response Spectra

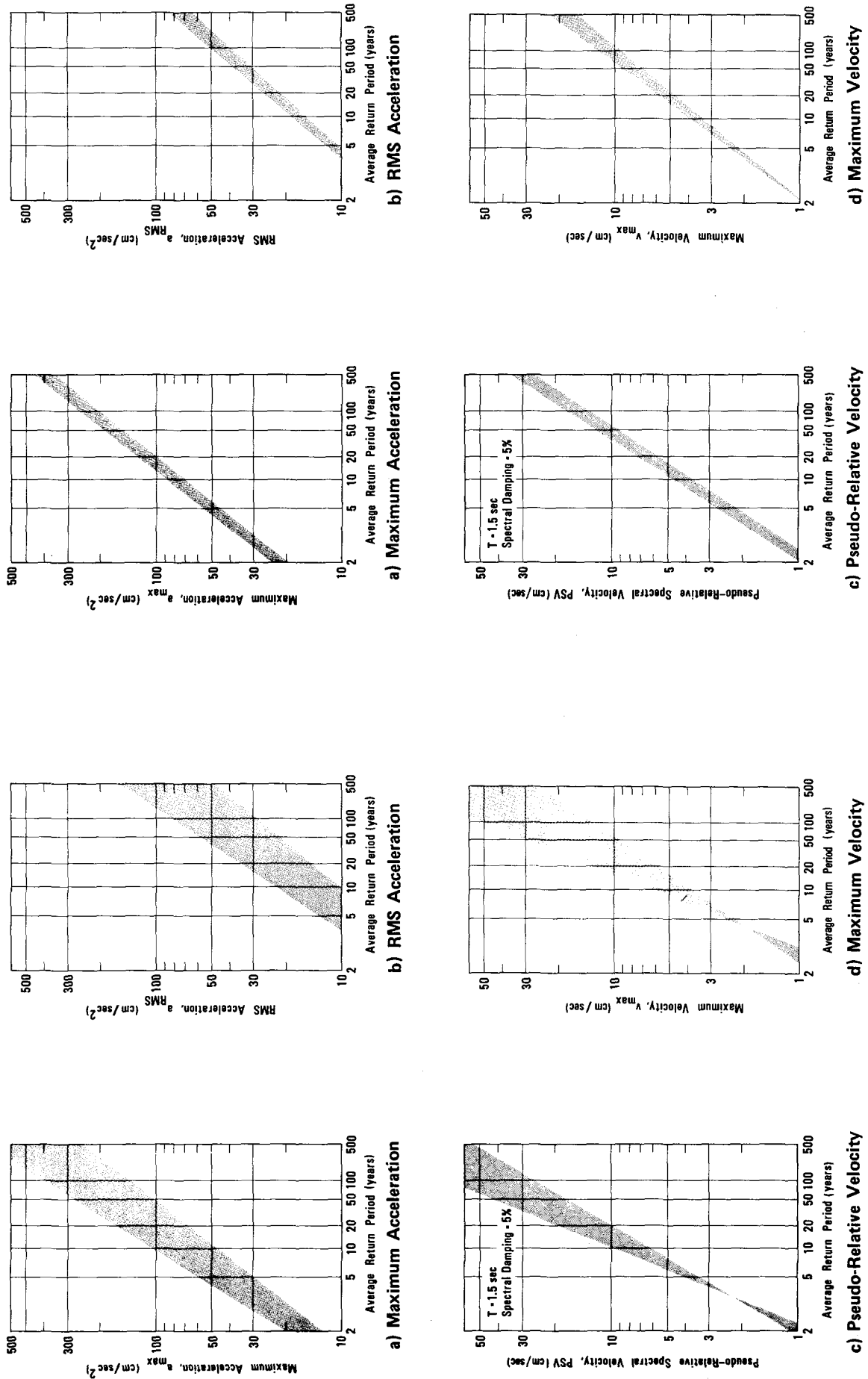


Fig. 3. Statistical Distribution of Mapped Seismic Exposure Parameters — Gulf of Alaska (Ref. 1)

Fig. 4. Statistical Distribution of Mapped Seismic Exposure Parameters — Lower Cook Inlet (Ref. 1)

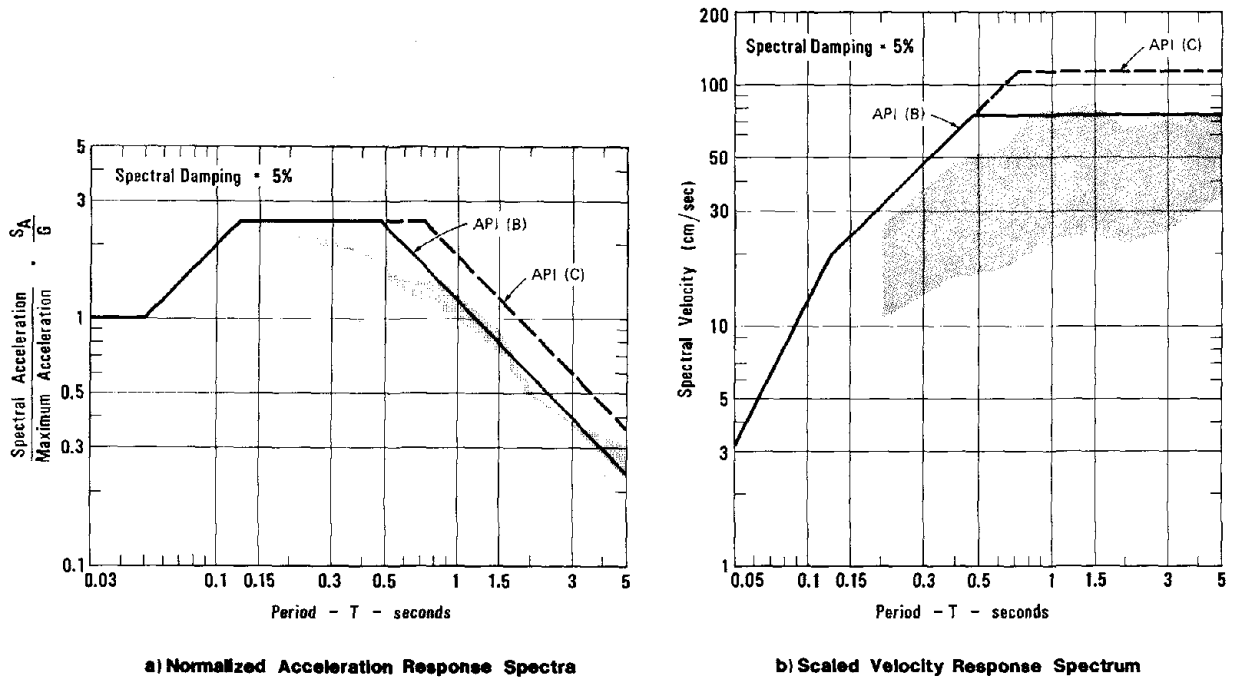


Fig. 5. Comparison Between Mapped and API (1978) Normalized and Scaled Response Spectra - Gulf of Alaska (Ref. 1)

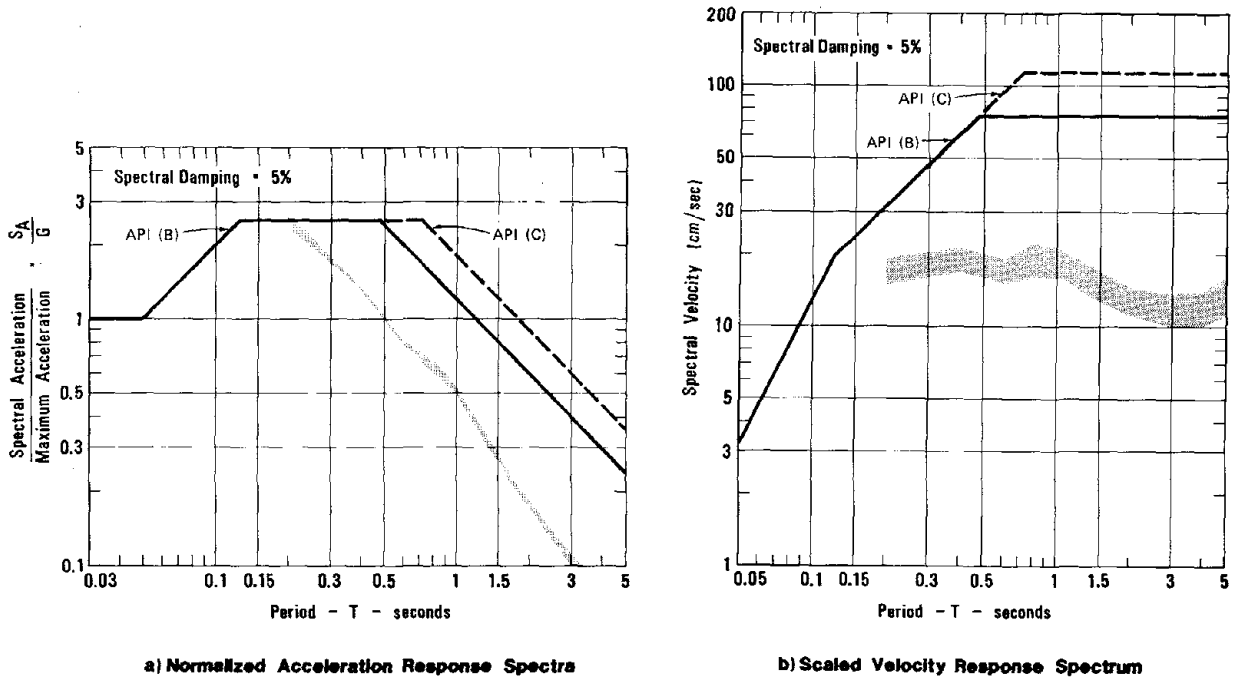


Fig. 6. Comparison Between Mapped and API (1978) Normalized and Scaled Response Spectra - Lower Cook Inlet (Ref. 1)



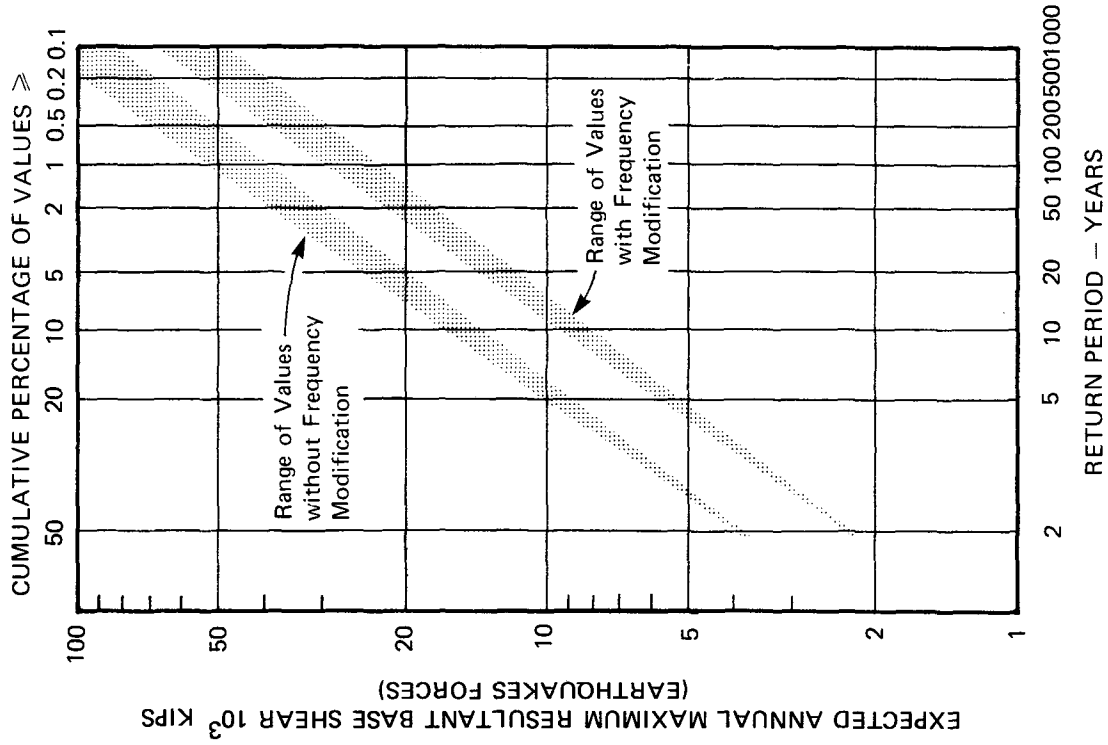


Fig. 8. Statistical Distribution of Earthquake Loading (Base Shear) - Lower Cook Inlet

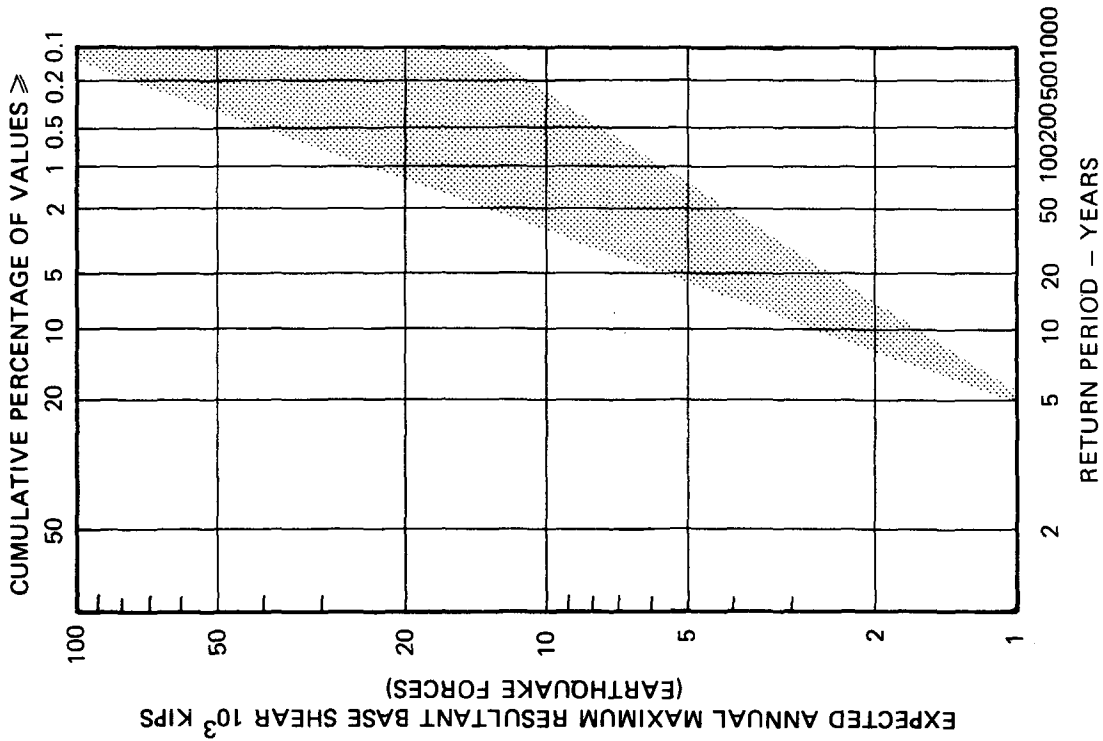


Fig. 7. Statistical Distribution of Earthquake Loading (Base Shear) - Gulf of Alaska

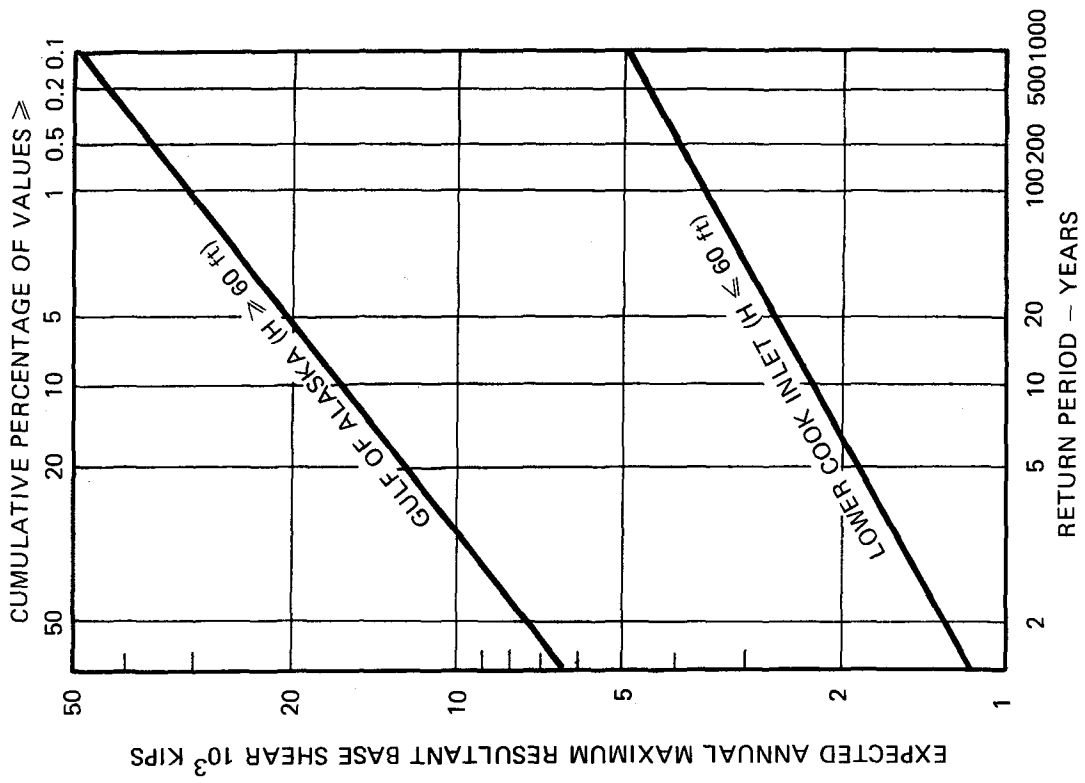


Fig. 10. Statistical Distribution of Storms Loading (Base Shear)

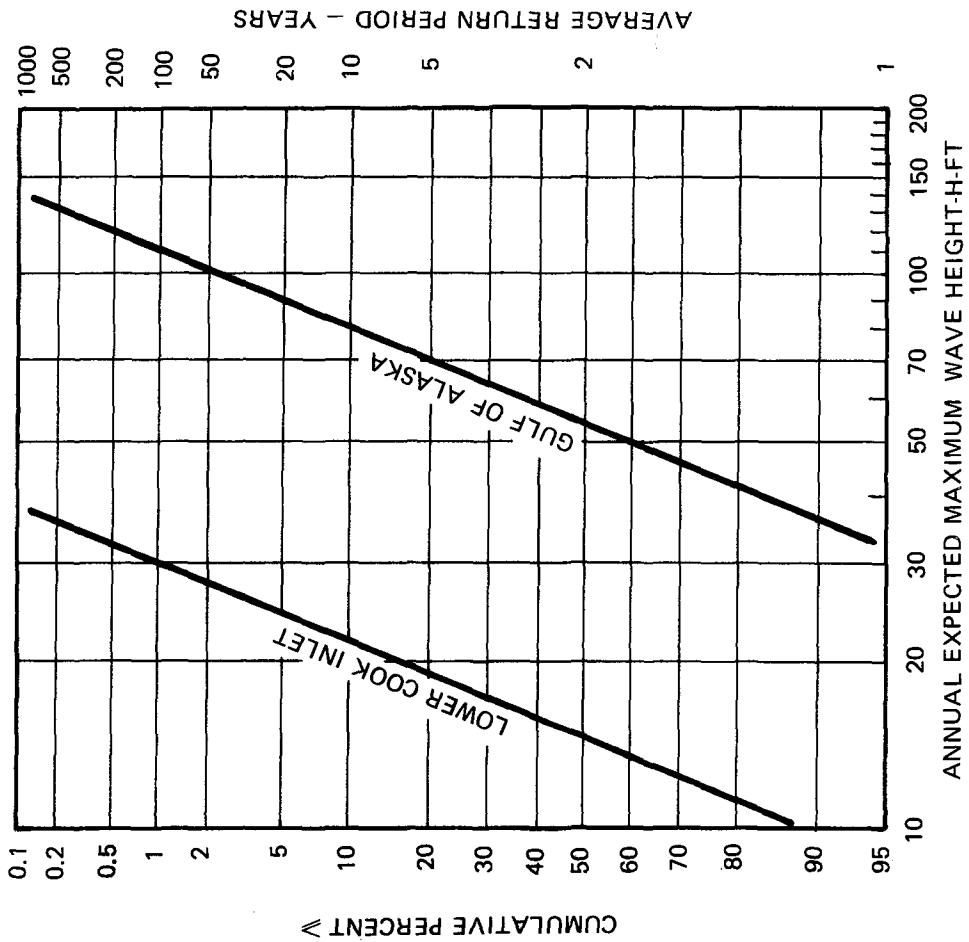


Fig. 9. Annual Expected Maximum Wave Height Versus Return Period

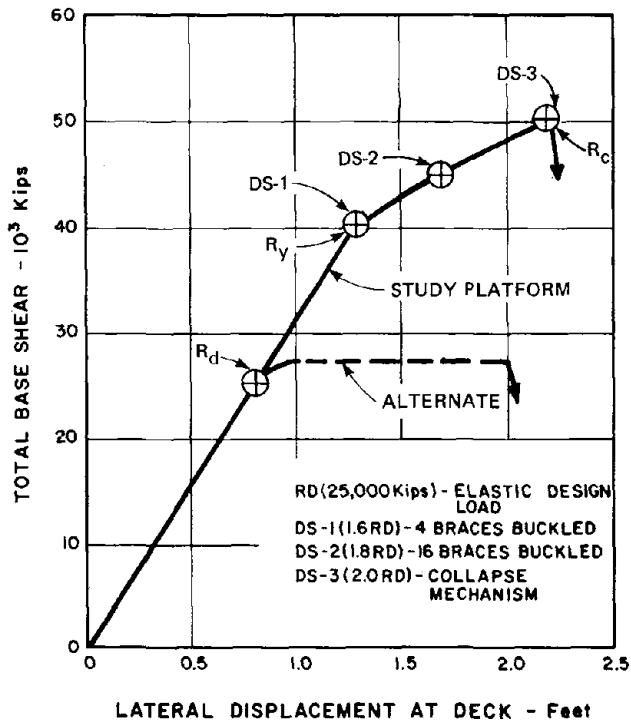


Fig. 11. Results of Static Inelastic Analysis of Study Platform

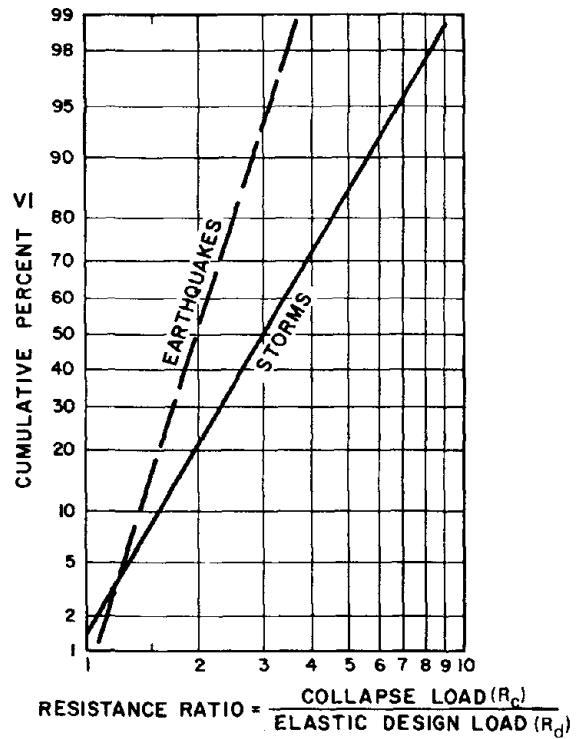


Fig. 12. Statistical Distribution of Resistance Capacity of Study Platform

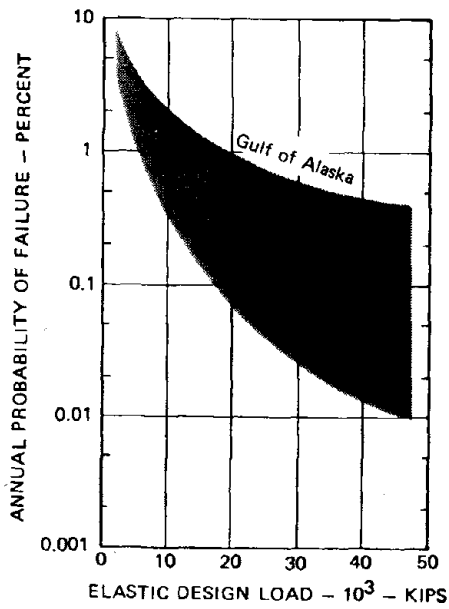


Fig. 13. Platform Reliability Under Earthquake Loading

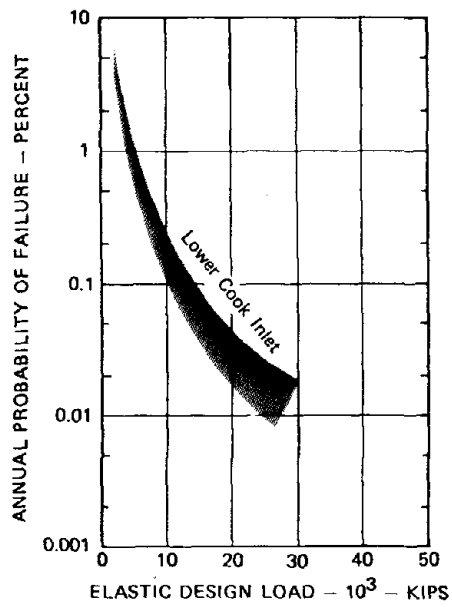


Fig. 14. Platform Reliability Under Earthquake Loading

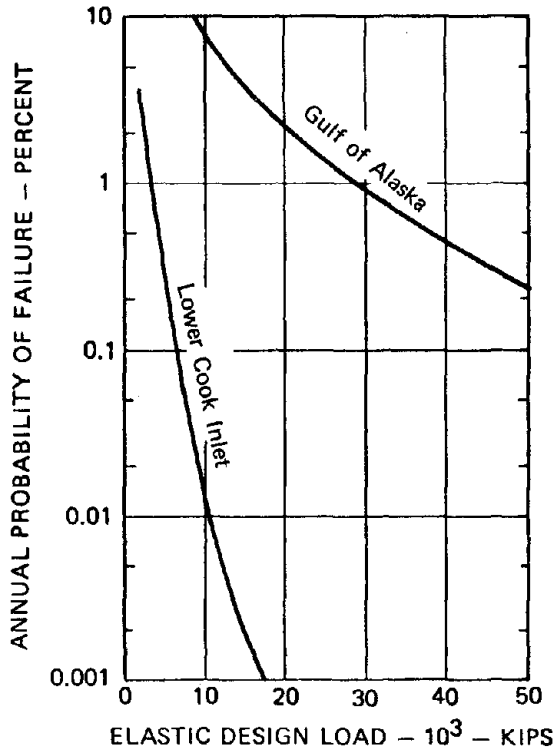


Fig. 15. Platform Reliability Under Storm Loading

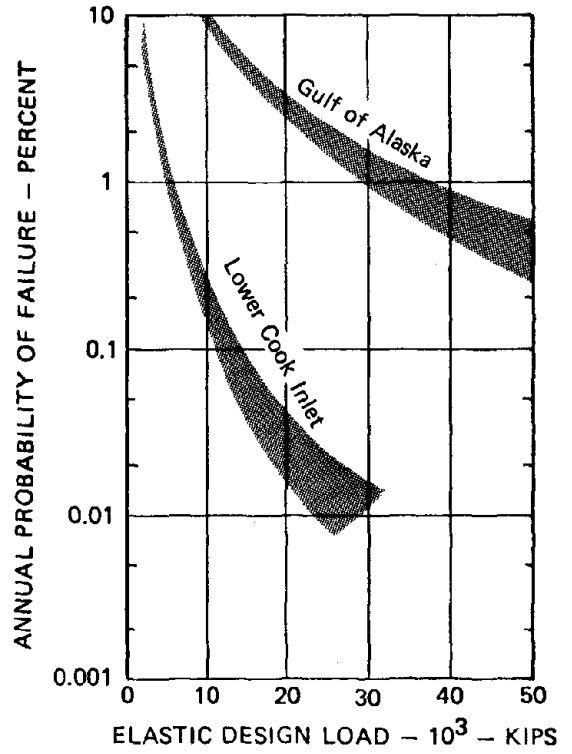


Fig. 16. Platform Reliability Under Combined Earthquake and Storm Loading

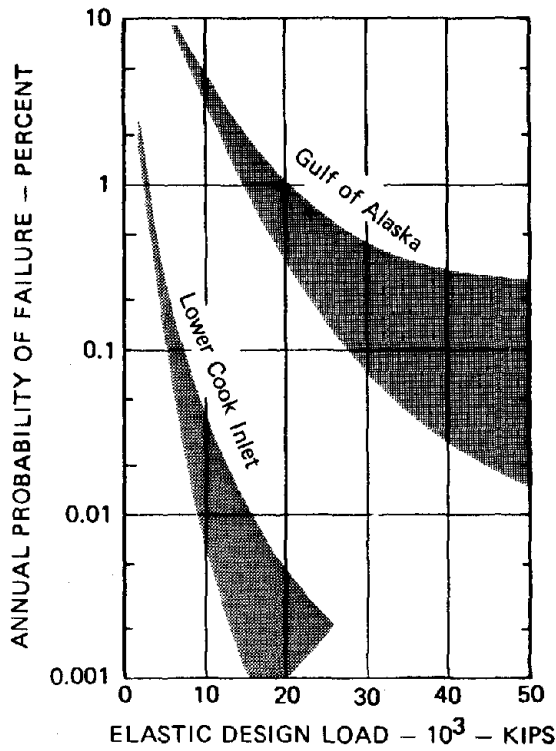


Fig. 17. Platform Reliability Under Combined Earthquake and Storm Loadings - Sensitivity Analysis - Modeling Uncertainties Effect

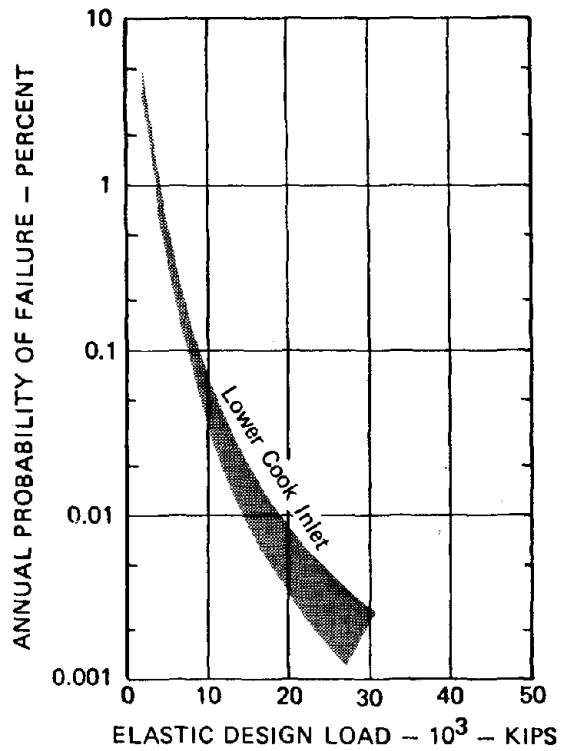


Fig. 18. Platform Reliability Under Combined Earthquake and Storm Loadings - Sensitivity Analysis - Frequency Filtering Effect

## PRELIMINARY MICROZONATION OF THE BALTIMORE CANYON LEASE AREA

by

J. A. Fischer<sup>I</sup> and C. T. Spiker<sup>II</sup>

## ABSTRACT

Deterministic analysis of known and postulated structure under the Atlantic Continental shelf together with tentative correlations with historical seismicity, suggest conservative design levels of Modified Mercalli Intensities of VI and VII for "strength" and "ductility" levels (respectively). Appropriate correlations show design levels of acceleration of 5 percent and 10 percent of gravity upon the generally "good" subbottom soils in the area. Expected variability of surficial (foundation) sediments necessitates future site specific analysis to confirm the near-surface effects on the character of the input vibratory ground motion to be used in anchoring design response spectra.

## INTRODUCTION

Petroleum exploration on continental shelf areas requires an assessment of possible earthquake-induced vibratory ground motion for purposes of engineering design of offshore structures. However, such assessments are usually limited by the sparse historical earthquake record and general lack of knowledge of geologic conditions in oceanic areas. Therefore, microzonation methodologies established in our land based work must be applied and/or extrapolated with an appropriate degree of conservatism to the offshore area of the installation.

Modern techniques require consideration of a variety of parameters. It is necessary to develop a state-of-the-art understanding of (1) plate tectonic theory; (2) the temporal and spatial distribution of historical earthquakes; (3) regional structure as prospective candidates for future seismic activity; (4) contemporary stress regime and relative brittleness of a region; (5) attenuation characteristics of the region; (6) local (near-surface) geologic conditions; and (7) regional characteristics displayed by time histories of historical events.

In well-instrumented, highly seismic areas like the west coast of the United States, the large data base acquired permits detailed investigation of these seismic parameters, so that relatively reliable relationships can be developed to explain and predict earthquake occurrence. In the eastern U.S., however, the relatively moderate seismic activity and lack of strong motion instrumentation prohibit the characterization of typical eastern events to a similar degree of reliability. Moreover, the identification of generating structures is postulatory at best since the detailed structural characteristics of the eastern "intraplate" tectonic regime is not as well understood as the "plate boundary" of the western

---

I Partner, Dames & Moore, Cranford, New Jersey.

II Senior Seismologist, Dames & Moore, Cranford, New Jersey.

U.S. For these reasons, we must utilize the historical record (some 400 years) of seismicity wherein the total data base is identified in terms of the Modified Mercalli Intensity (Damage) Scale. In this respect, the temporal and spatial distribution of historical seismicity defined in terms of damage is an invaluable guide in risk analysis since the more sophisticated investigations evolving from strong motion instrumental records are just not available.

#### METHODOLOGIES

Generally, there are two basic approaches which are applicable to seismic risk assessment in the eastern United States. The deterministic approach is emphasized by nuclear regulatory agencies. In this procedure one considers the recurrence of the maximum historical event associated with either a generating structure, or a defined source area (the area may be as large as a tectonic province) in order to place its recurrence with respect to a specific site. A standard statistical analysis, on the other hand, relies on a set of assumptions based on the available historical seismicity. These assumptions include a judgement concerning the upper bound (maximum possible) event for a given source area, the size and shape of the seismic source region, and in most cases, a random distribution of seismicity over this geometric source. These analyses nearly always base calculations on the probability of events larger than the maximum historical earthquake, which may not be deterministically justified in many cases. On the other hand, the deterministic approach ignores the time distribution and assumes the occurrence of the maximum historical event at some predetermined point (in relation to a specific site) on the basis of structural association or proximity of a limiting seismogenic zone. Applicable attenuation functions characteristic of the studied region are utilized in both approaches.

Once the maximum expected ground motion can be determined for a general locality on the basis of the methodologies discussed above, the local geologic conditions, as exemplified by soil conditions overlying bedrock at a specific site, can be investigated. Allowance for the effect of such site specific conditions on the incident seismic energy can be termed microzonation. In this sense we are limited in this exercise, since specific foundation parameters at sites in offshore continental shelf areas are not available.

#### PROCEDURE

For this study we have selected the general region of the Baltimore Canyon lease area as the subject site for illustrating a seismic risk assessment within the limits of the available detail. This area is shown on the attached Figure.

From a practical point of view, the statistical approach does not constitute a viable investigative tool for "microzonation" in offshore areas since a reliable data base is usually not available. It can be

used, however, as a basis for preliminary studies of a regional nature (21). This study employs the deterministic methodology historically utilized in the siting of critical structures, such as power plants, hospitals and dams.

## DETERMINISTIC CONSIDERATIONS

### Structure

Major structural features in the region are shown the Figure. The subject lease area lies within the northern half of the Baltimore Canyon Trough, a structural element of the Mid-Atlantic Outer Continental Shelf and upper continental slope. This structural depression in crystalline basement rock extends from Cape Hatteras, North Carolina to the Long Island platform, and probably resulted from tensional forces in the crust in Permian time which created a fault-bound, down-dropped "valley" in the basement rocks (13). Over this major depression, the sedimentary units of the emerged Coastal Plain to the west dip and thicken seaward as they pass under the continental margin onto the shelf. Off the New Jersey coast, the sedimentary wedge is intruded, eroded and domed (19). However, the last major intrusive movements have been dated in Cretaceous time (4). According to Schlee and others (19), the sedimentary wedge is interrupted at the edge of the shelf by deep-seated, high angle normal faulting which may have resulted in a horst-type feature beneath the continental slope.

A fracture or zone of weakness has been suggested by Dillon and Oldale (7) and is based on an inflection zone mapped on the basis of northward tilting, along strike, of four ancient shore lines defined on the Atlantic Shelf. A plot of the authors' basic data points identifies a broad axis for this flexure zone that aligns with a northwestward continuation of an off-shelf fracture zone suggested by offsets in magnetic anomalies at sea and disruption of the oceanic crust on deep, geophysical records (11). The trend of these features strikes northwest into north central New Jersey to a point where the largest historical earthquake was located (see Figure).

The well-known Kelvin Sea Mount trend (or Kelvin fault zone) has been tentatively correlated with several on-shore structural regimes. Both Diment and others (8) and Le Pichon and others (12) suggested that the trend of the sea mounts likely corresponds to a line of alkalic intrusions and earthquake epicenters extending from Boston to Montreal. This apparent "correlation" of epicenters from Boston to Montreal, when examined in light of the available geology and the best available earthquake locations, leaves much open to question. Significantly, Drake and Woodward (9) extended the Kelvin structural trend westward along the 40°N latitude. Emery (10) has delineated a linear offset in magnetic anomalies extending from the sea mounts across the shelf along this 40° parallel. According to Root and Hoskins (18), this 40° trend may be structurally related to an east/west-trending continental fault system in the onshore Appalachian uplands to the west (see Figure). They have postulated that this upland fault system is a continental feature which originated prior to opening of the Atlantic and which controlled the location of the subsequent transform faulting

(Kelvin fault) during the latest opening. The 40°N latitude line also coincides with the apparent right lateral displacement suggested by the Appalachian salient in southern Pennsylvania.

A north-south trending fault off Rhode Island extends for about 60 km, showing some 20 to 40 meters of displacement down to the east. This eastward dipping structure bears no apparent relationship to known faulting either on or off-shore (14).

Also, Sheridan and Knebel (20) report shallow faults in the upper sedimentary strata near the shelf edge off New Jersey revealed by high resolution seismic data. These structures indicate deep-seated faulting with offsets as much as 90 meters marking the transition from shelf to deep ocean. The northwest dip reported for these normal faults would suggest the horst-structure previously discussed. Additional minor faulting is reported on the inner and outer shelf area. The faults generally occur in clusters, show limited vertical displacement, and are generally attributed to continental slope-related gravity movements (16).

### Seismicity

The seismicity of the general region is shown on the Figure. The largest earthquakes in the Eastern United States are represented by the Cape Ann, Massachusetts Intensity VIII event of 1755, the Grand Banks, Newfoundland Intensity X event in 1929, the Charleston, South Carolina Intensity X event in 1886, and the Intensity VII events at Wilmington, Delaware (1871), Asbury Park, New Jersey (1927), New York City (1884, 1737), and a cluster of four events (VII) in the Connecticut basin. Off the coast, the historical record is sparse, showing eight random events of Intensity V and VI in the region under investigation. Reliable location of offshore events has only become possible since the advent of instrumentation in the East several decades ago. Moreover, there is usually some discrepancy between earthquake catalogs (Canada and the U.S.) so that a detailed review and interpretation of the historical record is mandatory for specific site studies. However, for the illustrative purposes of this study, all earthquakes reported by the major sources have been used.

### Structural Correlations

Eastern events larger than Intensity VII can be relegated to seismogenic zones or structures which preclude their consideration for the Mid-Atlantic lease area under discussion.

In 1929, more than 500 miles to the northeast, the Grand Banks earthquake (Intensity X) was reported to have cut submarine cables, generated tsunamis, while generally shaking the northeastern American continent. This event is considered to be associated with a discreet seismogenic regime and has not been a factor in siting studies for the northeastern coastal areas. Thus, there is no reason to postulate a recurrence of this event near the subject lease area. Similarly, the Charleston, South Carolina event, though historically controlling southeastern seismic risk



assessments to a large degree, has been restricted to a concentrated zone of activity in the immediate vicinity of Charleston. The Cape Ann, Massachusetts event has recently been reviewed and found to be associated with a tectonic regime responsible for the seismogenic zone in north-eastern Massachusetts.

However, the Intensity VII events near New York City; Asbury Park, New Jersey; and Wilmington, Delaware cannot be readily correlated with specific structure or zones of concentrated activity (although Fall Zone structure and/or oceanic fracture zones cannot be ruled out as localizing earthquake activity in this area). It has been suspected in the past that structures conforming to the general northeast trend of the Appalachian system were responsible for these on-shore events, but no active faulting has been adequately correlated with the seismicity.

If we assume that the location of the moderate, offshore events are reasonably determined, then possible correlations with the suggested offshore structure should be considered.

It should be pointed out, however, that offshore "structures" are less well-defined than are structures in the adjacent coastal areas. Also, the land-based tectonic regime has the advantage of some 400 years of seismic history with which to ascertain the seismogenic proclivity of the structures that are identified. Even with this advantage in data base, the tectonic character of the east coast remains somewhat postulatory, particularly as regards major crustal features.

The east coast magnetic anomaly corresponds generally to the strike of the continental slope, and thus, the eastern margin of the Baltimore Canyon Trough. Possibly three Intensity VI events and one Intensity V shock plot along this feature. If the slope is marked by deep-seated faulting as previously discussed, then the diffuse seismicity could be tentatively associated with this feature, and might result from minor adjustments of the ancient rift due to present-day seafloor spreading.

The northwest-trending extension of an oceanic fracture zone postulated by Klitgord (11) on the basis of magnetic anomalies can be tentatively traced shoreward by the flexure zone reported by Dillon and Oldale (7), which trends toward the Intensity VII earthquake epicenters in northern New Jersey and New York City. There is additional evidence based on geophysical interpretation of deep structures (11; in publication) that the oceanic fracture may be traceable under the slope.

The small (Intensity V) earthquake east of the lease area might be correlated with either of the suggested structural features. The Intensity V event off the south coast of Rhode Island can be spatially associated with the north-south faulting shown on the Figure. However, seismic profiles south of the structure, between Georges Bank and Baltimore Canyon troughs show no offsets of strata (14). Therefore, the seismogenic nature of this feature would not appear critical to the lease area.

If the postulated Kelvin structural trend along the 40° parallel is currently active, it may be responsible for the offshore events (Intensity V and VI) which have been located within 30 to 50 km of this trend, as well as the Asbury Park and Wilmington Intensity VII events on shore (see Figure).

In summary, causal relationships between the sparse seismicity in the shelf and coastal area and the postulated structures offshore are not convincing, but do suggest caution in assigning design events to this particular area.

### Design Earthquake

Conservative siting philosophy would require "floating" the Asbury Park, New Jersey Intensity VII event seaward. This shock and the Wilmington, Delaware Intensity VII, cannot be restricted solely to either the Coastal Plain (and shelf) or the Piedmont province to the west, as both events occur on the boundary between the two provinces. Thus, their consideration as floating events in either region would be applicable. However, the apparent low frequency of offshore earthquakes with maximum Intensities no higher than VI suggests that, for an acceptable level of risk for the life of the proposed offshore installations, consideration of a floating event as high as VII is not warranted. Nor is there a strong case at present for assigning a likely event as high as Intensity VII to the postulated structure trending northwest through the lease area, or the 40° structure trending east-west from the Kelvin fault zone. Although an actively-spreading Atlantic with attendant transform faulting is accepted today (20), there is no reliable evidence for youthful movements along either of these postulated structures. However, for a worst-case earthquake, the consideration of an Intensity VII as a result of movement along one of the suspected rifts is reasonable. It should be noted, however, that subsequent investigation during the course of exploration and development in the lease area may confirm more well-defined structures judged to be capable of relatively strong events. In such a case, consideration of an Intensity VII event along one of the structural trends might be required in the interest of conservatism.

On the basis of the above discussion, there is no justification at present for restricting the offshore or onshore earthquakes to the specific structures described. Therefore, for practical design purposes, the entire lease area may be deemed subject to occurrences of shocks no larger than the historical maximum (offshore) of Intensity VI which occur near both the northern and southern portions of the lease area. The recurrence of such an event at a particular site would have an extremely low order of probability as demonstrated by the historical record, and would supersede the attenuated effect of a recurrence of the New York/New Jersey Intensity VII events on shore.

The design Intensity of VI derived above is considered to be the maximum event which might affect an offshore installation during its useful life. In this respect, it will be used to calculate the design "strength level" as defined by the American Petroleum Institute (2) for seismic design

of offshore structures. Prudence dictates, however, that consideration be given to the translation of the 1927 Asbury Park event (VII) along a postulated fracture zone. An Intensity VII event along one of the structural trends is determined to be the maximum (rare, intense) earthquake leading to a ductility level for design (2).

#### VIBRATORY GROUND MOTION

Historically, the ground motion parameter utilized in seismic design and zonation studies has been the maximum level of acceleration in terms of percent of gravity (%g). Several correlations relating this parameter to Modified Mercalli Intensity (damage) are reported. Two recent correlations make use of the largest body of data and are currently accepted in the industry. For an API "strength" level Intensity VI design event, Trifunac and Brady (22) have calculated a mean peak horizontal acceleration on all materials of about 7% g. O'Brien and others (15), using worldwide data to supplement United States data, have calculated less than 5% g as an applicable mean for Intensity VI shaking.

Although scatter in the empirical data samples is large, these means are acceptable as a basic input to structural response analyses. Since both correlations use only the maximum peak amplitudes of measured ground acceleration, the effects of duration of motion, or cyclic loading are not accounted for. A damaging level of sustained vibratory ground motion would be lower than the peaks used in the correlations. In this respect, the correlations may be considered somewhat conservative as regards the real world. Considering the low order of probability of an Intensity VI event at any one specific site, we consider an acceleration level of 5% g to be adequately conservative as a "strength level" for design of offshore structures in the lease area.

API (2) recommends a Ductility level (rare, intense earthquake) twice that calculated for the Strength level. The resultant level of 10% g is compatible with the deterministically-derived worst-case earthquake of Intensity VII, similar to a recurrence, at the site, of the Wilmington or Asbury Park Intensity VII events. Correlations discussed above show a mean acceleration value for Intensity VII of 13% g (22), and 10% g (15). However, for the reasons stated above, 10% g is considered viable as a Ductility level in the subject lease area.

It is now thought (17, 5) that peak ground velocity and displacement are more critical to the design of large long-period offshore structures than is peak ground acceleration, the traditional land-based engineering design parameter. Trifunac and Brady (22) have calculated mean horizontal peak velocity levels of 7 and 13 cm/sec for the strength and ductility levels, respectively. For these design events they calculate displacements of 4 and 7 cm.

#### SOIL CONDITIONS

Geotechnical data obtained from explorations performed at a limited number of locations on the mid-Atlantic shelf can be used to approximate the soil conditions which can be expected to be encountered in the lease area (6).

A typical model for the shelf region shows a relatively thin (15 to 90 m) mantle of Quaternary sediments (Pleistocene and Holocene) overlying a thick Tertiary sequence (greater than 90 m) which may be divided into two broad categories: (a) Older Tertiary sediments consisting of thick deposits of dense sands and occasional layers of stiff clay, and (b) Younger Tertiary sediments consisting mainly of silts and clays. This model, although simplified, is believed to be applicable to most locations in the lease area. However, exceptions to this generalized model are to be expected in areas of deep buried channels and areas of cemented sediments. Thus, refinements in this generalized model would require detailed study and evaluation of the materials encountered at a particular site.

The indicated soil conditions over the inner and middle shelf regions are generally "strong materials" which should not pose unusual foundation problems. However, complex and variable soil conditions associated with the aforementioned buried channels may exist in some leases on the middle shelf areas. The outer shelf region appears to have significantly different foundation considerations. There is, at present, a general lack of knowledge concerning the nature of some of the Upper Tertiary sediments which are believed to be fine-grained slope deposits. These formations are encountered at shallow depths on the outer shelf areas, as are units of carbonate-cemented sandstones. The hydraulic and sedimentary processes responsible for mobility of the seabed thought to operate in the sand wave fields noted in some areas, are not well-defined.

In summary, soil conditions are marked by extreme variability over the lease area, and can significantly alter the character of incident ground motions at foundation level. Thus, detailed analysis of site specific soil properties are mandatory in establishing an effective microzonation of individual sites.

#### EXISTING STATISTICAL AND ZONATION STUDIES

As a check on the viability of the deterministic exercise, existing land-based probabilistic studies can be tentatively extrapolated offshore. Algermissen and Perkins (1) show that the coastal waters adjacent to the lease area should be subject to accelerations of less than 4 percent of gravity in rock or stiff soils with a 90% probability of not being exceeded in 50 years. Similarly, the Applied Technology Council (3) has calculated an effective acceleration and velocity contour map of the U.S., which, if extrapolated offshore, suggests that levels of acceleration and velocity of less than 5 percent of gravity and less than 7 cm/sec, respectively, should be expected with an 80 to 95% probability of not being exceeded in 50 years. This is applicable to the normal life of an offshore installation, and comparable to the "strength level" design. API (2) has generally zoned the Baltimore Canyon lease area as Zone 1, with a recommended strength level of 5 percent of gravity for engineering design.

#### RESULTS

Applied methodology confirms the following horizontal ground motion levels to be sustained on reasonably good foundation materials for the design earthquakes for the Baltimore Canyon lease area:

	<u>Acceleration</u> (% gravity)	<u>Velocity</u> (cm/sec)	<u>Displacement</u> (cm)
Strength Level	5	7	4
Ductility Level	10	13	7

Subsequent consideration of specific site foundation conditions and physical properties will result in a true microzonation of a particular lease block.

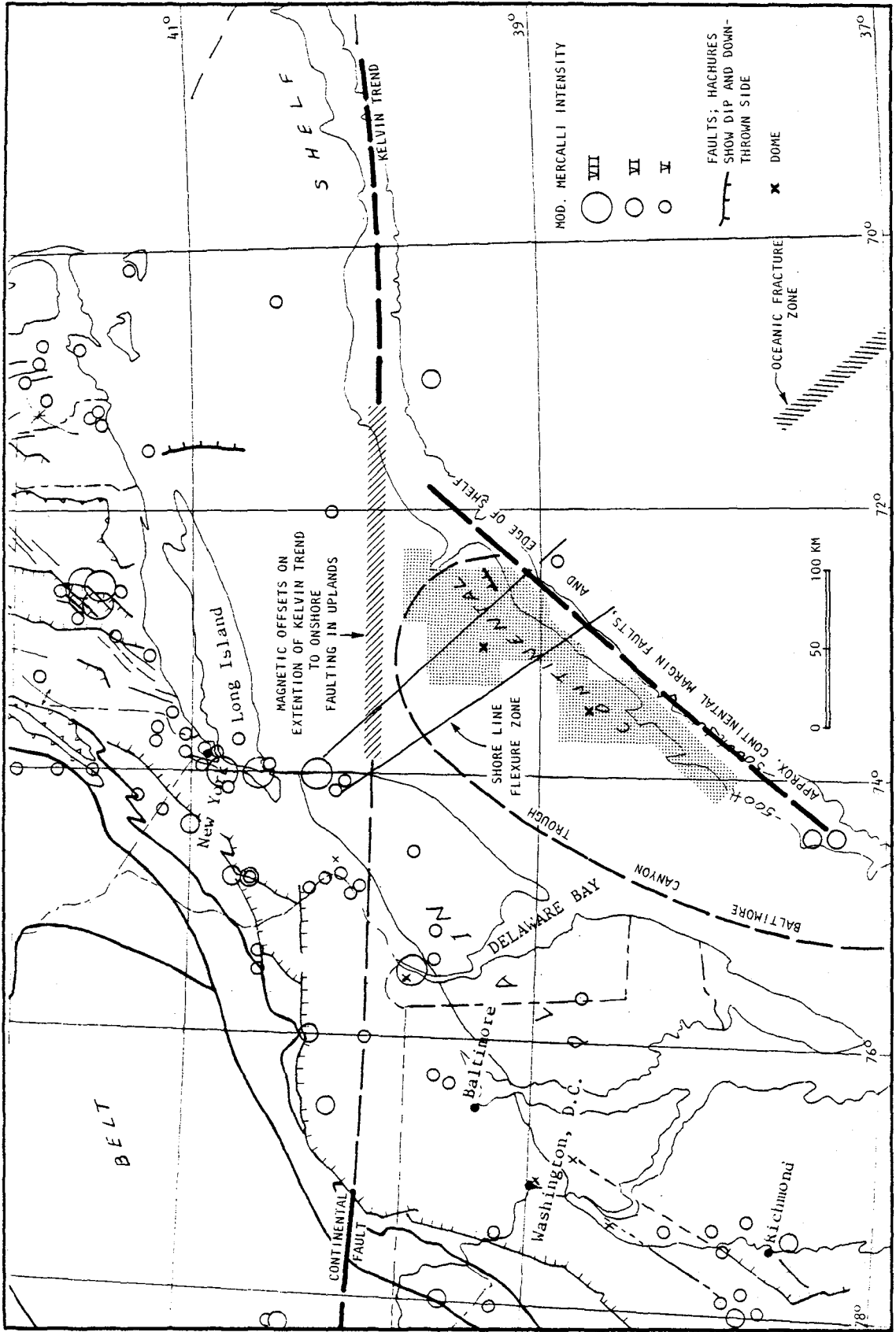
#### RECOMMENDATIONS

For preliminary planning purposes, the resultant levels of 5 and 10% of acceleration (strength and ductility levels, respectively) should be used to anchor appropriate response spectra derived from deconvolution of the soils column at a specific site. The possible ground motion amplification effect of thick, unconsolidated sediments is well documented and must be accounted for in final design assessments.

#### REFERENCES

1. Algermissen, S.T. and D.M. Perkins, 1976; A Probabilistic Estimation of Maximum Acceleration in Rock in the Contiguous United States; U.S. Geol. Sur. Open File Report 76-416; U.S. Dept. Interior.
2. API-RP-2A, 1976, A Statement of Position - Proposed Revisions to API-RP-2A for Earthquake Design; Mini Committee on Earthquake Design, June 14, 1976.
3. ATC-3, 1976, Working Draft of Recommended Comprehensive Seismic Design Provisions for Buildings; Prepared by Applied Technology Council, San Francisco, Calif.; Sponsored by Nat. Sci. Found. Research Applied to National Needs Program and Nat. Bur. Standards, Jan. 31, 1976.
4. Bureau of Land Management, 1977, Draft - Environmental Impact Statement: Proposed 1979 Outer Continental Shelf Oil and Gas Lease Sale Offshore the Mid-Atlantic States, OCS Sale #49, Vol. 1 of 3, U.S. Dept. of Interior.
5. Cornell, C.A. and E.H. Vanmarcke, 1975, Seismic Risk Analysis for Offshore Structures: Offshore Technology Conference, May 5-8, 1975, Houston, Texas; Paper No. 2350, Proceedings, Vol. III, p. 145-152.
6. Dames & Moore, 1974, Atlantic Generating Station - Units 1 and 2, Preliminary Safety Analysis Report, v. 2.
7. Dillon, W.P. and R.N. Oldale, 1977, Adjustment of the Late Quaternary Sea-Level Rise Curve based on Recognition of Large Glacio-Tectonic Movements of the Continental Shelf South of New England.
8. Diment, W.H., T.C. Urban, and F.A. Revetta, 1972, Some Geophysical Anomalies in the Eastern United States; in Robertson, E., ed., Nature of the Solid Earth, New York, McGraw-Hill Book Co., p. 544-572.

9. Drake, C.L. and H.P. Woodward, 1963, Appalachian Curvature, Wrench-faulting and Offshore Structures; New York Academy of Sci., Trans., Ser. 2., v. 26, p. 48-63.
10. Emery, K.O., 1966, Atlantic Continental Shelf and Slope of the United States - Geologic Background, U.S. Geol. Surv. Prof. Paper 529-A, U.S. Gov. Printing Office, Washington, D.C.
11. Klitgord, K., 1978, Personal Communication, U.S.G.S., Woods Hole, Mass.
12. LePichon, X., J.C. Sibuet, and J. Francheteau, 1977, The Fit of the Continents Around the North Atlantic Ocean, Tectonophysics, v. 38, p. 169-209.
13. Mattick, R.E., R.Q. Foote, N.L. Weaver, and M.S. Grim, 1974, Structural Framework of United States Outer Continental Shelf North of Cape Hatteras, Am. Assoc. Pet. Geol. Bull., 58(6), pt. 2, p. 1179-1190.
14. McMaster, R.L., 1971, A Triassic Fault on the Continental Shelf off Rhode Island, Geol. Soc. Am. Bull., v. 82, p. 2001-2004, July, 1971.
15. O'Brien, L.J., J.R. Murphy and J.A. Lahoud, 1977, The Correlation of Peak Ground Acceleration Amplitude with Seismic Intensity and Other Physical Parameters; Computer Sciences Corporation Report, NUREG-0143, prepared for U.S. Nuclear Regulatory Comm., March, 1977.
16. Offshore Navigation, Inc., 1976, Report to U.S.G.S. Conservation Division, Baltimore Canyon Sale 40 Area, Text 1-19 with Maps.
17. Page, R.A., 1975, Evaluation of Seismicity and Earthquake Shaking at Offshore Sites, Offshore Technology Conference, May 5-8, 1975, Houston, Texas, Paper No. OTC-2354, Proceedings, Vol. III, p. 179-190.
18. Root, S.I. and D.M. Hoskins, 1977; Lat 40°N Fault Zone, Pennsylvania: A New Interpretation, Geology, v. 5, p. 719-723, December.
19. Schlee, J., J.C. Behrendt, J.A. Crow, J.M. Robb, R.E. Mattick, P.T. Taylor, and B.J. Lawson, 1976, Regional Geologic Framework off the Northeastern United States, Amer. Assoc. Pet. Geol. Bull. 58(6), p. 926-951.
20. Sheridan, R.E. and H.J. Knebel, 1976, Evidence of post-Pleistocene faults on New Jersey Atlantic Outer Continental Shelf; Amer. Assoc. Pet. Geol. Bull., 60(7); p. 1112-1116.
21. Spiker, C.T. and J.A. Fischer, 1978, Offshore Seismic Risk in the Oil Patch, Central American Conference on Earthquake Engineering, Jan. 9-12, 1978, San Salvador, El Salvador, C.A.
22. Trifunac, M.D. and A.G. Brady, 1975, On the Correlation of Seismic Intensity Scales with Peaks of Recorded Strong Ground Motion, Bull. Seis. Soc. Amer., v. 65, No. 1, p. 139-162, February.



1340

**INTENTIONALLY BLANK**



SEISMIC RISK EVALUATION OF SOUTHERN CALIFORNIA  
COASTAL REGION

By

L. A. Selzer<sup>I</sup>, R. T. Eguchi<sup>II</sup>, T. K. Hasselman<sup>II</sup>

ABSTRACT

A seismic risk evaluation to identify design conditions for oil lease tracts in Southern California Coastal waters is presented. Earthquake design conditions are described by area maps showing expected peak ground acceleration, velocity and displacement contours together with response spectra for specific locations.

Expected peak ground motions were calculated using a Bayesian methodology which combines geological fault information with historical seismicity data. The geological model was developed from 123 major faults and the historical model from 6364 recorded earthquakes. Energy flux distributions were computed for both models. A linear statistical estimator was employed to revise the geological energy flux based on recorded earthquake data. Median log-linear attenuation laws were used to transform energy flux into isoseismals of peak ground motion.

Partitioning of seismic energy according to frequency was evaluated by analyzing strong motion accelerogram records. Record sets were selected to contain high energy and long duration features important to offshore structures. Normalized response spectra were derived from an analysis of accelerogram data sets and spectral ordinates were combined with ground motion values from the isoseismal maps to obtain response spectra for specific offshore locations. A probabilistic model was applied which enables expressing design spectra and isoseismal maps in terms of the probability of exceeding specified motions, or as a function of the return period for the specified motions.

INTRODUCTION

For several decades a major portion of offshore oil development has been concentrated in seismically benign areas such as the Gulf of Mexico. As a consequence little emphasis had been placed on earthquake design considerations for oil platforms. However, the planned and initial expansion of oil and gas exploration to the coastal waters of California and Alaska over the past few years has fostered a need for the development of earthquake design data. This need led to a study for the U. S. Geological Survey by The Aerospace Corporation (1) and a team of consultants. Results from that study pertaining to seismic design conditions for the coastal waters of Southern California are the subject of this paper.

---

I Aerospace Corporation, Los Angeles, California

II J. H. Wiggins Company, Redondo Beach, California

## STUDY AREA

The geographic focus of this study is the Southern California coastal region which is bounded to the north by 34° north latitude, to the south by the U. S. /Mexican border and to the east and west by west longitudes 117° 30 minutes and 120° respectively. While this is the area of primary interest, the risk maps cover a broader area including Southern California along with parts of Arizona and Mexico.

## SEISMIC DESIGN CONDITIONS

Earthquake risk is often described for design purposes by two characteristics. One indicating ground motion intensity (i. e. expected peak acceleration) and the other the frequency content of ground motion or the distribution of ground motion energy with frequency. These two characteristics are typically embodied in a design spectrum constructed by scaling spectral ordinates of a standard 1 g spectrum down (or up) in proportion to the expected peak ground acceleration. This practice is recognized to have many shortcomings. The most significant of these from an oil platform design standpoint is that it tends to overemphasize the importance of high frequency components of earthquake motion and as a result design spectra constructed in this manner are not well suited to oil platform design. Oil platforms even in moderately deep water (200 to 500 feet) are tall structures which tend to have lower mode frequencies falling in the peak ground displacement or velocity regions of design spectra. As such, platform response to ground motion tends to be dominated by the energy content in the lower frequency range. To account for this influence and to make use of all available information regarding past earthquakes as well as geological fault locations, a study of design conditions was undertaken incorporating the following features:

- Bayesian statistical techniques were applied to combine historical earthquake records and geological fault information in arriving at expected peak ground motions.
- Long duration and high energy earthquake ground motion records were selected from the strong motion data base and processed statistically to form normalized response spectral ordinate tables which are applicable to long period structures.
- Uncertainties inherent in earthquake occurrence, magnitude and location and motion attenuation and response amplification were treated probabilistically in arriving at site specific design conditions.

## SEISMIC RISK ANALYSIS

The use of both geological fault data and historical seismicity will provide the best possible estimate of future seismic activity for Southern California since a clear relationship exists between area tectonics and historical earthquake occurrences. Bayesian statistical techniques provide us with a rigorous mathematical basis for combining diverse information of this sort. The Bayesian analysis methodology adopted here is one developed by Hasselman, et. al. (6). It involves developing discrete source models of seismic energy release from geological data and historical seismicity, combining this information by employing Bayesian statistical techniques, and with the aid of conventional attenuation laws estimating future earthquake ground motions at discrete points.

The modeling process involves replacing theoretical sources consisting of line, point or area sources by an equivalent set of discrete point sources in a way analogous to the replacement of a structures continuous mass properties by a series of lumped masses. The process is begun by partitioning the area of interest to form a uniform grid as shown in Figure 1. Seismic energy emanating from individual grid areas is assumed concentrated at the area centers making these locations nodal points in the analysis. The rate of seismic energy release is calculated by employing two fundamental Guttenberg-Richter relationships (11). The first is the energy-magnitude relationship.

$$E = E_0 10^{1.5M} \quad (1)$$

Wherein  $M$  is the Richter magnitude and  $E_0$  is taken to be  $10^{11.5}$ . The second equation is the assumed log-linear relationship for earthquake frequency of occurrence.

$$\text{Log } N = a - bM \quad (2)$$

The variable  $N$  in this relationship is the cumulative frequency of occurrence or the number of earthquakes per year of Richter magnitude  $M$  or greater. The parameter  $a$  is the log of the frequency of all earthquakes of magnitude 0 and larger and will be referred to as "seismic intensity" or "seismicity." The constant  $b$  is the familiar magnitude distribution parameter. Given that the largest expected earthquake is the same for the entire region and the distribution of earthquake size (i. e. parameter  $b$ ) is constant for the entire region it can be shown (6) that seismic energy flux is simply related to the seismicity parameter by the following expression:

$$\dot{E} = \text{constant} \times 10^a \quad (3)$$

From this expression the energy flux for the  $i$ th grid area may be represented as

$$\dot{E}_i = \text{constant} \times 10^{a_i} \quad (4)$$

where  $a_i$  is the grid seismicity as defined in Figure 1. The practice of finding values for  $a$  and  $b$  in Equation 2 to fit historical data of earthquake occurrences as suggested by the insert in Figure 1 is common. However, as explained later it is also possible to use this log-linear relationship to find values of  $a$  and  $b$  based on geological fault information. Therefore, regardless of the source of seismicity parameter  $a$ , application of Equation 4 leads to an array of grid nodal points each assigned an energy flux. This array may be thought of as a plate of varying temperature having hot spots corresponding to locations of high seismic activity. Unfortunately, while the distribution of energy flux within the array paints an interesting picture of seismic activity which should correlate well with both the historical record and geological fault locations, it is hardly a form useful to platform designers. Platform designers must, of course, design their structures to withstand some maximum level of expected ground motion. To bridge the gap between the array of seismic energy flux and the needed definition of future ground motions involves several steps.

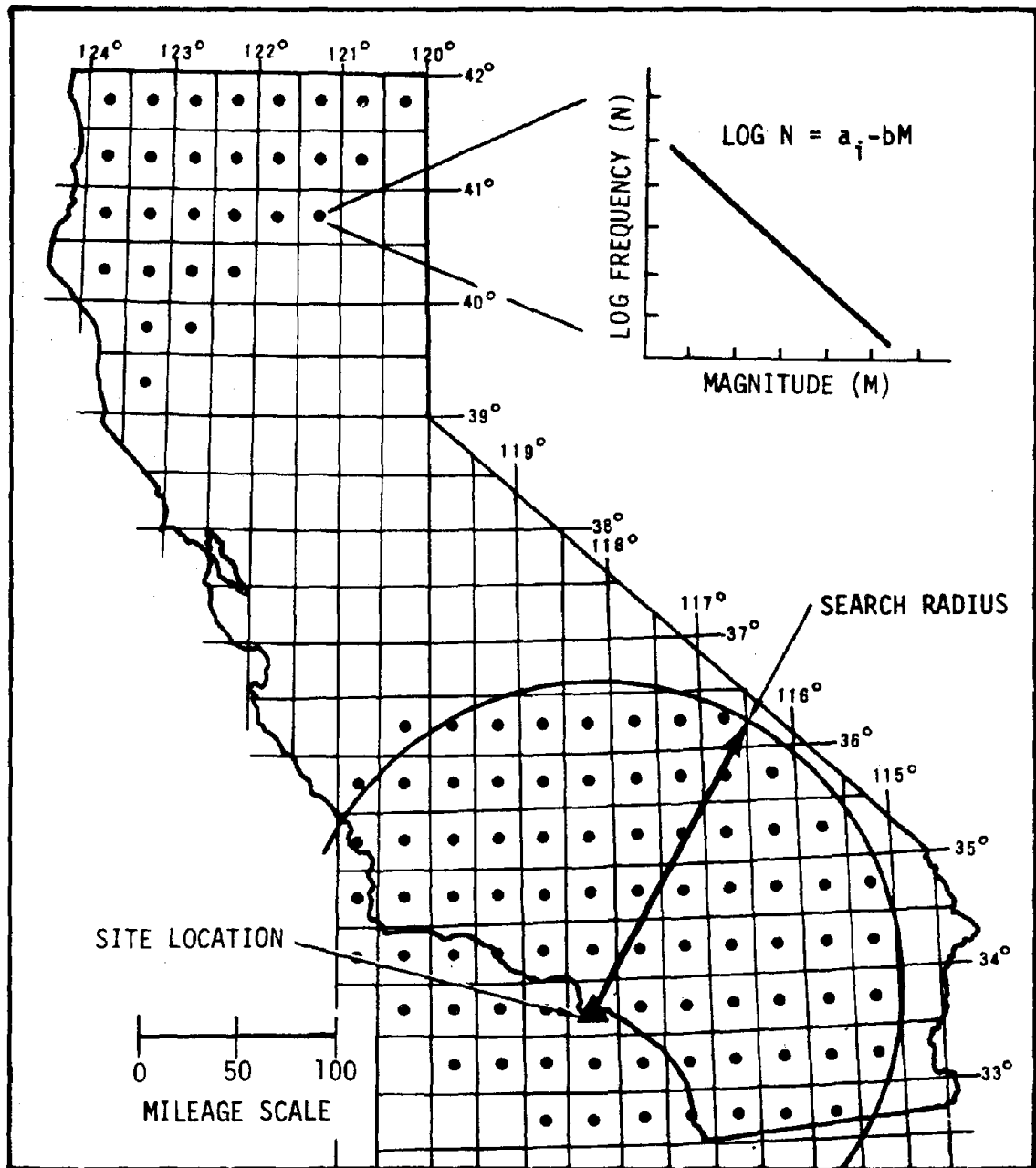


Figure 1. Discrete Source Modeling

First having chosen a site for investigation the total seismicity influencing that site must be established. This is approximated by selecting an appropriate search radius and summing the seismicity,  $a_i$ , from all grid areas within that search radius.

$$10^a = \sum_i 10^{a_i} \quad (5)$$

where  $a$  is now the total seismicity influencing the site in question. The search radius assumed for Southern California coastal waters is 200 miles.

Having determined the site related seismicity, ground motions are calculated by establishing a distance at which the energy release can be assumed to occur. This distance will be referred to as an "effective" hypocentral distance and is the distance giving the same distribution of ground motion for a specific site, as if all point sources within the radius of search were replaced by one "equivalent" point source. Calculation of this distance employs conventional ground motion attenuation equations of the form

$$\text{Log } X = C_1 + C_2 M - C_3 \text{ Log } R \quad (6)$$

where  $X$  represents either ground acceleration ( $A$ ), velocity ( $V$ ) or displacement ( $D$ ). The variable  $M$  denotes Richter magnitude and  $R$  the hypocentral distance from the energy source to site. Constants in the Equation  $C_1$ ,  $C_2$  and  $C_3$  are empirically derived from a regression of strong motion data and are different for each of the components of motion. Attenuation equations having the form represented by Equation 6 may be applied directly to the calculation of ground motions from a single earthquake of magnitude  $M$  at hypocentral distance  $R$ . Cornell (2) derived a method of using attenuation laws in conjunction with a more general description of seismic energy release (i. e. a theoretical type model) for calculating probabilistic values of ground acceleration, velocity and displacement. The procedure used here developed by Hasselman (6) is conceptually similar to Cornell's in that it is directly applicable to a multiplicity of discrete sources and involves the calculation of an "effective" hypocentral distance.

It can be shown using relationships for frequency of occurrence, (Equation 2), motion attenuation (Equation 6) and total site related seismicity (Equation 5) that an "effective" hypocentral distance,  $\bar{R}$ , for an array of discrete sources is

$$\bar{R} = \left[ \sum_i 10^{(a_i - a)} R_i^{-bC_3/C_2} \right]^{-C_2/bC_3} \quad (7)$$

In this equation  $R_i$  is the hypocentral distance from the site under investigation to the  $i^{\text{th}}$  grid area. Given the value for the effective hypocentral distance ( $\bar{R}$ ), Equations 2 and 6 may be used to derive frequency distributions for  $A$ ,  $V$  and  $D$ . These frequency distributions take the form

$$\text{Log } N = \left[ a + \frac{b}{C_2} (C_1 - C_3 \text{Log } \bar{R}) \right] - \frac{b}{C_2} \text{Log } X \quad (8)$$

This expression relating seismicity  $a$  and effective hypocentral distance  $\bar{R}$  provides a simple means of evaluating the frequency distribution of ground motions at a particular site. It is equally applicable to values of  $a$  and  $\bar{R}$  derived from historical data, geological fault information or a Bayesian combination of both.

Before turning to the application of this methodology to the Southern California region, it is interesting to note that Equation 8 has still another use, that of scaling ground motions from one return period to another. Given a Poisson process with return period  $T = 1/N$  from Equation 8 it is seen that ground motion levels  $X_1$  and  $X_2$  for respective return periods  $T_1$  and  $T_2$  exhibit the ratio

$$\frac{X_1}{X_2} = \left( \frac{T_1}{T_2} \right)^{C_2/b} \quad (9)$$

Thus, if the ground motion for a given return period is known, it can be readily scaled to another return period.

#### HISTORICAL DATA

The historical model represents the seismic environment in terms of recorded earthquake epicenters. In this analysis Richter magnitudes greater than and equal to 3.5 are considered. The primary source of historical earthquake information is the current NOAA earthquake data file which includes worldwide events from 1600 to 1976. For Southern California, 6364 events are recorded. The number of events in each one-half magnitude range from 3.5 to 8.0 were tabulated for regression analysis. In computing the number of events per year greater than a given magnitude a normalizing time span of 44.5 years (1932 - 1976) was used for all earthquakes of magnitudes less than 6.0. For magnitudes between 6.0 and 7.0 a span of 64.5 years (1912 - 1976) was used. Finally for magnitudes greater than 7.0, 124.5 years (1852 - 1976) was used. Fitting these data using the familiar log-linear frequency of occurrence relationship (Equation 2) results in the following:

$$\text{Log } N = 5.65 - 0.96M \quad (10)$$

The value of  $b = .96$  compares reasonably well with the .98 value computed for Southern California by Hileman (7). In calculating individual grid area seismicities,  $a_i$ ,  $b$  is held constant at .96.

#### GEOLOGICAL DATA

As mentioned earlier, geological fault evidence makes an independent assessment of seismic risk possible. The procedure for utilizing the geologic fault data is outlined here. Fault maps for Southern California were obtained from 3 available sources.

- Fault Map of California (8), Figure 2
- Preliminary Map Showing Recency of Faulting in Coastal Southern California (15), Figure 3
- Tectonic Map of North America (13), Figure 4

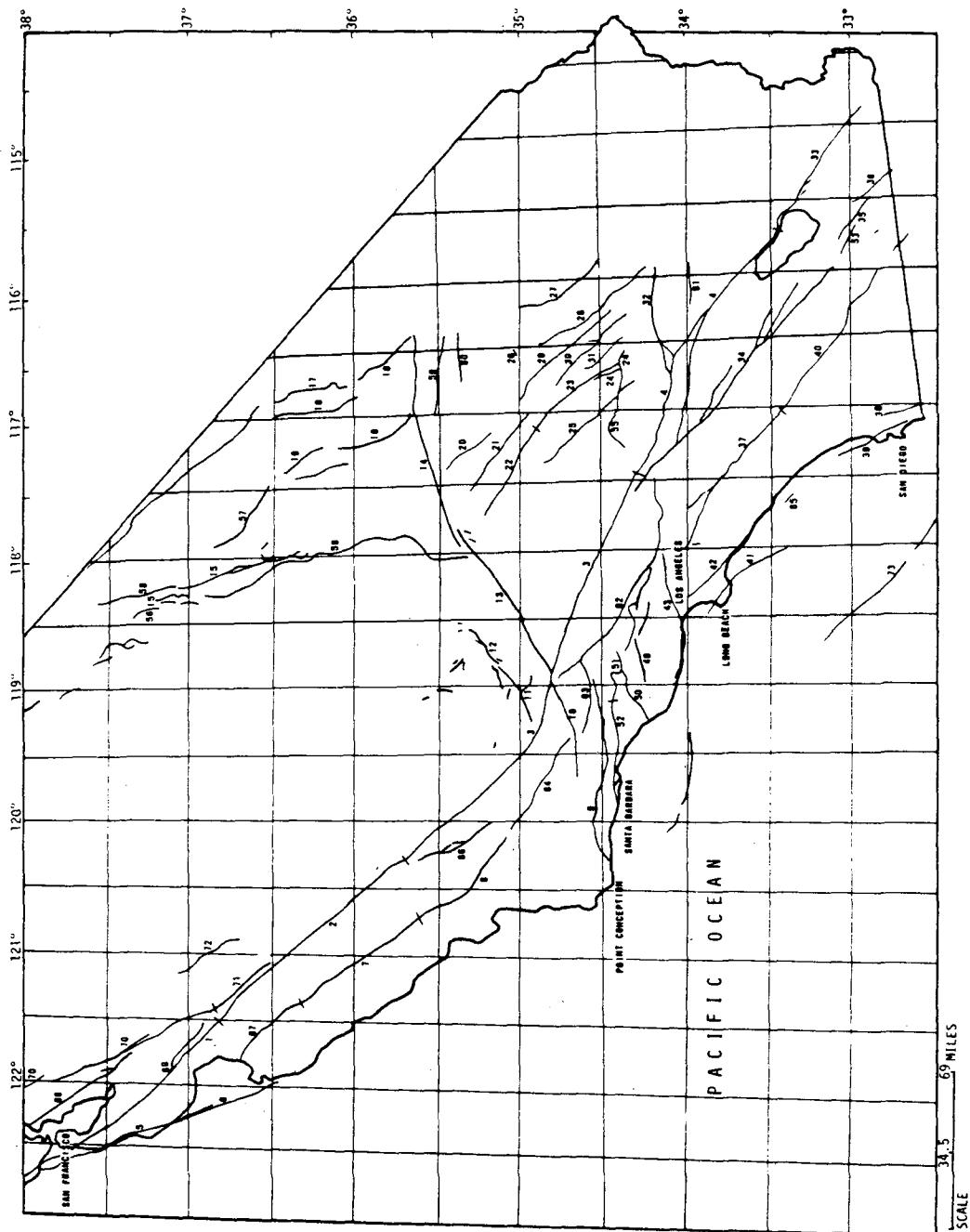


Figure 2. Fault Map of Southern California (Ref. 8)

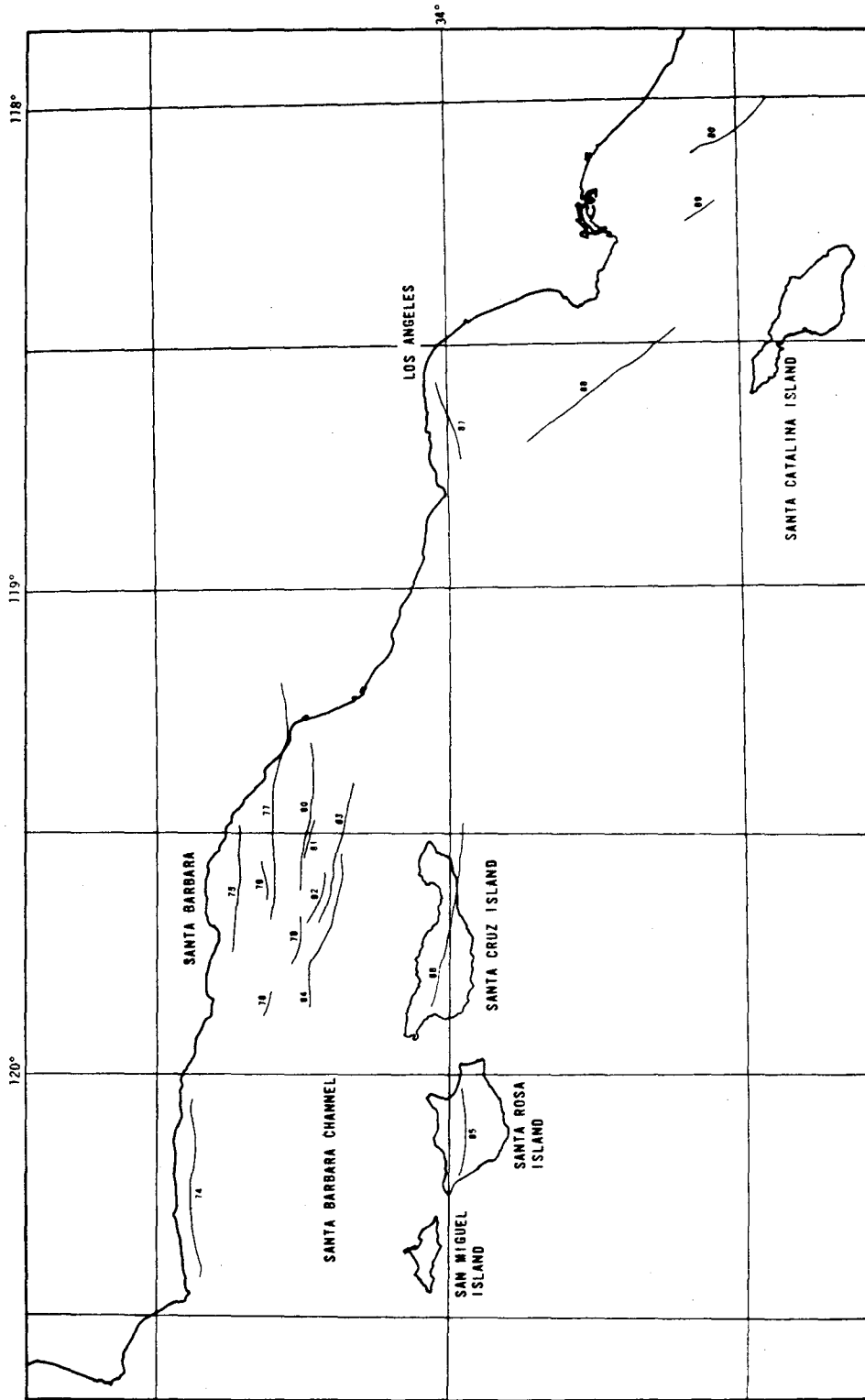


Figure 3. Offshore Fault Map of Southern California (Ref. 15)



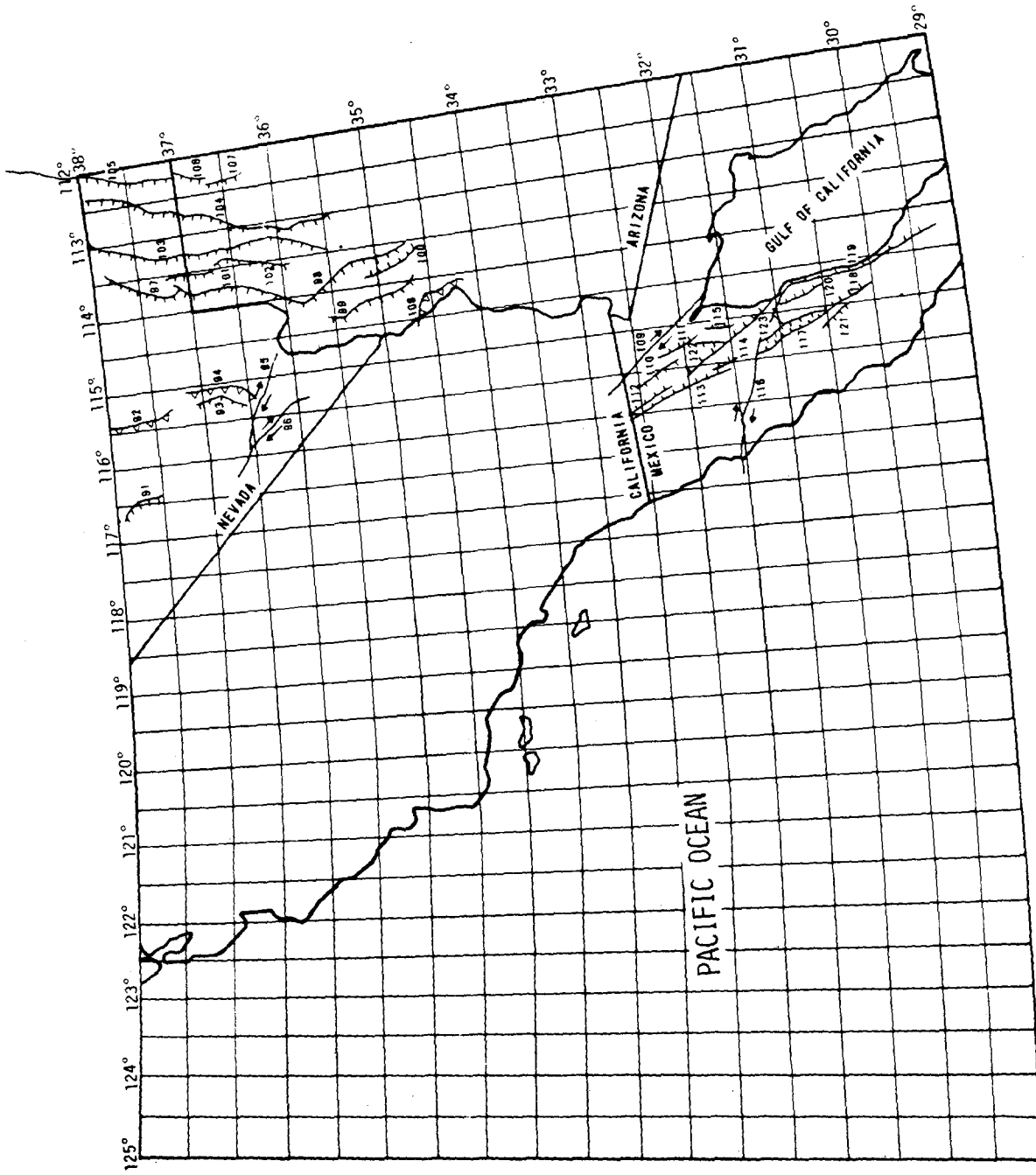


Figure 4. Fault Map of Nevada, Arizona, Utah and Northern Mexico (Ref. 13)

The overall source area extends from  $28.5^{\circ}$  to  $38.5^{\circ}$  N latitude and from  $111.5^{\circ}$  to  $125^{\circ}$  W longitude.

For all onshore California faults, the Jennings map was used, Figure 2. All faults showing historic or any Quaternary fault displacement are considered active and were selected for the geological model.

For offshore Southern California, all faults showing Historic, Holocene, Late Quaternary or Quaternary displacement were selected from the Ziony map, Figure 3.

For the major fault systems in Nevada, Arizona, Utah and Northern Mexico, the general Tectonic Map of North America was used, Figure 4.

For the entire area, 123 faults were selected and their characteristics tabulated. The tabulation includes fault length, maximum credible magnitude, logarithm of the total energy for that maximum magnitude, fault type, slip rate, maximum surface displacement, and the recurrence interval for the maximum credible earthquake.

Where given, the maximum credible magnitude,  $M_x$ , was taken directly from (5). Where no magnitude was provided, one was computed using the following procedure. First, an estimate of total fault length is obtained. Then depending on what type of movement the fault exhibits, a maximum magnitude is obtained from magnitude versus length of surface rupture relationships (3, 9). The surface rupture length was assumed to be one-half that of the total fault length (9, 12). Given the magnitude, the logarithm of energy was computed using Equation 1. However, since our interest is in energy flux, it is necessary to normalize the energy by an appropriate recurrence interval. For some of the major faults in Southern California this interval is given. However, for faults where a recurrence interval was not given an estimate was made based on strain and slip rate information following a procedure outlined by (14).

The result is an average return period computed for faults between Ventura and San Bernardino of approximately 150 years. Included are faults such as Oak Ridge, Sierra Madre, San Cayetano, Santa Susanna, Northridge and San Fernando.

Given a return period and magnitude, the desired energy flux may be computed. This energy flux is assumed to be uniformly distributed over the length of the fault. Referring to the grid map, Figure 1, it is common for several faults to intersect a particular grid area and for any given fault to intersect several areas. In order to establish an equivalent point source energy distribution, we shall make use of the indices  $i$  and  $j$ . Index  $i$  will be associated with grid area, while index  $j$  corresponds to an individual fault. The energy flux for each fault,  $E_j$ , is thereby apportioned to the grid areas which that fault intersects, in accordance with the assumption of a uniform energy distribution. If that portion of  $E_j$  falling in the  $i^{\text{th}}$  grid area is denoted by  $E_{ij}$ , then conservation of energy implies

$$\dot{E}_j = \sum_i \dot{E}_{ij} \quad (11)$$

Conversely, the total energy flux associated with the  $i^{\text{th}}$  grid area (resulting from a number of faults intersecting that area) will be

$$\dot{E}_i = \sum_j \dot{E}_{ij} \quad (12)$$

The total seismic energy flux,  $E_T$ , within a region encompassing many faults and grid areas is therefore,

$$\dot{E}_T = \sum_i \dot{E}_i = \sum_i \sum_j \dot{E}_{ij} \quad (13)$$

At this point we recognize the need to establish a basis of equivalence between energy flux, and the seismicity parameters,  $a$  and  $b$ , introduced earlier in Equation 2. This will enable us to relate the prior geological model with historical data.

The relationship adopted herein (6) is derived from

$$\dot{E} = \int_{-\infty}^{M_U} N'(M) E(M) dM \quad (14)$$

where  $M_U$  is taken to be 8.25 based on the presence of the San Andreas fault.  $N'(M)$  is the frequency density function corresponding to the cumulative frequency distribution of Equation 2.  $E(M)$  is given by Equation 1. It follows that

$$\text{Log } \dot{E} = \text{Log } E_0 + a + (1.5 - b) M_U + \text{Log} \left( \frac{b}{1.5 - b} \right) \quad (15)$$

Equation 15 is used for two different but related computations: (1) to convert values of  $a_i$  representing historical grid area seismicity to  $\log E_i$  for comparison with the seismic energy flux developed from the prior model, and (2) to convert total energy flux for a region,  $E_T$ , to a regional seismicity value,  $a$ . In terms of the present notation, Equation 15 therefore takes the two respective forms:

$$\text{Log } \dot{E}_i = a_i + \text{Log } E_0 + \text{Log} \left( \frac{b}{1.5 - b} \right) + (1.5 - b) M_U \quad (16a)$$

$$\text{Log } \dot{E}_T = a + \text{Log } E_0 + \text{Log} \left( \frac{b}{1.5 - b} \right) + (1.5 - b) M_U \quad (16b)$$

If we choose  $M_U$  to be the same in both equations, conservation of energy, i. e. Equation 12, implies that

$$10^a = \sum_i 10^{a_i}$$

This equation is recognized as being identical to Equation 5.

## ATTENUATION

Numerous relationships for how site ground motion attenuates with distance have been developed for Southern California. In this study, attenuation relationships developed by McGuire (10) are used. McGuire's data base utilized 70 strong motion records published by the California Institute of Technology. Only free field records were used and no more than seven records per earthquake or nine records per single site were incorporated.

These relationships are given below where  $A$  is the peak acceleration ( $\text{cm/s}^2$ ),  $V$ , peak velocity ( $\text{cm/s}$ ),  $D$ , peak displacement ( $\text{cm}$ ),  $M$ , Richter magnitude,  $R$  hypocentral distance ( $\text{km}$ ) and  $Y_s$  a site geology indicator which is 0 for rock sites and unity for soil sites.

$$\ln A = 3.40 + 0.89M - 1.17 \ln R - 0.20 Y_s \quad (17)$$

$$\ln V = -1.00 + 1.07M - 0.96 \ln R + 0.07 Y_s \quad (18)$$

$$\ln D = -2.72 + 1.00M - 0.63 \ln R + 0.12 Y_s \quad (19)$$

Soil is classified as any site underlain by alluvium or other soft material greater than 10 meters thick.

#### BAYESIAN ESTIMATION

As mentioned, a Bayesian estimate of peak ground motions is sought which embodies the combined geological and historical earthquake evidence consistent with the relative degrees of confidence in each. The Bayesian method of analysis presented in (6) is useful for this purpose. It involves taking a weighted average, on a grid-by-grid basis, of the energy flux computed separately from geological and historical data.

The notation

$$e = \text{Log } \dot{E} \quad (20)$$

is adopted for simplicity with subscript "p" denoting prior (geological) model and "o" denoting observed (historical) data. Bayesian estimates for grid area seismic energy flux are given as

$$e_i = \frac{\left(\frac{1}{\sigma_{p_i}}\right)^2 e_{p_i} + \left(\frac{1}{\sigma_{o_i}}\right)^2 e_{o_i}}{\left(\frac{1}{\sigma_{p_i}}\right)^2 + \left(\frac{1}{\sigma_{o_i}}\right)^2} \quad (21)$$

where  $\sigma_{p_i}$  and  $\sigma_{o_i}$  denote respectively the standard deviation on statistical estimates of  $e_{p_i}$  and  $e_{o_i}$ . The value of  $\sigma_{o_i}$  is obtained directly from regression analysis performed on historical data to obtain  $a_i$ .  $e_i$  is equal to  $a_i$  plus a constant as seen from Equation 16a. It follows that the standard deviation of  $e_i$  is also equal to the standard deviation of  $a_i$ .

A single value of  $\sigma_p$  is used for the geological model. Since energy for the geological model is computed from magnitude as a function of surface rupture length,  $\sigma_p$  is based on a regression of magnitude on fault length. The standard deviation on magnitude given by (5) is 0.5. Thus from Equation 1

$$\sigma_{p_i} = 1.5 (0.5) = 0.75 \quad (22)$$

It has been observed that  $\sigma_{o_i}$  may range from about 0.05 to 1.5, with a mean value of approximately 0.3. Corresponding (normalized) weighting factors given by

$$W_o = \frac{\left(\frac{1}{\sigma_o}\right)^2}{\left(\frac{1}{\sigma_p}\right)^2 + \left(\frac{1}{\sigma_o}\right)^2} \quad (23)$$

range, therefore, from about 0.2 to 1.0, with  $W_o = 0.86$  corresponding to  $\sigma_{oi} = 0.3$ . When there are no data in a particular grid area, it is assumed that  $W_o = 0$ . When there is no energy from the prior model in a particular grid area, it is assumed that  $W_o = 1$ . In general, it is found that whenever the data are adequate,  $e_{oi}$  prevails over  $e_{pi}$  in the weighted average.

Once the Bayesian estimates of energy flux, Equation 18, have been determined for each grid, the total seismic intensity parameter  $a$  for a site can be computed from Equations 16 and 5. The effective hypocentral distance  $\bar{R}$  is then determined from Equation 7.

### SEISMIC RISK MAPS

After computing the Bayesian  $a$ 's and  $\bar{R}$ 's, it is possible to calculate an array of ground motion values centered in individual grid areas using Equation 8. By feeding these results into a contour mapping routine, seismic risk maps showing isoseismal contours for peak ground acceleration, velocity or displacement may be produced.

Figures 5, 6 and 7 contain Bayesian peak ground acceleration, velocity and displacement isoseismals. These maps comprise a complete set and characterize the expected (475) year return period intensity of ground shaking based on a Bayesian combination of geological and historical data. In addition, two maps are shown for peak ground velocity, Figures 8 and 9. Figure 8 is developed from geological data while Figure 9 is developed from historical data. These maps are presented as an intermediate result to provide additional insight into the analysis. They may be compared individually with available fault maps and plotted earthquake epicenters. It is also important to note that the peak ground motions shown on the maps represent average soil conditions, exclusive of "rock." This is a direct result of having used McGuire's attenuation equation. The present map values can be modified for "rock" sites by applying the following scale factors derived from McGuire's results:

$$A_r = 1.22 A_s \quad (24a)$$

$$V_r = .932 V_s \quad (24b)$$

$$D_r = .887 D_s \quad (24c)$$

The subscripts  $s$  and  $r$  denote "soil" and "rock" respectively.

### MOTION SPECTRAL AMPLIFICATION

Having estimated for California coastal waters, the expected intensity of ground motion the next step is to establish a spectral description of the

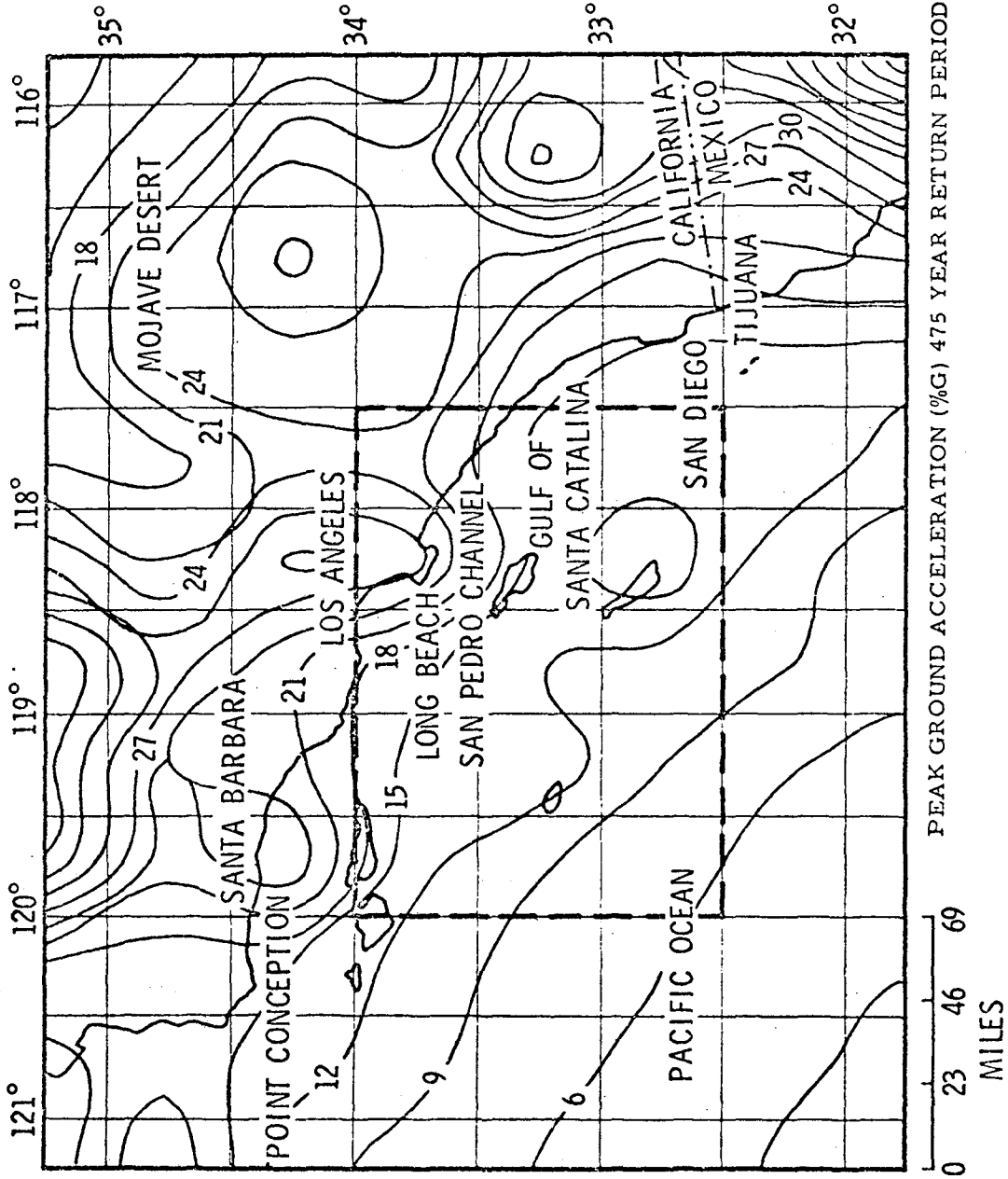


Figure 5. Seismic Risk Map for Southern California Bayesian Estimate -- Acceleration

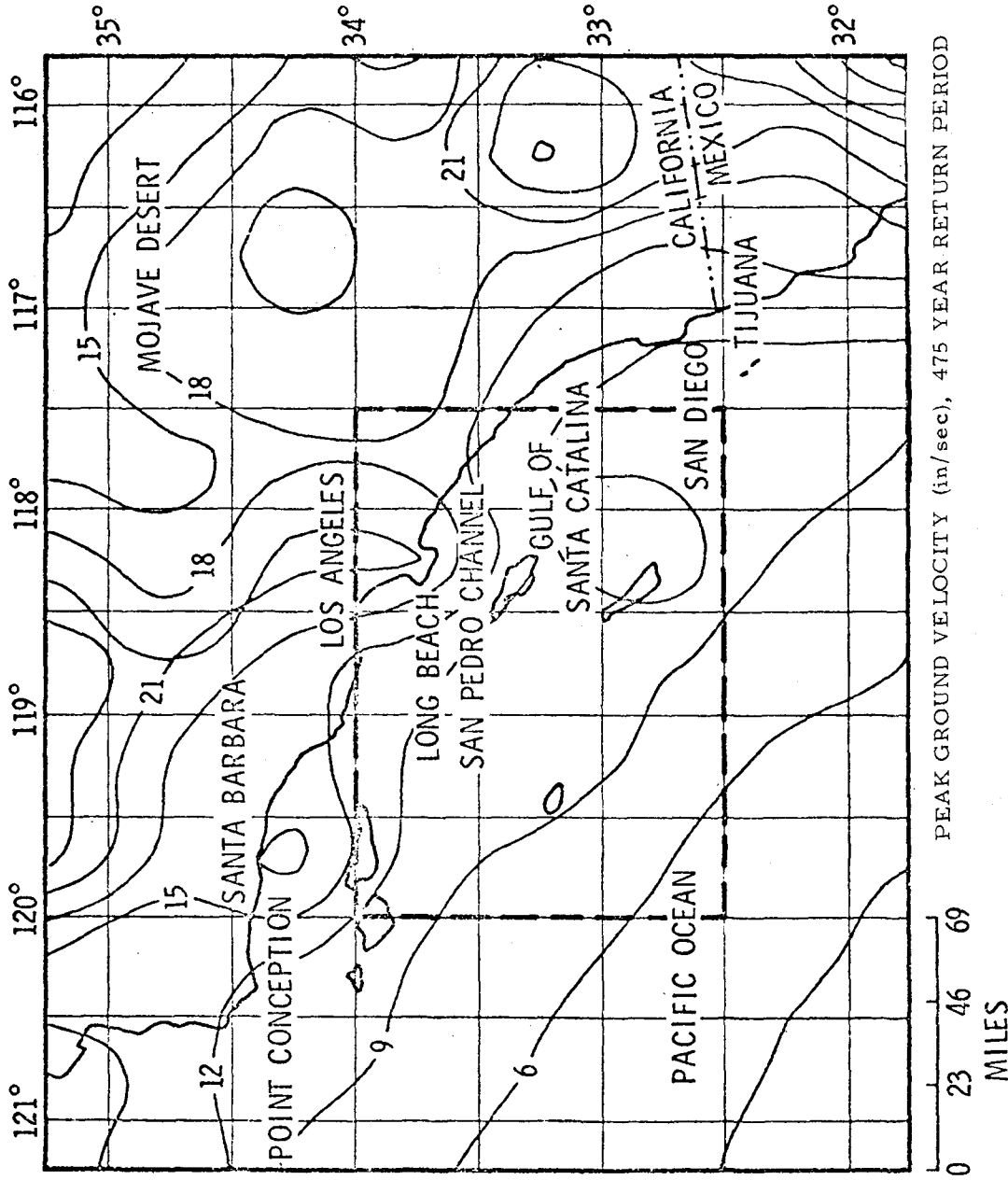


Figure 6. Seismic Risk Map for Southern California Bayesian Estimate -- Velocity

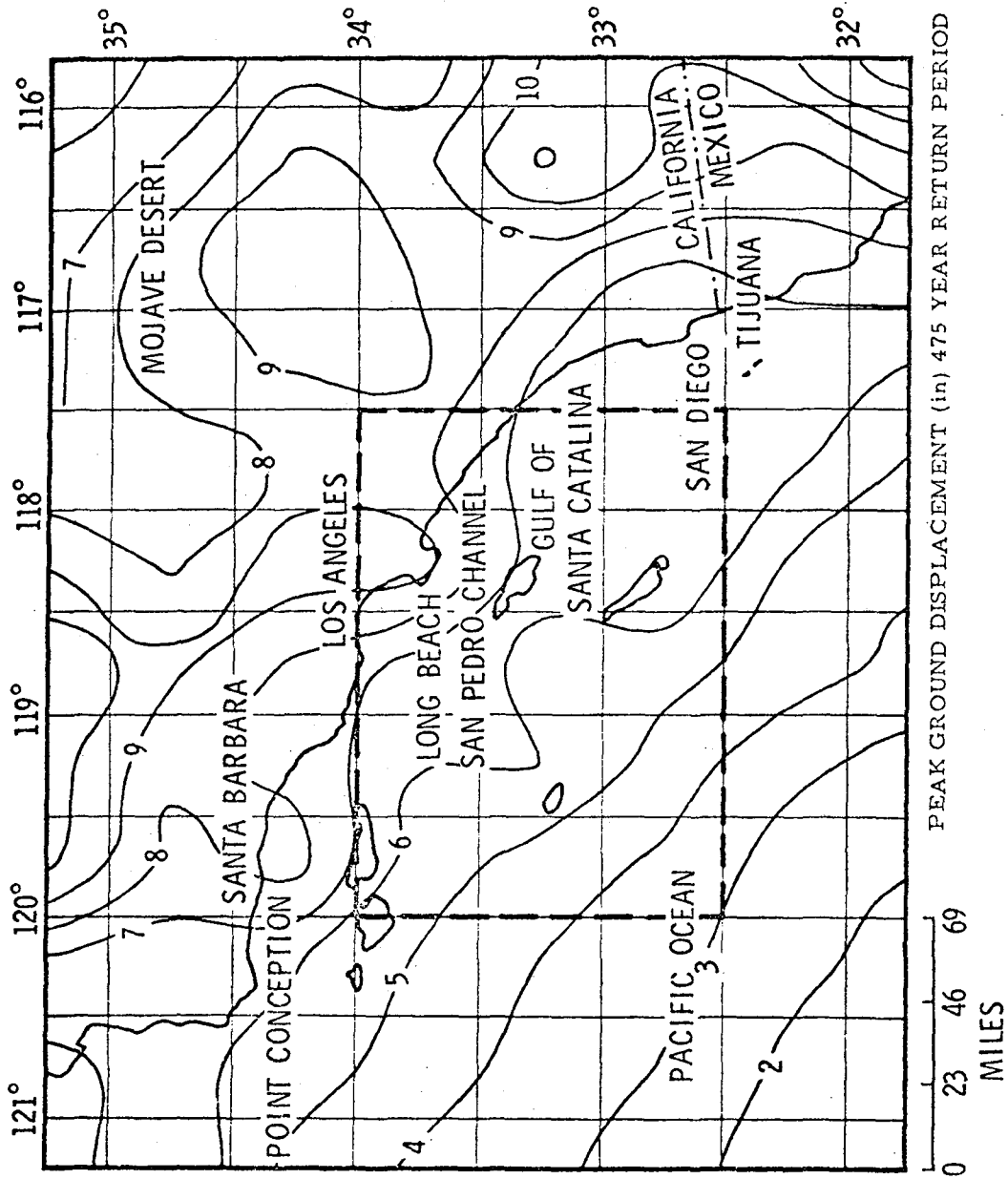


Figure 7. Seismic Risk Map for Southern California Bayesian Estimate--Displacement



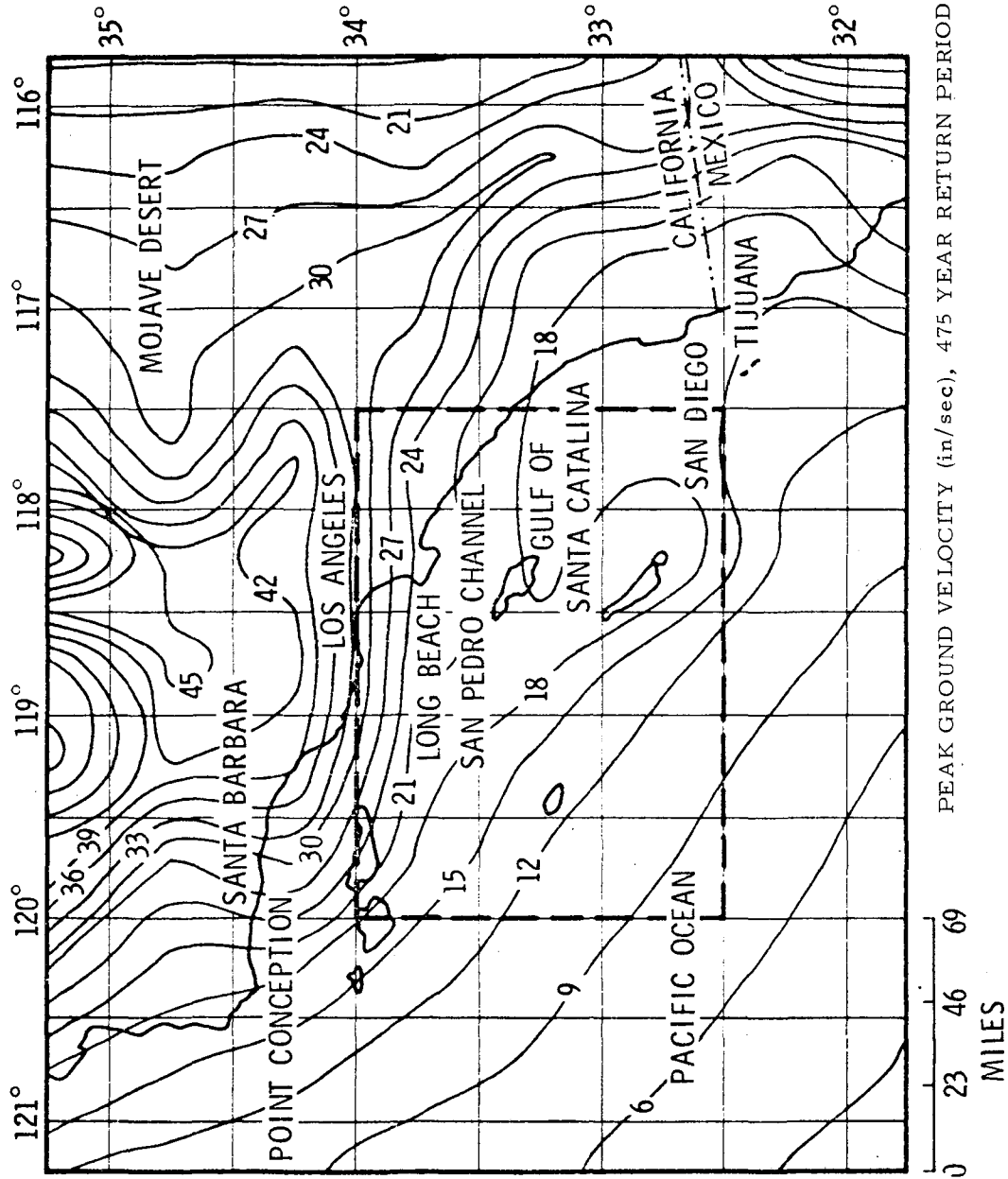


Figure 8. Seismic Risk Map for Southern California Coast  
Prior Geological Model - Velocity

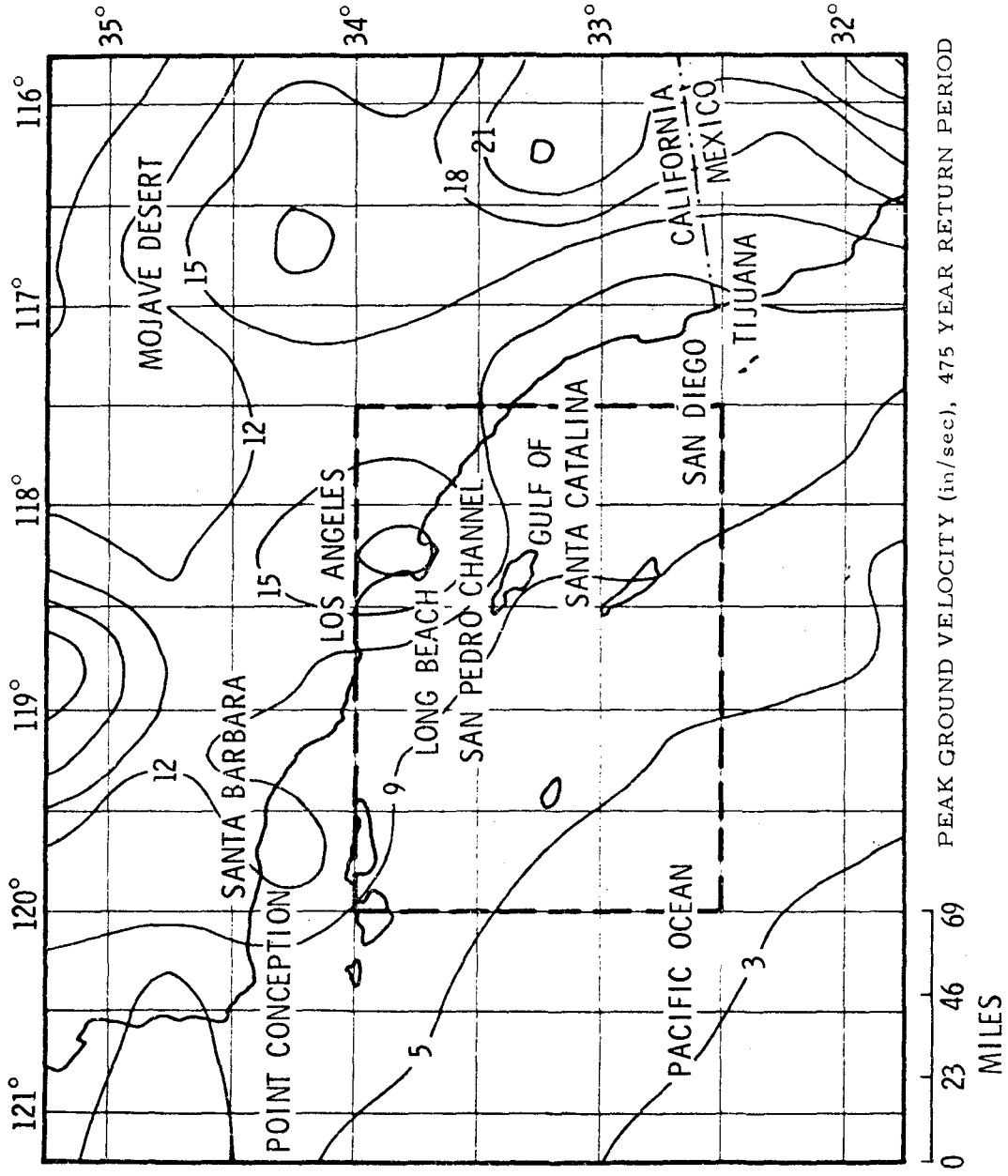


Figure 9. Seismic Risk Map for Southern California Coast  
Historical Data -- Velocity

motion which is applicable to offshore structures. This was done in a study by Mohraz and Eskiĵian (4); the important features of which are summarized here.

Mohraz and Eskiĵian selected ground motion records from 987 accelerograms on the current Cal Tech tapes (16) and processed these records to obtain spectral amplification ratios. Since offshore structures are typically long period, their design will be governed by low frequency, high intensity and long duration earthquake ground motions. For this reason care was taken to select records with long duration and high energy. Thus the following selection criteria were applied:

1. All structurally amplified records such as those taken on upper floors of buildings were eliminated.
2. All vertical records were eliminated.
3. All records with maximum acceleration less than .05 g were eliminated.
4. To obtain the desired influence of duration, all records with less than 5 seconds between the first and last .05 g peak were eliminated.
5. Finally, of the surviving records those with less than average energy were eliminated.

The remaining records were sorted according to the geology of the recording instrument site. The classification scheme selected is consistent with McGuire's attenuation laws used in establishing ground motion intensity. It divides the records into two groups: (1) "rock" sites having rock at the surface or rock overlain by less than 10 meters of soil and (2) "soil" sites having soil layers greater than 10 meters in depth.

These record sets were analyzed to determine amplification spectra and ground motion ratios. The method used is similar to that employed in (4) and involves calculating from spectral velocity records provided on the Cal Tech tapes, spectral acceleration and displacement values. The result is a curve of spectral acceleration, velocity and displacement as a function of frequency for each selected record. These curves are individually normalized using the maximum record value. At this point, a regression of spectral values from the collection of records is performed at discrete frequencies. The spectral values are assumed to be log-normally distributed. Finally, the results are averaged over frequency ranges of 0.1 to 0.3 hertz, 0.3 to 3 hertz and 3 to 8 hertz to provide displacement, velocity and acceleration spectral amplification ratios. This process as well as record selection is graphically illustrated in Figure 10.

The results from this analysis are shown for each site classification in Tables 1, 2 and 3. Tables 1 and 2 provide spectral amplification ratios for different values of structural damping and assuming log-normal frequency distributions of the data. Table 3 provides ground motion ratios for the same set of records.

Variations were made in the record selection process to examine the influence of geology, duration, energy and the presence or absence of San Fernando records. From these variations the following observations were made:

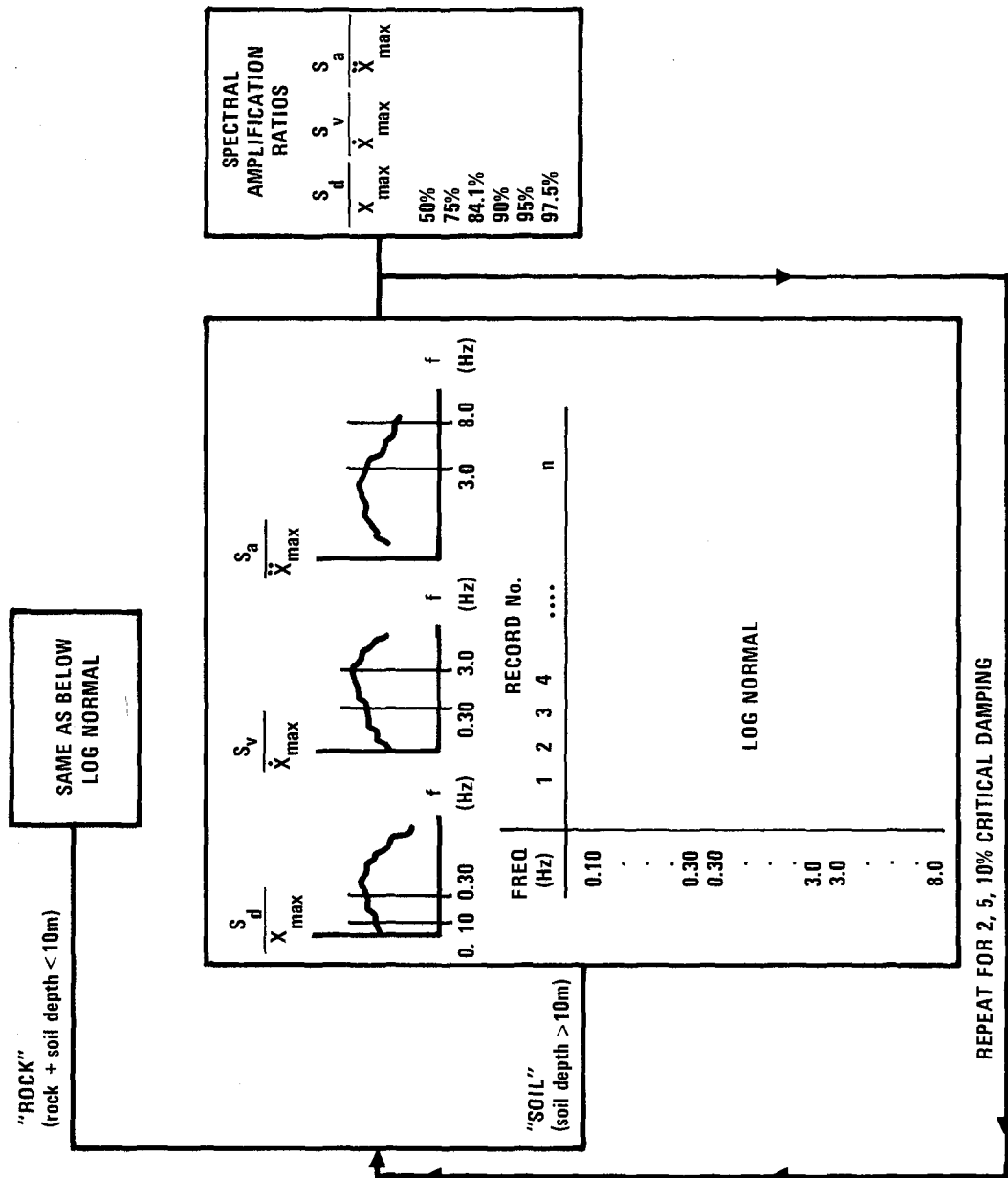


Figure 10. Analysis Methodology

- ELIMINATE:
1. VERTICAL RECORDS
  2. ALL STRUCTURALLY AMPLIFIED RECORDS
  3. PEAK  $\ddot{X} < 0.05 \text{ g/s}$
  4. PEAK  $\ddot{X} > 0.05 \text{ g/s}$  BUT DURATION BETWEEN PEAKS  $< 5.0 \text{ sec}$

ELIMINATE: RECORDS WHOSE ENERGY CONTENT

$$\int_{0.333}^{8.0} \left( \frac{F(\omega)}{F(\omega)_{max}} \right)^2 dT < \text{MEAN}$$

Table 1

## Spectral Amplification Ratios

"Rock" Sites (Rock plus soil less than 10 meters)

Amplification Ratio	LOG-NORMAL						Damping Ratio
	50%	75%	84.1%	90%	95%	97.7%	
$S_d/\dot{X}_{max}$	2.73	3.24	3.52	3.79	4.16	4.57	2%
	2.39	2.78	2.99	3.18	3.46	3.76	5
	2.00	2.27	2.41	2.55	2.73	2.93	10
$S_v/\ddot{X}_{max}$	1.67	2.09	2.34	2.58	2.92	3.03	2
	1.32	1.61	1.78	1.93	2.15	2.39	5
	1.04	1.23	1.34	1.45	1.59	1.75	10
$S_a/\ddot{X}_{max}$	2.78	3.57	4.03	4.49	5.16	5.93	2
	2.12	2.64	2.94	3.23	3.65	4.12	5
	1.70	2.06	2.27	2.46	2.74	3.05	10

Table 2

## Spectral Amplification Ratios

"Soil" Sites (Soil depth greater than 10 meters)

Amplification Ratio	LOG-NORMAL						Damping Ratio
	50%	75%	84.1%	90%	95%	97.7%	
$S_s/\dot{X}_{max}$	2.67	3.21	3.52	3.80	4.20	4.64	2%
	2.30	2.72	2.95	3.16	3.46	3.78	5
	1.92	2.20	2.39	2.54	2.75	2.98	10
$S_v/\ddot{X}_{max}$	1.60	2.00	2.22	2.44	2.76	3.10	2
	1.26	1.53	1.69	1.83	2.04	2.27	5
	0.99	1.19	1.29	1.39	1.54	1.69	10
$S_a/\ddot{X}_{max}$	3.04	3.71	4.08	4.43	4.93	5.47	2
	2.28	2.69	2.91	3.12	3.41	3.73	5
	1.80	2.06	2.20	2.33	2.51	2.69	10

Table 3

## Ground Motion Ratios (Log-Normal)

	"Rock" Sites		"Soil" Sites	
	50%	84.1%	50%	84.1%
d/a	23	34	34	49
v/a	48	69	56	78
ad/v <sup>2</sup>	3.93	6.38	4.11	6.00

1. For the long duration high energy record sets, spectral amplifications for "soil" sites were found to be greater than those for "rock" sites in the frequency range below 2.5 hertz. These findings are consistent with those from earlier works as reported in (4). In the process of examining the "soil" and "rock" site influence it was determined that amplification ratios are quite sensitive to shallow layers of soil making it extremely important to exercise caution when classifying sites.

2. The duration of accelerogram records was found to have a smaller influence on response spectral amplification than had been expected. However, it was determined that the ground motion ratios (i.e.  $d/a$ ,  $v/a$  and  $ad/v^2$ ) are quite sensitive to duration with larger velocity and displacement ratios associated with the longer duration records.

3. The higher energy records produced larger spectral amplifications in the velocity and displacement regions as anticipated.

4. Elimination of records from the San Fernando event as well as elimination of short duration and low energy records resulted in too few records upon which to draw any conclusions.

#### SITE DESIGN SPECTRA

Having established spectral amplification ratios for long period offshore structures, the next and final step in the process of describing the coastal seismic design environment is to prepare site specific design spectra. The process involves combining peak ground motions for a selected site from the Eguchi-Hasselmann study (3) with spectral amplifications computed in the Eskijian-Mohraz study (4).

Within the framework of the present analysis, separate spectral amplification factors are applied to peak ground acceleration, velocity and displacement to produce corresponding response spectrum characteristics, namely peak values of pseudo-acceleration, pseudo-velocity, and pseudo-displacement. The amplification factors, Tables 1 and 2, are denoted by  $G_X$  where X represents either peak ground acceleration, velocity or displacement. Pseudo-response, denoted by Y, is then computed by multiplying the peak ground motion value, X (defined by Figures 5, 6 and 7, for example), by the amplification factor,  $G_X$ , as

$$Y = G_X X \quad (25)$$

Since the amplification factors defined in Tables 1 and 2 are empirically derived from strong motion accelerograms (and integrated accelerograms), they are considered as random variables. In particular, the lognormal distribution is assumed for  $G_X$  (3). In addition, based on previous work (10), a lognormal distribution has been adopted for X which represents the variability in attenuation. Based on these distributions, it follows that Y will have a lognormal distribution with parameters

$$\mu_{\ln Y} = \mu_{\ln G_X} + \mu_{\ln X} \quad (26a)$$

$$\sigma_{\ln Y}^2 = \sigma_{\ln G_X}^2 + \sigma_{\ln X}^2 \quad (26b)$$

where  $\mu$  represents the mean value of the parameter and  $\sigma$  the standard deviation.

The probability that the random variable,  $Y$ , will not exceed some given value,  $y$ , during a period of time,  $t$ , is given by

$$F_{Y,t}(y) = \exp \left[ -\nu_0 t [1 - F_Y(y)] \right] \quad (27)$$

where,  $Y$  is the largest pseudo-response value (e.g., pseudo-acceleration, pseudo-velocity or pseudo-displacement) to occur during an exposure period of  $t$  years, and  $\nu_0$  is the mean rate of arrival of all events greater than some lower bound  $y_0$ . Equation 27 is based on the assumption that the occurrence of earthquakes can be modeled by a Poisson process and that earthquake magnitudes are exponentially distributed.  $F_Y(y)$  is given by

$$F_Y(y) = \int_{y_0}^{\infty} \phi \left( \frac{\ln y - \mu \ln Y}{\sigma \ln Y} \right) f_{\bar{Y}}(\bar{y}) d\bar{y} \quad (28)$$

where,

$$f_{\bar{Y}}(\bar{y}) = b_X y_0^{b_X} \bar{y}^{-(b_X+1)} \quad (29)$$

and where  $b_X = b/C_2$ .  $C_2$  and  $b$  are the constants in the attenuation Equation (6) and the frequency of occurrence Equation (2) relationships, respectively.

Probabilities of non-exceedance for various response values can then be obtained by integrating Equation 28 for various values of  $y$  and inputting those results into Equation 27. A more detailed discussion of this analysis is presented in Reference (17) along with the results of a parametric study involving  $\sigma \ln Y$  and  $b/C_2$ .

Consider as an example a site off the coast at  $33^\circ$  N latitude and  $118^\circ$  W longitude. The design spectrum for this site is obtained as follows: from the Bayesian seismic risk maps peak ground motions ( $X$ ) for a 475 year return period of 15%  $g$  acceleration, 12 inches per second velocity and 6.5 inches displacement are read from Figures 5, 6 and 7 respectively. With these peak ground motions and having verified that the site soil conditions correspond to the classification used in preparing the maps, the next step is to combine the peak ground motions ( $X$ ) with spectral amplification factors ( $G_X$ ) as described previously to account for the uncertainties embodied in each.

Following the described procedure pseudo-response spectrum ordinates are calculated, Figure 11, as a function of probability of non-exceedance or return period. With the selection of the desired risk level (probability that the ground motions will not be exceeded during the structures lifetime) a design spectrum may be plotted for the site in question on tripartite graph paper using the spectral ordinates. An example of such a design spectrum is shown in Figure 12. It provides the desired description of the seismic design conditions for that specific site.

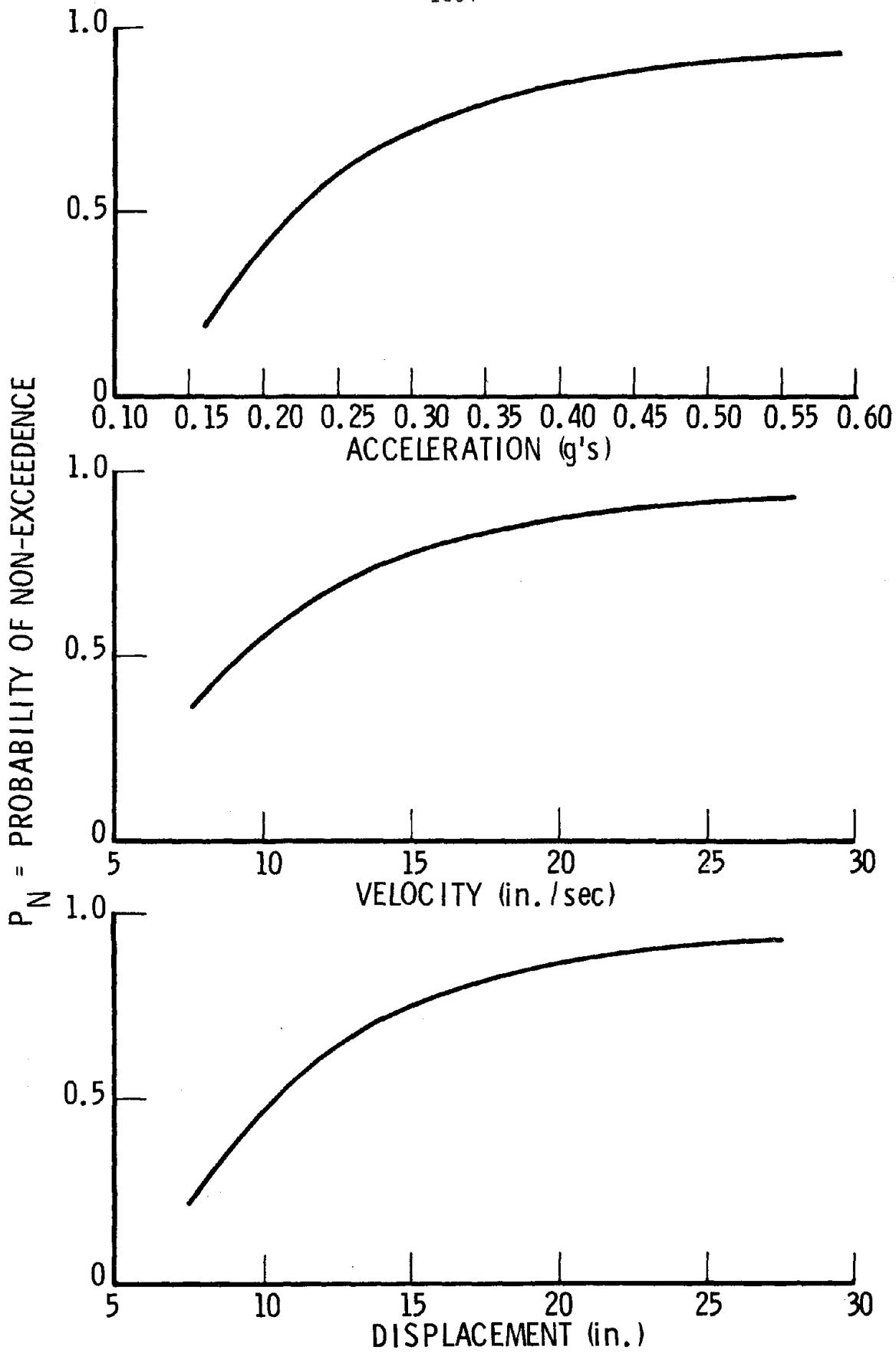


Figure 11. Spectral Ordinates for Southern California (lat  $33^{\circ}\text{N}$ , long  $118^{\circ}\text{W}$ ). Soil Site, 5% Damping, 50 Yr. Life



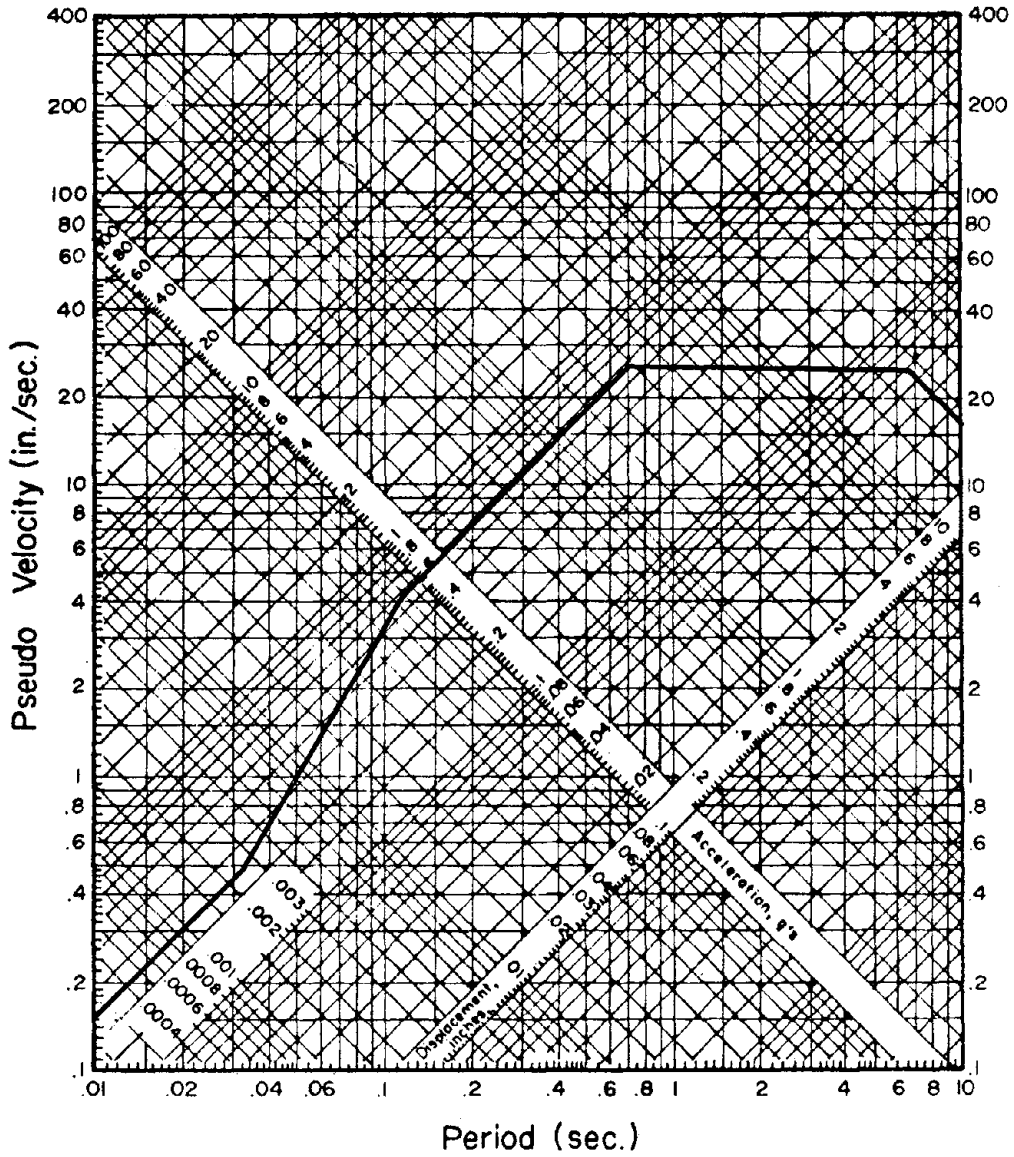


Figure 12. Design Spectrum Southern California (lat  $33^{\circ}$  N, long  $118^{\circ}$  W)  
 5% Damping; 475 Year Return Period Soft Site

## CONCLUSIONS

Conclusions drawn from this study fall into complementary categories - methodology and its application to the problem at hand. The methodology described has three prominent features.

1. Modeling techniques related to seismic energy flux allow both geological data and historical data to be processed in the same way to develop seismic risk maps.

2. Bayesian statistical estimation is used with a prior estimate of seismic energy flux based on geological data. Historical data which sample the actual energy flux over a limited period of time are introduced to revise the initially estimated seismic energy flux distribution. Seismic risk maps are then developed by the above mentioned procedure.

3. Probabilistic analysis is based on median ground motion values depicted on seismic risk maps. Statistically derived uncertainties on attenuation laws and pseudo-response amplification factors are subsequently incorporated to produce response spectra which depend either upon return period or probability of exceedance.

This methodology has been applied to the coastal waters of Southern California as well as to frontier oil lease tract areas off the coast of Alaska and the mid-Atlantic states (1). The application of this methodology has produced the following results:

1. A statistical regression analysis of all historical data available on the current NOAA data tapes within a radius of several hundred miles surrounding each study area to determine the parameters of the Richter equation.

2. Numerically indexed fault maps for Southern California where each fault is listed by number in a corresponding table giving such information as length of fault, type of fault, maximum magnitude, slip rate, maximum surface displacement and recurrence interval associated with the maximum magnitude.

3. Seismic risk maps depicting median peak ground velocity for a 475 year return period computed independently for the geological model and the available historical data on the NOAA data file.

4. Bayesian seismic risk maps depicting median peak ground acceleration, velocity and displacement for a 475 year return period. These maps reflect the combined results of geological and historical data weighted in accordance with the relative degrees of statistical confidence determined for each.

5. Normalized response spectral ordinate tables which reflect long duration and high energy ground motion and are applicable to long period structures.

6. Design spectra for selected sites based on a probabilistic combination of uncertainties resulting from motion attenuation, response amplification as well as earthquake occurrence, magnitude and location.

## REFERENCES

1. Aerospace Report No. ATR-77(7626-01)-7, "Environmental Design Data for Gulf of Alaska, Mid-Atlantic and Southern California Outer Continental Shelf Regions," Summary Final Report, Prepared for the United States Geological Survey by The Aerospace Corporation, December, 1977.
2. Cornell, C. A., "Engineering Seismic Risk Analysis," Bull. Seis. Soc. Am., Vol. 58, No. 5, pp 1583-1606, October, 1968.
3. Eguchi, R. T., and Hasselman, T. K., "Seismic Risk Mapping for Frontier Lease Tract Areas," Appendix B to Environmental Design Data for Gulf of Alaska, Mid-Atlantic and Southern California Outer Continental Shelf Regions, Summary Final Report, Prepared for the United States Geological Survey by The Aerospace Corporation, December, 1977.
4. Eskijian, M. L., and Mohraz, B., "Horizontal Spectral Amplification Ratios for Offshore Platforms," Appendix C to Environmental Design Data for Gulf of Alaska, Mid-Atlantic and Southern California Outer Continental Shelf Regions, Summary Final Report, Prepared for the United States Geological Survey by The Aerospace Corporation, December, 1977.
5. Greenfelder, R. W., "Maximum Credible Rock Accelerations From Earthquakes in California," Map Sheet 23, California Division of Mines and Geology, State of California, 1974.
6. Hasselman, T. K., Chrostowski, J. D., and Wiggins, J. H., "A Bayesian Approach for Mapping Earthquake Intensity," Presented at ASCE National Convention, San Francisco, Calif., October 17-21, 1977. Submitted for Publication to ASCE J. Structural Division.
7. Hileman, J. A., Allen, C. R., and Nordquist, J. M., "Seismicity of the Southern California Region - 1 January 1932 to 31 December 1972," Contribution No. 2385, Div. Geol. Planetary Sciences, California Institute of Technology, 1973.
8. Jennings, C. W., "Fault Map of California," Geologic Data Map No. 1, California Division of Mines and Geology, State of California, 1975.
9. Mark, R. K., "Application of Linear Statistical Models of Earthquake Magnitude versus Fault Length in Estimating Maximum Expectable Earthquakes," Geology, Vol. 5, pp 464-466, August, 1977.
10. McGuire, R. K., "Seismic Ground Motion Parameter Relations," The Use of Probabilities in Earthquake Engineering, ASCE Fall Convention and Exhibit, Preprint 2913, San Francisco, California, 1977.
11. Richter, C. F., Elementary Seismology, W. H. Freeman and Co., 1958.
12. Slemmons, D. B., "Faults and Earthquake Magnitude," State-of-the-Art for Assessing Earthquake Hazards in the U.S. - Report 6, Misc. Paper S-73-1, U. S. Army Engineer Waterways Experiment Station, 1977.

13. United States Geological Survey, "Tectonic Map of North America," 1969.
14. Wallace, R. E., "Earthquake Recurrence Intervals on the San Andreas Fault," Geol. Soc. Am. Bull. Vol. 81, pp 2875-2890, October, 1970.
15. Ziony, J. I., Wentworth, C. M., Buchanan-Banks, J. M., and Wagner, H. C., "Preliminary Map Showing Recency of Faulting in Coastal Southern California," Misc. Field Studies Map MF-585, USGS, 1974.
16. Hudson, D. E. et. al., (1971 - 1975) Analysis of Strong Motion Earthquake Accelerograms - Digitized and Plotted Data, Volume II. Corrected Accelerograms and Integrated Ground Velocity and Displacement Curves, Parts A through Y. Earthquake Engineering Research Laboratory, California Institute of Technology, Pasadena, California.
17. Hasselman, T. K. and Eguchi, R. T., "A Simple Method for Incorporating the Uncertainty of Attenuation and Spectral Amplification in Seismic Risk Analysis," International Symposium on February 4, 1976. Guatemalan Earthquake and the Reconstruction Process, Guatemala, May 14 - 19, 1978.



approach used to derive current criteria response spectra which presupposes independence of response spectrum ordinates (e.g., References 1, 2, and 3). Current criteria response spectra have mean value ordinates calculated at each frequency by the assumption of independent spectral ordinates and normalization by the PGA. For example, analyses to determine criteria response spectra compute a normalized ordinate at 2 Hertz from say 30 different response spectra, and these 30 ordinates at 2 Hertz are studied separately from the adjacent ordinates at 1.99, 2.01 Hertz and all other frequencies.

Assuming that each earthquake record is unique, shape parameters are used to quantify the mean value and variance functions of each of the response spectra. It is shown that the instrumental PGA is one of several shape parameters and that a wide variety of spectral shapes can be quantified numerically in terms of these shape parameters. The large variability in these shape parameters provides one of the keys to developing statistically reliable site specific design criteria.

## THEORY

The typical characteristics of a response spectrum are shown in Figure 1 in which the ordinate is spectral acceleration, SA, on a linear scale and the abscissa is period, T, on a logarithmic scale. Such a plot magnifies the region of interest for most engineered facilities.

An empirical approach has been employed in this paper to provide mean value and variance functions that fit a wide variety of response spectra. The mean value response spectra function is made up of five parameters, and is written

$$\overline{SA} = C1 \cdot e^{-(C2 \cdot T)} + C3 \cdot T^{C4} \cdot e^{-(C5 \cdot T)} \quad 1$$

in which  $\overline{SA}$  is the mean value spectral acceleration, T is the period in seconds, and C1 through C5 are constants to be determined from analysis of the data.

The first term of this function has the shape shown in Figure 2 where parameter C1 corresponds to the PGA, and C2 is determined essentially by a simple statistical analysis of the response spectra data in the period range of 5 to 10 seconds. The second term of equation 1, which is also shown in Figure 2, has a smooth rise from zero at zero period to a peak and then a rapid decay with an increase in period. The three parameters of the second term are determined by employing a multiple-nonlinear regression analysis in which the function is fit to the response spectra data to minimize the squared error.

Figure 1 shows the resulting mean value response spectrum superimposed on the 18 May 1940 El Centro response spectrum, N-S component for 5 percent damping. Though the variance data about the mean value function has not been completely processed to date, it has been observed that the absolute difference between the actual and mean value spectral ordinates are of the same basic shape as the mean value function. Thus, it will be a simple matter to specify a mean plus one or two standard deviation response spectrum curve in the same form as equation 1.

It was found after computing the five parameters, C1 through C5, for several earthquake spectra that it was more convenient for comparison pur-

poses to rewrite equation 1 in terms of a set of parameters which have a more physical interpretation in regard to the mean value curve. By defining  $X_1$  as the period at which the peak mean value spectral ordinate occurs,  $X_2$  as the peak mean value spectral ordinate, and  $X_3$  as the relative spread of the mean value curve as measured by the distance of the inflection point from the peak divided by  $X_1$ , equation 1 may be rewritten

$$SA = C_1 \cdot e^{-(C_2 \cdot T)} + \left( \frac{X_2 - C_1 \cdot e^{-(C_2 \cdot X_1)}}{X_1 (1/X_3^2) \cdot e^{-(1/X_3^2)}} \right) \cdot T^{(1/X_3^2)} \cdot e^{-(T/(X_1 \cdot X_3^2))} \quad 2$$

## DATA ANALYSIS

Thirteen El Centro events for which response spectra are recorded were used in the analysis and are listed in Table 1 along with their dates, locations and magnitudes and epicentral distances. Figure 3 graphically shows the location of the thirteen epicenters and the location of the recording station. The seven recording stations which obtained records of the 27 June 1966 Parkfield earthquake and whose corresponding response spectra were analyzed are listed in Table 2 along with their site locations and epicentral distances. Figure 4 shows the geographical relationship of the Parkfield earthquake epicenter and the location of each of the seven recording stations. Data given in Tables 1 and 2 has been obtained from "Earthquake History of the United States" (Ref. 4) and Hileman and Allen (Ref. 5).

A computer program was developed for the automated processing of response spectra data obtained from NTIS computer tapes (Ref. 6). This program was used to investigate the previously defined characteristics,  $C_1$ ,  $C_2$ ,  $X_1$ ,  $X_2$ ,  $X_3$ , for the five percent damped response spectra data corresponding to the recorded events of Tables 1 and 2. An additional calculation of the root mean square difference between the regressed mean value function and the response spectra data has been made for each directional component processed. The value was then normalized by the PGA (i.e.,  $C_1$ ) and is included along with the other pertinent results of the analyses.

## RESULTS OF THE ANALYSES

Results of the mean value response spectra nonlinear regression analyses are given in Tables 3 and 4. Parameters  $C_1$ ,  $C_2$ ,  $X_1$ ,  $X_2$ ,  $X_3$  are listed in Tables 3 and 4 for 13 earthquakes recorded at Station No. 117, El Centro, and the Parkfield earthquake of 27 June 1966 recorded at seven stations, respectively. In addition, typical mean value spectra are plotted in Figures 5 and 6 for the El Centro station and in Figures 7 and 8 for the Parkfield earthquake.

These figures and tables indicate several things:

1. The El Centro site spectra are, on the average, broader than those produced by the Parkfield earthquake. The average value of  $X_3$ , which is a relative measure of spread, is 0.80 for the El Centro site, whereas it is 0.64 for the Parkfield earthquake response spectra.
2. The period of the peak mean value response,  $X_1$ , is quite variable for different earthquakes and for the same earthquake recorded at different stations. It appears, also, that  $X_1$  does not correlate well with epicentral distance.

3. In all but one case listed in Tables 3 and 4 the mean vertical response spectra have peaks occurring at smaller periods (higher frequencies) than the horizontal components.

One of the more interesting results of the analysis to date is shown in Figure 9, in which the peak ground acceleration,  $C_1$ , is plotted against the peak of the mean value response spectra,  $X_2$ , for the N-S component of the earthquakes recorded at the El Centro site. The correlation coefficient between these two parameters is 0.989. For the E-W component it is 0.995 and for the vertical component it is 0.989. A similar computation for the Parkfield earthquake gives a correlation coefficient of 0.986 for the horizontal components and 0.971 for the vertical components.

## CONCLUSIONS

Based on the preliminary results presented in this report and additional work in progress, it appears that the chosen mean value function provides a satisfactory fit to the data and that the five constants of that equation plus a variance function provide a satisfactory sufficient statistic. That is, the values of these parameters provide detailed quantified measures by which response spectra can be compared, correlations developed, and criteria analysed on a site specific basis.

Although the peak spectral ordinate is very highly correlated with the peak ground acceleration, the period at which the peak ordinate is found is highly variable and appears to be uncorrelated with epicentral distance.

The wide band characteristics of the response spectra for 13 earthquakes recorded at the El Centro site are quite similar while more narrow band characteristics are found in the spectra of the Parkfield event recorded at several different sites.

Although many more studies remain to be done, it has been shown that peak ground acceleration by itself is not a satisfactory sufficient statistic for response spectra. In addition, no standard shape exists for a universal criteria. Sufficient data are available to develop the basic characteristics of site specific criteria response spectra including the uncertainties in all the parameters.



## REFERENCES

1. Newmark, N. M., Blume, J. A., Kapur, K. K., "Seismic Design Spectra for Nuclear Power Plants," J. Power Division., Proc. ASCE, Vol.99, No. PO2, 287-303 (November, 1973).
2. Seed, H. B., Ugas, C., and Lysmer, J., "Site-Dependent Spectra for Earthquake-Resistant Design," Earthquake Engineering Research Center, University of California, Berkeley, Report No. EERC 74-12, November, 1974.
3. Applied Technology Council "An Evaluation of a Response Spectrum Approach to Seismic Design of Buildings," ATC-2 Report, San Francisco, California, 1974.
4. "Earthquake History of the United States," Publication 41-1 Revised Edition (Through 1970), U.S. Department of Commerce, National Oceanic and Atmospheric Administration, Environmental Data Service, Boulder, Colorado, 1973.
5. Computer Tape NIS159 and NIS160, National Information Service for Earthquake Engineering, Earthquake Engineering Research Center, University of California at Berkeley, Richmond, California, 1978.
6. Hileman, James A., Allen, Clarence R., and Nordquist, John M., "Seismicity of the Southern California Region 1 January 1932 to 31 December 1972," Seismological Laboratory, California Institute of Technology, Pasadena, California, 1973.

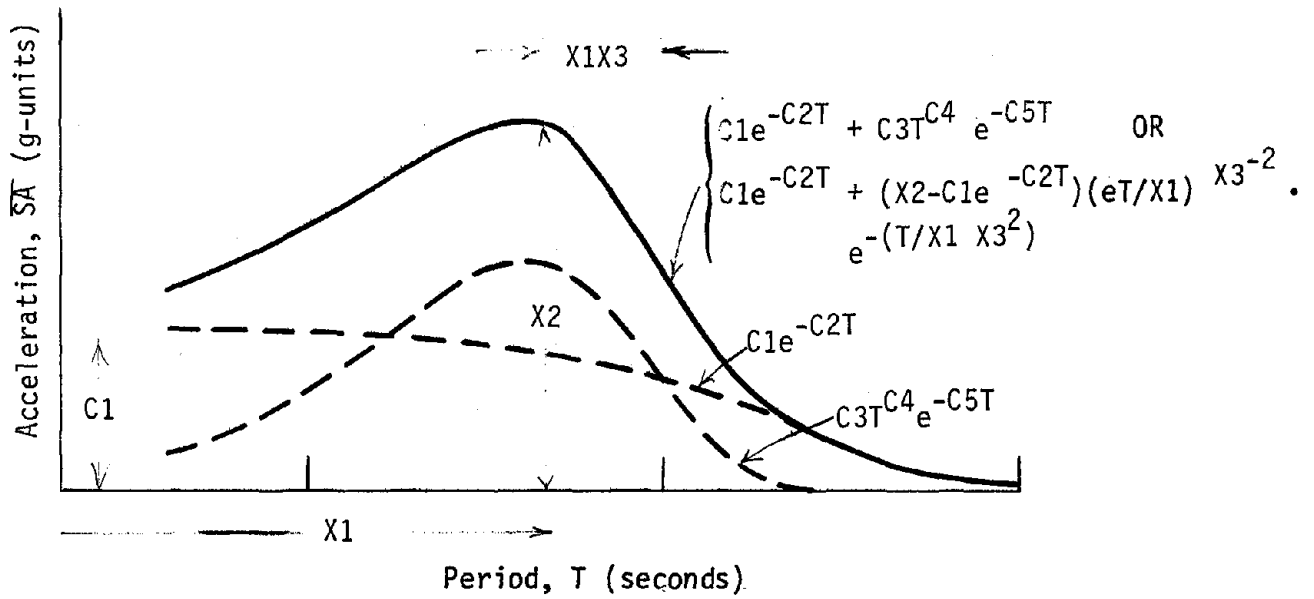


FIGURE 2 MEAN VALUE RESPONSE SPECTRA FUNCTION

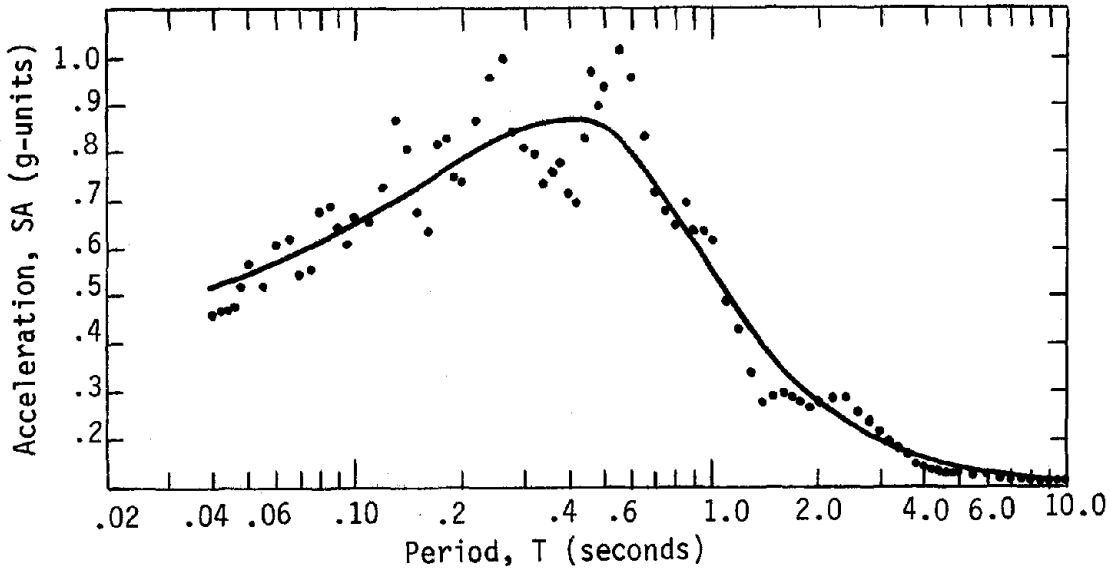


FIGURE 1 RESPONSE SPECTRA WITH MEAN RESPONSE SPECTRA SUPERIMPOSED -- FIVE PERCENT DAMPING, EL CENTRO RECORDING STATION 1940 N-S COMPONENT

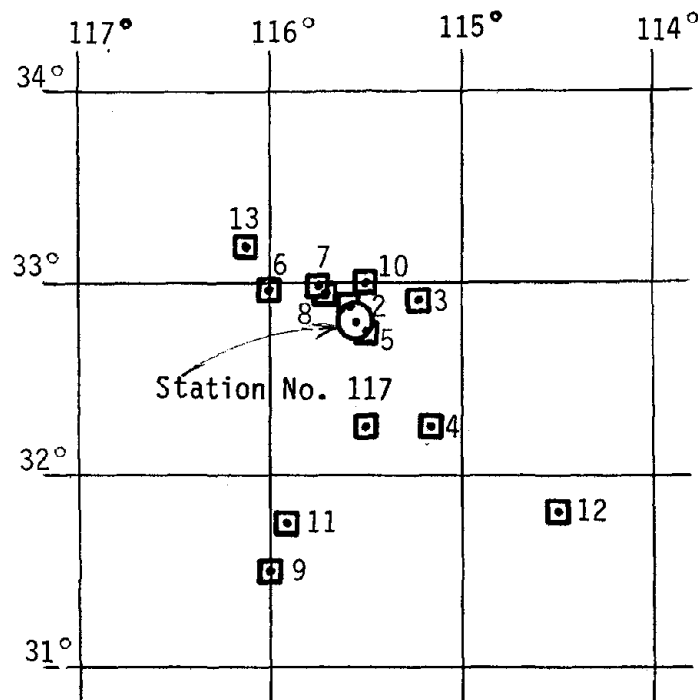


FIGURE 3 GEOGRAPHICAL LOCATION OF EARTHQUAKES RECORDED AT STATION No. 117,  
EL CENTRO IMPERIAL VALLEY IRRIGATION DISTRICT

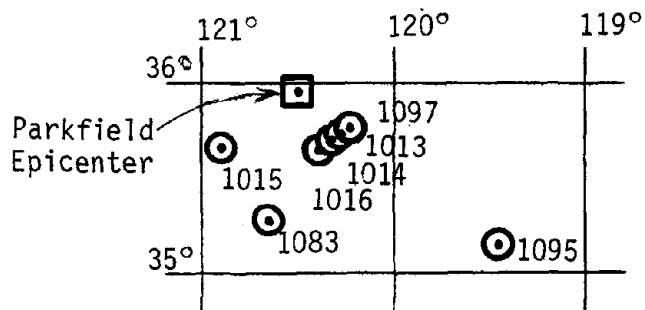
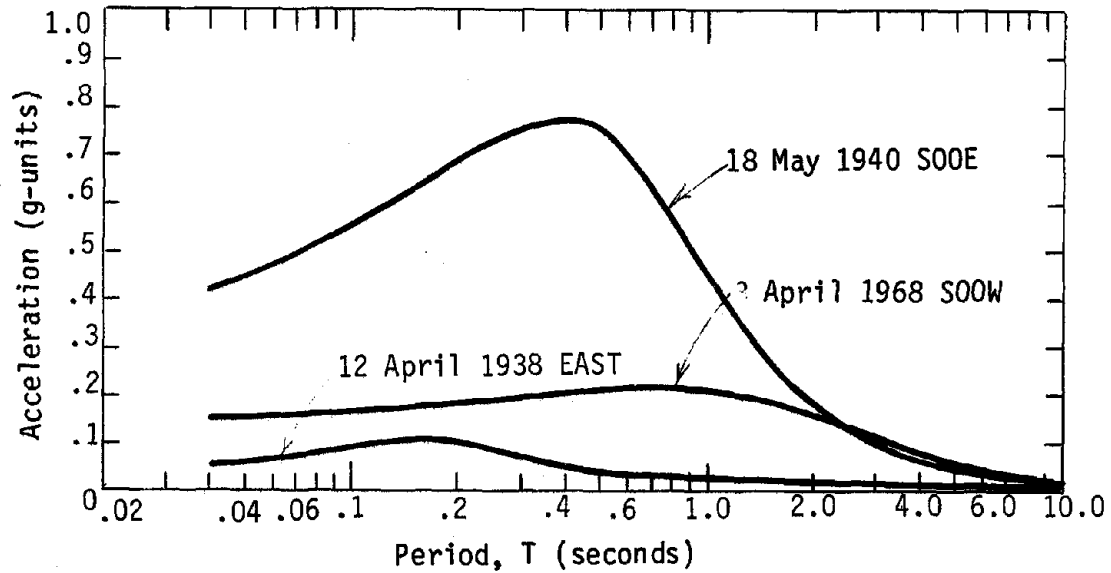
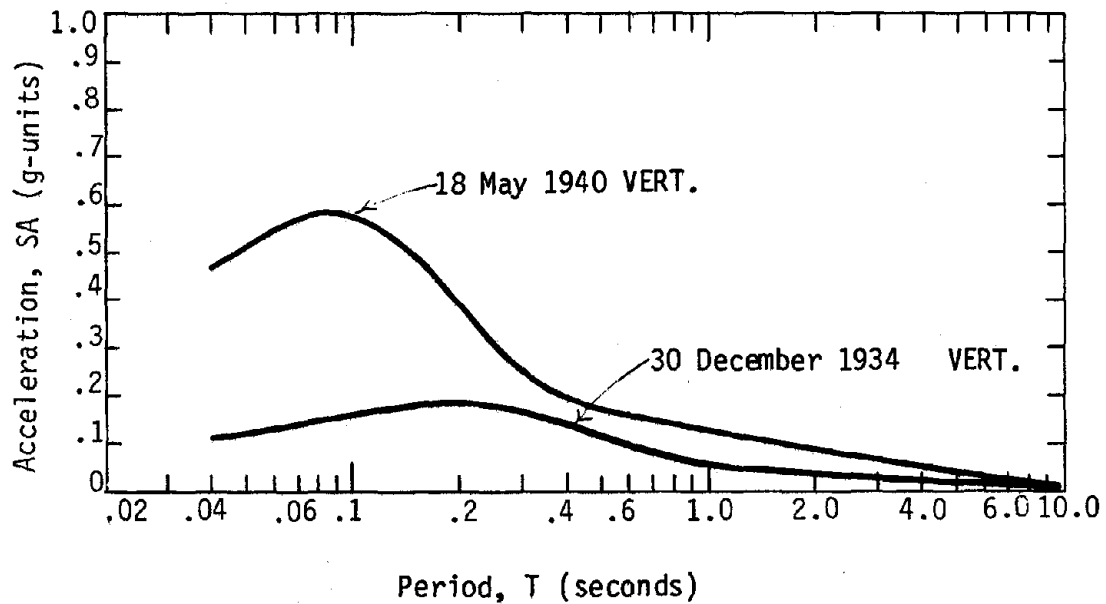


FIGURE 4 GEOGRAPHICAL LOCATION OF RECORDING STATIONS  
RECORDING THE PARKFIELD EARTHQUAKE, 27 JUNE 1966



**FIGURE 5 TYPICAL MEAN VERTICAL RESPONSE SPECTRA -- FIVE PERCENT DAMPING**  
EL CENTRO RECORDING STATION



**FIGURE 6 TYPICAL MEAN VERTICAL RESPONSE SPECTRA -- FIVE PERCENT DAMPING**  
EL CENTRO RECORDING STATION

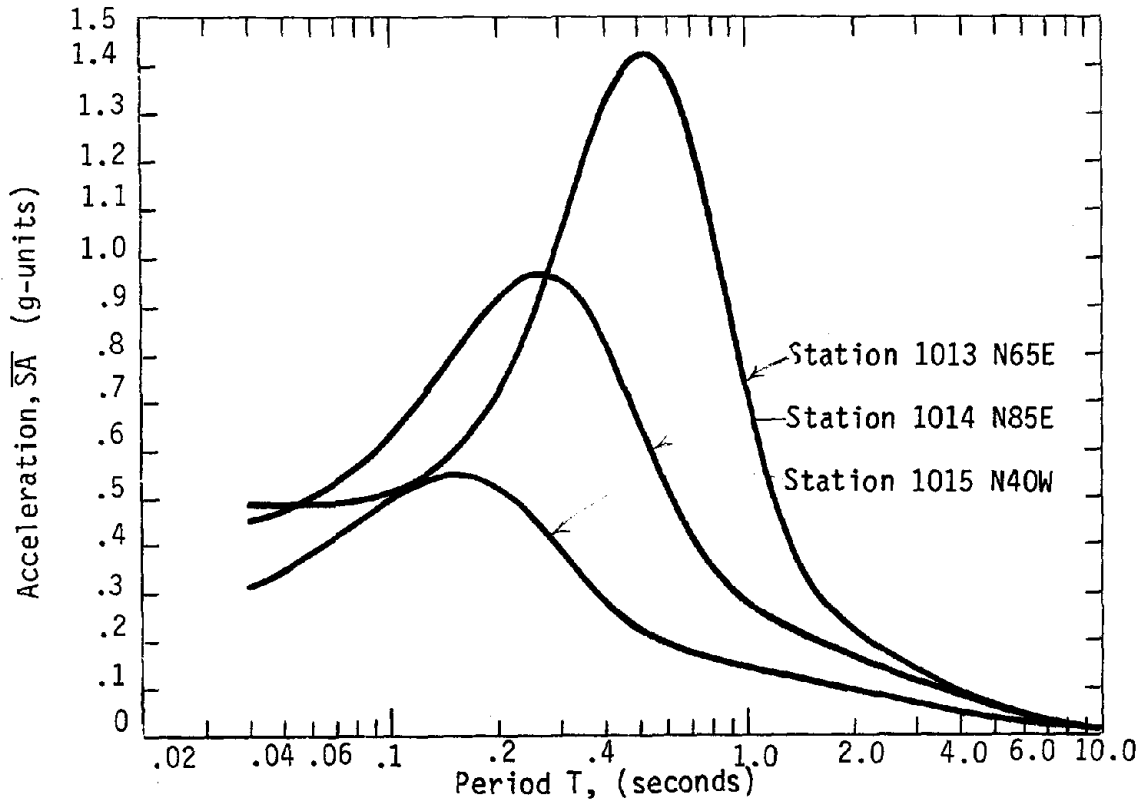


FIGURE 7 TYPICAL MEAN HORIZONTAL RESPONSE SPECTRA --  
 PARKFIELD EARTHQUAKE, 27 JUNE 1966 -- FIVE PERCENT DAMPING

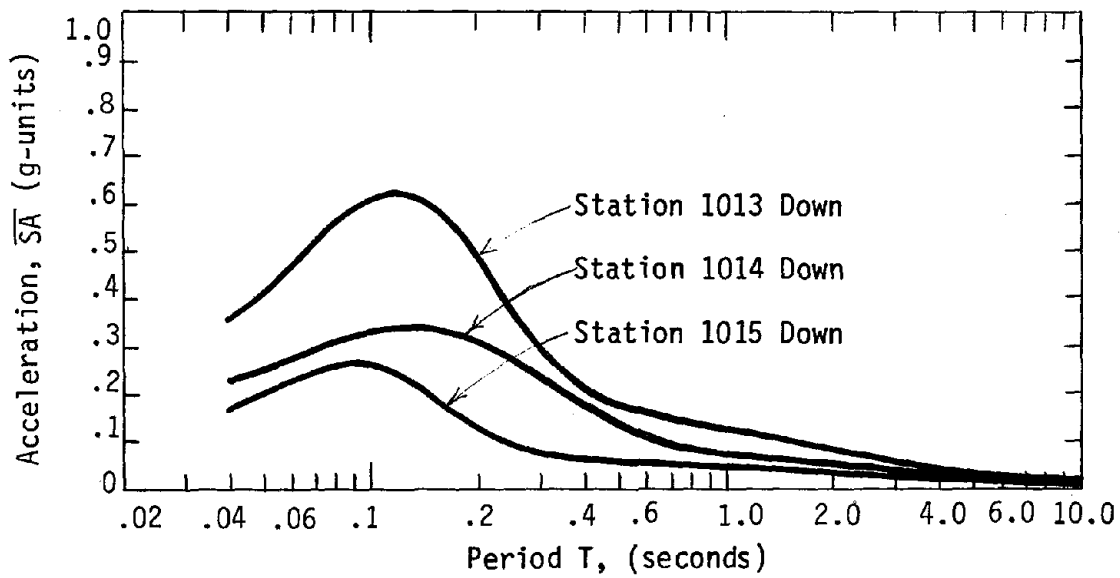


FIGURE 8 TYPICAL VERTICAL RESPONSE SPECTRA --  
 PARKFIELD EARTHQUAKE, 27, JUNE 1966 -- FIVE PERCENT DAMPING

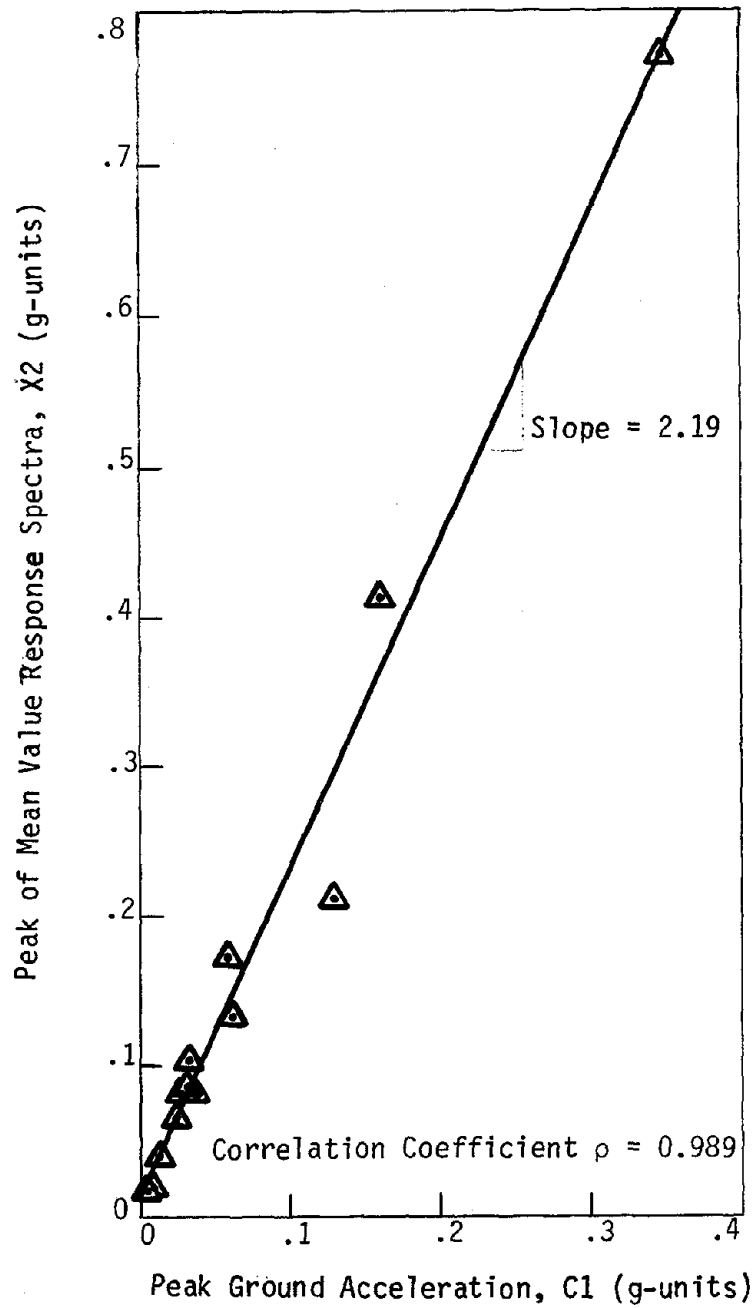


FIGURE 9 CORRELATION BETWEEN PEAK GROUND ACCELERATION  
AND PEAK OF MEAN RESPONSE SPECTRA EL CENTRO RECORDING STATION No. 117  
NORTH SOUTH COMPONENTS FIVE PERCENT DAMPING

TABLE 1 EARTHQUAKES RECORDED AT STATION NO. 117,  
EL CENTRO IMPERIAL VALLEY IRRIGATION DISTRICT

No.	Date	Location	Epicentral Coordinates		Magnitude (RM)	Epicentral Distance (km)
			N. Lat.*	W. Long.*		
1	30 December 1934	South of Calexico	32.25	115.5	6.5	61.1
2	12 April 1938	Imperial Valley	32.9	115.6	3.0	10.0
3	5 June 1938	Imperial Valley	32.9	115.2	5.0	33.0
4	6 June 1938	Imperial Valley	32.25	115.2	4.0	70.7
5	18 May 1940	Southeast of Imperial Valley	32.7	115.5	6.7	8.5
6	21 October 1942	Near Borrego Valley	33.0	116.0	6.5	46.1
7	23 January 1951	Near Calipatria	33.0	115.7	5.6	26.8
8	13 June 1953	Imperial Valley	32.9	115.7	5.5	23.0
9	12 November 1954	Baja California	31.5	116	6.3	150.4
10	16 December 1955	Near Brawley	33.0	115.5	4.3	22.9
11	9 February 1956	Baja California	31.8	115.9	6.8	121.5
12	7 August 1966	Gulf of California	31.8	114.5	6.3	148.3
13	8 April 1968	South of Ocotillo Wells	33.2	116.1	6.4	69.4

TABLE 2 MULTIPLE RECORDINGS OF PARKFIELD EARTHQUAKE,  
27 JUNE 1966 (5.6 RM)

No.	Station Location	Station No.	Station Coordinates		Epicentral Distance (km)
			N. Lat.*	W. Long.*	
1	Cholame, Shandon, CA Array No. 2	1013	35.73	120.29	30.0
2	Cholame, Shandon, CA Array No. 5	1014	35.70	120.33	30.2
3	Cholame, Shandon, CA Array No. 8	1015	35.67	120.90	43.1
4	Cholame, Shandon, CA Array No. 12	1016	35.64	120.40	33.0
5	Tembler, CA, No. 2	1097	35.75	120.26	30.6
6	San Luis Obispo Rec. Bldg., CA	1083	35.28	120.67	71.8
7	Lincoln School Tunnel, Taft, CA	1095	35.15	119.45	129.0

\* Degrees

TABLE 3 RESULTS OF ANALYSES, EARTHQUAKES RECORDED AT  
STATION NO. 117, EL CENTRO

<u>No.</u>	<u>Year</u>	<u>Component</u>	<u>RMS/PGA</u>	<u>C1 (g)</u>	<u>C2 (Hz)</u>	<u>X1 (sec)</u>	<u>X2 (g)</u>	<u>X3</u>
1	1934	SOOW	0.24	0.160	0.429	0.266	0.413	0.93
		S9OW	0.22	0.182	0.429	0.295	0.412	0.78
		VERT	0.26	0.069	0.281	0.200	0.183	0.88
2	1938	NORTH	0.26	0.029	0.375	0.175	0.081	0.71
		EAST	0.21	0.050	0.348	0.155	0.108	0.54
		UP	0.33	0.022	0.350	0.101	0.036	0.86
3	1938	NORTH	0.33	0.034	0.514	0.140	0.082	0.51
		EAST	0.31	0.027	0.522	0.122	0.053	1.02
		UP	0.27	0.013	0.414	0.108	0.043	0.40
4	1938	NORTH	0.28	0.009	0.319	0.166	0.019	0.70
		UP	0.33	0.004	0.205	0.107	0.012	0.57
5	1940	SOOE	0.20	0.348	0.402	0.400	0.772	0.90
		S9OW	0.20	0.214	0.232	0.433	0.529	0.81
		VERT	0.33	0.210	0.425	0.088	0.583	0.82
6	1942	NORTH	0.19	0.060	0.170	0.272	0.173	0.63
		EAST	0.22	0.047	0.185	0.331	0.113	0.74
		UP	0.19	0.026	0.400	0.167	0.073	0.63
7	1951	NORTH	0.27	0.031	0.340	0.368	0.085	0.78
		EAST	0.26	0.028	0.351	0.461	0.097	0.62
		UP	0.34	0.014	0.328	0.144	0.035	0.72
8	1953	NORTH	0.39	0.007	0.178	0.305	0.016	0.75
		EAST	0.39	0.037	0.410	0.455	0.085	1.03
		UP	0.21	0.017	0.360	0.138	0.047	0.59
9	1954	NORTH	0.23	0.025	0.364	0.674	0.065	0.59
		EAST	0.19	0.028	0.332	0.615	0.058	0.81
		UP	0.27	0.007	0.225	0.338	0.014	1.09
10	1955	NORTH	0.22	0.064	0.417	0.281	0.134	0.84
		EAST	0.20	0.072	0.511	0.207	0.153	0.75
		UP	0.28	0.058	0.523	0.094	0.082	0.83
11	1956	SOOW	0.37	0.033	0.247	0.517	0.104	0.85
		S9OW	0.28	0.051	0.247	0.611	0.137	0.75
		VERT	0.50	0.013	0.204	0.330	0.030	1.24
12	1966	NORTH	0.38	0.014	0.169	0.574	0.040	0.87
		EAST	0.47	0.015	0.184	0.583	0.038	0.91
		UP	0.48	0.005	0.076	0.846	0.014	1.19
13	1968	SOOW	0.22	0.130	0.235	0.871	0.211	1.12
		S9OW	0.43	0.057	0.116	0.683	0.132	1.14
		VERT	0.23	0.030	0.222	0.210	0.092	0.52



TABLE 4 RESULTS OF ANALYSES, MULTIPLE RECORDINGS OF  
PARKFIELD EARTHQUAKE, 27 JUNE 1966 (5.6 RM)

<u>No.</u>	<u>Station No.</u>	<u>Component</u>	<u>RMS/PGA</u>	<u>C1 (g)</u>	<u>C2 (Hz)</u>	<u>X1 (sec)</u>	<u>X2 (g)</u>	<u>X3</u>
1	1013	N65E	0.28	0.489	0.411	0.533	1.424	0.52
		DOWN	0.45	0.206	0.482	0.121	0.618	0.66
2	1014	N05W	0.25	0.355	0.537	0.319	0.910	0.56
		N85E	0.25	0.434	0.484	0.275	0.974	0.61
		DOWN	0.38	0.119	0.498	0.141	0.336	0.88
3	1015	N50E	0.29	0.237	0.440	0.158	0.552	0.67
		N40W	0.27	0.275	0.501	0.199	0.702	0.57
		DOWN	0.45	0.079	0.453	0.092	0.265	0.58
4	1016	N50E	0.31	0.053	0.262	0.201	0.151	0.58
		N40W	0.31	0.064	0.257	0.180	0.151	0.64
		DOWN	0.39	0.045	0.380	0.151	0.150	0.62
5	1097	N65W	0.18	0.269	0.546	0.273	0.820	0.45
		S25W	0.32	0.347	0.536	0.301	0.826	0.58
		DOWN	0.15	0.132	0.555	0.182	0.265	0.52
6	1083	N36W	0.23	0.015	0.266	0.278	0.037	0.64
		S54W	0.19	0.012	0.341	0.206	0.028	0.95
		VERT	0.30	0.006	0.221	0.266	0.016	0.61
7	1095	N21E	0.25	0.008	0.071	0.612	0.024	0.78
		S69E	0.26	0.011	0.177	0.683	0.027	0.82
		UP	0.21	0.006	0.160	0.587	0.016	0.58

1382

**INTENTIONALLY BLANK**

## INELASTIC SEISMIC DESIGN CONSIDERATIONS

## FOR OFFSHORE PLATFORMS

by

Damodaran Nair<sup>I</sup>, Jay B. Weidler<sup>I</sup> and Robert A. Hayes<sup>I</sup>

## ABSTRACT

The ability of offshore platforms to withstand extreme earthquakes is examined in terms of the inelastic energy absorption capacity. The important considerations in the design of platforms are shown to be the inelastic behavior of platform elements such as beam-columns and struts, the behavior of the panels and the overall behavior of the platform itself. The intensity of the extreme earthquake which the platform can withstand is estimated by equating the ultimate energy absorption capacity of the platform to the earthquake input energy. The postelastic behavior and the energy absorption capacity of platforms is exemplified by analyzing a typical frame. It is shown that properly designed conventional platforms can absorb substantial amounts of energy by inelastic action. By varying the local characteristics of the platform, it is demonstrated that in addition to the overall energy absorption capacity, the local behavior of the platform must also be examined to arrive at meaningful results.

## INTRODUCTION

Earthquake -resistant design philosophy for offshore platforms is based on the dual design criteria (1,2). Accordingly, a platform is designed to behave elastically under a level of earthquake intensity which has a moderate probability of occurring during the life of the structure, and to behave inelastically when subjected to extreme ground motions. The rationale for the dual design philosophy can be related to the ability of well proportioned structures to absorb substantial amounts of energy by inelastic action.

One obvious method of assessing the survivability of platforms to severe ground motions is to establish the intensity of ground motion associated with the extreme earthquake and then to perform nonlinear time history analysis to determine the response

---

<sup>I</sup> Offshore Structures Department, Brown & Root, Inc.  
Houston, Texas

of the platforms. However such an approach has only limited value when applied to complex structural systems such as offshore platforms. This is because of the difficulties in adequately predicting the characteristics of future earthquakes as well as our inability to accurately model all the relevant aspects of inelastic structural behavior. A less refined but more meaningful method for design applications is currently being used for offshore platforms. The primary objective of this approach is to ensure that the platform has a specified minimum amount of energy absorption capacity beyond the design level which will enable it to withstand a stronger earthquake than the one for which it was designed.

The principal objectives of this paper are twofold: First, the ability of platforms to survive strong ground motions is examined in terms of the inelastic energy absorption capacities of platforms. In particular the salient aspects of the behavior of platform elements such as struts and beam-columns and those of the platform itself are discussed and the ultimate energy absorption capacity of the platform is related to the spectral velocity of the ground motion. Second, inelastic platform behavior is illustrated by analyzing typical two dimensional frames and guidelines are presented for proportioning platforms which will have significant amounts of postelastic energy absorption capacity.

#### IMPORTANT ASPECTS OF INELASTIC BEHAVIOR

Vibratory motion of the ground during an earthquake feeds energy into the platform. Part of the earthquake energy is dissipated through damping in the structure, water and soil and the rest is stored in the structure in the form of kinetic energy of motion of the mass and, for elastic behavior, in the form of strain energy of deformation of platform components. However, if the ground motions are severe enough inelastic action will occur in parts of the structure with the associated plastic energy dissipation. If the structure can absorb sufficient amount of energy through plastic deformation, it is obvious that such a structure can undergo an extreme earthquake without collapse.

It is generally recognized that the energy absorption capacity of a structure is a good index of its survivability to severe ground motions (17-24). This information, when supplemented with the behavior of platform components such as beam-columns and struts as well as the performance of subassemblages of elements called panels, provides a meaningful technique to evaluate the behavior of platforms to earthquakes. The behavior of elements and panels is designated as local behavior and the behavior of the platform itself is called the overall behavior.

## LOCAL BEHAVIOR

The structural elements which make up a platform can be grouped into two main categories: struts and beam-columns. The vertical diagonal braces are mainly subjected to axial forces and their behavior can be modeled by struts. The jacket legs, horizontal braces, deck columns etc. carry both axial load and moment and their behavior is modeled by beam-columns. The above distinction permits one to model the most salient features of each category more accurately.

Inelastic Behavior of Struts - The behavior of structural members under axial tensile loading is well defined (3,4). However their behavior under compressive loading is much more complex. Assuming that the local buckling characteristics of tubular members have been accounted for (5,6), the column buckling loads can be determined as discussed in References 3 and 4. The postbuckling behavior of struts is significant in determining the energy absorption capacity. Both experimental and analytical investigations have been performed recently to define the postbuckling behavior of struts and this information is available in References 7-11.

In the inelastic modeling of struts under tensile loading, the limited axial ductility (about 15-20) should be recognized. The axial member ductility is defined as the ratio of the maximum axial elongation the member can sustain to the maximum elastic deformation. A failure criterion based on energy absorption such as the one presented in Reference 9 provides a meaningful algorithm for determining the limiting capacities of compressive struts.

Inelastic Behavior of Beam-Columns - A fundamental requirement for satisfactory postelastic behavior is that the tubular member should have sufficient rotational capacity before ovalization or local buckling to permit the formation of a plastic hinge. Recent tests with steels having a yield strength of 36 ksi demonstrated that tubes with a  $D/t$  ratio of 36 ( $1300/F_y$ ) or less possess sufficient plastic hinge rotation capacity prior to local buckling and can develop fully plastic moment capacity (9). Tubes with  $D/t$  ratios up to 48 also have considerable ductility - three to ten times the yield deformation. References 12-16 deal with the inelastic behavior of tubular members in bending.

Inelastic Behavior of Panels - The behavior of subassemblages of elements is the next step in the evaluation of the inelastic behavior of the platforms. A panel herein is defined as the portion of the platform between two horizontal braces, including the horizontals. Evaluation of the energy absorption capacity of the panel will ensure that each part of the platform has a specified minimum energy absorption capacity and that there are no weak links in the structure. The importance of recognizing the panel behavior is illustrated in the example presented in a later section.

## OVERALL PLATFORM BEHAVIOR

As mentioned earlier, the total energy absorption capacity of the platform is a good index of the overall inelastic behavior of the platforms due to strong motion earthquakes. An alternate index is the overall ductility ratio. This is defined as the ratio of the maximum useful average lateral deflection of the top level of the platform (deck) to the deflection of the same level under design conditions. The maximum useful lateral deflection for this purpose can be selected based on considerations of platform stability under gravity and buoyancy loads or platform collapse. Platform collapse in turn can be defined based on collapse mechanisms, an estimate of repair damage or from considerations of functional failure.

## RESERVE CAPACITY OF PLATFORMS

An estimate of the reserve capacity of platforms to strong ground motions can be obtained by finding the ultimate energy absorption capacity of the platform. The above process involves two steps: (1) estimating the ultimate energy absorption capacity of the platform; (2) determining the relationship between the energy absorption capacity and the intensity of ground motion it can sustain.

Ultimate Energy Absorption Capacity - Static inelastic analysis has been used in the past to investigate the postelastic behavior of offshore platforms (24,25). A static lateral load pattern is derived based on the design level response spectra and the dynamic characteristics of the platform. Incremental static analysis is performed under increasing amounts of lateral loads and account is taken of the yielding members. This process is continued until the platform collapses. The energy absorption capacity of the platform corresponding to each set of lateral loads can be computed either from external loads and joint displacements or in terms of the energy absorption of each element of the platform. The energy absorption corresponding to the collapse load is called the ultimate energy absorption capacity.

Relation Between Energy Absorption Capacity and Intensity of Ground Motion - Let  $E_d$  represent the energy absorption capacity of a platform corresponding to the design level earthquake.  $E_d$  can be computed by a static analysis using deflections and loads corresponding to the design level earthquake or it can be computed as the combined strain energy due to each of the significant modes of vibration of the structure. A comparison of the energies computed by the above two approaches is given in a later section. Let  $E_u$  be the energy absorption capacity of the platform at collapse as defined in an earlier section.

The maximum energy contained in an elastic single degree of freedom system of mass  $m$  will be (17,18)

$$E = \frac{1}{2} m S_v^2 \quad (1)$$

in which  $S_v$  is the spectral velocity of the applied component of ground motion. For multi degree of freedom systems having a total mass  $M$ ,

the maximum energy transmitted by a component of ground motion can be approximated by

$$E_d = \frac{1}{2} M S_{vd}^2 \quad (2)$$

In Eq. 2,  $S_{vd}$  is the spectral velocity associated with the significant mode and for the design level of ground motion. Eq. 2 assumes that the spectral velocities associated with the various modes are equal. Figure 1 shows the response spectrum recommended in Ref. 1. It can be seen that the spectral velocity is constant in the range of periods of practical importance for offshore platforms (.5-5 seconds). Eq. 2 gives an upperbound estimate of the energy transmitted to the structure by the ground motion.

Let  $S_{vu}$  represent the spectral velocity corresponding to the severe ground motion for the constant velocity spectral region. The minimum energy absorption required of the structure to withstand the extreme earthquake is then given by

$$E_u = \frac{1}{2} M S_{vu}^2 \quad (3)$$

Studies of simple systems reported in References 19-22 shows that Eq. 3 gives a conservative estimate of the energy being transmitted to the structure. A relation between the spectral velocity of the design level earthquake and that for the extreme earthquake which will cause platform collapse can be written as

$$S_{vu} = S_{vd} \sqrt{\frac{E_u}{E_d}} \quad (4)$$

Eq. 4 can be interpreted as follows: A platform designed elastically for the level of ground motion represented by a spectral velocity  $S_{vd}$  and a corresponding energy absorption capacity of  $E_d$ , can undergo without collapse a more intense ground motion represented by the spectral velocity  $S_{vu}$ , if the ultimate energy absorption capacity of the structure is  $E_u$ . Eq. 4 presents a method by which the energy absorption capacities of platform can be used to get an estimate of the severity of ground motion it can undergo.

The above discussion is based on the assumption that the structure is excited by a single component of ground motion. If there is more than one component of excitation involved, the above equations should be modified to account for these effects.

#### EXAMPLE PLATFORM

Structure - The inelastic behavior of offshore platforms is illustrated by analyzing the two dimensional frame shown in Figure 2. This frame represents an exterior bent of an eight-legged platform designed for drilling and production operations in the Santa Barbara Channel. The platform was designed to withstand elastically an intensity of ground motion having an effective peak acceleration of 0.25G and the design spectrum is identified as spectrum B in Figure 1. The fundamental period of the bent under design conditions is 1.5 seconds.

For purposes of nonlinear analysis the jacket legs and horizontals were modeled as beam-columns whereas the diagonal braces were modeled as struts. The behavior of the struts is idealized as shown in Figure 3(a) and the moment-axial force interaction diagram for the tubular beam columns is shown in Figure 3(b). The yield strength of the steel is 36 ksi and the member sizes are as shown in Figure 2.

Method of Analysis - The inelastic behavior of the bent was investigated by performing an incremental static analysis of the platform under a prescribed distribution of lateral loads in combination with the gravity and buoyancy loads. The lateral force distribution was derived by performing a response spectrum analysis of the platform using spectrum B in Figure 1. The RMS lateral force distributions are shown by solid lines in Figure 2. The magnitude of the above set of forces was increased to initiate inelastic action in the various platform elements. The analysis was continued until small increase in lateral loads produced a significant amount of lateral deflection.

#### PRESENTATION AND DISCUSSION OF RESULTS

The average lateral deflection of elevation +71 versus the base shear (defined as the sum of lateral forces) is shown plotted in Figure 4(a). The deflected shape of the structure for selected loading stages is also shown plotted in Figure 4(b). The following inelastic events are identified. Point A in Figure 4(a) denotes the design level condition. Point B denotes the onset of the first inelastic event in which the brace member 4 reaches its buckling capacity and starts losing its strength, according to the pattern shown in Figure 3(a). The lateral loads were decreased to the level shown by point C in order to offset the decreasing capacity of member 4. The drop in lateral load is explained by the fact that the increase in axial tension of member 5 is more than offset by the drop in the compressive load of member 4. An analysis procedure that accounts for the local stiffness changes in the platform due to inelastic events and the consequent redistribution of lateral loads may not exhibit a drop in the lateral load. After the compression member reaches point 3 shown in Figure 3(a), the lateral loads are again increased. Point D in Figure 4(b) corresponds to the stage when member 5 reaches its yield capacity. Further increases in lateral loads cause compression member 9 to buckle and the behavior follows the same pattern as explained for the top panel. After the failure of braces in the top two panels, small increase in lateral loads caused excessive deflections in the structure and the analysis was stopped.

Typical deflection patterns are shown plotted in Figure 4(b). The energy absorption of the bent was calculated for each of the loading stages and is shown plotted in Figure 4(a). It may be noted that the ultimate energy absorption capacity,  $E_u$ , of the platform in the present case is 7.5 times as much as the energy corresponding to the design level earthquake. Using Eq. 4, it is predicted that the platform has enough reserve capacity to withstand, without collapse, a ground motion 2.7 times the design intensity of ground motion.



The energy absorption capacity of the platform corresponding to the design level earthquake was computed by using the static load pattern shown in Figure 2. An alternate approach is to compute the strain energy associated with each of the significant modes of response and then to combine the energies by the root mean square rule. This resulted in a design level energy which is only 51% of the energy computed by the previous method. This further increases the ratio of the energy absorption capacity of the platform at design level to its capacity at collapse.

Change in Loading Pattern - It is the usual practice (24,25) to derive the lateral load pattern based on the elastic stiffness of the structure and to maintain the same pattern throughout the analysis. With changing stiffness of the structure, the load distribution also changes. This effect is investigated by computing the lateral force distribution corresponding to stage D of the inelastic events. This distribution is shown by dashed lines in Figure 2. The elastic natural period of the platform at this stage is 2 seconds. It may be noted that there are substantial changes in the lateral force distributions when major inelastic events occur.

Another assumption made in the above analysis was that the horizontal braces remain elastic. This restriction was removed and a new series of analyses were performed in which member 3 formed plastic hinges at both ends. There were no major changes in the base shear versus deflection diagram.

#### PLATFORM WITH "SOFT" BOTTOM PANEL

The inelastic behavior of the platform studied in the earlier sections was re-examined after introducing the following modifications. The top panel was strengthened by increasing the wall thickness of the diagonals from 3/8" to 1/2". The bottom panel was softened by decreasing the size of the diagonal braces from 22"  $\emptyset$  x 5/8" wall thickness to 20"  $\emptyset$  to 1/2" wall thickness. The base shear vs deck deflection for the revised frame is shown in Figure 5(a) and in Figure 5(b) are shown the deflection configurations of the platform at selected stages of loading. The energy absorption capacity of the modified frame is also shown in Figure 5(a). In this frame the inelastic action started in the diagonal braces of the bottom panel and propagated upwards to the panel above that. By softening the bottom panel and initiating the inelastic action in the bottom panel, the energy absorption capacity of the platform is almost doubled. The increased energy absorption capacity of the bottom story has been recognized in the design of buildings for some time (26). Ref. 26 presents a detailed investigation of this concept and points to the several disadvantages of having a weak link in the bottom part of the structure.

It is obvious that from considerations of the overall energy absorption capacity, the second frame with a soft bottom panel is attractive. However, unless the inclusion of such a weak link is intentional,

it should be avoided in usual design practice. It should be mentioned that in the above analysis the pattern of lateral loads was kept the same as for elastic level. It is expected that inelastic action in the bottom panel would produce substantial changes to the above pattern and should be considered in the evaluation of the energy absorption capacity. Furthermore in order to provide a complete description of the energy absorption capacities of platforms, evaluation of the capacity of the panels is also needed. Such panel behavior will point out the presence of weak links in the structure.

Offshore platforms are usually designed by equally important considerations other than earthquake such as storm loadings, installation requirements, etc. As such there are situations in which certain panels are relatively weak compared to others which are designed by, say, an installation consideration. The examination of the panel behavior provides the designer an opportunity to build uniform reserve capacities into various platform elements.

#### CONCLUSIONS

1. A method is presented to evaluate the inelastic energy absorption capacities of platforms and to relate this information to the intensity of ground motion the platform can undergo.
2. Conventional platforms of the template type have excellent inelastic energy absorption capacity to survive extreme earthquakes without collapse.
3. A procedure which consists of determining the overall inelastic energy absorption capacity of the platform and the inelastic behavior of the individual panels provides a means by which the ability of platforms to undergo extreme earthquakes can be evaluated.
4. Based on the present study as well as others yet unreported, it seems that the reserve capacity of platforms to withstand extreme earthquakes can be greatly increased by proper sizing of members and panels. Furthermore, a design strategy which leads to desirable postelastic behavior is to limit the inelastic action to the diagonal braces alone and to keep the jacket legs and deck columns elastic.

## REFERENCES

1. American Petroleum Institute, Recommended Practice for Planning, Designing, and Constructing Fixed Offshore Platforms (API RP 2A), Ninth Edition, November 1977.
2. Nair, V.V.D., "Aseismic Design of Offshore Platforms," Proceedings of the ASCE Geotechnical Engineering Division Specialty Conference Earthquake Engineering and Soil Dynamics, Vol. II, pp. 660-684, June 19-21, 1978, Pasadena, California,
3. Sherman, D.R., "Tentative Criteria for Structural Applications of Steel Tubing and Piping," American Iron and Steel Institute, SP 604-876-7-5-M-MP, 1976.
4. Structural Stability Research Council, Guide to Stability Design Criteria for Metal Structures, Edited by Johnston, B.G., John Wiley & Sons, 1976, pp. 261-329.
5. Bouwkamp, J.G., "Buckling and Post-Buckling Strength of Circular Tubular Sections," Offshore Technology Conference, Paper No. OTC 2204, 1975, pp. 583-591.
6. Miller, C.D., "Buckling of Axially Compressed Cylinders," Journal of the Structural Div., ASCE, Vol. 103, March 1977, pp. 695-721.
7. Higginbotham, A.B., and Hanson, R.D., "Axial Hysteretic Behavior of Steel Members," Journal of the Structural Division, ASCE, Vol. 102, No. ST7, 1976, pp. 1365-1381.
8. Kahn, L.F., and Haonson, R.D., "Inelastic Cycles of Axially Loaded Steel Members," Journal of the Structural Division, ASCE, Vol. 102, No. ST5, 1976, pp. 947-959.
9. Marshall, P.W., et. al., "Inelastic Dynamic Analysis of Tubular Offshore Structures," Offshore Technology Conference, Paper No. OTC 2908, 1977, pp. 235-246.
10. Prathuangsit, D., et. al., "Axial Hysteretic Behavior with End Restraints," Journal of the Structural Division, ASCE, Vol. 104, June 1978, pp. 883-896.
11. Jain, A.K., et. al., "Inelastic Response of Restrained Steel Tubes," *ibid*, pp. 897-910.
12. Chen, W.R., and Ross, D.A., "Behavior of Fabricated Tubular Columns under Biaxial Bending," ASCE National Water Resources and Ocean Engineering Conv., San Diego, Calif. Reprint 2659, April 1976.
13. Ross, D.A., and Chen, W.R., "Tests of Fabricated Tubular Columns," ASCE National Water Resources and Ocean Engineering Convention, San Diego, Calif. April 1976, Reprint 2736.

14. Sherman, D.R., "Tests of Circular Steel Tubes in Bending," *Journal of the Structural Division, ASCE*, Vol. 102, No. ST11, 1976, pp. 2181-2195.
15. Wagner, A.L., et. al., "Ultimate Strength of Beam-Columns," *Journal of the Structural Division, ASCE*, Vol. 103, No. ST11, 1977, pp. 9-24.
16. Popov, E.P., and Bertero, V.V., "Cyclic Loading of Steel Beams and Connections," *Journal of the Structural Division, ASCE*, Vol. 99, June 1973, pp. 1189-1204.
17. Housner, G.W., "Limit Design of Structures to Resist Earthquakes," *Proceedings of the First World Conference on Earthquake Engineering, San Francisco, 1956.*
18. Housner, G.W., "The Plastic Failure of Frames During Earthquakes," *Proceedings of the Second World Conference on Earthquake Engineering, Tokyo, Japan, 1960.*
19. Berg, G.V., and Thomaides, S.S., "Energy Consumption by Structures in Strong-Motion Earthquakes," *Proceedings of the Second World Conference on Earthquake Engineering, Tokyo, Japan, 1960.*
20. Goel, S.C., and Berg, G.V., "Inelastic Earthquake Response of Tall Steel Frames," *Journal of the Structural Div., ASCE*, Vol. 94, August 1968, pp. 1907-1934.
21. Sun, C.K., et. al., "Gravity Effect on Single-Degree Inelastic System," *Journal of the Engineering Mechanics Division, ASCE*, Vol. 99, Feb. 1973, pp. 183-200.
22. Bazan, E., and Rosenblueth, E., "Seismic Response of One Story X-Braced Frames," *Journal of the Structural Division, Vol. 100, Feb. 1974, pp. 489-493.*
23. Blume, J.A., "A Reserve Energy Technique for the Earthquake Design and Rating of Structures in the Inelastic Range," *Proceedings of the Second World Conference on Earthquake Engineering Tokyo, Japan, 1960.*
24. Gates, W.E., et. al., "Analytical Methods for Determining the Ultimate Earthquake Resistance of Fixed Offshore Structures," *OTC Paper No. 2751, Offshore Technology Conference, Houston, Texas, 1977.*
25. Kallaby, J., and Millman, D.N., "Inelastic Analysis of Fixed Offshore Platforms for Earthquake Loading," *Paper No. OTC 2357, Offshore Technology Conference, 1975, pp. 215-226.*
26. Chopra, A.K., et.al., "Earthquake Resistance of Buildings with a Soft First Story," *International Journal of Earthquake Engineering and Structural Dynamics, Vol. 1, 1973, pp. 347-355.*

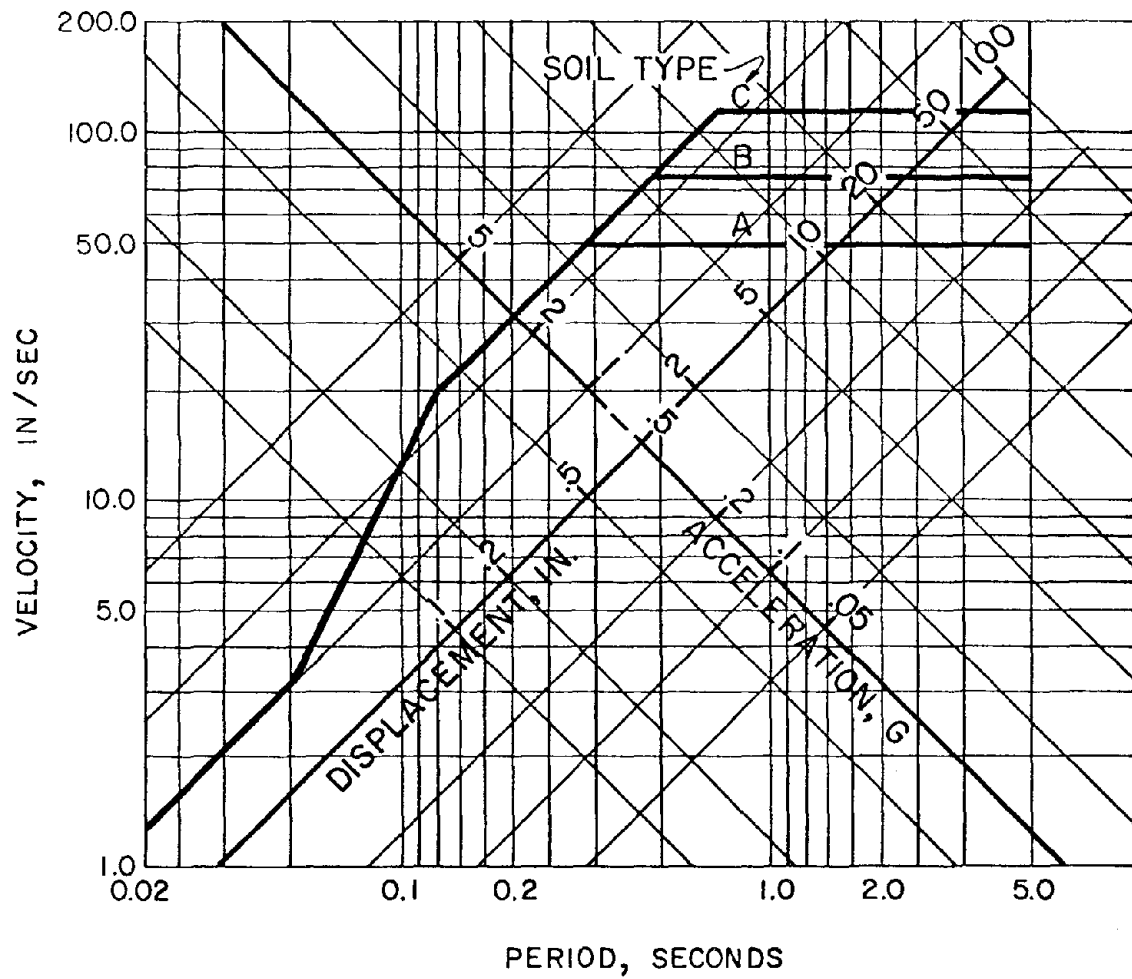


FIGURE 1 - RESPONSE SPECTRA NORMALIZED TO 1.0 G

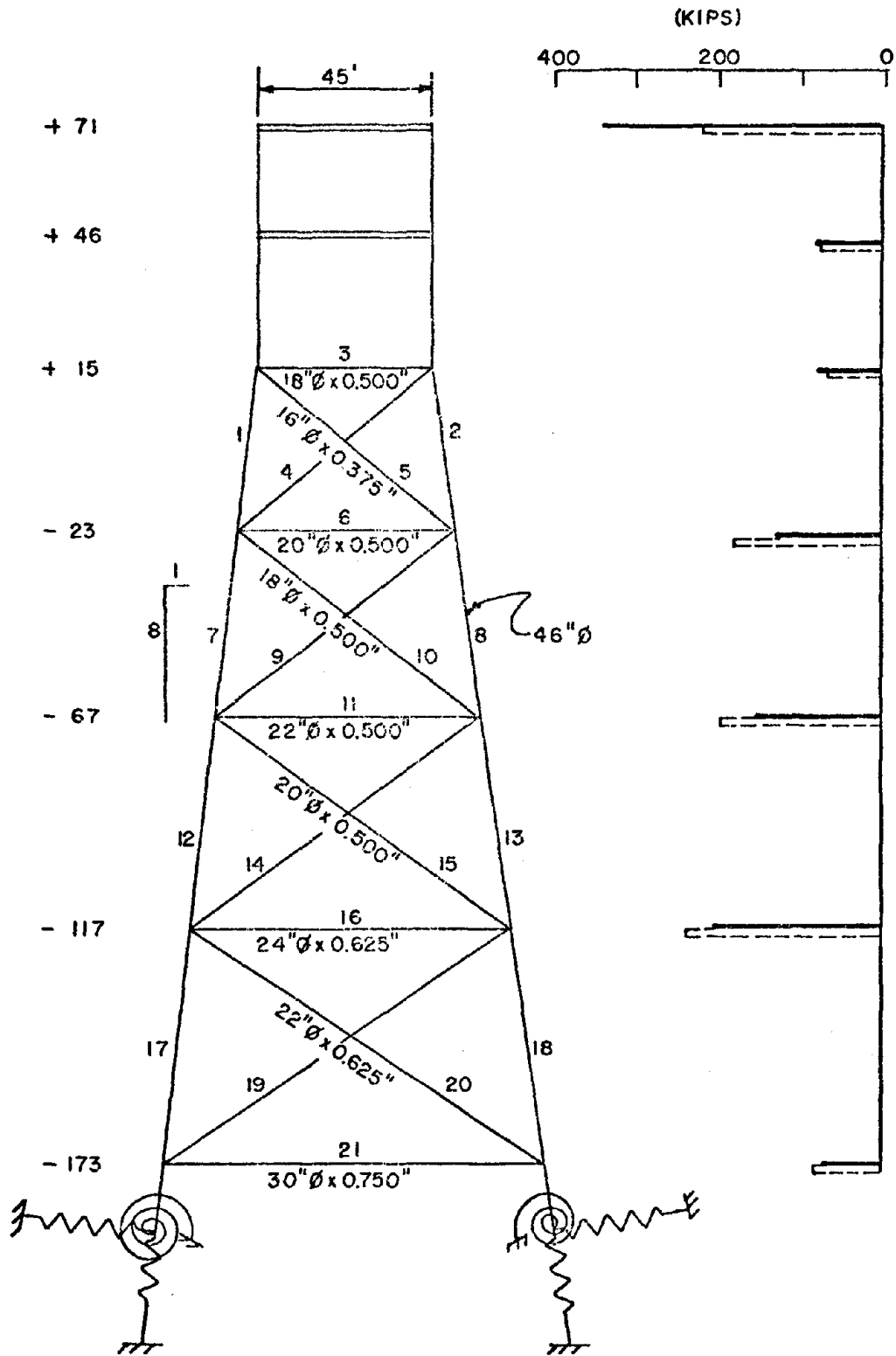
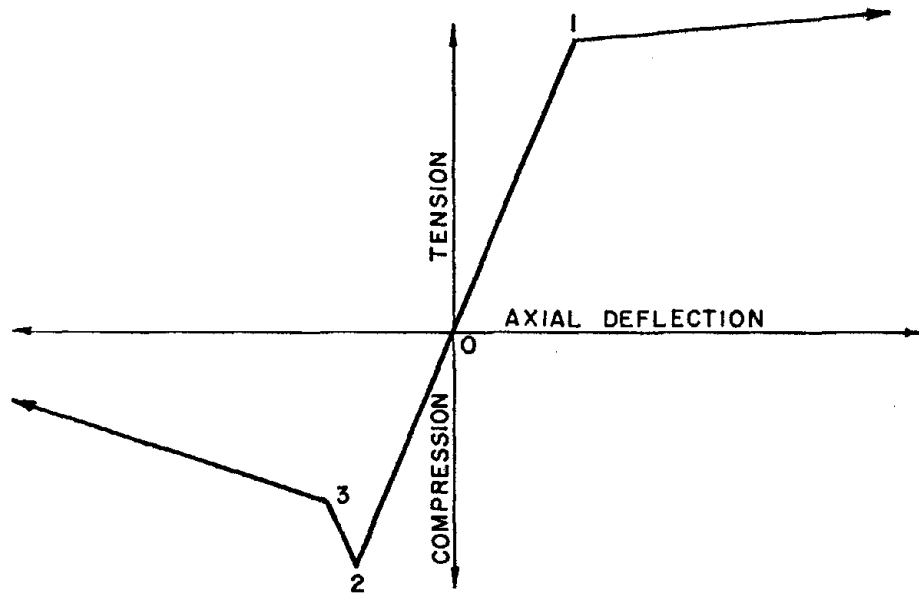
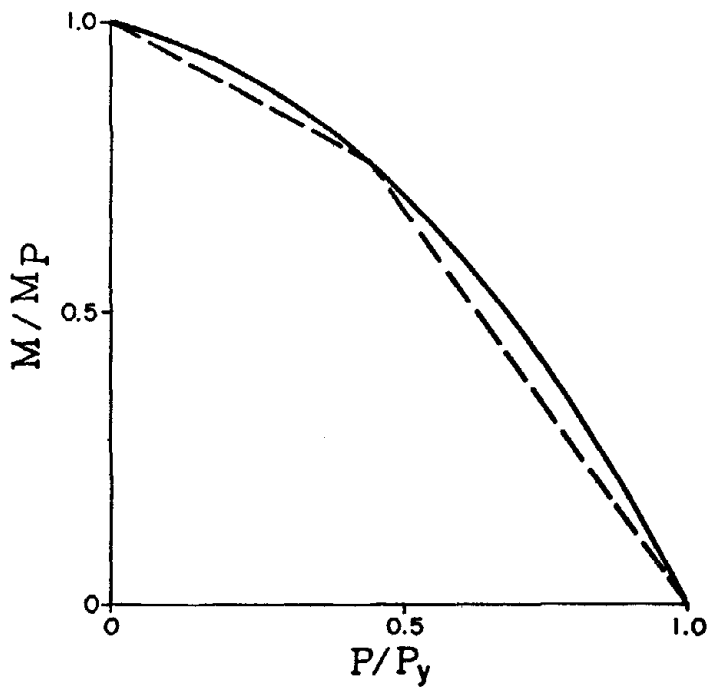


FIGURE 2 - EXAMPLE PLATFORM

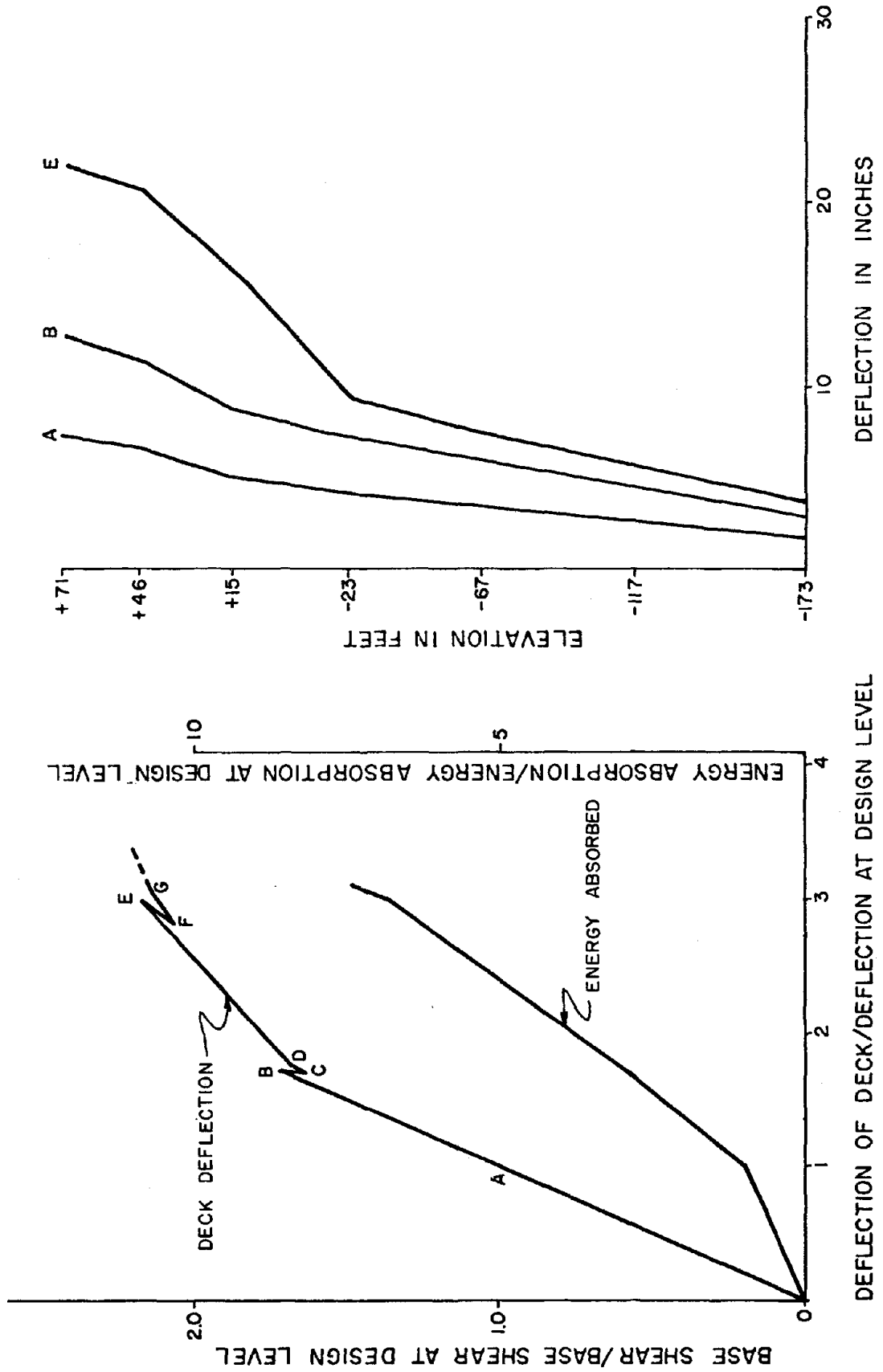


(a) BEHAVIOR OF STRUTS



(b) BEHAVIOR OF BEAM-COLUMNS

FIGURE 3



DEFLECTION OF DECK/DEFLECTION AT DESIGN LEVEL

FIGURE 4



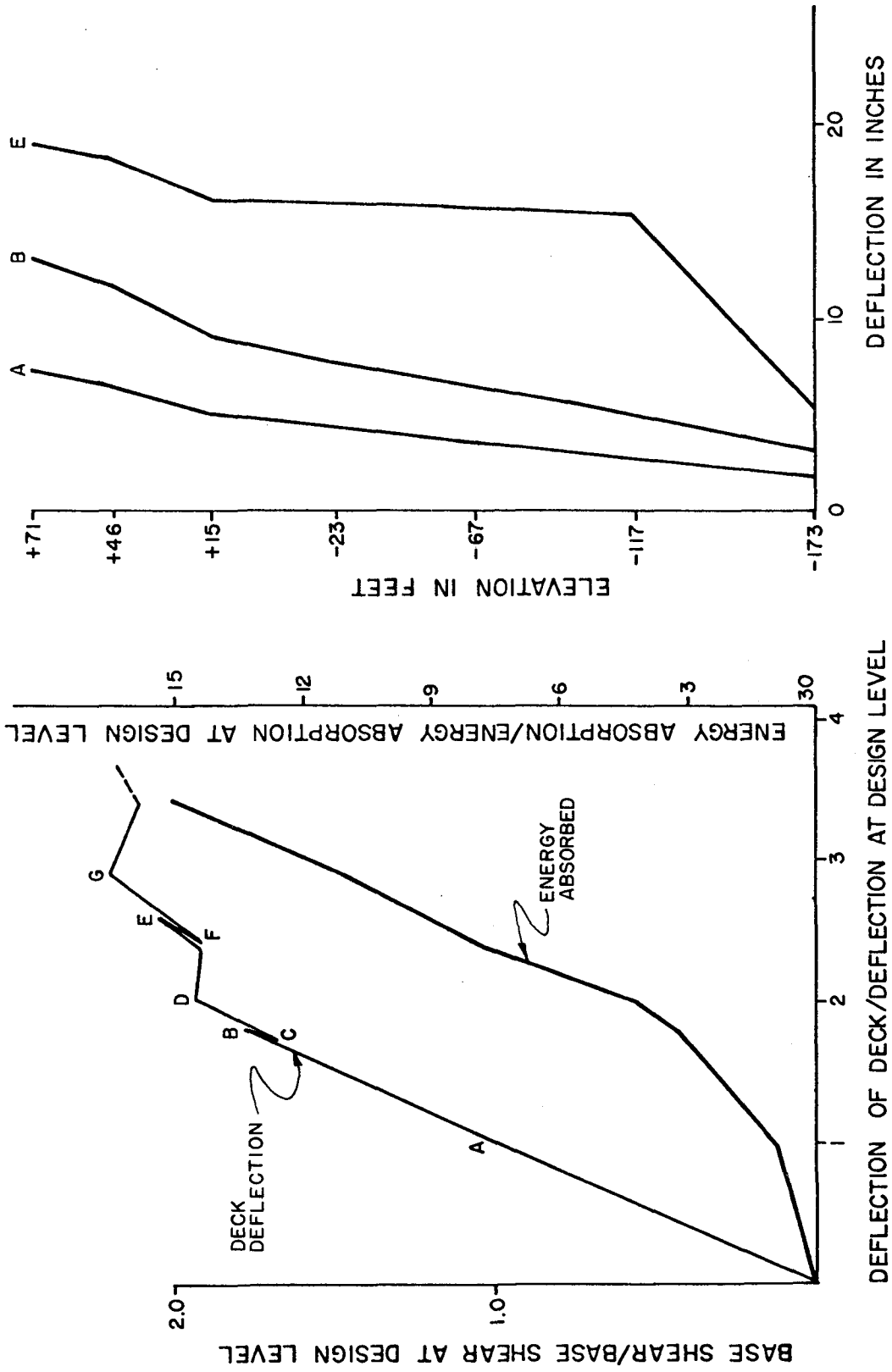


FIGURE 5

1398

**INTENTIONALLY BLANK**

THE INFLUENCE OF MICROZONATION ON THE RELIABILITY-BASED  
DESIGN OF OFFSHORE STRUCTURES

by

H. Kappler<sup>I</sup> and G.I. Schuëller<sup>II</sup>

ABSTRACT

In this paper a reliability concept is proposed, in which the microzoning effect is introduced as a corrective factor to the probability distribution of the earthquake load intensity. The frequency of earthquake occurrence for particular sites under investigation is modeled by a Poisson process. In a numerical example the concept is applied to a fixed (template) offshore platform located in a seismic active area and in a water depth of 100 m (300 ft), a depth in which usually the governing design load type - either waves or earthquake - cannot be distinguished easily beforehand. It is shown that in areas where, according to the seismic mapping, the wave load is expected to be the governing design load, due to the microzoning effect, the earthquake load can yield lower reliability values.

INTRODUCTION

The determination of regional seismicity for both onshore and offshore areas has received increasing attention in the past. These studies generally result in seismic probability maps, showing contours of intensities which correspond to a given return period, say 100 years etc.. It is a fact that the models leading up to these maps imply intensity attenuation relations which are valid for firm ground. However, additional factors, such as local soil conditions (soil stratigraphy), topographic irregularities (hill or slope formations) and local geological formations may also influence the intensity distribution and the frequency content of earthquakes. For the latter effect - which is generally called microzonation or microregionalization - may be accounted for by locally transforming the intensities of a map of regional seismicity. Although there are a number of objections to this rather simplified method to be raised (1), due to its clarity in application it is nevertheless employed widely by practising structural engineers.

---

I Research Associate of Civil Engineering, Technische Universität München, Munich, Germany

II Lecturer of Civil Engineering, Technische Universität München, Munich, Germany

It should be mentioned at this point that the actual structural risk has to be determined by combining the likelihood of the seismic activity, i.e. its frequency of occurrence and intensity, and the uncertainty inherent in the response and the material properties of the structure. As the characteristics of occurrence of natural events such as earthquakes is random in nature, their likelihood of occurrence may be determined by utilizing stochastic processes. For calculating the structural response, given an earthquake of a particular intensity distribution, response spectral, random vibrational and/or time history methods may be applied. The theory of structural reliability is to be applied for taking into account the statistical scatter of material properties such as yield limit etc..

In addition to the earthquake threat, offshore structures are also subjected to storm generated waves, which particularly in the North Sea and in the Gulfs of Mexico and Alaska have proven to be very severe. A proper structural design procedure of offshore structures - such as for example fixed production platforms - has to include the risk analysis due to both natural hazards. Depending on the respective conditions, either the earthquake loading or the wave loading may be the governing design parameter. It is shown in this paper that for certain conditions where - according to wave height and regional seismicity maps - the wave loading proves to be the governing design parameter, due to the influence of microzoning effect, i.e. the transformation of the earthquake intensity for a particular potential construction site under consideration, the earthquake loading leads to larger structural failure probabilities, i.e. higher risks.

#### THE RELIABILITY CONCEPT

As it was already mentioned in the previous section, that due to the random characteristics of natural hazards - such as severe storms and earthquake - an economical and safe design of offshore structures requires the utilization of probabilistic methods. Furthermore, the statistical properties of the construction materials used have also to be incorporated in the analysis, particularly in areas where data is scarce. This can be accomplished by applying Bayesian methods as shown in (1,2,3). An alternative approach which is followed here is using classical reliability theory (4,5) which makes use of objective statistical estimates. In this context it should be pointed out that, provided sufficient data is available, the Bayesian updating procedure does yield the same answers as the classical statistical approach.

For both storm and the earthquake hazards, identical reliability procedures may be used. Hence in the following, the development of the analysis in general terms deals with the occurrence of particular events representing the occurrence of these hazards. For forecast purposes the occurrence of these events may be modeled by stochastic processes. It is reported that, for natural hazards with high load intensities as a consequence, the Poisson process is an appropriate model. Statistical evidence

also seem to support this assumption (7,8). The probability of occurrence of  $n$  events within a particular time range  $[0,t]$  can therefore be expressed as

$$p(n|v,t) = \frac{(vt)^n e^{-vt}}{n!} \quad (1)$$

In the above equation is  $v$  the mean rate of event occurrence and can be statistically estimated by using historical data. An event may be defined as a storm and/or earthquake occurrence exceeding a certain lower bound threshold. In other words, a load event which is likely to cause damage to the structure.

After having decided on a model to predict events on a long-term basis, one has to determine the probability distribution of the loads caused by these events, i.e. the conditional load distributions. These distributions may be obtained by fitting theoretical distributions to observed data. Physical and statistical arguments permit the desired extrapolation beyond the data range.

Finally the statistical information of the material properties has to be introduced in the model. Again, similar arguments as in the load case have to be used to accept a particular theoretical distribution, which permits probability statements within ranges in which no data have been observed. This is an extremely important aspect, for generally structures are to be designed for loads greater and strengths smaller than those which have been observed in the past. The failure probability of a structure conditioned on a particular event type is visualized in Fig. 1 below.

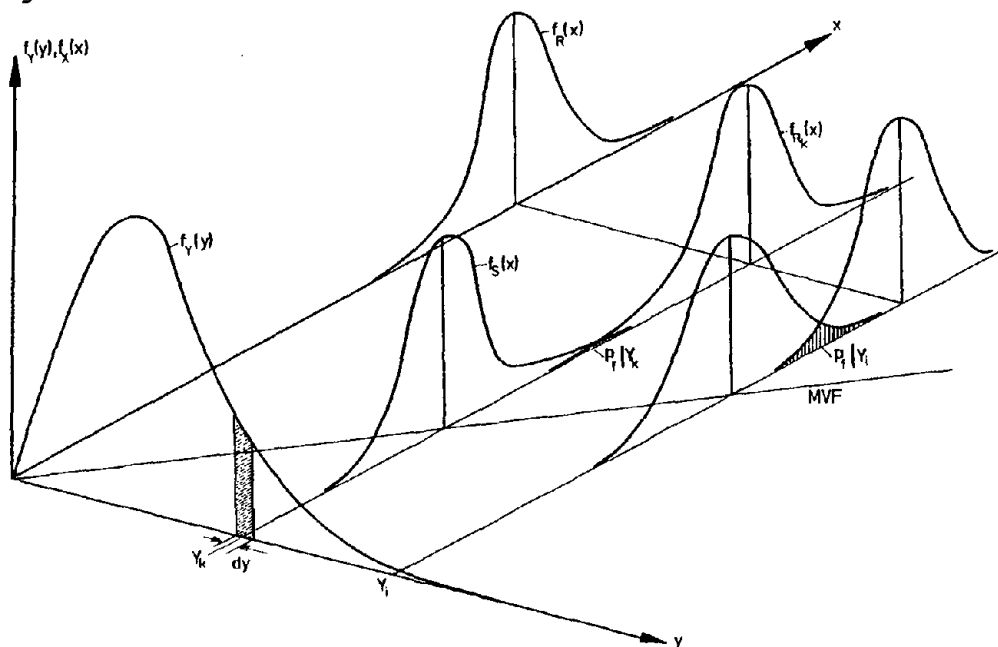


Fig. 1 - Schematic sketch of conditional structural failure probability

In the figure above  $f_Y(y)$  represents the distribution of the load intensity, given the event;  $f_S(x)$  accounts for the uncertainties which arise when calculating the force distributions, given  $f_Y(y)$ ;  $f_R(x)$  stands for the probability distribution of the structural resistance. The conditional failure probability for each  $Y_K$  dy results from the convolution of  $f_S(x)$  and  $f_R(x)$ , i.e.

$$p_f|Y_K = \int_0^{\infty} F_{R_K}(x) \cdot f_{S_K}(x) dx \quad (2)$$

The probability of survival of the structure, given the load intensity  $Y_K$  is then

$$L|Y_K = 1 - p_f|Y_K \quad (3)$$

Integrating over all possible conditional load intensities which may occur during the event E results in the following expression

$$L|E = \int_0^{\infty} L|Y_K \cdot f_{Y_K}(y) dy \quad (4)$$

which is a conditional probability. Assuming statistical independence between the probability of the event occurrence and its effect, which is expressed in equ.(4) one obtains for the probability of survival within a particular period  $[0, t]$

$$L_T(t) = \sum_{\text{all } n} (L|E) \cdot p(n|\nu, t) \quad (5)$$

inserting for the Poisson assumption the occurrence probability of the event (i.e. equ. (1)), this yields (9)

$$L_T(t) = \sum_{n=0}^{\infty} \frac{(\nu t)^n e^{-\nu t}}{n!} \left[ \int_0^{\infty} L|Y_K \cdot f_{Y_K}(y) dy \right]^n \quad (6)$$

Recall that  $\nu$  is the mean rate of occurrence of the event E.

#### THE CHOICE OF DESIGN CRITERIA

Depending on various factors, i.e. structural system, the environmental conditions, the water depth etc., either the earthquake or the storm wave loading may generate the design governing parameters. There is also the possibility of the combination of both, an event, which has been recognized as less severe by

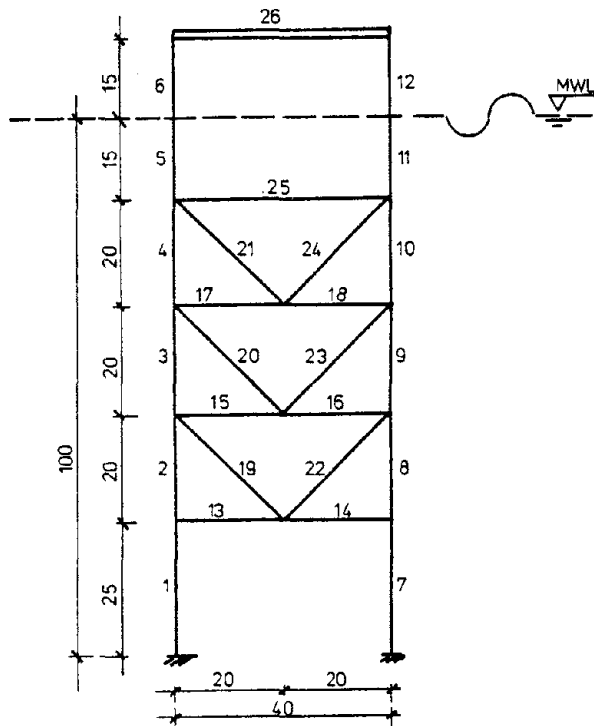
other investigators (10). It will therefore be neglected.

With respect to the *storm* wave design criteria one first has to calculate from historical records the mean rate of occurrence of detrimental storms in the given area for which the structure is to be designed for. Following this investigation, the estimated wave height distributions for given storm conditions have to be determined. For this, the Rayleigh or the Fisher Tippett type I or III distributions are used. Note that the wave height distribution corresponds to  $f_Y(y)$  of Fig. 1. The load distribution  $f_S(x)$  expresses the uncertainties inherent in the wave force calculations, i.e. the statistical scatter of the wave forces given a wave with particular characteristics (11,12). For this type of distribution the log-normal fits best to actual wave force data. From this it becomes clear that each wave causes a particular threat to the structure. The relative importance of each wave in this respect is scaled by its probability of occurrence. One, of course, has to consider all possible waves contained in the storm generated sea state (see equ.(6)).

The frequency of occurrence of the *earthquake* loading may also be modeled by a Poisson process (7). The distribution of the maximum intensities ( $f_Y(y)$ ) may be modeled by a Gumbel (Fisher Tippett type I) distribution(2). The distribution of the structural response,  $f_S(x)$ , may be determined by using time- or frequency-oriented methods. Utilizing the time history method one either has to apply simulation procedures to produce sufficient sample records, or one has to introduce severe assumptions, such as stationarity and ergodicity in order to be able to make statistical statements about the response. Applying the power spectral method the assumption about the normal (Gaussian) property of the input has to be made for a statistical interpretation of the response, the latter being also normally distributed under the assumption of linear structural behavior. Again, each earthquake with a particular "maximum" intensity causes a particular hazard to the structures. An integration over the probability distribution over all possible intensities (equ.(6)) yields the failure - or if so desired - survival probability with reference to the design life.

#### NUMERICAL EXAMPLE

The procedure suggested in the previous section will now be exemplified by carrying out a numerical example. For this purpose a template platform located in a water depth of 100 m as schematically sketched in Fig. 2 is used. The typical member sizes are listed in Table 1. Structural steel St52 is utilized. The coefficient of variation of the yield limit is assumed to be 0.08. The lognormal as well as the Weibull distribution are appropriate modelling distributions.



Member No.	Type	Outer $\phi$ [m]	Wall thickness t [m]
1÷12,26	84" $\phi$ 4.0	2.134	0.1016
13,14	42" $\phi$ 3.0	1.067	0.0762
15÷25	30" $\phi$ 1.2	0.762	0.0305

Table 1: Member sizes of sample structure as shown in Fig. 2

The structure is assumed to be located in the northern part of the Gulf of Alaska. For the purpose of pointing out the influence of microzonation, two different sites are investigated, i.e. Kayak Island and Pamplona sites respectively. For both sites a water depth of 100m is assumed. Their

Fig. 2: Schematic sketch of template platform as used in the numerical example

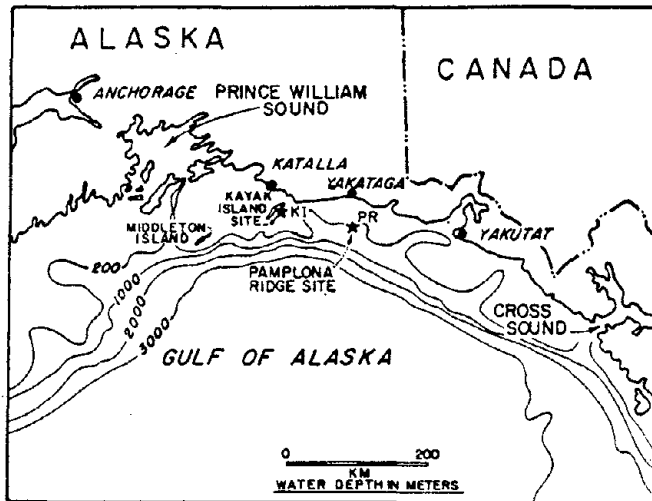


Fig. 3: Geographic location of sites under investigation, after (13)

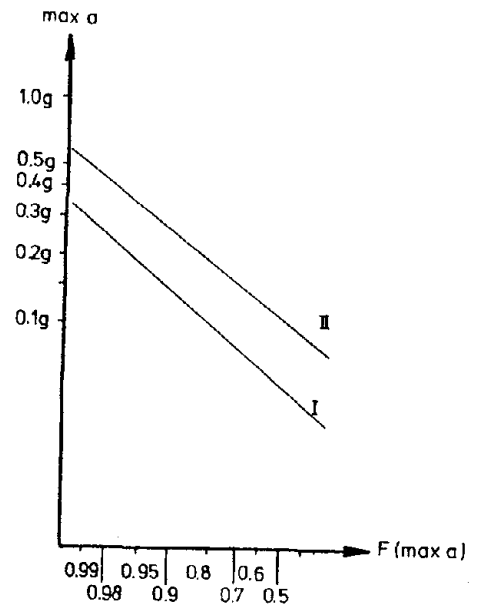


Fig. 4: Distribution of seismic activities for sites (I.Kayak Island, II.Pamplona Ridge;after Bea (13)).



expected seismic activities, as reported previously by Bea (13), are shown in Fig. 4. The intensity distribution in terms of maximum accelerations,  $\max a$ , reveal a Gumbel (Fisher Tippett type I) distribution (see Fig. 4). The ratio of their modal values, however, is 2.2. This aspect will be discussed later on.

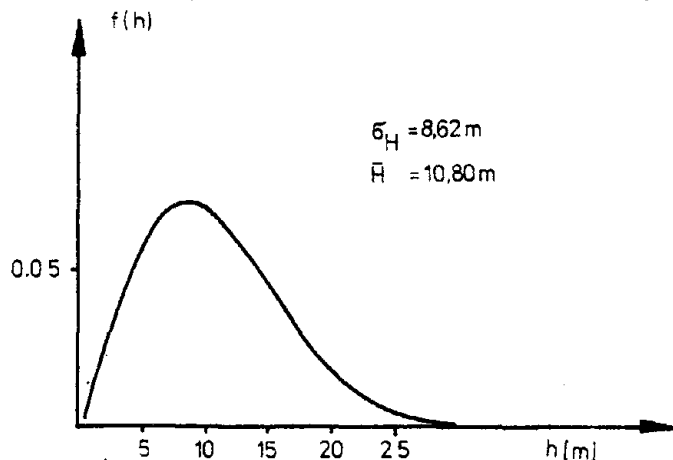


Fig. 5: Wave conditions to be expected during severe storm deduced from information reported in ref. (13).

The mean rate of occurrence of earthquakes with a magnitude larger than 3.5 is reported to be  $\nu=0.43$  per year for the entire region (13). The storm wave conditions represented by the Rayleigh distribution - as shown in Fig. 5 - has also been deduced from the information reported in ref. (13). Particular long-term storm records are not available for the sites. However, a storm occurrence mean rate of 0.2 per year seems to be reasonable to assume. The load analysis of the platform is based on Stokes' 5th order wave theory and drag and mass coefficient are chosen to be 0.6 and 1.2 respectively.

A coefficient of variation of wave loading of 0.3 is used. A respective value of 0.08 has been utilized for the structural resistance. Both variables have been modelled by lognormal distributions. It should be noted that an efficient method for choosing member sizes of platforms on the basis of platform risk has been suggested by Choi and Kappler (14). If, for example, the platform has to be designed for a life of 25 years, the risk of failure  $F_T(t)$  for this period of time is calculated to be  $3 \cdot 10^{-3}$ . Note that  $F_T(t) = 1 - L_T(t)$ . The latter expression is to be determined by evaluating equ. (6). The failure probability refers to the jacket failure. Furthermore it is based on the "weakest link" assumption

The corresponding earthquake analysis reveals failure rates of  $2.2 \cdot 10^{-3}$  and  $1.4 \cdot 10^{-2}$  for the Kayak Island and Pamplona Ridge site respectively. The dynamic analysis has been carried out by scaling the El Centro earthquake record. The first three structural frequencies are 0.81, 1.6 and 3.85 Hz. It is interesting to note that a design wave of  $H=25$  m and an horizontal acceleration of 0.4 g yield similar conditional failure probabilities,  $p_f$ .

## CONCLUSIONS

The analysis as carried out in the previous section reveals quite an interesting aspect with respect to the influence of microzoning effects on the design. For both sites - Kayak

Island and Pamplona Ridge - a regional seismicity information in terms of seismic maps would provide identical seismic design information. If the structure would be designed for the Kayak Island site the storm wave and the earthquake hazard would yield almost the same failure rates. In other words, no particular choice can be made about which type of hazard is governing the design. However, there is a considerable difference in the result if the platform has to be erected in the vicinity of the Pamplona site. For the latter site, the expected failure rate increases by more than one order of magnitude. For this site the earthquake loading is clearly the design governing parameter. Needless to say that for each hazard mostly different members are the main contributors to the ultimate failure rate. For example, for the storm wave hazard, member numbers 1,7,19,20 seem to be most critical. For the earthquake loading mainly member numbers 1 and 7 contribute to the conditional failure probability. Although no attempt is made here to investigate the physical reasons of the microzoning effect, i.e. the local geological formations, topographic irregularities or local soil conditions, its effect on the resulting structural reliabilities underlines the importance of developing such procedures for cases, where insufficient data - in terms of ground movement - is available. A comparison of the distribution of the ground accelerations for the two sites reveals that the microzonation effect might be included by using a corrective factor. This factor may be expressed as the ratio of the modal values of the acceleration distributions.

#### ACKNOWLEDGEMENT

This research is partially supported by the Deutsche Forschungsgemeinschaft which is gratefully acknowledged by the authors.

#### BIBLIOGRAPHY

- (1) NEWMARK, N.M. and E. ROSENBLUETH: "Fundamentals of Earthquake Engineering", Prentice Hall, Inc., Englewood Cliffs, N.Y., 1971.
- (2) ESTEVA, L.: "Seismicity", in "Seismic Risk and Engineering Decisions", Ed.: C. Lomnitz and E. Rosenblueth, Elsevier Publ. Camp., N.Y., 1976, pp 179-224.
- (3) WHITMAN, R.V. and C.A. CORNELL: "Design", in "Seismic Risk and Engineering Decisions", Ed.: C. Lomnitz and E. Rosenblueth, Elsevier Publ. Co., N.Y., 1976, pp 339-380.
- (4) FREUDENTHAL, A.M.: "Safety and the Probability of Structural Failure", Transactions, ASCE, Vol. 121, Proc. Paper 2843, 1956, pp 1337-1397.

- (5) FREUDENTHAL, A.M., J.M. GARRELTS and M. SHINOZUKA: "The Analysis of Structural Safety", J.Struct.Div., Proc. ASCE, Vol. 92, No. ST1, Feb., 1966, 267-325.
- (6) SCHUËLLER, G.I. and R.F. SCHWARZ: "Some Aspects of the Reliability-Based Design of Reactor Containment Structures", Journ.Nucl.Engr.Des., Vol.37, No. 2, May, 1976, pp 299-305.
- (7) BENJAMIN, J.R.: "Probabilistic Models for Seismic Force Design", J.Struct.Div., ASCE, Vol. 94, No. ST5, Paper 5950, 1968.
- (8) RUSSELL, L.R. and G.I. SCHUËLLER, "Probabilistic Models for Texas Gulf Coast Hurricane Occurrences", Prepr.Offshore Techn.Conf., Vol.I, p.177-190, Houston 1971, also in: J. Petroleum Techn., March, 1974, p.279-288.
- (9) SCHUËLLER, G.I. and H.S. CHOI: "Offshore Platform Risk Based on a Reliability Function Model", Proc. Offshore Tech. Conf., pp 473-479, Houston, May, 1977.
- (10) YANG, J.N. and A.M. FREUDENTHAL: "Reliability Assessment of Offshore Platforms in Seismic Regions", Proc., 2nd Int. Conference Struct.Safety Rel., (ICOSSAR'77), Ed.:H. Kupfer, M. Shinozuka and G.I. Schuëller, Werner Verlag, Düsseldorf, Germany, 1977, pp 247-266.
- (11) SCHUËLLER, G.I. and H.C. SHAH: "A Probabilistic Approach to Determine Wave Forces on Ocean Pile Structures", Proc. 13th Coast.Engr.Conf., Vol. III, pp 1683-1701, Vancouver B.C., Canada, 1972.
- (12) KIM, Y.Y. and H.C. HIBBARD: "Analysis of Simultaneous Wave Force and Water-Particle Velocity Measurements", Offshore Tech. Conf., Paper No. 2192, Houston, May 1975.
- (13) BEA, R.G.: "Earthquake Criteria for Platforms in the Gulf of Alaska", Proc., Offsh.Tech.Conf., Paper No. 2675, Houston, May, 1976.
- (14) CHOI, H.S. and H. KAPPLER: "An Application of Reliability Function Model to Estimate Offshore Platform Risk at an Early Stage of Design", Proc., Offshore Tech.Conf., Paper No. 3106, pp 473-483, May, 1978, Houston, Texas.

1408

**INTENTIONALLY BLANK**

## ASEISMIC DESIGN CONSIDERATIONS FOR CONCRETE GRAVITY PLATFORMS

by

B.J. Watt<sup>1</sup> and R.C. Byrd<sup>2</sup>

## ABSTRACT

The dynamic response characteristics of concrete gravity platforms are contrasted with those of typical land-based structures as well as with the more conventional space-frame offshore platform concept. The nature and importance of structure-water interaction and soil-structure interaction are discussed in terms of both experimental and analytical results. A design approach based on a two level ground shaking criterion is suggested as the soundest procedure at this time. The special seismicity considerations relating to concrete gravity platforms are highlighted.

## INTRODUCTION

Concrete gravity production platforms as used by the oil industry in the North Sea are very different from other engineering structures. This is because of their shape, size, mass, buoyancy and other characteristics described in this paper. The dozen large platforms of this type which have been installed to date are all located in the North Sea, a seismic province of relatively low activity (1). Several oil companies studied the applicability of this concept in areas of high seismicity such as the Gulf of Alaska (2). The disappointing drilling results from that area have led to a slackening of interest in the concrete gravity platform concept in the U.S.A., reinforced by the apparent high cost of such systems, based on the North Sea experience. Nevertheless, many of the areas scheduled to be leased for offshore development in the next decade are characterized by environments which are distinctly unfavorable to piled systems. Gravity platforms have a real, if somewhat limited future in the development of certain offshore areas. It is appropriate at this conference to review their needs when considering the problems of microzonation offshore. Future data acquisition and processing programs should be designed to incorporate the characteristics of these structures which are not always identical with those of more conventional platform systems.

## OBJECTIVES

Earthquake occurrences offshore are associated with a number of phenomena including tsunamis, submarine landslides and ground shaking. This paper is limited to the latter phenomenon, and has the following objectives.

---

<sup>1</sup> President, Brian Watt Associates, Inc., Houston, Texas.

<sup>2</sup> Senior Supervising Engineer, Brian Watt Associates, Inc. Houston, Texas.

- Describe the main features of gravity platform dynamic response.
- Identify the special characteristics of free-field ground motion which are important to gravity platforms.
- Describe a realistic design approach.

## CHARACTERISTICS

Concrete is a construction material which readily lends itself to the adoption of many different structural forms to solve the same engineering problem. The diversity among reinforced concrete and prestressed concrete bridge designs is evidence of this. Figure 1 shows typical North Sea platform configurations but it is to be expected that as new areas are developed significantly different platform shapes may evolve. For the purposes of this discussion, the most common structure type deployed to date will form the focus. This is shown in Figure 1(a) and consists of a large base caisson supporting several legs consisting of concrete towers which in turn support a steel deck which houses the drilling and production facilities.

Apart from the obvious consideration of water depth, the size of such a system depends on several other factors including payload carried to location, water depths available for construction and other items not immediately associated with the installation location. Base diameters of 300 to 400 ft., overall heights to deck level of 600 ft., and dry concrete weights in excess of 300,000 tons are not uncommon. Not only are the global dimensions of such structures large in comparison with typical land-based systems, but the individual structural components are also somewhat different from land-based systems. In particular, the need to resist very high hydrostatic pressures results in wall and slab thicknesses which are typically in excess of 3 ft. and sometimes significantly more.

One of the most significant differences between such structures and other offshore as well as land-based systems is the extremely large mass which participates in dynamic response to earthquakes. The total mass of the platform system comprises the self weight of the structure, the mass of water contained within the structure as well as an equivalent "added mass" of ambient fluid which participates in the dynamic response. For the case of horizontal excitation, these latter two factors can contribute three times as much mass as is contributed by the self weight of the structure alone.

Another important feature is the buoyancy of the structure, particularly where foundation behavior is concerned. The soil below the mudline is subjected to the buoyant weight of the structure system. This effect, when coupled with the much larger mass, means that the same structure would respond very differently if it were installed on two nominally identical sites, one of which was dry and the other submerged.

Finally, the functional application of these structures as drilling and production platforms means that their ability to tolerate relative movement between structure and foundation is different from that of most other types of construction.

#### STRUCTURE-WATER INTERACTION

The subject of structure-water interaction can be summarized as the problem of describing the pressure field in the surrounding water in the presence of dynamic boundaries which are in turn coupled to the water pressure field.

There are four basic mechanisms which are involved in determining the water pressure field surrounding a dynamic structure:

- Compressibility of the water.
- Turbulence created by flow separation around the structure.
- The local disturbance created by the structure attempting to accelerate the fluid at its boundary.
- The generation of surface waves by the motion of the structure.

We can show that the effect of compressibility is unimportant when the velocity of structure motion is small relative to the speed of sound in water (approximately 4720 fps) as is generally the case (4). We will thus confine our discussion to the last three effects.

It is convenient for the purpose of response analysis to describe the influences of the fluid pressure field in terms of force coefficients which can be related to the dry structure characteristics and which allow the consideration of fluid influences as part of the dynamic analysis. This process involves integrating the various pressure field effects in three dimensions and producing net force coefficients which are frequency dependent in the general case.

#### Drag Force

The forces due to form drag are proportional to the cross-sectional area of the structure component and the square of the relative velocity between the structure and fluid. We will not attempt to describe this force relationship in detail here since it is generally well known, but we would like to make some comments about its treatment.

It can be shown (5) that the ratio of the drag force to the inertia force, which we shall consider below, can be written approximately as the ratio of the amplitude of relative motion to the

diameter of the structure component,  $a/D$ ; the horizontal relative motion being the sum of ground motion and structure response motion, while the vertical relative motion consists of response only. It is clear that the drag force is small compared to the inertial force for most offshore gravity structures in earthquakes and can reasonably be ignored. However, for structures which are to be built in very deep water, this might not be true for members in the upper part of the structure and it should be checked carefully. This force cannot be ignored in general for exposed risers or the smaller components of space-frame structures.

### Inertia Forces

The two structure-water interaction effects under discussion can both be described as inertial force effects and both influences can be contained in the same influence coefficient, which for convenience only, is often normalized by the mass of the water displaced by the structure envelope. We use the term "inertial" here in referring to forces which are in phase or 180 degrees out of phase with the structure acceleration.

It should also be noted that the wave generation pressure disturbance contains a component which is ninety degrees out of phase with structure acceleration and is essentially a damping factor. This may become important for large structures at low frequencies, but can be ignored in general with little effect. This damping term amounts to a radiation of energy from the system by surface waves.

The net result, in general, of the inertia related fluid effect is to increase the mass of the structure component for response purposes, thus the term "added mass" coefficient. It should also be noted that the same effect causes an "added load" term to be placed on the right-hand side of the dynamic equation and in general the mass portions of these terms are not equal, as will be noted below.

Figure 2 shows the calculated inertia coefficient, including the effect of wave generation, compared with measured coefficient values from tests that were recently concluded at the University of California at Berkeley (5). These data point out a number of important characteristics of the acceleration related fluid forces:

- ° They are almost independent of frequency over a wide range.
- ° They can be calculated very accurately under some conditions.
- ° Wave generation has an increasing effect at lower frequencies, making the total coefficient frequency dependent and of decreasing magnitude toward the



lower frequencies. The fluid effect becomes a "subtracted mass" at very low frequencies, corresponding to the region where significant quantities of energy are radiated away in waves.

The details of these tests are contained in (5) and the analytical formulation was taken from (4). They will not be discussed here except to say that the total inertia coefficient is plotted versus a dimensionless frequency parameter which relates the wave generation force to the local disturbance force. It can be seen that the two forces are opposite in sign and effectively cancel each other in the case where:

$$\frac{\omega^2 \sqrt{DH}}{g} = 3.142$$

and,     D = structure diameter  
           H = structure height  
            $\omega$  = excitation frequency  
           g = gravity

The same test series (5) revealed that the vertical inertial behavior could be calculated accurately as well, showing that there are no major non-linearities in the solutions to the hydrodynamic equations of motion as applied to large submerged offshore structures during earthquakes. However, the tests also revealed that the "added load" for vertical motion of a totally submerged structure should be calculated using the entire mass of the water column above the structure, not the inertia coefficient due to relative motion of the structure on its foundation, as shown in Figure 3. The question of vertical excitation will be discussed in more detail later.

An example of the magnitudes of the vertical and horizontal inertia ("added mass") coefficients is shown in Figure 4.

Powerful analytic tools are available to deal with this aspect of offshore structure dynamics. However, the dynamic coefficient formulations are often misused. See (4) for a more detailed discussion on the use of "added mass" coefficients for flexible tower structures.

One more important area where little is known is in the influence or coupling, of the individual towers of a multi-towered structure. This is a subject of current research.

It may be concluded that the earthquake forces due to the fluid can be calculated quite accurately in many cases using available analytical techniques to derive the influence coefficients, provided that the other aspects of the problem, including the foundation, are understood. An example of the agreement between measured and calculated forces that is possible under laboratory conditions is shown in (5).

## STRUCTURE-SOIL INTERACTION

The importance of soil-structure interaction has been clearly recognized for the analysis of the earthquake response of nuclear reactors. However, there is no consensus as to the most desirable method of simulating the behavior and for analyzing the total system response (6). Soil-structure interaction effects are equally pronounced in the case of gravity platforms (3), (7), (8) and it is clear that a sensible prediction of earthquake loads in both structure and foundation cannot be achieved without a careful dynamic analysis which embodies an adequate treatment of the interaction phenomena.

Two interaction features need to be considered. The first and most obvious is the so-called "inertial" interaction resulting from the fact that both structure and soil participate in the earthquake motion and each has its own stiffness, mass and damping characteristics which will contribute to the response of the ensemble. The problem has been studied using the so-called impedance or superposition approach (3) for the case of linear foundation behavior, as well as by means of the linear iterative finite element method and by using a non-linear hysteretic formulation (8).

All methods have demonstrated the importance of the soil flexibility and damping behavior in determining the overall system response. A significant characteristic for all analysis cases reported thus far is the tendency toward a sliding mode of failure of the foundation. In fact, high shear stresses will develop beneath the structure base even for reasonably low excitation levels. The data in Figure 5 are from a linear iterative finite element analysis (9) and show the reduction in shear modulus for both the free field and the coupled structure-foundation cases.

The other factor to be taken into account is the kinematic interaction resulting from the rigidity of the structure and its size in relation to the wave lengths of the free field excitations. A theoretical procedure for evaluating the kinematic interaction effect between a large circular disc and an elastic half space traversed by a horizontally propagating shear wave is presented in (9) while (10) presents measured data which suggest that these effects are responsible for a considerable degree of filtering of high frequency components of the free field motion. The theory in (9) was used to evaluate the likely effects on gravity structures and the results were discussed in (11). As shown in Figure 6 of this paper, for a large gravity structure, the presence of a large rigid caisson can effectively filter out much of the earthquake energy associated with frequencies higher than one Hertz. While the effect acts toward reducing the translational motion of the structure, it is also associated with torsional driving which lessens the advantages implied by the results in Figure 6. However, as reported in (11), the net effect appears to be a reduction in earthquake induced motions.

The advantages and limitations of the various available analysis procedures are reviewed in (8) and (11). Both the linear iterative and impedance approaches are limited to relatively low level excitations and are not suitable for the case of extreme magnitude earthquakes. The other existing analysis methods and constitutive models are also somewhat limited and there is need for a fully three dimensional non-linear analysis capability which represents a realistic simulation of the physical phenomena. The constitutive model developed in (12) may represent an interesting approach to the earthquake problem as well as to the wave problem for which it was originally formulated.

#### TYPICAL RESPONSE BEHAVIOR

The presence of a very large mass and a low center of gravity for the structure mean that the modal participation factors are very different from those of a typical high rise building. Fundamental periods are usually in the range 2.5 to 6 seconds depending on size and water depth and a significant foundation contribution to the response is apparent over the first three modes, all of which may have periods longer than 0.8 seconds. Although the first mode is dominated by cantilever distortion of the upper structure together with a small amount of foundation rocking, it is the second mode which usually makes the major contribution to foundation shear. A similar trend has also been noted for steel gravity platforms as well as certain space-frame offshore platforms.

An important consequence of the long period of response of these platforms is their reaction to the long period components in many natural accelerograms. This would tend to make peak structure response relate more to the duration of the excitation than to its maximum acceleration. A number of natural and artificial records have been analyzed and in most cases the peak platform response occurs towards the end of the earthquake and well after the period of initial hard shaking as shown in Figure 7. It is therefore essential not to truncate records too soon when analyzing these systems, particularly when considering inelastic response.

#### PROBABLE FAILURE MODES

A study of the response of typical concrete gravity platforms to both design level and survivability level earthquakes showed that some damage could be incurred by the structure without leading to collapse. As far as foundation stability was concerned, the dominant mode of failure is sliding along a fairly shallow failure surface. This type of sliding failure acts so as to uncouple the structure from the foundation and to attenuate the structural response. This can only be achieved at the expense of damage in the foundation and the key issue is whether this damage is acceptable or whether it is associated with a total collapse mechanism. The studies which have been carried out (8) provide analytical

evidence that although sliding will occur, the magnitude will be acceptable. For example, the results of subjecting a typical platform in 600 feet of water to a free field excitation with a peak velocity of 40 inches per second, resulted in relative slip between 6 to 10 inches for a range of soil conditions. If the dynamically induced foundation forces had been used to conduct a general bearing capacity analysis, in many instances failure would have been predicted as shown in Figure 8. The dynamic analyses have shown the irrelevance of conventional bearing capacity approaches to earthquake problems with structures of this kind. They also showed that there was little danger of a collapse due to overturning for the kinds of structures and foundations considered.

As far as the structure itself is concerned, the base caisson is subjected to reasonably high shear forces and since reinforced concrete structures do not have acceptable behavior in the shear mode, it is the authors' contention that they should be designed such that failure will not initiate in shear, but rather in flexure as is the case in conventional building design practice. Studies of typical flexural yielding characteristics for the platform legs indicated acceptable moment-curvature relationships and the non-linear dynamic analyses reported in (8) showed that although yielding in flexure could take place under the most extreme ground shaking on hard ground sites, the total damage would be acceptable and would involve tensile yielding of the reinforcement with little or no crushing of concrete.

#### VERTICAL EXCITATION

To the authors' knowledge, no comprehensive analysis of the vertical excitation and response behavior of gravity platforms has been undertaken. Certainly, there do not appear to be any published details in the general literature.

At first sight, the problem appears quite severe with respect to foundation stability. This is due to the fact that the structure imposes its buoyant weight at the mudline under normal conditions, but that during dynamic response to earthquakes, the effective mass of the system includes not only the real mass of the concrete structure itself, but the very large additional mass of contained fluid and the surrounding water which together represent a mass which will be typically seven or eight times as large as that implied by the buoyant weight of the structure at rest. This implies, for example, that a "lift off" condition could be achieved if the structure experienced a vertical acceleration relative to the ground of as little as  $1/8$  g, compared with the 1 g situation for a structure on land. This is rather misleading and it is necessary to examine the mechanics of the system in general before jumping to rapid conclusions about the importance of vertical excitation.

One of the most important factors, as usual, is the free-field excitation. The horizontal studies on kinematic interaction referred to earlier have shown that it is not just the magnitude but also the wave length and direction of propagation which are important with regard to assumptions about free field motions. This is also true for the case of vertical excitation. The usual assumption is that the site is excited in phase at all points in the plan area under consideration. This implies that a pressure wave is transmitted to the water by the soil body wave at the mudline. For the case of a large area or, for that matter, for the situation arising when surface waves (at the mudline) occur, a different situation occurs in which there is a variation of force along the mudline and hence, the inducing of varying foundation stresses, even in the absence of a structure. Conceptually, the situation is analogous to that of wave induced instability (13).

Let us now consider the case of a gravity structure which is fully submerged. A rather idealized representation of this was presented in Figure 3, for the case of an in phase vertical excitation.

The total force on the foundation for the general case of a compliant foundation can be written (5):

$$F_z = [M + \rho C_{zz}^m H A] \ddot{z} + [M + \rho \Delta H A] \ddot{v}_g \quad [2]$$

where:

H = structure height

A = top and bottom area of the structure,

M = total mass of the structure including enclosed fluid and concrete

$\Delta H = h - H$ , where h is water depth  
= height of the water columns above the structure, or depth of submergence,

$C_{zz}^m$  = vertical "added mass" (inertia) coefficient

$\ddot{v}_g$  = vertical ground acceleration

$\ddot{z}$  = vertical structure response acceleration relative to the moving foundation

$\rho$  = density of water

Dividing by the area of the base yields the average pressure on the foundation.

$$q = \frac{F}{A} = \left[ \frac{M}{A} + \rho C_{zz}^m H \right] \ddot{Z} + \left[ \frac{M}{A} + \rho \Delta H \right] \ddot{V}_g \quad [3]$$

The pressure on the bottom adjacent to the structure, assuming in-phase excitation, is given by:

$$p = \rho h \ddot{V}_g \quad [4]$$

The pressure that is of concern for foundation failure is the difference between [3] and [4], or:

$$\Delta p = \left[ \frac{M}{A} + \rho C_{zz}^m H \right] \ddot{Z} + \left[ \frac{M}{A} - \rho H \right] \ddot{V}_g \quad [5]$$

It should be noted that the first term on the right hand side of [5] would disappear for a rigid foundation. However, the importance of the vertical inertia coefficient and the relative response in general are readily apparent.

The magnitude of the pressure that would be exerted on the top of the structure is given by:

$$q' = \rho C_{zz}^m H \ddot{Z} + \rho \Delta H \ddot{V}_g \quad [6]$$

The importance of the first term in Equation [5] and [6] will depend on the frequency of the excitation, i.e., proximity to resonance. The second term is directly proportional to water depth and can represent a significant force for the deeper installation locations. The experiments of (5) have verified that Equation [6] does indeed represent the pressure on the top of the structure in an average sense. The pressure distribution would, of course, not be uniform over the top surface of the structure.

The consequences of these pressure relationships for structures must be viewed in light of typical design procedures and the expected structure system/ground acceleration relationships. Looking first at Equation [5], the differential foundation pressure, one can show that the first term decreases rapidly for excitation frequencies greater than  $\sqrt{2}$  times the vertical mode frequency. For this case the differential pressure is less than that which would be exerted by the structure on dry land, since the effective mass is reduced by the mass of the displaced water. The pressure is

seen to be independent of water depth for excitation far from resonance. For structures which are excited near resonance in the vertical mode, the differential pressure term can become quite large and would likely exceed the equivalent dry structure load by a considerable amount due to the added mass of water. As seen in Figure 4, the vertical inertia coefficient increases with depth of submergence.

Considering the question of lift-off, we can see that this is not possible until the amplitude of the differential pressure exceeds the pressure due to gravity acting on the effective submerged mass of the system. This can occur when the following relationship is satisfied.

$$1 > \frac{[M - \rho H] [g - \ddot{V}_g]}{[M + \rho C_{zz}^m H] \ddot{Z}} \quad [7]$$

It can be noted that increased ground acceleration and increased added mass from the water decrease the relative response acceleration required for lift-off. It is, however, unlikely that lift-off conditions could be satisfied except in extremely large magnitude shaking near the resonant frequency of the soil-structure system. Nevertheless, these conditions should be examined.

Considering the dynamic pressure on the structure top, Equation [6], we see that the ratio of this pressure to hydrostatic is:

$$\frac{\text{Dynamic}}{\text{Hydrostatic}} = \frac{C_{zz}^m H \ddot{Z} + \Delta H \ddot{V}_g}{\Delta H g} \quad [8]$$

The dynamic pressure can exceed hydrostatic as resonance is approached or for large values of ground excitation. The degree to which this would be a problem would depend on whether or not the structure was initially designed for hydrostatic pressure. It can be seen that the relative importance of added mass effects decreases with increased depths of submergence.

The above evaluations have incorporated the rather sweeping assumption that all ground accelerations are in phase. The fact that structure response and ground acceleration are not in phase for real soils has also not been discussed and this would change the impact of the relative acceleration ( $\ddot{Z}$ ) somewhat. Nevertheless, a careful investigation of the question of vertical excitation is warranted from the mechanics of the problem as described above. The assumption of uniform, in phase, vertical excitations needs careful consideration. It is rather unlikely that this

would hold over an area of 700 to 1,000 feet in diameter, as would be necessary for consideration of the foundation stability problem. It is anticipated that kinematic interaction effects will be important and it is clear, therefore, that any useful information on the characteristics of motion at the mudline will be an important factor in the validity of any force prediction.

#### RECOMMENDED DESIGN APPROACH

In reviewing the above information, it can be seen that there are uncertainties in the prediction of dynamic response of the system even before considering the uncertainties with regard to free field motions for the site in question. When one adds to this the uncertainties regarding the earthquake response of the types of structural elements which are used in very large concrete gravity structures, it is clear that any design approach must take cognizance of this. It has become increasingly recognized in the field of aseismic design that the post-yield behavior of the structure is of paramount importance in ensuring survivability during a rare, intense earthquake. The approach adopted by the more progressive building codes as well as that used by the American Petroleum Institute for steel platform structures (14) is to specify a ductility requirement for the structure. In other words, the structure is designed for a so-called elastic or design level earthquake but in addition, it is required to exhibit certain ductility characteristics which will enable it to survive a more serious earthquake which is herein referred to as the survivability event.

It is the authors' contention that we do not know sufficient about the dynamic response of concrete gravity platforms during severe earthquakes to make general rules at this time concerning ductility requirements. The preliminary studies referred to earlier in this paper have suggested that adequate ductility can be provided but it is premature to use the results of these limited studies as the basis for general ductility requirements. Recognizing that there is a difference between designing for earthquakes and waves and recognizing furthermore the advantages of ductility and the need for this during the extreme event, the American Concrete Institute has adopted a two level design criterion in its recommended practice for the design of offshore concrete structures (15). The criteria are stated in general terms as follows:

- a) Design the structure and foundation for the design level earthquake, using a standard limit state approach.
- b) Check that the structure-foundation system will endure the survivability level earthquake without collapse.



The overall design procedure to ensure a safe aseismic structure can be considered in the following steps:

1. Seismicity study.
2. Site response study.
3. Selection of Design Criteria.
4. Dynamic Analysis.
5. Stress Analysis.
6. Evaluation of Failure Modes.
7. Satisfying Ductility Requirements.
8. Development of Aseismic Design Details.

The above steps are discussed in some detail in Appendix B of (15) which was prepared by the first author of this paper. Items 1 and 2 are of particular interest for this conference.

#### SPECIAL SEISMICITY CONSIDERATIONS

From the previous discussions, it is clear that there are a number of factors which are of importance to gravity platforms. Many of these unfortunately, are beyond the current state of the art, but it is worth summarizing them as follows:

1. Assessment of the importance of the water overburden in determining the free field response at the mudline.
2. The relationship between horizontal and vertical excitation both in terms of magnitude as well as phasing.
3. Considerations of long period components of ground shaking in both vertical and horizontal excitations.
4. Variations in ground motions across the site especially as these will affect kinematic interaction between structure and soil.
5. Means for developing both design level and survivability level earthquakes.

Most of these questions will have to be tackled in some detail before a major structure is installed in a highly active seismic province.

#### CONCLUSIONS

The response of concrete gravity platforms to earthquakes would appear from the analyses conducted to date to be different in many respects from land-based structures as well as from the conventional steel jacket offshore platform. The long response periods of typical large gravity platforms means that they

are sensitive to the long period components which occur in natural accelerograms and care should be taken when corrections are applied for machine error that the long periods components are not filtered out. Kinematic interaction would appear to be significant and a better definition of site wide free field behavior is needed. The tendency for foundation sliding means that there is also a need for improved understanding on the phasing of horizontal and vertical excitations. Finally, in view of the limited experience to date, it appears necessary at this stage to conduct dynamic analyses for both the design level and survivability level earthquakes. The latter requirement not only poses an additional analytical burden in coping with a non-linear problem, but also creates the need for defining so-called survivability level earthquakes.

#### REFERENCES

1. Hoeg, K. (1978): Personal communication regarding unpublished study of seismicity of North Sea platform installation areas, by The Norwegian Geotechnical Institute.
2. Ove Arup and Partners (1975): "Gulf of Alaska Concrete Platform Study - Final Report", Technical Report to Shell Oil Company, Atlantic Richfield Company, and Mobil Oil Corporation, April, 1975. (PROPRIETARY)
3. Penzien, J., and Tseng, W. S. (1978): "Three Dimensional Dynamic Analysis of Fixed Offshore Platforms", Numerical Methods in Offshore Engineering, Zienkiewicz, O. C. et. al., Ed., John Wiley, London, 1978.
4. Liaw, C - Y., and Chopra, A. K. (1973): "Earthquake Response of Axisymmetric Tower Structures Surrounding by Water", Report No. EERC 73-25, Earthquake Engineering Research Center, University of California, Berkeley, June, 1978.
5. Byrd, R. C. (1978): "A Laboratory Study of the Fluid Structure Interaction of Submerged Tanks and Caissons in Earthquakes", Report No. EERC 78/08, Earthquake Engineering Research Center, University of California, Berkeley, June 1978.
6. ASCE (1976): "Analyses for Soil Structure Interaction Effects for Nuclear Power Plants", Report by the Ad Hoc Group on Soil-Structure Interaction, Nuclear Structures and Material Committee of Struc. Div., ASCE, Final Draft, April, 1976.
7. Watt, B.J.; Boaz, I. B. and Dowrick, D. J. (1976): "Response of Concrete Gravity Platforms to Earthquake Excitation", OTC 2673, Proc. Offshore Technology Conference, Houston, Texas; May, 1976
8. Watt, B. J., et. al. (1978): "Earthquake Survivability of Concrete Platforms", OTC 3159, Proc. Offshore Technology Conference; Houston, Texas; May, 1978.

9. Wolf, J. P. (1975): "Seismic Response to Traveling Shear Waves including Soil-Structure Interaction with Base Mat Uplift", Proc. of Specialist Meeting on the Anti-Seismic Design of Nuclear Installations, Nuclear Energy Agency, OEDC; Paris, 1975.
10. Crouse, C. B. (1978): "Prediction of Free-field Earthquake Ground Motions", Proc. ASCE Geotechnical Eng. Division Conference on Earthquake Engineering and Soil Dynamics, Vol. I, 1978.
11. Watt, B. J.(1978): Summary of discussions on "Gravity Platforms", ASCE Earthquake Engineering and Soil Dynamics Conference, Pasadena, California, June, 1978.
12. Prévost, J-H. (1978): "Plasticity Theory for Soil Stress-Strain Behavior", Paper submitted to ASCE Eng. Mech. Div., 1978.
13. Henkel, D.J. (1970): " The Role of Waves in Causing Submarine Landslides", Geotechnique, 20, 1970.
14. API (1978): "Recommended Practice for Planning, Designing and Constructing Fixed Offshore Platforms", API RP2A, Ninth Edition, American Pet. Institute; Dallas, Texas; November 1977.
15. ACI (1978): "Recommended Practice for Fixed Offshore Structures, Final Draft, App. B., Design for Earthquakes", ACI Rec. Pract. No. 357, American Concrete Institute, 1978.

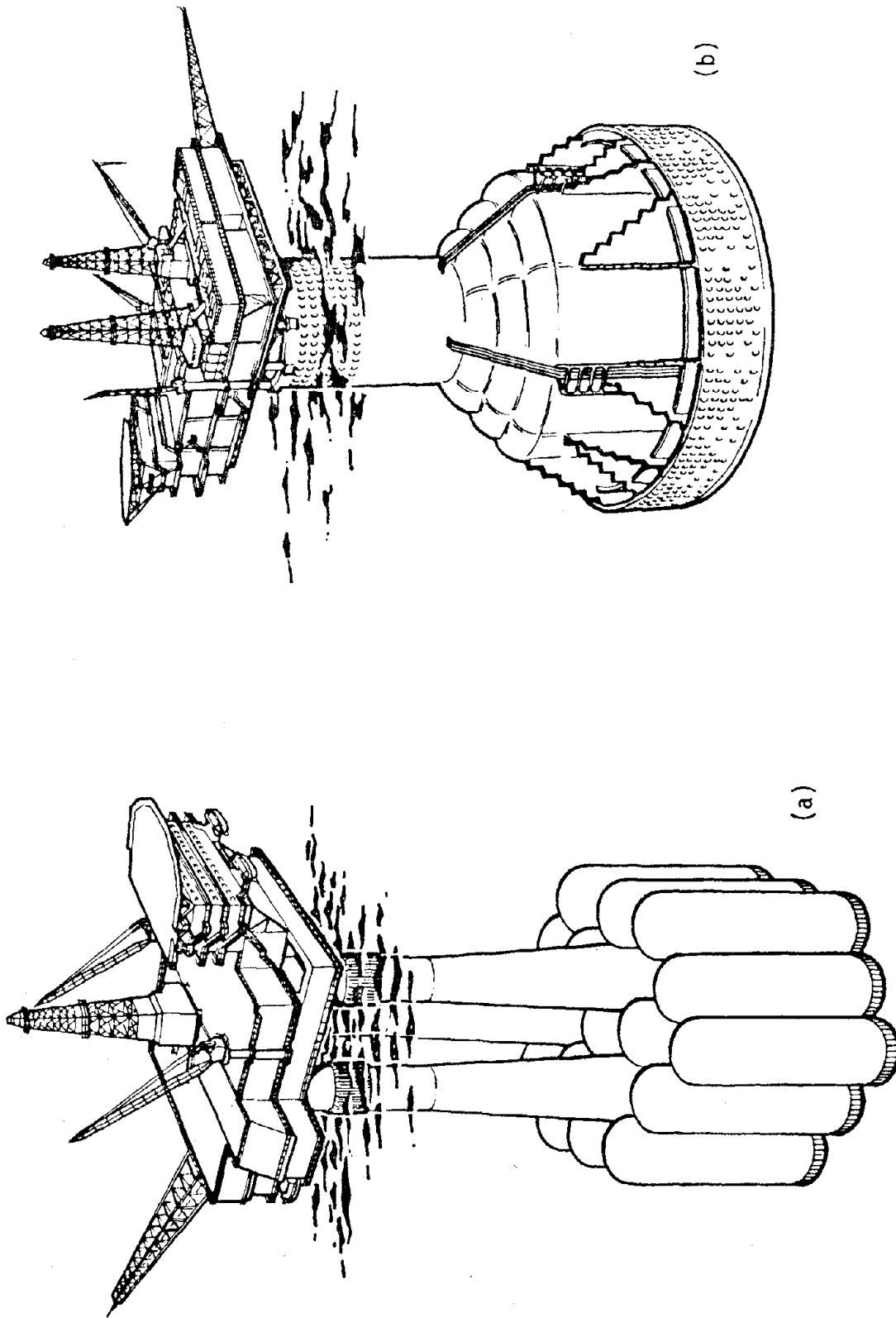


FIGURE 1: TYPICAL GRAVITY PLATFORMS

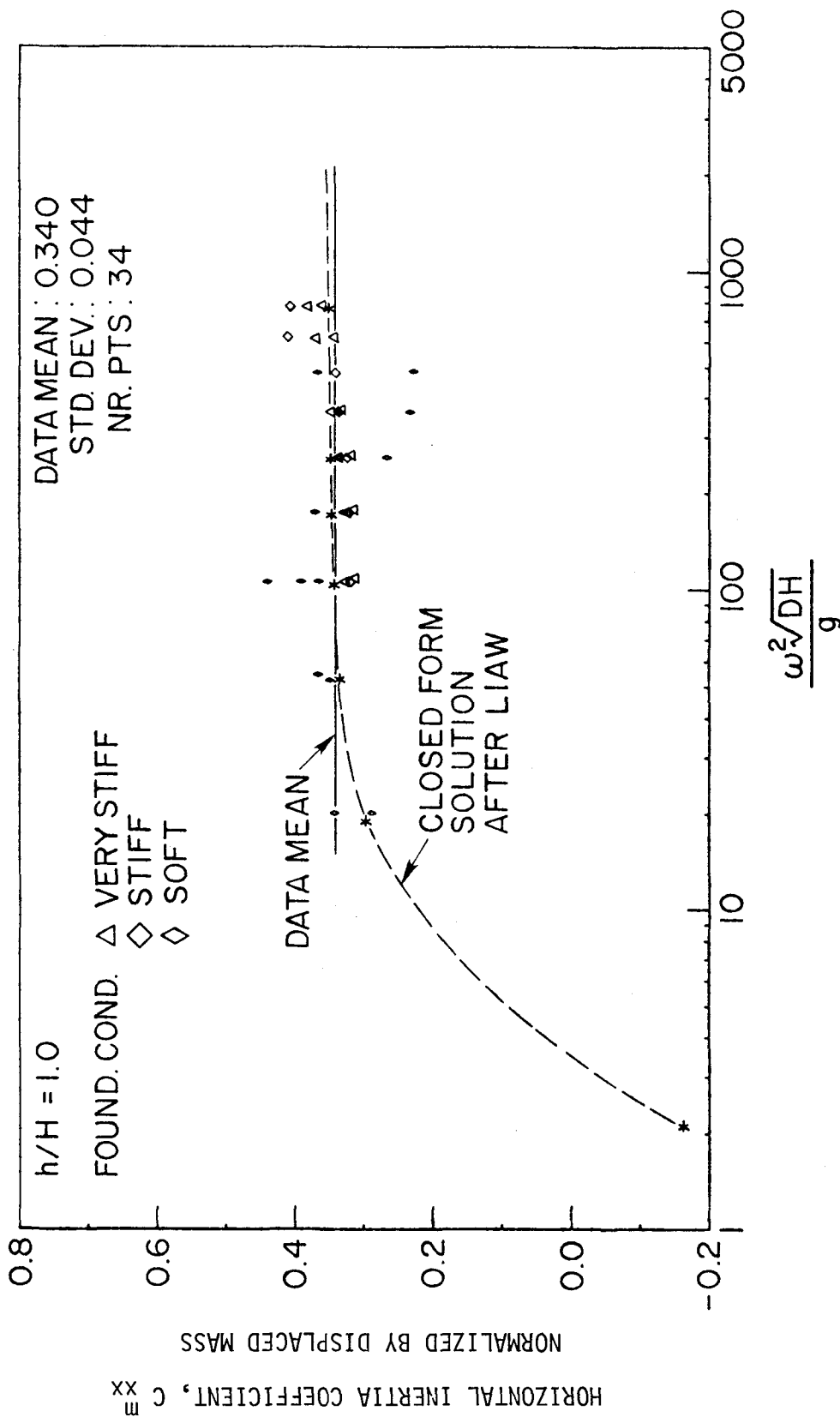
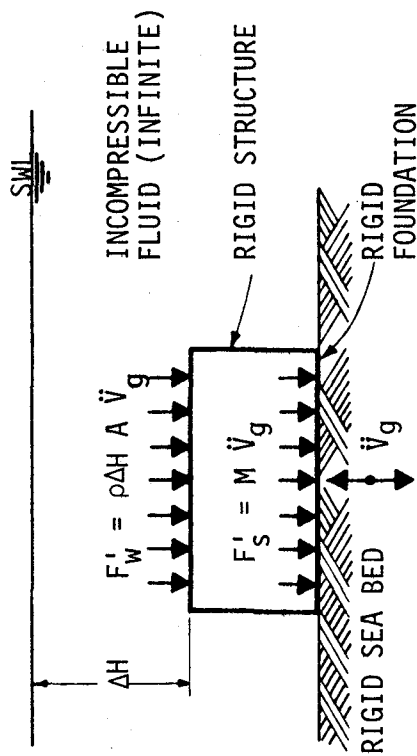


FIGURE 2: CALCULATED AND MEASURED HORIZONTAL INERTIA COEFFICIENTS VERSUS DIMENSIONLESS FREQUENCY FOR A SURFACE PIERCING CYLINDRICAL STRUCTURE,  $H/D = .43$ ,  $D = 262$  FT.

(1) FOUNDATION EXCITATION ONLY

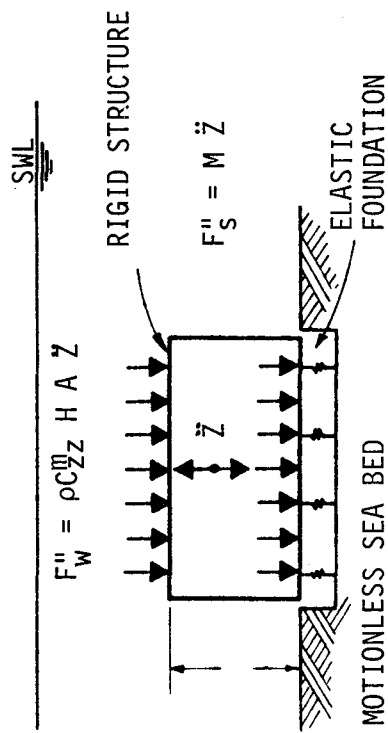


$$F'_z = (M + \rho \Delta H A) \ddot{v}_g$$

FORCE DUE TO RIGID BODY MOTION

+

(2) RELATIVE MOTION ONLY



$$F''_z = (M + \rho C_{zz}^m H A) \ddot{z}$$

FORCE DUE TO RELATIVE MOTION

=

TOTAL HYDRODYNAMIC FORCE

FIGURE 3: VERTICAL HYDRODYNAMIC FORCE REPRESENTATION

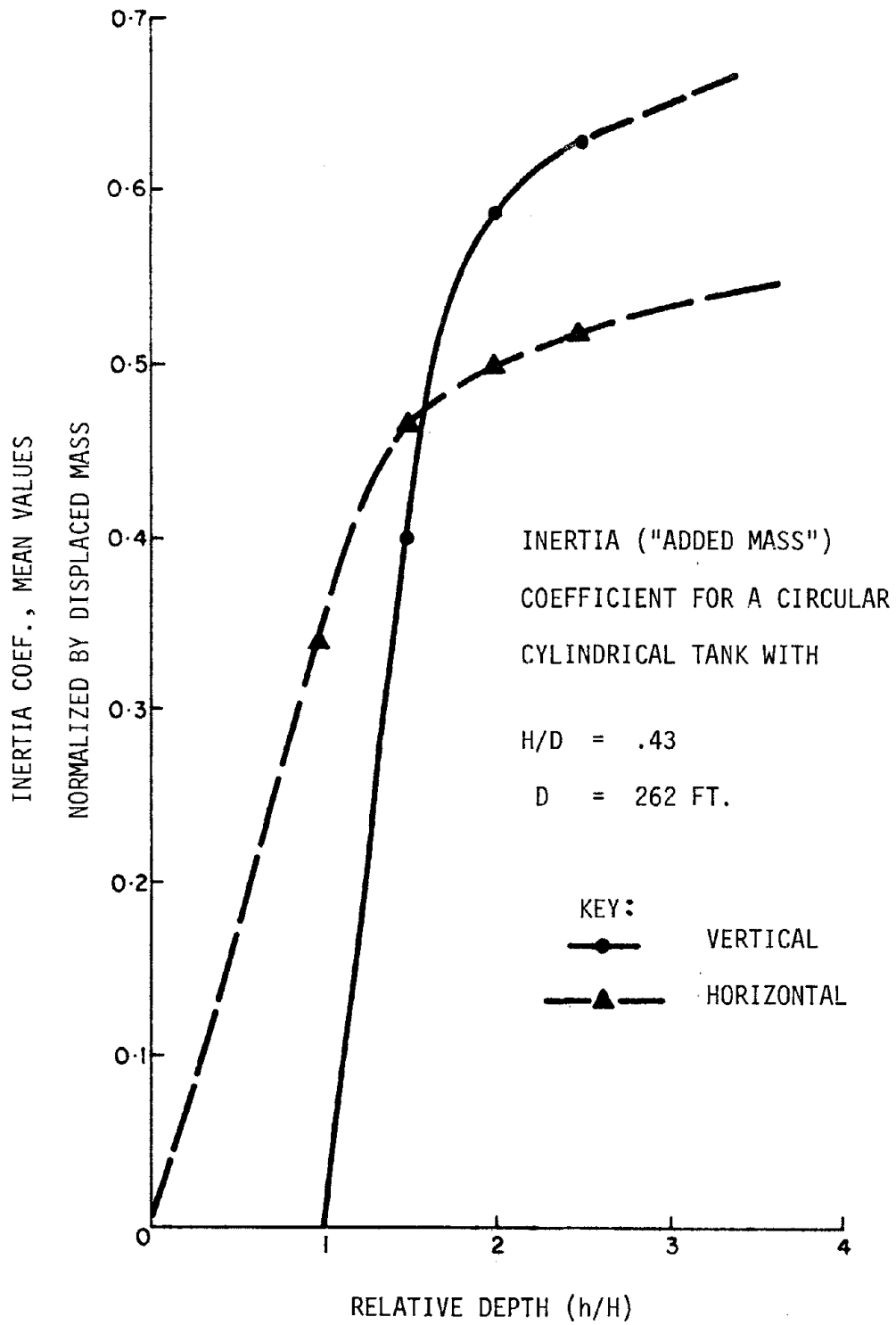


FIGURE 4: MEAN HORIZONTAL AND VERTICAL INERTIA COEFFICIENT VERSUS RELATIVE WATER DEPTH

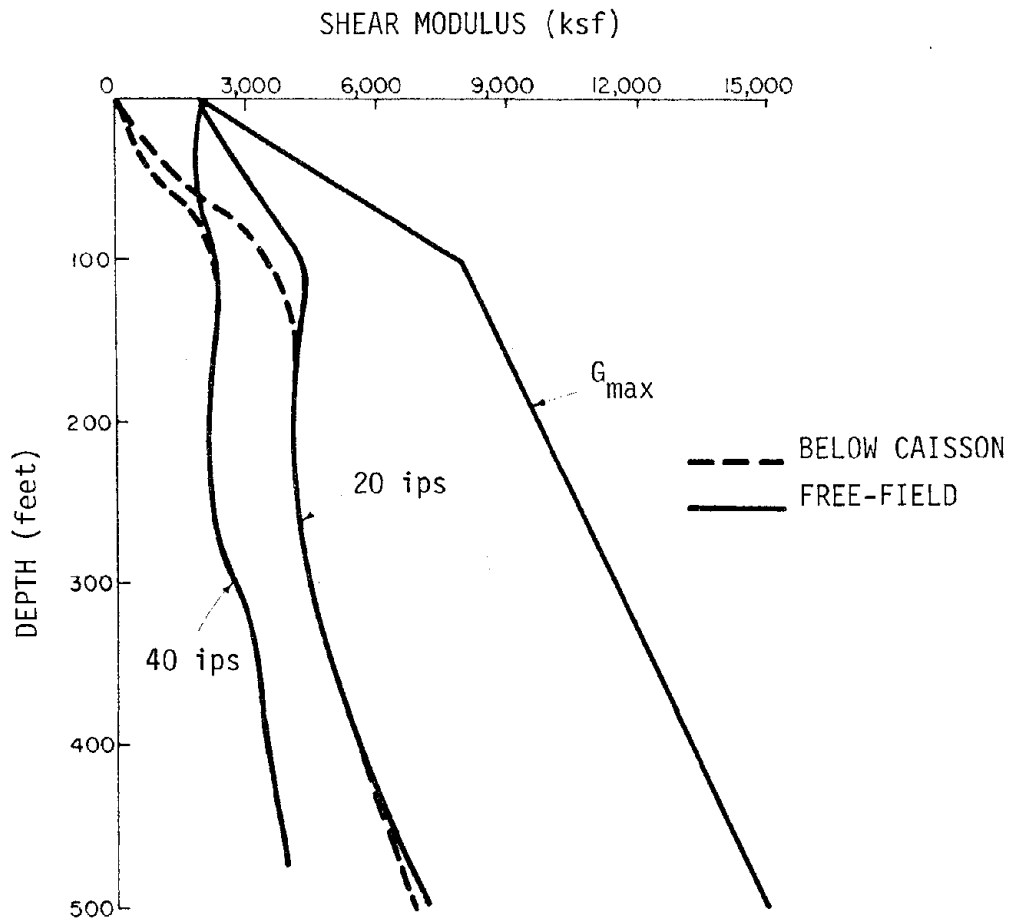


FIGURE 5 REDUCTION IN SOIL SHEAR MODULI FOR PEAK FREE-FIELD VELOCITIES OF 20 AND 40 INCHES/SEC.



1429

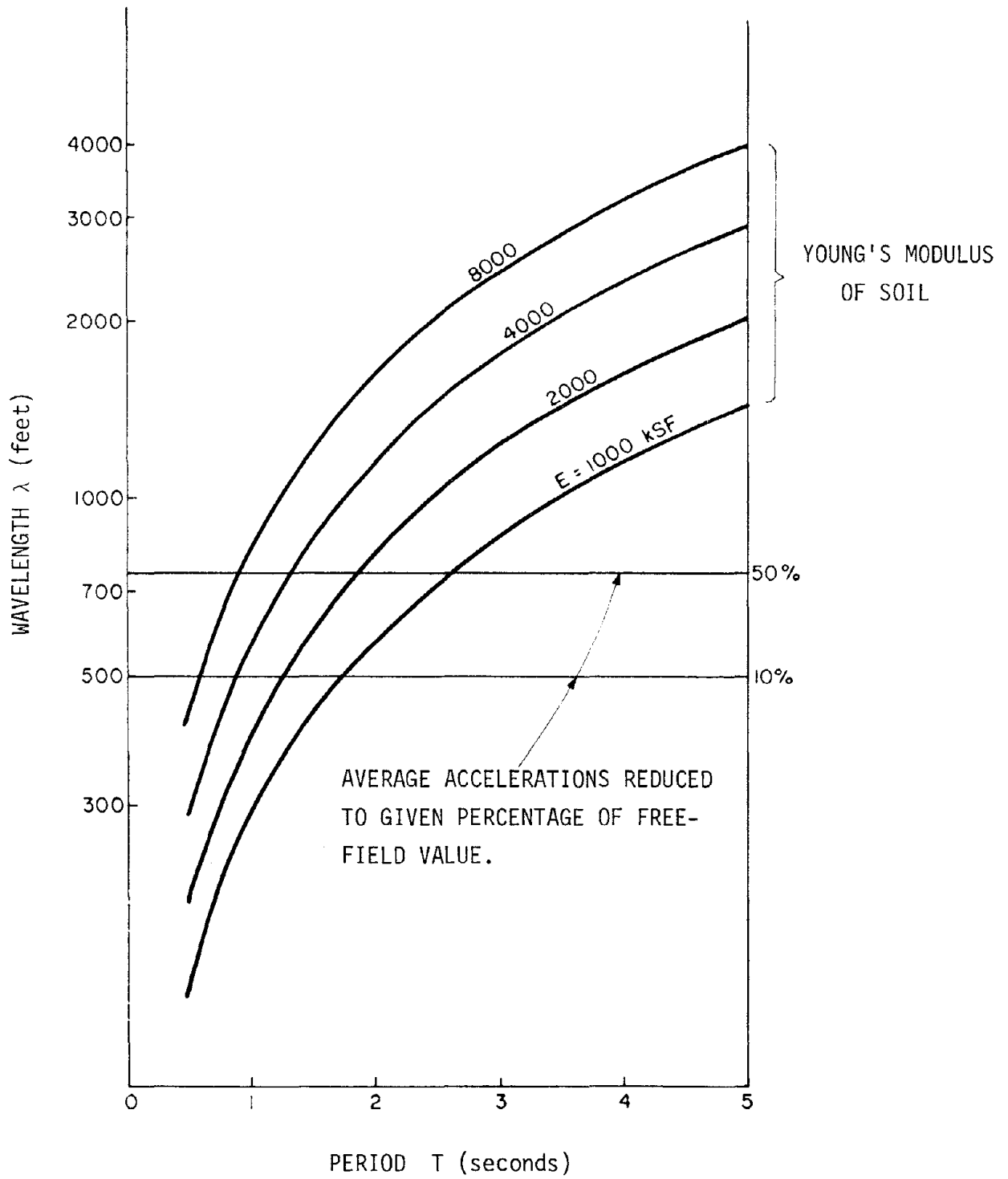


FIGURE 6 KINEMATIC REDUCTION OF ACCELERATION BY 450 FEET DIAMETER RIGID DISC

1430

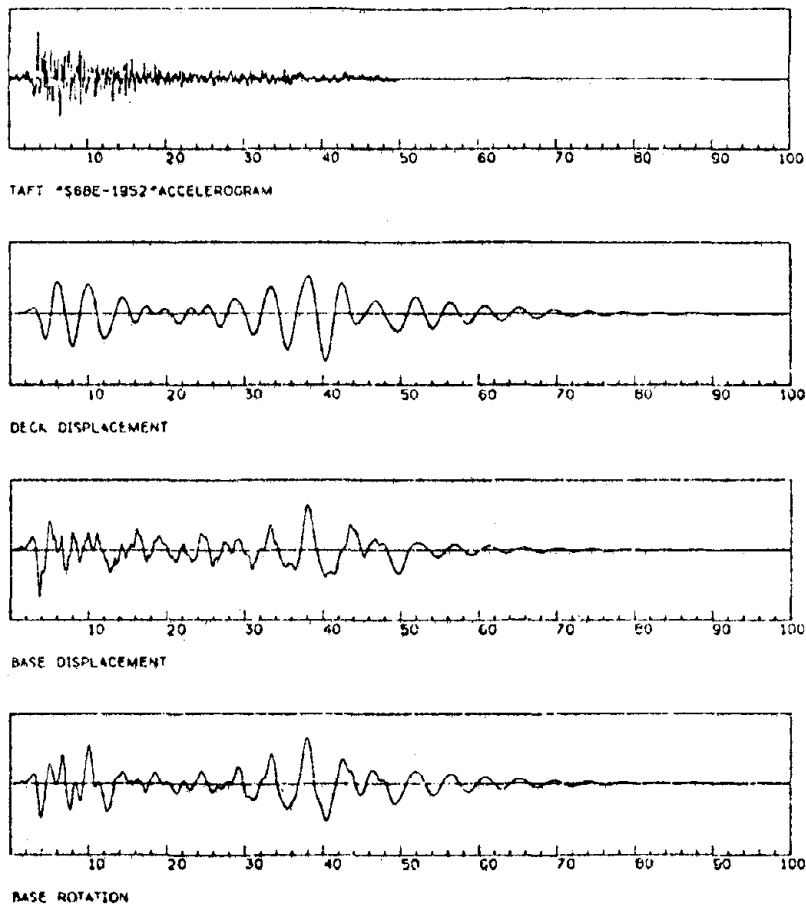
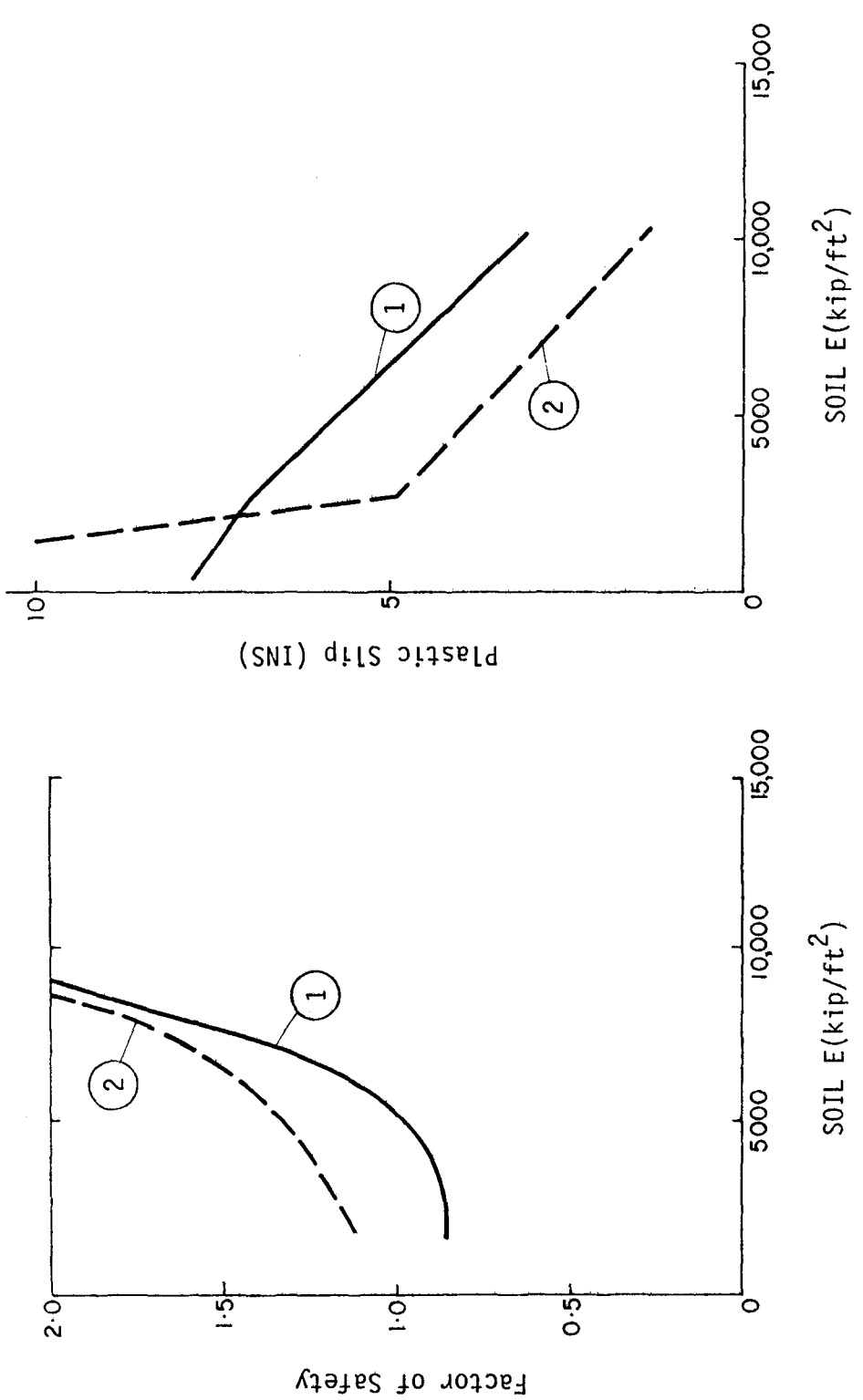


FIGURE 7: RESPONSE OF GRAVITY PLATFORM TO TAFT 1952 S69 E ACCELEROGRAM

1431



(a) Safety Factors from Conventional Stability Analysis

(b) Plastic Slip from Nonlinear Dynamic Analysis

FIGURE 8: FOUNDATION STABILITY

1432

INTENTIONALLY BLANK

## SITE EFFECTS ON MICROZONATION IN OFFSHORE AREAS

By

Y. Moriwaki<sup>I</sup> and E. H. Doyle<sup>II</sup>

## ABSTRACT

Earthquake ground motions at three selected sites in a typical offshore environment are compared using a combination of empirical and analytical procedures. The selected sites consist of rock, soft clay or stiff clay. Ground response analyses are conducted using a one-dimensional procedure that incorporates the nonlinear stress-strain behavior of the clay and accounts for modulus degradation during cyclic loading. The analytical results are compared to available empirical relationships to assess the trends obtained by either procedure. The results can be used to provide reasonable means for establishing general seismic zonation or for site specific studies.

## INTRODUCTION

Microzonation of offshore areas requires the assessment of possible earthquake response at different sites. Perhaps the most important part of this assessment consists of "predicting" earthquake motions which, at a given site, are affected by many factors including earthquake source mechanism, the nature of the transmission path, regional geology and topography, and local site conditions. This paper focuses on the effect of local subsurface (soil) conditions on the seismic response of essentially horizontal ground. While the effect of local site conditions on earthquake motions appears to be complicated (1, 6), there is considerable evidence that a seismic motion is modified by soil deposits of various stiffnesses (10, 15). Furthermore, it is not surprising that a softer and deeper soil deposit in general appears to cause a greater change in seismic motions (13). Assessment of the potential effects of local soil conditions on the seismic response of horizontal ground for microzonation and design purposes in offshore areas is necessary for many projects.

This paper discusses a method of one-dimensional seismic response analysis especially suited for clayey sites. Two hypothetical deep clayey sites, one soft and the other stiff, typically encountered in offshore areas and a rock site are used for illustrating the potential effects of site conditions on seismic response.

---

I Project Engineer, Woodward-Clyde Consultants, San Francisco, California  
II Senior Research Engineer, Shell Development Co., Houston, Texas

## METHODS OF SITE RESPONSE ASSESSMENT

There are two basic procedures to assess the nature of earthquake response at a given site for engineering purposes, an empirical procedure and an analytical procedure. Empirical procedures are based on some statistical summary of recorded earthquake motions and generally provide some quantities related to earthquake motions including peak values (acceleration, velocity and displacement) as well as spectral values. These quantities may be a function of any combination of variables such as earthquake magnitude, distance to some representation of earthquake source and local site conditions. These empirical procedures, if used appropriately, should provide reasonable values of peak earthquake ground motion parameters and spectral ordinates, statistically incorporating many of the uncertainties involved in seismic events. However, microzonation in the general sense may require some site specific seismic response as well as additional information such as peak shear stresses induced in the ground and the nature of deformations caused by shaking.

There are basically two types of one-dimensional, shear-beam type analytical procedures in common use at present, equivalent linear and nonlinear. A typical equivalent linear procedure is represented by SHAKE (12) which uses the complex response method to perform damped elastic analyses. Strain compatible modulus and damping values obtained by an iterative process are used to approximate the nonlinear behavior of soils. There are a number of nonlinear analytical procedures presently in usage including DESRA (3), CHARSOIL (16), and DCHARM (4). Each of these procedures uses a backbone curve (a hyperbolic relation for DESRA and a Ramberg-Osgood relation for CHARSOIL and DCHARM) and the Masing criterion to track nonlinear dynamic stress-strain variations. The equations of motion are integrated in the time domain using the Newmark method (11) for DESRA and the method of characteristics for CHARSOIL and DCHARM. Reduction in modulus mainly due to excess pore water pressure increase can be incorporated in all of these analyses by methods based on the volume change and rebound characteristics of the soil for DESRA, on an assumed relationship between shear modulus and constrained modulus for a version of CHARSOIL (8), and on the experimentally obtained relationship between modulus and the number of cyclic loadings for DCHARM. For clayey soils, since some of the parameters necessary in DESRA and CHARSOIL for modulus reduction due to cyclic loading may be difficult to measure or assess, the DCHARM approach based on easily obtainable plots from a series of cyclic tests appears to be a useful alternative.

## METHOD OF ANALYSIS INCORPORATED IN DCHARM

The nonlinear, degrading stress-strain model used in DCHARM can be specified based on the results of a series of strain-controlled (constant-strain) cyclic loading tests (4, 5). The basic model consists of the following: a) an initial backbone curve and the Masing criterion; b) degradation of the backbone curve under constant-strain cyclic loading; and c) extension of the degradation concept to transient cyclic loading conditions.

### Initial Backbone Curve and Masing Criterion

The initial backbone curve is described mathematically using a Ramberg-Osgood model:

$$\frac{\gamma}{\gamma_y} = \frac{\tau}{\tau_y} + \alpha \left( \frac{\tau}{\tau_y} \right)^R \quad (1)$$

where  $\gamma$  = shear strain,

$\tau$  = shear stress,

$\gamma_y$  = reference shear strain,

$\tau_y = G_{\max} \gamma_y$  and  $G_{\max}$  is the maximum shear modulus, and

$\alpha, R$  = Ramberg-Osgood parameters.

In addition to the backbone curve, a set of rules based on the Masing criterion is required to specify the hysteretic stress-strain behavior of clay for transient cyclic loading (11). The Masing criterion basically means that the branches of the hysteretic curve are a two-fold magnification of the backbone curve.

In obtaining a Ramberg-Osgood curve, the parameters in Eq. 1 ( $\gamma_y, \tau_y, \alpha, R$ ) have to be specified to fit experimental stress-strain (backbone curve) data as well as damping-strain data (5).

### Degradation of Backbone Curve Due to Constant-Strain Cyclic Loading

Degradation Index,  $\delta$ : The degradation of a hysteresis loop in a constant-strain cyclic loading tests can be viewed as the degradation of the initial backbone curve (see Fig. 1). The degraded, new backbone curves have stresses which at a given cyclic strain level, are a fraction,  $\delta$ , (called degradation index), of the initial stresses. A degraded backbone curve is expressed mathematically as:

$$\frac{\gamma}{\gamma_y} = \frac{\tau}{\delta \tau_y} + \left( \frac{\tau}{\delta \tau_y} \right)^R \quad (2)$$

t-parameter: The plot of secant modulus,  $G$ , versus number of cycles,  $N$  from a constant-strain cyclic test on cohesive soils generally results in a straight line on a log-log plot as shown in Fig. 2. The negative slope of this line is referred to as the degradation parameter  $t$ . The linear relationship of  $\log G_s$  versus  $\log N$  can be expressed as follows:

$$G_{SN} = G_{S1} N^{-t} \quad (3)$$

where  $G_{SN}$  = Nth cycle secant modulus, and  $G_{S1}$  = first cycle secant modulus, both at a given strain level.

Since setting  $\delta = G_{SN}/G_{S1}$  is consistent with the definition of degradation index,  $\delta$ , Eq. 3 is equivalent to:

$$\delta = N^{-t} \quad (4)$$

By conducting a number of strain-controlled cyclic tests at different strain levels, the  $t$ -parameter can be obtained as a function of cyclic shear strain. Available data on several types of cohesive soils suggest a relationship of the following form:

$$t = \frac{\gamma}{a + b \gamma^c} \quad (5)$$

where  $a$ ,  $b$ ,  $c$  = constants which are determined from test results.

#### Extension of Degradation Concept to Arbitrary Cyclic Loading Conditions

A backbone curve and the Masing criterion completely define the stress-strain behavior of a soil element during an arbitrary cyclic loading but without any accommodation for degradation. On the other hand, using Eqs. 4 and 5, a prediction of  $\delta$  throughout a constant cyclic strain test is possible. However, in order to predict  $\delta$  during transient cyclic loading, an additional assumption is required. For transient loading, the model assumes that the value of degradation index,  $\delta$ , corresponding to each new half-cycle (defined by two successive zero-crossings of the stress-time history, say BC (see Fig. 3(a)), depends only on two parameters (5): a) the value of degradation index for the previous cycle say  $\delta_{AB}$ ; and b) the absolute value of the maximum strain developed during the previous cycle, say  $|\gamma_{AB}|$  (see Fig. 3(b)).

Then, from Eq. 4:

$$\delta_{AB} = \left( \frac{n_{AB}}{2} \right)^{-t_{AB}} \quad (6)$$



where  $t_{AB}$  can be obtained from  $|\gamma_{AB}|$  and Eq. 5, and  $n_{AB}$  is the number of half cycles at cyclic strain level of  $|\gamma_{AB}|$  required to attain  $\delta_{AB}$ . Since it takes an additional half cycle to reach BC from AC in Fig. 3, the degradation index for the new half cycles,  $\delta_{BC}$ , can be expressed as:

$$\delta_{BC} = \delta_{AB} \left[ 1 + \left( \frac{\delta_{AB}}{2} \right)^{1/t_{AB}} \right]^{-t_{AB}} \quad (7)$$

Thus the model assumes that, at any given time during an arbitrary cyclic loading, the effect of all previous cycling is completely represented by the current value of degradation index  $\delta$ .

#### SEISMIC RESPONSE OF SELECTED SITES

Seismic response of three typical offshore sites consisting of rock, 200 ft of stiff clay and 200 ft of soft clay is compared using a combination of empirical (15) and analytical procedures. A summary of the soil profiles and the Ramberg-Osgood and degradation parameters used in the analyses are provided in Table 1. Two sets of the Ramberg-Osgood parameters were selected, set (a) and set (b). The Ramberg-Osgood parameters used for set (a) were obtained based on a series of strain-controlled cyclic direct simple shear tests on a soft clay emphasizing modulus behavior at high strains ( $\approx 0.1\%$ ) resulting in a reasonable representation of the measured modulus reduction curve but somewhat high damping values compared to measured data. The Ramberg-Osgood parameters used for set (b) were calculated based on the Seed-Idriss sand reduction curve (14) which appears to be representative of initial backbone curves of some clayey soils. For the analyses, the 1952 Taft S69E (IIA004 Caltech Designation) motion and the 1935 Helena N90E (IIB025 Caltech Designation) motion were input at bedrock level with the peak acceleration scaled to 0.3g or 0.6g.

Absolute acceleration response spectra (5% damping) at the ground surface using DCHARM with degradation option for stiff and soft sites and the assumed rock motion (Taft) scaled to a peak acceleration of 0.3g are shown in Fig. 4. The Ramberg-Osgood parameters of set (a) (Table 1) were used in these analyses. The stiff site amplified the input motion while the soft site greatly attenuated the input motion except for  $T \geq 3$  sec. The results for Taft 0.6g input motion at bedrock (not presented herein) are similar to those shown in Fig. 4 except the response spectrum for the stiff site was generally lower than that for the rock site and the attenuation of motion for the soft site relative to the rock site was even greater than that for the case shown in Fig. 4.

In assessing the soil properties for response analyses, low strain modulus value of a given site often can be reasonably chosen based on available shear strength data, shear wave measurements, etc. The modulus reduction curve is often more difficult to choose without cyclic laboratory tests and consequently, in the absence of laboratory test results, some published average reduction curve such as the Seed-Idriss curve (Ramberg-Osgood parameters set (b)) is often used. The effect of variation in the modulus reduction curve for the stiff site is illustrated in Fig. 5 by two response spectra, one corresponding to using Ramberg-Osgood parameters set (a) and the other corresponding to using Ramberg-Osgood parameters set (b). While there are some large differences in some period ranges, neither response spectrum is higher or lower throughout the entire period range and the overall characteristics of the two spectra are similar.

Also shown in Fig. 5 are the average empirical spectra for stiff sites and deep cohesionless sites developed by Seed, Ugas and Lysmer (15). The peak ground acceleration value used in scaling the empirical spectra was 0.32g to provide a reasonable match with the DCHARM results in the high frequency range. As can be seen from Fig. 5, DCHARM spectra in general appear to be consistent with the empirical data except for the period range between 0.4 sec to 1 sec. As the input Taft motion (see Fig. 4) is not particularly rich in this period range, high response in this period range appears to be site specific. Although for simplicity, a comparison with only the Seed, Ugas and Lysmer empirical curves was made, similar observations would have resulted if other empirical curves were used.

A comparison of spectra obtained by DCHARM for the soft site with the two sets of Ramberg-Osgood parameters and average empirical spectrum for soft to medium stiff clay sites (15) is shown in Fig. 6. Note that the DCHARM response spectrum obtained using the Ramberg-Osgood set (b) shows a significantly higher response compared to that obtained using the Ramberg-Osgood set (a) in the period range between 0.6 sec to 4 sec. Also note that both DCHARM results show a significantly higher response compared to average empirical results for periods longer than approximately 1.5 sec. The difficulty in using empirical data for soft sites has been recognized previously (2, 15). For offshore structures which usually have relatively long periods, site-specific effects on response in the long period range are an important consideration.

The effect of input motion on the response of the soft site is shown in Fig. 7. Helena input motion, which is not as rich as Taft in the long period range and which is of relatively short duration, suppressed the response of the soft site in the long period range. Although not presented herein, the effect of input motion on the response of the stiff site is similar to what is shown in Fig. 7.

The response spectra for the soft site from DCHARM with and without modulus degradation are shown in Figs. 8 and 9 for Ramberg-Osgood parameters sets (a) and (b), respectively. In these analyses, modulus degradation reduces the response in the period range shorter than approximately 4 sec and increases the response in the longer period range.

The results presented in Figs. 4 through 9 were obtained assuming that the bedrock underlying the soil deposit is rigid and using the rock input at the soil-rock interface. This assumption is typical for most current nonlinear analytical procedures (3, 4, 16). Incorporation of the elasticity of the bedrock can be readily made, however, as suggested by Joyner and Chen (7). The program DCHARM was modified accordingly to take the elasticity of the bedrock into account and the rock input motion was used as a rock outcrop motion (similar to what is currently done in a SHAKE analysis) instead of a soil-rock interface motion.

The effects of incorporating the elasticity of the bedrock (the rock was assumed to have a shear wave velocity of 4,000 fps) for the stiff site and using Ramberg-Osgood parameters set (b) are illustrated in Fig. 10. The main effects appear to be at  $T = 0.8 \pm$  approximately 0.2 sec, where the spectral ordinates are reduced when the elasticity of the bedrock is incorporated in the analysis. This trend is similar to that observed in similar comparisons for equivalent linear analyses (eg, 12), where the spectral ordinates are also reduced at the fundamental period of the soil deposit. For the case shown in Fig. 10, the fundamental period of the soil deposit is approximately 0.8 to 0.9 sec.

#### SUMMARY AND DISCUSSION

In this study, the seismic response of three postulated offshore sites, consisting of rock, 200 ft of stiff clay, and 200 ft of soft clay, was compared using analytical and empirical procedures. Ground response analyses of the stiff clay and soft clay soil profiles were made using a one-dimensional, nonlinear analysis procedure that incorporates cyclic modulus degradation. Response spectra of seafloor motions were obtained from the analyses and compared with spectra of the input rock motions and with average site-dependent spectra derived from statistical analyses of recorded data.

In the analytical studies, it was found that the stiff-site profile generally amplified moderately intense input rock motions and generally attenuated very intense input rock motions. The soft-site profile greatly attenuated low-period motions and amplified long-period motions for moderate to very intense input rock motions.

The general trends from ground response analyses were found to be similar to those shown by empirical data. However, the studies also illustrated that local site effects can result in large differences from empirically-derived average spectra in some period ranges. Such differences were more pronounced for the soft site than for the stiff site analyzed.

In general, a relatively large range of responses might be expected for "soft-site" profiles because of the wide range of subsurface profiles and soil properties that could be included in a "soft-site" classification and the sensitivity of the soil dynamic properties to the intensity of the input motions. This consideration and the fact that soft soil sites tend to amplify response in the long-period range indicate the importance of analytically evaluating site-specific effects for long-period offshore structures. It may also be noted that such analyses can provide other response quantities often needed for engineering evaluations, such as shear stresses and relative displacements within the soil profile.

The analytical studies described herein also examined the effects on response of variations in the characteristics of the input motion (amplitude, frequency content, duration), dynamic soil properties including cyclic degradation properties, and flexibility of the rock underlying the soil deposit. It was shown that variations in these factors can influence response, thus indicating the need for careful selection of input parameters and for parametric studies.

## REFERENCES

1. Crouse, C. B. (1978) "Prediction of Free-Field Earthquake Ground Motions," Proceedings of the ASCE Geotechnical Engineering Division Specialty Conference, Earthquake Engineering and Soil Dynamics, Pasadena, California.
2. Faccioli, E. "Response Spectra for Soft Soil Sites," Proceedings of the ASCE Geotechnical Engineering Division Specialty Conference, Earthquake Engineering and Soil Dynamics, Pasadena, California.
3. Finn, W. D., Byrne, M., and Martin, R. "Seismic Response and Liquefaction of Sands," Journal of the Geotechnical Engineering Division, ASCE, Vol. 102, No. GT8.
4. Idriss, I. M., Dobry, R., Doyle, E. H., and Singh, R. D. (1976) "Behavior of Soft Clays under Earthquake Loading Conditions," Proceedings, 8th Annual Offshore Technology Conference, Houston, May 3-6.
5. Idriss, I. M., Dobry, R., and Singh, R. D. (1978) "Nonlinear Behavior of Soft Clays During Seismic Loading," Journal of Geotechnical Engineering Division, ASCE, Vol. 104.
6. Jennings, P. C. (1973) "The Effect of Local Site Conditions on Recorded Strong Earthquake Motions," Proceedings, 42nd Annual Convention, Structural Engineers Association of California.
7. Joyner, W. B., and Chen, A. T. F. (1975) "Calculation of Nonlinear Ground Response in Earthquakes," Bulletin of Seismological Society of America, Vol. 65, No. 5.
8. Liou, C. P., Streeter, V. L., and Richart, F. E. (1976) "A Numerical Model for Liquefaction," ASCE National Convention, Philadelphia, Specialty Session, Liquefaction Problems in Geotechnical Engineering, Preprint No. 2752.
9. Martin, P. P. (1975) "Nonlinear Methods for Dynamic Analysis of Ground Response," Thesis presented to the University of California at Berkeley, California, in partial fulfillment of the requirements for the degree of Doctor of Philosophy.
10. Mohraz, B. (1976) "A Study of Earthquake Response Spectra for Different Geological Conditions," Bulletin of Seismological Society of America, Vol. 66, No. 3, pp. 915-936.

11. Newmark, N. M., and Rosenblueth, E. "Fundamentals of Earthquake Engineering," Prentice-Hall, Inc., Englewood Cliffs, New Jersey, 1971.
12. Schnable, P. B., Lysmer, J., and Seed, H. B. (1972) "SHAKE - A Computer Program for Earthquake Response Analysis of Horizontally Layered Site," Report No. EERC 72-12, Earthquake Engineering Research Center, University of California, Berkeley.
13. Seed, H. B., and Idriss, I. M. (1970) "Analysis of Ground Motions at Union Bay, Seattle during Earthquake and Distant Nuclear Blasts," Bulletin of Seismological Society of America, Vol. 60, No. 1.
14. Seed, H. B., and Idriss, I. M. (1970) "Soil Moduli and Damping Factors for Dynamic Response Analyses," Report No. EERC 70-10, University of California Earthquake Engineering Research Center, Berkeley, December 1970.
15. Seed, H. B., Ugas, C., and Lysmer, J. (1976) "Site Dependent Spectra for Earthquake-Resistant Design," Bulletin Seismological Society of America, Vol. 66, No. 1, pp. 221-244.
16. Streeter, V. L., Wylie, E. B., and Richart, R. E. (1974) "Soil Motion Computations by Characteristic Method," Journal of the Geotechnical Engineering Division, ASCE, Vol. 100, No. GT3, March 1974.

Table 1 - SUMMARY OF SOIL PROFILES

Ramberg-Osgood Parameter See (Eq. 1)

Set (a)  $R = 5.0$        $\alpha = 2.0$        $\gamma_y = 0.02\%$   
 Set (b)  $R = 2.3$        $\alpha = 1.3$        $\gamma_y = 0.02\%$

Degradation Parameter See (Eq. 5)

Soft Site:  $t = \frac{\gamma}{2.7 + 1.54\gamma}$       Stiff Site:  $t = \frac{\gamma}{5.4 + 3.08\gamma}$

Soft Site			Stiff Site		
Thickness (ft)	Maximum Shear Modulus, $G_{max}$ (ksf)	Viscosity, $\eta$ (ksf-sec)	Thickness (ft)	Maximum Shear Modulus, $G_{max}$ (ksf)	Viscosity, $\eta$ (ksf-sec)
6.9	335	2.84	20.1	3922	13.16
7.5	402	3.41	22.8	5053	16.96
8.2	477	4.05	25.6	6330	21.24
8.8	547	4.64	28.2	7719	25.91
9.2	603	5.12	31.1	9381	31.48
10.1	725	6.15	34.3	11422	38.33
10.7	806	6.84	37.9	13882	46.59
11.6	961	8.15			
12.4	1100	9.33			
13.1	1224	10.38			
14.2	1432	12.15			
15.0	1602	13.59			
16.3	1890	16.03			
17.3	2133	18.09			
18.6	2450	20.78			
20.0	2855	24.22			

\*Viscosity corresponds to 2% low strain damping

Total unit weight of soil,  $\gamma_t = 120$  pcf for all

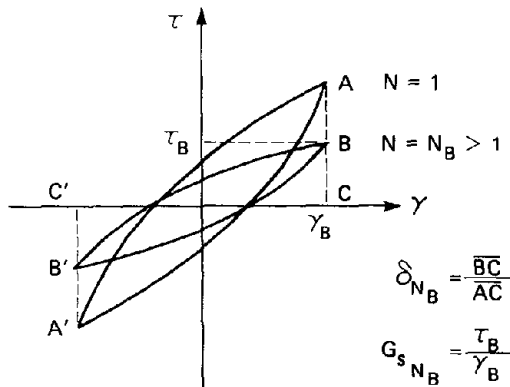


Fig. 1 Constant-Strain Cyclic Test

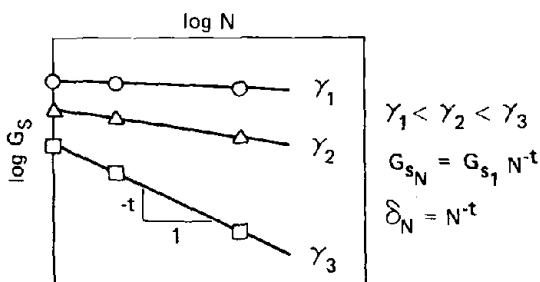


Fig. 2  $G_s$  versus  $N$  from Constant-Strain Cyclic Tests

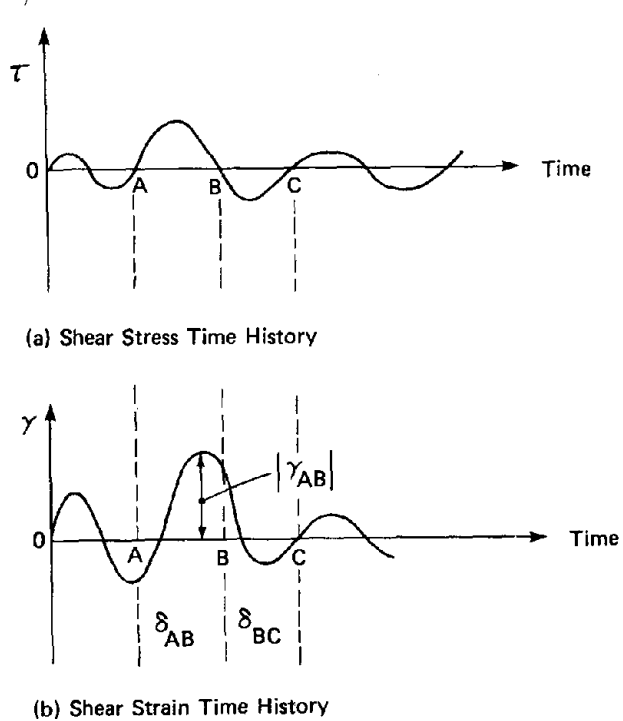


Fig. 3 Existing Model: Degradation Under Arbitrary Loadings

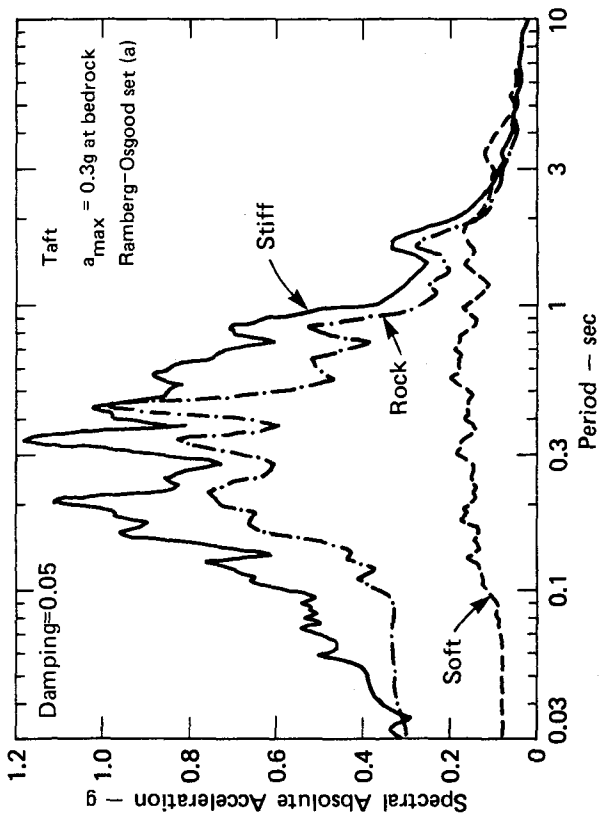


Fig. 4 Effects of Site Conditions on Response Spectra at Surface

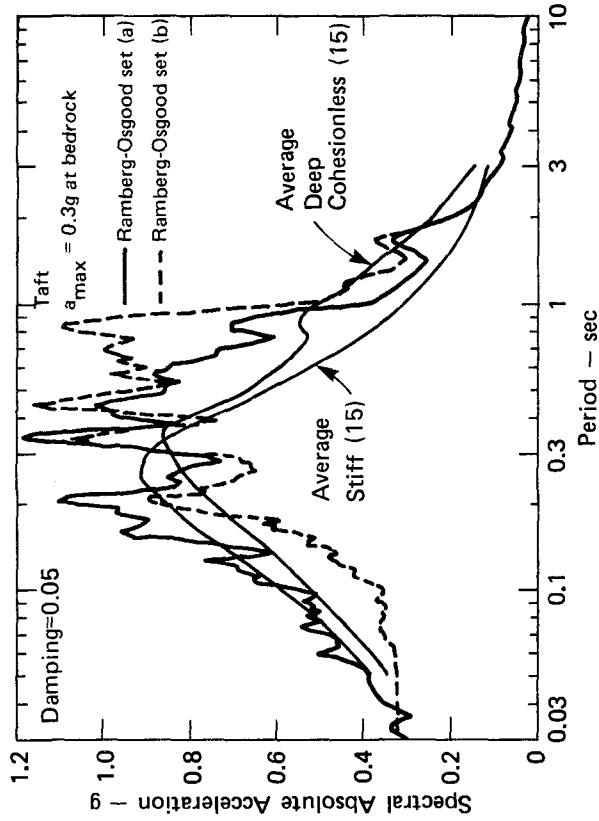


Fig. 5 Surface Response Spectra of Stiff Site: Effects of Backbone Curves and Comparison with Empirical Data

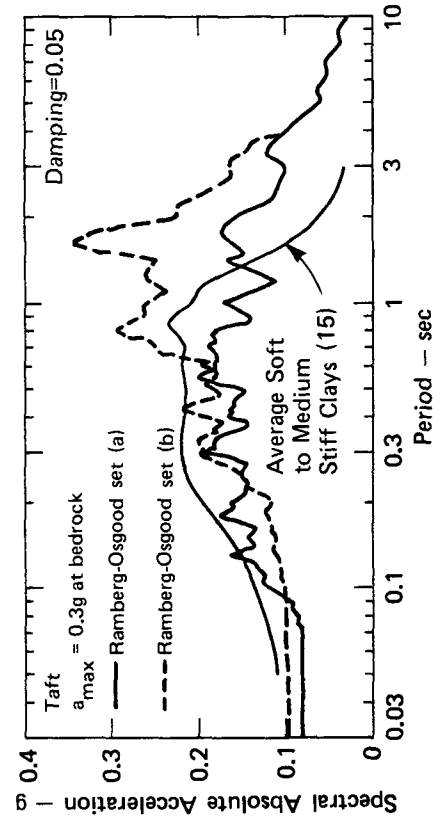


Fig. 6 Surface Response Spectra of Soft Site: Effects of Backbone Curves and Comparison with Empirical Data

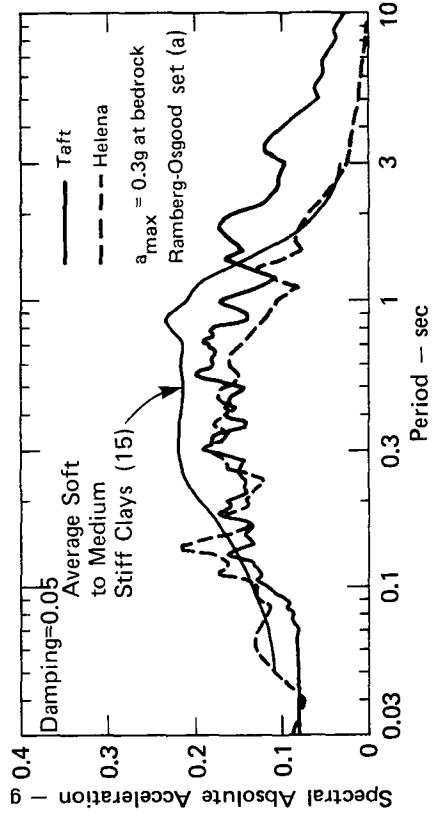


Fig. 7 Surface Response Spectra of Soft Site: Effects of Input Earthquakes



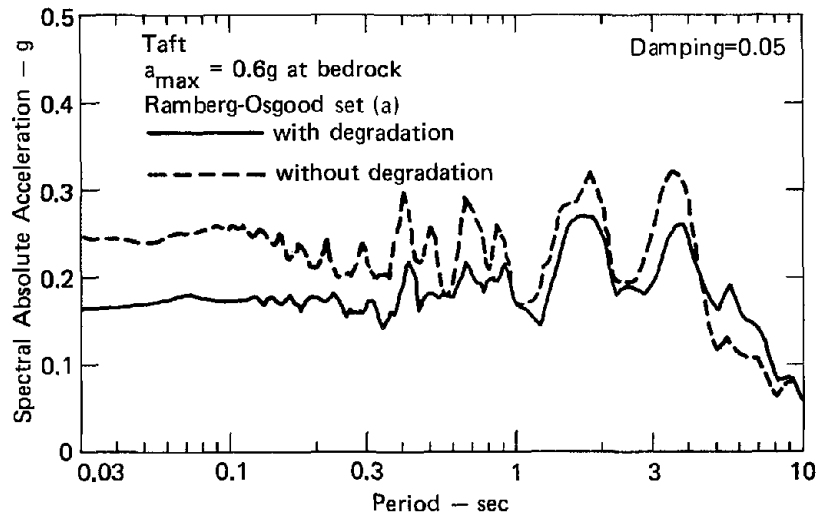


Fig. 8 Surface Response Spectra of Soft Site: Effects of Degradation

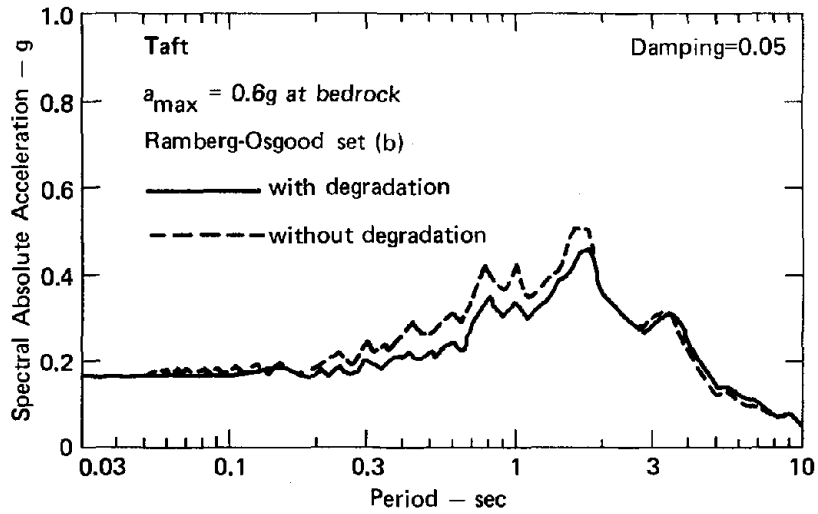


Fig. 9 Surface Response Spectra of Soft Site: Effects of Degradation

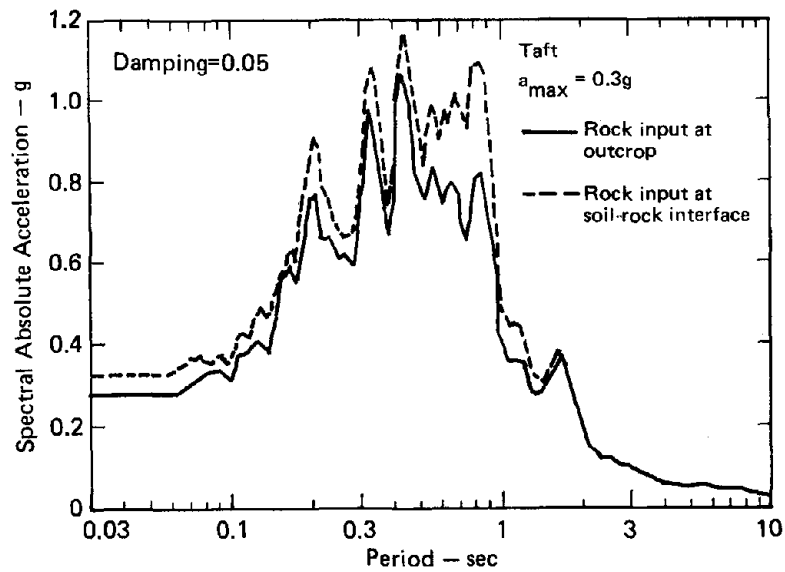


Fig. 10 Surface Response Spectra of Stiff Site: Effects of Incorporating Elasticity of Bedrock into Analysis

1446

**INTENTIONALLY BLANK**

IMPORTANCE OF SURFACE WAVES IN STRONG GROUND  
MOTION IN THE PERIOD RANGE OF 1 TO 10 SECONDS

by

H. J. Swanger<sup>I</sup> and D. M. Boore<sup>II</sup>

ABSTRACT

Analysis of the El Centro recordings of the 1968 Borrego Mountain, California, earthquake suggests that nearly all of the first 40 sec. of the largest motion in the 2 to 10 sec. period range can be described quite well by surface waves. In contrast to most engineering practice, it is this period range that is of particular concern in the design of offshore structures. The experience with the Borrego Mountain earthquake recordings suggests that surface waves will be an important component of the ground motion at the periods of interest to engineers and that existing techniques for computing surface wave characteristics can be applied to the prediction of ground motions in the offshore geologic environment, where data are not currently available. Synthesis of surface wave motion in crustal models similar to those which might be expected in a continental shelf suggest that the long period characteristics of motion are controlled not only by near surface soil characteristics, but also by the characteristics of the bedrock below. Differences in the bedrock structure with depth may result in differences in the ground response of possibly a factor of four or more. Gradients in seismic velocity with depth can amplify a wide period range. Sharp contrasts at depths as large as a few kilometers can cause strong resonances in the surface waves at particular periods. These results suggest that for long period design problems, one cannot assume that all rock structures are alike in response characteristics. More meaningful site classification may be in terms of regional geology or depth to basement, rather than surface lithology.

INTRODUCTION

Attention usually is restricted to seismic body waves in studies of effects of earthquakes on man-made structures. In most cases damage is limited to areas near the earthquake epicenter, and the majority of the ground motion appears to be a result of body waves, which seem to contain the bulk of the energy in the period ranges generally of interest for engineering purposes, less than 1 second. The response of a structure to incident body wave ground motion from below can be predicted fairly reliably. Not all ground motion from an earthquake, however, is due to body waves. Seismic surface waves (Love waves and Rayleigh waves) can contribute significantly to surface motion. Rayleigh waves can exist whenever a free surface is present. Love waves will be generated whenever shear velocities increase with depth. Even though surface waves are just superpositions of body waves, their characteristics are

---

I Graduate student of Geophysics, Stanford University, Stanford, California; now at Systems, Science, and Software, La Jolla, California.  
II Assistant Professor of Geophysics, Stanford University, Stanford, California; now at U.S. Geological Survey, Menlo Park, California.

difficult to view with the same perspective as with body waves, and generally in seismic interpretation we differentiate between the two phenomena.

There are several practical reasons for limiting interest to body waves. As mentioned, body waves are thought to have the bulk of the energy near a source. The frequency content in surface waves is generally thought to be too low to be of engineering interest. Experience has shown that the high frequency characteristics of the motion observed are controlled by near surface layering very close to the site, implying that scattered waves and wave guides may be of little importance.

Despite these practical arguments, there are reasons which suggest that surface waves and surface wave-like phenomena may be important in certain circumstances. Many engineering structures of interest have relatively long resonant periods (1-10 sec.) including very tall buildings, offshore drilling platforms, and virtually any structure of large dimensions. At these periods, surface wave motion may be larger than body wave motion at intermediate distances (tens to hundreds of km.). Because of dispersion, the duration of shaking might be quite long, and lateral strains, often not accounted for in design, may be caused by surface waves propagating with relatively low horizontal velocities.

Throughout the data set of strong ground motion recordings there are a number of instances where surface wave-like effects are seen. Trifunac (1971) gave strong arguments for surface waves in the recordings of the 1940 Imperial Valley earthquake. Anderson (1974) showed that the largest accelerations in a few of the recordings of the 1966 Parkfield, Calif., earthquake, are in time intervals consistent with surface wave arrivals. The displacement recording at El Centro, Calif., from the 1968 Borrego Mountain earthquake is dominated by what appears to be well-dispersed surface-waves (Figure 1). Hanks (1975), using rotated displacement records, points out numerous cases of dispersed waves in the period range of 2-8 sec. for the 1971 San Fernando earthquake.

All of the observations mentioned above are based on qualitative analyses; though these observations seem to fit some characteristics of surface wave-like effects, no one has verified that this motion is consistent with our knowledge of what surface wave motion should be for the given source and media characteristics. This is important to verify, because if indeed these observations do fit classical theory, we can then apply classical theory to estimate potential design motion for site specific cases (Herrmann and Nuttli, 1975a,b). This is especially important in evaluating hazards in an offshore environment where we have no strong-motion data to rely on when choosing criteria for design motion.

#### EL CENTRO RECORDING OF THE BORREGO MOUNTAIN EARTHQUAKE

To determine whether surface wave methods are useful in strong motion problems, we examined the displacement recording at El Centro of the 1968 Borrego Mountain, California, earthquake (Swanger and Boore, 1978). The ground motion at El Centro was recorded simultaneously on

a standard accelerograph and a Gardner Displacement Meter with a resonant period of approximately 6 seconds. The displacement meter response showed considerable motion at the long periods for a duration of over one minute, and the characteristics of time history suggest that the majority of the motion may be due to surface waves. This is a particularly good test case for applying surface wave methods since the earth structure near the site is known quite well from seismic refraction work and the structure appears to be nearly plane-layered near the site.

Using a source model and layered earth model chosen from independent sources, synthetics were computed for comparison to the observed displacement motion. Figure 2 shows the observed and computed motion for varying source characteristics. The source model chosen for use has only two independent quantities, the rupture velocity and moment, and the moment was chosen to match the value of observed peak displacement. The fit is quite good, even for a wide range of source details. This suggests the overall character of the recording is controlled by the media response and only weakly determined by the source characteristics. It is important to note that the layered earth model chosen contained no near surface soils. Even though there are surficial soils at El Centro, they have almost no effect on the long-period character of the observed motion. The characteristics are controlled by surface waves resonating in the entire sedimentary basin.

#### MOTION ON A CONTINENTAL SHELF

The observations at El Centro suggest that surface waves are important in the long period response of sedimentary structures, and the comparison shown implies that surface wave methods work quite well at describing the response. Next we will show some examples of what type of response one might expect in a geologic structure for which we have no data: a continental shelf. The continental shelf has a number of structural features which may be conducive to the formation of surface waves. The sedimentary cover usually extends to depths in excess of 5 km. Seismic velocities in such material will generally increase significantly with depth. Such gradients in velocity can trap waves near surface. Sharp contrasts in velocity may exist within the sedimentary system where such units of different ages overlay one another. Continental shelf environments usually have rather deep soil cover as well. The details of the long period response will depend strongly on the detailed characteristic of the media. Here we can only give some examples of what general ground motion characteristics might be expected on a continental shelf, and how these characteristics might be different from those observed onshore.

First, we compare the long period response of a "typical" continental shelf to a "typical" onshore rock site. The continental shelf model chosen contains 100 m of soft soils with properties resembling San Francisco Bay mud and 8 km of sediments with seismic velocity with depth following Faust's law (Faust, 1951). The upper 8 km of the onshore models has velocities approximately that of granite. The layered model for the two structures were the same below 8 km. Love wave motion in each model was computed at various distances from equivalent sources. Enough modes were included to model all significant surface wave motion for periods greater than 1.5 sec. Figure 3 shows

pseudo-velocity response spectra of computed transverse motion at 50 and 100 km from a source of approximate magnitude  $M_S=7.5$ . The peaks and troughs in the spectra are largely source effects rather than due to media response. The major feature in the comparison is that the overall amplitude of the longer periods is amplified on the shelf by a factor of 3 to 4.

One might assume that the controlling feature in the shelf model will be the 100 m of soft soil (with shear velocities on the order of 100 m/s). To check this, we computed the ground motion in the shelf model without any surface soils for comparison to the original motion. Figure 4 shows the ratio of pseudo-velocity spectra for motion on the shelf with and without surface soils. The variation seen here is much smaller than the factor of 3 or 4 shown in the previous comparison. At least for the period range where the calculations account for most of the ground motion periods greater than 2 sec., the shelf structure amplifies the motion considerably and amplification is controlled by the velocity below the rock-soil interface, not the soils.

It has been shown that the gradients in seismic velocity can amplify a large period band. We might expect that a sharp contrast at depth may cause resonance of a narrow period band. As an example, we computed motion for a model constructed from published refraction data off Kodiak Island, Alaska. The model contains a contrast at a depth of 1.9 km where shear and compressional velocity approximately double. No surface soils are included. Figure 5 shows computed horizontal and vertical Rayleigh wave motion at 40 km epicentral distance from an 8 km deep source. Note the peculiar character of the vertical component. The vertical motion is almost monochromatic and has its largest motion when the horizontal component is relatively quiet. The vertical pseudo-velocity response (Figure 6) reveals a strong resonance at about 4 or 5 sec. periods. Such peculiar time histories of motion may be important in the non-linear response of structures.

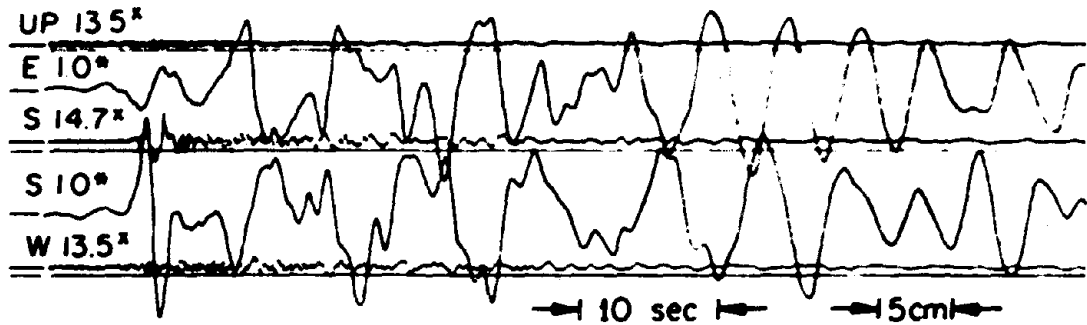
## CONCLUSIONS

It has been shown that surface wave contributions to ground motion may be a controlling feature in determining amplitudes of long period strong ground motion. Calculations indicate that the long period motion may be enhanced in sedimentary geologies where gradients in velocity with depth are present. Sharp contrasts in velocity with depth can cause resonances similar in nature to those in near-surface soils. Ground motion at the long periods is due to waves with wavelengths so long that often near-surface soil will not influence their characteristics.

Specific considerations may be required in specifying design motion for long period structures. If existing data are to be used for specifying rock motion characteristics, it may be important to use only observations made in a geologic environment similar to the site on a regional scale. For off-shore design, the most useful information will come from onshore observations in deep sedimentary basins like the Los Angeles Basin or the California Central Valley.

## REFERENCES

- Anderson, John (1974) A dislocation model for the Parkfield earthquake: Bull. Seism. Soc. Am. 64, 671-686.
- Faust, L. Y (1951) Seismic velocity as a function of depth and geologic time: Geophysics 16, 192-206.
- Hanks, T. C. (1975) Strong ground motion of the San Fernando, California, earthquake: Ground displacements: Bull. Seism. Soc. Am. 65, 193-225.
- Herrmann, R. B. and O. W. Nuttli (1975a) Ground-motion modelling at regional distances for earthquakes in a continental interior, I. theory and observations: Earthq. Eng. and Struct. Dyn. 4, 49-58.
- Herrmann, R. B. and O. W. Nuttli (1975b) Ground-motion modelling at regional distances for earthquakes in a continental interior, II. effect of focal depth, azimuth, and attenuation: Earthq. Eng. and Struct. Dyn. 4, 59-72.
- Swanger, H. J. and D. M. Boore (1978) Simulation of strong-motion displacements using surface-wave modal superposition: Bull Seism. Soc. Am. 68, 907-922.
- Trifunac, M. D. (1971) A method for synthesizing realistic strong ground motion: Bull Seism. Soc. Am. 61, 1739-1753.



(\*) Sensitivity in cm/g; (\*) Static magnification.

Figure 1.--El Centro recording of the 1968 Borrego Mountain earthquake on accelerograph (traces 1, 3, and 5) and Carder displacement meter. The amplitude scale can be derived from the listed sensitivities and the peak amplitudes of  $120 \text{ cm/sec}^2$  and  $5.7 \text{ cm}$  on the S acceleration and displacement traces (U.S. Earthquakes, Dept. of Commerce, 1968).



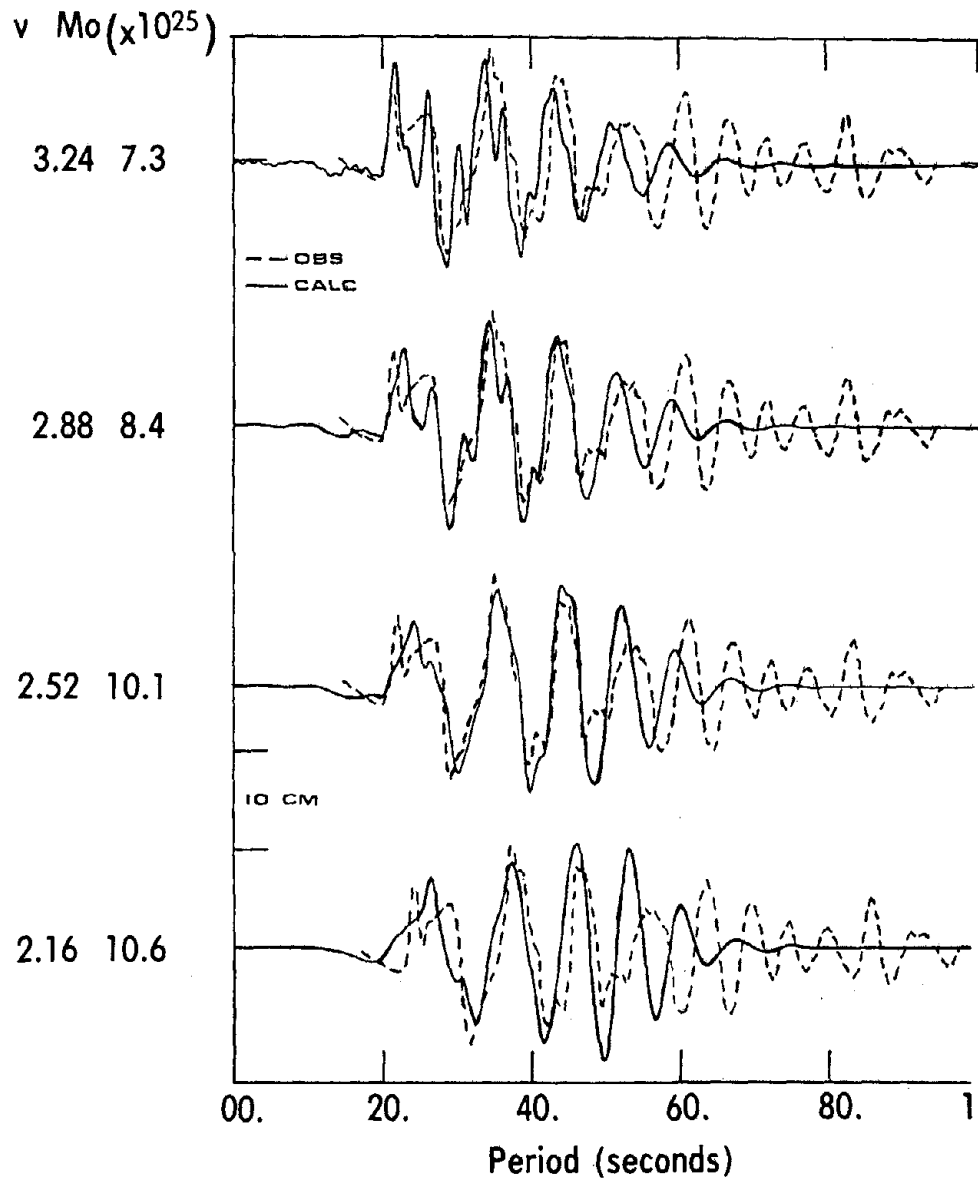


Figure 2.—Observed and calculated waves for a series of rupture velocities (in km/s) and seismic moments (in dyne-cm).

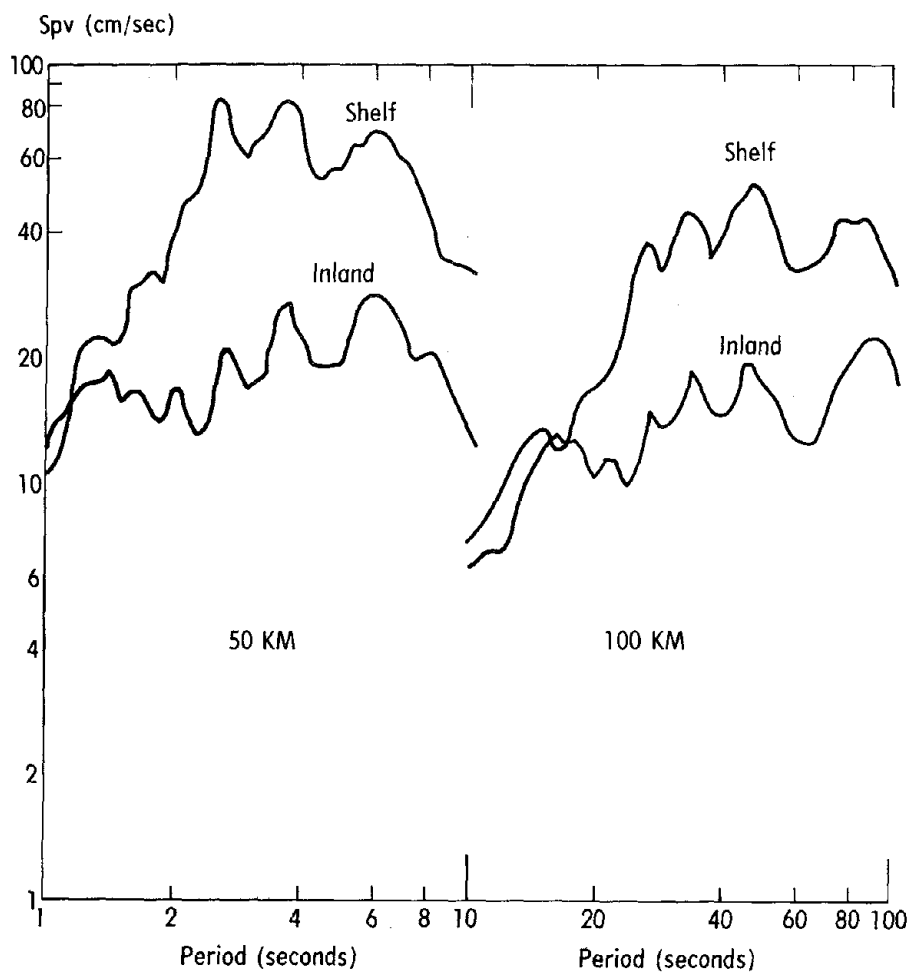


Figure 3.-Pseudo-relative velocity response ( $S_{pv}$ ) at 5% damping for surface wave motions recorded at 50 and 100 km for propagation across different geologic structures.

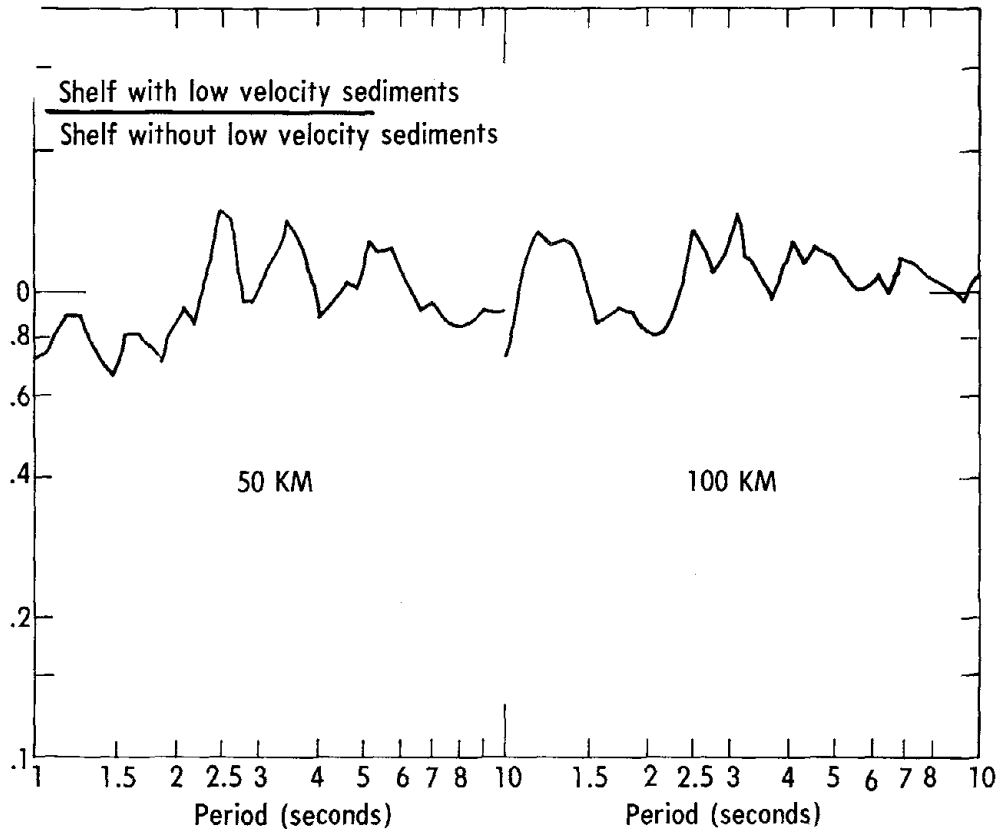


Figure 4.-Ratio of 5% damped  $S_{pv}$  at 50 and 100 km for a shelf with and without a surface layer.

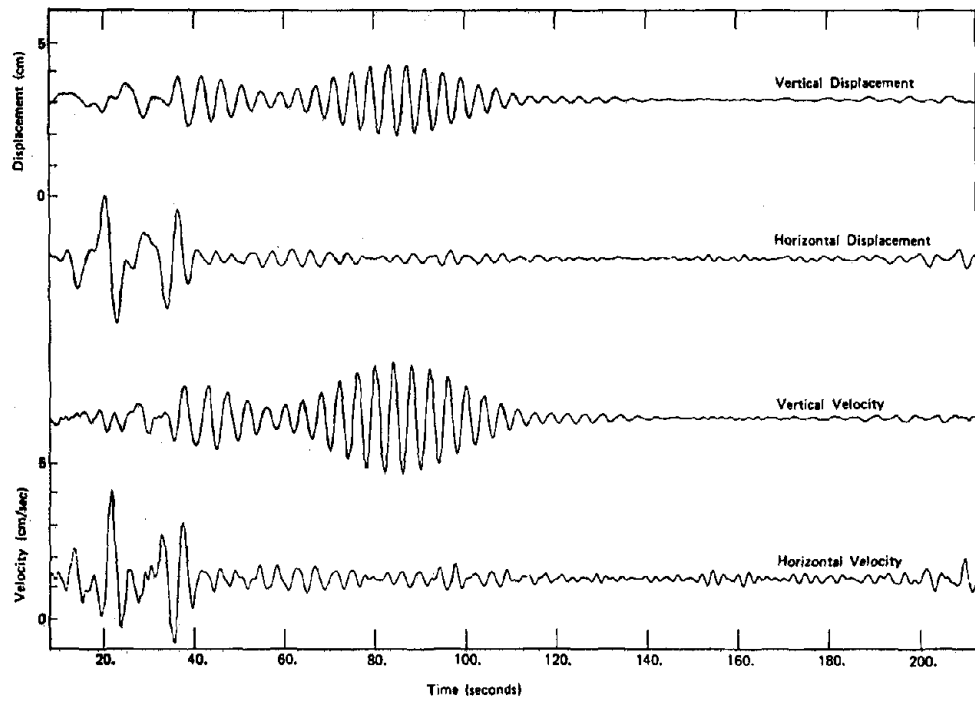


Figure 5.-Rayleigh wave displacement and velocity at 40 km for a source at 8 km depth.

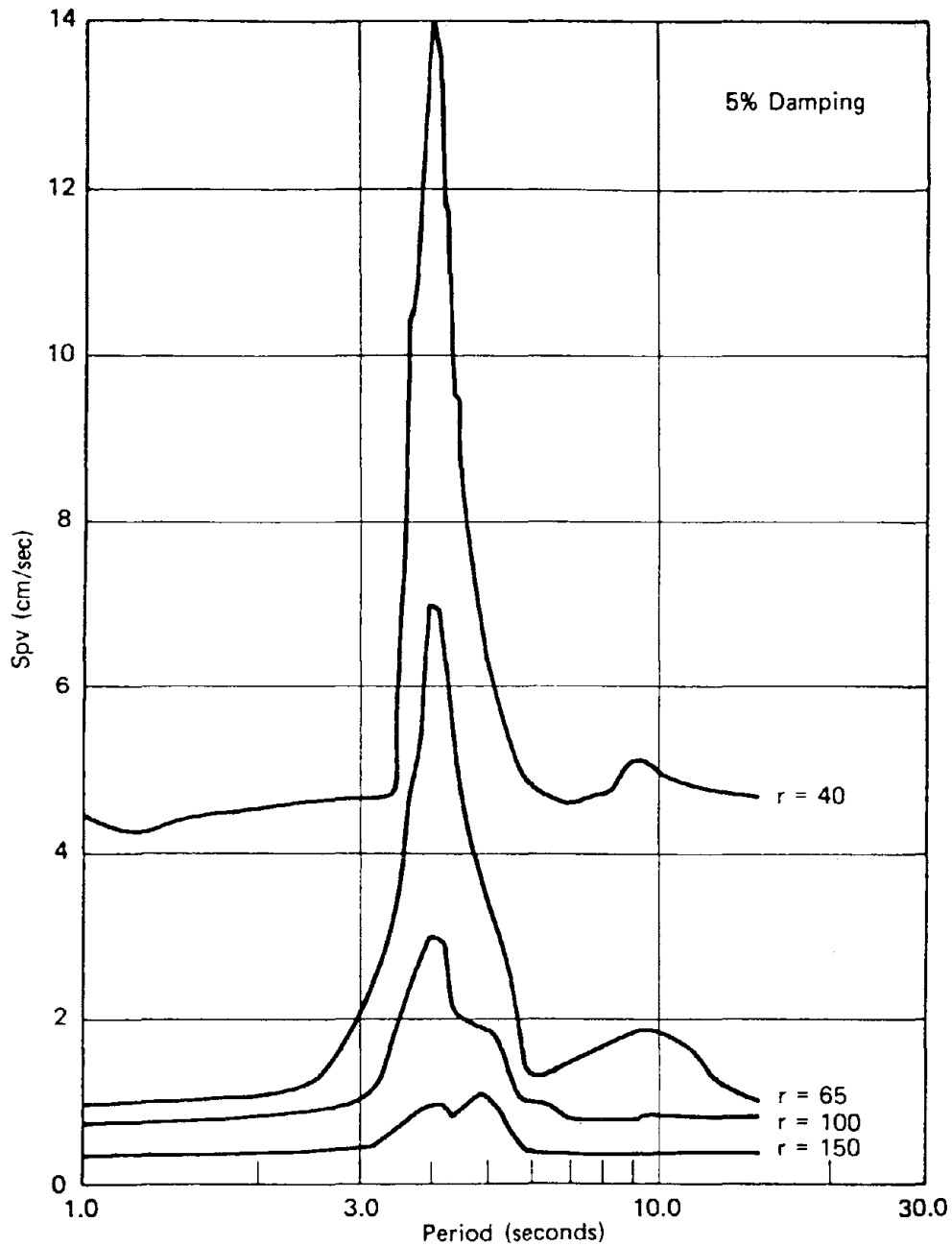


Figure 6.— $S_{pv}$  for vertical component of Rayleigh waves, at various distances with the source and geologic model used in Figure 5. Note the narrow-band resonance due to the sharp change in geologic properties with depth.

1458

**INTENTIONALLY BLANK**

## GUIDELINES FOR DESIGN OF OFFSHORE STRUCTURES FOR EARTHQUAKE ENVIRONMENT

by

I

II

J. Kallaby and W. W. Mitchell

## ABSTRACT

Earthquake hazard and its effects on siting of offshore platforms are examined. The nature of the earthquake loading and how it is applied to the structure is presented. The design philosophy underlying the API-RP2A provisions in the editions since 1976 is reviewed, and the directions for future guidelines are discussed. The behavior of systems and components is considered with respect to building ductility into a platform structure.

## THE EARTHQUAKE ENVIRONMENT

Earthquakes have been the subject of several major concerted private and government studies recently. These studies have been aimed at a better understanding of the seismological aspects of earthquakes as well as the analysis and design of structures to perform better during strong earthquakes. During these last few years, concern for public safety from earthquake hazard acquired national stature and serious funding was appropriated by the federal government for more comprehensive approach to this hazard. Several of these awards are given through the National Science Foundation (1).

## PLATFORM SITING

The siting of an offshore platform is rarely determined on the basis of high or low probability of earthquake occurrence. It is determined by the optimum location for development drilling of a hydrocarbon structure already shown to have commercial reserves. It is not unusual that such structures are geologically associated with faulting that may still be active. Hydrocarbon structures are, fortunately, usually large enough to allow a margin for siting to avoid direct placement on a fault. Such placement on or immediately adjacent to a fault should be avoided. Just how close a structure can be placed to a fault depends to a large degree on the ability of the proposed type of structure to withstand the ground motions the fault can generate at the site.

A preliminary and general guide for evaluating the earthquake hazard of a proposed platform site offshore U.S. Coastal waters is given by the API-RP2A (2). These guidelines are being updated to reflect a developing

---

I Brown & Root, Inc., Houston, Texas

II Standard Oil Co. of California, San Francisco, California

state of the art and results of recent studies. Revisions have been proposed of the hazard map for the next edition of RP2A. These proposed revisions are shown in Figure 1. To estimate the response of a proposed platform structure to the proposed site hazard, response spectra for three different soil types given by RP2A (2) are reproduced in Figure 2. It is essential that the designer views these guidelines as an effort at macrozonation whereas platform design would normally be based on a microzonation or site specific study. Such a study, recommended by RP2A, examines the proposed platform site to determine its risk or hazard and to establish several of the design parameters to be used in the study.

#### EARTHQUAKE DESIGN PHILOSOPHY

The vast majority of onshore structures located in earthquake prone regions are designed by code requirements such as those of the Uniform Building Code (3) which is used in the western states. These codes require that structures be designed for a system of static applied lateral loading. This loading is scaled in intensity depending on the period of the structure in its fundamental mode and is derived from an assumed response spectrum based on experience with performance of buildings. These requirements are generally based on the recommendations of the Structural Engineers Association of California (4).

The early offshore production platforms installed in seismically active areas such as the Santa Barbara Channel were designed in accordance with procedures established for seismic design of buildings. Subsequent developments in understanding the response of structures to earthquakes and development of computer programs for complex structural analysis have led to the application of dynamic analysis procedures for the seismic design of major structures. Dynamic analysis is used extensively for nuclear plant design and has been used to some extent for high-rise buildings. Seismic dynamic analysis was first applied to offshore platforms for the Hondo platform located in the Santa Barbara Channel with designs starting in 1969 and to the Maui A platform located offshore New Zealand with designs starting in 1973.

In 1969, the American Petroleum Institute (API) first published its Recommended Practice for Planning, Designing and Constructing Fixed Offshore platforms, RP2A. The early editions of RP2A, although suggesting that a dynamic analysis be made, presented the Uniform Building Code static design procedure for seismic design. The 7th Edition of RP2A, published in January 1976, was the first edition to present criteria for dynamic analysis. The criteria is being modified and expanded with developing state of the art.

Formulation of the API procedure for dynamic analysis considered procedures for design of nuclear plants, the Hondo platform developed by Housner and Jennings in 1969 (5), and the Maui A platform (6). The procedure includes provisions for design of platforms intended to insure no significant structural damage for the level of earthquake shaking which has a reasonable likelihood of not being exceeded during the life of the platform. These are termed the Strength Requirements. In addition, Ductility Requirements are included to insure that the platform has sufficient energy absorption capacity to prevent its collapse during rare



intense earthquake motions, although structural damage may occur. Currently, the latter criteria are satisfied by demonstrating that the platform can sustain, without collapse, twice the deck level deflection that it experiences under the Strength Requirements. In the next edition it is planned to modify this to require that the platform absorb at least four times the amount of energy absorbed under the Strength Requirements.

The analysis for the Strength Requirements calls for a description of ground motion to be used in the design. This may be in the form of ground motion records or time histories or in the form of a response spectrum depending on the analysis method the designer chooses to use. Usually the intensity and characteristics of the seismic ground motion used for the Strength Requirements are determined by site specific studies, and it is planned to give greater emphasis to such studies in the next edition of RP2A. For the case where site specific studies have not been made, however, RP2A includes seismic design criteria. These are in the form of G factors, the ratio of effective horizontal ground acceleration to gravitational acceleration, which are specified for various seismic zones (Figure 1), and normalized response spectra for several soil types (Figure 2). The seismic zone is determined from a zonation map of the United States. The 1976 edition of RP2A was based on the Uniform Building Code, which itself is based on historical earthquake damage levels. Subsequently zonation maps were developed for U.S. coastal waters based on seismic risk. The map for the 48 contiguous states is based largely on the work of Algermissen and Perkins (7). The planned next edition of RP2A will present a revised map for Alaska based largely on a seismic exposure study performed for a group of petroleum industry companies operating in Alaska, (Figure 1).

Future developments of the seismic design criteria in RP2A are not clearly defined at this time. For the next several years, they are most likely to consist of refinements of the current criteria and its expansion to cover other than steel framed platforms, to which the current criteria is limited. One likely major change is the eventual replacement of the current Ductility Requirements with guidelines for building ductility into a platform structure. The current analytical requirements are included to encourage a better understanding of the post yield and post buckling behavior of braced tubular steel structures. A better understanding has been gained for other common types of structures, such as buildings. Since the analytical methods necessary to demonstrate ductility are complex and at present costly to use, it is hoped that with experience gained from the ongoing analyses, guidelines for building ductility into a platform can be established, and the need for analytical requirements eliminated.

#### DYNAMIC VS. STATIC LOADING

As pointed out, offshore platforms designed in accordance with the present guidelines of RP2A, are to be analyzed using dynamic response techniques to account for the behavior of the platform during an earthquake, whereas building codes use static loads for analysis.

The major differences between the above two approaches are discussed (8), and summarized below:

1. Dynamic analysis considers the variation of the applied load with time while static is independent of time.
2. Dynamic analysis considers accelerations developed in a structure due to time varying deflections which, in turn, by d'Alembert's principle, create inertia forces which tend to oppose that motion. Static analysis does not deal with inertia forces.

Thus the magnitude of the inertia forces developed depends on the rate of change of the ground and platform displacement as well as the mass, stiffness and damping of the platform. Since these same forces determine the displacement of the structure, which in turn, affects the magnitude of the forces, it is necessary to formulate equations of equilibrium by use of differential equations.

#### EQUATIONS FOR DYNAMIC EQUILIBRIUM

The equilibrium equations for the nodal points in a linear structural frame at any instant in time,  $t$ , are a set of linear equations of the following form:

$$F_t = M\ddot{U} + C\dot{U} + KU \dots\dots\dots(1)$$

where  $F_t$  is the generalized time dependent load;  $M$ ,  $C$  and  $K$  are the generalized mass, damping and stiffness matrices; and  $\ddot{U}$ ,  $\dot{U}$  and  $U$  are the generalized acceleration, velocity and displacement at the node. The structure matrix is formed by combination of the various matrices of the structural elements.

In the case of prescribed base motion Eq. 1 becomes

$$-M\ddot{U}_b = M\ddot{U}_r + C\dot{U}_r + KU_r \dots\dots\dots(2)$$

where  $U_r$  is the relative displacement of the node with respect to the base or

$$U_r = U - U_b \dots\dots\dots(3)$$

#### EVALUATION OF DYNAMIC PROPERTIES

The dynamic properties of the structure are evaluated by allowing the structure to vibrate freely with or without damping. In the case of free damped vibration, this is done by setting  $F_t$  in equation 1 equal to 0. Dividing the resulting equation by the generalized mass,  $M$ , gives the damped free vibration of a single degree of freedom system or, for each mode  $n$ , of a multidegree of freedom system.

$$\ddot{U}_n + 2\xi_n \omega_n \dot{U}_n + \omega_n^2 U_n = 0 \dots \dots \dots (5)$$

where  $\xi_n$  is the damping ratio of the specified damping to the critical damping and is defined by

$$\xi_n = \frac{C_n}{2M_n\omega_n} \dots \dots \dots (6)$$

and  $\omega_n$  is the circular frequency defined by

$$\omega_n = \left(\frac{K_n}{M_n}\right)^{\frac{1}{2}} \dots \dots \dots (7)$$

Calculation of the mode shapes,  $\phi_n$ , requires solution of the generalized eigen-value problem where

$$K_n\phi_n = \omega_n^2 M_n\phi_n \dots \dots \dots (8)$$

#### MAGNITUDE OF EARTHQUAKE GENERATED FORCES

The sizing of members and joints of a platform controlled by earthquake criteria, is dictated by the magnitude of the inertia forces. This magnitude is influenced to a large degree by the following factors:

1. The Earthquake Event: This is measured by the intensity, frequency content and duration of the event. Usually, larger forces are generated by higher intensity and higher frequency events, and more destructive displacements are generated by longer durations.
2. The Stiffness of the Structure: In general, the stiffer structures generate larger forces. However, as a structure undergoes significant inelastic deformation, its response to earthquake motions is diminished. Present API RP2A guidelines (2), require a platform structure to maintain its stability through prescribed ductility excursion.
3. The Mass of the Platform: The larger the mass the larger the inertia forces. However, increasing the mass increases the natural periods of the platform which in turn reduce the forces. Usually, increasing the mass will increase the forces. It should also be pointed out that the mass of the deck equipment and supplies may vary significantly for the short duration drilling period as compared to the long duration production period. This should be considered in the risk evaluation and establishment of the site specific design criteria. This differentiation is presently left by the RP2A guidelines in the hands of the owner and his qualified consultants.

4. The Added Mass: The added mass is the apparant increase in the mass of the platform due to its presence in water. This increase may vary between 10% and 50% of the platform mass, including enclosed water, and invariably tends to increase the inertia forces. This increase is mitigated by the resulting longer platform period and the damping effect of interaction between structure and surrounding water. The added mass is variable and depends on the size of the member, its location relative to the water surface and the orientation of its longitudinal axis to the accelerating water particles. For the typical jacket or template type structures, the added mass may conservatively be assumed as the mass of the displaced water for members whose long axis is transverse to the direction of motion and may be neglected if the motion is parallel to the axis. The API RP2A recommend these values but encourages use of other values for structures such as gravity platforms based on analysis and confirmation tests as appropriate.

#### BEHAVIOR OF STRUCTURES UNDER EARTHQUAKE LOADINGS

The predicted response of offshore platforms to strong earthquake ground motion has been calculated in a number of analytical studies and for several actual structures which have been or are planned to be installed. Most of the actual designs and some of the studies have used three dimensional analytical models of the structure with representations of the piles and pile-soil interaction included. Both the time history and the response spectrum method of analysis have been used. The analyses have been made using computers to determine the characteristics of the structural system and the response to the design ground motions.

Analyses have been reported for platforms in water depths up to 850 feet, (Platform Hondo). Platform response is significantly affected by the load deflection behavior of the foundation in the horizontal direction and in the vertical direction. For analyses where the response of the platform structure is within the elastic range, as in the case of Strength design, the overall response is predominantly governed by the first transverse bending modes for the shallower structures and by the first two transverse bending modes for deeper structures. Vertical response is significant for portions of the structure such as the deck, legs and piles. Torsional response is important for structures which are unsymmetrical in layout or mass distribution. The natural periods of vibration of the predominant modes for the reported analyses generally lie between 1.0 and 5.0 seconds. Consequently, structural response has been dominated by peak ground motion velocity rather than peak ground motion acceleration. For Platform Hondo, for example, little difference in peak response was reported (10) between the response to the 1971 Pacoima Dam ground motion record having a peak acceleration of 1.20 g and the response to the 1940 El Centro ground motion record scaled to a about 0.30 g peak acceleration. Thus, using averaged response spectra based on ground acceleration for design, it is important that the effective ground acceleration be used for scaling the design spectra rather than peak acceleration.

Several predictions have been made of the response of platforms following the initial yielding or buckling of structural members. Kallaby and Millman (6) presented a static analysis procedure for making such predictions. The procedure includes an algorithm based on tests made at the University of California at Berkeley for the post-buckling behavior of tubular compression members (9). The procedure was applied to the Maui A Platform, a four-leg self-floating platform containing k-braced, diagonally braced and x-braced panels. The analytical model yielded first in an X-braced panel. The lateral load capacity of the platform continue to increase until one of the diagonal braces in a K-braced frame buckled. Following the buckling of the brace, other horizontal braces and vertical legs in the vicinity of the buckled brace yielded and other diagonal and horizontal braces at the same level on the opposite side buckled, resulting in a significant decrease in lateral load carrying capacity of the structure. The analysis was carried to a deflection at the deck level of 1.37 times that when first yield was experienced, at which point the lateral load carrying capacity had been reduced about 30 percent. Deflection at first yield is not the same as the deflection under the Strength Requirement earthquake and is usually larger.

Delflache et al (10) presented results of the analysis of Platform Hondo for which the design criteria required demonstration of structure ductility beyond the elastic range. The platform is an eight-leg structure with X-bracing in two-legged bents and diagonal bracing in opposite directions in four-legged bents. Thus, a portion of the shear at each level is carried in diagonal tension members regardless of the direction of the induced earthquake loading. The results of the analysis show increasing load carrying capacity of the structure with deflections in excess of 1.25 times the deflection at first yield. The calculated post-yield deflection was more than twice the deflection calculated for the structure for the level of ground motion having a significant probability of occurrence within the life of the structure.

Marshall, Gates et al (11, 12) presented the results of inelastic analyses of a two dimensional X-braced frame. Criteria are presented for the post-yield and post-buckling behavior of members, including criteria for degradation of load carrying capacity in compression of members under cyclic loading. Criteria are also presented for terminating the failure of members developing plastic hinges.

The two dimensional frame as originally proportioned lost considerable horizontal load carrying capacity after initial buckling of the compression diagonal because the horizontal braces buckled before the stress load could be transferred to the tension diagonal. In the word of the authors, "Once the horizontal struts buckled, all the significant diagonal braces...buckled or yielded, "unzipping" the primary lateral force resisting system." When the size of the horizontal braces was increased, a significant improvement in post-yield behavior of the structure was noted. In an X-braced frame, the horizontal braces are very lightly loaded when the tension and compression braces are sharing the lateral load equally. However, when inelastic behavior occurs in the diagonals, the loads in the horizontal braces increase substantially in order to redistribute the shears. For the originally proportioned structure, a substantial

reduction in lateral load carrying capacity occurred when the deflection at the deck exceeded 1.36 times the deflection at first yield. The modified structure maintained a high lateral load carrying capacity through a deflection 3.0 times that at first yield. The corresponding amount of energy absorbed was over five times that absorbed at first yield. Even greater ductility may have been achieved had the strength of the horizontal braces been increased further.

#### DESIGN OF TUBULAR JOINTS FOR EARTHQUAKE ENVIRONMENT

Joints that tie major framing together such as legs and main bracing elements are critical to the adequate performance of a platform in earthquake zones 3, 4, and 5. It is suggested that such joints maintain their load carrying capacity well beyond first yield. This is done by limiting the diameter to thickness ( $D/t$ ) ratio of the members forming the joint. Fortunately, such limitation does not change the platform steel tonnage significantly. It is usually less than 1% in a typical template.

Several recent studies have attempted to determine the plastic rotational capacity of tubular members (13,14). Present RP2A (2) guidelines limit joints that may be required to maintain their capacity through substantial inelastic deformation to a  $D/t$  ratio of  $1300/F_y$  based on earlier work. Sherman (13) indicates that joints with  $D/t$  ratios of  $1700/F_y$  also demonstrate ductility ratios of 3 to 10 times yield deformation which may be adequate for the majority of the joints which are not expected to undergo substantial inelastic rotation. Tubes with  $D/t$  ratios of  $2700/F_y$  and  $3600/F_y$  buckled shortly after reaching yield, and RP2A requires a maximum  $D/t$  ratio of  $3300/F_y$  for joints designed to preclude local buckling prior to yield.

#### GUIDELINES FOR BUILDING DUCTILITY INTO A PLATFORM STRUCTURE

Results of previous platform studies and designs suggest guidelines for building ductility into platforms which, if followed, might eliminate the need to perform a nonlinear analysis to demonstrate ductility. In general, these guidelines would assure good overall structure ductility and would provide assurance against premature load member and joint failure before the overall structure ductility is attained. Several important guidelines are already noted in RP2A. These include:

- . Requirements for maximum diameter to thickness ( $D/t$ ) ratios for tubular members which are subject to inelastic deformation under a rare intense earthquake. These limitations have been established from the results of laboratory tests and are intended to avoid local buckling within the members.
- . A suggestion that connections of primary members be designed to develop a strength in excess of that of the member. It is planned to strengthen this guideline in the next edition of RP2A by requiring that for seismically active areas, joints

for primary structural members be designed for either the tensile yield load or the compressive buckling load of the members framing into a joint, as appropriate for the ultimate behavior of the structure.

Other guidelines which might be developed to assure good ductility include:

- A requirement that vertical bracing systems be established such that a portion of the lateral shear forces within the structure at any level be carried by a member in tension regardless of the direction of the force. The tension brace should not be dependent on the stability of a companion compression brace, such as in a k-braced frame, to develop the full tensile yield stress in the member. If such a framing system is not feasible at a particular level within the structure, the bracing in that level should be designed using lower allowable stresses. Elsewhere, to the extent practical, the diagonal bracing members throughout the structure should be designed to have nearly the same level of stress with respect to yield under earthquake loading in order to avoid limiting inelastic deformation to one area of the structure only. Horizontal members in vertical bracing systems should be designed to transmit the forces required to develop the full yield capacity of the tension braces in the panel immediately below, assuming that diagonal compression braces are ineffective.
- More conservative slenderness ratio limitations for primary members than required in non-seismic areas. Kallaby (15) has suggested specific limitations for braced and unbraced framing. Good design practice has shown that  $Kl/r$  for braced framing be between 80 and 100 for braced framing and between 70 and 90 for unbraced framing. These limitations are desirable to attain improved post-buckling behavior of compression members as demonstrated by laboratory tests of statically loaded members. The benefits of lower slenderness ratios should be confirmed by cyclic testing of tubular frames.

#### ACKNOWLEDGEMENT

The authors wish to acknowledge their appreciation to Dr. J. B. Weidler, Brown & Root Offshore Structures Department for his valuable comments.

## BIBLIOGRAPHY

1. National Science Foundation, Division of Advanced Environmental Research and Technology, Summary of Awards, Fiscal Year 1977, Rann, NSF 77-74, Washington, D.C.
2. American Petroleum Institute, Recommended Practice for Planning, Designing, and Constructing Fixed Offshore Platforms, API-RP2A, Ninth Edition, November 1977, Dallas, Texas.
3. International Conference of Building Officials, Uniform Building Code, 1976 Edition, Whittier, California.
4. Structural Engineers Association of California, Recommended Lateral Force Requirements and Commentary, 1975, San Francisco, California.
5. Housner, G. W. and Jennings, P. C., Earthquake-Resistant Design of Drilling Towers in the Santa Barbara Channel, June 1968.
6. Kallaby, J. and Millman, D., Inelastic Analysis of Fixed Offshore Platforms for Earthquake Loadings, Offshore Technology Conference Proceedings, OTC Paper 2357, 1975, Houston, Texas.
7. Algermissen, S. T. and Perkins, D. M., A Probabilistic Estimate of Maximum Acceleration in Rock in the Contiguous United States, Open File Report 76-416, United States Geological Survey, 1976.
8. Kallaby, J., Design Considerations for Fixed Platform, Part 1, Special Earthquake Engineering Report, Ocean Engineering, September 15, 1976, Dallas, Texas.
9. Bouwkamp, J. G., Buckling and Post-Buckling Strength of Circular Tubular Sections, Offshore Technology Conference Proceedings, OTC Paper 2204, 1975, Houston, Texas.
10. Delflache, M. L., Glassrock, M. S., Hayes, D. A. and Ruez, W. J., Design of the Hondo Platform for 850-Foot Water Depth in the Santa Barbara Channel, Offshore Technology Conference Proceedings, OTC Paper 2960, 1977, Houston, Texas.
11. Gates, W. E., Marshall, P. W. and Mahin, S. A., Analytical Methods for Determining the Ultimate Earthquake Resistance of Fixed Offshore Structures, Offshore Technology Conference Proceedings, OTC Paper 2751, 1977, Houston, Texas.
12. Marshall, P. E., Gates, W. E. and Anagnostopoulos, S., Inelastic Dynamic Analysis of Tubular Offshore Structures, Offshore Technology Conference Proceedings, OTC Paper 2908, 1977, Houston, Texas.
13. Sherman, D. R., Tests of Circular Steel Tubes in Bending, Journal of the Structural Division, ASCE, Vol. 102, No. ST11, 1976.



14. Sherman, D. R., Tentative Criteria for Structural Applications of Steel Tubing and Piping, American Iron and Steel Institute, SP 604-876-7-5 M-MP, 1976.
15. Kallaby, J., Considerations for Analysis and Design of Piled Offshore Structures in Severe Earthquake Environment, Offshore Technology Conference Proceedings, OTC Paper 2748, 1977, Houston, Texas.

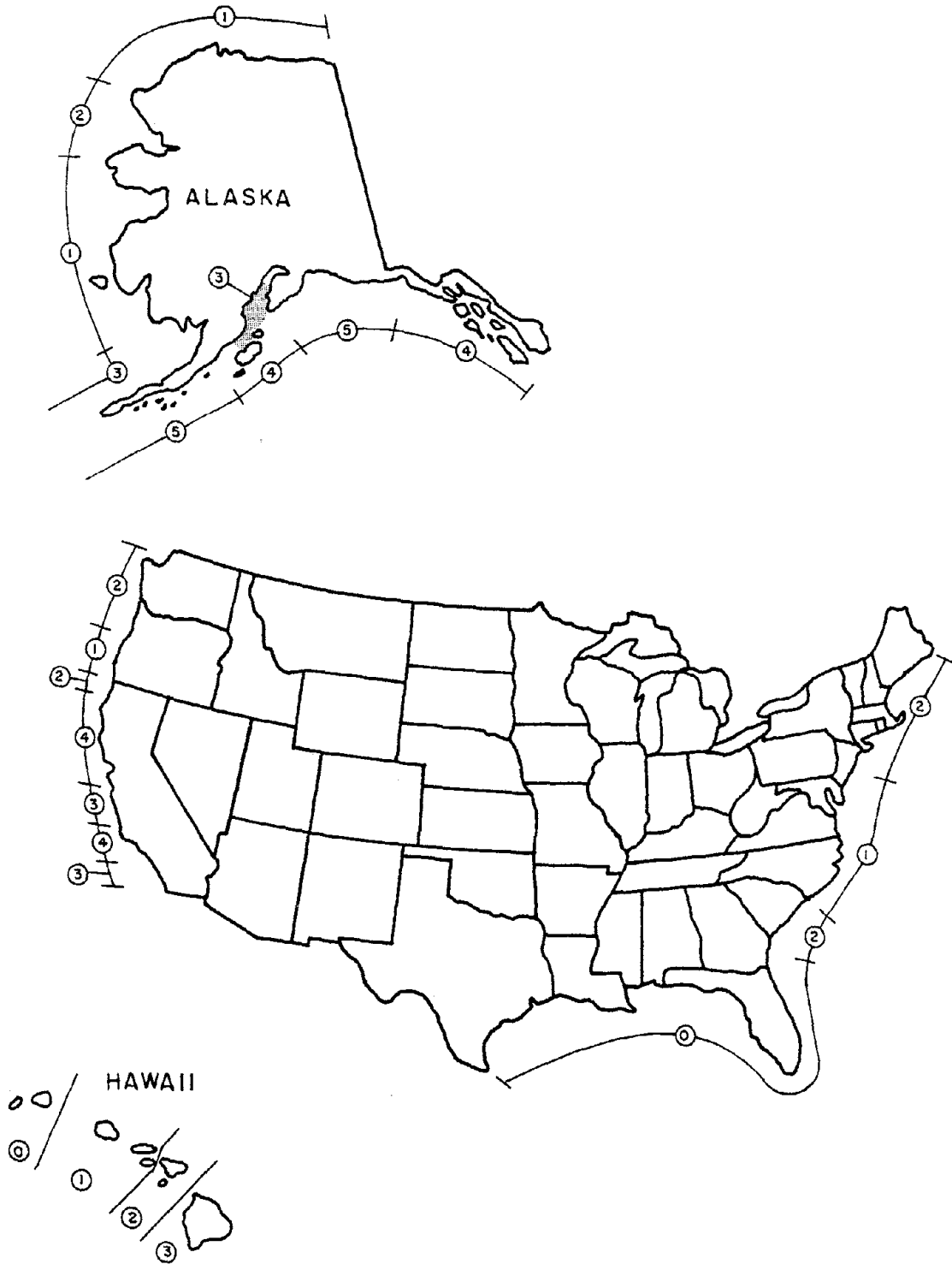
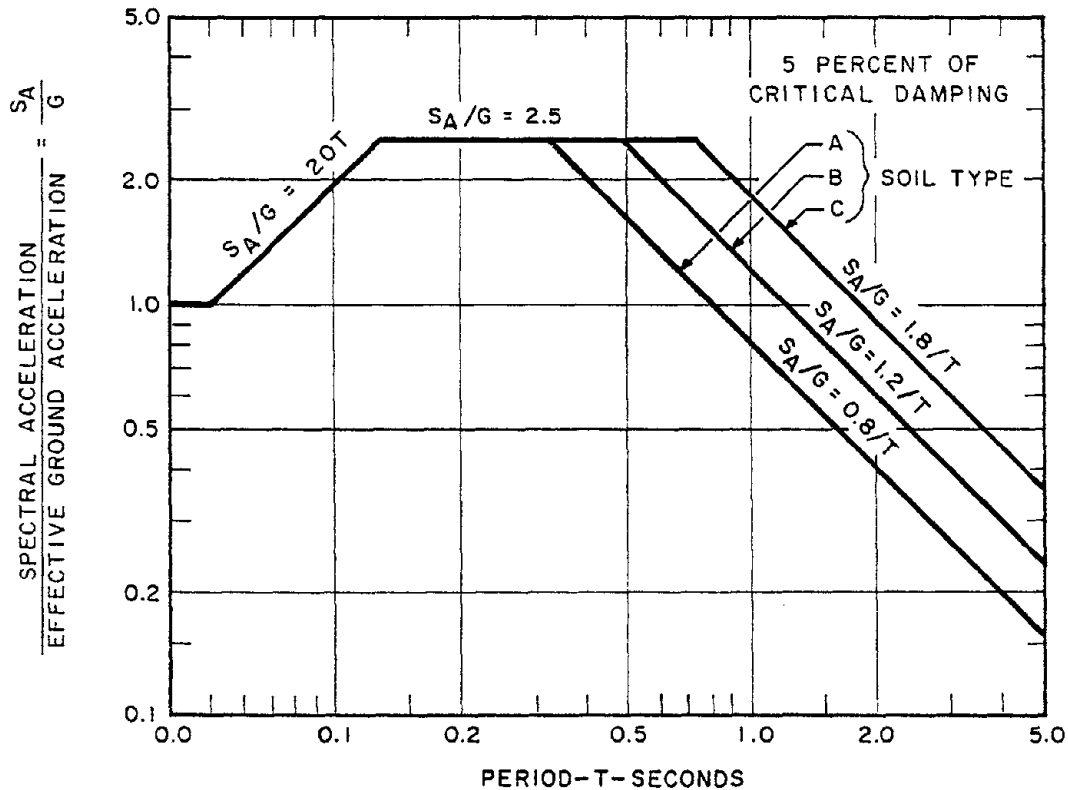


FIGURE 1: PROPOSED SEISMIC RISK MAP OF UNITED STATES COASTAL WATERS



$S_A$  = SPECTRAL ACCELERATION

$S_V = \frac{T}{2\pi} S_A$  = SPECTRAL VELOCITY

$S_D = \frac{T^2}{4\pi^2} S_A$  = SPECTRAL DISPLACEMENT

### SOIL TYPE

- A. Rock - crystalline, conglomerate, or shale-like material generally having shear wave velocities in excess of 3000 ft/sec (194 m/sec).
- B. Shallow Strong Alluvium - Competent sands, silts and stiff clays with shear strengths in excess of about 1500 psf (72 kPs), limited to depths of less than about 200 feet (61 m), and overlying rock-like materials.
- C. Deep Strong Alluvium - Competent sands, silts and stiff clays with thicknesses in excess of about 200 feet (61 m) and overlying rock-like materials.

FIGURE 2: RESPONSE SPECTRA NORMALIZED TO 1.0 GRAVITY

1472

INTENTIONALLY BLANK

1473

***URBAN PLANNING, SOCIO-ECONOMICS***

***AND GOVERNMENT RESPONSIBILITY***

***SESSION***

1474

INTENTIONALLY BLANK

1475

THE POLICY AND ADMINISTRATIVE IMPLICATIONS OF  
SEISMIC MICROZONATION: TOWARD LOGIC OR CONFUSION?

by

Robert A. Olson  
Seismic Safety Commission  
Sacramento, California

INTRODUCTION

It is evident from the literature on "microzonation" that (1) there is no universally accepted definition of the term, and (2) the policy implications of seismic microzonation have not been clearly recognized.

The underlying assumption of this paper is that the quest to develop microzonation techniques and apply them has implications for public policy and decision-making, especially as such techniques relate to the regulation of land and the application of construction codes and standards. This paper is limited to clarifying some of the issues that may have to be faced when, and if, attempts are made to implement the principles and procedures of microzonation through the policy process.

From the viewpoint of public policy, "microzonation" appears to be a process consisting of several techniques used to evaluate the seismic, geologic, and soils characteristics of areas as large as perhaps a multi-state region or as small as a building site for the purpose of determining the potential susceptibility of damage to structures from earthquakes. Logically, the next step would be to apply more or less stringent practices, standards and procedures on the use of land and construction. If reasonably correct, this definition allows a look at the application of "microzonation" in earthquake hazard reduction programs and a review of two actual and a fictitious earthquake that further illustrate some of the issues inherent in the possible use of microzonation.

THE APPLICATION OF "MICROZONATION" IN EARTHQUAKE HAZARD REDUCTION

The literature indicates microzonation has evolved from a strong desire to reduce the understanding of world seismicity to smaller and smaller units. Researchers have produced intensity, isoseismal, seismic risk, epicenter, expected peak acceleration, geologic, soils, and similar maps for the world, continents and parts thereof including countries, regions within countries, and even smaller areas. Some of these products affect decision-making, and nearly all of them are based on different information, assumptions, and qualifications. A special concern is where the boundaries are between seismic regionalization and microzonation.

For research purposes and in their appropriate contexts these maps and similar data are important tools. However, if the full array was shown to a group of users, such as representatives from local planning, zoning and building permitting and inspection agencies, one can hypothesize that there would be both concern and confusion about how to apply them technically and equitably in various regulatory programs.

Gaus and Sherif (1972) stated the intended application of microzonation when they said:

...the process of zoning of earthquake effects has been discussed without giving consideration to the factors which might enter into a zoning procedure or what, importantly, is the appropriate size of a zone as determined by the needs of the ultimate users of such procedures. In the past it has been common to draw up maps showing earthquake zones; however, these zones have generally covered large areas in which an entire country might typically be divided into three zones. This is adequate for presenting the expected range of various sizes of earthquakes, but is not really adequate for the user who is responsible for the detailed design of a structure. Events in various earthquakes such as the one which shook Caracas, Venezuela in 1967 illustrated the effects of amplification and interaction which can occur in local regions and for particular structures. From this one can infer the need for a more detailed zoning procedure of microzonation to serve as a guide for safer land use and construction. A microzonation procedure would provide the general guidelines to be followed in a region and would form the basis for regulations for most structures. (Emphasis added)

In another paper, Bostrom and Sherif (1972) further discussed the policy implications of microzonation when they noted that:

The application of microzonation in practice supposes a willingness on the part of the public and owners of new construction to expend limited sums of money in the short term in order to effect a long-term saving in money and lives. Regulation is necessary because the expenditure required in zonation and adaptation must be expended by agencies other than those reaping the long term savings. For this reason, it has become apparent that adequate regulations in the form of a quantifiable zonation and a uniform building code will only be accepted in so much as their intention is fully understood, and the general benefit appreciated.

Some earthquake hazard reduction programs in California do recognize relative seismicity within the State. A few examples are worthy of summary since they involve the use of microzonation to some degree.

The regulations governing public school construction since 1933 under the provisions of the Field Act now recognize relative seismicity by using zones which are demarcated by cultural features, such as county lines, highways, or others. It is proposed that the regulations which control the construction of new hospitals and related facilities statewide, under the Hospital Seismic Safety Act, recognize relative seismicity by following the same procedure. Currently, only one zone is used.

The "Tentative Provisions for the Development of Seismic Regulations for Buildings" prepared by the Applied Technology Council approach the problem by establishing a "Seismicity Index" which gives design values for each county in the United States. Thus, such values could be easily applied by government.

The process used by the Engineering Criteria Review Board of the Bay Conservation and Development Commission typifies another process. Charged with regulating the use of land around the perimeter of San Francisco Bay,



the Commission relies upon the Board to recommend as part of the permit process the standards to be followed in the siting, design and construction of a given facility. This involves the consideration of geologic, seismic, soils and design factors for a particular building site. The Board's recommendations almost always become stipulations in the permit granted by the Commission.

The Uniform Building Code recognizes relative seismic risk on a national scale through its zoning map. The 1976 version shows two zones in California. The State usually adopts it as a minimum under the provisions of the Earthquake Protection Law, and local governments usually do the same with some modifications. However, codes are administered on the basis of political boundaries, and although very little data exists, it appears that where local governments are uncertain about which zone they should use, they select one and apply it uniformly.

The insurance industry has taken a similar approach to the ATC in applying seismic risk in California. Twenty-nine counties are included in Zone 3, and the balance of the State is in Zone 1 for earthquake insurance rating purposes. This approach also recognizes both the earthquake hazard and administrative realities.

Thus, in earthquake hazard reduction programs administered or regulated by State and local governments in California there is no uniformity, and microzonation is not consciously used as a technical program for making decisions.

#### CASE STUDIES ILLUSTRATE THE ISSUES

The Santa Rosa, California earthquake of 1969, the actual measurement of ground motion on a small scale basis, and a fictitious scenario prepared for a workshop on earthquake hazardous buildings demonstrate the issues that may confront policy makers when they try to implement administrative and regulatory measures based on seismic microzonation.

Studies by Steinbrugge and others showed that damage from the October 1, 1969 Santa Rosa, California earthquakes was not distributed evenly throughout the city, nor was the varying damage pattern fully explainable by soil-structure interaction. Pockets of damage were observed within the city limits that implied that the shaking was greater in some areas than others (see Figure 1).

Although some of the damage occurred to structures built prior to the city's first use of lateral force requirements in the Uniform Building Code, it is clear that the construction of most buildings was regulated by some version of the UBC. Thus, given this propensity for varying damage patterns and the uniform application of the code, what issues would face both the City Council and the Building Department if microzonation techniques were to be used in the city as a means of limiting future earthquake damage?

First, except for individual site studies which would probably be uneconomical for most structures, could the expected damage zones within the city be defined clearly enough to be administered logically? What controversy and extra costs are implied when differing standards may be required for individual buildings or different sections of town? Can the



# SANTA ROSA AND VICINITY

### LEGEND

- U.S. HIGHWAY NUMBER
- STATE HIGHWAY NUMBER
- BLDG. NUMBER
- SCHOOL
- ONE-WAY STREET

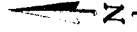
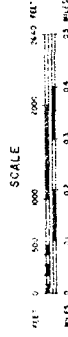
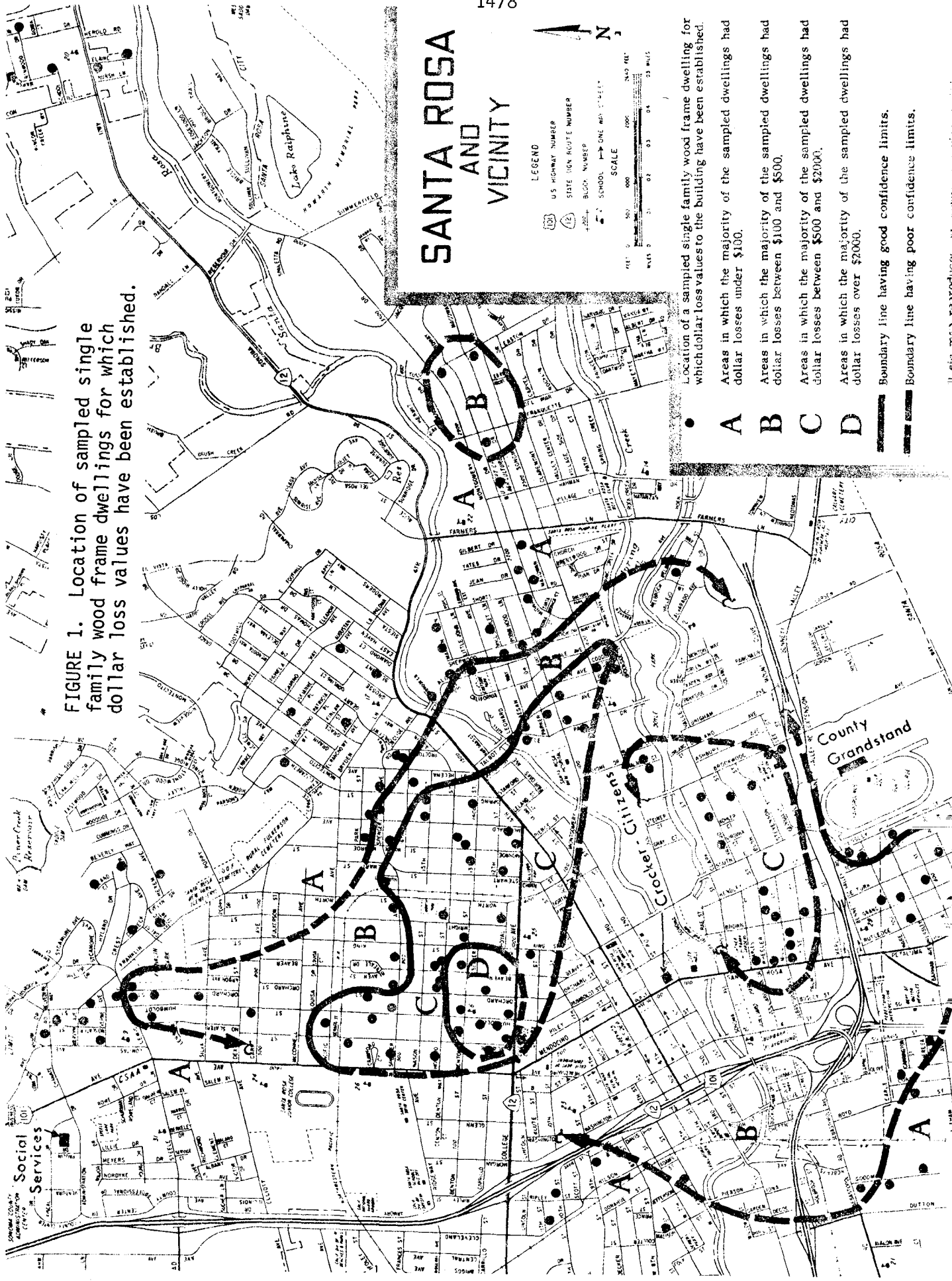


FIGURE 1. Location of sampled single family wood frame dwellings for which dollar loss values have been established.

- Location of a sampled single family wood frame dwelling for which dollar loss values to the building have been established.
- Areas in which the majority of the sampled dwellings had dollar losses under \$100.
- Areas in which the majority of the sampled dwellings had dollar losses between \$100 and \$500.
- Areas in which the majority of the sampled dwellings had dollar losses between \$500 and \$2000.
- Areas in which the majority of the sampled dwellings had dollar losses over \$2000.
- Boundary line having good confidence limits.
- Boundary line having poor confidence limits.

A B C D



techniques themselves support such finite applications? After the next earthquake, would the damage be "equalized" between one zone and another? Conversely, would there be controversy and liability associated with damage to structures built to the more stringent requirements in one zone that failed to perform as well as those in a "less hazardous" zone nearby? Lastly, would the application of microzonation techniques assure that structures respond appropriately to all possible damaging earthquakes that could affect the city?

This last concern has been recognized by Richter when he discussed the many variables, including cultural ones, that may relate to damage in cities. He noted:

Regionalization of a large city presents special problems, which depend in close detail on the character of the ground. Where there are appreciable differences of level, the hilly and elevated areas, for which earthquake risk is generally less, are normally occupied by residences and small business. The principal business and industrial centers, and of course harbor development, are usually on lower ground, which may be sandy, alluvial, or even marshy. This lower ground is often also occupied by dilapidated residential sections, with numerous old structures which are fire and disease traps as well as earthquake risks.

Local spots of artificial fill, replacing old ponds or rubbish pits, or originating in grading uneven ground, are danger areas difficult to detect without careful study of old records.

Alcock used the ground responses from the 1969 Rulison nuclear gas stimulation explosion in Colorado to study the distribution of damage to structures in the town of Grand Valley. Without going into the details, the ground motion produced by the explosion was equivalent to a 5.3 magnitude (Richter) earthquake, and there was correlation between the ground motion and damage (see Figure 2):

The correlation of ground resonance, structure location, and damages is shown in Figure 2. An analysis of this data shows that of the 92 structures located in sites where the ground resonance is greater than 12.5 Hz, 26 structures had architectural damage. Of the 92 structures located on sites with a ground resonance of less than 12.5 Hz, 54 structures suffered architectural damage. The structures in Grand Valley are fairly typical of the area being one and two story wood frame with a few concrete block, brick and masonry buildings.

One then is confronted with the following question: If microzonation techniques are valid and if they had been used to regulate construction in the city, would the results of the earthquake have been the same or different, and if different, how much? In other words, would the application of microzonation have been judged an effective public policy?

"Santa Luisa," California, a fictitious city created by the Seismic Safety Commission for the purpose of evaluating the policy implications of abating earthquake hazardous buildings, provides a useful example for studying the potential implications of microzonation for the policy process.

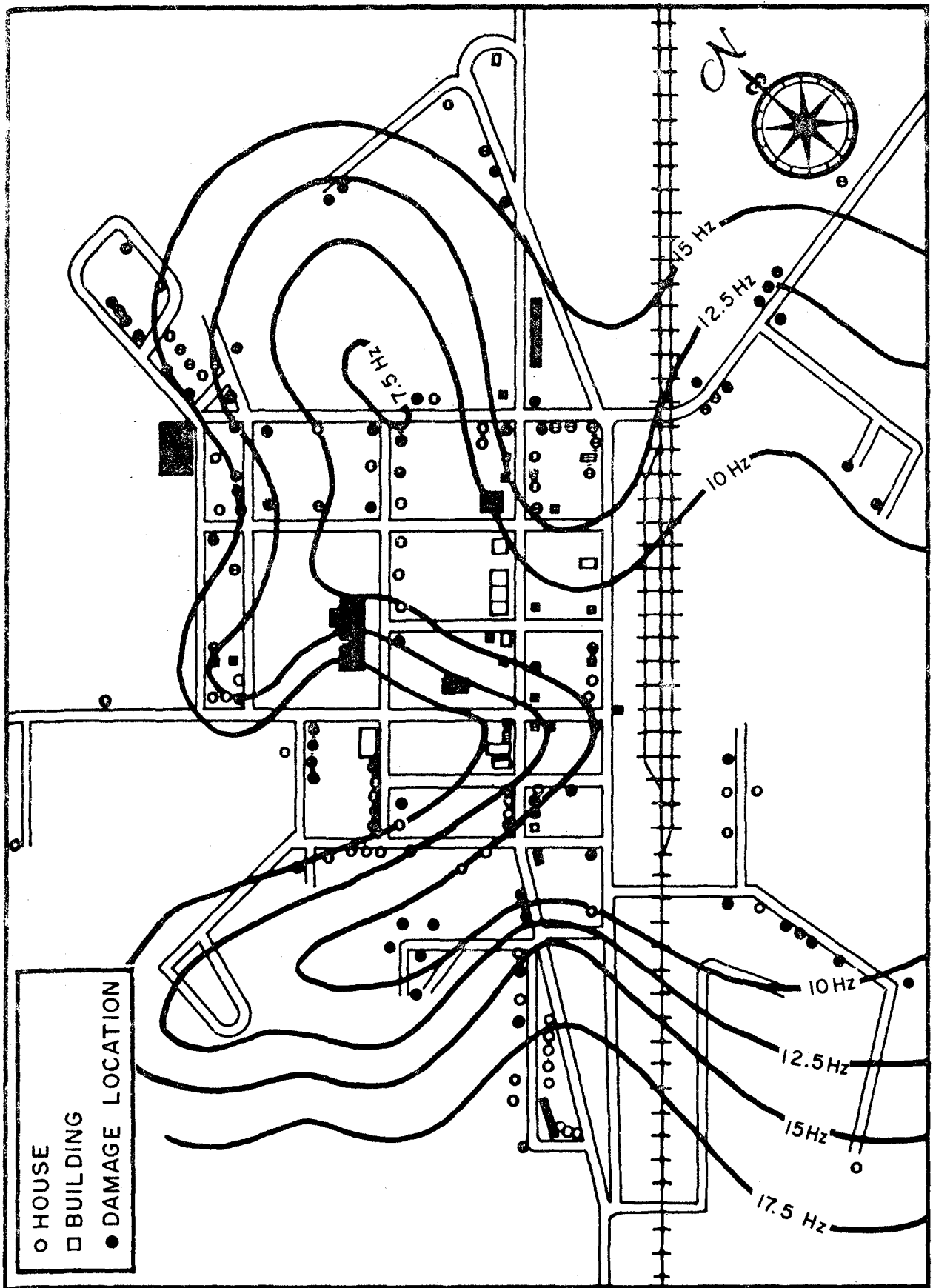


Figure 2. Correlation of Ground Resonance and Damage Pattern

It was postulated that 150,000 people lived in the city, which has experienced several damaging earthquakes in historic times. Two active faults, one traversing part of the city, have been the principal causes. Of great concern was that 14.2 percent of the residents lived in multiple family units, a majority of which were built prior to 1942. Some of these buildings had been damaged by a previous earthquake.

Local hazard reduction programs included adoption and enforcement of the Uniform Building Code, completion of a seismic safety element for the city's general plan, enforcement of the provisions of the Special Studies Zones Act which requires geologic reports for major structures proposed to be built in the two fault zones, the beginning of a process to inventory and systematically inspect older buildings in the downtown area, and initial drafting of a local ordinance to abate hazardous buildings. Illustrative maps are enclosed (Figures 3,4,5,6) which show the Special Studies Zones, historic epicenters and fault breaks, expected seismic ground response, and estimated building damage levels for a "1906 type" earthquake.

Assuming the city's staff has heard of seismic microzonation, consulted experts, and has presented a proposed ordinance to the City Council of "Santa Luisa" that would require the use of microzonation techniques in conjunction with the UBC to control planning and construction in the city, questions such as the following will have to be addressed before a program is implemented.

1. Are the techniques sufficiently adequate to be applied accurately and reliably?
2. Why should this be required, who will benefit, and how will the costs - public and private - be distributed?
3. How does this differ from what the city is doing already?
4. Is it feasible to establish this as a general policy that would be institutionalized and administered on a regular basis?
5. What processes, staff and consultants would be required for the program?

These examples have been used to illustrate the policy-oriented questions that can be expected when the application of seismic microzonation techniques is proposed. They revolve around issues of capability, effectiveness, ease of administration, costs and benefits, and integration with other efforts to reduce earthquake hazards. Such issues should be anticipated so that the policy implications are understood well enough to be answered.

## CONCLUSION

Bostrom and Sherif (1972) set the stage for concluding observations regarding the application of seismic microzonation when they said:

Zonation resolves itself into risk estimation. To a certain extent a society is progressive in proportion to the risks it is willing to take. It is infeasible to eliminate the earthquake risk altogether, but it turns out that one's view of what is an acceptable

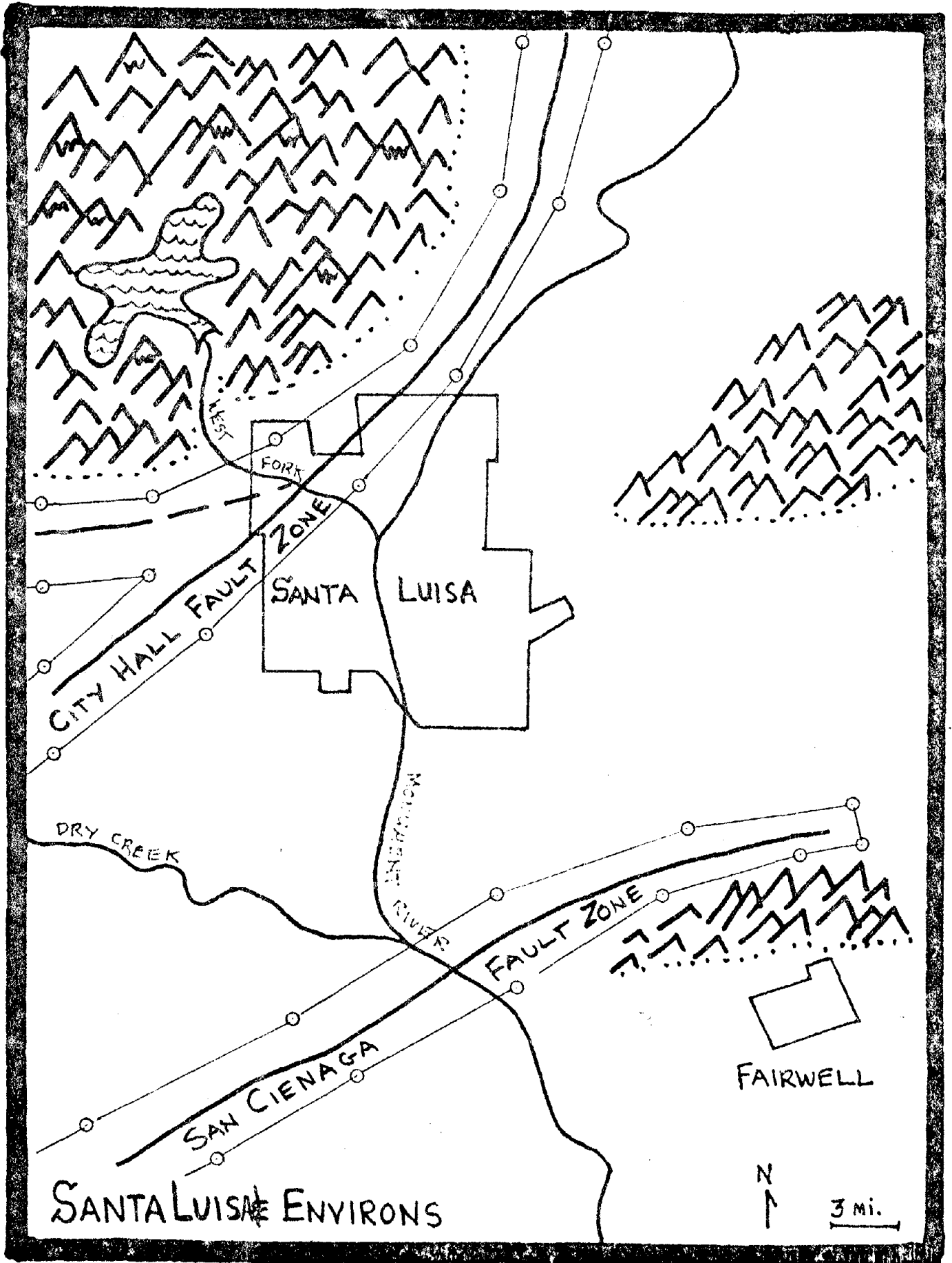


FIGURE 3. Hazard Map 1 (Special Studies Zones)

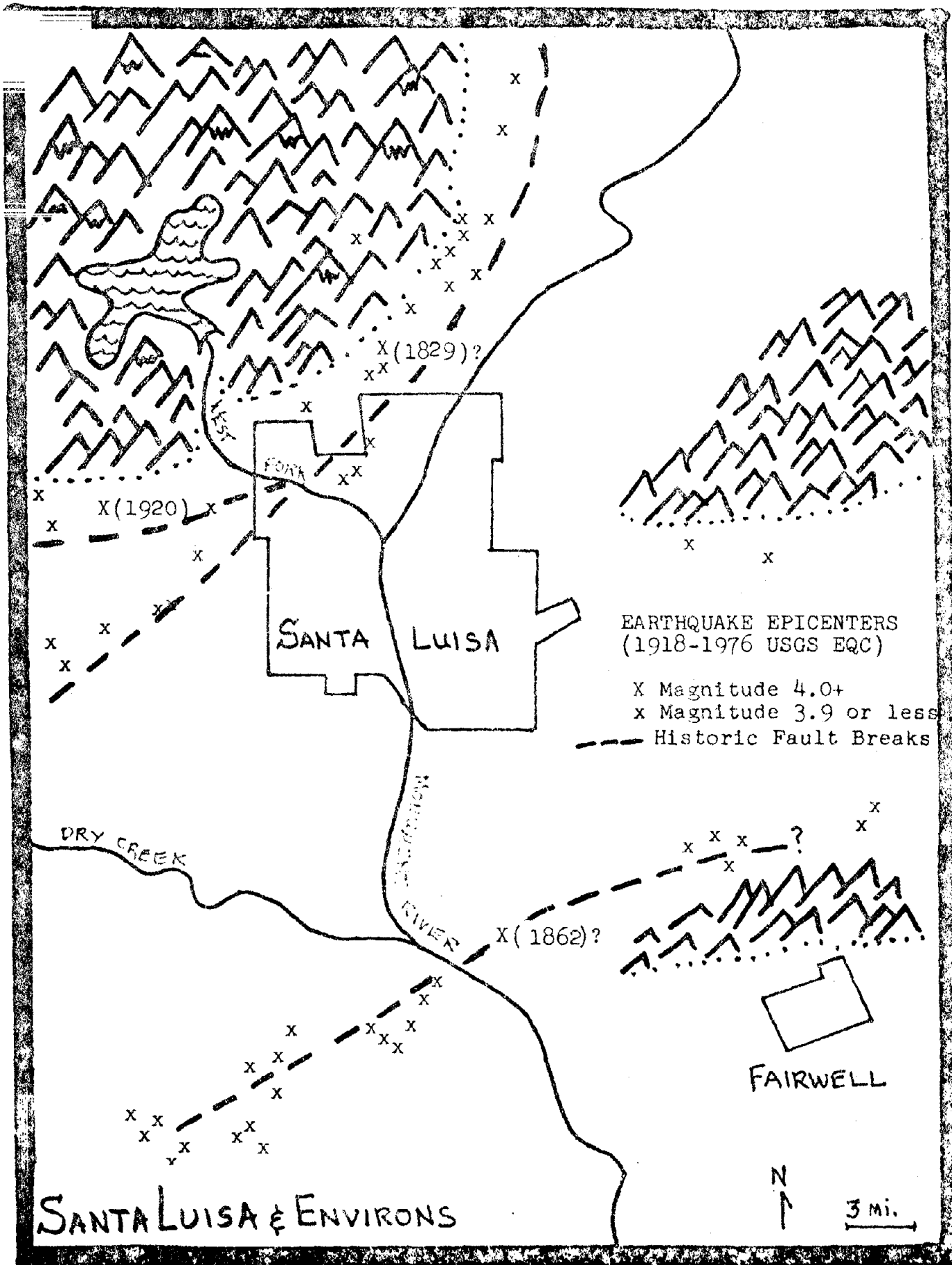


FIGURE 4. Hazard Map 2 (Epicenters & Fault Breaks)

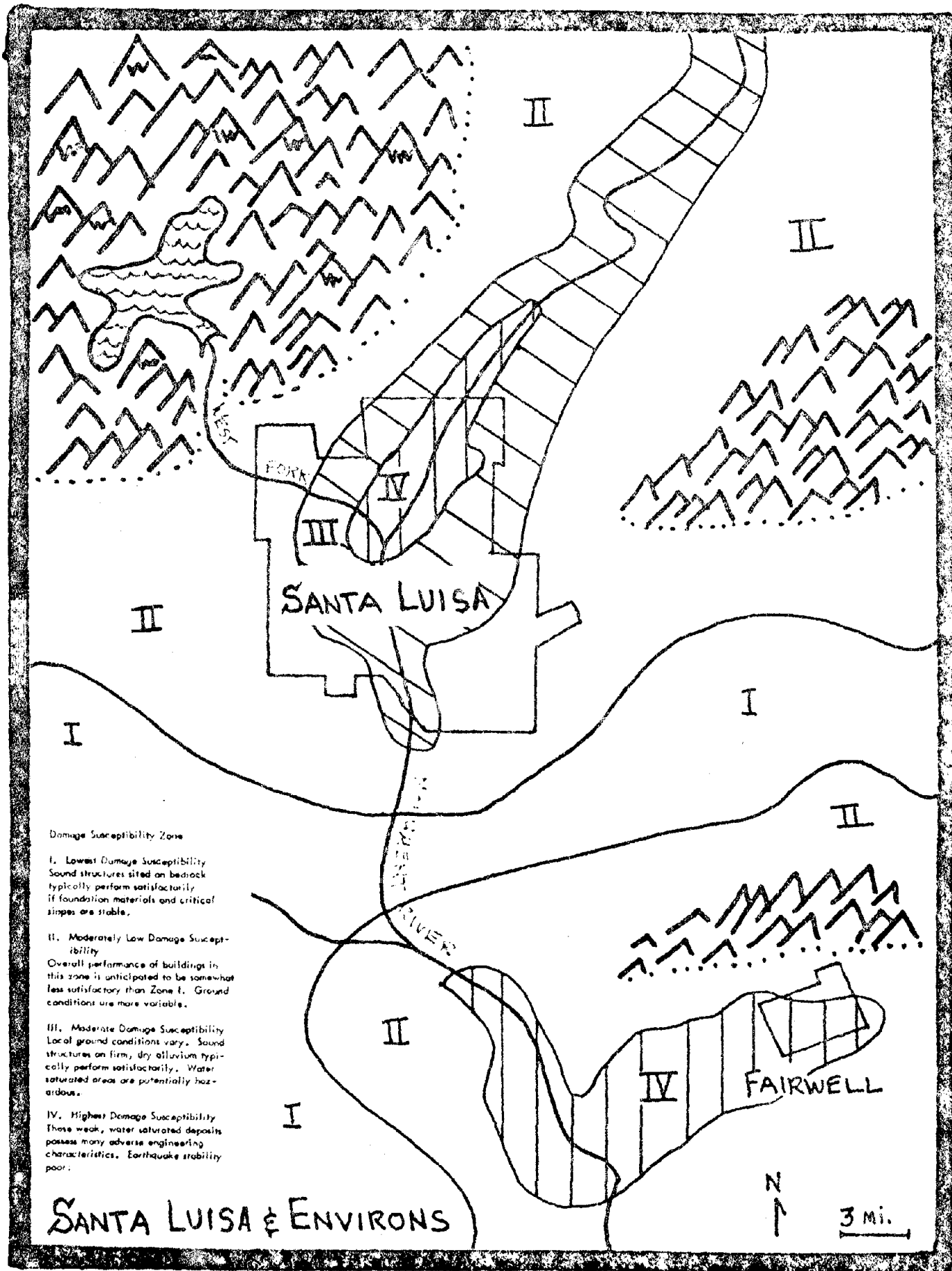


FIGURE 5. Hazard Map 3 (Seismic Ground Response)



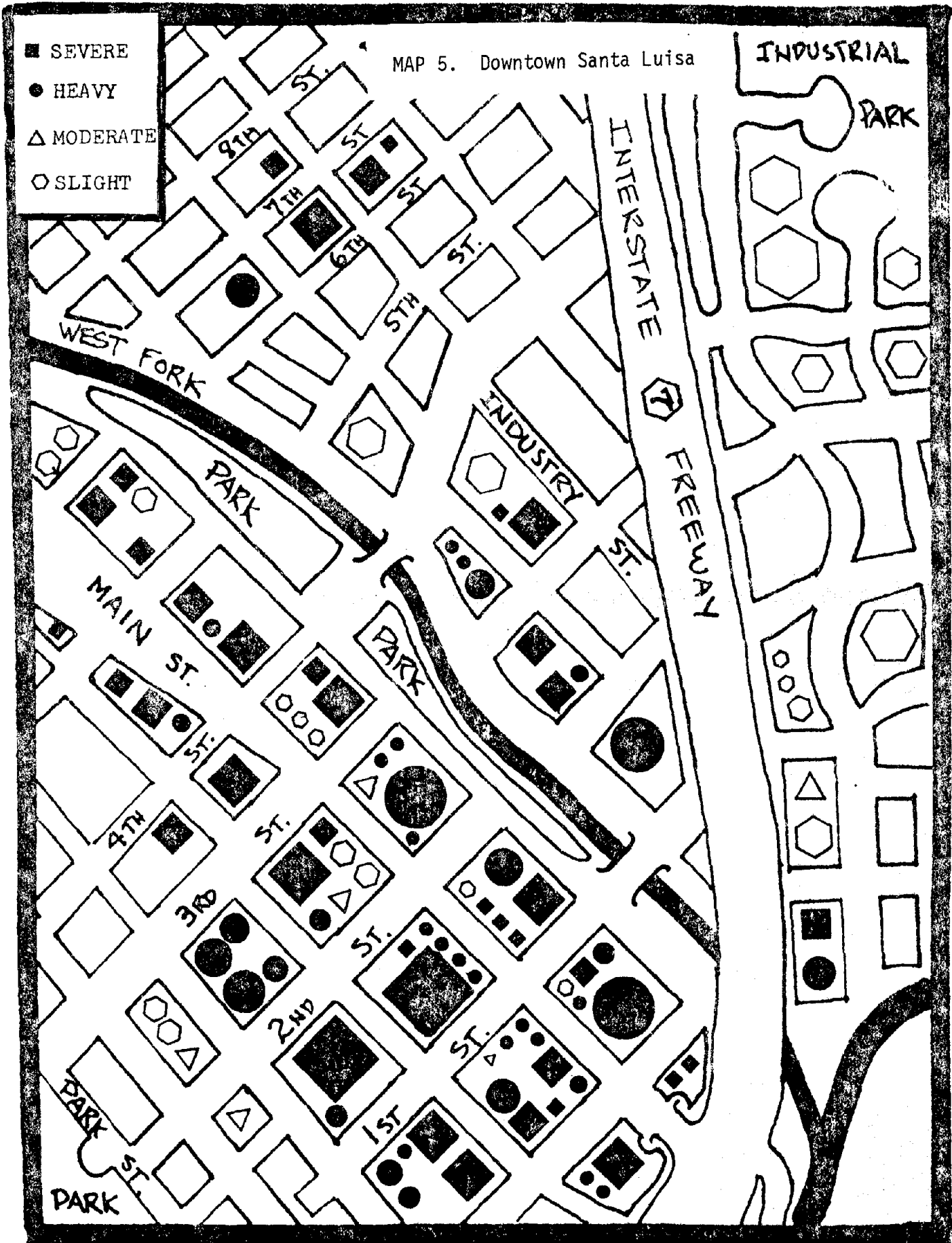


FIG. 6. ESTIMATED BUILDING DAMAGE LEVELS FOR A "1906 TYPE" EARTHQUAKE

risk is dependent upon whether one is an insurer, for instance, or a seller of real estate. The question then to be faced is: "How do we arrive at a system acceptable to all interests; and quantifiable?"

The balancing of competing interests, particularly where there is an issue involving governmental authority and private freedom, is achieved through the political process. The implementation of microzonation techniques to control land use and construction is such an issue and will become politicized.

Thus it is worthwhile to review major public policy questions so that there is both an appreciation of and attention to them by researchers who may be involved in the design of microzonation techniques. First, some programs already include recognition of relative seismicity, and how would microzonation techniques differ from or modify them? Second, how would such techniques be integrated into current hazard reduction efforts? Third, what are the potential impacts of microzonation, and how are they distributed? Last, can the state-of-the-art assure equitable, reliable, and justifiable results? These are significant questions.

REFERENCES

1. Alcock, Dr. E.D., "Grand Valley Colorado; A Microzonation Case History," Proceedings of the International Conference on Microzonation, Seattle, Washington, 1972, pp. 299-306.
2. Applied Technology Council, Tentative Provisions for the Development of Seismic Regulations of Buildings, National Bureau of Standards Special Publication 510, Washington, D.C., 1978
3. Barozangi, Muawia and James Dorman, "World Seismicity Maps Compiled from ESSA, Coast and Geodetic Survey, Epicenter Data, 1961-67", Bulletin of the Seismological Society of America, Vol 59, No. 1, February, 1969, pp. 369-380.
4. Bostrom, R.C. and M.A. Sherif, "United States Microzonation Procedures," Proceedings of the International Conference on Microzonation, Seattle, Washington, 1972, pp. 183-210.
5. Division of Mines and Geology, State of California, Urban Geology Master Plan for California, Bulletin 198, Sacramento, California, 1973.
6. Gaus, Michael P. and M.A. Sherif, "Zonation and Microzonation", Proceedings of the International Conference on Microzonation, Seattle, Washington, 1972, pp. 3-12.
7. Insurance Services Office, personal correspondence, May, 1978.
8. Richter, C.F., "Seismic Regionalization," Bulletin of the Seismological Society of America, Vol. 49, No. 2, April, 1959, pp. 123-162.
9. Richter, C.F., "Seismic Regionalization or Zoning: Revision," Proceedings of the International Conference on Microzonation, Seattle, Washington, 1972, pp. 267-282.
10. Seismic Safety Commission, State of California, selected unpublished materials for the "Hazardous Buildings Workshop, October 19-21, 1977," Sacramento, California.
11. Steinbrugge, Karl V., et. al., The Santa Rosa, California, Earthquakes of October 1, 1969, U.S. Department of Commerce, Environmental Science Services Administration, Rockville, MD., 1970.

1488

**INTENTIONALLY BLANK**

## TOWARD A MEASURE OF SOCIO-SEISMICITY

by

Mitchel Abolafia<sup>I</sup> and Alan L. Kafka<sup>II</sup>

## ABSTRACT

Most seismic risk maps rely on a composite of historical seismicity and tectonic principles to estimate earthquake risk in a specific region. Despite the increasing sophistication of such maps, a concern with life and property requires the inclusion of social variables, such as population and structural density, in the estimation of seismic risk. It is evident that a magnitude 7.0 earthquake in a highly populated region will cause far more damage than an earthquake of the same magnitude in a sparsely populated region.

Using data from the U.S. Census of Population and Housing, this paper suggests several measures which unite social and seismic variables. Estimates of persons per square mile and the percent of single family housing structures in a region are weighted against the risk of earthquakes in a cross-section of major risk regions in the United States. The variation in socio-seismicity between places with equivalent seismic risk is interpreted in terms of its relevance for policy planning. This new measure, if applied to the entire United States, would extend and improve the usefulness of seismic risk maps.

## INTRODUCTION

As the trends of urbanization and industrialization spread throughout the world, the density of man's built environment grows ever greater. The accompanying movement of population from farmland to the cities not only places large numbers of people in close proximity, it concentrates them in hospitals, factories, schools, and apartments, all of which are frequently multi-level structures. While the consequences of urbanization and industrialization have often been a general improvement in health and welfare, they have also brought an unanticipated consequence; the possibility that a natural hazard would decimate the densely built environment and its human occupants.

Coincident with the increasing density of multi-level structures has been the development of complex social institutions which function to organize the efforts of large numbers of people in the major facets of social life; e.g., industry, government, education, etc. This ability to organize, if applied properly, could allow societies to compensate for the increasing threat from earthquakes. Such compensation would require a concerted mobilization similar to that of previous societal efforts in public health and education. As in these previous efforts, a set of standards would have to be set and enforced.

---

I Graduate Student, Department of Sociology, State University of New York, Stony Brook, N.Y.

II Graduate Student, Seismology, Dept. of Earth & Space Sciences, State University of New York, Stony Brook, N.Y.

Even the most technologically sophisticated societies are learning that their environment can never be completely predicted or controlled, but they are also learning that political, economic, and technological tools can be harnessed to reduce the misfortune which has so often characterized man's experience with natural hazards. One such tool is the determination of seismic risk in a region and the development of feasible plans for the protection of life and property. The concept of socio-seismicity extends our understanding of seismic risk through the consideration of its social correlates with the intention of ultimately broadening its applications.

#### SEISMIC RISK AND SOCIO-SEISMIC RISK

In this paper we address only the social aspects of earthquake risk. We make no attempt to deal with the tectonic or seismic principles involved in creating a seismic risk map. While we are aware of the difficulties involved in the interpretation of such maps (3), we have bypassed these issues to rely on the most sophisticated and frequently used of seismic risk maps. Specifically, we will be using the 1969 earthquake risk map of S. T. Algermissen shown in Fig. 1 (1). A short review of the principles involved in creating this map is in order. The map's primary assumption is that future earthquakes will occur in the vicinity of previously recorded seismic disturbances. The level of risk at any point on the map is based on two variables. The first is the maximum observed earthquake intensity at that point. The second variable is a measure of the amount of energy released at that point (based on magnitude) in all known past earthquakes. By superposing these two variables, the map takes into account not only the amount of energy released, but also the fact that seismic energy appears to attenuate differently in the eastern United States than it does in the western United States (2). Using these variables, four levels of risk were identified. The continental United States was then divided into risk zones, labelled 0 to 3, where 0 is the lowest risk and 3 is the highest.

Our first effort to add social variables to the estimate of seismic risk involved superposing a population density map of the United States (4) on Algermissen's map (see Fig. 2). This offered us a first gross view of how the population is distributed in earthquake prone regions. The density values are for counties in terms of their population per square mile. The black regions are zones of extremely high population density with 250 or more persons per square mile. The heavily and lightly stippled regions are zones of high earthquake risk where population density is 50 to 249.9 and less than 50, respectively. Although all of the shaded regions appear as "major risk" (zone three) regions on Algermissen's map, we find substantial variation within these regions when population density is considered. The significance of this variation is in terms of its human consequence. While the probability that a major earthquake will occur may be just as high in a stippled zone as in a black one, the effect in terms of the threat to life and property will vary considerably. Further research is needed to determine the parameters of this variation.

Admittedly, Fig. 2 is only a first approximation to a measure of socio-seismicity. In order to effectively microzone a region for earthquake risk, a multivariate measure must be developed. To this end, we have constructed a socio-seismic index (SSI) consisting of three variables: population density, structural density, and seismic risk. Data

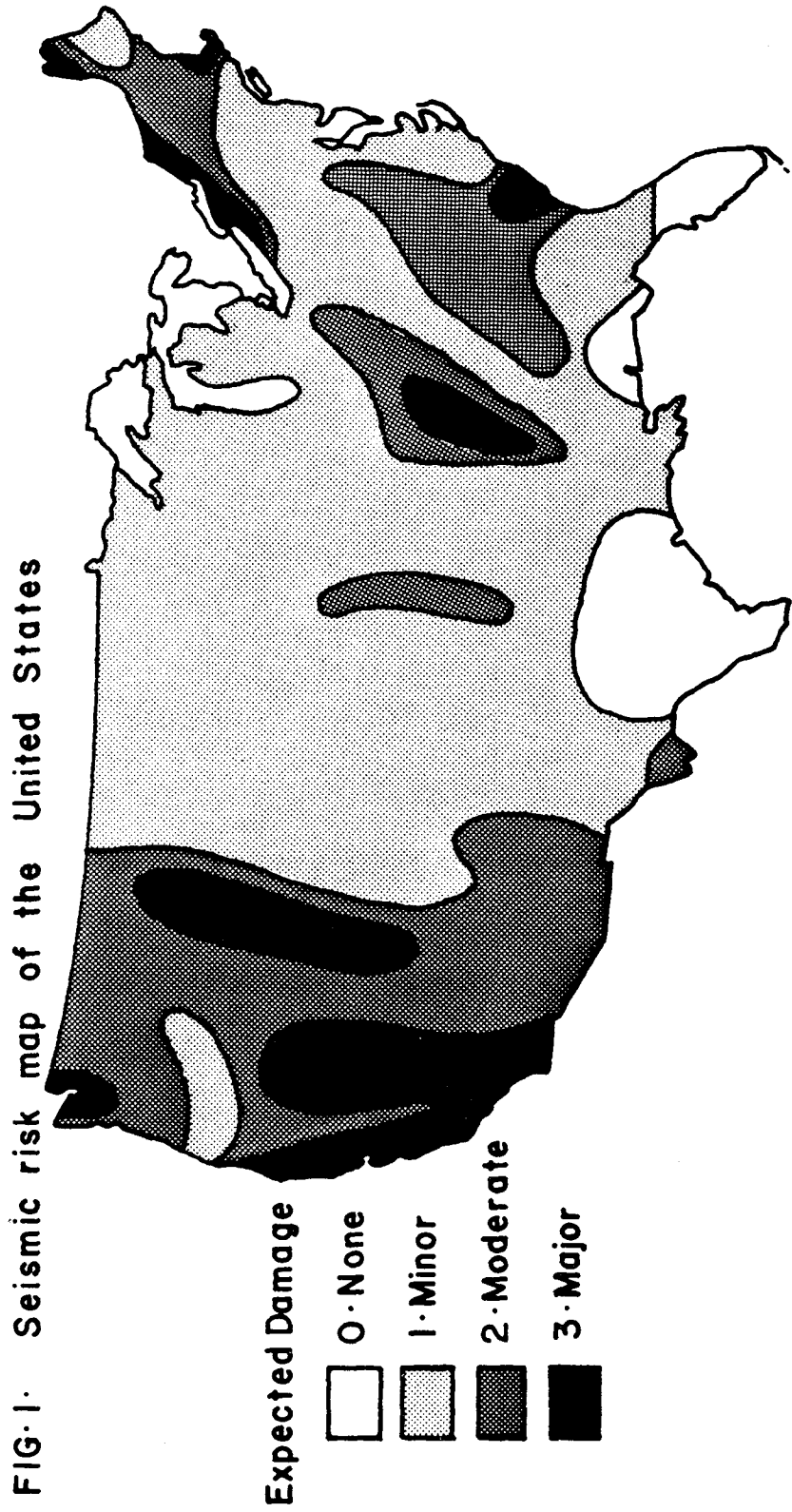
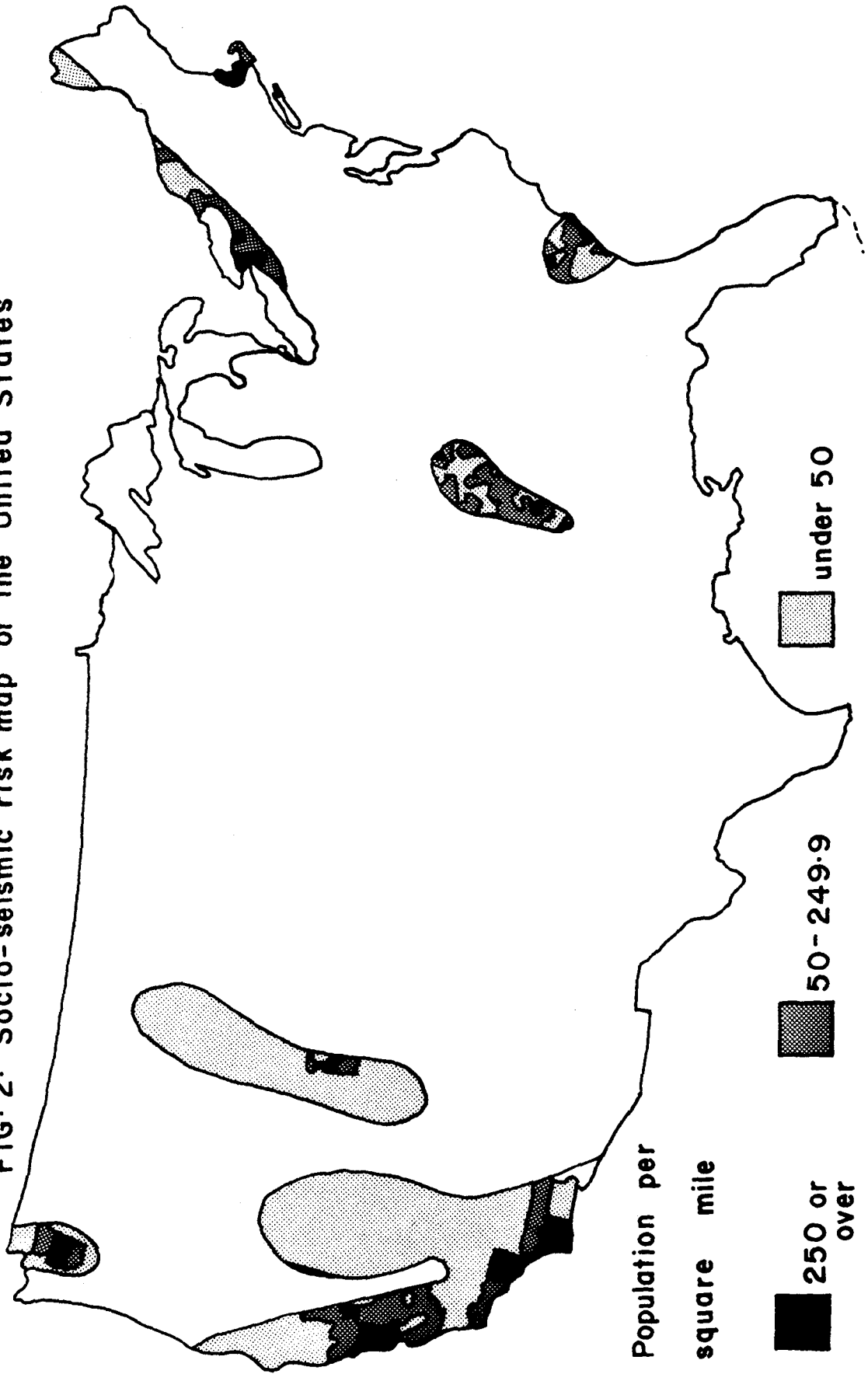


FIG. 1. Seismic risk map of the United States

Published in 1969 (ESSA / Coast and Geodetic Survey)

FIG. 2. Socio-seismic risk map of the United States





for the first two variables were obtained from the U.S. Census in the form of persons per square mile and percent of housing in single unit structures in places with 2500 or more residents (4, 5). The seismic risk variable was taken directly from Algermissen's map. For purposes of illustration the SSI will be applied to a sample of high risk cities in the U.S. and to a detailed mapping of southern Los Angeles County.

The SSI was constructed by first gathering data for the twenty-seven cities shown in Table 1 and for the fifty-eight localities in the part of southern Los Angeles County shown in Fig. 3. The means and standard deviations of the two social variables were calculated for the localities in Table 1 and Fig. 3 separately. Using these statistics, an index ranging from 1 through 4 was created for each variable. The SSI was constructed by adding the index values of each locality for both social variables. (Note that the seismic variable may be excluded from our calculations because it is constant.) The resulting SSI values, ranging from 2 through 8 (lowest to highest risk), are shown in Table 1 and Fig. 3. Although the map of southern Los Angeles County reveals sharp distinctions between neighboring regions, the reader is cautioned that these discontinuities are, in part, artifacts of political boundaries. Real differences in socio-seismic risk are likely to be more gradual. The values of the index are then interpreted as approximations, subject to refinement, of the socio-seismic risk at any point on the map.

#### DISCUSSION AND CONCLUSIONS

The socio-seismic index described above represents a first step toward increasing the usefulness of seismic risk maps. This usefulness could be further increased by the inclusion of other relevant variables. Among these are: the age of construction in an area, the type of construction, and the percent of elderly and disabled in an area. Localized socio-seismic maps could be drawn to include such geophysical characteristics as frequency of occurrence of earthquakes and local geologic structure and faulting patterns. The development of multivariate indices and comprehensive maps will offer communities a more useful estimate of the risk to their area.

We are convinced that socio-seismic risk maps can become valuable tools in the hands of business and government planners, but we must caution that they are designed for very specific purposes. A socio-seismic index does not predict the likelihood of an earthquake. Reliable earthquake prediction is still in its infancy. At this point responsible scientists can only hope to make their fellow citizens and their government aware that a potential for disaster exists in their area. Socio-seismicity can then serve two purposes: to indicate the magnitude of risk to an already built environment, and to plan for future development in low density areas. The development of socio-seismic maps for all major risk areas might serve as an incentive to organize action in local communities.

Such action may take several forms. The most immediate form would be disaster relief. Communities, once they are aware of the threat to life, should be organized for prompt response. This would include not only provision for food, shelter, and medicine, but also pre-tested plans for dealing with gas line breakage, massive fires, and large scale evacuation. The most far-reaching but most difficult application of socio-seismic risk estimates is in the area of land use planning. This would include restricting the use of high risk areas through zoning as well as an improve-

TABLE 1

## Socio-Seismicity in a Sample of Major Risk Cities\*

<u>Location</u>	<u>Population per Square Mile</u>	<u>% in one unit Structures</u>	<u>Socio- Seismic Index</u>
San Francisco, CA	15,764	33.7	8
Boston, MA	13,936	14.7	8
Buffalo, NY	11,205	27.7	8
Somerville, MA	21,653	10.4	8
St. Louis, MO	10,167	34.1	7
Santa Monica, CA	10,637	29.1	7
Rochester, NY	8,072	43.0	7
Worcester, MA	4,721	33.8	6
Anchorage, Alaska	2,965	38.2	6
Charleston, S.C.	3,892	46.6	5
Niagara Falls, N.Y.	6,389	53.6	5
Salt Lake City, Utah	2,966	55.3	5
Missoula, Mont.	3,734	62.8	5
Seattle, Wash.	6,350	59.8	5
Los Angeles, CA	6,077	52.0	5
Santa Barbara, CA	3,744	56.3	5
Honolulu, HA	3,872	46.5	5
Carbondale, Ill.	4,305	57.3	5
Memphis, Tenn.	2,868	68.9	4
Paducah, Ky.	2,658	72.5	4
Ogden, Utah	3,293	67.3	4
Reno, Nev.	2,405	55.8	4
Cairo, Ill.	1,846	74.8	3
Riverside, CA	1,959	78.9	3
San Diego, CA	2,199	64.9	3
New Madrid, Mo.	680	84.3	2

\* Population statistics are available in the U.S. Census of Population, Summary, Table 31, 1970. Structural statistics are found in the U.S. Census of Housing, State Volumes, Tables 1 and 23, 1970. Seismicity is based on the map published by the U.S. Coast and Geodetic Survey (1).

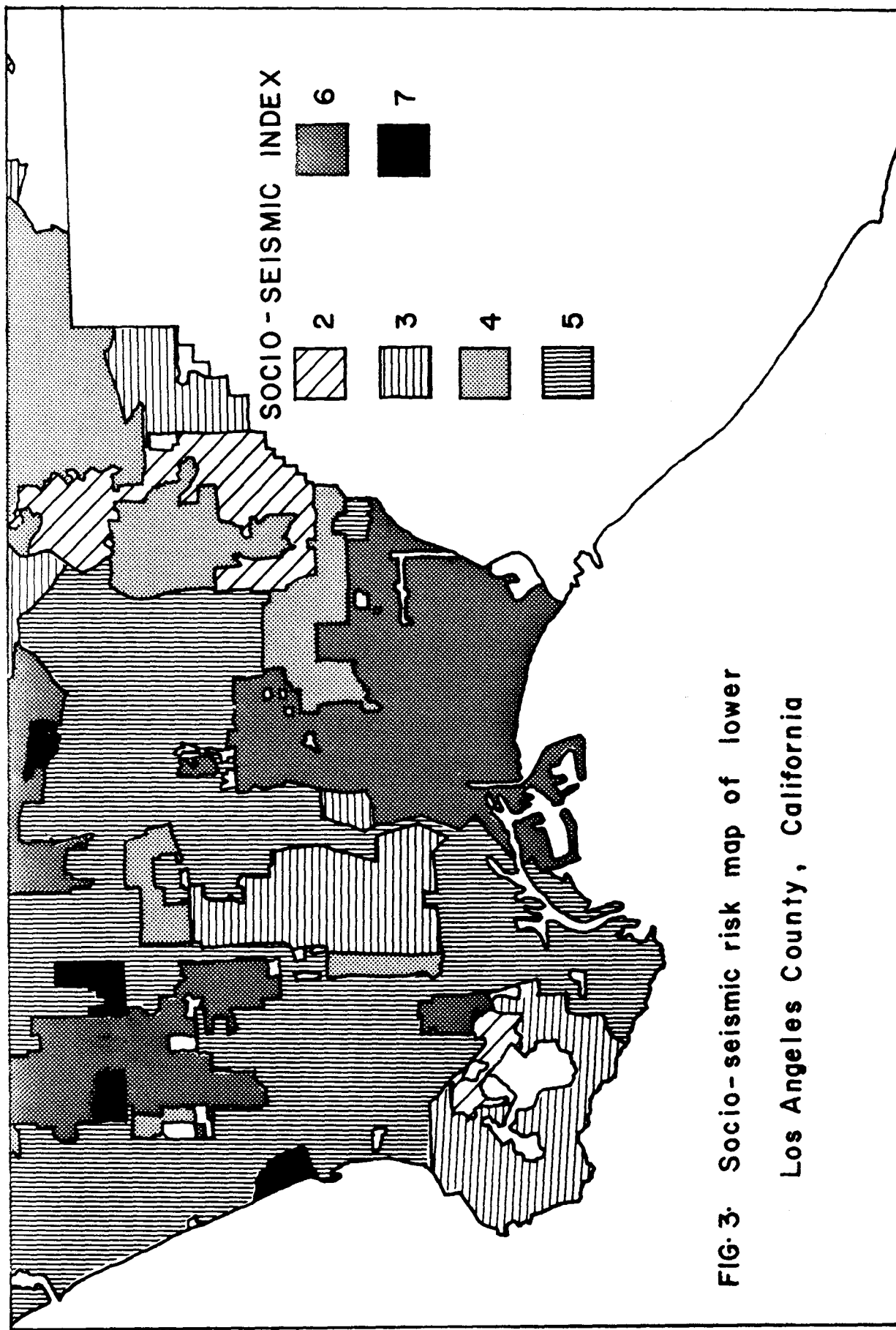


FIG. 3. Socio-seismic risk map of lower Los Angeles County, California

ment in construction practices through an up-grading of the building codes.

The difficulties involved in land use planning are numerous. Most obviously, those places with the highest socio-seismic risk are dense social, political, and economic environments that cannot be easily altered. Boston and San Francisco are unlikely to rezone their central business districts, although some rezoning is becoming more feasible through urban renewal. Less developed areas, on the edge of a metropolis, may still be able to shift their predominant character to some safe use. An alternative to rezoning is the purchase or condemnation by government of the areas most prone to landslide and liquefaction, but in most cases purchase is too costly and condemnation too politically unpopular.

The reduction of risk from earthquakes is likely to prove most elusive inside our central cities. Older structures, those which most frequently house the elderly and the poor, are among the most dangerous structures in an earthquake. While it is true that engineers are devising methods by which aging structures can be reinforced, building owners cannot be expected to assume the full cost of reinforcing such structures and occupants cannot simply be displaced. A solution will require creative legislation so that the burden of risk reduction is born equitably.

Regardless of the region, the benefit of land use planning for socio-seismic risk will be difficult to realize. The long tradition of resistance to government sponsored land use planning will be the major obstacle to the reduction of earthquake risk. The resistance is based on the threat of rezoning to those who own property in high risk regions. Property owners argue that rezoning is a violation of their right to develop their land as they see fit. Specifically, they fear that land values will be decreased by rezoning. The state could use its police power to enforce zoning and building codes or its right of eminent domain to take the land, but the development of any comprehensive land use plan will certainly be resisted by those committed to the maintenance of the present urban ecology.

As Figures 2 and 3 make clear, socio-seismic risk regions do not conform to political boundaries. Since earthquakes do not distinguish between city, county, and state jurisdiction, intergovernmental cooperation and regional planning are necessary for earthquake risk reduction. For this purpose regional seismic zone commissions could be created to oversee development in high risk areas. Alternatively, federal agencies, such as the U.S. Geological Survey, could provide local planning boards with technical assistance, thereby preserving local autonomy. It is organized efforts such as these that will provide the basis for an effective response to the threat of earthquake. It is with these efforts in mind that we urge the development of more comprehensive measures of socio-seismicity.

#### REFERENCES

1. Algermissen, S. T., Earthquake History of the United States, ed. by J. L. Coffman and C. A. vonHake, NOAA Publication 41-1, 1973.
2. Nuttli, O. W., Seismic wave attenuation and magnitude relations for eastern North America, J.G.R., 78, 876-885, 1973.
3. Perkins, D. M., Seismic risk maps, Earthquake Information Bulletin,

Vol. 6, No. 6, 1974.

4. U.S. Bureau of the Census, 1970 Census of the Population, Government Printing Office, Washington, D.C., 1973.

5. U.S. Bureau of the Census, 1970 Census of Housing, Government Printing Office, Washington, D.C., 1973.

1498

**INTENTIONALLY BLANK**

AN EVALUATION STUDY ON THE DISTRIBUTION  
OF PROPERTY LOSSES CAUSED BY EARTHQUAKES

by

Eiichi Kuribayashi<sup>I</sup> and Tadayuki Tazaki<sup>II</sup>

ABSTRACT

The authors have employed a statistical model in order to evaluate the property losses valued in money caused by earthquakes and compared them of various kinds of facilities. Using money value for evaluating the seismic losses is convenient to compare the losses of various kinds of facilities, although the evaluation method for the existing property and its loss relatively depends upon the administrative policy in addition to the engineering judgement.

The property loss was assumed to be evaluated by multiplying the existing property in the quake-influenced area and the loss ratio. The loss ratio was represented as the function of the magnitude of an earthquake, epicentral distance and subground condition. Subground condition was simplified into two categories (i.e. alluvial, and diluvial and tertiary). The existing property was estimated from the National Wealth Survey of Japan.

The data of eighteen earthquakes occurred in Japan since 1923 was used in this analysis.

1. Introduction

Better understanding of the scale and distribution of disasters in future earthquakes, which may not be avoided only by physically technological countermeasures, is necessary in earthquake disaster mitigation programs. If areas vulnerable to earthquakes are identified in advance, relevant administrations can take the predisaster countermeasures such as retrofitting vulnerable structures, reallocating lifeline facilities and disseminating permeably disaster risk potentials to residents. Additionally as for post-disaster countermeasures, those activities as surveying the damage, rescuing and rehabilitating concentratively are very efficiently applicable. Therefore estimating accurately the scale and distribution of earthquake disasters is very effective in both pre- and post-disaster countermeasures for disaster mitigation measures, which should optimize the limited resources.

Quantitative estimations of earthquake disasters have been carried out for existing wooden houses (1)~(4), bridges (5) and underground pipes (6). In order to express the amount of losses, various kinds of indexes are used such as the equivalent ratio of razed houses for the wooden houses, damaged spots per service line for underground pipes respectively. However commonly usable index is necessary to evaluate the total loss of disasters and to compare them of various kinds of facilities. The property loss valued in money meets with this requirement.

The authors have investigated the evaluation method of property loss distribution by analyzing eighteen of historical earthquake in Japan.

---

I Chief, Earthquake Engineering Section, Public Works Research Institute,  
Ministry of Construction, JAPAN

II Research Engineer, do

## 2. Methodology of the Analysis

The authors assumed a ratio of property losses caused by earthquake as an index of earthquake disasters. The property loss ratio can be defined as a ratio between property losses (l) and existing assets (w) valued in money respectively, and expressed as the functions of earthquake magnitudes, epicentral distances and subground conditions as follows,

$$D_I = G_I 10^{\alpha M + \beta \Delta}, \quad (1)$$

$$D_{II} = G_{II} 10^{\alpha M + \beta \Delta}, \quad (2)$$

where the suffixes of I and II means older subgrounds than diluvial deposits and younger than alluvium respectively and,

$G_I, G_{II}$  : constants for the subground types, I and II,

M : earthquake magnitudes in Richter scale,

$\Delta$  : epicentral distances in km,

$\alpha, \beta$  : constants.

The ratio is to be evaluated in accordance with the subground condition as shown in Fig.1(A). The existing assets distribute independently from it like in Fig.1(B). The property loss caused by an earthquake can be evaluated by multiplying the existing assets and the ratio as shown in Fig.1(C).

The constants were determined by correlating actual property losses and the estimation of the losses of eighteen earthquakes occurred in Japan since 1923.

A total property loss (L) in each earthquake can be estimated by summing up the losses of each mesh ( $l_i$ ) which is appropriately divided into,

$$L = \sum_i l_i = \sum_i \{ \delta_i (D_I)_i + (1 - \delta_i) (D_{II})_i \} w_i \quad (3)$$

where

$w_i$  : existing assets,

$(D_I)_i$  : property loss ratio in subground type I,

$(D_{II})_i$  : property loss ratio in subground type II,

$l_i$  : loss in mesh i,

$\delta_i$  : identification index  $\begin{cases} 1 & \text{for subground type I in mesh } i \\ 0 & \text{for subground type II in mesh } i. \end{cases}$

As shown in Ref.(7) it can be said that the assets correlate with the population in each district in Japan,

$$A_T = 2.77 \cdot P - 0.891 \quad (4)$$

$A_T$  : Gross tangible fixed assets in trillion yen (1970),

P : Population in million (1970).

Accordingly the assets at each mesh were estimated from the relationships between the assets and local populations as shown in the following.

In Eq.(4), the regression constant of 0.891 is negligible compared to the assets. Then Eq.(3) becomes:

$$L = \sum_i \{ \delta_i (D_I)_i + (1 - \delta_i) (D_{II})_i \} W \frac{p_i}{P} \quad (5)$$

where

W : National wealth in yen,

P : Population of Japan,

$p_i$  : Population of mesh i.

The population of mesh i ( $p_i$ ) was estimated from the average population density of the quake-damaged area, which was obtained from the sum of the population and area of the municipalities suffered from an earthquake.



Therefore,

$$\begin{aligned} L &= \frac{W}{P} \frac{P_D}{A_D} \sum_i \{ \delta_i (D_I)_i + (1 - \delta_i) (D_{II})_i \} a_i \\ &= \frac{W}{P} \frac{P_D}{A_D} \sum_i \{ \delta_i G_I + (1 - \delta_i) G_{II} \} 10^{\alpha M + \beta \Delta_i} a_i \end{aligned} \quad (6)$$

where

$P_D$  : Population of the quake-damaged area,

$A_D$  : Area of the quake-damaged area in  $\text{km}^2$ ,

$a_i$  : Area of mesh  $i$  in  $\text{km}^2$ ,

$\Delta_i$  : Epicentral distance of the center of the mesh (km).

Fig.2 shows the procedure to estimate the losses caused by an earthquake as stated above.

The mesh used in this analysis was made to coincide with that of a hundred times of the National Land Information Mesh Data of National Land Agency.

The loss was summed up within the area where damage possibly occurred as shown in Eq.(7).(8)

$$\log R = 0.5 M - 1.5 \quad (7)$$

where

$R$  : Radius of the area where damage possibly occurred in km,

$M$  : Magnitude in Richter scale.

The unknown constant  $G_I$ ,  $G_{II}$ ,  $\alpha$  and  $\beta$  were determined by minimizing the difference of the sum of square of  $\log(\frac{LPAD}{WPDA})$  and its estimate  $\log(\frac{LPAD}{WPDA})$ .

$$\sum_j \{ \log(\frac{LPAD}{WPDA})_j - \log(\frac{LPAD}{WPDA})_j \}^2 \rightarrow \text{Min} \quad (8)$$

$J$  : Suffix to denote earthquake  $j$

$a$  : Average area of a mesh in  $\text{km}^2$

### 3. Data Used in this Analysis

#### 3.1 National Wealth

National Wealth Survey has been conducted 12 times until 1970 in Japan usually in every 5 years. However there exists a twenty year blank of survey before and after World War II. In order to interpolate the national wealth during the blank years, it was estimated from the relationship to the gross national product (GNP) as shown in Eq.(9). (7).

$$\log_{10} W = 1.03 + 0.937 \log_{10} N \quad (\text{unit : million yen}) \quad (9)$$

$N$  : Gross National Product.

#### 3.2 Population and Area of the Damaged Area

The population and area of the damaged area to be used in Eq.(6) were the sum of those of municipalities which were involved within the radius ( $R'$ ) given by Eq.(10). The radius  $R'$  corresponds to the area, within which the seismic intensity of Japan Meteorological Agency is expected to be greater than V. (9)

$$\log_{10} R' = 0.5M - 1.85 \quad (10)$$

$M$  : Magnitude in Richter scale.

The data of population and area as of 1970 were used. The local population must have changed, but the ratio of the population of Japan and that of the damaged area, which was used in Eq.(6), is considered to have changed little.

#### 3.3 Subground Condition

Each mesh was classified into subground type I or II according to the Reference (10). Fig.3 shows an example of the classification of subground in

northern part of Japan.

### 3.4 Earthquakes Used in the Analysis

Eighteen earthquakes, whose recorded property losses are listed in Table 1, were used in this analysis. The influence of inflation were not taken into consideration of the loss value, because both the loss and existing assets were valued in current price.

### 4. Results of the Analysis

The regression formulas for Eq.(1) and (2) were introduced as follows:

$$D_I = 7,9 \times 10^{-7} \times 10^{0.62M} - 0.0028\Delta \quad (11)$$

$$D_{II} = 1.9 \times 10^{-6} \times 10^{0.62M} - 0.0028\Delta \quad (12)$$

$$6.1 \leq M \leq 8.1$$

The multiple correlation coefficient by Eq.(13) was 0.82,

$$R = \sqrt{1 - \frac{\sum_j \left\{ \left( \frac{LPA}{WP_D a} \right)_j - \widehat{\left( \frac{LPA}{WP_D a} \right)_j} \right\}^2}{\sum_j \left\{ \left( \frac{LPA}{WP_D a} \right)_j - \overline{\left( \frac{LPA}{WP_D a} \right)_j} \right\}^2}} \quad (13)$$

where

$\overline{\left( \frac{LPA}{WP_D a} \right)}$  : Average of  $\frac{LPA}{WP_D a}$  for all earthquakes,

$\widehat{\left( \frac{LPA}{WP_D a} \right)_j}$  : Regression estimate calculated by Eq.(11) and (12) for earthquake j.

Fig.4, 5 show the value of  $D_I$  and  $D_{II}$ . As far as the multiple correlation coefficient concerned, the regression formulas can be considered to estimate the property losses caused by an earthquake.

### 5. Comparison of Property Loss among Lifeline Facilities

Fig.6 shows the breakdown of the social capital according to the National Wealth Survey of 1970. If the composition of the social capital can be assumed to be constant for a decade before 1970, the ratio calculated by Eq.(14) of various kinds of lifeline facilities for eight earthquakes in Japan from 1961 till 1970 represents the individual loss ratios of facilities.

$$\text{Individual loss ratio} = \frac{I_k P}{W_k P_D} \quad (14)$$

$I_k$  : Loss valued in money of facility k,

$W_k$  : Existing assets of facility k

= National wealth as of the year of the earthquake

x  $\frac{\text{Assets of facility k as of 1970}}{\text{National wealth as of 1970}}$

Fig.7 - 14 show the relationships between the individual loss ratio of various kinds of facilities and the total property loss.

The procedure to evaluate the loss value is not always completely the same in each facilities. However it tends to be that the loss ratios of building and highway facility are almost the same as that of the total property loss. The loss ratios of agriculture, river and harbor facilities are higher than the total. The loss ratios of electric power, telecommunication and water supply facilities are lower than that of the total, but they gradually reach the same level as the ratio itself comes to a greater

value. (See Fig.15)

## 6. Conclusions

By this analysis following conclusions can be made.

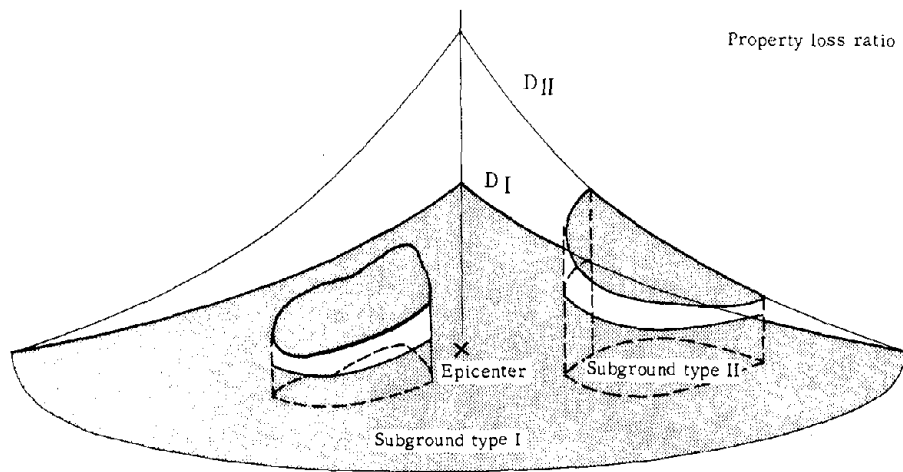
- (1) The property loss can be used as the index elucidating satisfactorily the scale of the earthquake disaster.
- (2) The property loss can be estimated from the magnitude of the earthquake, epicentral distance and subground condition.
- (3) By comparing the property loss of various kinds of lifeline facilities, buildings and highway facilities are likely to suffer the average property loss. Agricultural, river and harbor facilities are likely to suffer greater loss than the average. Electric power, telecommunication and water supply facilities are likely to suffer less property loss.

## 7. References

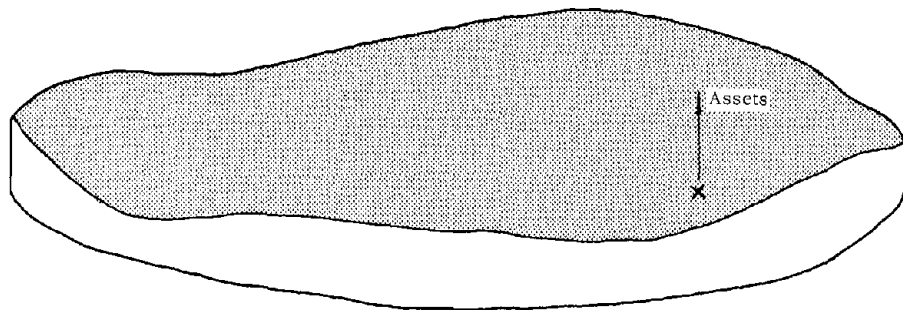
- All references listed below are written in Japanese except (7).
- (1) H. Kawazumi : Damage Distribution and Earthquake in Tokyo, Architecture Magazine, 773, 1951
  - (2) S. Omote, S. Miyamura : Relationships between Damage Distribution in Earthquake in Yokohama and Nagoya City, and Subground Conditions, Architecture Magazine, 773, 1951
  - (3) E. Kuribayashi, et al. : Investigation on the Damage of Fukui, Yebino and Izuhan-to-oki Earthquakes, Technical Memorandum of PWRI No.1196, March 1976
  - (4) E. Kuribayashi, et al. : Investigation on the Estimation Method of Razed Houses and Fire Distribution Caused by Earthquakes, Technical Memorandum of PWRI No.1256, May 1977
  - (5) T. Katayama : A Methodology to Estimate the Bridge Capability against Earthquake, Journal "Column"
  - (6) K. Kubo, et al. : Quantitative Analysis of Seismic Damage to Buried Pipelines, Proc. of the 4th Japan Earthquake Engineering Symposium, 1975
  - (7) E. Kuribayashi, et al. : An Evaluation Study on the Distribution Characteristics of Property Losses Caused by Historical Earthquakes, 10th Joint Meeting of UJNR, May 1978
  - (8) M. Katsumata : Earthquake Magnitude and the Area Possibly to Suffer Damage. Proc. of the Spring Session of Seismological Society of Japan, 1977
  - (9) T. Usami : List of the Earthquakes Caused Damage in Japan, Tokyo University Press
  - (10) Economic Planning Agency and National Land Agency : Classified Maps of Subground

Table 1 Property Loss Caused by Earthquakes

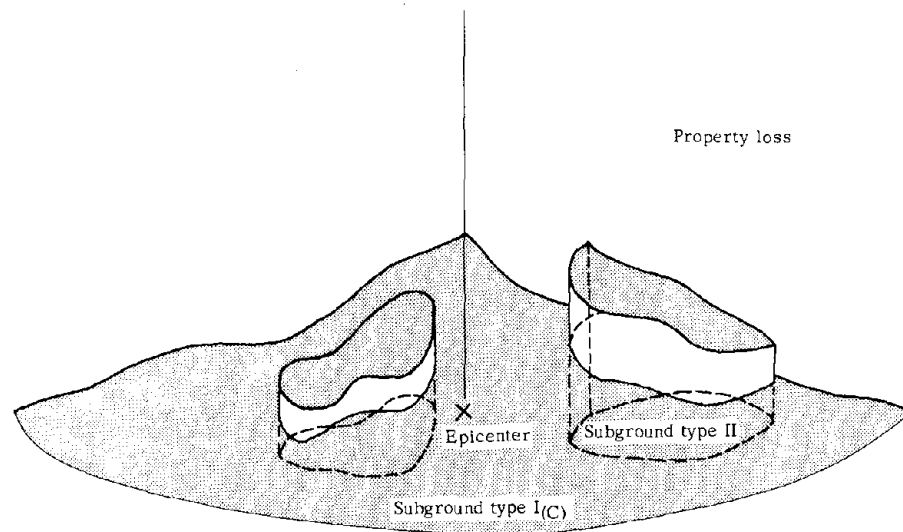
Earthquake	Year	Magnitude	Property Loss (Unit: million yen)	Estimated National Wealth (Unit: million yen)
Kanto	1923	7.9	5,500	77,000
Kita-Tajima	1925	6.5	89	78,000
Kita-Tango	1927	7.5	82.18	68,000
Kita-Izu	1930	7.0	25.46	63,000
Shizuoka	1935	6.3	10.32	96,000
Oga	1939	7.0	7.73	182,000
Tottori	1943	7.4	160	337,000
Nankai (Kochi Pref.)	1946	8.1	2,792	2,206,000
Fukui	1948	7.3	305,000	11,120,000
Imaichi	1949	6.7	3,500	13,860,000
Tokachi-oki	1952	8.1	15,183	24,200,000
Hyuganada	1961	7.0	163	70,380,000
Miyagiken-hokubu	1962	6.5	4,049	77,500,000
Niigata (Niigata Pref.)	1964	7.5	130,000	103,700,000
Yebino	1968	6.1	8,876	178,200,000
Tokachi-oki	1968	7.9	58,395	178,200,000
Tokachi-oki (Hokkaido Pref.)	1968	7.9	11,356	178,200,000
Tokachi-oki (Aomori Pref.)	1968	7.9	47,039	178,200,000
Nemuro-hanto-oki	1973	7.4	3,925	365,400,000
Ohitaken-chubu	1975	6.4	4,493	482,700,000



(A)



(B)



(C)

Fig. 1 Abstract of Property Loss Evaluation Caused by Earthquakes

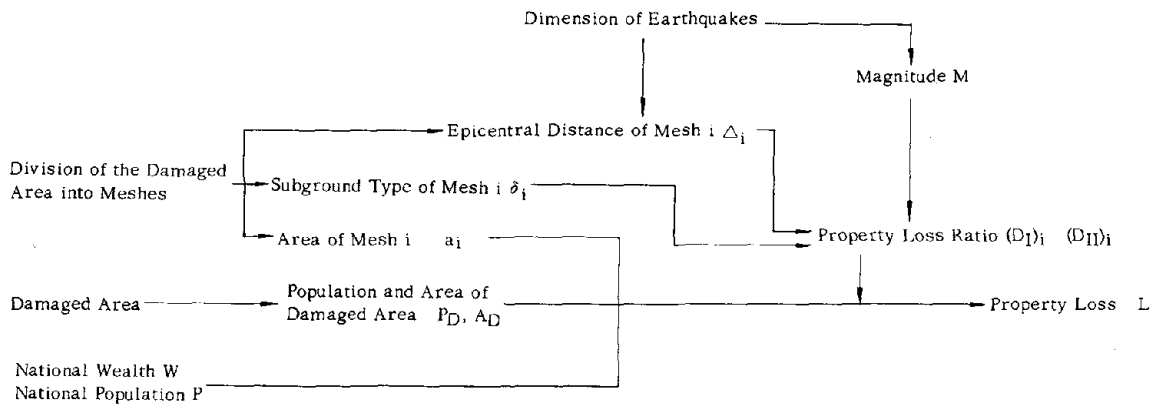


Fig. 2 Flow Chart to Evaluate Property Loss



Fig. 3 An Example of Subground Types

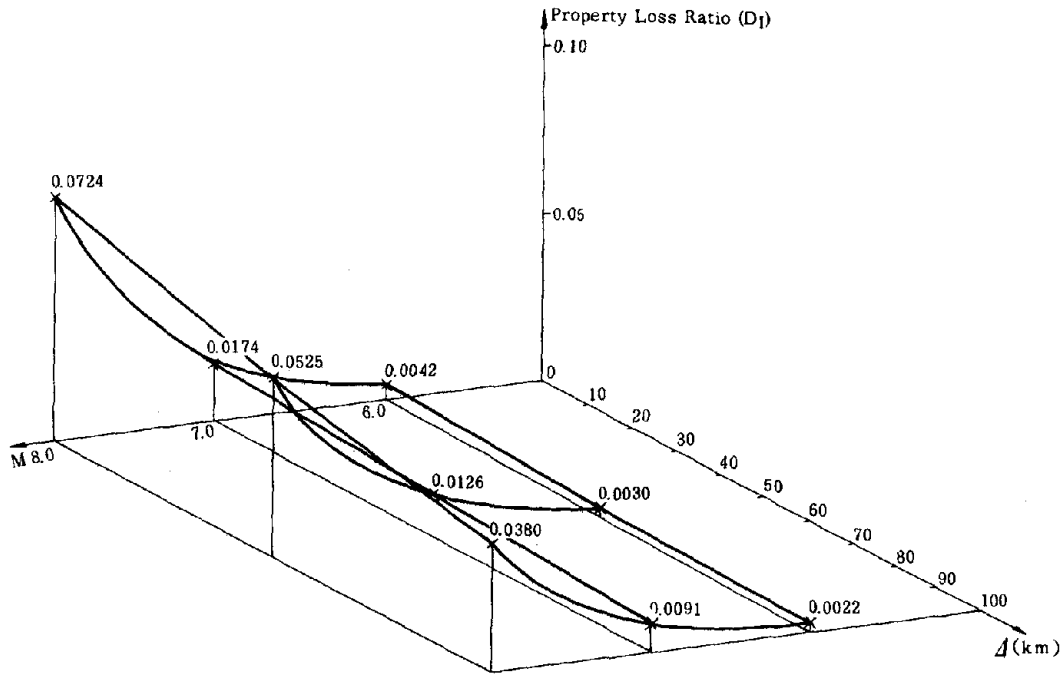


Fig. 4 Relationship between Magnitude, Epicentral Distance and Property Loss Ratio (Subground Type I)

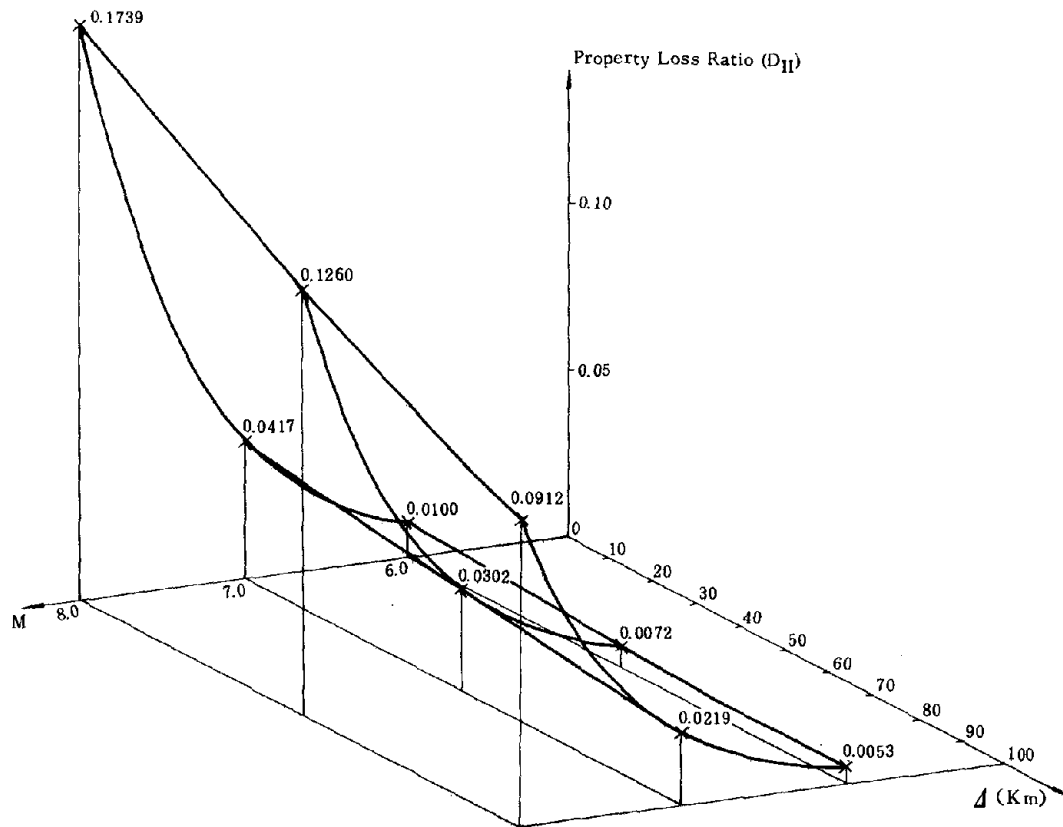


Fig. 5 Relationship between Magnitude, Epicentral Distance and Property Loss Ratio (Subground Type II)

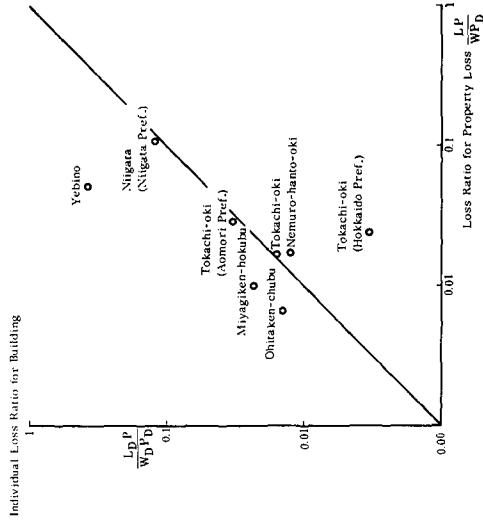


Fig. 7 Relationship between Loss Ratios of Property Loss and of Building

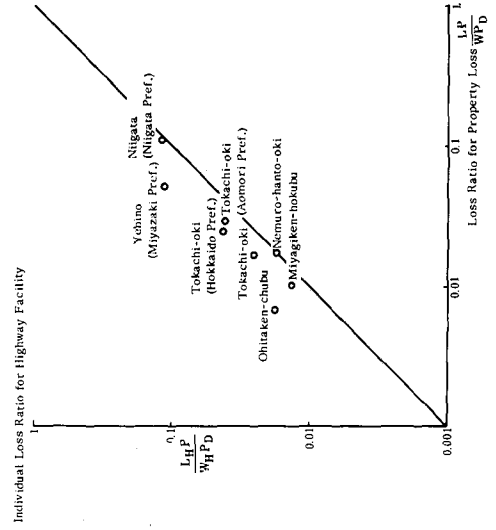


Fig. 8 Relationship between Loss Ratios of Property Loss and of Highway Facility

Social Capital (82,715 billion yen)	
32,876.2 bil. yen	Assees of Public Corporations (39.7)
	Transportation (44.2)
	Electric Power (24.7)
	Telecommunication (14.8)
21,827 bil. yen	Water Supply (13.7)
	Gas Supply (2.6)
	Education (49.4)
	Public Organizations (16.6)
	Religion (12.4)
	Medical Service (11.0)
20,986.3 bil. yen	Cooperation (8.1)
	Public Insurance (2.5)
	Highway (38.7)
	Agriculture, Fishery, Forestry (26.5)
	River (19.9)
	Harbor (9.9)
7,769.8 bil. yen	Others (5.0)
	Governmental Assets (9.4)
Central (29.8)	
Local (70.2)	

( ) : percentage.

Fig. 6 Breakdown of Social Capital in 1970 National Wealth Survey



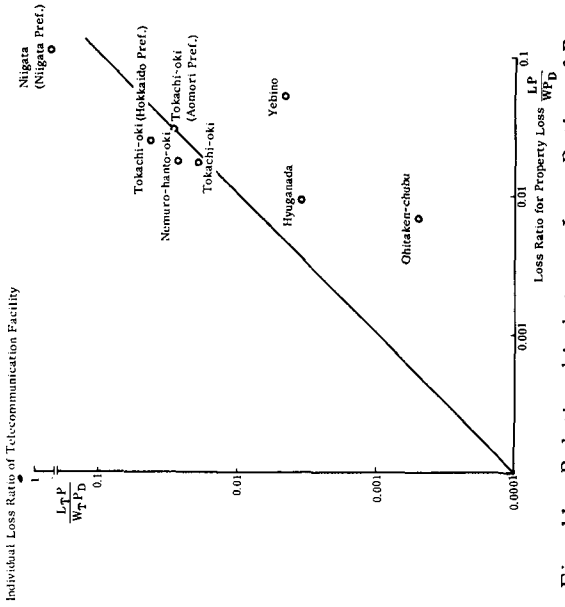


Fig. 11 Relationship between Loss Ratios of Property Loss and of Telecommunication Facility

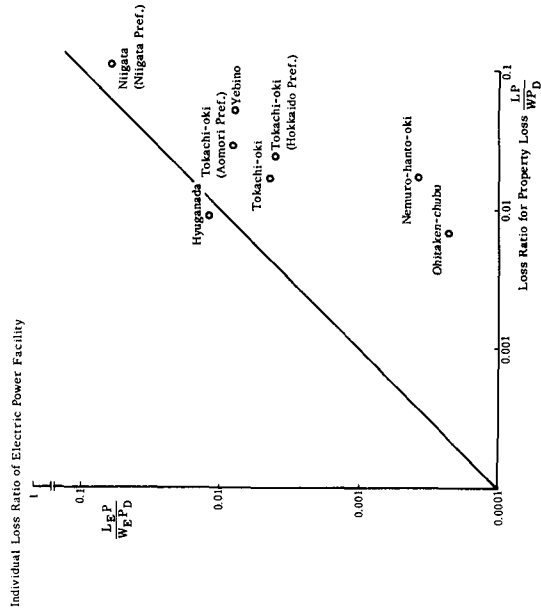


Fig. 12 Relationship between Loss Ratios of Property Loss and of Electric Power Facility

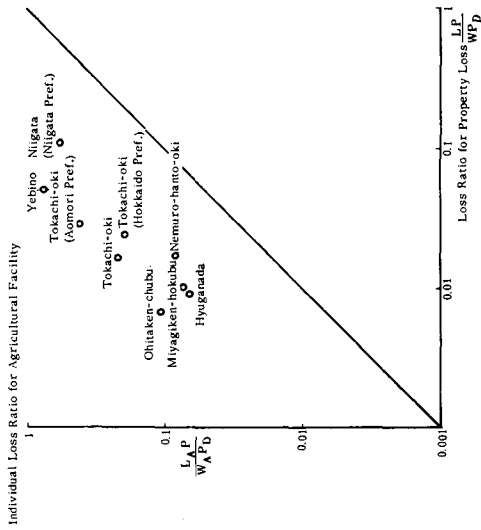


Fig. 9 Relationship between Loss Ratios of Property Loss and of Agricultural Facility

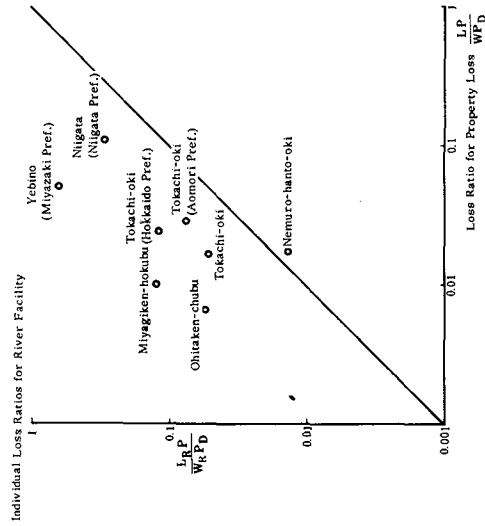


Fig. 10 Relationship between Loss Ratios of Property Loss and of River Facility

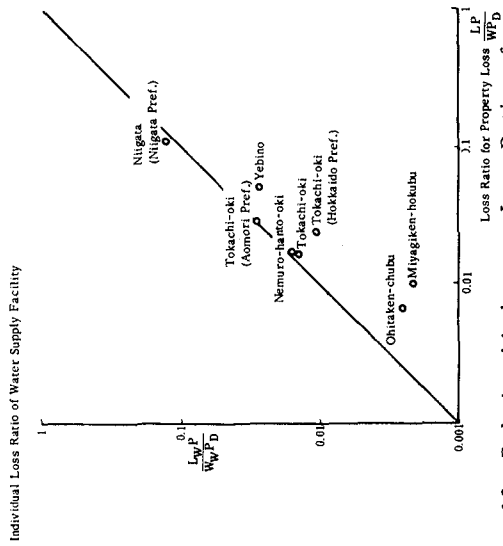


Fig. 13 Relationship between Loss Ratios of Property Loss and of Water Supply Facility

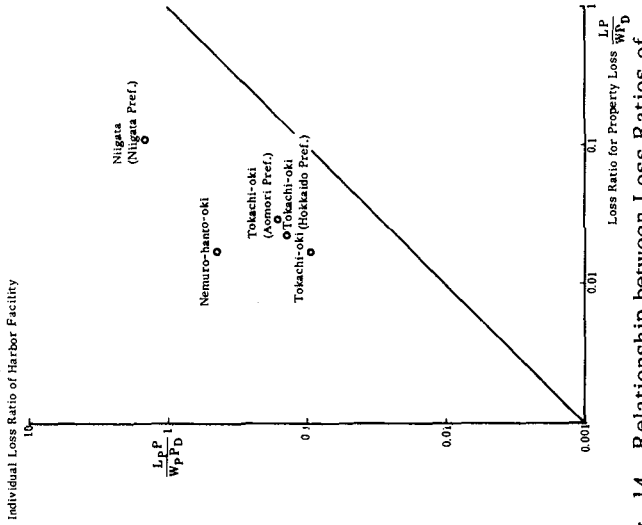


Fig. 14 Relationship between Loss Ratios of Property Loss and of Harbor Facility

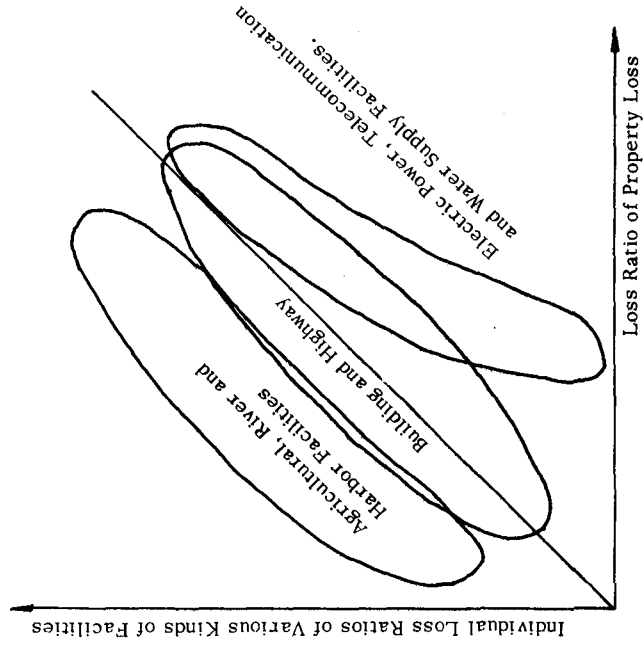


Fig. 15 Characteristics of Individual Loss Ratios of Various Kinds of Facilities

POTENTIAL FOR INFLATED BUILDING  
COSTS AFTER DISASTERBY  
Dr. Harold C. Cochrane<sup>1</sup>

## ABSTRACT

The earth movement in the Palmdale vicinity has created a great deal of concern among public administrators both in California and in Washington. This fact has given renewed momentum to legislation allocating funds for community preparedness and additional monitoring of the region's seismicity. The question as to why earthquake proofing techniques, land use management plans and other damage mitigating adjustment have not been more widely accepted has once again gained the attention of public officials. This theoretical piece seeks to assess the benefits to be derived from these adjustments, but not simply from the vantage point of loss reduction. It can be shown that under certain circumstances resulting from moderate and strong earthquakes, significant reconstruction bottlenecks and material shortages are likely. The paper presents a model of optimal adjustment to the earthquake hazard, given the recognition that a potential for a construction inflation exists. The model formulated to explore this facet of the hazard problem extends the work of Russell (1970) and Howe and Cochrane (1976). The results demonstrate that more stringent building codes and land use guidelines are economically justifiable once inflation is brought into the analysis.

Introduction

The past decade seemed to spark renewed concern for the hazard earth movements pose not only to cities in California, but Boston and other East Coast communities as well. During this period, mapping of earthquake faults was accelerated; earthquake prediction and modification studies were intensified and socioeconomic assessments of earthquake predictions and events were begun. The results of these studies, although not complete, have yielded a great deal of insight into the nature of the catastrophic event, its potential and its consequences. Yet a careful review of the literature published to date reveals a remarkable lack of attention to the problem of inflation after disaster. This lack of interest could merely reflect the fact that many of the nation's recent disasters--the San Fernando earthquake, for example--have not given rise to any significant price spiral.

By overlooking the potential for price increases in the building trades, policy makers have been deprived of one more argument for the implementation of more stringent building codes and land use guidelines. Specifically, the benefits derived from each of these hazard adjustments are not simply the reduction in expected losses measured in predisaster dollars. Reduction in losses reflecting replacement cost, post-event, is the only meaningful measure of these benefits. The next large Los Angeles earthquake will destroy or damage over \$25 billion worth of property. Yet, the entire State

---

<sup>1</sup>Associate Professor of Economics, Colorado State University. Funding for this research was provided by the National Science Foundation (NSF grant No. 76-24169).

of California could at best muster enough construction talent to replace only half of this lost capital in a year's time. This discrepancy between available resources and that required for rebuilding the city is likely to stimulate severe price dislocations, the extent of which may be matched only by the soaring inflation experienced now in certain Alaskan boom towns.

Economists have for some time recognized that the adjustment of an economy's capital stock cannot be undertaken instantaneously. That is, it may well be desirable to expand the stock of capital (housing, equipment, and so on) and the cash resources may even be available. Yet, if the desired expansion is large enough, then it may be physically impossible to meet the planned rate of expansion. For example, suppose that the price of natural gas were deregulated tomorrow and, as a result, prices for this resource rose threefold. It would not be surprising if the demand for substitute forms of heating--solar panels, for example--would be great. However, this industry is still in its infancy and most probably would not be able to meet the new demand for its product without expanding its level of operations. Such expansion will in most industries require years to complete and as a result it may be on the order of years before the demand for these panels could be met.

The imbalance between demand and supply would, in the short run, cause prices to climb. Their rise does not necessarily indicate profiteering. It simply indicates that in attempting to supply the demanded commodity, firms are forced to employ mixes of capital and labor which may be viewed as inefficient from the standpoint of the long run. If the commodity in short supply happened to be construction equipment and labor, then it is likely that rebuilding costs will escalate as the existing equipment is used more intensively and labor is forced to work long shifts commanding overtime pay. This more intensive use of existing local resources may be insufficient to meet the requirements of the disaster-stricken area. As dissatisfaction with the pace of the effort mounts, it is quite likely that outside interests will begin moving into the area to expand the pool of construction talent. However, these contractors may be leaving other areas of the state which also are expressing their demands for housing. In order to bid these resources away from uses elsewhere, disaster victims may be forced to pay premium wages reflecting the cost of transporting labor and equipment in addition to maintaining labor on-site.

Incorporation of these factors into a general model of capital expansion has been carried out by Gould (1968), Treadway (1969), and Lucas and Prescott (1971). Combining this body of knowledge with a theoretical framework developed by Russell (1970) and extended by Howe and Cochrane (1976) yields a model of rational adjustment to natural hazards. The model demonstrates that the optimal level of earthquake proofing or land use regulation is heightened if the potential for building inflation is recognized.

#### Housing Market Response to Disaster

What is meant by "inflation" in this paper is simply the rise in construction costs flowing from excess demand placed on that industry.

Rudimentary economics suggests that a disaster, in reducing the supply of housing, will cause the price of structures spared damage to rise. This escalation in price serves as a signal for contractors, both from within the region as well as those outside, to begin restoring the stock of homes. The amount of construction talent brought into the region depends upon the cost. If the disaster causes the price of homes to inflate by 10 percent, then it is difficult to justify a 20 percent increase in cost; those faced with the decision about purchasing housing will likely turn to used homes. Hence, there may be some limit on the amount of building activity observed. Such a limit is governed by the type of shortages which materialize and how this shortage influence cost.

This process is basically how the market will function. There are, of course, other factors involved: the amount of aid provided victims; insurance in force; the impact of the disaster on employment--to mention the more obvious. Demand for housing is governed not only by its price but also by the income and wealth position of prospective buyers. If the disaster destroys a high proportion of a person's wealth, it is unlikely that this same individual will have the resources to enter the housing market (especially if he was not insured). Similarly, if the disaster causes substantial unemployment, then the demand for housing will soften; fewer individuals will meet lender's requirements. In either case, the reduced stock of housing will not trigger large price changes. In turn, little construction talent will be induced into the disaster stricken area.

The above description highlights the functioning of the housing market. It does not, however, address the problem of how the potential for escalating costs influences the optimal choice of protective measures. Analysis of this subject requires a slightly different model which is developed in the next section. Before doing so, however, a few notes of caution are in order. First, the optimal choice of protection is only justified in the eyes of the economist. That is, it is a level which balances the loss reduction afforded by the adjustment against its cost. Some decision makers may behave in such a fashion but many may not. Hence, the levels discussed in the following section should be treated as optimal from the standpoint of a society that is interested in efficient use of its resources.

#### Model of Adjustment to Natural Hazards

From a purely economic standpoint, the employment of earthquake proofing techniques would result in two types of benefits, one private and one public. The traditional method of evaluating the desirability of these measures is to compare the cost of their implementation with their effectiveness in reducing losses. Hence, the choice facing the individual decision maker is: do the benefits offset the costs? However, it is possible that in the wake of certain large-scale disasters the costs of reconstruction will be inflated by critical shortages of labor and material. If this possibility were recognized by those contemplating the use of more stringent building designs, then it is likely that such designs would stand a better chance of adoption. This can be shown with the aid of the following analytical model.

It is assumed that the costs of strengthening buildings and the losses one could sustain in the event of a large earthquake respond to building strength in the following fashion:

Figure 1 Here

The costs of protection increase with the level of protection while the losses decline. The dashed line shows the sum of costs and losses and indicates that level of design which minimizes this sum ( $x^*$ ). It can be shown, with a minimal amount of calculus, that  $x^*$  occurs at that point where the marginal reduction in losses is just matched by the marginal addition to costs, as  $x$  changes.

$$(1) \quad \frac{\partial C}{\partial x} = \frac{\partial L}{\partial x}$$

However, if the disaster is of sufficient size, then the losses should include an adjustment for rising cost of repair. This can be accomplished by attaching a building trades constraint to the cost-loss model just described. The sum of the costs and losses would be:

$$(2) \quad F(x, X, \lambda, \bar{y}) = f_1(x) c(\bar{y}, x, X) - c(\bar{y}, x) \\ + \lambda \{f_2[N f_1(x) c(\bar{y}, x)] - X\}$$

where:  $f_1(x)$  is a damage function relating adjustment level (building strength) to percentage of structure value damaged in any event.  $[\partial f_1(x)]/\partial x < 0$ .

$c(\bar{y}, x, X)$  is the cost of repair assuming: the square footage of the structure is fixed at  $\bar{y}$ ; a given adjustment level  $x$ ; and an inflationary impact given by  $X$ .  $\partial c/\partial x > 0$ ,  $\partial c/\partial X > 0$ .

$c(\bar{y}, x)$  is the initial building cost with some level of proofing techniques incorporated.

$\{f_2[N f_1(x) c(\bar{y}, x)] - X\}$  captures the influence of the building trades constraint.  $X$ , the bottleneck cost, is sensitive to the number of structures damaged ( $N$ ), the damage function ( $f_1(x)$ ) and the cost of repair ( $c(\bar{y}, x)$ ).

$\lambda$  is the lagrangian multiplier.

Minimizing (2) with respect to  $x$  yields two possible solutions, each depending upon the value of  $\lambda$ . In general:

$$(3) \quad \frac{\partial F(x, X, \lambda, \bar{y})}{\partial x} = 0 \\ 0 = \frac{\partial f_1(x)}{\partial x} c(\bar{y}, x, X) + \frac{\partial c(\bar{y}, x, X)}{\partial x} f_1(x) \\ + \frac{\partial c(\bar{y}, x)}{\partial x} + \lambda N b \left[ \frac{\partial f_1(x)}{\partial x} c(\bar{y}, x) + \frac{\partial c(\bar{y}, x)}{\partial x} f_1(x) \right]$$

where:  $b$  is a constant of proportionality which relates damages to congestion costs.

The constraint may or may not come into play in the final solution, i.e.,  $\lambda = +$  or  $\lambda = 0$ . If  $\lambda = 0$ <sup>1/</sup> we have

$$(4) \quad 0 = \left[ \frac{\partial f_1(x) c(\bar{y}, x, X)}{\partial x} + \frac{\partial c(\bar{y}, x, X) f_1(x)}{\partial x} \right] + \frac{\partial c(\bar{y}, x)}{\partial x}$$

(4) indicates that in the absence of the construction constraint, the decision maker will select that level of protection for which the marginal reduction in damage (the term in brackets) just offsets the marginal cost increases.<sup>2/</sup> If  $\lambda = +$ , then the first order conditions for a minimum are:

$$(5a) \quad \frac{\partial F}{\partial x} = 0 = \frac{\partial f_1(x) c(\bar{y}, x, X)}{\partial x} + \frac{\partial c(\bar{y}, x, X) f_1(x)}{\partial x} + \frac{\partial c(y, x)}{\partial x} + \lambda N b \left[ \frac{\partial f_1(x) c(\bar{y}, x)}{\partial x} + \frac{\partial c(\bar{y}, x) f_1(x)}{\partial x} \right]$$

$$(5b) \quad \frac{\partial F}{\partial X} = 0 = [f_1(x) \frac{\partial c(\bar{y}, x, X)}{\partial X}] - \lambda$$

$$(5c) \quad \frac{\partial F}{\partial \lambda} = 0 = N b [f_1(x) c(\bar{y}, x)] - X$$

If construction externalities (bottlenecks) enter into the problem then

$$(6) \quad \lambda = + = f_1(x) \frac{\partial c(\bar{y}, x, X)}{\partial X}$$

This implies that  $\partial c(y, x, X)/\partial X$  is positive, i.e., the construction constraint will affect losses. Substituting (6) into (5a) yields

<sup>1/</sup>  $\lambda = 0$  when  $\partial F/\partial X = 0$ . Since  $\partial F/\partial X = f_1(x) \frac{\partial c(\bar{y}, x, X)}{\partial X} - \lambda$  and  $f_1(x) > 0$ , then  $\partial c(\bar{y}, x, X)/\partial X = 0$ . This means that costs are insensitive to bottlenecks, at least as far as the decision maker is concerned.

<sup>2/</sup> The term in brackets contains two components--the reduction in damages and the added cost of repair resulting from increasing building strength. The reduction in damages must override any cost increases in order for strengthened buildings to have any appeal at all.

$$(7) \quad 0 = \frac{[\partial f_1(x) c(\bar{y}, x, X)]}{\partial x} + \frac{\partial c(\bar{y}, x, X) f_1(x)}{\partial x} \\ + \frac{\partial c(\bar{y}, x)}{\partial x} + [f_1(x) \frac{\partial c(y, x, X)}{\partial X}] \quad \text{N b} \quad \frac{[\partial f_1(x) c(\bar{y}, x)]}{\partial x} + \frac{\partial c(\bar{y}, x) f_1(x)}{\partial x}$$

It is the presence of the last term which creates a difference between the optimal solution which ignores bottlenecks, and one in which rising repair solution costs are recognized. The last term in (7) can be shown to be always positive.<sup>3/</sup> This indicates that the slope of the loss relation is greater than that of the cost function. In order for optimality to be obtained,  $x$  must increase, thereby increasing  $c(\bar{y}, x)/x$ . This conclusion is illustrated in Figure 2 where the most efficient level of production rises from  $x_1^*$  to  $x_2^*$ .

Figure 2 Here

### Evidence of Inflation

In order to test the hypothesis that escalating building costs would follow certain disasters, housing market data were collected from past disaster sites.<sup>4/</sup> By looking at the time history of prices we could determine whether the disaster contributed to inflation in this sector. For one site, Darwin, Australia, accurate information on building costs were obtained so they too were included in the analysis. At the time of this paper's preparation, a full analysis of the data had not been completed. The material to follow is, therefore, only suggestive of the type of presentation that will be made at the conference.

Tentative findings point to inflationary pressures over and above that expected without disaster. The results for Darwin are presented in some detail because more effort has been devoted thus far to this part of the study. Just as important, the data base included both housing sales and costs.

In December of 1974, a cyclone passed directly over the capital city of Australia's Northern Territory. Within eight hours, the town's housing stock had been diminished from 12 thousand single-unit homes to 4 thousand; 8 thousand were completely demolished. Because of an acute housing shortage

---

<sup>3/</sup>  $f_1(x_1)$  is positive and  $\partial c(\bar{y}, x, X)/\partial X$  is negative.  $\frac{\partial c(y, x)}{\partial x} f_1(x)$  is less than  $\frac{\partial f_1(x) c(\bar{y}, x)}{\partial x}$ . Hence, the term in brackets will be negative.

<sup>4/</sup> The sites chosen include--Darwin, Australia (Cyclone, 1974); Rapid City, South Dakota (Flash Flood, 1972); Wilkes-Barre, Pa. (Flood, 1972); San Fernando, Calif. (Earthquake, 1971); New Orleans, La. (Hurricane, 1965); and Corning, New York (Flood, 1972).



and the fact that Darwin is so distant from other major population centers of Australia, it was decided that this site would provide some useful insights into the problem of post-disaster inflation.

The immediate post-disaster period saw a rapid rise in material and labor cost stemming from critical shortages in both. The extent to which labor costs increased is difficult to document, although the indices presented in Figure 3 show a rise which differs markedly from other areas of Australia. As shown, growth in Northern Territory wages has lagged

Figure 3 Here

consistently behind the remainder of Australia except for the immediate post-disaster period, indicated by the shaded area. For approximately one year, the trend reversed indicating a shortage in construction labor in the Darwin area.

A graph of housing costs (Figure 4) show that inflation in the building sector was well established prior to 1975. In 1972, the average contract price for a three bedroom home was approximately \$13 thousand; by 1974

Figure 4 Here

the costs had risen to \$21 thousand, an increase of 62%. When comparing the trend after the disaster with that of costs elsewhere in Australia, it becomes evident that the Northern Territory has experienced a sharper rise in prices since 1975. The lower curve shows the growth in building costs if the rate of change in such costs, Australia-wide, is used to indicate the "normal" rate of inflation in the construction sector.

The drop in the average contract price from 1976 reflects both a relaxation in the building codes and a more plentiful supply of labor. The original code implemented in late 1975 proved to add almost \$11 thousand to the price of the average three bedroom house. It quickly became apparent that given the existing housing market in Darwin there were only a limited number of people that could afford to pay for such a change in housing costs. As a result, the code was modified in the subsequent year to permit less expensive yet effective cyclone resistant designs. At the same time, facilities became available to accommodate the influx of tradesmen from the South. Up to June of 1975, a permit stipulating that individuals entering have a place of residence was required to enter Darwin. This discouraged some but not all subcontractors from expanding the supply of reconstruction talent.

A separate study of costs conducted by the Darwin Reconstruction Commission concluded that the remoteness of Darwin contributed 20 percent to the price of an average residential structure. These added costs reflected: airfare, lodging in a contractor's camp, materials transport costs, premium wages, and set-up costs for new contractors. All of these, except for material transport, are directly chargeable to the bottlenecks encountered in the effort to rapidly rebuild the city. In short, of 20 percent increased costs, 17 percent was attributable to these so called bottleneck problems.

By taking both this 17 percent increase and the added materials and labor required to meet the new building codes to the "normal" inflationary trend, Darwin's cost changes can be nearly reproduced.

The real estate market emerged very slowly following the cyclone, the first sales commencing after a lapse of almost six months. Records for the period January 1975 to June 1977 showed several distinct trends, some of which could have been predicted while others are still unsatisfactorily explained. The original intent for including the housing market in the study was that post-disaster pressure on building costs should be reflected in price changes for the existing housing stock. The rapid return of Darwin's residents, at least in theory, should have driven up prices on the limited amount of housing that survived the storm. One would expect the extent of such increases to mirror any escalation in building costs. At least in theory disaster victims would treat new and old housing (less physical depreciation and quality differences) as close substitutes. Hence, escalating costs of building materials would shift demand toward the existing housing stock thereby causing a rise in prices there.

To test this possibility, real estate sales records were summarized to provide the following information:

- \*sales price
- \*date of sale
- \*predisaster assessed value
- \*post-disaster assessed value, and
- \*condition of the structure upon sale (whether it had been repaired to predisaster or post-disaster code)

The factors that proved to be most useful in forecasting sales price were predisaster assessed value and condition of the structure upon sale. The date of sale did not significantly alter selling price.

This by itself is a curious result since a plot of selling prices over time should have revealed a growth path compounding at a rate of approximately eight percent per year, at least for the period of the early and middle 70's. One explanation for the failure of time to influence sales price could be the simultaneous shift in both supply and demand. The swift return of population placed pressure on the housing market, while the relatively rapid program of rebuilding expanded the housing stock. The interaction of these two forces diminished the influence of time. If either supply of housing or demand had been relatively stable during this period, it is quite likely that time would have turned out to be a significant factor. For example, if the population had returned sooner, the price of the housing stock surviving the storm would have escalated to reflect the scarcity. As rebuilding commenced and the number of available structures expanded, the price would have fallen to a path representative of the "normal" growth in materials and labor costs.

These results suggest that the period of reconstruction created a market for moderately priced homes, especially those that embodied the improved construction methods. Homes in the upper price ranges did not increase in value to even keep pace with inflation in building costs. These

observations seem to suggest that an inflationary trend existed after the cyclone, which exceeded that to be expected by normal building price increases. But the trend was very uneven, centering mostly in the market for low and moderate priced housing. A number of realtors interviewed tended to support this finding.

### Implications for Government Policy

The potential for inflation in the wake of disaster points to the need for a careful review of alternative ways of diminishing these impacts. Competing policies can be conveniently divided into those that are implemented pre-event and those which are directed to the reconstruction period. Earthquake proofing, land use management, and a mandatory hazard insurance program are obvious ways of reducing potential construction bottlenecks. Price control guidelines, distribution of stockpiled material, tax breaks, outright government grants, and a priority system for reconstruction represent a sample of post-event possibilities.

Given the framework developed above, it is possible to examine each of those policies and speculate about the consequences of their adoption. The introduction of earthquake proofing technology was shown above to relieve pressure on the building trades industry and thereby reduce the post-disaster losses experienced by the homeowner. The social desirability of proofing was enhanced further by the fact that if implemented, fewer resources would be diverted from economic uses elsewhere.

Adoption of either more stringent building codes or land use planning of fault zones has generally come in response to disaster. Major pieces of legislation have resulted from every one of California's major earthquakes. Regulations concerning fire followed on the heels of the 1906 San Francisco quake. School safety provisions were enacted after Long Beach (1933). Hospital safety was the subject of intense scrutiny in the wake of San Fernando (1971). There are several explanations for this observation, but much of the blame for not pursuing a more carefully thought-out program lies in the public's perception of low probability events. There is now good reason to suspect that individuals have a great deal of difficulty processing information about events the chances of which are less than one in one hundred of occurring.<sup>5/</sup> This finding could also explain the relatively little interest observed in earthquake insurance. Less than 5 percent of all homeowners in California now carry any form of earthquake coverage. The model developed above is equally applicable to the insurance problem.

If insurance is made mandatory, premium payments would be linked directly to proofing technology adopted as well as the structure's location with regard to hazardous faults. The premium could reflect as well, the bottleneck constraint illustrated above. Even though the homeowner may still be subject to the same ignorance or may wish to assume that others

---

<sup>5/</sup>A recently completed study on hazard insurance by Kunreuther (1976) demonstrates this problem.

have proofing in effect, he will be forced to internalize these factors. The insurance company could set premium payments based upon all relevant costs including bottleneck costs. The homeowner is free to compare the cost of proofing with the reduction in premium payments. The homeowner may then adopt that level of  $x$  for which:

$$(8) \quad 0 = \frac{\partial c(\bar{y}, x)}{\partial x} + P$$

$P$  here is the premium payment that is reduced by added protection  $x$ . It is in other words the marginal savings on insurance. Optimal protection occurs at a level of  $x$  which causes the marginal costs to just equal the marginal savings. Now the insurance company can set  $P$  so that:

$$(9) \quad P = \left[ \frac{\partial f_1(x)}{\partial x} c(\bar{y}, x, X) + \frac{\partial c(\bar{y}, x, X)}{\partial x} f_1(x) \right] \\ + \left[ f_1(x) \frac{\partial c(\bar{y}, x, X)}{\partial x} \right] Nb \left[ \frac{\partial f_1(x)}{\partial x} c(\bar{y}, x) + \frac{\partial c(\bar{y}, x)}{\partial x} f_1(x) \right].$$

Inserting (9) and (8) we are given (7), which yields the socially optimal level of adjustment to the hazard. If for some reason voluntary purchase of insurance accelerated, then these same cost increases will be an important consideration in the establishment of premiums. If those companies marketing insurance do not include this factor, claims may exceed reserves.

A tax incentive is readily incorporated into the model. If the homeowner does not recognize the potential for inflation, then the optimal adjustment level, as he sees it, is  $x_1^*$  in Figure 2. In order to induce him to move to  $x_2^*$ , a tax incentive can be applied to those expenditures designed to strengthen buildings. This grant will lessen the private costs of adjusting to the hazard and induce a shift in optimal protection level toward  $x_2^*$ . The result is that government bears part of the cost of protection but this expenditure yields a net return to society shown in Figure 5.

#### Figure 5

At that point in time when the large-scale event materializes, the focus of public policy must of course switch to the question of what to do about the mounting pressure being exerted on the construction industry. The framework thus far presented does provide some insight here as well. Price guidelines will serve to diminish the reservoir of construction resources. Those contractors located at some distance from the disaster site may be unwilling to move operations if the added costs are not reimbursable. This reduction in the pool of construction talents will prolong the recovery effort.

Stockpiled material could soften any escalation in building costs, particularly for those items which could turn out to be in very short supply. This strategy may be very costly, however, since the interest costs over a 50- to 100-year period are quite substantial.

Outright cash grants to individuals may help lessen their burden, but they will not solve the basic problem, which is a shortage of critical resources. In fact, what may happen could turn out to be counterproductive. The added cash flowing into the affected area may just accelerate cost increases, providing the capital to bid away resources from more remote areas around the state.

A priority system for reconstruction appears, at least on the surface, to have the most potential of any of the post-disaster possibilities thus far discussed. Rather than permitting the market to allocate effort to different uses, a priority system could be established to indicate those demands which must be met first. For example, only those property owners who experience a complete loss would be given access to limited construction resources. After completing those construction requirements, partial losses would be attended to.

#### References

- Gould, John P.  
 1968 "Adjustment Costs in the Theory of Investment of the Firm,"  
Review of Economic Studies, 35, pp. 47-57.
- Howe, Charles W. and Harold C. Cochrane  
 1976 "A Decision Model for Adjusting to Natural Hazard Events With  
 Application to Urban Snow Storms," The Review of Economics  
 and Statistics, 58, pp. 50-58.
- Kunreuther, Howard, et al.  
 1976 Limited Knowledge and Insurance Protection: Implications for  
 Natural Hazard Policy, Final Report to the National Science  
 Foundation, Grant ATA73-03 064-A03.
- Lucas, Robert E. and Edward C. Prescott  
 1971 "Investment Under Uncertainty," Econometrica, 39, pp. 659-681.
- Russell, Clifford S.  
 1970 "Losses from Natural Hazards," Land Economics, 66, pp. 383-393.

FIGURE 1

OPTIMAL ADJUSTMENT TO NATURAL PHENOMENA

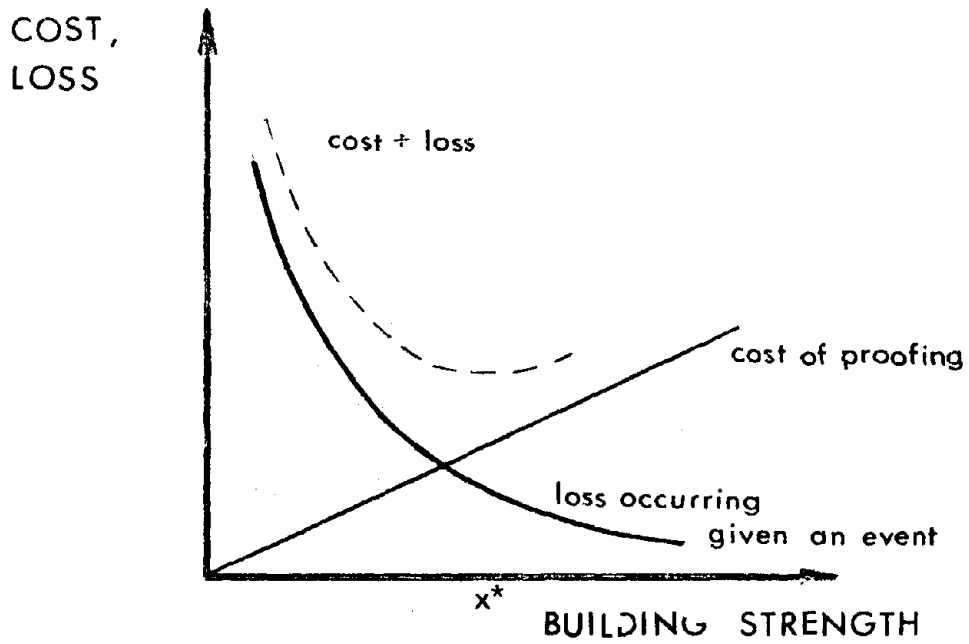


FIGURE 2

OPTIMAL ADJUSTMENT TO NATURAL PHENOMENA: INFLATION INCLUDED

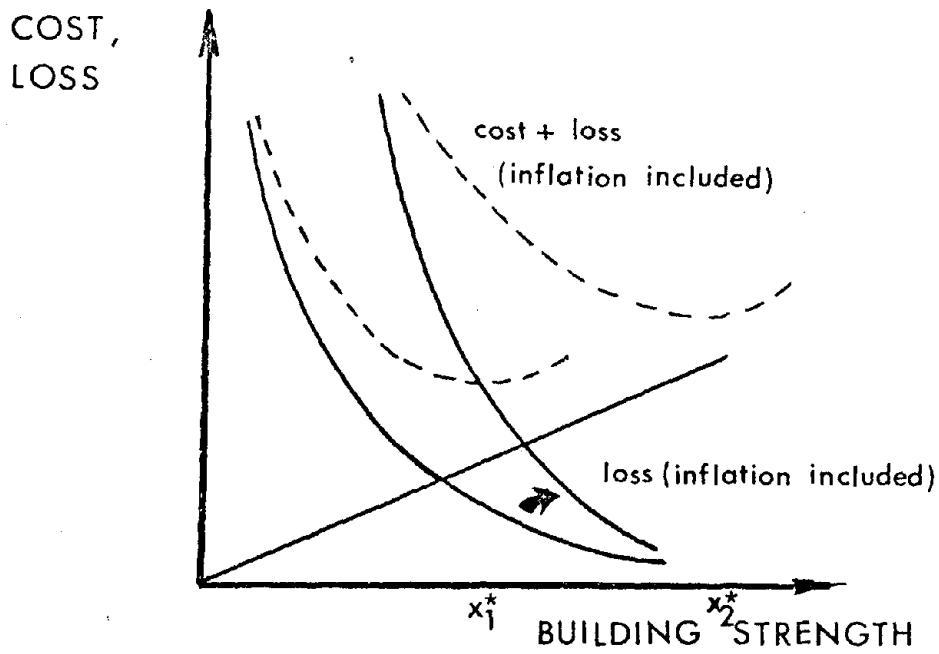
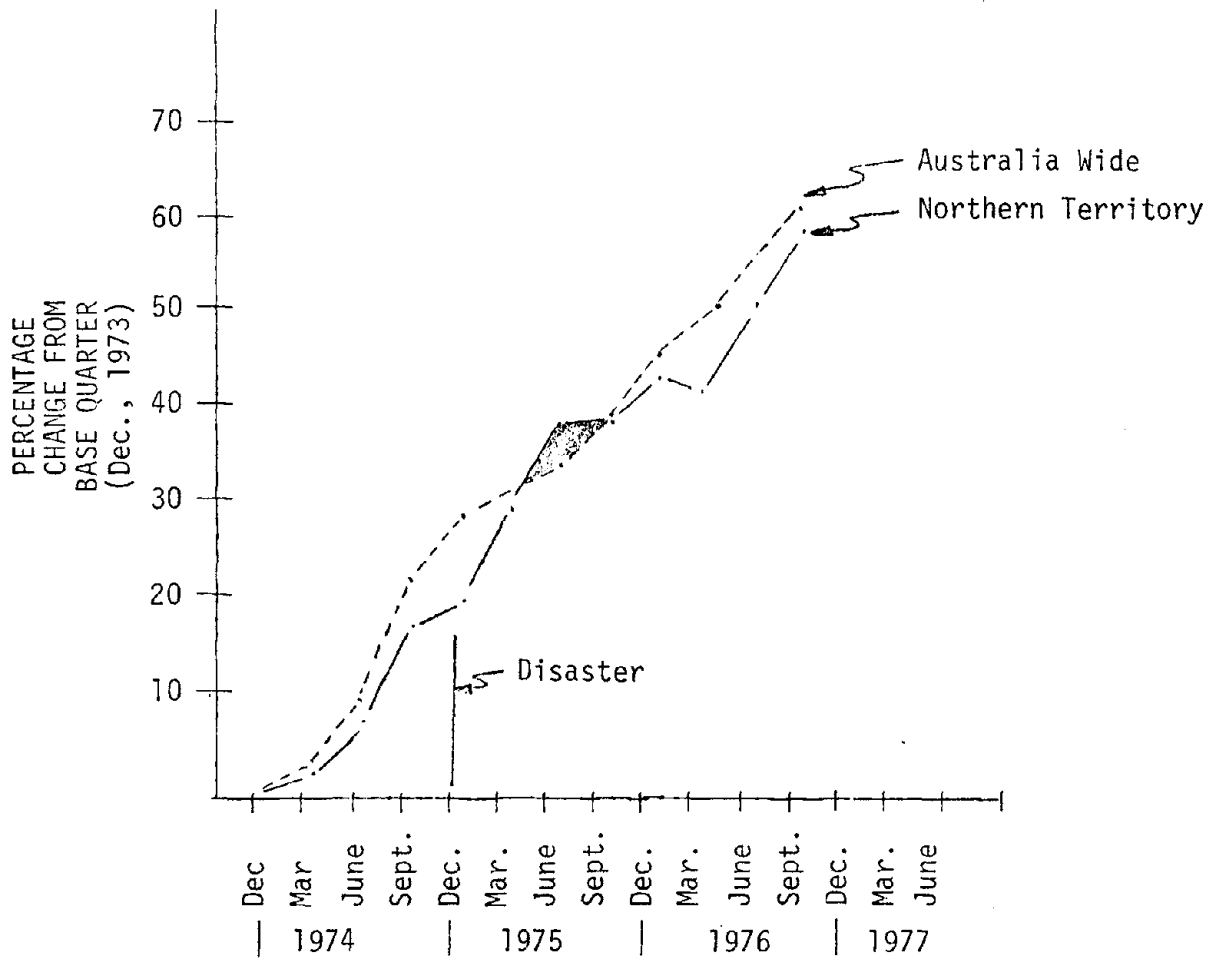


FIGURE 3  
 CHANGE IN AVERAGE WEEKLY EARNINGS OF  
 WORKERS  
 NORTHERN TERRITORY CONTRASTED WITH AUSTRALIA



CONSTRUCTION COSTS AFTER THE CYCLONE

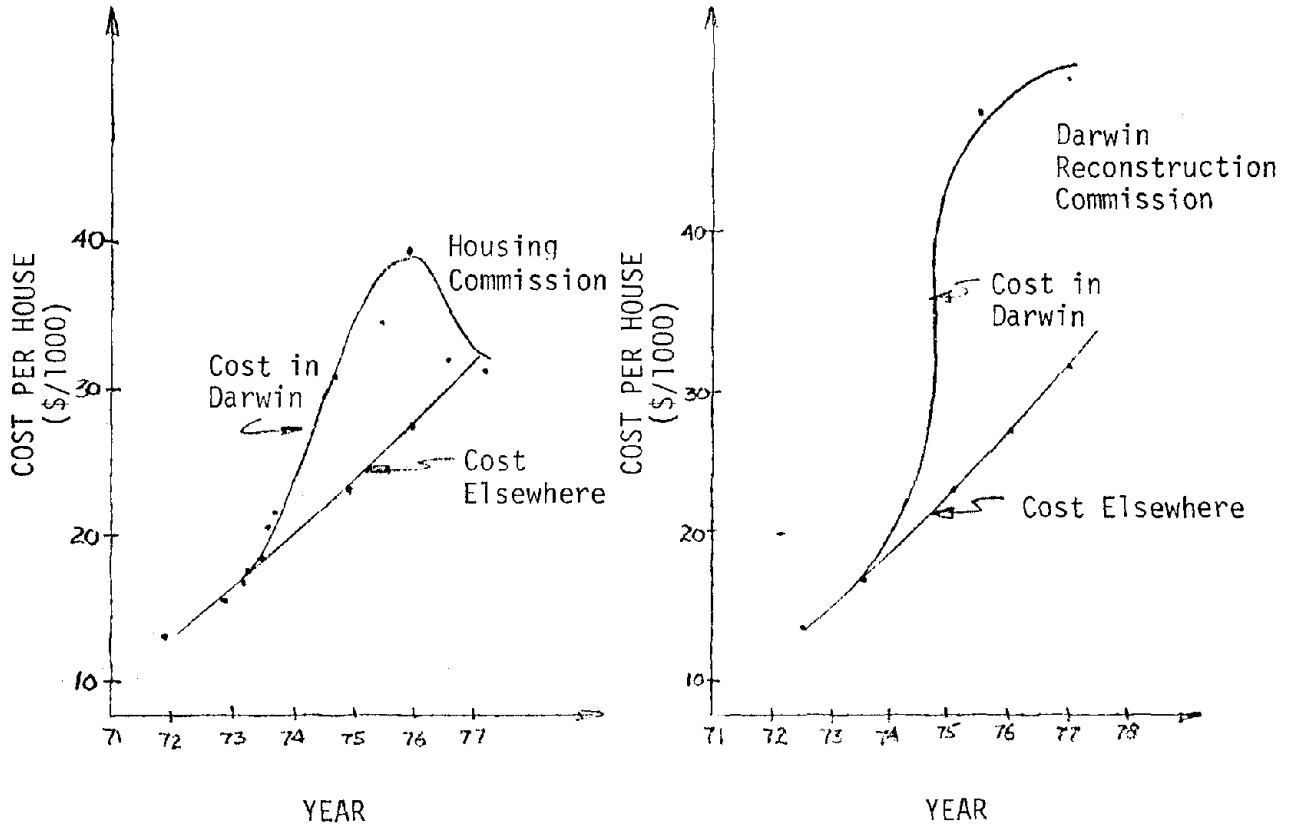
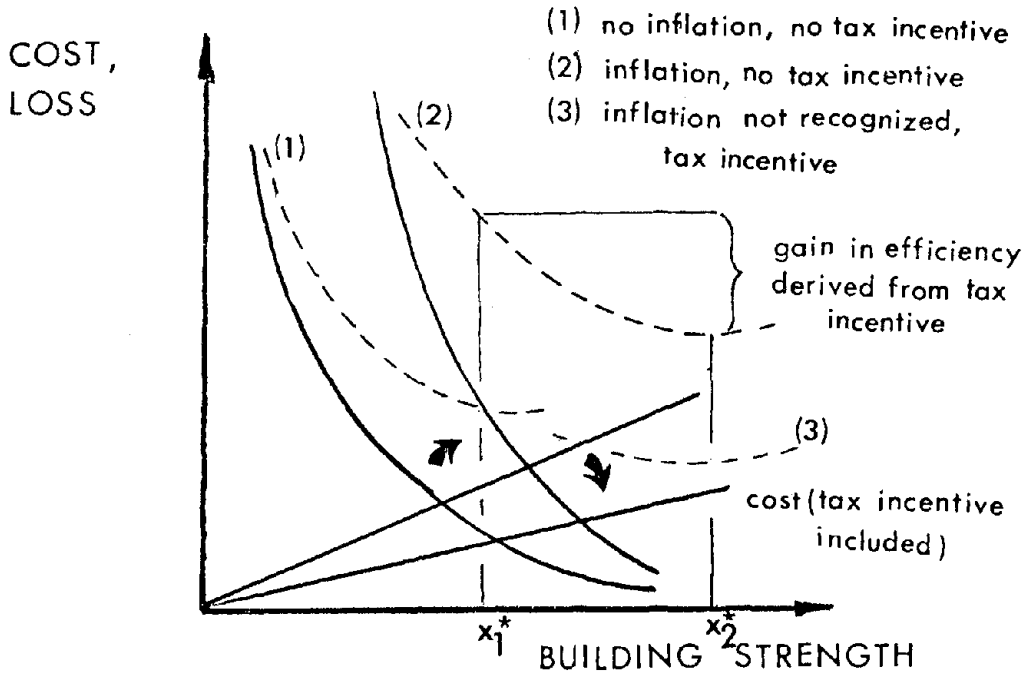


FIGURE 5

OPTIMAL ADJUSTMENT TO NATURAL PHENOMENA: TAX INCENTIVES INCLUDED





## EARTHQUAKE AND INSURANCE

by

Robert Themptander<sup>I</sup>

## ABSTRACT

This paper deals with some of the problems that the insurance industry presently will have to face in connection with earthquake insurance. Additional future problems arising from the foreseen development of earthquake prediction are touched upon. In a few cases possible solutions are indicated.

## INTRODUCTION

Glamourless as most insurance activities may seem to be, there are some greatly challenging areas involved. One example is problems in connection with insuring or reinsuring the earthquake peril. In the following some of these problems will be touched upon. The approach to earthquake insurance has been different in different parts of the world. What is regarded as a problem in some countries may thus be much less pronounced or not even noticeable in others. Some problems, however, seem to be of an almost world-wide nature.

## PROBLEMS

There seems to be a clear difference in people's awareness of the earthquake risk and the windstorm risk. This is not surprising. The seasonal return pattern of storm appearances, public forecastings and warning systems as well as rescue plans all contribute to a more or less continuous reminding of the wind risk. In respect of earthquakes it has so far been quite different. In most people's mind a great earthquake is remote until it actually occurs. For some time after a catastrophic quake the awareness is high but too soon it is again fading. The time of high awareness coincides perfectly with the period just following a strong earthquake and its aftershocks, when the likelihood for a new one is at a minimum. A few decades later there is a new generation, for which a major earthquake is something their parents may still talk of, but which is not likely to occur to them.

Thus even people living in highly earthquake-prone areas show a remarkably low interest in insuring their property against the earthquake risk. In most Latin-American countries, for instance, less than 10 % of private dwellings and contents are covered, and in many countries this figure falls below 5 %. Even in highly developed California one finds similar low insurance interest despite all the extensive earthquake research which is going on in this state.

It is difficult to believe that a majority of the uninsured are in fact lacking knowledge about the very real risk. As a consequence the phenomenon can in many cases be classified as fatalism. Sometimes, however, it must no doubt be pure negligence, and it is surprising indeed to learn how many homeowners and householders in Latin-America, even well off people, completely abstain from buying any kind of insurance coverage for their property, fire as well as earthquake.

---

I Vice President and Actuary, Skandia Insurance Company, Stockholm, Sweden

One might also presume that a share of the population do trust that if a catastrophe occurs, their own government and sources from abroad will contribute to a great extent to indemnifying uninsured victims, the more so since that kind of support is far from unusual.

However, not only property owners' attitudes are of importance. In many seismically active countries no earthquake coverage is provided by the insurance industry or - as in Japan - is provided only on a highly reduced basis.

The aforesaid clearly indicates that only a small share of the economic loss in an earthquake today will be paid by insurance arrangements, a fact which was also demonstrated after recent catastrophes. Only some 10 % of the actual losses in Nicaragua on December 23, 1972 and in Guatemala on February 4, 1976 were payable under insurance contracts, and almost nothing was insured of the Italian catastrophe on May 6, 1976 and the Rumanian on March 4, 1977.

This is, of course, most unsatisfactory from the indemnification point of view, though it does relieve the insurance world from facing an otherwise obvious problem. If most property and business interruption interests were insured the present worldwide private insurance capacity would be far from sufficient to absorb the risk.

The total value of surplus funds presently held by property/casualty insurance companies on a worldwide basis can be estimated at 50-60 billion US dollars. Legal minimum solvency requirements probably add up to at least 2/3 of actual surplus funds and insurance companies with a careful underwriting would certainly not take the risk of loosing the entire remaining 1/3 in one single catastrophic event. One may assume that a loss of some 10 billion US dollars in one single event would be bad enough for the total insurance industry<sup>I</sup>, and that global capacity would be available only if every insurance company in the world participate with its full capacity, in covering the top catastrophe exposures, such as in the Los Angeles, San Francisco, Mexico City or Tokyo areas. In practice a lot of companies do not participate in reinsuring foreign catastrophic risks so the maximum capacity available is further reduced.

This deficit in worldwide capacity will most probably last for many years to come. The rapid growth in value concentration in highly populated areas, inflationary effects etc. will continue, and the profitability in the insurance/reinsurance business is rarely good enough to enable the surplus funds to keep pace with the growth in catastrophe potential.

Other factors do contribute to the limitation of worldwide capacity. One is the low frequency of supercatastrophes. Memory is too short not only among the insured population, but also insurance companies do to some extent fall in the same trap. In lines of insurance characterized by extremely low frequency of extremely large losses the premium level generally tends to become insufficient, although for long periods of time the profitability seems to be good. Primary companies hesitate to give away too much

---

I It is delicate to quantify the amounts mentioned here. However, their indicated magnitude seems to be realistic.

of this "profit" to their reinsurers, so reinsurance conditions tend to deteriorate by increasing commissions, by extending profit commission also to catastrophe premium etc. Reinsurers who are aware of the long term loss potential certainly abstain from engaging themselves to their full capacity.

Another factor of importance is the distribution method commonly used for insurance and reinsurance. An insured risk is often by a broker placed with several insurance companies and a reinsurer in his turn is via different brokers offered participation in treaty business as well as facultative shares emanating from different primary companies. Eventually the reinsurers retrocede part of their portfolios to other reinsurers. The same risk or treaty may partly be scuffled around the world via a number of reinsurers, brokers and underwriting agencies before it eventually is kept by the last company in a long chain. On top of all this most companies buy catastrophe covers to protect their net retained portfolios, and such catastrophe covers are spread among important international reinsurers already engaged in the chain. This creates complicated problems for a reinsurer who wants to estimate his true total exposure in an area that in an earthquake can be hit by intensities of, say, MM VI or stronger. Needless to say, it will be even more difficult to estimate what probable maximum loss he will suffer. Such uncertainties make a cautious reinsurer anxious to maintain a certain security margin and not utilize his theoretical maximum capacity in anyone area. It is true that less careful reinsurers no doubt will engage themselves without conscious apprehension, but many of these will fail to pay their underwritten share of a supercatastrophe in full. The same will no doubt come true in respect of many primary insurers, having been too optimistic.

After a destructive earthquake at least domestic insurers and reinsurers will no doubt also suffer from a substantial indirect strain on their surplus funds. Their assets (liability funds as well as surplus) are probably to a great extent invested in real estates, shareholding in industrial companies etc. located in the affected area. These assets are vulnerable to a substantial decrease in value after a major earthquake, even if the property behind the investments is completely undamaged. People may prefer to move to another area, an industry may suffer economically from lack of normal supply from other, damaged industries etc. At the same time as the liability funds (loss reserves) increase by the quake, the total assets may thus decrease. This will put a double squeeze on the surplus funds.

What, then, can be done to make available a sufficiently high overall capacity to insure whoever wants to protect his property and other economic interests?

As already said, the governments after a national catastrophe are greatly involved, not only in rescuing activities, but also to a large extent in economic support to suffering people. The indemnification is thus provided by insurance companies and the government. The present split is however probably not the most efficient.

One solution has already since long been tested in the US for flood insurance.

Another solution, which in recent years has been discussed in Australia, would be to introduce a governmental system for insuring national hazards. It was suggested that the insurance companies should collect a catastrophe premium, compulsory coupled with the fire policy, on behalf of the government. The companies should keep a small fee and deliver the rest of the premium to a government administered catastrophe fund. The fund should retain a small share of the catastrophe risk, 5,000,000 A \$ per event and reinsure the unlimited excess liability with the worldwide insurance industry.

Such a program would however still leave the capacity problem for the insurance industry unsolved.

A better solution, based on cooperation between governments and the insurance industry, would probably be the following:

- The banks should ask for earthquake insurance as well as fire insurance before giving mortgage loans.
- The insurance companies should write earthquake insurances as usual in combination with fire policies.
- The insurance companies aggregate liability should be limited in anyone earthquake (main shock and related aftershocks together) to a fixed but high amount per country, being adequate in relation to the afore-said surplus situation, say 5 billion dollars anyone occurrence for US-domiciled companies.
- Any amounts that may exceed the limit decided upon should be guaranteed by the government.

Such a system could work rather well. The banks could, by requiring earthquake insurance, increase the insured sector substantially. The insurance companies do have the organization and capability to settle losses and, after the infrequent supercatastrophes, the government would reimburse them any amounts in excess of the fixed limit.

Whether or not such schemes come true, much can be done to improve the insurance industry's capability to absorb a growing exposure to the earthquake risk. The tax legislations are in most countries rather shortsighted. Sweden is in most respects a "high tax" country, but the tax rules for insurance companies are foresighted and logical. The companies are allowed to load premiums and loss reserves up to high amounts taxdeductible, thus building up substantial "hidden" catastrophe reserves to be used when the loss experience turns to a severely bad one. Colombia and Mexico are on their way in the same direction having stipulated that 80 and 60 percent respectively of the earthquake premiums have to be put aside each year to an accumulating earthquake fund, and that these dispositions should be taxfree.

There is, in fact, no sense in having to pay tax on what seems to be profit from the earthquake premium during years without damaging events. The effects of such a taxation is even disastrous. What happens during say a 50 years return period between two damaging earthquakes is, that only 50 % of the premium can be funded, if the corporate tax is 50 %. This means that either the insureds must be charged twice the premium needed, or the insurers will lose money. To charge double premium would only increase the population's reluctance to buy earthquake coverage even more. Hopefully the governments will realize that the premium for the catastrophe business should be funded without a prior heavy taxation.

Thus insurers and reinsurers already today have to tackle some intricate problems related to earthquake coverages. It is however easy to envision one future problem which may very well outweigh the present ones. That is the situation which will arise when fairly reliable earthquake predictions will be publicly announced, also for major quakes.

All insurance operations are based on the assumptions that neither the insured nor the insurer knows when a loss will occur, but that the losses should occur in accordance with some kind of stochastic process for which the mean value, and preferably the variance, of the loss distribution can be fairly well estimated.

Already before "the prediction era" earthquake insurance falls a little outside these conditions. It is true that insureds or insurers do not know when a loss will occur, but the frequency of damaging quakes in anyone area is so low that the rating procedure is hardly a pure actuarial or statistical task. Statistical data are too inadequate. Professor Clarence R. Allen has pointed out<sup>1</sup> that sometimes geologic records of the Holocene epoch, or even of the entire Quaternary period provide better knowledge about the seismicity of any given region than actual statistical records.

However, when successful prediction will be possible also the first condition will no longer be fulfilled. It seems evident that such predictions will be possible in the near future, perhaps in 10 to 20 years time. Such a development should deserve full support from the insurance industry, although a voluntary earthquake insurance system no longer will be possible. A voluntary system would result in an even less demand for coverage as long as no strong quake is predicted, whereas the demand would increase tremendously in an area when a prediction has been issued. At that time the insurance companies will certainly not be able to accept new liabilities to any premium rates but such as will in turn be unacceptable to the insureds. It may still be possible to insure high quality earthquake resistant buildings against an unexpected total - or nearly total - loss, since for such buildings the destruction ratio might be regarded as random.

---

I Earthquake Information Bulletin, Volume 10, Number 1

It is however, difficult to suggest a general solution although some kind of semi-compulsory coverage seems to become unavoidable. To collect enough premiums to cover the earthquake losses only by payments made from areas where a quake is known to be more or less imminent will anyway not be possible.

Also other lines of insurance may be affected by earthquake prediction, although more indirectly. A reliable prediction will be followed up by warnings and some loss preventing measures will be taken. For instance, people living or working in buildings of weak construction will hopefully be moved to safer places. In most cities large areas thus will be evacuated for some time.

Public response to warnings has been studied in connection with other potentially dangerous events such as floods, hurricanes and tornadoes. The common opinion is<sup>I</sup> that people will react calmly and optimistically and to a great extent continue their daily life. Very little panic is expected. It is however probable that some measures will have to be taken to avoid, or at least limit possible effects of various criminal activities in larger evacuated areas. In all big cities there is an obvious risk for looting and burglary surges under such extraordinary conditions.

#### CONCLUSIONS

The first important insurance markets to become affected by successful predictions are probably the US and Japan where the possibilities for sufficient instrumentation seem to be the best. The US insurance market is by far the largest and makes up for roughly 50 % of the total world market. Although the insurance industry does not need very long time to adjust its products in accordance with the foreseeable development it is therefore important that representatives of local insurers and international reinsurers keep themselves well informed in order to find future solutions which will provide effective protection and utilize the available insurance capacity as far as possible. The importance of an organization like Insurance Services Office can in this connection not be stressed enough.

---

I Earthquake Prediction and Public Policy, National Academy of Sciences, Washington D.C. 1975

# The U. S. Geological Survey's Role in Geologic-Related Hazards Warning

by D. R. Nichols and R. A. Matthews<sup>I</sup>

## ABSTRACT

In response to the Disaster Relief Act of 1974 and subsequent delegations of authority, and under the authority of its Organic Act, the U. S. Geological Survey published in the Federal Register a description of its capabilities for predicting geologic-related hazardous events and proposed procedures for providing such information to government officials and the general public. Three levels of geologic-related hazard information were defined: Notice of Potential Hazards; Hazard Watch; and Hazard Warning.

Although the procedures have not been formally adopted, examples of four potential hazards have been brought to the attention of public officials during the past 18 months: (a) a rockfall in Billings, Montana, (b) an active fault in Ventura, California, (c) potential hazards from ground fissuring and faulting in Las Vegas Valley, Nevada; and (d) a landslide near Kodiak, Alaska.

In these cases, the Geological Survey's role was essentially one of identifying and documenting a hazard and communicating technical information. Recommendations or orders to take defensive action are issued by officials of State and local government, where the police and public safety authority rests in our governmental system.

## INTRODUCTION

Although the U. S. Geological Survey has been investigating geologic-related hazards for much of its 100-year history, except for the present Earthquake Hazard Reduction Program, it has not had formal programs directed at hazard identification with the objective of providing warnings for State or local governments. Nevertheless, where volcanic, landslide, subsidence, and other hazards have been identified and mapped incidental to other mapping programs within the Survey, such information has been brought to the attention of concerned officials in the past.

With the passage of the Disaster Relief Act of 1974 and the redelegation of authorities contained in Section 202(b), 202(c), and 202(d) of that Act, first to the Secretary of the Department of Housing and Urban Development, then to the Secretary of Interior, and finally to the Director of the Geological Survey, the Survey developed proposed procedures for warning and preparedness for geologic-related hazards. These procedures, based on the authority provided under the Survey's Organic Act, are outlined in a statement published in the Federal Register on April 12, 1977 (Volume 42, No. 70).

## PROCEDURES

The Federal Register statement describes the Survey's capabilities

<sup>I</sup>Hazards Information Coordinator and Deputy Hazards Information Coordinator, respectively, U. S. Geological Survey, Reston, Virginia.

to predict hazardous events, which are defined as those geologic processes and conditions that could result in harm to people and property. These include earthquakes, volcanic eruptions, landslides, mudflows, subsidence, and glacier-related phenomena, such as the release of glacier-dammed lakes and rapid ice surges or retreats. The statement also notes that the present capability of scientists to predict hazardous events varies greatly with the type of event and with regard to its time, place, and magnitude of effects. The Federal Register statement summarizes the state-of-the-art in predicting each type of these events and emphasizes that, except for earthquakes, there is no comprehensive national program to identify, map, or evaluate geologic-related hazards. It does note, however, that when and where information is obtained, the U. S. Geological Survey will attempt to authenticate it and communicate such information to appropriate State, local, and Federal authorities and to the public.

#### Hazard Identification

When a potentially hazardous event, process, or condition is identified by a Survey employee during the course of carrying out official duties and responsibilities, the employee is asked to document the potential hazard as precisely and completely as possible. As a minimum, the documentation should describe:

- (a) geologic, hydrologic, or other pertinent conditions that exist;
- (b) factors that indicate that such conditions constitute a potential hazard;
- (c) location or area that may be affected;
- (d) estimated severity and time of occurrence, if such estimates are justified by available information;
- (e) other pertinent supporting data, including estimates of the size of the population likely to be affected and, if appropriate, the number and types of structures likely to be affected;
- (f) possible mitigating measures, if appropriate, and their potential effectiveness; and
- (g) where possible, a listing of the names of authorities known to have principal responsibility for health, safety, and welfare in the area likely to be affected (i.e., Mayor, City Engineer, Department of Public Works, County Manager, or, if multicounty or multistate, Governors and Offices of Emergency Services) and Federal agencies having installations, structures, or activities in the area.

#### Hazard Evaluation

Three levels of geologic-related hazard information were defined in the Federal Register statement: (1) Notice of potential hazard.--The



communication of information on the location and possible magnitude of geologic effects of a potentially hazardous geologic event process, or condition.

(2) Hazard watch.--The communication of information, as it develops from a monitoring program or from observed precursor phenomena, that a potentially catastrophic event of generally predictable magnitude may be imminent in a general area or region and within an indefinite time period (possibly months or years).

(3) Hazard warning.--The communication of information (prediction) as to the time (possibly within days or hours), location, and magnitude of a potentially disastrous geologic event or process.

These terms refer to the issuance of technical information to officials responsible for public safety and to the news media.

Information pertaining to potentially hazardous conditions or events is submitted to a carefully selected scientific evaluation panel for review of the scientific basis for the hazard identification. Such panels may be established formally, such as the Survey's Earthquake Prediction Council (now being reconstituted as the National Earthquake Prediction Council), which relies on scientific expertise pertaining to a specific type of hazard; or informally with membership changing according to the need for topical or areal expertise consistent with different types or areas of potential hazard. Upon review of the evidence, the evaluation panel transmits its finding and recommendations to the Director. The panel may find that: (a) a hazard to life or property is unlikely or insufficiently defined to justify a Notice of Potential Hazard without additional information; (b) a potential hazard to life or property exists; (c) the potential hazard exists and that monitoring by the Geological Survey could lead to better definition of location or magnitude, extent, or timing of hazard; or (d) the hazard conditions are sufficiently well-defined as to location, magnitude, and time to warrant the issuance of a Hazard Watch or Hazard Warning.

Similarly, the Director will undertake to have reviewed and evaluated identifications or predictions of potentially hazardous events made by scientists outside the Geological Survey as deemed appropriate or upon the request of the head of a concerned State or Federal agency. The requestor will be notified promptly of the findings of the evaluation panel and, if appropriate, a Notice of Potential Hazard, Hazard Watch, or Hazard Warning will be issued.

#### Communication

The procedures to be followed by the U. S. Geological Survey in documenting and verifying information on potential hazards and in transmitting it to government officials and the public depend on (1) the apparent urgency in releasing information in order to save lives and property, (2) whether the information was developed as an objective of a Survey project, incidental to a project, or unrelated to a specific project but in connection with official duties. The procedures outlined

are intended to transmit such information as soon as possible consistent with sound scientific review.

In rare instances the initial identification of a hazardous event may be made while the event is in process or when it is likely to occur so soon that no time is available to contact a Geological Survey office. If a Survey employee observes such an immediate hazard that presents a clear risk to life and property, and there does not appear to be sufficient time to contact a responsible Survey official for scientific evaluation and policy review, the employee should make every reasonable effort to communicate the observations immediately and directly to the affected parties and appropriate local public officials.

In most instances, however, there will be sufficient time to provide a thorough scientific review and evaluation before communicating the information to appropriate public officials.

Transmittal of such information is commonly as a letter, followed by a news release. The letter includes a description of the geologic and hydrologic conditions that exist, the factors that suggest such conditions constitute a potential hazard, and the location or area they may affect. In most instances it will not be possible to estimate the severity of the hazard or the time it might occur. Where potentially hazardous conditions are monitored by the Geological Survey, local, State, and Federal authorities will be informed periodically of the results of such investigations. Technical assistance, to the extent possible, will be extended as requested by these officials to assist in developing possible mitigation measures.

Notices of Potential Hazard, Hazard Watches, and Hazard Warnings to government agencies will also include: (a) the statement of the authority of the Geological Survey for issuing the Notice, Watch, or Warning; (b) copies of scientific papers or authentication reports that form the basis of the Notice, Watch, or Warning; (c) an offer to consult with any reviewers that the governor or governors of affected States may wish to appoint; (d) an offer to provide appropriate technical assistance within areas of expertise in the Geological Survey in evaluating possible geologic hazards as it may effect people and property; (e) a statement of what additional steps, if any, the Geological Survey proposes to take to better define the degree or area of hazard; and (f) a list of all parties to whom the Notice, Watch, or Warning is being transmitted.

#### ACTIVITIES TO DATE

Upon publication of the Federal Register statement, letters were transmitted to the governors of all 50 States and Territories and to some 75 Federal agencies inviting them to designate representatives with whom the Geological Survey could develop specific procedures for transmitting information on geologic-related hazards. Only three States failed to name a representative. Of those named, 25 are with State Offices of Civil Defense or Disaster Preparedness, 18 are with State Geological Surveys, seven are members of governor's staff, three are from State Departments of Natural Resources, two are from State Planning

offices, one from a State Institute for Environmental Quality, and one is with the State university; several States named two representatives. Since then, we have met with representatives from 18 states and other officials as appropriate, in groups of two to four States at a time to work out detailed procedures tailored to the interests of each State. We have normally invited representatives from National Oceanic and Atmospheric Administration, the Federal Disaster Assistance Administration, and on two occasions, the Environmental Protection Agency, to these meetings. In general, the procedures that have evolved follow the pattern established with the State of California. The Survey's Hazards Information Coordinator will telephone the designated State representative to provide advance notice that a hazard communication is under consideration; where time permits, a draft of a letter will be sent to the State representative for comments. If the representative is not the State Geologist, a copy of the draft will also be sent to him. The State will then provide their response, which will be included with the recommendations of the evaluation panel and the Hazards Information Coordinator, and will be sent to the Director.

If the Director decides to issue a Notice, Watch, or Warning, an official letter will be sent to the State representative with copies to all affected State agencies, such as the State Geological Survey, the State Engineer, and the Department of Transportation; the State's Senators and Congressional representatives whose districts are effected; and the mayors and chairmen of Boards of Supervisors of affected local jurisdictions. A news release for general circulation will be issued simultaneously or shortly after the official notice. Copies of the letter and documentation will also be sent to designated representatives of all Federal agencies that have facilities in the affected area or that have loan or grant programs to the State(s), local jurisdiction(s), and organizations in the affected area.

Pending adoption of final procedures, official Hazard Notices, Watches, or Warnings are not being issued. Nevertheless, letters that are generally in accordance with the procedures described in the Federal Register have been sent to four jurisdictions and are examples of what would constitute a Notice of Potential Hazard. The first was to the Mayor of Billings, Montana, notifying him of a potential rockfall on the bluffs of the Yellowstone River where a block of rock, weighing approximately 20,000 tons, appears to be moving outward and endangering three to eight residences below.

The second letter was to the State Geologist of California, who has responsibility under the Alquist-Priolo Special Study Zone Act, to designate areas of active and potentially active faulting. In this case, the Survey transmitted an MF map that showed the location of the Ventura fault, which passes through Ventura, California. The accompanying text provides evidence that the fault has been active within the last 6,000 years. State law requires that the State Geologist designate such faults as active and delineate a special studies zone a quarter mile wide or less on either side of the active traces. A third letter and accompanying open-file report was sent to the Nevada State representative describing potential faulting and fissuring accompanying differential subsidence along pre-existing faults in the alluvium of Las Vegas

Valley. Should differential subsidence continue, it could result in increased fissuring and movement along pre-existing faults which would endanger the foundation of structures built across them. The most recent letter and open-file report was sent to the State of Alaska's representative describing a large landslide extending from sea level to 1,100 feet above Kodiak Harbor. Portions of the landslide, which is a half mile wide and more than 180 feet thick, are currently moving slowly. If the entire mass were to fail suddenly, perhaps triggered by an earthquake or an extremely heavy rainfall, it could generate a sea wave comparable to the tsunami that struck Kodiak during the 1964 Alaskan earthquake in which more than 24 billion dollars damage occurred and two people lost their lives (Kachadoorian and Plafker, 1967, p. F17).

Several examples illustrate what might constitute a Hazard Watch. One involved alerting State and local officials of a possible flank eruption of Mauna Loa volcano during 1978. Survey personnel are monitoring the volcano and have participated with State and local officials in pre-eruption planning. Another example is the visit of the Director, in 1976, to notify Governor Brown's office of the uplift along the San Andreas fault in southern California and of the monitoring activities being planned. The Survey, in cooperation with the National Geodetic Survey and State and local agencies, has resurveyed the area and has installed numerous instruments to detect possible precursory indicators of earthquakes. A third example is the notification of State, local, and Federal officials of the increased activity of Mount Baker in 1975, which resulted in a number of measures to limit human occupation of potential hazard areas (Frank, Meir, and Swanson, 1977, p. 39-41). Subsequent monitoring indicated a lower level of risk and restrictions were lifted.

There are no examples of predictions having been made that would constitute a Hazard Warning as defined in the Federal Register. However, if Mauna Loa continues to perform according to past history, such a warning could be issued to the State and the city of Hilo.

In addition to meeting with State and Federal representatives to develop specific procedures for communicating information of geologic hazards, the Geological Survey plans to conduct workshops in areas affected by identified geologic-related hazards to help public officials and the public understand the nature of the hazard and possible mitigation measures that could be undertaken to reduce risk. We are also preparing leaflets, pamphlets, circulars, and a 30-minute movie to help the public and governmental officials understand the nature of geologic hazards and measures by which they could avoid or mitigate the effects.

#### PROBLEMS

The Survey recognizes that providing earth-science information in accordance with its expertise is only the first of the inputs needed by State and local governments and the public in mitigating the effects of geologic hazards. The actual adoption of the most effective mitigation measures by local authorities will result from a cooperative effort by agencies at all governmental levels and by nongovernmental organizations.

and the public. Decisions for adoption of such mitigation measures should be based upon a broad range of earth-science, engineering, and socio-economic information.

Our experience to date in communicating information on geologic-hazards to Federal and State governments has been generally positive. Most are quite receptive to the Federal government and the Survey undertaking this role and are pleased to cooperate. However, local government recipients of such information have been much less enthusiastic. They are faced with two principal problems. First, they lack the technical expertise to assess the specific risk involved and the funding to develop possible engineering solutions to the risks where such may be economically feasible. Second, local governments are also faced with the possibility that, given the information, they may be liable for any failure to reduce the hazard. Unfortunately, funds from State and Federal agencies are generally not available to assist in hazard mitigation until after a disaster has occurred.

The Program we have described is in the developmental stage and will be modified as time and experience dictate. We are attempting to assess the effects and results of the program as it proceeds and to monitor socioeconomic research on hazard warnings to help guide our efforts. Several areas of needed improvement have been identified. First is the possible need for more explicit legislative authority, coupled with an amendment to the Federal Tort Liability Act to exempt the Survey from liability for the issuance of warnings. Such exemption may be needed to avoid law suits seeking compensation for losses to individuals or a community as a result of a warning. It would also avoid liability for not issuing warnings of events of which we have no fore knowledge. The Survey is also in the process of drafting a charter for a National Earthquake Prediction Evaluation Council to expand the expertise available for evaluating earthquake predictions.

#### REFERENCES

- Frank, David, Meir, M. F., and Swanson, D., 1977, Assessment of increased thermal activity at Mount Baker, Washington, March 1975-March 1976: U. S. Geological Survey Professional Paper 1022A, p. A1-A49.
- Kachadoorian, Reuben and Plafker, George, 1967, "Effects of the Earthquake of March 27, 1964 on the communities of Kodiak and nearby islands": U. S. Geological Survey Professional Paper 542F, p. F1-F41.









## INDEX OF AUTHORS

- Abdel-Ghaffar, A.M. ....II-1037  
 Abolafia, M. ....III-1489  
 Acharya, H.K. ....I-379  
 Alarcón, E. ....II-921  
 Aki, K. ....II-1051  
 Akky, M.R. ....III-1307  
 Algermissen, S.T. ....I-291, 497  
 Alonso, J.L. ....I-523  
 Alt, J.N. ....II-669  
 Anderson, J.G. ....I-559  
 Apsel, R. ....II-693  
 Arango, I. ....II-983  
 Archuleta, R.J. ....I-255  
 Arya, A.S. ....II-865  
  
 Ballard, R.F. Jr. ....II-1013  
 Bazán, E. ....II-657  
 Bea, R.G. ....III-1307  
 Bell, E.J. ....I-471  
 Bell, J.W. ....I-471  
 Benjamin, J.R. ....III-1369  
 Bertero, V.V. ....III-1145  
 Bhatia, S.K. ....II-839  
 Bolt, B.A. ....II-617  
 Boore, D.M. ....I-255; III-1447  
 Borchardt, R.D. ....I-229, 241  
 Botsai, E.E. ....I-193  
 Brabb, E.E. ....I-229, 303  
 Brune, J. ....II-1051  
 Byrd, R.C. ....III-1409  
  
 Campbell, K.W. ....II-1063  
 Chandrasekaran, A.R. ....III-1157  
 Chen, J.H. ....III-1169  
 Chen, P.C. ....III-1169  
 Clayton, D.N. ....II-983  
 Cluff, L.S. ....I-135, 457, 535;  
     II-669; III-1281  
 Cochran, H.C. ....III-1511  
 Cooper, S.S. ....II-1013  
 Crouse, C.B. ....II-1117  
  
 Delfosse, G.C. ....III-1223  
 Deza, E. ....I-341  
 Dezfulian, H. ....II-873  
 Dobry, R. ....II-945  
 Dominguez, J. ....II-921  
 Donovan, N.C. ....I-55  
 Doyle, E.H. ....III-1433  
 Duke, C.M. ....II-1025  
  
 Eguchi, R.T. ....III-1341  
 England, R. ....II-813  
 Eskijian, M.L. ....III-1257  
 Esteva, L. ....II-657  
  
 Finn, W.D.L. ....II-839  
 Fischer, J.A. ....I-329; III-1329  
 Frazier, G.A. ....II-693  
 Fumal, T.E. ....I-241  
 Furuya, T. ....II-1001  
  
 Gardner, W.S. ....II-945  
 Gibbs, J.F. ....I-241  
 Glass, C.E. ....I-509  
 Goto, N. ....II-793  
 Grant, W.P. ....II-983  
  
 Hadjian, A.H. ....III-1199  
 Hall, W.J. ....III-1235  
 Harp, E.L. ....I-279, 353  
 Hart, E.W. ....II-635  
 Hart, G.C. ....III-1135  
 Hasselman, T.K. ....III-1341  
 Hattori, S. ....I-421  
 Hayes, R.A. ....III-1383  
 Hays, W.W. ....I-497; II-753  
 Helmberger, D.V. ....I-27  
 Herd, D.G. ....I-231  
 Herrera, I. ....II-813  
 Hisada, T. ....III-1187  
 Hutton, J.R. ....I-179  
  
 Idriss, I.M. ....I-457; III-1281  
 Isenberg, J. ....II-911  
 Ishibashi, I. ....I-81  
 Ishihara, K. ....II-897  
 Iwasaki, T. ....II-705, 885; III-1211  
 Iwasaki, Y.T. ....I-445  
  
 Jaén, H. ....I-341  
 Jennings, P.C. ....I-27  
 Joyner, W.B. ....I-255  
  
 Kafka, A.L. ....III-1489  
 Kagami, H. ....II-793  
 Kallaby, J. ....III-1459  
 Kao, C.S. ....I-367  
 Kappler, H. ....III-1399  
 Katayama, T. ....I-606; II-705  
 Kawashima, K. ....II-705; III-1211  
 Keefer, D.K. ....I-279, 353  
 King, E.J. ....I-267  
 King, J. ....II-1051  
 King, K.W. ....I-497  
 Kircher, C. ....III-1369  
 Kisslinger, C. ....I-3  
 Kobayashi, H. ....I-588; II-825  
 Kockelman, W.J. ....I-303  
 Kogan, J. ....I-341  
 Kudo, K. ....II-765

- Kuribayashi, E. ....III-1499  
 Kuroiwa, J. ....I-341  
  
 Lagorio, H.J. ....I-193  
 Lam, I. ....II-1089  
 Liang, G.C. ....II-1025  
  
 Mahin, S.A. ....III-1145  
 Mándrescu, N. ....I-399  
 Marcuson, W.F. III ....II-1013  
 Mardiross, E. ....II-739  
 Martín, A. ....II-921  
 Martin, G.R. ....II-1089  
 Matthews, R.A. ....III-1531  
 Mau, S.T. ....I-367  
 McWhorter, J.G. ....I-329  
 Midorikawa, K. ....I-547  
 Midorikawa, S. ....I-588; II-825  
 Miletì, D.S. ....I-179  
 Miller, R.D. ....I-497  
 Milne, W.G. ....I-323  
 Miranda, J.C. ....III-1223  
 Mitchell, W.W. ....III-1459  
 Moazami-Goudarzi, K. ....I-391  
 Mohraz, B. ....III-1257  
 Morgan, J.R. ....III-1235  
 Moriwaki, Y. ....III-1433  
 Mukerjee, S. ....II-865  
 Murakami, S. ....I-547  
 Murphy, V.J. ....I-153  
  
 Nair, D. ....III-1383  
 Nandakumaran, P. ....II-865  
 Negmatullaev, S.Kh. ....II-681  
 Nemat-Nasser, S. ....II-957  
 Nersesov, I. ....II-1051  
 Newmark, N.M. ....III-1235  
 Nichols, D.R. ....III-1531  
 Nishi, M. ....II-971  
 Noda, T. ....II-971  
 Nowack, R.L. ....I-485  
  
 Ogawa, K. ....II-897  
 Ohsaki, Y. ....III-1187  
 Ohta, T. ....III-1187  
 Ohta, Y. ....II-793  
 Okahara, M. ....II-1001  
 Olson, R.A. ....III-1475  
 Oweis, I.S. ....II-777  
  
 Packer, D.R. ....I-457  
 Page, W.D. ....II-669  
 Parhikhteh, H. ....I-391  
 Paris, F. ....II-921  
 Patwardhan, A.S. ....I-485, 535;  
 III-1281, 1291  
 Paul, D.K. ....III-1157  
  
 Perkins, D.M. ....I-267  
 Perkins, J.B. ....I-315  
 Petrovski, J. ....I-413; III-1269  
 Ploessel, M.R. ....II-647  
 Power, M.S. ....II-801  
 Prager, S.R. ....II-873  
 Preston, R.F. ....I-267  
 Prothero, W. ....II-1051  
 Puri, V.K. ....II-865  
  
 Remmer, N.S. ....I-215  
 Rogers, A.M. ....II-753  
 Rojahn, C. ....II-681; III-1135  
 Roth, W.H. ....II-1105  
  
 Sabina, F.A. ....II-813  
 Sadigh, K. ....II-801  
 Saeki, M. ....II-705  
 Sánchez-Sesma, F.J. ....II-729  
 Savage, W.U. ....II-669  
 Schell, B.A. ....I-571  
 Schuëller, G.I. ....III-1399  
 Schwartz, D.P. ....I-457  
 Scott, R.F. ....II-1037  
 Seleznyov, G.S. ....II-681  
 Self, G. ....II-1051  
 Selzer, L.A. ....III-1341  
 Seo, K. ....I-588  
 Shakal, A.F. ....II-717  
 Sherif, M.A. ....I-81  
 Shibata, H. ....I-612  
 Shima, E. ....I-433  
 Shioi, Y. ....II-1001  
 Shokooh, A. ....II-957  
 Shpilker, G. ....II-1051  
 Simpson, D.W. ....II-681  
 Singh, R.D. ....II-945  
 Spiker, C.T. ....III-1329  
 Steinbrugge, K.V. ....I-203, 291  
 Sugimura, Y. ....II-933  
 Swan, F.H. III ....I-457  
 Swanger, H.J. ....III-1447  
 Sweet, J. ....II-693  
  
 Tai, M. ....I-445  
 Tanimoto, K. ....II-971  
 Tatsuoka, F. ....II-885  
 Tazaki, T. ....III-1499  
 Themptander, R. ....III-1525  
 Tillson, D.D. ....I-485  
 Tinsley, J.C. ....I-267  
 Tocher, D. ....II-669  
 Tohno, I. ....I-600  
 Tokida, K. ....II-885  
 Tokimatsu, K. ....I-600; II-853  
 Toksöz, M.N. ....II-717  
 Traubenik, M.L. ....II-1105

Trexler, D.T. ....I-471  
Trifunac, M.D. ....I-559  
Tsai, C.F. ....II-1089  
Ts'ao, H.S. ....II-1077  
Tucker, B. ....II-1051  
Tuel, D.G. ....I-279  
Turner, B.E. ....II-1117

Urbina, L. ....I-523

Vaid, Y.P. ....II-839  
Valera, J.E. ....II-1105  
Vaughan, D.K. ....II-911  
Veletsos, A.S. ....I-111

Watabe, M. ....III-1187  
Watt, B.J. ....III-1409  
Webster, F.A. ....III-1369  
Weichert, D.H. ....I-323  
Weidler, J.B. ....III-1383  
Werner, S.D. ....II-1077  
Whitman, R.V. ....III-1247  
Wieczorek, G.F. ....I-279, 353  
Wiggins, R.A. ....II-693  
Wilson, R.C. ....I-353  
Wu, F.T. ....II-701

Yasuda, S. ....II-885  
Yoshikawa, S. ....I-445  
Yoshimi, Y. ....I-600; II-853  
Youd, T.L. ....I-267  
Youngs, R.R. ....II-801

